

**EVALUATION OF STEEL I-SECTION BEAM AND BEAM-COLUMN
BRACING REQUIREMENTS BY TEST SIMULATION**

Ajinkya M. Lokhande and Donald W. White

Research Report
to the
American Institute of Steel Construction

School of Civil and Environmental Engineering
Georgia Institute of Technology

May 2015

TABLE OF CONTENTS

	Page
LIST OF TABLES	v
LIST OF FIGURES	vii
ABSTRACT	xv
CHAPTER 1 INTRODUCTION.....	1
1.1 PROBLEM STATEMENT AND OBJECTIVES	1
1.2 RESEARCH METHODS EMPLOYED IN THIS WORK.....	6
1.3 ORGANIZATION.....	10
CHAPTER 2 OVERALL STUDY DESIGN.....	11
2.1 STUDY INVARIANTS	11
2.2 OVERVIEW OF STUDY VARIABLES AND PROBLEM NAMING CONVENTION.....	13
2.2.1 <i>Member Type</i>	13
2.2.2 <i>Type of Loading</i>	14
2.2.3 <i>Bracing Type and Number of Intermediate Braces</i>	17
2.2.4 <i>Unbraced Length</i>	18
2.2.5 <i>Bracing Stiffness Ratios for Combined Lateral and Torsional Bracing</i>	19
2.3 EXAMPLE NAMING.....	25
CHAPTER 3 FINITE ELEMENT PROCEDURES	27
3.1 GENERAL MODELING CONSIDERATIONS	27
3.2 MODELLING OF BRACES	30
3.3 MATERIAL PROPERTIES	30
3.4 RESIDUAL STRESSES	32
3.5 BENCHMARK STUDIES	34
3.5.1 <i>Beam Benchmark Study</i>	34
3.5.2 <i>Column Benchmark Study</i>	37
3.6 GEOMETRIC IMPERFECTIONS IN BEAMS	39
3.7 GEOMETRIC IMPERFECTIONS IN BEAM-COLUMNS.....	44
3.7.1 <i>Beam-Columns with Point (Nodal) Lateral or Shear Panel (Relative) Lateral Bracing Only, Provided Only on One Flange</i>	44
3.7.2 <i>Beam-Columns with Combined Torsional and Lateral Bracing</i>	47

CHAPTER 4	BEAMS SUBJECTED TO MOMENT GRADIENT LOADING	49
4.1	OVERVIEW	49
4.2	DETAILED STUDY DESIGN	49
4.3	BEAM RIGIDLY-BRACED STRENGTHS	53
4.4	SUMMARY OF THE ANSI/AISC 360-10 BEAM BRACING EQUATIONS CONSIDERED IN THIS RESEARCH	55
4.5	RESULTS	61
4.5.1	<i>Beams with Moment Gradient 1 Loading, Basic Bracing Cases.....</i>	<i>61</i>
4.5.2	<i>Beams with Moment Gradient 1 Loading, Combined Bracing Cases, Positive Bending.....</i>	<i>68</i>
4.5.3	<i>Beams with Moment Gradient 1 Loading, Combined Bracing Cases, Negative Bending.....</i>	<i>75</i>
4.5.4	<i>Beams with Moment Gradient 2 Loading, Basic Bracing Cases.....</i>	<i>77</i>
4.5.5	<i>Beams with Moment Gradient 2 Loading, Combined Bracing Cases</i>	<i>82</i>
4.5.6	<i>Beams with Moment Gradient 3 Loading.....</i>	<i>88</i>
CHAPTER 5	BEAMS WITH TOP FLANGE LOADING.....	99
5.1	OVERVIEW	99
5.2	DETAILED STUDY DESIGN	99
5.3	RESULTS	100
CHAPTER 6	BEAM-COLUMNS SUBJECTED TO UNIFORM BENDING MOMENT	109
6.1	OVERVIEW	109
6.2	DETAILED STUDY DESIGN	109
6.3	RECOMMENDED BEAM-COLUMN BRACING REQUIREMENTS.....	113
6.3.1	<i>Beam-Columns with Lateral Bracing Only on the Flange in Flexural Compression and with $P_{ft}/P_{fc} < 0$.....</i>	<i>114</i>
6.3.2	<i>Beam-Columns with Lateral Bracing Only on the Flange in Flexural Compression and with $P_{ft}/P_{fc} > 0$.....</i>	<i>114</i>
6.3.3	<i>Beam-Columns Restrained by a Combination of Lateral and Torsional Bracing.....</i>	<i>115</i>
6.4	RESULTS	116
6.4.1	<i>Beam-Columns with Lateral Bracing Only on the Flange in Flexural Compression and with $P_{ft}/P_{fc} < 0$.....</i>	<i>116</i>
6.4.2	<i>Beam-Columns with Lateral Bracing Only on the Flange in Flexural Compression and with $P_{ft}/P_{fc} > 0$.....</i>	<i>130</i>
6.4.3	<i>Beam-Columns Restrained by a Combination of Lateral and Torsional Bracing.....</i>	<i>138</i>

CHAPTER 7 BEAM-COLUMNS SUBJECTED TO MOMENT GRADIENT LOADING	179
7.1 OVERVIEW	179
7.2 DETAILED STUDY DESIGN	179
7.3 RESULTS	183
7.3.1 <i>Beam-Columns with Point Lateral Bracing Only on the Flange in Flexural Compression, Subjected to Moment Gradient 1 Loading</i>	183
7.3.2 <i>Beam-Columns with Combined Lateral and Torsional Bracing, Subjected to Moment Gradient 1 Loading</i>	189
7.3.3 <i>Beam-Columns with Point Lateral Bracing Only on the Flange in Flexural Compression, Subjected to Moment Gradient 2 Loading</i>	220
7.3.4 <i>Beam-Columns with Combined Lateral and Torsional Bracing, Subjected to Moment Gradient 2 Loading</i>	223
CHAPTER 8 SUMMARY AND CONCLUSIONS	237
APPENDIX	247
REFERENCES	285

LIST OF TABLES

	Page
Table 1.1. Bracing graphics key.	3
Table 2.1. Naming convention for cases studied in this research.	14
Table 4.1. Comparison of rigidly-braced strengths for beams with Moment Gradient 1 loading and $n = 1$	54
Table 4.2. Comparison of rigidly-braced strengths for beams with Moment Gradient 1 loading and $n = 2$	54
Table 4.3. Comparison of rigidly-braced strengths for beams with Moment Gradient 2 loading and $n = 1$	54
Table 4.4. Comparison of rigidly-braced strengths for beams with Moment Gradient 3 loading and $n = 1$	55
Table 4.5. Comparison of rigidly-braced strengths for beams with Moment Gradient 3 loading and $n = 2$	55
Table 4.6. Comparison of β_{br} to β_{F98} and β_{F96} and summary of brace forces at $\beta = \beta_{br}$ for Moment Gradient 1 basic bracing cases.	67
Table 4.7. Comparison of β_{br} to β_{F98} and β_{F96} and summary of braced forces at $\beta = \beta_{br}$ for Moment Gradient 2 basic bracing cases with transverse loading at the beam centroid.	80
Table 5.1. Comparison of β_{br} to β_{F98} and β_{F96} and summary of brace forces at $\beta = \beta_{br}$ for Moment Gradient 2 basic bracing cases involving top flange loading.	104
Table 6.1. Brace stiffnesses β_{F96L} and β_{brL} and brace forces as a percentage of $(M/h_o + P/2)$ for beam-columns with lateral bracing only on the flange in flexural compression and with $P_{fi}/P_{fc} < 0$	129
Table 6.2. Brace stiffnesses β_{F96L} and β_{brL} and brace forces as a percentage of $(M/h_o + 2.5P)$ for beam-columns with lateral bracing only on the flange in flexural compression and with $P_{fi}/P_{fc} > 0$	137
Table 6.3. Brace stiffnesses β_{F96L} and β_{brL} and brace forces as a percentage of P for beam-columns with combined torsional and lateral bracing.	171
Table 6.4. Brace stiffnesses β_{F96T} and β_{brT} and torsional brace force as a percentage of $(M/h_o + P/2)$ for beam-columns with combined torsional and lateral bracing.	173
Table 7.1. Brace stiffnesses β_{F96L} and β_{brL} , and brace forces as a percentage of $(M/h_o + P/2)$ for beam-columns with Moment Gradient 1 loading, lateral bracing only on the flange in flexural compression, and $P_{fi}/P_{fc} < 0$	188
Table 7.2. Brace stiffnesses β_{F96L} and β_{brL} and point lateral brace forces as a percentage of P for beam-columns with Moment Gradient 1 loading and combined lateral and torsional bracing.	214

Table 7.3. Brace stiffnesses β_{F96T} and β_{brT} and torsional brace forces as a percentage of $(M/h_o + P/2)$ for beam-columns with Moment Gradient 1 loading and combined lateral and torsional bracing.....	216
Table 7.4. Peak load as a percentage of the rigidly-braced strength when $\beta_L = \beta_{brL}$	219
Table 7.5. Peak load as a percentage of the rigidly-braced strength when $\beta_T = \beta_{brT}$	219
Table 7.6. Brace stiffnesses β_{F96L} and β_{brL} and brace forces as a percentage of $(M/h_o + P/2)$ for beam-columns with Moment Gradient 2 loading, lateral bracing only on the flange in flexural compression and $P_{ft}/P_{fc} < 0$	223
Table 7.7. Brace stiffnesses β_{F96L} and β_{brL} and brace forces as a percentage of P for beam-columns with Moment Gradient 2 loading and combined lateral and torsional bracing.....	232
Table 7.8. Brace stiffnesses β_{F96T} and β_{brT} and torsional brace forces as a percentage of $(M/h_o + P/2)$ for beam-columns with Moment Gradient 2 loading and combined lateral and torsional bracing.....	233

LIST OF FIGURES

	Page
Figure 1.1. Point (Nodal) lateral bracing with $n = 1$	3
Figure 1.2. Shear panel (relative) lateral bracing with $n = 2$	3
Figure 1.3. Point torsional bracing with $n = 1$	3
Figure 1.4. Combined point torsional and point (nodal) lateral bracing with $n = 1$	4
Figure 1.5. Combined point torsional and shear panel (relative) lateral bracing with $n = 2$	4
Figure 1.6. Example maximum strength knuckle curve.	7
Figure 1.7. Example brace force versus brace stiffness curve.....	8
Figure 1.8. Example bracing stiffness interaction plot for combined bracing cases with lateral bracing on the flange in flexural compression.....	9
Figure 1.9. Example bracing stiffness interaction plot for combined bracing cases with lateral bracing on the flange in flexural tension.....	10
Figure 2.1. Moment Gradient 1 (MG1).	15
Figure 2.2. Moment Gradient 2 (MG2).	15
Figure 2.3. Moment Gradient 3 (MG3).	15
Figure 2.4. Load at centroid.....	16
Figure 2.5. Top flange loading.....	16
Figure 2.6. Torsional to lateral bracing stiffness interaction ratios (TLBSRs) for beams subjected to positive bending.....	21
Figure 2.7. Torsional to lateral bracing stiffness interaction ratios (TLBSRs) for beams subjected to negative bending.....	22
Figure 2.8. Naming convention example, test B_MG2pt_NB_n1_Lb5.....	25
Figure 3.1. Load application - axial load and moment.	28
Figure 3.2. Representative finite element model.	29
Figure 3.3. Steel stress-strain curve assumed in the structural analysis.	31
Figure 3.4. Lehigh residual stress pattern (Galambos and Ketter, 1959).	33
Figure 3.5. Results of beam benchmark study for uniform bending.	34
Figure 3.6. Results of beam benchmark study for Moment Gradient 2 loading.....	36
Figure 3.7. Out-of-straightness in the weak-axis bending direction for the benchmark study column.....	37
Figure 3.8. Results of the column benchmark study without local buckling imperfections.....	38
Figure 3.9. Results of the column benchmark study considering local buckling imperfections. .	39

Figure 3.10. Flange initial out-of-plane displacements corresponding to the imperfection pattern for the single-curvature bending cases in beams containing one intermediate brace point.....	41
Figure 3.11. Flange initial out-of-plane displacements corresponding to the imperfection pattern for the single-curvature bending cases in beams containing two intermediate brace points.....	41
Figure 3.12. Flange initial out-of-plane displacements corresponding to the imperfection pattern for the reversed-curvature bending cases in beams containing one intermediate brace point.....	43
Figure 3.13. Flange initial out-of-plane displacements corresponding to the imperfection pattern for the reversed-curvature bending cases in beams containing two intermediate brace points.....	43
Figure 3.14. Imperfection pattern for beam-columns with lateral bracing only, bracing only on the flange in flexural compression, and one intermediate brace point.....	45
Figure 3.15. Imperfection pattern for beam-columns with lateral bracing only, bracing only on the flange in flexural compression, and two intermediate brace points.....	46
Figure 3.16. End view of imperfection pattern for members with a single lateral brace only on the top flange, shown for three different effective flange force ratios.....	46
Figure 3.17. Imperfection pattern for beam-columns with combined lateral and torsional bracing and one intermediate brace point.....	47
Figure 3.18. Imperfection pattern for beam-columns with combined lateral and torsional bracing and two intermediate brace points.....	48
Figure 4.1. Beam knuckle curves and brace force vs. brace stiffness plots for point (nodal) lateral bracing cases with $n = 1$ and Moment Gradient 1 loading.....	64
Figure 4.2. Beam knuckle curves and brace force vs. brace stiffness plots for shear panel (relative) lateral bracing cases with $n = 2$ and Moment Gradient 1 loading.....	65
Figure 4.3. Beam knuckle curves and brace force vs. brace stiffness plots for point torsional bracing cases with $n = 1$ and Moment Gradient 1 loading.....	66
Figure 4.4. Brace force vs. the Load Proportionality Factor for B_MG1p_RB_n2_Lb5 with $\beta_L = \beta_{brL}$	67
Figure 4.5. Point (nodal) lateral and point torsional bracing stiffness interactions for Moment Gradient 1 loading and $n = 1$ (B_MG1p_CNTB_n1* and B_MG1n_CNTB_n1*).....	69
Figure 4.6. Shear panel (relative) lateral and point torsional bracing stiffness interactions for Moment Gradient 1 loading and $n = 2$ (B_MG1_CRTB_n2* and B_MG1n_CRTB_n2*)....	70
Figure 4.7. Point torsional and point lateral force tuples (M_{br}, P_{br}) corresponding to different combinations of recommended point (nodal) lateral and point torsional bracing stiffnesses from Fig. 4.5 for Moment Gradient 1 loading and $n = 1$ (B_MG1p_CNTB_n1* and B_MG1n_CNTB_n1*).....	73
Figure 4.8. Point torsional and shear panel lateral force tuples (M_{br}, V_{br}) corresponding to different combinations of recommended shear panel lateral and point torsional bracing	

stiffnesses from Fig. 4.6 for Moment Gradient 1 loading and $n = 2$ (B_MG1p_CRTB_n2* and B_MG1n_CRTB_n2*).	74
Figure 4.9. Beam knuckle curves and brace force vs. brace stiffness plots for point (nodal) lateral bracing cases with $n = 1$, Moment Gradient 2, and centroidal loading.	78
Figure 4.10. Beam knuckle curves and brace force vs. brace stiffness plots for torsional bracing cases with $n = 1$, Moment Gradient 2, and centroidal loading.	79
Figure 4.11. Brace force vs. the Load Proportionality Factor for B_MG2pc_TB_n1_Lb5 with $\beta = 80$ kip/in.	81
Figure 4.12. Point (nodal) lateral and point torsional bracing stiffness interactions for Moment Gradient 2, centroidal loading and $n = 1$ (B_MG2*c_CNTB_n1*).	83
Figure 4.13. Brace forces corresponding to different combinations of point (nodal) lateral and point torsional bracing stiffnesses used in the interaction plots for Moment Gradient 2 loading and $n = 1$ (B_MG2*c_CNTB_n1*) in Fig. 4.11.	84
Figure 4.14. Point lateral brace force vs. the Load Proportionality Factor for the case in Fig. 4.13a (B_MG2pc_CNTB_n1_Lb5_TLBSR1) where the lateral brace force at peak load is 1.8 % of P .	85
Figure 4.15. Point lateral brace force vs. the Load Proportionality Factor for the critical case in Fig. 4.13b (B_MG2nc_CNTB_n1_Lb5_TLBSR0.33) where the lateral brace force is 3.0 % of P and the torsional brace moment is 3.8 % of M at the peak load.	86
Figure 4.16. Point torsional brace force vs. the Load Proportionality Factor for the critical case in Fig. 4.13b (B_MG2nc_CNTB_n1_Lb5_TLBSR0.33) where the lateral brace force is 3.0 % of P and the torsional brace force is 3.8 % of M at the peak load.	86
Figure 4.17. Beam knuckle curves and brace force vs. brace stiffness plots for point torsional bracing cases with $n = 1$ and Moment Gradient 3 loading.	89
Figure 4.18. Point (nodal) lateral and point torsional bracing stiffness interaction for Moment Gradient 3 loading, $n = 1$ and $L_b = 15$ ft (B_MG3_CNTB_n1_Lb15*).	91
Figure 4.19. Beam knuckle curves and brace force vs. brace stiffness plots for combined point (nodal) lateral and point torsional bracing cases with $n = 1$, Moment Gradient 3 loading and $L_b = 15$ ft.	92
Figure 4.20. Brace forces corresponding to different combinations of point (nodal) lateral and point torsional bracing stiffnesses used in the Fig. 4.18 interaction plots for Moment Gradient 3 loading and $n = 1$ (B_MG3_CNTB_n1_Lb15*).	94
Figure 4.21. Shear panel (relative) lateral and point torsional bracing stiffness interaction for Moment Gradient 3 loading, $n = 2$ and $L_b = 15$ ft (B_MG3_CRTB_n2_Lb15*).	95
Figure 4.22. Beam knuckle curves and brace force vs. brace stiffness plots for combined shear panel (relative) lateral and point torsional bracing cases with $n = 2$, Moment Gradient 3 loading and $L_b = 15$ ft.	96
Figure 4.23. Brace forces corresponding to different combinations of shear panel (relative) lateral and point torsional bracing stiffnesses used in the Fig. 4.21 interaction plots for Moment Gradient 3 loading and $n = 2$ (B_MG3_CRTB_n2_Lb15*).	98

Figure 5.1. Beam knuckle curves and brace force vs. brace stiffness plots for point (nodal) lateral bracing cases with $n = 1$, Moment Gradient 2, and top flange loading.	102
Figure 5.2. Beam knuckle curves and brace force vs. brace stiffness plots for point torsional bracing cases with $n = 1$, Moment Gradient 2, and top flange loading.	103
Figure 5.3. Brace force vs. the Load Proportionality Factor for B_MG2pt_TB_n1_Lb5 with $\beta_T = \beta_{brT}$	105
Figure 5.4. Point (nodal) lateral and point torsional bracing stiffness interactions for Moment Gradient 2, top flange loading and $n = 1$ (B_MG2pt_CNTB_n1*)......	106
Figure 5.5. Brace forces corresponding to different combinations of point (nodal) lateral and point torsional bracing stiffnesses used in the interaction plots for Moment Gradient 2 loading and $n = 1$ (B_MG2*t_CNTB_n1*) in Fig. 5.3.	107
Figure 5.6. Point torsional brace force vs. the Load Proportionality Factor for the case B_MG2nt_CNTB_n1_TLBSR1 in Fig. 5.5b where torsional brace force at peak load is 5.1 %.....	108
Figure 6.1. brace force vs. brace stiffness plots for point (nodal) lateral bracing cases with $n = 1$, uniform bending with an effective flange force ratio $P_{ft}/P_{fc} \leq 0$, and $L_b = 5$ ft.	117
Figure 6.2. Beam-column knuckle curves and brace force vs. brace stiffness plots for point (nodal) lateral bracing cases with $n = 1$, uniform bending with an effective flange force ratio $P_{ft}/P_{fc} \leq 0$, and $L_b = 10$ ft.....	119
Figure 6.3. Beam-column knuckle curves and brace force vs. brace stiffness plots for point (nodal) lateral bracing cases with $n = 1$, uniform bending with an effective flange force ratio $P_{ft}/P_{fc} \leq 0$, and $L_b = 15$ ft.....	121
Figure 6.4. Beam-column knuckle curves and brace force vs. brace stiffness plots for shear panel (relative) lateral bracing cases with $n = 2$, uniform bending with an effective flange force ratio $P_{ft}/P_{fc} \leq 0$, and $L_b = 5$ ft.	123
Figure 6.5. Beam-column knuckle curves and brace force vs. brace stiffness plots for shear panel (relative) lateral bracing cases with $n = 2$, uniform bending with an effective flange force ratio $P_{ft}/P_{fc} \leq 0$, and $L_b = 10$ ft.	125
Figure 6.6. Beam-column knuckle curves and brace force vs. brace stiffness plots for shear panel (relative) lateral bracing cases with $n = 2$, uniform bending with an effective flange force ratio $P_{ft}/P_{fc} \leq 0$, and $L_b = 15$ ft.	127
Figure 6.7. Beam-column knuckle curves and brace force vs. brace stiffness plots for point (nodal) lateral bracing cases with $n = 1$, uniform bending with an effective flange force ratio $P_{ft}/P_{fc} > 0$, and $L_b = 5$ ft.	131
Figure 6.8. Beam-column knuckle curves and brace force vs. brace stiffness plots for point (nodal) lateral bracing cases with $n = 1$, uniform bending with an effective flange force ratio $P_{ft}/P_{fc} > 0$, and $L_b = 10$ ft.	132
Figure 6.9. Beam-column knuckle curves and brace force vs. brace stiffness plots for point (nodal) lateral bracing cases with $n = 1$, uniform bending with an effective flange force ratio $P_{ft}/P_{fc} > 0$, and $L_b = 15$ ft.	133

Figure 6.10. Beam-column knuckle curves and brace force vs. brace stiffness plots for shear panel (relative) lateral bracing cases with $n = 2$, uniform bending with an effective flange force ratio $P_{ft}/P_{fc} > 0$, and $L_b = 5$ ft.	134
Figure 6.11. Beam-column knuckle curves and brace force vs. brace stiffness plots for shear panel (relative) lateral bracing cases with $n = 2$, uniform bending with an effective flange force ratio $P_{ft}/P_{fc} > 0$, and $L_b = 10$ ft.	135
Figure 6.12. Beam-column knuckle curves and brace force vs. brace stiffness plots for shear panel (relative) lateral bracing cases with $n = 2$, uniform bending with an effective flange force ratio $P_{ft}/P_{fc} > 0$, and $L_b = 15$ ft.	136
Figure 6.13. Beam-column knuckle curves and brace force vs. brace stiffness plots for combined point (nodal) lateral and torsional bracing cases with $n = 1$, uniform bending with lateral bracing on the flange in flexural compression, and $L_b = 5$ ft.	139
Figure 6.14. Beam-column knuckle curves and brace force vs. brace stiffness plots for combined point (nodal) lateral and torsional bracing cases with $n = 1$, uniform bending with lateral bracing on the flange in flexural compression, and $L_b = 15$ ft.	142
Figure 6.15. Beam-column knuckle curves and brace force vs. brace stiffness plots for combined point (nodal) lateral and torsional bracing cases with $n = 1$, uniform bending with lateral bracing on the flange in flexural tension, and $L_b = 5$ ft.	145
Figure 6.16. Beam-column knuckle curves and brace force vs. brace stiffness plots for combined point (nodal) lateral and torsional bracing cases with $n = 1$, uniform bending with lateral bracing on the flange in flexural tension, and $L_b = 15$ ft.	148
Figure 6.17. Beam-column knuckle curves and brace force vs. brace stiffness plots for combined shear panel (relative) lateral and torsional bracing cases with $n = 2$, uniform bending with lateral bracing on the flange in flexural compression, and $L_b = 5$ ft.	151
Figure 6.18. Beam-column knuckle curves and brace force vs. brace stiffness plots for combined shear panel (relative) lateral and torsional bracing cases with $n = 2$, uniform bending with lateral bracing on the flange in flexural compression, and $L_b = 15$ ft.	156
Figure 6.19. Beam-column knuckle curves and brace force vs. brace stiffness plots for combined shear panel (relative) lateral and torsional bracing cases with $n = 2$, uniform bending with lateral bracing on the flange in flexural tension, and $L_b = 5$ ft.	161
Figure 6.20. Beam-column knuckle curves and brace force vs. brace stiffness plots for combined shear panel (relative) lateral and torsional bracing cases with $n = 2$, uniform bending with lateral bracing on the flange in flexural tension, and $L_b = 15$ ft.	166
Figure 6.21. Point lateral brace force vs. the Load Proportionality Factor for BC_UMp_CNTB_n1_Lb5_FFR1 corresponding to a point lateral brace stiffness of $\beta_{brL} = 33.82$ kip/in from Eq. (6-5) and a point torsional brace stiffness of $\beta_{brT} = 26.20$ from Eq. (6-7).	175
Figure 6.22. Point lateral brace force vs. the Load Proportionality Factor for BC_UMn_CNTB_n1_Lb5_FFR-0.67 corresponding to a point lateral brace stiffness of $\beta_{brL} = 4.64$ kip/in calculated from Eq. (6-5) and a point torsional brace stiffness of $\beta_{brT} = 12.09$ from Eq. (6-7).	176

Figure 6.23. Point lateral brace force vs. the Load Proportionality Factor for BC_UMp_CNTB_n1_Lb15_FFR-0.67 corresponding to a point lateral brace stiffness $\beta_{brL} = 0.68$ kip/in from Eq. (6-5) and a point torsional brace stiffness $\beta_{brT} = 10.16$ kip/in.....	177
Figure 7.1. Beam-column knuckle curves and brace force vs. brace stiffness plots for point (nodal) lateral bracing cases with $n = 1$, Moment Gradient 1 loading, and $L_b = 5$ ft.....	184
Figure 7.2. Beam-column knuckle curves and brace force vs. brace stiffness plots for point (nodal) lateral bracing cases with $n = 1$, Moment Gradient 1 loading, and $L_b = 15$ ft.....	185
Figure 7.3. Beam-column knuckle curves and brace force vs. brace stiffness plots for shear panel (relative) lateral bracing cases with $n = 2$, Moment Gradient 1 loading, and $L_b = 5$ ft.	186
Figure 7.4. Beam-column knuckle curves and brace force vs. brace stiffness plots for shear panel (relative) lateral bracing cases with $n = 2$, Moment Gradient 1 loading, and $L_b = 15$ ft. ..	187
Figure 7.5. Beam-column knuckle curves and brace force vs. brace stiffness plots for combined point (nodal) lateral and torsional bracing cases with $n = 1$, Moment Gradient 1 loading with lateral bracing on the flange in flexural compression, and $L_b = 5$ ft.	190
Figure 7.6. Beam-column knuckle curves and brace force vs. brace stiffness plots for combined point (nodal) lateral and torsional bracing cases with $n = 1$, Moment Gradient 1 loading with lateral bracing on the flange in flexural compression, and $L_b = 15$ ft.	192
Figure 7.7. Beam-column knuckle curves and brace force vs. brace stiffness plots for combined point (nodal) lateral and torsional bracing cases with $n = 1$, Moment Gradient 1 loading with lateral bracing on the flange in flexural tension, and $L_b = 5$ ft.....	194
Figure 7.8. Beam-column knuckle curves and brace force vs. brace stiffness plots for combined point (nodal) lateral and torsional bracing cases with $n = 1$, Moment Gradient 1 loading with lateral bracing on the flange in flexural tension, and $L_b = 15$ ft.....	196
Figure 7.9. Beam-column knuckle curves and brace force vs. brace stiffness plots for combined shear panel (relative) lateral and torsional bracing cases with $n = 2$, Moment Gradient 1 loading with lateral bracing on the flange in flexural compression, and $L_b = 5$ ft.	198
Figure 7.10. Beam-column knuckle curves and brace force vs. brace stiffness plots for combined shear panel (relative) lateral and torsional bracing cases with $n = 2$, Moment Gradient 1 loading with lateral bracing on the flange in flexural compression, and $L_b = 15$ ft. ..	202
Figure 7.11. Beam-column knuckle curves and brace force vs. brace stiffness plots for combined shear panel (relative) lateral and torsional bracing cases with $n = 2$, Moment Gradient 1 loading with lateral bracing on the flange in flexural tension, and $L_b = 5$ ft.....	206
Figure 7.12. Beam-column knuckle curves and brace force vs. brace stiffness plots for combined shear panel (relative) lateral and torsional bracing cases with $n = 2$, Moment Gradient 1 loading with lateral bracing on the flange in flexural tension, and $L_b = 15$ ft.....	210
Figure 7.13. Point lateral brace force vs. the Load Proportionality Factor for BC_MG1n_CNTB_n1_Lb15_FFR-0.5 corresponding to a point lateral brace stiffness $\beta_{brL} = 1.46$ kip/in from Eq. (6-5) and a point torsional brace stiffness $\beta_{brT} = 13.46$ kip/in from Eq. (6-7).	218

Figure 7.14. Beam-column knuckle curves and brace force vs. brace stiffness plots for point (nodal) lateral bracing cases with $n = 1$, Moment Gradient 2 loading, and $L_b = 5$ ft.	221
Figure 7.15. Beam-column knuckle curves and brace force vs. brace stiffness plots for point (nodal) lateral bracing cases with $n = 1$, Moment Gradient 2 loading, and $L_b = 15$ ft.	222
Figure 7.16. Beam-column knuckle curves and brace force vs. brace stiffness plots for combined point (nodal) lateral and torsional bracing cases with $n = 1$, Moment Gradient 2 loading with lateral bracing on the flange in flexural compression, and $L_b = 5$ ft.	224
Figure 7.17. Beam-column knuckle curves and brace force vs. brace stiffness plots for combined point (nodal) lateral and torsional bracing cases with $n = 1$, Moment Gradient 2 loading with lateral bracing on the flange in flexural compression, and $L_b = 15$ ft.	226
Figure 7.18. Beam-column knuckle curves and brace force vs. brace stiffness plots for combined point (nodal) lateral and torsional bracing cases with $n = 1$, Moment Gradient 2 loading with lateral bracing on the flange in flexural tension, and $L_b = 5$ ft.	228
Figure 7.19. Beam-column knuckle curves and brace force vs. brace stiffness plots for combined point (nodal) lateral and torsional bracing cases with $n = 1$, Moment Gradient 2 loading with lateral bracing on the flange in flexural tension, and $L_b = 15$ ft.	230
Figure 7.20. Point lateral brace force vs. the Load Proportionality Factor for BC_MG2n_CNTB_n1_Lb5_FFR-0.5 corresponding to a point lateral brace stiffness of $\beta_{brL} = 9.56$ kip/in from Eq. (6-5) and a point torsional brace stiffness of $\beta_{brT} = 15.26$ kip/in from Eq. (6-7).	235
Figure 7.21. Point torsional brace force vs. the Load Proportionality Factor for BC_MG2n_CNTB_n1_Lb5_FFR-0.5 corresponding to a point lateral brace stiffness of $\beta_{brL} = 9.56$ kip/in from Eq. (6-5) and a point torsional brace stiffness of $\beta_{brT} = 15.26$ kip/in from Eq. (6-7).	235
Figure A.1. Beam knuckle curves and brace force vs. brace stiffness plots for combined point (nodal) lateral and torsional bracing cases with $n = 1$, Moment Gradient 1 loading with lateral bracing on the flange in flexural compression, and $L_b = 5$ ft.	248
Figure A.2. Beam knuckle curves and brace force vs. brace stiffness plots for combined point (nodal) lateral and torsional bracing cases with $n = 1$, Moment Gradient 1 loading with lateral bracing on the flange in flexural compression, and $L_b = 15$ ft.	250
Figure A.3. Beam knuckle curves and brace force vs. brace stiffness plots for combined point (nodal) lateral and torsional bracing cases with $n = 1$, Moment Gradient 1 loading with lateral bracing on the flange in flexural tension, and $L_b = 5$ ft.	252
Figure A.4. Beam knuckle curves and brace force vs. brace stiffness plots for combined point (nodal) lateral and torsional bracing cases with $n = 1$, Moment Gradient 1 loading with lateral bracing on the flange in flexural tension, and $L_b = 15$ ft.	254
Figure A.5. Beam knuckle curves and brace force vs. brace stiffness plots for combined shear panel (relative) lateral and point torsional bracing cases with $n = 2$, Moment Gradient 1 loading with lateral bracing on the flange in flexural compression, and $L_b = 5$ ft.	256

Figure A.6. Beam knuckle curves and brace force vs. brace stiffness plots for combined shear panel (relative) lateral and point torsional bracing cases with $n = 2$, Moment Gradient 1 loading with lateral bracing on the flange in flexural compression, and $L_b = 15$ ft. .	259
Figure A.7. Beam knuckle curves and brace force vs. brace stiffness plots for combined shear panel (relative) lateral and point torsional bracing cases with $n = 2$, Moment Gradient 1 loading with lateral bracing on the flange in flexural tension, and $L_b = 5$ ft.	262
Figure A.8. Beam knuckle curves and brace force vs. brace stiffness plots for combined shear panel (relative) lateral and point torsional bracing cases with $n = 2$, Moment Gradient 1 loading with lateral bracing on the flange in flexural tension, and $L_b = 15$ ft.	265
Figure A.9. Beam knuckle curves and brace force vs. brace stiffness plots for combined point (nodal) lateral and torsional bracing cases with $n = 1$, Moment Gradient 2 loading with lateral bracing on the flange in flexural compression, intermediate transverse load applied at centroid of the mid-span cross-section, and $L_b = 5$ ft.	268
Figure A.10. Beam knuckle curves and brace force vs. brace stiffness plots for combined point (nodal) lateral and torsional bracing cases with $n = 1$, Moment Gradient 2 loading with lateral bracing on the flange in flexural compression, intermediate transverse load applied at centroid of the mid-span cross-section, and $L_b = 15$ ft.	270
Figure A.11. Beam knuckle curves and brace force vs. brace stiffness plots for combined point (nodal) lateral and torsional bracing cases with $n = 1$, Moment Gradient 2 loading with lateral bracing on the flange in flexural tension, intermediate transverse load applied at centroid of the mid-span cross-section, and $L_b = 5$ ft.	272
Figure A.12. Beam knuckle curves and brace force vs. brace stiffness plots for combined point (nodal) lateral and torsional bracing cases with $n = 1$, Moment Gradient 2 loading with lateral bracing on the flange in flexural tension, intermediate transverse load applied at centroid of the mid-span cross-section, and $L_b = 15$ ft.	274
Figure A.13. Beam knuckle curves and brace force vs. brace stiffness plots for combined point (nodal) lateral and torsional bracing cases with $n = 1$, Moment Gradient 2 loading with lateral bracing on the flange in flexural compression, intermediate transverse load applied at top flange of the mid-span cross-section, and $L_b = 5$ ft.	276
Figure A.14. Beam knuckle curves and brace force vs. brace stiffness plots for combined point (nodal) lateral and torsional bracing cases with $n = 1$, Moment Gradient 2 loading with lateral bracing on the flange in flexural compression, intermediate transverse load applied at top flange of the mid-span cross-section, and $L_b = 15$ ft.	278
Figure A.15. Beam knuckle curves and brace force vs. brace stiffness plots for combined point (nodal) lateral and torsional bracing cases with $n = 1$, Moment Gradient 2 loading with lateral bracing on the flange in flexural tension, intermediate transverse load applied at top flange of the mid-span cross-section, and $L_b = 5$ ft.	280
Figure A.16. Beam knuckle curves and brace force vs. brace stiffness plots for combined point (nodal) lateral and torsional bracing cases with $n = 1$, Moment Gradient 2 loading with lateral bracing on the flange in tension, intermediate transverse load applied at top flange of the mid-span cross-section, and $L_b = 15$ ft.	282

ABSTRACT

The ANSI/AISC 360-10 Appendix 6 provisions provide limited guidance on the bracing requirements for beam-columns. In cases involving point (nodal) or shear panel (relative) lateral bracing only, these provisions directly sum the corresponding strength and stiffness requirements for column and beam bracing. According to the Appendix 6 Commentary, this approach is expected to be conservative. However, in many practical beam-column bracing situations, the implications of simply summing the column and beam requirements are not clear. This is due to the impact of the lateral bracing position and the transverse load position through the cross-section depth, as well as the fact that both torsional and lateral restraint can be important attributes of the general beam-column bracing problem. Due to these factors, the simple addition of the column and beam bracing requirements is not necessarily conservative.

For cases involving torsional bracing combined with point (nodal) or shear panel (relative) lateral bracing, the ANSI/AISC 360-10 provisions simply state that “the required strength and stiffness shall be combined or distributed in a manner that is consistent with the resistance provided by the element(s) of the actual bracing details.” However, no guidance is provided on what constitutes a consistent combination or distribution of these bracing requirements. In fact, only limited guidance is available in the broader literature regarding the appropriate handling of combined lateral and torsional bracing even for I-section beams. Nevertheless, combined lateral and torsional bracing is quite common, particularly for beam-columns, since it is rare that separate and independent lateral bracing systems would be provided on both flanges of an I-section member. More complete guidance is needed for the proper consideration of combined lateral and torsional bracing of I-section beams and beam-columns in structural design.

This research focuses on a reasonably comprehensive evaluation of the bracing strength and stiffness requirements for doubly-symmetric I-section beams and beam-columns using refined Finite Element Analysis (FEA) test simulation. The research builds on recent simulation studies of the basic bracing behavior of beams subjected to uniform bending. Various cases of beam members subjected to moment gradient are considered first. This is followed by a wide range of studies of beam-column members subjected to constant axial load and uniform bending as well as constant axial load combined with moment gradient loading. A range of unbraced lengths are considered resulting in different levels of plasticity at the member strength limit states. In addition, various bracing configurations are addressed including point (nodal) lateral, shear panel (relative) lateral, point torsional, combined point lateral and point torsional, and combined shear panel lateral and point torsional bracing.

CHAPTER 1 INTRODUCTION

1.1 Problem Statement and Objectives

ANSI/AISC 360-10 Appendix 6 (AISC 2010a) provides equations for design of stability bracing for columns, beams and beam-columns. These equations address both strength and stiffness requirements for the bracing components. This research aims to evaluate the accuracy of the Appendix 6 provisions for beam members subjected to moment gradient loading, including the consideration of transverse load height effects. It also aims to provide recommendations for design of lateral and combined lateral and torsional bracing systems for beams and beam-columns. This study is part of an overall research program to investigate the stability bracing behavior of beam and beam-column members, and to provide recommendations for potential improvements to AISC 360 Appendix 6.

This research builds on recent FEA test simulation studies by Prado and White (2015) on the basic stability bracing behavior of beams subjected to uniform bending. These investigators studied the influence of the number of intermediate braces on beam bracing requirements. They also evaluated the impact of inelasticity on bracing requirements, by studying members with unbraced lengths, L_b , close to the AISC L_p and L_r limits as well as within the intermediate range of the AISC inelastic lateral-torsional buckling strength equations. Based on the AISC 360-10 Chapter F provisions, when $L_b \leq L_p$, I-section beams fail in uniform bending by what can be categorized as plastic lateral-torsional buckling, where the “maximum plateau” flexural resistance of the member is developed. Furthermore, when $L_p \leq L_b \leq L_r$, these members fail by inelastic lateral-torsional buckling. Finally, when $L_b > L_r$, the flexural strength limit state under uniform bending moment is elastic lateral-torsional buckling.

Prado and White (2015) showed that the AISC 360-10 Appendix 6 equations work well in many cases, especially when they are used with the various refinements given in the Specification

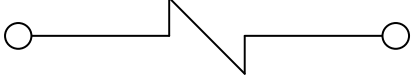
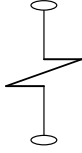
Commentary. However, improvements were recommended for some situations. In addition, Prado and White (2015) studied the benefits of combined lateral and torsional bracing of beams. They considered both lateral bracing at the level of the compression flange as well as at the level of the tension flange in combination with torsional restraint.

Since Prado and White (2015) only addressed beams subjected to uniform bending, one of the objectives of this research is to build on this work by studying the impact of moment gradient on the beam bracing requirements. Another objective is study the impact of transverse load height and to evaluate the performance of the ANSI/AISC 360-10 Appendix 6 (AISC 2010a) Commentary equations in capturing this effect. Lastly, a central objective of this work is the evaluation of the bracing behavior for beam-columns subjected to both uniform bending as well as moment gradient loading. The various bracing types considered in this work are as follows:

- Point (nodal) lateral bracing,
- Shear panel (relative) lateral bracing,
- Point torsional bracing,
- Combined point (nodal) lateral and point torsional bracing, and
- Combined shear panel (relative) lateral and point torsional bracing.

Table 1.1 summarizes the graphical symbols used in this work to represent the three basic types of bracing: point lateral, shear panel lateral and point torsional. The member configurations considered in this research for each of these bracing types are summarized in Figs. 1.1 through 1.5. The variable n in Figs. 1.1 through 1.5 indicates the number of intermediate braces. The member end lateral bracing is not shown in these figures. The member ends are torsionally simply-supported in all the studies conducted in this research. That is, the members are free to bend in the major- and minor-axis directions and they are free to warp at their ends. The end lateral displacements and torsional rotations are rigidly restrained.

Table 1.1. Bracing graphics key.

Brace Type	Graphical Symbol
Point (Nodal) lateral brace	
Shear panel (Relative) lateral brace	
Point torsional brace	

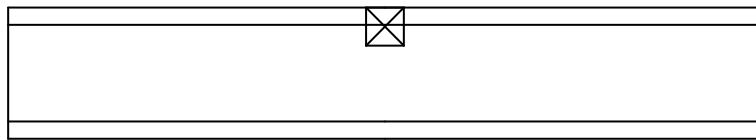


Figure 1.1. Point (Nodal) lateral bracing with $n = 1$.

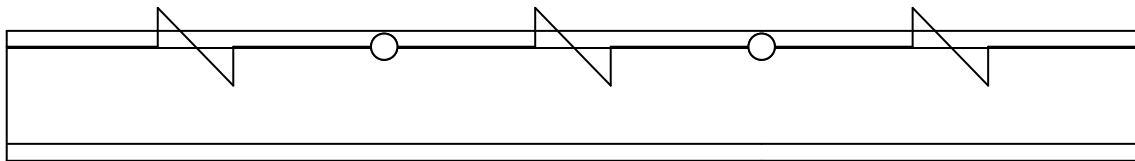


Figure 1.2. Shear panel (relative) lateral bracing with $n = 2$.

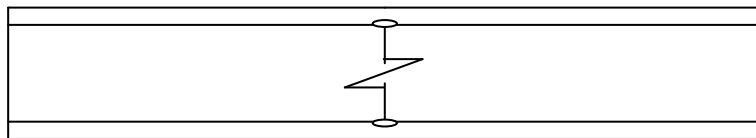


Figure 1.3. Point torsional bracing with $n = 1$.

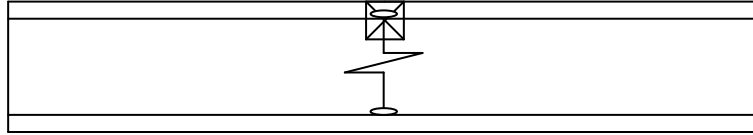


Figure 1.4. Combined point torsional and point (nodal) lateral bracing with $n = 1$.

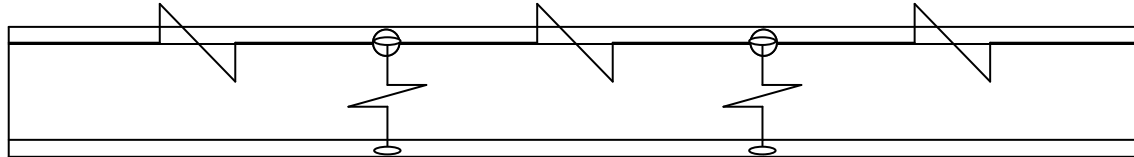


Figure 1.5. Combined point torsional and shear panel (relative) lateral bracing with $n = 2$.

Prado and White (2015) did not study the bracing requirements for members subjected to combined axial load and bending moment. Furthermore, the AISC 360-10 Appendix 6 provisions provide limited guidance on bracing requirements for beam-columns. In cases involving point (nodal) or shear panel (relative) lateral bracing only, these provisions directly sum the corresponding strength and stiffness requirements for column and beam bracing. According to the Appendix 6 Commentary, this approach is expected to be conservative. However, in many practical beam-column bracing situations, the implications of simply summing the column and beam requirements are not clear. This is due to the impact of the lateral bracing position and the transverse load position through the cross-section depth, as well as the fact that both torsional and lateral restraint can be important attributes of the general beam-column bracing problem. Due to these factors, the simple addition of the column and beam bracing requirements is not necessarily conservative. For cases involving torsional bracing combined with point (nodal) or shear panel (relative) lateral bracing, the ANSI/AISC 360-10 provisions simply state that “the required strength and stiffness shall be combined or distributed in a manner that is consistent with the resistance provided by the element(s) of the actual bracing details.” However, no guidance is provided on what constitutes a consistent combination or distribution of these bracing

requirements. Therefore, one of the major objectives of this research is to evaluate the bracing behavior and provide recommendations for design of stability bracing for beam-column members.

It is rare that beam-column members would be provided with independent lateral bracing on both flanges. In some cases, lateral bracing would be provided only on the flange in flexural compression; however, it is more common for general beam-columns to have a combination of lateral and torsional bracing. Therefore, another major objective of this research is to study the requirements for combined lateral and torsional bracing, and to provide recommendations for proper design of combined bracing systems for beams as well as beam-columns. From prior research (Prado and White 2015; Tran 2009), it is known that the behavior of combined bracing systems is different for cases where the lateral bracing is on the flange in flexural compression versus cases where the lateral bracing is on the flange in flexural tension. Hence, both positive and negative bending, i.e., cases involving compression on the laterally-braced flange and cases in which the laterally-braced flange is in tension, are studied in this research.

In summary, the main objectives of this research are:

- To evaluate the physical behavior and the performance of the ANSI/AISC 360-10 Appendix 6 equations in accounting for the effect of moment gradient on the bracing requirements for beams, including the consideration of basic point lateral, shear panel lateral, and point torsional bracing systems as well as combined lateral and torsional bracing.
- To evaluate the associated physical behavior and the performance of the AISC 360-10 Appendix 6 equations in accounting for transverse load height effects.
- To provide recommendations for the design of torsional and/or lateral bracing systems for beam-column members subjected to uniform major-axis bending.

- To provide recommendations for design of torsional and/or lateral bracing systems for beam-column members subjected to moment gradient loading.

1.2 Research Methods Employed in this Work

This research involves the use of refined finite element analysis (FEA) test simulation methods to determine the load-deflection and limit load response of beams and beam-columns, and their bracing systems, considering the influence of initial geometric imperfections, residual stress effects, and the overall spread of plasticity throughout the volume of the members. The members are modeled using shell finite elements, and thus the FEA models are capable of capturing overall member buckling, local buckling and distortional buckling influences as applicable for the cases studied. The general purpose finite element analysis software ABAQUS version 6.13 (Simulia 2013) is used throughout this work. Details of the FEA models are discussed in Chapter 3.

These refined test simulations are used to generate knuckle curves and brace force versus brace stiffness plots. Knuckle curves are basically plots of the member strength as a function of the brace stiffness. Knuckle curves have been used in prior research, e.g. Stanway et al. (1992a & b), Yura and Phillips (1992), Yura et al. (1992), Yura (1995), Helwig and Yura (1999), White et al. (2009), Bishop (2013), and Prado and White (2015), for assessing the behavior of stability bracing. Knuckle curves showing the maximum strength or limit load of physical members having initial geometric imperfections and residual stresses are useful in assessing the impact of different characteristics of stability bracing for design. This is because, for strength limit states design, one is interested in the maximum strength behavior of the physical geometrically imperfect elastic/inelastic member or structure.

Figure 1.6 shows an example maximum strength knuckle curve. The specific numerical values for the abscissa and ordinate are immaterial to the discussion of the general knuckle curve characteristics. Generally, maximum strength knuckle curves asymptote to a horizontal line,

corresponding to the resistance of the rigidly-braced structure, as the bracing stiffness is increased. Depending on the specific bracing characteristics, the knuckle curve can have a very gradual or a more abrupt approach to the rigidly-braced strength.

Also of significant importance to stability bracing design is the variation of the brace strength requirements as a function of the provided brace stiffness. Figure 1.7 shows an example plot of this type. The required brace strength requirement is defined as the maximum force developed in the subject bracing components at the limit load of various simulated tests. Again, the specific values of the ordinate and abscissa are not important to the discussion of the general characteristics here. The bracing strength requirement increases from zero, for zero stiffness (i.e., no bracing) to a maximum value at an intermediate bracing stiffness typically close to or slightly smaller than the stiffness corresponding to the knuckle in the knuckle curve. The required brace force (or the maximum of the brace forces when there are multiple braces) then tends to reduce with increasing brace stiffness beyond this value.

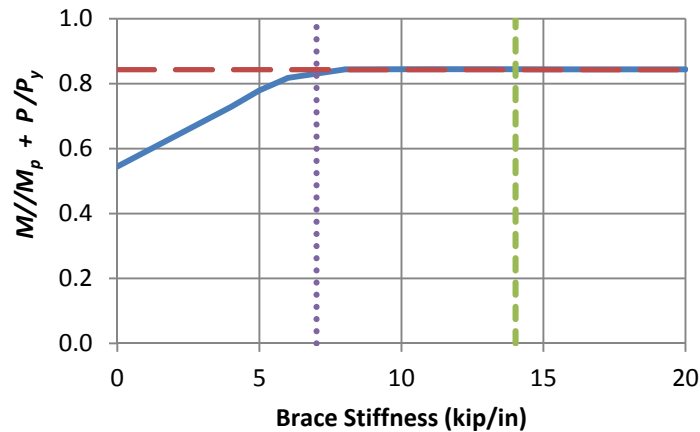


Figure 1.6. Example maximum strength knuckle curve.

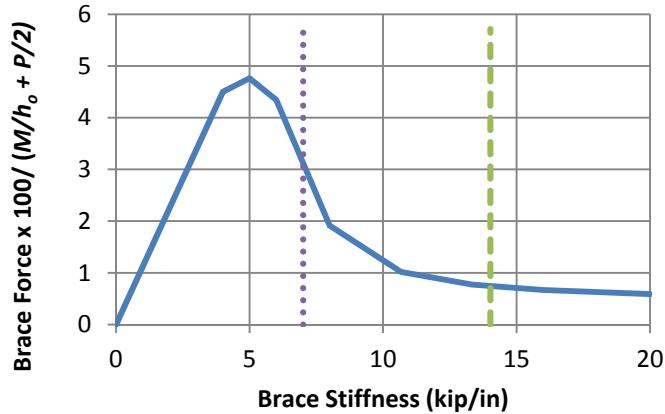


Figure 1.7. Example brace force versus brace stiffness curve.

As discussed in Section 1.1, one of the major objectives of this research is to provide recommendations for design of combined lateral and torsional bracing, considering the interaction between the separate bracing stiffnesses. As such, this research addresses questions such as: How much torsional bracing is required in combination with a particular amount of lateral bracing to effectively brace a beam or a beam-column?

One way of interpreting the results of combined torsional and lateral bracing cases is by plotting stiffness interaction curves. Figures 1.8 and 1.9 show example bracing stiffness interaction plots for combined torsional and lateral bracing with the lateral bracing placed on the flange in flexural compression and in flexural tension respectively. The bracing stiffness values plotted in the interaction plots are determined as the intersection points of the knuckle curves with the strengths corresponding to 98 and 96 % of the rigidly-braced strengths. The separate 98 and 96 % strength interaction curves in Figs. 1.8 and 1.9 are shown to highlight the nature of the asymptotic strength gain in the knuckle curves with increases in the brace stiffness as the member resistance approaches the rigidly-braced strength.

Based on a complete assessment of their data regarding the requirements for full bracing of beams subjected to uniform moment loading, Prado and White (2015) recommend that the bracing stiffnesses required to develop 96 % of the rigidly-braced member strength are appropriate targets for definition of the “fully-braced” member resistances, that is, the member resistances corresponding to lateral-torsional buckling of the beam members between the braced points. In this research, this criterion is used to assess the full bracing requirements for moment gradient loading on beams and for uniform bending and moment gradient loading of beam-columns.

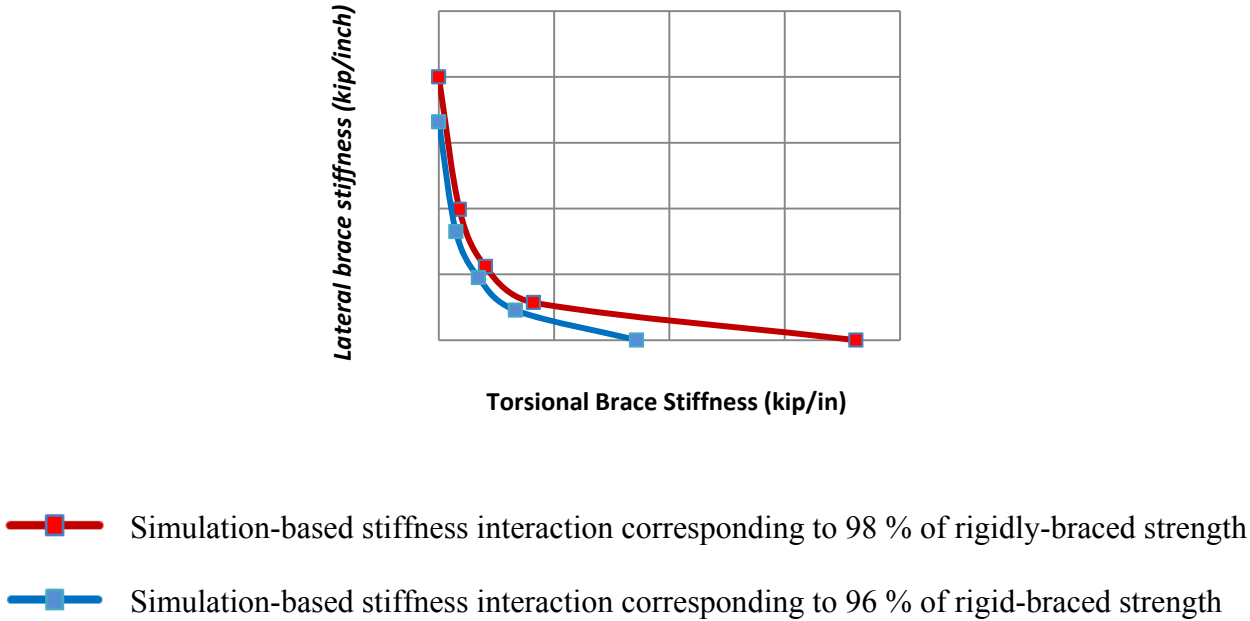
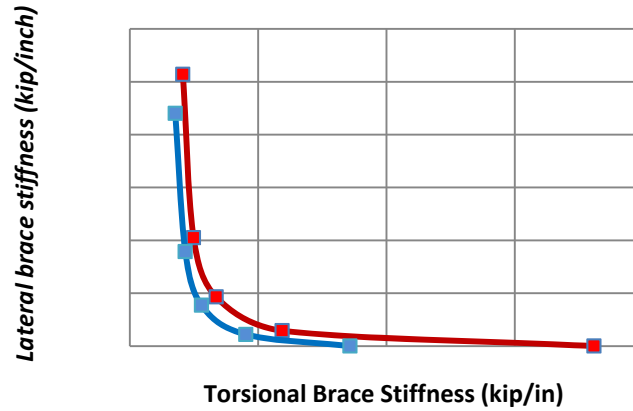


Figure 1.8. Example bracing stiffness interaction plot for combined bracing cases with lateral bracing on the flange in flexural compression.



- Simulation-based stiffness interaction corresponding to 98 % of rigidly-braced strength
- Simulation-based stiffness interaction corresponding to 96 % of rigidly-braced strength

Figure 1.9. Example bracing stiffness interaction plot for combined bracing cases with lateral bracing on the flange in flexural tension.

1.3 Organization

Chapter 2 reviews the overall design of this research study. Chapter 3 explains the details of the FEA procedures employed for the test simulations conducted in this work. Chapters 4 through 7 explain the results for the various loading and bracing configurations considered. Chapter 4 addresses beams subjected to moment gradient loading and Chapter 5 addresses the influence of transverse load height for beam members. Chapter 6 then addresses beam-columns subjected uniform bending moment and Chapter 7 addresses beam-columns subjected to moment gradient loading. Chapter 8 provides a summary and conclusions.

CHAPTER 2 OVERALL STUDY DESIGN

2.1 Study Invariants

The invariants in the study design of the current research are as follows:

- The steel material is A992 Grade 50. The member yield strengths are taken as $F_y = 50$ ksi, and the elastic modulus E is taken as 29,000 ksi. Additional material stress-strain assumptions are discussed in Section 3.3.
- A W21x44 section is adopted as a representative “beam-type” wide flange section (i.e., W sections with d/b_f greater than about 1.7). In general, it may be useful to consider the behaviour of column-type wide flange sections as well; however, the present studies focus on the bracing of beam-type sections. It is possible that the bracing stiffness and strength requirements will not be sensitive to whether the cross-section is a beam or a column type. The essential dimensions and properties of the W21x44 section are $b_f = 6.5$ in, $t_w = 0.35$ in, $d = 20.7$ in, $t_f = 0.45$ in, $A = 13$ in², I_{yc} (lateral moment of inertia of the compression flange) $\approx I_y/2 = 10.35$ in⁴, and h_o (distance between the flange centroids) $= d - t_f = 20.25$ in.
- The focus is on equally-spaced and equal-stiffness braces throughout this work, such that the fundamental bracing behaviour targeted by Appendix 6 of the ANSI/AISC 360-10 Specification (AISC 2010a) can be assessed, and basic extensions of this behaviour pertaining to beams and beam-columns can be studied.
- The member ends are rigidly braced in the out-of-plane lateral direction at both flanges and the end cross-sections are constrained to enforce Vlasov kinematics (plane sections remain plane with the exception of warping, i.e., cross-bending, of the flanges due to torsion), and no distortion of the cross-section profile. The flanges are free to warp and bend laterally at the member ends, i.e., the member ends are torsionally simply-supported.

- For members subjected to axial load, the axial force is constant along the member length.
- The beam minimum rigidly-braced strengths from test simulations with different bracing conditions (defined subsequently in Section 4.3) are used as the required moments to estimate the beam bracing stiffness requirements from the AISC Appendix 6 and other design equations. Point torsional bracing generally gives a slightly smaller beam rigidly-braced strength. This is associated with the fact that torsional bracing restrains twist, but it does not restrain the overall lateral movement of the cross-section in the out-of-plane direction. In addition, all the required stiffnesses and strengths are determined as nominal values, that is, the resistance factors ϕ in the AISC equations are all taken equal to 1.0. For beam columns, the moments and axial forces used for estimation of bracing stiffness are determined by using the rigidly-braced strength for each specific bracing configuration (i.e., the member strength obtained if each of the bracing components is replaced by a zero displacement constraint).
- The Lehigh pattern (explained subsequently in Section 3.4) is utilized to represent the member initial residual stress effects in all cases.
- In all the bracing studies in this research, the geometric imperfections specified are an out-of-alignment equal to the maximum AISC (2010b) Code of Standard Practice tolerance of $L_b/500$ at the critical brace location, a member out-of-straightness of $L_b/2000$ (one-half of the maximum AISC Code of Standard Practice tolerance) in the critical unbraced lengths, and an imperfection pattern resulting approximately in the greatest demand on the critical brace. The specifics of the geometric imperfections are discussed in detail in Sections 3.6 and 3.7.

2.2 Overview of Study Variables and Problem Naming Convention

The study is divided into four major parts:

- a) Beams subjected to moment gradient loading.
- b) Beams with an intermediate transverse load applied at the compression flange, to investigate load height effects.
- c) Beam-columns subjected to constant axial load and uniform bending moment.
- d) Beam-columns subjected to constant axial load and moment gradient loading.

The overall scope and content of these studies can be understood succinctly by considering the naming convention for the various specific cases. This naming convention is summarized in Table 2.1. The names of the test cases are created by assembling the phrases from each of the columns of this table. The columns of Table 2.1 are explained in the following subsections.

A full factorial study design would make the number of cases to be studied extremely large. Therefore, for each of the four major tasks listed above, a targeted number of study cases is selected. The subsequent Chapters 4 through 7 explain the details regarding the selection of specific study cases.

2.2.1 Member Type

In column (a) of Table 2.1, ‘B’ represents a beam type member and ‘BC’ represents a beam-column type member.

Table 2.1. Naming convention for cases studied in this research.

Member Type (a)	Type of loading (b)	Bracing type (c)	Number of intermediate braces (d)	Unbraced length (e)	Torsional to Lateral Bracing stiffness ratio (f)	Flange force ratio (g)
B BC	UMp	NB	n1	Lb5	TLBSR5.67	FFR-0.67
	UMn	RB	n2	Lb10	TLBSR4	FFR-0.5
	MG1p	TB		Lb15	TLBSR1	FFR-0.33
	MG1n	CNTB			TLBSR0.33	FFR0
	MG2pc	CRTB			TLBSR0.25	FFR0.5
	MG2pt				TLBSR0.11	FFR1
	MG2nc					
	MG2nt					
	MG3					

2.2.2 Type of Loading

Column (b) of Table 2.1 outlines the various loading conditions considered in this research. These are discussed in detail below.

2.2.2.1 Uniform Bending and Moment Gradient Loading

The identifier ‘UM’ stands for Uniform Bending Moment, and ‘MG1’, ‘MG2’ and ‘MG3’ represent the various moment gradient cases (varied over the full length of the member) as illustrated in Figs. 2.1 through 2.3.

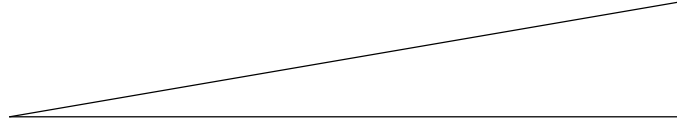


Figure 2.1. Moment Gradient 1 (MG1).



Figure 2.2. Moment Gradient 2 (MG2).

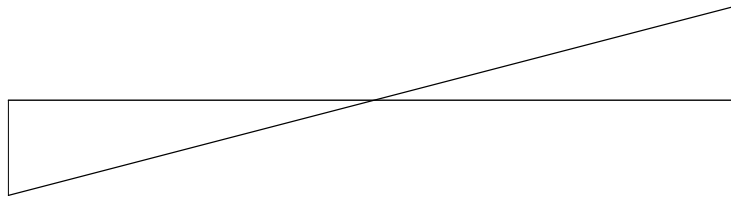


Figure 2.3. Moment Gradient 3 (MG3).

2.2.2.2 Positive and Negative Bending

One of the objectives of this research is to evaluate the benefit of combined lateral and torsional bracing for beams and beam-columns with:

- a) Lateral bracing on the flange in flexural compression (these cases are referred to as positive bending)
- b) Lateral bracing on the flange in flexural tension (these cases are referred to as negative bending)

Both positive and negative bending are considered for the beams and beam-columns having combined lateral and torsional bracing. In column (b) of Table 2.1, the identifier 'p' represents positive bending and 'n' represents negative bending.

2.2.2.3 Load Position

To evaluate the impact of transverse load height on the stability bracing demands, the following cases are considered:

- a) Load at centroid
- b) Top flange loading

In column (b) of Table 2.1, the identifier ‘c’ represents centroidal loading and ‘t’ represents top flange loading. These cases involve a concentrated load applied at the mid-span of the member, producing the MG2 moment diagram shown in Fig. 2.2. The load positions are illustrated in Figs. 2.4 and 2.5. Two-sided bearing stiffeners having the dimensions 3.075 in x 0.45 in are assumed at the mid-span load location in these tests.

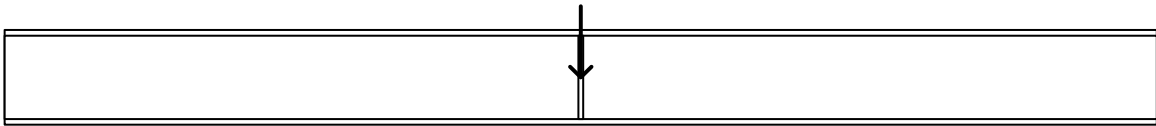


Figure 2.4. Load at centroid.

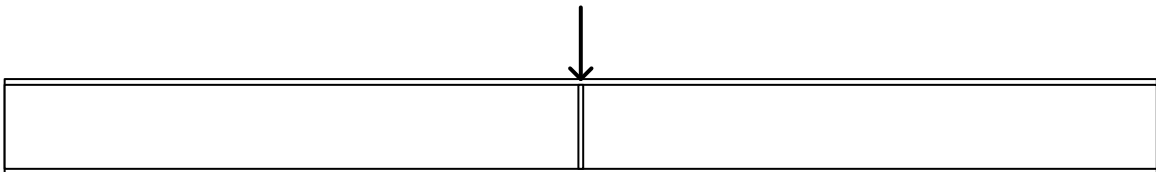


Figure 2.5. Top flange loading.

2.2.3 Bracing Type and Number of Intermediate Braces

The various bracing types and the number of intermediate brace locations considered in this research are illustrated in Figs. 1.1 through 1.5. In column (c) of Table 2.1, ‘NB’ represents point (nodal) lateral bracing, ‘RB’ represents shear panel (relative) lateral bracing, ‘TB’ represents point torsional bracing, ‘CNTB’ represents combined point (nodal) lateral and torsional bracing and ‘CRTB’ represents combined shear panel (relative) lateral and point torsional bracing. It should be noted that in all the cases considered in this research, the lateral bracing is placed only on the top flange in these elevation views.

As discussed in Section 1.1, Prado and White (2015) addressed the influence of the number of intermediate braces on the bracing requirements. Therefore, consideration of this effect is not the main focus of this research. The point (nodal) lateral bracing as well as the combined point (nodal) lateral and torsional bracing cases are considered here only for $n = 1$ (one intermediate brace location). Shear panel (relative) lateral bracing as well the combined shear panel (relative) lateral and torsional bracing cases are considered only for $n = 2$ (two intermediate brace locations). Because of the presence of rigid out-of-plane bracing at the member ends, the behavior of shear panel (relative) lateral bracing with $n = 1$ is actually identical to that of point (nodal) lateral bracing with $n = 1$. Therefore, the current work effectively addresses $n = 1$ and 2 for cases involving shear panel lateral bracing, but just $n = 1$ for cases involving point lateral bracing. Again, Prado and White (2015) addressed the impact of a larger number of intermediate brace points on the bracing response, but only in the context of beams subjected to uniform bending. In column (d) of Table 2.1, ‘n1’ indicates one intermediate brace point and ‘n2’ indicates two intermediate brace points.

The moment gradient (C_b) factors used for the critical unbraced lengths in performing the AISC Appendix 6 calculations are determined from Eq. (C-F1-1) of the AISC 360-10 Commentary, and are as follows for $n = 1$:

MG1: $C_b = 1.30$

MG2: $C_b = 1.75$

MG3: $C_b = 1.75$

For $n = 2$, the following moment gradient factors employed are:

MG1: $C_b = 1.18$

MG2: The moment gradient 2 case with $n = 2$ is not considered.

MG3: $C_b = 1.43$ (for moment gradient 3, the bracing is sized based on the outer unbraced lengths, which have the largest moment).

It should be noted that C_b enters into the AISC Appendix 6 bracing provisions only in the torsional bracing stiffness and strength equations. One question of interest in this research is the impact of considering the moment gradient effect in the torsional bracing equations versus the lack of considering this effect in the point lateral and shear panel lateral bracing equations.

2.2.4 Unbraced Length

Prado and White (2015) evaluated the impact of member inelasticity on the bracing requirements by studying W21x44 members with three different unbraced lengths (5 ft, 10 ft and 15 ft). To prevent the number of cases from becoming extremely large, most of the studies in this research are conducted only for unbraced lengths of 5 and 15 ft. The length $L_b = 5$ ft is close to the anchor point $L_p = 4.45$ ft of the AISC beam LTB strength curve for W21x44 members with $F_y = 50$ ksi. Therefore, this unbraced length corresponds to development of a flexural “plateau strength” equal to the plastic moment capacity, M_p , for the W21x44 section. In addition, this value corresponds to $L_b/r_y = 47.6$ for Grade 50 W21x44 members, which is a reasonably short unbraced length that leads to extensive spread of yielding throughout the member prior to a weak-axis flexural buckling failure as a column. The length $L_b = 15$ ft is slightly larger than the anchor point $L_r = 13$ ft of the AISC beam LTB strength curve for Grade 50 W21x44 members. Furthermore,

this unbraced length corresponds to $L/r_y = 128.7$ for these types of members, which slightly exceeds the length $4.71\sqrt{E/F_y}$ corresponding to the transition between inelastic and elastic column flexural buckling per the AISC column strength curve (AISC 2010a). Therefore, the members with $L_b = 5$ ft tend to be heavily plastified at their ultimate strength condition, and the members with $L_b = 15$ ft and a small C_b (moment gradient) factor are dominated by elastic stability behavior. A small number of members with $L_b = 10$ ft are considered in this work. These intermediate length members fail, as columns, beams or beam-columns, by inelastic buckling after significant spread of yielding through the member cross-sections. In column (e) of Table 2.1, Lb5, Lb10, and Lb15 represent unbraced lengths of 5 ft, 10 ft and 15 ft respectively.

2.2.5 Bracing Stiffness Ratios for Combined Lateral and Torsional Bracing

2.2.5.1 Torsional to Lateral Bracing Stiffness Ratios for Beams

As discussed in Section 1.2, one way of interpreting the results of combined lateral and torsional bracing is by plotting stiffness interaction diagrams. Different torsional to lateral bracing stiffness ratios need to be considered to generate these bracing stiffness interaction plots.

For positive bending cases (i.e., where the lateral bracing is on the flange in flexural compression), the Torsional to Lateral Bracing Stiffness Ratios (TLBSRs) listed in Table 2.2 are considered in this work. The variables referenced in this table are as follows:

β_L = Provided lateral bracing stiffness

β_T = Provided torsional bracing stiffness

β_{Lo} = Required lateral bracing stiffness for full bracing per the AISC 360-10 Appendix 6 (AISC 2010a) rules, including the refinements specified in the Appendix 6 Commentary, assuming the member is laterally braced only.

β_{T_0} = Required torsional bracing stiffness for full bracing per the AISC 360-10 Appendix 6 (AISC 2010a) rules, including the refinements specified in the Appendix 6 Commentary, assuming the member is torsionally braced only.

Table 2.2. Torsional to Lateral Bracing Stiffness Ratios (TLBSRs) for beams subjected to positive bending.

β_T / β_{T_0}	β_L / β_{L_0}	$(\beta_T / \beta_{T_0}) / (\beta_L / \beta_{L_0})$
0.80	0.20	4.00
0.50	0.50	1.00
0.20	0.80	0.25

Full bracing is defined as a case that has sufficient stiffness and strength to develop the maximum member buckling resistance based on an effective length equal to the unbraced length between the brace points (i.e., an effective length factor of $K = 1$). For prismatic members braced by equally-spaced braces, full bracing produces a buckling mode in which the member bends in alternate directions in adjacent unbraced lengths and has inflection points at each of the brace locations. Full bracing can refer to an ideal member buckling resistance, or it can refer to the nominal or design buckling resistance of the physical member having generally unavoidable initial geometric imperfections. The bracing stiffness necessary to develop the maximum fully-braced resistance of the physical geometrically imperfect member, and to limit the corresponding brace forces to certain specified limits, is generally larger than the stiffness required to attain the fully-braced eigenvalue buckling resistance of the ideal geometrically perfect member.

The TLBSR values for positive bending cases are illustrated in the form of an x-y plot in Fig. 2.6. The values 4, 1, and 0.25 shown adjacent to the dashed lines in Fig. 2.6 are the slopes of the corresponding lines. This slope is the TLBSR (i.e., $\text{TLBSR} = (\beta_T / \beta_{T_0}) / (\beta_L / \beta_{L_0})$). Thus, $\text{TLBSR} = 4$ indicates that:

- The initially targeted and provided lateral bracing stiffness is 0.8 times the base required lateral bracing stiffness as per AISC 360-10 Appendix 6 (AISC 2010a) rules including refinements specified in the Appendix 6 Commentary, and
- The initially targeted and provided torsional bracing stiffness is 0.2 times the base required torsional bracing stiffness as per AISC 360-10 Appendix 6 (AISC 2010a) rules including refinements specified in the Appendix 6 Commentary.

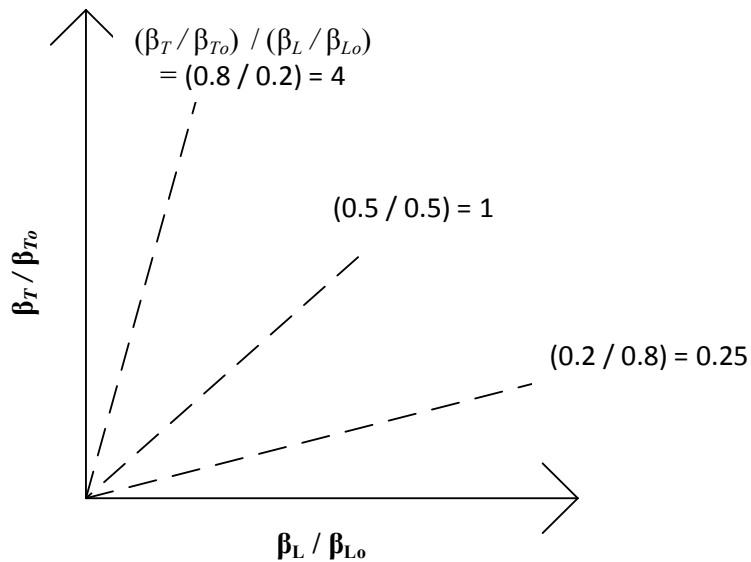


Figure 2.6. Torsional to lateral bracing stiffness interaction ratios (TLBSRs) for beams subjected to positive bending.

When generating the knuckle curves corresponding to each TLBSR, the magnitude of torsional and lateral bracing stiffnesses in the test simulations is varied such that the TLBSR is kept constant. Therefore, the above “initially targeted” values are only used in setting the TLBSR. Bracing knuckle curves and brace force versus brace stiffness curves are generated in all cases by varying both bracing stiffnesses such that the TLBSR is held constant at the selected values.

For negative bending cases (i.e., where the lateral bracing is attached to the flange in flexural tension), the Torsional to Lateral Bracing Stiffness Ratios (TLBSRs) listed in Table 2.3 are considered in this work. These TLBSR values are illustrated in the form of an x-y plot in Fig. 2.7.

In column (f) of Table 2.1, ‘TLBSR’ stands for Torsional to Lateral Bracing Stiffness Ratio. The number following ‘TLBSR’ represents the specific value of the ratio, $(\beta_T / \beta_{T0}) / (\beta_L / \beta_{L0})$.

Table 2.3. Torsional to Lateral Bracing Stiffness Interaction Ratios (TLBSRs) for beams subjected to negative bending.

β_T / β_{T0}	β_L / β_{L0}	$(\beta_T / \beta_{T0}) / (\beta_L / \beta_{L0})$
0.85	0.15	5.67
0.50	0.50	1.00
0.25	0.75	0.33
0.10	0.90	0.11

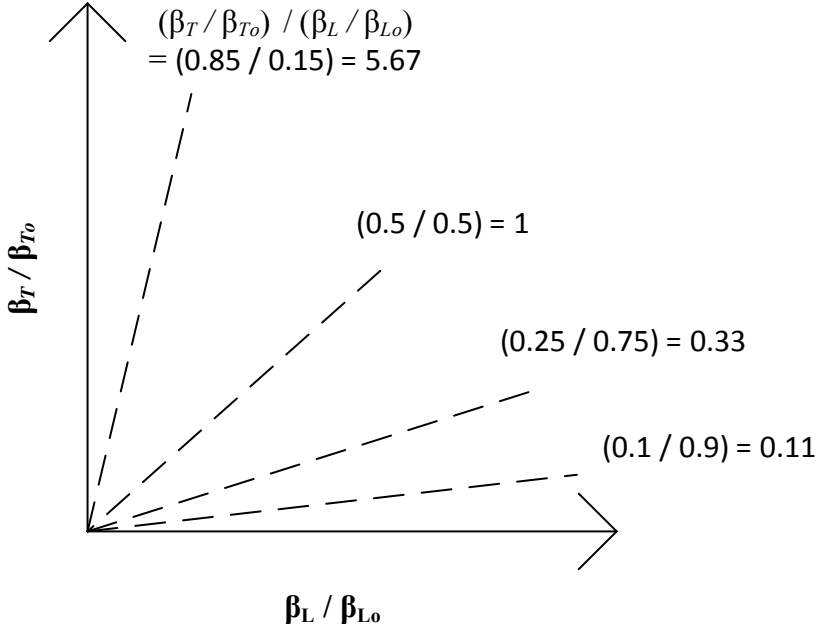


Figure 2.7. Torsional to lateral bracing stiffness interaction ratios (TLBSRs) for beams subjected to negative bending.

2.2.5.2 Torsional to Lateral Bracing Stiffness Ratios (TLBSRs) and Flange Force Ratios (FFRs) for Beam-Columns

To define a study design for bracing of beam-columns, one needs to select more than just the Torsional to Lateral Bracing Stiffness Ratios (the TLBSRs). One also needs to identify a measure of the member axial force to the member bending moment. This attribute of the current study is quantified by the effective Flange Force Ratio (FFR). The FFR is the ratio of the effective axial force transmitted by each flange, neglecting any contributions from the member web. That is, in this research, which uses doubly-symmetric W21x44 sections for all of the members, the effective flange force in the member flange loaded in flexural compression is taken as

$$P_{fc} = P / 2 + M_{max} / h_o$$

where P is the member axial force, taken as positive in compression, M_{max} is the first-order maximum internal moment, and h_o is the distance between the flange centroids. Similarly, the effective flange force for the flange loaded in flexural tension is

$$P_{ft} = P / 2 - M_{max} / h_o$$

Therefore, the effective Flange Force Ratio is

$$\text{FFR} = P_{ft} / P_{fc}$$

This ratio is positive when both flanges support a net axial compression, and it is negative when the moment causes a net tension in the flange loaded in flexural tension. The following effective flange force ratios are considered for beam-columns subjected to uniform bending in this research: -1, -0.67, -0.33, 0, 0.5, and 1. The following effective flange force ratios are considered for beam-columns subjected to moment gradient loading: -1, -0.5, 0, 0.5, and 1. These ratios are selected such that the following three situations are studied:

- a) One flange in net overall compression and other flange in net overall tension,
- b) One flange in net overall compression and other flange subjected net zero force, and
- c) Both flanges in net overall compression.

Column (g) of Table 2.1 shows the different designations for the flange force ratios used in this research. In this column, ‘FFR’ stands for the Flange Force Ratio and the number following ‘FFR’ represents the ratio P_{ft}/P_{fc} . The FFR value of -1 actually corresponds to the beam loading cases, i.e., axial force of zero, Case (a) above is addressed by FFR = -0.67 and -0.33, Case (b) corresponds to FFR = 0, and Case (c) is addressed by FFR = 0.5 and 1.

A full factorial study design with different bracing stiffness ratios and effective flange force ratios would make the number of cases to be considered extremely large. Hence a scheme of designing the lateral bracing for a load equal to the axial load, P , and the torsional bracing for a load equal to $(M_{max}/h_o + P/2)$ is evaluated in this work for beam-columns having combined torsional and lateral bracing. Other rules are considered for members in which only the flange subjected to flexural compression is laterally braced. The above rule stems from the fact that the torsional brace is ineffective at providing overall lateral bracing against column flexural buckling under the axial load, but the axial load has some influence on the torsional bracing stiffness and strength requirements. The $P/2$ term is an ad hoc addition to account for the amplification in the torsional brace demand due to the combined axial and moment loading.

In practice, an engineer would encounter situations where the lateral bracing may be very stiff or very flexible, e.g., a roof or wall diaphragm composed of stiff precast concrete panels and other cases where the lateral bracing may be relatively flexible, e.g., standing-seam roof panels. In such cases, the lateral bracing would need to be designed generally to accommodate the member axial force. If the lateral bracing stiffness is larger than the minimum requirement to develop the member axial force, then the design would be considered conservative with respect to the lateral bracing, according to the above rule. Varying the TLBSRs in a manner other than that indicated

by the above minimum requirements, e.g., to consider any potential beneficial effects of additional lateral bracing stiffness for relieving the torsional bracing stiffness demands for beam-columns, is not considered in this research. Various general TLBSRs are considered for beams in this research, as discussed in the previous Section 2.2.5.1.

2.3 Example Naming

As indicated above, the various specific beam-column cases studied in this research are named based on the identifiers listed in Table 2.1. For example, the case B_MG2pt_NB_n1_Lb5 has the loading and geometry shown in Fig. 2.8. This member is a beam, with Moment Gradient 2 loading (resulting in the moment diagram shown in Fig. 2.3), positive bending moment (causing compression on the top flange, where the lateral bracing is provided, transverse load applied at the level of the top flange, nodal (point) lateral bracing with one intermediate brace location, and 5 ft unbraced length between the braced points. In this case, the TLBSR and FFR identifiers are left blank, since these parameters are not relevant to a beam with point lateral bracing. The member end conditions, not shown, are torsionally simply-supported (out-of-plane lateral bending and warping of the flanges free, but out-of-plane lateral displacements and twisting constrained by rigid supports).

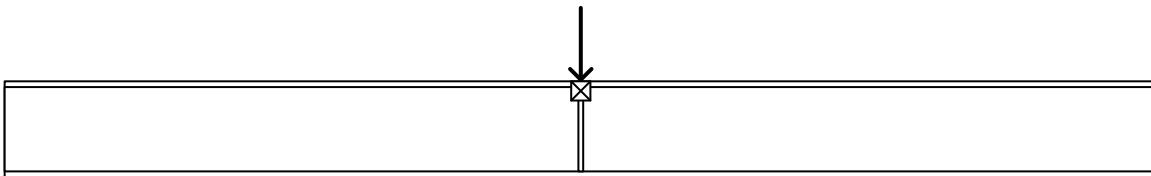


Figure 2.8. Naming convention example, test B_MG2pt_NB_n1_Lb5.

CHAPTER 3 FINITE ELEMENT PROCEDURES

3.1 General Modeling Considerations

The test simulation studies conducted in this research are directed at modelling the overall load-deflection response up to and beyond the peak load capacity of various member and bracing configurations, considering the influence of initial geometric imperfections, residual stress effects, and the overall spread of plasticity throughout the volume of the members. The members are modeled using shell finite elements, and thus the FEA models are capable of capturing general overall member buckling, local buckling and distortional buckling influences as applicable for the cases studied. The different bracing components are modeled using elastic spring elements. Axial load and bending moments are applied at the member ends via concentrated longitudinal axial forces at the web flange junctures. Figure 3.1 shows a representative case for a beam-column subjected to uniform bending. Multi-point constraints are applied at the member end cross-sections to enforce Vlasov kinematics at these locations. That is, plane sections are constrained to remain plane in the web as well as in the flanges at the member ends, but the flanges are allowed to rotate freely and independently about a vertical axis through the web. Therefore, warping of the flanges is effectively unrestrained at the member ends. The specific multi-point constraint equations are defined in detail by Kim (2010).

In addition, the vertical displacement of all points on the top and bottom flange are constrained to be equal to the vertical displacement at the corresponding web-flange juncture at each end of the member, such that there is no distortion of the cross-section profile at the member ends.

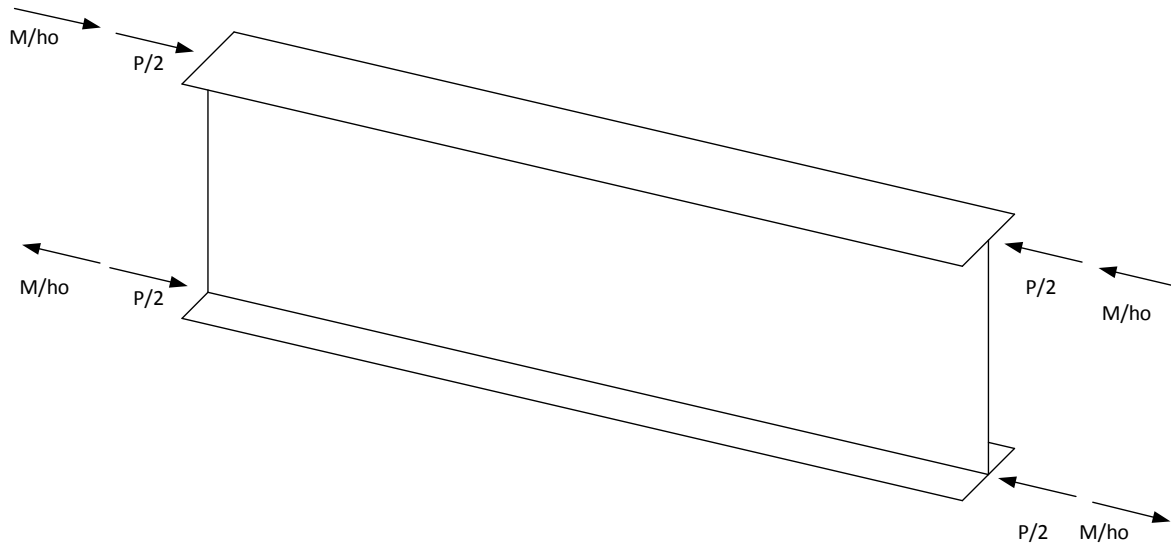


Figure 3.1. Load application - axial load and moment.

Because of the application of multi-point constraints at the member ends, the above member end loads do not cause any stress concentrations. The member is supported at one end in the plane of bending by constraining the vertical and longitudinal displacements to zero at the bottom web-flange juncture, and at the other end in the plane of bending by constraining just the vertical displacement at the bottom web-flange juncture to zero. The lateral (out-of-plane) displacements at the member ends are constrained to zero at each web-flange juncture and throughout the height of the web. Self-weight of the member is not included in the analysis.

The general purpose finite element analysis software ABAQUS version 6.13 (Simulia 2013) is used throughout this research. The four-node S4R shell element is used to model both the flanges and the web of the member. The S4R element is a general purpose large strain quadrilateral element which uses a single point numerical integration over its area combined with an algorithm for stabilization of the corresponding spurious zero-energy modes. Twelve elements are used across the width of the flanges and sixteen elements are used through the depth of the web of the W21x44 members in these studies. An aspect ratio of 1 to 1 is implemented for all the elements in the web. The flange elements are the same length dimensions as the web elements along the

longitudinal direction of the member. Figure 3.2 shows a representative finite element model. A five point Simpson's rule is applied for integration of the stresses through the thickness of the shell element. The Riks method is used to perform the incremental-iterative non-linear load-deflection analyses.

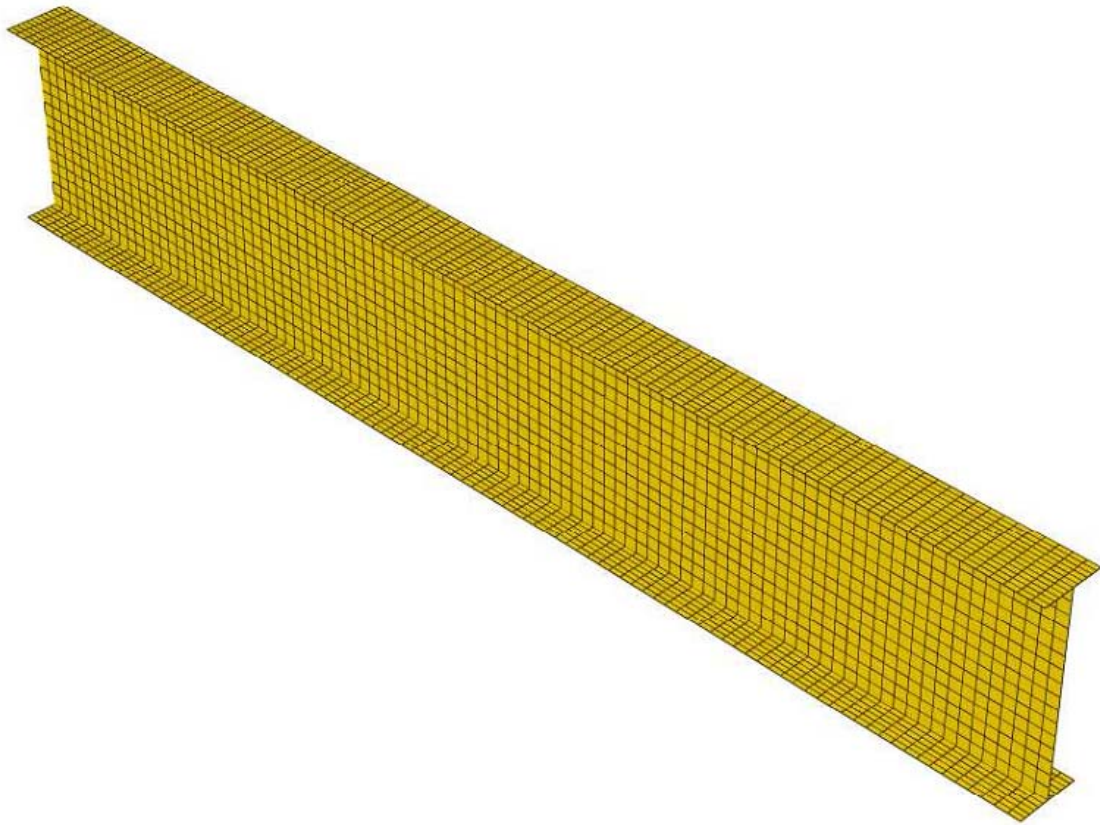


Figure 3.2. Representative finite element model.

Initial residual stresses are specified via a user-defined FORTRAN subroutine. Geometric imperfections are introduced by performing a pre-analysis of the member in which displacements corresponding to the desired geometric imperfection pattern are imposed at various control points and the member is allowed to elastically deform between these points. The deflections from the pre-analysis are then applied as an initial imperfection on the geometry of the member in its zero load condition in subsequent test simulation load-deflection analyses. The member is taken as

stress and strain-free in this initial imperfect geometry at the beginning of the test simulation, with the exception of the residual stresses.

Force equilibrium is not strictly maintained when the residual stresses are introduced on the imperfect member geometry. The residual stresses are self-equilibrating only on the perfect geometry of the member. As such, a first step of the test simulation analysis is conducted in which the residual stresses are allowed to equilibrate. This results in a relatively small change to the member geometry. This ‘equilibrium step’ is followed by a second step of the test simulation analysis in which load is applied to the member.

3.2 Modelling of Braces

ABAQUS provides two types of spring elements which are used to simulate the bracing components in this research. All the bracing components are modelled as linear elastic springs. Point (nodal) lateral bracing is simulated with the spring type 1 element, which is a grounded spring element. Shear panel (relative) bracing is simulated using the spring type 2, which is a spring element that resists relative displacements in a specified coordinate direction between the nodes it connects. In addition, nodal torsional bracing is implemented via the use of the spring type 2 element.

3.3 Material Properties

The material properties of the steel are modelled in all the test simulation studies of this research using the stress-strain curve shown in Fig. 3.3. All the members are assumed to be homogenous and the yield stress of steel, F_y , is taken as 50 ksi. The modulus of elasticity, E is taken as 29000 ksi. The material is modelled with a small tangent stiffness within the yield plateau region of $E/1000$ up to a strain-hardening strain of $\epsilon_{sh} = 10\epsilon_y$, where ϵ_y is the yield strain of the material. Beyond this strain, a constant strain-hardening modulus of $E_{sh} = E/50$ is used up to the ultimate stress level of $F_u = 65$ ksi. The material is modelled as perfectly plastic beyond this point.

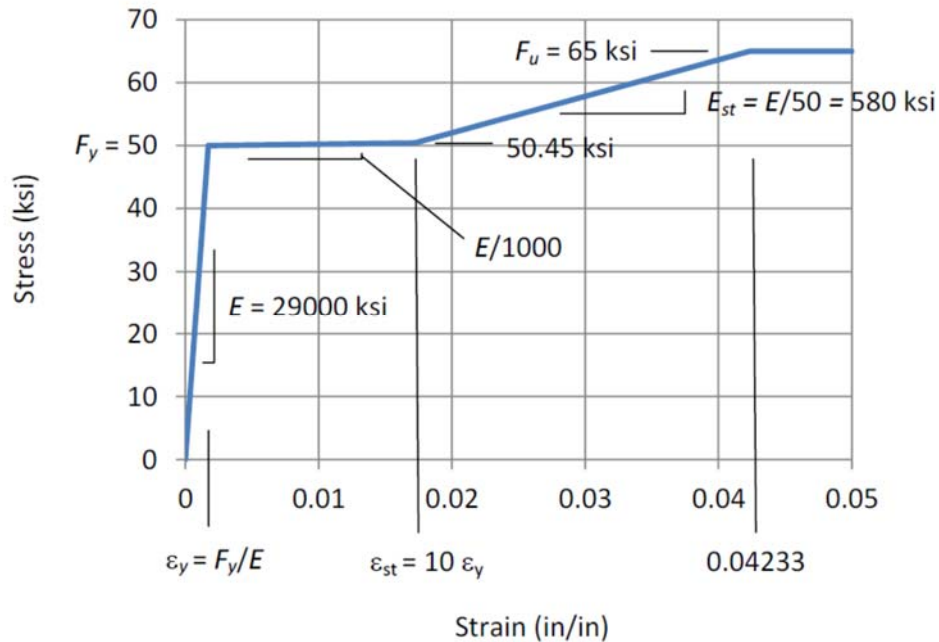


Figure 3.3. Steel stress-strain curve assumed in the structural analysis.

The above stress-strain curve is used to define the plastic hardening as a function of the equivalent plastic strain for a J2 incremental flow theory of plasticity material model in ABAQUS. Isotropic hardening is assumed for the evolution of the yield surface upon plastic straining.

Since the S4R element in ABAQUS is a large strain formulation, this element actually interprets the input stress versus plastic strain curve associated with Fig. 3.3 as the true stress versus log strain response. However, for the maximum strains commonly experienced at the limit load of the test simulations, the difference between the uniaxial true-stress versus log strain and engineering stress versus engineering strain is small. The stress-strain curve shown in Fig. 3.3 is a reasonable representation of the true-stress true-strain response of structural steel for stresses up to the level of F_u . The maximum stresses experienced in the simulations are well within this limit for the studies considered in this work.

3.4 Residual Stresses

Residual stresses are introduced into rolled structural steel members by uneven cooling after rolling operations, as well as by mill straightening. Flame cutting and welding causes residual stresses in welded I-section members. One of the most commonly accepted models used to represent nominal residual stresses in hot-rolled I-section members is the Lehigh residual stress pattern shown in Fig. 3.4. This pattern has a constant residual tension in the web and a self-equilibrating stress distribution in the flanges with a maximum residual compression of $0.3F_y$ at the tips of the flanges and a linear variation in stress between the flange tips and the above residual tension value at the web-flange juncture. The residual stresses are constant through the thickness of the flange and web plates. The Lehigh residual stress pattern (Galambos and Ketter, 1959) is considered commonly to provide an accurate to relatively conservative assessment of residual stress effects on the inelastic buckling response of rolled wide flange members. The potential conservatism is due to the attribute that the flanges contain a net compressive residual force that is balanced by the web residual tension. The Lehigh residual stress pattern is assumed in all of the studies conducted in this research.

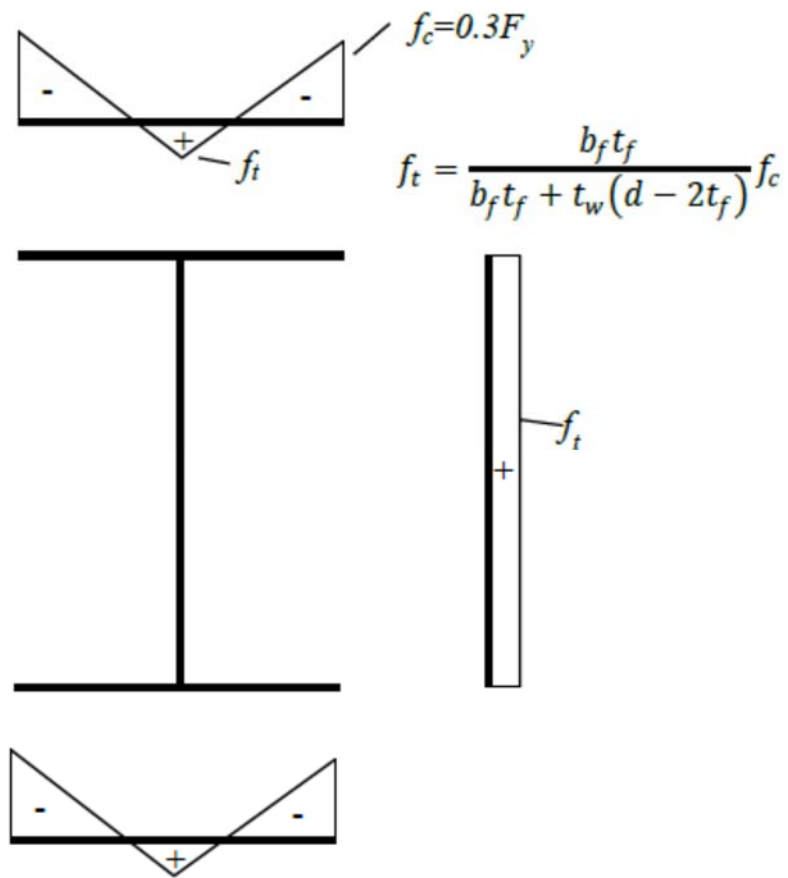


Figure 3.4. Lehigh residual stress pattern (Galambos and Ketter, 1959).

3.5 Benchmark Studies

Benchmark studies for columns and beams are presented below to illustrate how the capacities obtained from test simulations compare with the strengths predicted by the ANSI/AISC 360 Specification (AISC 2010a) as well as the Eurocode 3 Standard (CEN 2005).

3.5.1 Beam Benchmark Study

The results of a beam benchmark study for uniform bending, conducted by Prado and White (2015), is shown in Fig. 3.5. The modelling approach is exactly the same as that used for all of the cases in this research. The beams studied here are simply-supported members with no intermediate lateral bracing. A sweep of the compression flange with maximum amplitude of $L/1000$ at the mid-span is used, where L is the overall span length in the plane of bending.

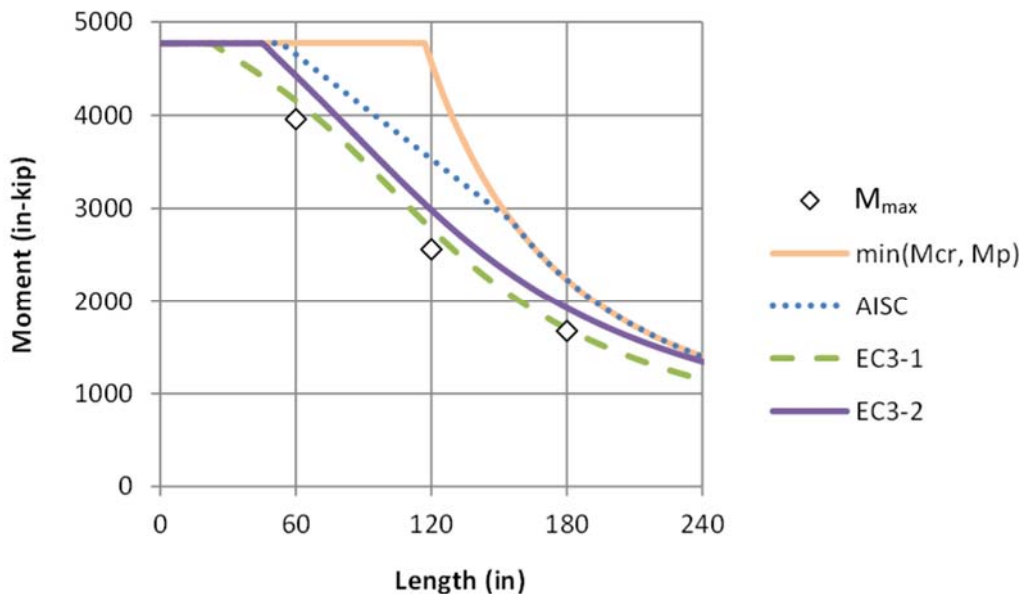


Figure 3.5. Results of beam benchmark study for uniform bending.

In Fig. 3.5, the maximum strengths determined from the test simulations (M_{max}) are compared to the elastic buckling capacity, capped by the plastic moment of the W21X44 cross-section, as well as to the ANSI-AISC 360-10 and the Eurocode 3 (CEN 2005) predicted strengths. Two curves are shown from the Eurocode 3 provisions, one corresponding to general I-section members (EC3-1) and the second providing an enhanced strength estimate intended for application with rolled I-section members and members with a cross-section similar to rolled I-sections (EC3-2). It can be observed that the test simulation strengths are closest to the EC3-1 curve. This is to be expected since the EC3-1 strength curve was developed largely from extensive test simulation studies similar to the studies conducted here, but with a residual stress pattern that is not quite as damning as the Lehigh residual stress pattern. The use of the Lehigh residual stress pattern reduces the member capacities slightly in comparison to the EC3-1 curve. The EC3-2 and AISC strength curves were developed considering extensive collections of experimental data. Generally, the maximum strengths obtained from test simulations, using typical nominal residual stress patterns along with geometric imperfections set at maximum fabrication and construction tolerances, tend to be smaller on average compared to the strengths from experimental tests. One reason for this behavior is the fact that the imperfections and residual stresses in the experimental tests (and assumed to occur in practice) are not as large as the nominal values typically assumed in simulation studies.

Figure 3.6 shows beam benchmark study results for a representative moment gradient loading case (MG1 in Fig. 2.1) with rigid lateral bracing on the compression flange at the mid-span of the member. The curves in this figure are based on the use of a moment gradient factor C_b of 1.3 for the right-hand critical unbraced length and a $C_b = 1.75$ for the non-critical left-hand unbraced length. Using these C_b values and the approximate procedure recommended by Nethercot and Trahair (1976), the effective length factor for lateral torsional buckling of the right-hand unbraced length is $K = 0.88$ (accounting for the restraint provided by the left-hand non-critical unbraced length to the right-hand critical unbraced length). When $C_b = 1.3$ and $K = 0.88$ are used to evaluate

the LTB strength of the right-hand segment, the prediction from the AISC strength curves is equal to the theoretical elastic LTB capacity, M_{cr} , capped by the section plastic moment resistance M_p , with the exception of a small deviation close to the length where M_{cr} reaches M_p . Conversely, the two Eurocode strength predictions show a substantial reduction in strength relative to the AISC predictions. The test simulation strengths are again close to the Eurocode 3 predictions, but in this case, the correlation with the rolled I-section EC3-2 curve is somewhat better than with the general I-section EC3-1 curve. The reason for the improved prediction by the EC3-2 curve can be explained as being due to an additional factor, referred to as f in Eurocode 3, which better accounts for the effect of moment gradient on the inelastic buckling resistance. One can observe that the test simulation predictions are slightly conservative relative to the EC3-2 curve. This is due to the conservative nature of the Lehigh residual stress pattern compared to the base residual stresses utilized in the Eurocode 3 developments. Nevertheless, at the shortest unbraced length considered in this work (i.e., $L_b = 5$ ft), the beam develops the fully-plastic bending resistance of the cross-section, M_p .

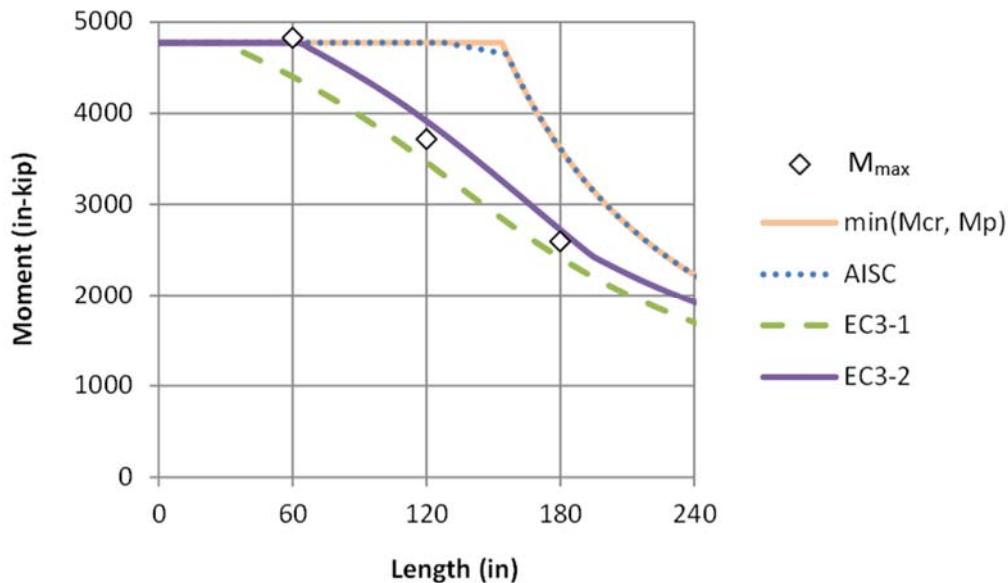


Figure 3.6. Results of beam benchmark study for Moment Gradient 2 loading.

3.5.2 Column Benchmark Study

The following column benchmark studies are performed using the W21X44 section. The members are flexurally and torsionally simply-supported and have no intermediate brace points. Warping and lateral bending are free at the member ends. The modelling approach is exactly the same as that used for all of the studies in the above section and in the simulations conducted in this research. An out of straightness of $L/1000$ is used in the weak-axis bending direction as illustrated by Fig. 3.7, where L is the total length of the column.

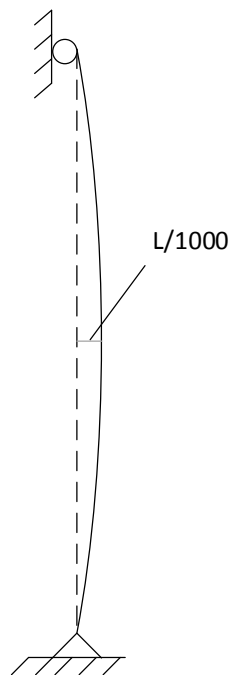


Figure 3.7. Out-of-straightness in the weak-axis bending direction for the benchmark study column.

Figure 3.8 shows the results from this benchmark study for 5 ft, 10 ft and 15 ft long columns. The designation EC3 indicates the applicable Eurocode 3 (CEN 2005) column curve whereas AISC indicates the AISC 360-16 (AISC 2016) column curve. The AISC 360-16 column curve is the same as in the (AISC 2010) Specification, with the exception of the handling of the influence of the W21x44 slender web under uniform axial compression. The 2016 Specification handles slender web effects under uniform axial compression via a streamlined unified effective area

approach. This procedure leads to some reduction in the axial capacity for shorter columns, but reduces to no effect on the axial resistance of longer columns.

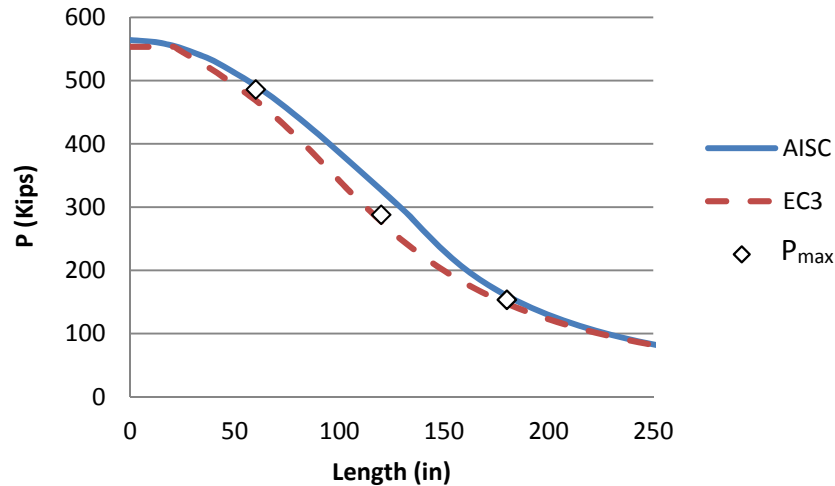


Figure 3.8. Results of the column benchmark study without local buckling imperfections.

With the exception of one isolated set of cases described subsequently at the end of Section 3.7.2, the FEA simulation studies throughout this report generally do not include any consideration of local buckling type imperfections in the W21x44 members. To gage the effect of this modeling decision, i.e., to determine the effect of local buckling imperfections on the column capacities, the above column benchmark study is repeated with the inclusion of local buckling imperfections. The local buckling imperfections are determined by performing an elastic Eigenvalue buckling pre-analysis of the member subjected to the concentric axial compression. These imperfections are then combined with the sweep of the member in the weak-axis bending direction, illustrated in Fig. 3.7, to define an initial strain-free imperfect geometry of the column. The shape of the local buckling mode having the smallest eigenvalue is selected and scaled such that the maximum web out-of-flatness is $h/72$. This value is a common fabrication tolerance for welded I-section members (MBMA 2006). The ASTM A6 tolerances for W shapes do not specify any limit on the web out-of-flatness. The resulting flange tilt within the above buckling mode is well within the ASTM A6 flange tilt tolerance of 5/16 inch, corresponding to $d > 12$ in. Figure 3.9 shows the results for the

column strengths after the local buckling imperfections are included. One can observe that the strength of the 5 ft long W21x44 column ($F_y = 50$ ksi) is reduced from 486 kips to 430 kips. However, the maximum strengths of the columns having the longer unbraced lengths are practically unchanged due to the inclusion of the local buckling imperfections (the reductions are 3.13 % and 0.33 % for 10 ft and 15 ft unbraced lengths respectively). In effect, for the longer unbraced lengths, the member response is dominated by overall flexural buckling.

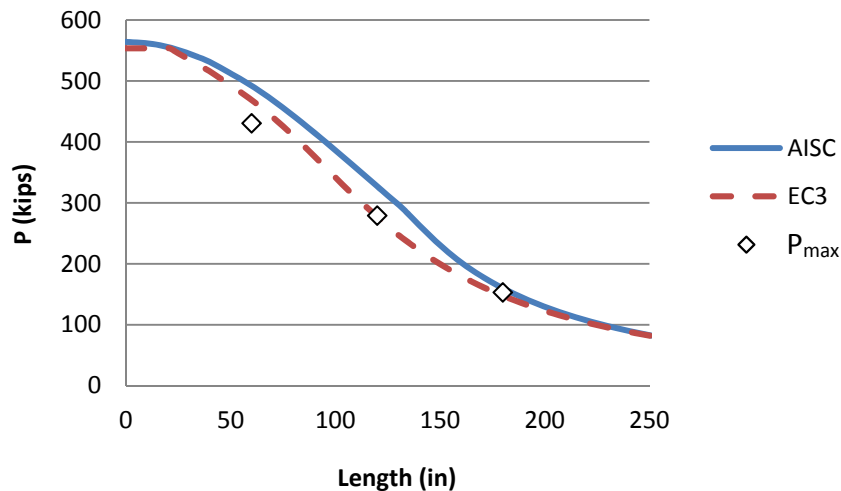


Figure 3.9. Results of the column benchmark study considering local buckling imperfections.

3.6 Geometric Imperfections in Beams

Wang and Helwig (2005) found that the largest brace forces in fully-braced beams are produced for all practical purposes by giving the compression flange at the brace point having the largest internal moment an out-of-plane initial displacement, leaving the other brace points at their perfect geometry position, and leaving the tension flange straight. Furthermore, to create a maximum out-of-alignment along the compression flange equal to the limit of $1/500$ specified in the AISC (2010b) Code of Standard Practice, this out-of-plane initial displacement is taken as $L_b/500$.

In addition to the above out-of-alignment of the brace points, an out-of-straightness of the compression flange of $L_b/2000$ is imposed in opposite directions on each side of the above critical brace location in this work. This additional “sweep” of the compression flange is applied to avoid cases where the imperfect geometry is completely symmetric about the critical brace location, thus ensuring that the beam fails ultimately in an “S” shape with an inflection point at the brace locations in the test simulations (assuming full bracing). Cases in which the geometry is completely symmetric about the critical brace point, and in which this type of additional out-of-straightness is not modelled, can fail in an unrealistic symmetrical mode about the critical brace location. This can result in larger member strengths and brace force demands than would be expected for the physical member. The value $L_b/2000$ is selected as a reasonable value for the compression flange out-of-straightness that is less than the AISC (2010b) Code of Standard Practice limit of $L_b/1000$, and for which the overall imperfection in the unbraced length where the out-of-alignment and out-of-straightness are additive is only slightly larger than that obtained if the compression flange were simply allowed to bend between the brace points based on the offset of $L_b/500$ imposed at the critical brace location.

Figures 3.10 and 3.11 show the imperfection patterns (the out-of-plane lateral displacement of the compression flange) for beams that are subjected to single-curvature major-axis bending (no reversal of the sign of the moment within the span). Figure 3.10 shows the imperfection pattern for beams having one intermediate brace and Fig. 3.11 shows the pattern for beams having two intermediate brace locations. The symbol ‘X’ on the elevation views of the members in these figures indicates the brace point location. Various single curvature bending cases are considered in this research, as discussed in Section 2.2.2. As noted above, the imperfection is applied to the compression flange and the tension flange is constrained to remain straight for these cases. As described in Section 3.1, these imperfections are imposed in a pre-analysis and are then inserted as an initial strain-free deflection relative to the perfect member geometry in the FEA simulation studies. The desired initial lateral displacements of the compression flange are specified at the

critical brace point and at the middle of the unbraced lengths on each side of the brace point in the pre-analysis. In addition, zero lateral displacement is specified at the corresponding locations on the tension flange in the pre-analysis. In the pre-analysis, the member is allowed to elastically deform between these locations where the imperfection values are specified. All the corresponding nodal displacements are then inserted as a strain-free initial deflection for the FEA simulations.

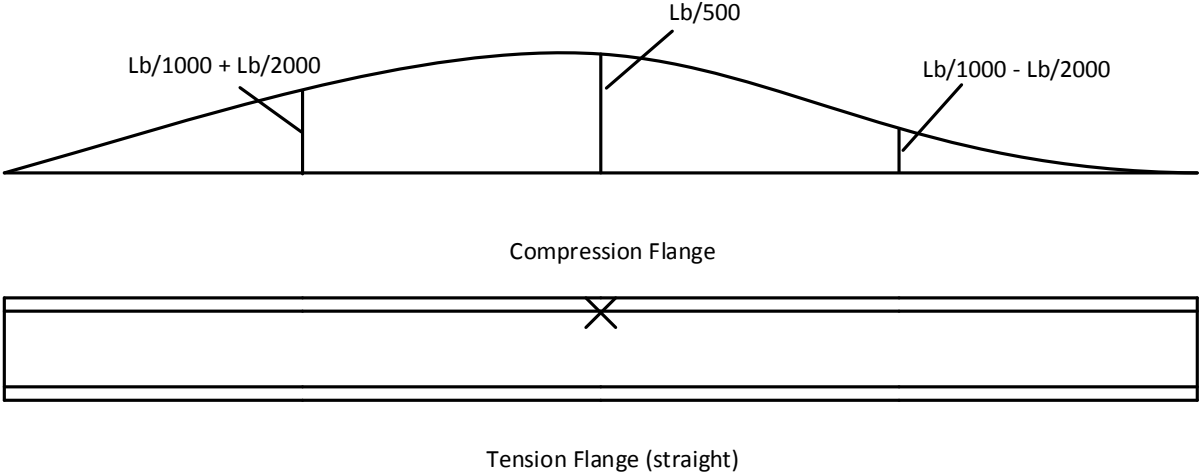


Figure 3.10. Flange initial out-of-plane displacements corresponding to the imperfection pattern for the single-curvature bending cases in beams containing one intermediate brace point.

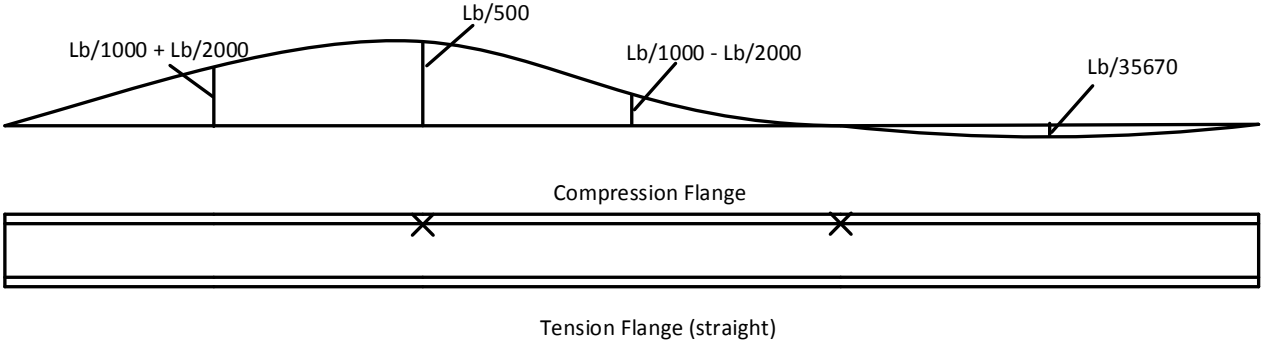


Figure 3.11. Flange initial out-of-plane displacements corresponding to the imperfection pattern for the single-curvature bending cases in beams containing two intermediate brace points.

In the cases with two intermediate braces, the compression flange lateral displacement at the middle of the unbraced length further away from the critical brace location is determined from an elastic frame analysis of a prismatic beam with the above displacements imposed at the critical brace location and the middle of the unbraced lengths on each side of this brace. The left-most intermediate brace point is taken as the critical brace location in Fig. 3.11. The value for the elastic deflection obtained at the middle of the right-most “non-critical” unbraced length (actually a small displacement of only $L_b/35670$) is then imposed on the compression flange of the beam in this unbraced length in the ABAQUS pre-analysis.

It should be noted that the above imperfections are focused on cases in which the members are fully-braced, or in which the members are partially braced but the brace stiffness is approaching the full bracing stiffness. For members with two intermediate braces and relatively flexible partial bracing, the critical geometric imperfections are generally different. For instance, in the limit that the intermediate brace stiffnesses are zero, the critical geometric imperfection would involve a single sweep of the compression flange along the entire length of the member. The studies in this research are focused predominantly on cases with full or near full bracing.

For beams with the Moment Gradient 3 loading (reverse curvature bending), the imperfection pattern shown in Fig. 3.12 is used when the beam has a single intermediate brace point. Figure 3.13 shows the initial imperfection pattern when the beam has two intermediate brace locations. For fully reversed curvature bending, since both the top and bottom flange are subjected to flexural compressive forces, the out-of-plane flange displacements are scaled by 0.5 to limit the initial torsional rotation to a maximum value of $(L_b/500)/h_o$ between the top and bottom flange at the critical brace point location. This is the de facto standard torsional imperfection considered for the development of the torsional bracing stiffness requirements in AISC Appendix 6.

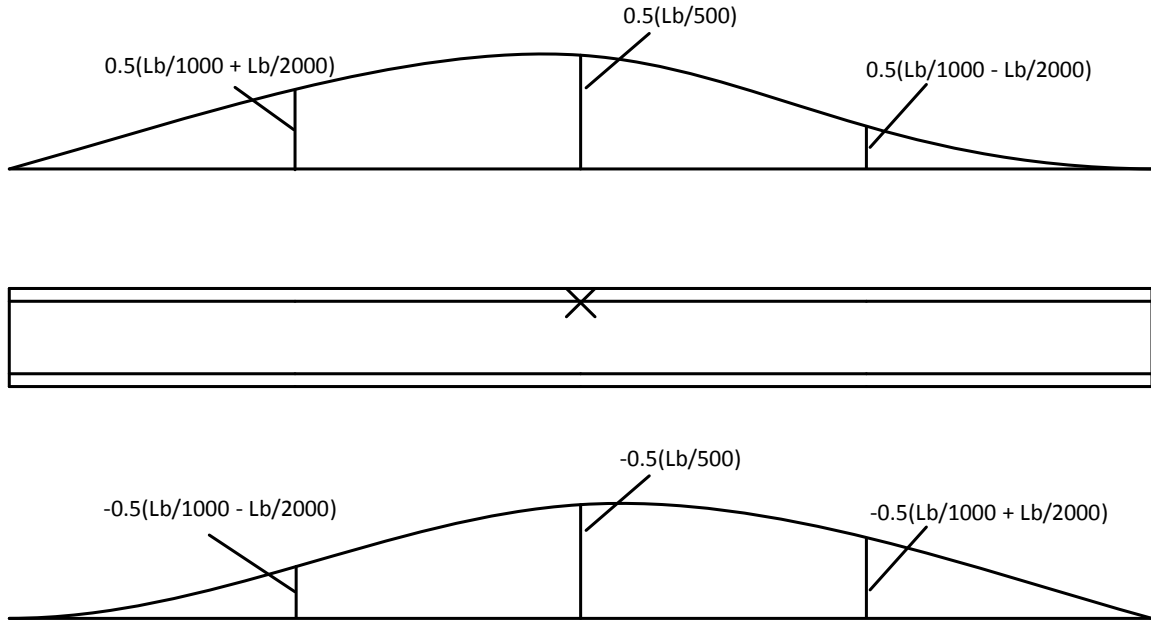


Figure 3.12. Flange initial out-of-plane displacements corresponding to the imperfection pattern for the reversed-curvature bending cases in beams containing one intermediate brace point.

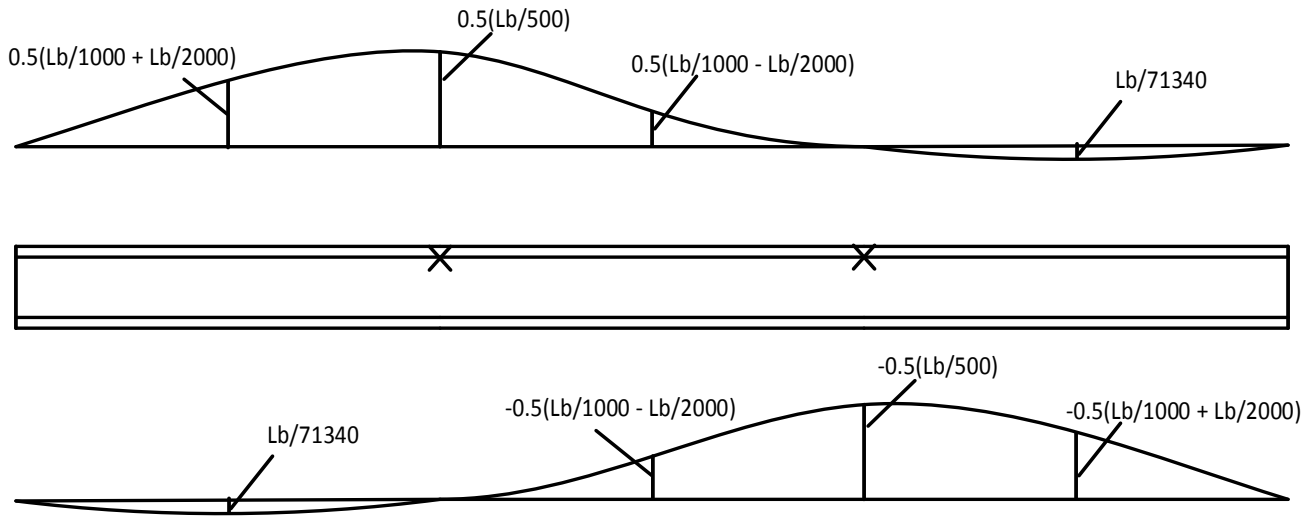


Figure 3.13. Flange initial out-of-plane displacements corresponding to the imperfection pattern for the reversed-curvature bending cases in beams containing two intermediate brace points.

3.7 Geometric Imperfections in Beam-Columns

For beam-columns the critical imperfection pattern is taken to depend on the type of bracing as well as the ratio of effective flange force in the flange in flexural tension P_{ft} to effective flange force in the flange in flexural compression P_{fc} . In the limit that the axial force goes to zero, the critical imperfection should correspond to that described above for beams. However, in the limit that the bending moment goes to zero, the critical imperfection should involve brace point out-of-alignment and out-of-straightness in both flanges. This attribute of the geometric imperfections is addressed in this work by making the imperfections a function of the effective Flange Force Ratio (FFR). The bracing types considered in this research are discussed in Section 2.2.3 and the ratio of the effective flange forces is discussed in Section 2.2.5.2. Imperfection patterns for beam-columns with lateral bracing only and with combined lateral and torsional bracing are discussed separately in the following subsections.

3.7.1 Beam-Columns with Point (Nodal) Lateral or Shear Panel (Relative) Lateral Bracing Only, Provided Only on One Flange

For beam-columns with bracing only on the flange in flexural compression, when P_{ft} / P_{fc} is less than or equal to zero, the member is more like a beam type member because only one flange is in net compression. For these cases the critical imperfection pattern is taken to be the same as that for beams, as shown in Figs. 3.10 through 3.13. However, when P_{ft} / P_{fc} is greater than zero, the member acts more like a column because both flanges are in net compression. For these cases the imperfection pattern for the flange in flexural compression is specified as shown in the above figures. However, since the other flange is subjected to a net axial compression and is unbraced over the full length of the member, its imperfection is specified as a single-wave sweep with a maximum deviation from the perfect geometry at the mid-span of the member. The magnitude of this sweep is varied from zero to $L/2000$ (where L is the full member length) as a linear function of P_{ft}/P_{fc} , using the imperfection factor (IF) as described below.

The imperfection pattern for beam-columns with lateral bracing only, and with the bracing provided on only one flange, is as shown in Figs. 3.14 and 3.15. The imperfection factor (IF) is taken as a bilinear function of P_{fi}/P_{fc} in this research. If $P_{fi}/P_{fc} \leq 0$, then IF is taken equal to zero (IF = 0), i.e., the imperfections are the same as if the member were a beam with zero axial loading. If $P_{fi}/P_{fc} > 0$, then IF is taken equal to P_{fi}/P_{fc} , i.e., as the net axial compression becomes larger in the unbraced flange, the out-of-straightness of this flange is linearly increased. In the limit that the member is loaded in pure axial compression with zero bending moment, the sweep of the unbraced flange is taken as $L/2000$. Therefore, the out-of-straightness of the bottom flange, i.e., the flange subjected to flexural tension, is equal to $2L_b/2000 = L_b/1000$ for the cases with a single intermediate brace point (Fig. 3-14) and it is equal to $3L_b/2000 = L_b/667$ for the cases with two intermediate brace points (Fig. 3-15). Figure 3.16 shows end views of the resulting imperfect geometry of the above members with $n = 1$ for three different effective flange force ratios (-0.33, 0.5, and 1). The “non-critical” unbraced length is the one closest to the camera.

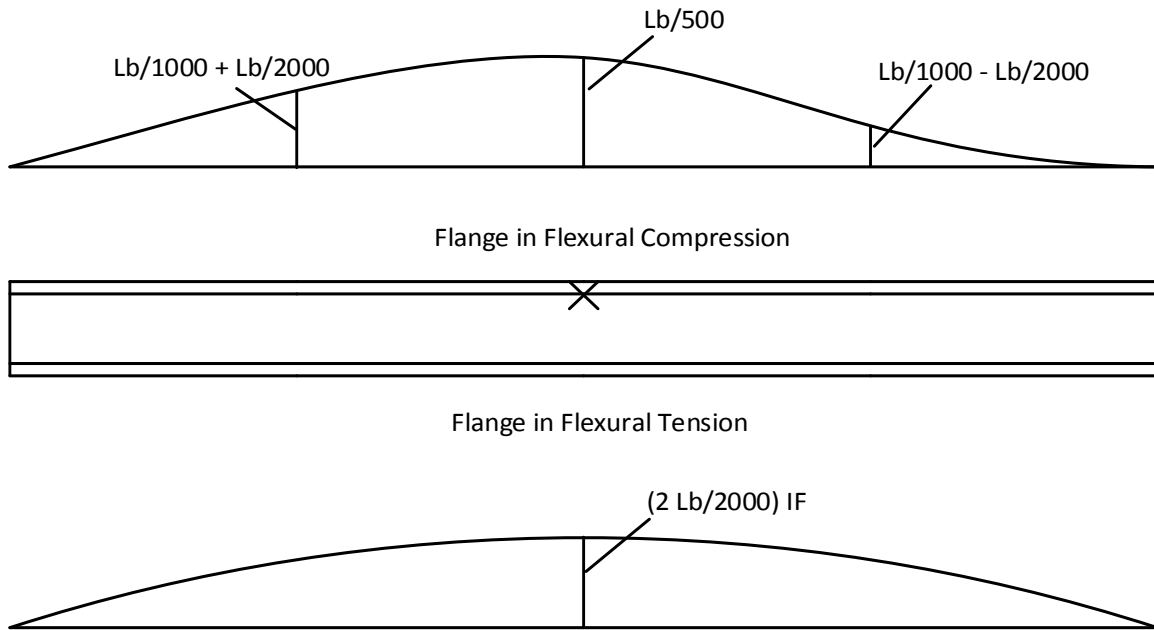


Figure 3.14. Imperfection pattern for beam-columns with lateral bracing only, bracing only on the flange in flexural compression, and one intermediate brace point.

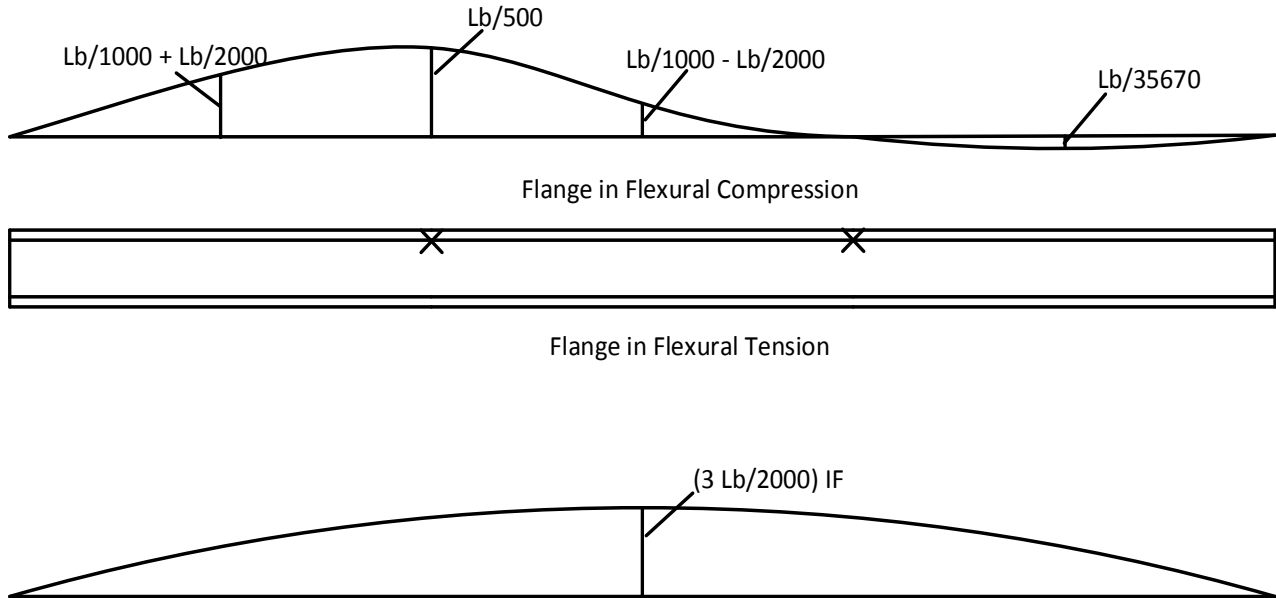


Figure 3.15. Imperfection pattern for beam-columns with lateral bracing only, bracing only on the flange in flexural compression, and two intermediate brace points.

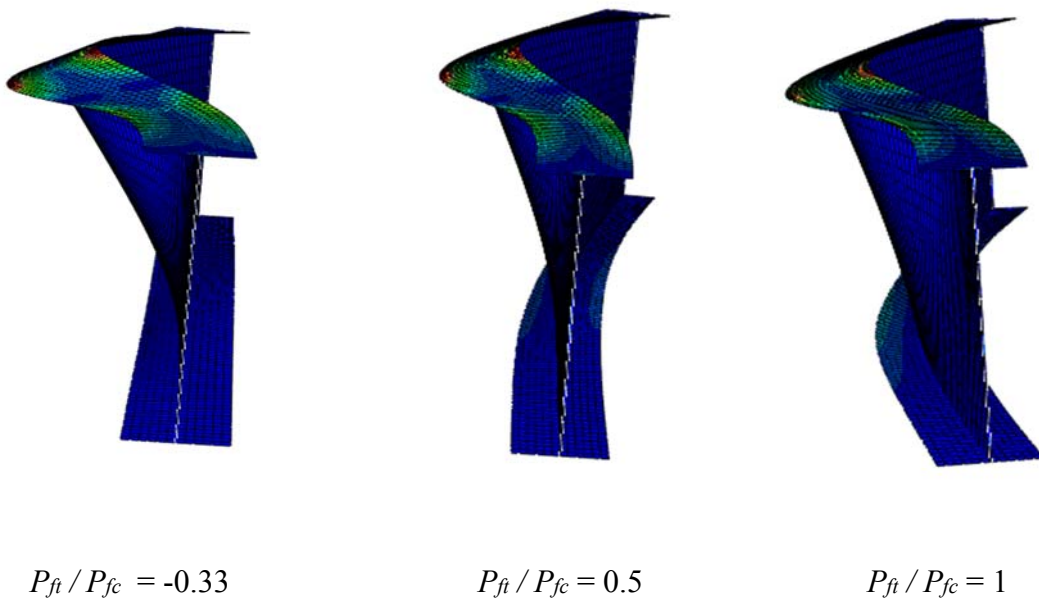


Figure 3.16. End view of imperfection pattern for members with a single lateral brace only on the top flange, shown for three different effective flange force ratios.

3.7.2 Beam-Columns with Combined Torsional and Lateral Bracing

For beam-columns with both flanges braced via combined torsional and lateral bracing, if P_{ft}/P_{fc} is less than or equal to zero, the member is more like a beam type member because only one flange is in net compression. For these cases the imperfection pattern is taken to be the same as that for beams. However, if P_{ft}/P_{fc} is greater than zero, the member behaves more like a column because both of its flanges are in net compression. For these cases, the imperfection pattern for the flange in flexural compression is taken to be the same as that for the compression flange in beams. Furthermore, since the other flange is also braced and is subjected to a net compression, it also uses the same imperfection pattern as the compression flange. However, the magnitude of the imperfection is taken as proportional P_{ft}/P_{fc} . In the limit that P_{ft}/P_{fc} approaches zero, the member imperfection is identical to the beam case. However, in the limit that the member is subjected to pure axial compression, such that P_{ft}/P_{fc} approaches 1.0, identical imperfections are specified for both of the flanges. The imperfection patterns for beam-columns with combined bracing are summarized in Figs. 3.17 and 3.18.

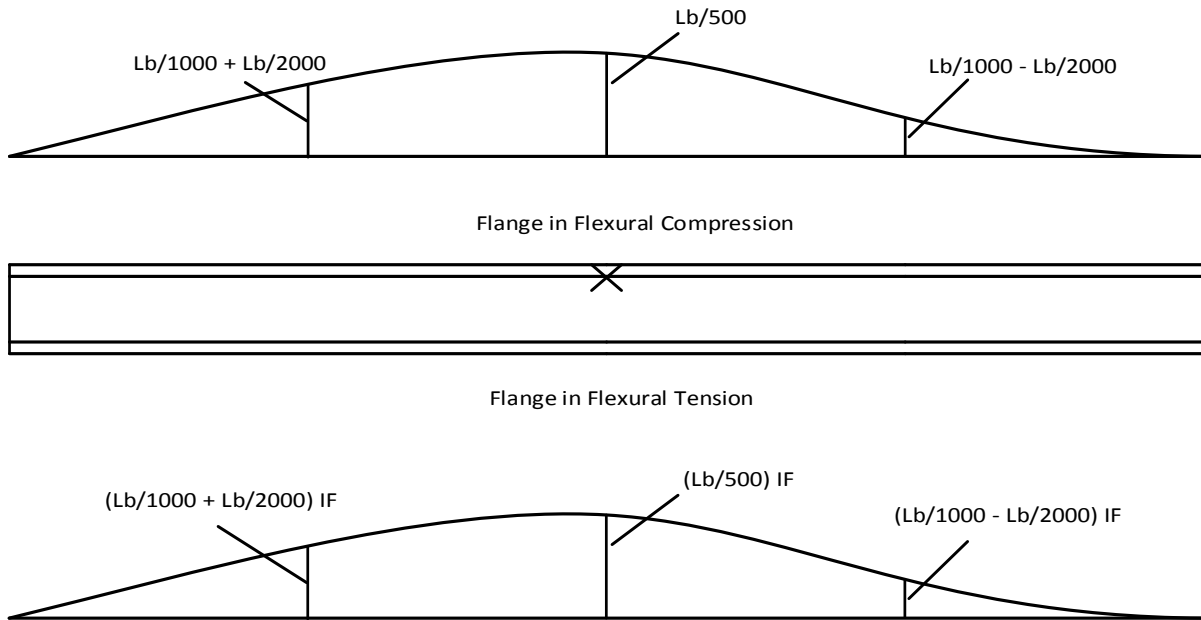


Figure 3.17. Imperfection pattern for beam-columns with combined lateral and torsional bracing and one intermediate brace point.

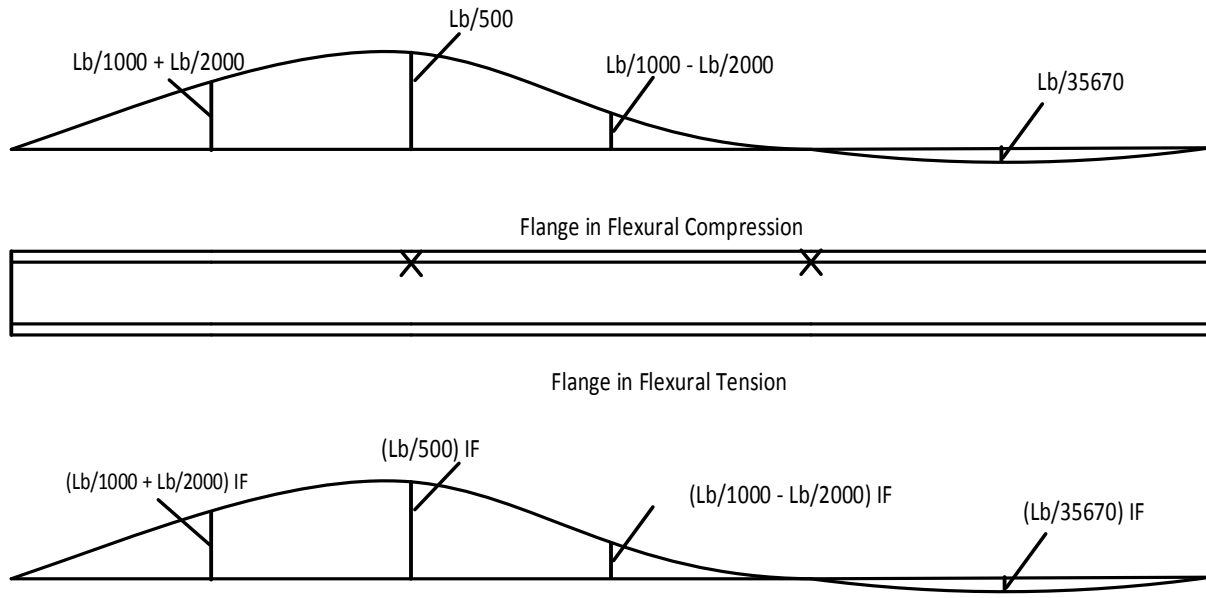


Figure 3.18. Imperfection pattern for beam-columns with combined lateral and torsional bracing and two intermediate brace points.

In cases where negative bending moment is applied, causing compression on the bottom flange (i.e., the flange opposite from the one containing the lateral bracing, and therefore, the one restrained laterally only via the torsional bracing) then the imperfection patterns in the above figures are switched between the top and bottom flanges.

In the FEA simulation studies conducted in this research, the beam-columns with 5 ft unbraced lengths and Moment Gradient 1 loading experienced difficulty in converging in some of the cases. To solve this problem, and to consider the impact of web local buckling displacements on the member resistance, local buckling imperfections were added to the above imperfections for all of the Moment Gradient 1 cases with $L_b = 5$ ft. The local buckling imperfections were determined by conducting a separate elastic eigenvalue buckling pre-analysis using the beam-column loading (i.e., the axial load and the Moment Gradient 1 loading). None of the other FEA simulation cases studied in this research considered member local buckling imperfections.

CHAPTER 4 BEAMS SUBJECTED TO MOMENT GRADIENT LOADING

4.1 Overview

This chapter addresses the first major objective of this research, evaluation of the bracing of beams with moment gradient loading. Section 4.2 gives details of the cases considered. Top flange loading effects are excluded in this chapter but are considered subsequently in Chapter 5. Section 4.3 discusses the member rigidly-braced strengths. Section 4.4 summarizes the ANSI/AISC 360-10 bracing design equations considered in this research. Section 4.5 presents the test simulation results.

4.2 Detailed Study Design

The cases considered in this research to study the bracing requirements for beams subjected to moment gradient loading are listed below. The case naming convention is explained in Sections 2.2 and 2.3. The cases considered for the Moment Gradient 1 loading, single curvature bending with an applied moment on one end and zero moment on the opposite end of the beam, are as follows.

- Positive moment loading, basic bracing types:

B_MG1p_NB_n1_Lb5
B_MG1p_NB_n1_Lb15
B_MG1p_RB_n2_Lb5
B_MG1p_RB_n2_Lb15
B_MG1p_TB_n1_Lb5
B_MG1p_TB_n1_Lb15

- Positive moment loading, combined point (nodal) lateral and point torsional bracing:

B_MG1p_CNTB_n1_Lb5_TLBSR4
B_MG1p_CNTB_n1_Lb5_TLBSR1
B_MG1p_CNTB_n1_Lb5_TLBSR0.25
B_MG1p_CNTB_n1_Lb15_TLBSR4
B_MG1p_CNTB_n1_Lb15_TLBSR1
B_MG1p_CNTB_n1_Lb15_TLBSR0.25

- Positive moment loading, combined shear panel (relative) lateral and point torsional bracing:

B_MG1p_CRTB_n2_Lb5_TLBSR4
B_MG1p_CRTB_n2_Lb5_TLBSR1
B_MG1p_CRTB_n2_Lb5_TLBSR0.25
B_MG1p_CRTB_n2_Lb15_TLBSR4
B_MG1p_CRTB_n2_Lb15_TLBSR1
B_MG1p_CRTB_n2_Lb15_TLBSR0.25

- Negative moment loading, combined point (nodal) lateral and point torsional bracing:

B_MG1n_CNTB_n1_Lb5_TLBSR5.67
B_MG1n_CNTB_n1_Lb5_TLBSR1
B_MG1n_CNTB_n1_Lb5_TLBSR0.33
B_MG1n_CNTB_n1_Lb5_TLBSR0.11
B_MG1n_CNTB_n1_Lb15_TLBSR5.67
B_MG1n_CNTB_n1_Lb15_TLBSR1
B_MG1n_CNTB_n1_Lb15_TLBSR0.33
B_MG1n_CNTB_n1_Lb15_TLBSR0.11

- Negative moment loading, combined shear panel (relative) lateral and point torsional bracing:

B_MG1n_CRTB_n2_Lb5_TLBSR5.67
B_MG1n_CRTB_n2_Lb5_TLBSR1
B_MG1n_CRTB_n2_Lb5_TLBSR0.33
B_MG1n_CRTB_n2_Lb5_TLBSR0.11
B_MG1n_CRTB_n2_Lb15_TLBSR5.67
B_MG1n_CRTB_n2_Lb15_TLBSR1
B_MG1n_CRTB_n2_Lb15_TLBSR0.33
B_MG1n_CRTB_n2_Lb15_TLBSR0.11

The following cases are considered for the Moment Gradient 2 loading, transverse load applied at the centroid of the cross-section at the mid-span of the beam.

- Positive moment loading, basic bracing types:

B_MG2pc_NB_n1_Lb5
B_MG2pc_NB_n1_Lb15
B_MG2pc_TB_n1_Lb5
B_MG2pc_TB_n1_Lb15

- Positive moment loading, combined point (nodal) lateral and point torsional bracing:

B_MG2pc_CNTB_n1_Lb5_TLBSR4
B_MG2pc_CNTB_n1_Lb5_TLBSR1
B_MG2pc_CNTB_n1_Lb5_TLBSR0.25
B_MG2pc_CNTB_n1_Lb15_TLBSR4
B_MG2pc_CNTB_n1_Lb15_TLBSR1
B_MG2pc_CNTB_n1_Lb15_TLBSR0.25

- Negative moment loading, combined point (nodal) lateral and point torsional bracing:

B_MG2nc_CNTB_n1_Lb5_TLBSR5.67
B_MG2nc_CNTB_n1_Lb5_TLBSR1
B_MG2nc_CNTB_n1_Lb5_TLBSR0.33
B_MG2nc_CNTB_n1_Lb5_TLBSR0.11
B_MG2nc_CNTB_n1_Lb15_TLBSR5.67
B_MG2nc_CNTB_n1_Lb15_TLBSR1
B_MG2nc_CNTB_n1_Lb15_TLBSR0.33
B_MG2nc_CNTB_n1_Lb15_TLBSR0.11

Finally, the following cases are considered for the Moment Gradient 3 loading, reverse curvature bending.

- Basic torsional bracing:

B_MG3_TB_n1_Lb5
B_MG3_TB_n1_Lb15

- Combined point (nodal) lateral and point torsional bracing:

B_MG3_CNTB_n1_Lb15_TLBSR4
B_MG3_CNTB_n1_Lb15_TLBSR1
B_MG3_CNTB_n1_Lb15_TLBSR0.25

- Combined panel (relative) lateral and point torsional bracing:

B_MG3_CRTB_n2_Lb15_TLBSR4
B_MG3_CRTB_n2_Lb15_TLBSR1
B_MG3_CRTB_n2_Lb15_TLBSR0.25

4.3 Beam Rigidly-Braced Strengths

For beams with a given number of intermediate brace locations, there is a slight difference in the rigidly-braced strengths as a function of the bracing type (point lateral, shear panel lateral, point torsional, etc.). In this research, the beam rigidly-braced strength for a given number of intermediate braces ($n = 1$ or 2) is taken as the minimum of the rigidly-braced strengths obtained for the different bracing types. A separate rigidly-brace strength is used for $n = 1$ versus $n = 2$. This philosophy simplifies the comparison of the study results. It should be noted that the AISC Specification (AISC 2010a) predicts only one strength for the different bracing types considered for a given value of n . In all of the cases considered, the minimum rigidly-braced strength is obtained when torsional bracing is used alone, without any combination with lateral braces. Generally, the rigidly-braced strengths are only slightly different for the different bracing types, but the differences are measurable. As noted previously in Section 2.1, the minimum rigidly-braced member strength is used as the required moment when estimating the beam bracing stiffness requirements from the AISC Appendix 6 (AISC 2010a) equations and other bracing design equations.

Tables 4.1 and 4.2 give the rigidly-braced strengths for the Moment Gradient 1 loading with $n = 1$ and $n = 2$ respectively. Similarly, Table 4.3 gives the rigidly-braced strengths for the Moment Gradient 2 cases. Tables 4.4 and 4.5 give the rigidly-braced strengths for the Moment Gradient 3 cases with $n = 1$ and $n = 2$.

Table 4.1. Comparison of rigidly-braced strengths for beams with Moment Gradient 1 loading and $n = 1$.

	$L_b = 5$ ft	$L_b = 15$ ft
Combined point (nodal) lateral and point torsional bracing	4827 kip-inch	2671 kip-inch
Point (nodal) lateral bracing	4824 kip-inch	2594 kip-inch
Point torsional bracing	4798 kip-inch	2409 kip-inch

Table 4.2. Comparison of rigidly-braced strengths for beams with Moment Gradient 1 loading and $n = 2$.

	$L_b = 5$ ft	$L_b = 15$ ft
Shear panel (relative) lateral and point torsional bracing	4738 kip-inch	2476 kip-inch
Shear panel (relative) lateral bracing	4737 kip-inch	2449 kip-inch
Point torsional bracing	4691 kip-inch	2197 kip-inch

Table 4.3. Comparison of rigidly-braced strengths for beams with Moment Gradient 2 loading and $n = 1$.

	$L_b = 5$ ft	$L_b = 15$ ft
Combined point (nodal) lateral and point torsional bracing	4989 kip-inch	3152 kip-inch
Point (nodal) lateral bracing	4989 kip-inch	3149 kip-inch
Point torsional bracing	4913 kip-inch	3069 kip-inch

Table 4.4. Comparison of rigidly-braced strengths for beams with Moment Gradient 3 loading and $n = 1$.

	$L_b = 5$ ft	$L_b = 15$ ft
Combined point (nodal) lateral and point torsional bracing	4981 kip-inch	3501 kip-inch
Point torsional bracing	4968 kip-inch	3422 kip-inch

Table 4.5. Comparison of rigidly-braced strengths for beams with Moment Gradient 3 loading and $n = 2$.

	$L_b = 15$ ft
Combined point (nodal) lateral and point torsional bracing	2975 kip-inch
Point torsional bracing	2650 kip-inch

4.4 Summary of the ANSI/AISC 360-10 Beam Bracing Equations Considered in this Research

In this research, the point and panel lateral bracing stiffness requirements per AISC are obtained from Eq. (C-A-6-5), in the Appendix 6 (AISC 2010a) Commentary, with $C_b P_f$ taken equal to M_{max}/h_o , where M_{max} is taken as the beam minimum rigidly-braced strength presented in Section 4.3. More generally, M_{max} is the maximum flexural strength required of the beam within the unbraced length corresponding to the shear panel under consideration, or the largest of the required flexural strengths within the unbraced lengths adjacent to the point brace under consideration. In addition, the stiffness requirements are expressed without the consideration of the resistance factor (ϕ), or other words with ϕ taken equal to 1.0, to facilitate the direct comparison with FEA test simulation results. Given these specific substitutions, AISC Eq. (C-A-6-5) may be written as

$$\beta_{brL} = \frac{2N_i(M_{max} / h_o)C_{iL}C_d}{L_b} \quad (4-1)$$

where the additional variables are defined as:

$N_i = 1.0$ for shear panel (relative) bracing

$= (4 - 2/n)$ for point (nodal) bracing

$n =$ number of intermediate braces

$h_o =$ distance between the centroids of the compression and tension flanges

$C_{iL} =$ lateral bracing transverse load height factor

$= 1.0$ for centroidal loading

$= 1 + 1.2/n$ when the transverse load is applied at the flange level and is detrimental to the member stability (this occurs when the transverse load is applied normal to the flange at the flange level, in the plane of the web, and is directed toward the beam cross-section shear center from its point of application)

$C_d =$ double curvature factor, which accounts for the potential larger demands on the lateral bracing in unbraced lengths containing inflection points, applied only to the point brace closest to the inflection point or to the panel brace corresponding to the unbraced length containing the inflection point as well as the panel brace in the unbraced length closest to the inflection point.

$= 1 + (M_s / M_L)^2$ in the above cases where the C_d factor is applicable

$= 1.0$ otherwise

M_s = absolute value of the maximum moment causing tension in the braced flange within the overall length composed of the unbraced length containing an inflection point and the adjacent unbraced length closest to the inflection point

M_L = absolute value of the maximum moment causing compression in the braced flange within the overall length composed of an unbraced length containing an inflection point and the adjacent unbraced length closest to the inflection point

L_b = unbraced length within the shear panel under consideration, or adjacent to the point brace; when unbraced lengths adjacent to a point brace have different M_{max}/L_b values, the larger value should be used in the calculation of the required brace stiffness.

As noted at the beginning of Section 4.3, the above definition of M_{max} as the minimum rigidly-braced strength obtained in the FEA test simulations for the different bracing types simplifies the comparison to the bracing requirements to the study results by focusing on the use of just one value for the member resistance.

It should be noted that the above equation is generally accepted as a reliable estimate of the bracing stiffness necessary to provide “full bracing” to a beam member. That is, Eq. (4-1) gives an estimate of the bracing stiffness necessary to develop the AISC beam capacity calculated based on the specified unbraced lengths between the brace points L_b (i.e., based on a lateral-torsional buckling effective length factor $K = 1$). In addition, the “ideal full bracing stiffness” for point lateral and shear panel lateral bracing may be estimated as one-half of the required value from Eq. (4-1). The ideal full bracing stiffness may be considered conceptually as the stiffness value necessary to develop M_{max} if the initial beam geometry is perfectly straight and the beam is loaded ideally within the plane of major-axis bending.

The following values of the above variables are calculated, considering the different loading and bracing conditions evaluated in this research:

- For point lateral bracing, $N_i = 2$ for $n = 1$ and $N_i = 3$ for $n = 2$.
- For the Moment Gradient 2 cases with top flange loading, not considered in this chapter but evaluated subsequently in Chapter 5, $C_{iL} = 2.2$ for $n = 1$ and $C_{iL} = 1.6$ for $n = 2$.
- For the Moment Gradient 3 cases with $n = 1$, $M_S/M_L = 1$ and therefore $C_d = 2$, whereas for $n = 2$, $M_S/M_L = 1/3$ and therefore $C_d = 1.11$.

The AISC lateral bracing strength requirements are calculated in this research using Eqs. (C-A-6-6a) and (C-A-6-6b), in the Appendix 6 (AISC 2010a) Commentary, for shear panel (relative) and point (nodal) lateral bracing respectively. These equations may be written as

$$V_{br} = 0.004(M_{\max} / h_o) C_{iL} C_d \quad (4-2)$$

for shear panel bracing, which gives the panel shear force strength requirement normal to the axis of the beam, and

$$P_{br} = 0.01(M_{\max} / h_o) C_{iL} C_d \quad (4-3)$$

for point bracing, which gives the direct point (nodal) brace strength requirement normal to the axis of the beam.

A refined estimate of the required lateral bracing strength can be obtained by multiplying the right-hand side of the above by Eq. (C-A-6-1) from the Appendix 6 (AISC 2010a) Commentary,

$$\frac{1}{2 - \frac{\beta_{brL}}{\beta_{act}}} \quad (4-4)$$

This equation accounts for the fact that the second-order amplification of the initial out-of-alignment at the brace points (Δ_o) due to the stability effects is smaller as the “actual” brace stiffness, β_{act} , is increased relative to the minimum required brace stiffness, β_{brL} . A detailed

derivation of Eq. (4-4) as well as an explanation of these AISC Appendix 6 (AISC 2010a) equations, with all the Commentary refinements included (but with an emphasis on applications with uniform bending moment), can be found in Chapter 2 of Prado and White (2015).

In this research, the required point torsional bracing stiffness for full bracing is expressed as an equivalent shear panel (relative) lateral bracing stiffness oriented vertically between the two flanges of the I-section member. This approach of considering the torsional bracing as an equivalent relative lateral bracing, but between the two flanges rather than between two points along the same flange, is discussed in detail in Chapter 2 of Prado and White (2015). The required AISC torsional bracing stiffness, expressed in this form, is obtained simply by dividing AISC Eq. (A-6-11) by h_o^2 . Furthermore, as explained by Prado and White (2015), Eq. (A-6-11) divided by h_o^2 may be written in the following form:

$$\beta_{brT} = \pi^2 \left[\frac{\left(\frac{M_{max}}{C_b h_o} \right)}{P_{ef,eff}} \right] \left[\frac{\left(\frac{M_{max}}{C_b h_o} \right)}{L_b} \right] \frac{n_T + 1}{n_T} C_{iT} \quad (4-5)$$

where the terms not already defined above in the context of Eq. (4-1) are:

C_b = equivalent uniform moment factor for the critical unbraced length; generally M_{max}/C_b should be taken as the maximum value from the unbraced lengths adjacent to the point brace (the C_b values used for the different study cases in this research are presented in Section 2.2.3)

$P_{ef,eff}$ = effective elastic lateral buckling resistance of the beam compression flange based on the unbraced length between the braces

$$= \frac{\pi^2 E (I_{eff} / 2)}{L_b^2}, \text{ equal to } \frac{\pi^2 E I_{yc}}{L_b^2} \text{ for a doubly-symmetric I-section}$$

I_{yc} = out-of-plane lateral bending moment of inertia of the compression flange

n_T = number of intermediate torsional braces along the beam length

C_{IT} = torsional bracing load height factor accounting, for the effects of the height of any transverse loads relative to the depth of the member cross-section

= 1.2 when the transverse loading is applied at the flange level in the direction that is detrimental to the member stability; this occurs when the transverse load is directed toward the member shear center from its point of application

= 1.0 otherwise

The format of Eq. (4-5) is different than the corresponding Eq. (A-6-11) in AISC 360-10. However, when C_{IT} is taken conservatively as 1.2, this equation gives identical results to Eq. (A-6-11) divided by h_o^2 . The form shown in Eq. (4-5) is useful for emphasizing the contribution from the beam to the resistance of brace point movement via the term $P_{ef,eff}$. Of importance to a number of the subsequent discussions, β_{brT} in Eq. (4-5) is 2.0 times what is commonly referred to as the “ideal full bracing stiffness,” defined as the bracing stiffness necessary to develop the moment capacity M_{max} before a hypothetical member with zero initial imperfections would fail out-of-plane by buckling between the braced locations.

The required torsional brace strength is estimated in this research by using the refined Eq. (C-A-6-8) of the AISC Appendix 6 Commentary, which may be written in the form

$$M_{br} = \beta_{brT} h_o^2 \theta_o \quad (4-6)$$

where β_{brT} is the required torsional bracing stiffness expressed as an equivalent shear panel (relative) bracing stiffness between the two I-section flanges, given by Eq. (4-5), h_o is the distance

between the I-section flange centroids, $\theta_o = \frac{L_b}{500h_o}$ is the assumed initial twist imperfection, and

M_{br} is the torsional moment strength requirement for the point torsional brace. The shear (or shear couple) force in the equivalent shear panel (relative) brace between the flanges is obtained by dividing M_{br} by h_o .

Prado and White (2015) find that Eq. (4-6) does not work well as a predictor of the torsional bracing strength requirements in I-section beams subjected to uniform moment. In addition, they state that Eq. (4-4) does not work well in predicting the variation in the torsional brace forces at the member strength limit as a function of the torsional brace stiffness. They find that an ad-hoc modifier

$$\frac{1}{\sqrt{2 - \frac{\beta_{br}}{\beta_{act}}}} \quad (4-7)$$

combined with a base torsional brace strength requirement of 2 %, gives a reasonably good estimate of the torsional brace strength requirements for $\beta > \beta_{br}$. Furthermore, Prado and White (2015) observe that a brace force requirement of 2 % of M_{max} (i.e., $0.02M_{max}$) provides an accurate to conservative estimate of the brace forces required to develop 95 % or greater of the load capacity from the test simulations in all cases (i.e., for all brace stiffness values) in I-section beams subjected to uniform bending moment.

The reduction in the torsional bracing strength requirement for $\beta > \beta_{br}$ given by Eq. (4-7) is relatively small. Therefore, only the simpler base torsional bracing strength requirement of $0.02M_{max}$ and the torsional brace strength requirement from Eq. (4-6) are evaluated in this research.

4.5 Results

The results for the various beam moment gradient loading cases are discussed in the following subsections.

4.5.1 Beams with Moment Gradient 1 Loading, Basic Bracing Cases

The results for the Moment Gradient 1 loading cases are shown for the basic point and panel lateral bracing cases and for the point torsional bracing cases in Figs. 4.1 through 4.3 respectively. Figures 4.1 through 4.3 show the knuckle curves and brace-force versus brace stiffness curves for

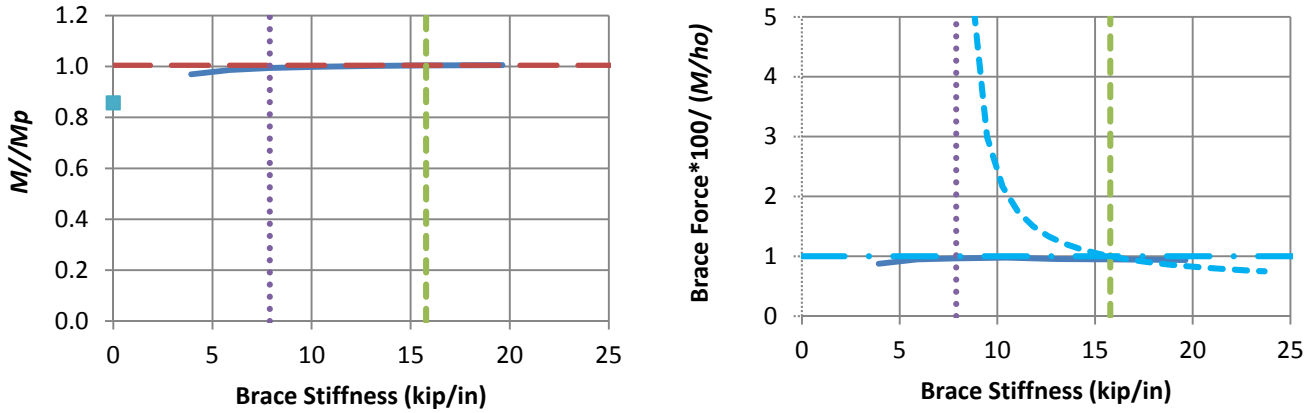
these studies. The term M in the plots is the maximum moment along the length of the member at the member limit load (i.e., at the member flexural capacity) in these and all the subsequent test simulation plots. This moment is normalized by the W21x44 section plastic moment capacity, $M_p = 4770$ in-kip, in the knuckle curve plots. The required brace force (measured at the test limit loads) is reported as a percentage of the equivalent flange force, M/h_o , in all cases.

Table 4.6 compares the bracing stiffness results from Figs. 4.1 through 4.3 to the corresponding estimates from the AISC bracing equations presented in Section 4.4 and reports the maximum brace forces as a percentage of M/h_o for the tests with lateral brace stiffness $\beta_L = \beta_{brL}$ or torsional brace stiffness $\beta_T = \beta_{brT}$. The torsional bracing stiffnesses are reported in this table as the equivalent relative lateral bracing stiffness values (in units of kip/in). The following observations can be gleaned from Table 4.6 and Figs. 4.1 to 4.3 regarding the bracing stiffness requirements:

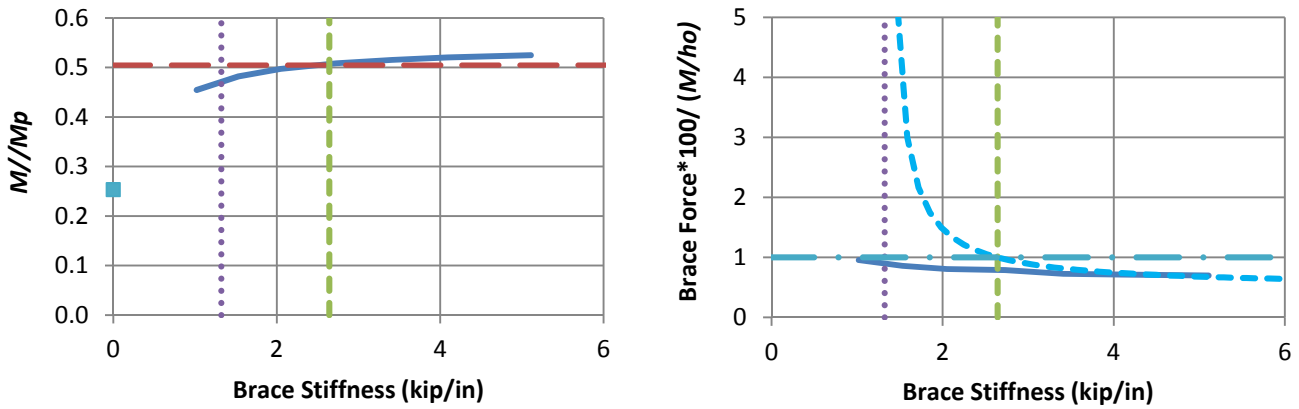
- The AISC Appendix 6 β_{br} equations provides a conservative estimate of the stiffnesses required to reach either 96 % or 98 % of the rigidly-braced strength, shown as β_{F96} and β_{F98} , for all of the beams considered here. This is consistent with the results reported by Prado and White (2015) for beams subjected to uniform bending.
- For the beams with $L_b = 5$ ft, all of the ratios β_{br}/β_{F96} values are larger than 2.0, meaning that the estimated ideal bracing stiffness values of one-half of the required full bracing stiffness are sufficient for the beams to develop 96 % of their rigidly-braced strengths. In these cases, the beams experience significant distributed yielding prior to reaching their maximum strength.
- For the 15 ft unbraced lengths, where the beam response is more dominated by elastic stability effects, the bracing stiffness required to reach 96 % of the rigidly-braced strength is slightly larger than the ideal full bracing stiffness values from AISC 360-10 (i.e., the β_{br}/β_{F96} values are somewhat smaller than 2.0).

Regarding the AISC bracing required strength estimates, the brace force versus brace stiffness plots and the summary results reported in Table 4.6 show the following:

- The point lateral (nodal) brace strength requirements are estimated accurately by the AISC Appendix 6 (AISC 2010a) equations for brace stiffnesses at and above β_{brL} .
- The brace force - brace stiffness plot in Fig. 4.2b and the corresponding entry in Table 4.6 show that the maximum panel brace strength requirements are slightly underestimated by the current AISC Eq. (4-2) for $\beta_L \geq \beta_{brL}$ for the case with the longer unbraced length. However, the AISC prediction is accurate if the base required brace force is increased from 0.4 % to 0.5 % of the corresponding flange force M_r/h_o . This is again consistent with the results reported by Prado and White (2015) for beams subjected to uniform bending.
- The brace force - brace stiffness plot in Fig. 4.2a shows that the maximum panel brace force at the test limit loads for the 5 ft case is underestimated by the AISC brace strength Eq. (4-2). Table 4.6 reports that the maximum shear panel brace force is 0.68 % in this problem at the limit load in the test corresponding to $\beta_L = \beta_{brL}$. However, close inspection of the brace force versus applied load curves from the different tests shows that a brace strength requirement of 0.5 % is sufficient to develop very close to the test limit load for $\beta \geq \beta_{br}$. Figure 4.4 shows the brace force versus the Load Proportionality Factor for the B_MG1p_RB_n2_Lb5 case with $\beta_L = \beta_{brL}$. (The Load Proportionality Factor is the fraction of a specified reference load that has been applied at a given stage of the structural analysis.) From this figure, it can be observed that a brace strength requirement of 0.5 % is sufficient to develop a member strength very close to the test limit load. By combining the results in Fig. 4.4 with the knuckle curve value at $\beta_L = \beta_{brL}$ in Fig. 4.2a, one can conclude that 97 % of the beam's rigidly-braced strength is developed in this critical case.



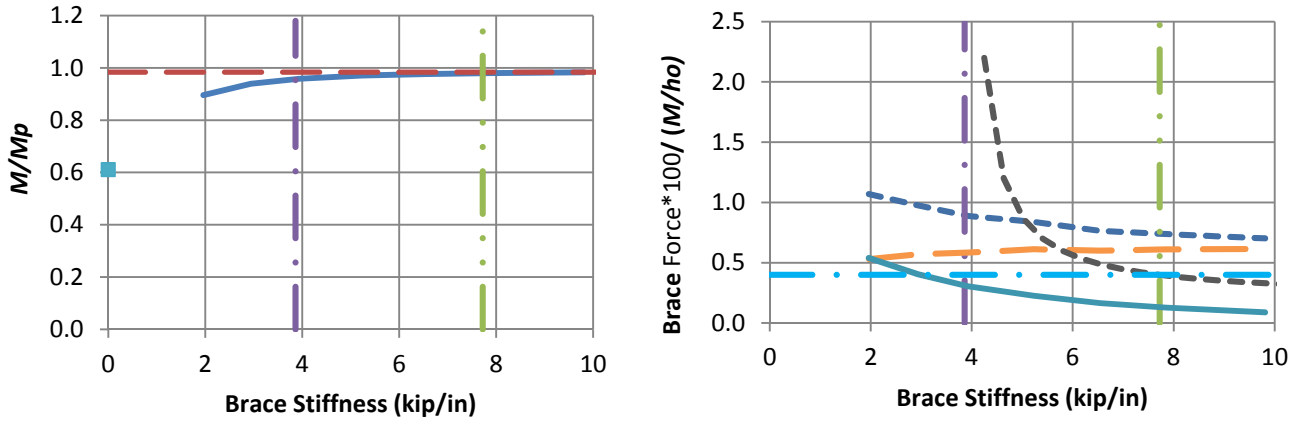
a) B_MG1p_NB_n1_Lb5



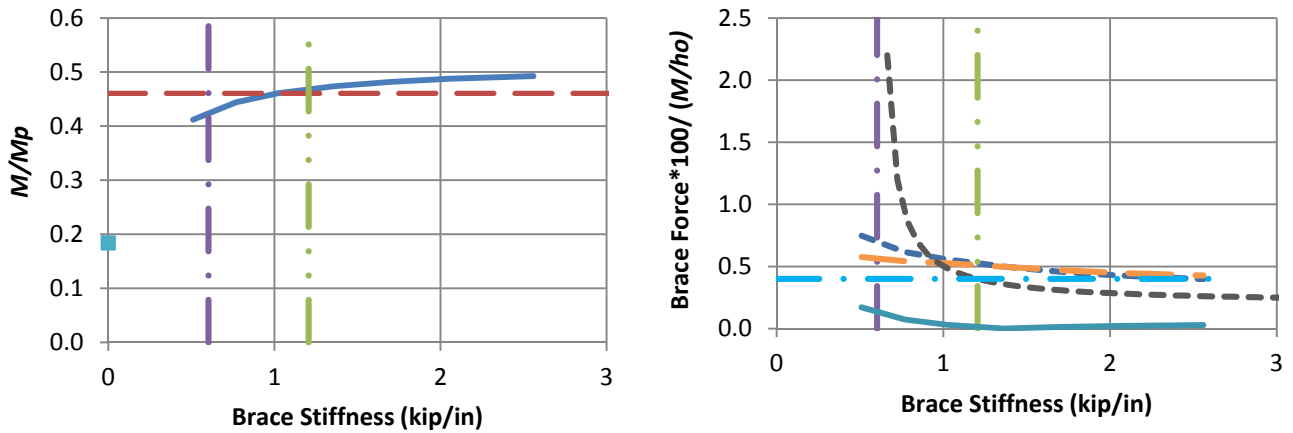
b) B_MG1p_NB_n1_Lb15

- Test simulation results
- - Rigidly-braced strength
- AISC ideal full bracing stiffness
- - $\beta_{brL} = 2x$ AISC ideal full bracing stiffness
- Test simulation strength at zero brace stiffness
- • Base AISC required strength corresponding to $\beta_L = \beta_{brL}$
- - • Refined estimate of required strength using Eqs. (4-1) and (4-4)

Figure 4.1. Beam knuckle curves and brace force vs. brace stiffness plots for point (nodal) lateral bracing cases with $n = 1$ and Moment Gradient 1 loading.



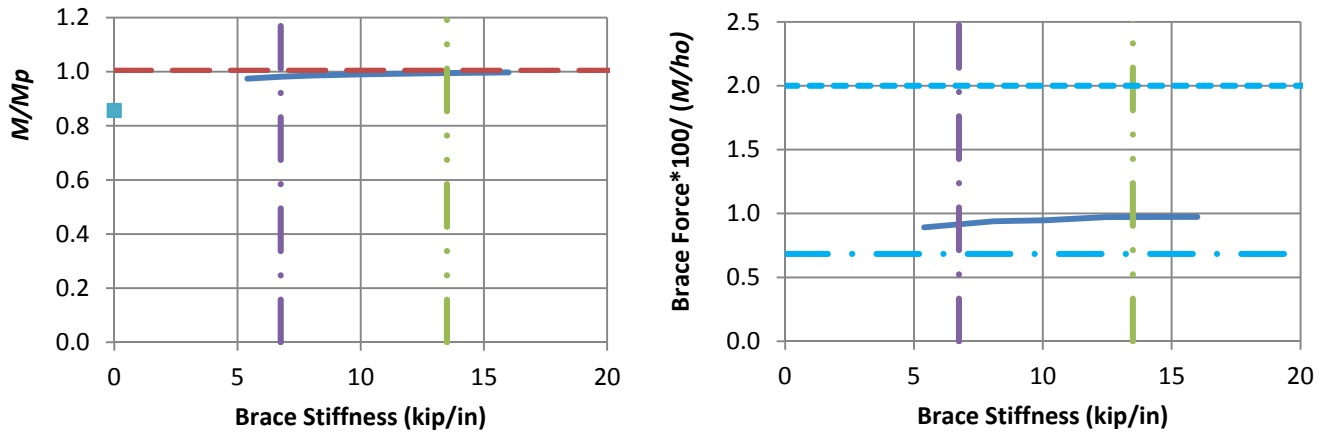
a) B_MG1p_RB_n2_Lb5



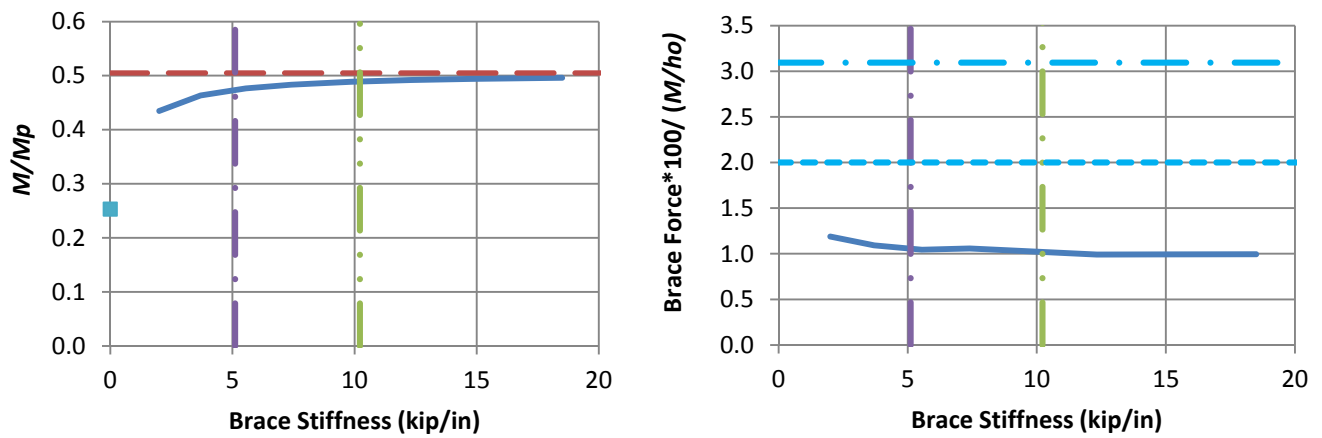
b) B_MG1p_RB_n2_Lb15

- Test simulation results
- • AISC ideal full bracing stiffness
- • $\beta_{brL} = 2 \times$ AISC ideal full bracing stiffness
- - - Left end panel shear force
- Right end panel shear force
- Middle panel shear force
- Test simulation strength at zero brace stiffness
- • Base AISC required strength for $\beta_L = \beta_{brL}$
- - - Refined estimate of required strength from Eqs. (4-1) and (4-4)

Figure 4.2. Beam knuckle curves and brace force vs. brace stiffness plots for shear panel (relative) lateral bracing cases with $n = 2$ and Moment Gradient 1 loading.



a) B_MG1p_TB_n1_Lb5



b) B_MG1p_TB_n1_Lb15

- Test simulation results
- • AISC ideal full bracing stiffness
- • $\beta_{brT} = 2x$ AISC ideal full bracing stiffness
- Test simulation strength at zero brace stiffness
- • Base AISC required strength corresponding to $\beta_T = \beta_{brT}$
- - - Recommended required strength of 2 %
- - - Rigidly-braced strength

Figure 4.3. Beam knuckle curves and brace force vs. brace stiffness plots for point torsional bracing cases with $n = 1$ and Moment Gradient 1 loading.

Table 4.6. Comparison of β_{br} to β_{F98} and β_{F96} and summary of brace forces at $\beta = \beta_{br}$ for Moment Gradient 1 basic bracing cases.

Case	β_{F98} (kip/in)	β_{F96} (kip/in)	β_{br} (kip/in)	β_{br}/β_{F96}	Brace force as a percentage of M/h_o at $\beta = \beta_{br}$
B_MG1p_NB_n1_Lb5	5.70	3.80	15.80	4.16	1.00
B_MG1p_NB_n1_Lb15	2.00	1.60	2.60	1.62	0.80
B_MG1p_RB_n2_Lb5	4.50	3.20	7.80	2.44	0.68
B_MG1p_RB_n2_Lb15	0.90	0.80	1.20	1.50	0.55
B_MG1p_TB_n1_Lb5	7.80	5.00	13.40	2.68	1.00
B_MG1p_TB_n1_Lb15	16.40	8.10	10.20	1.26	1.00

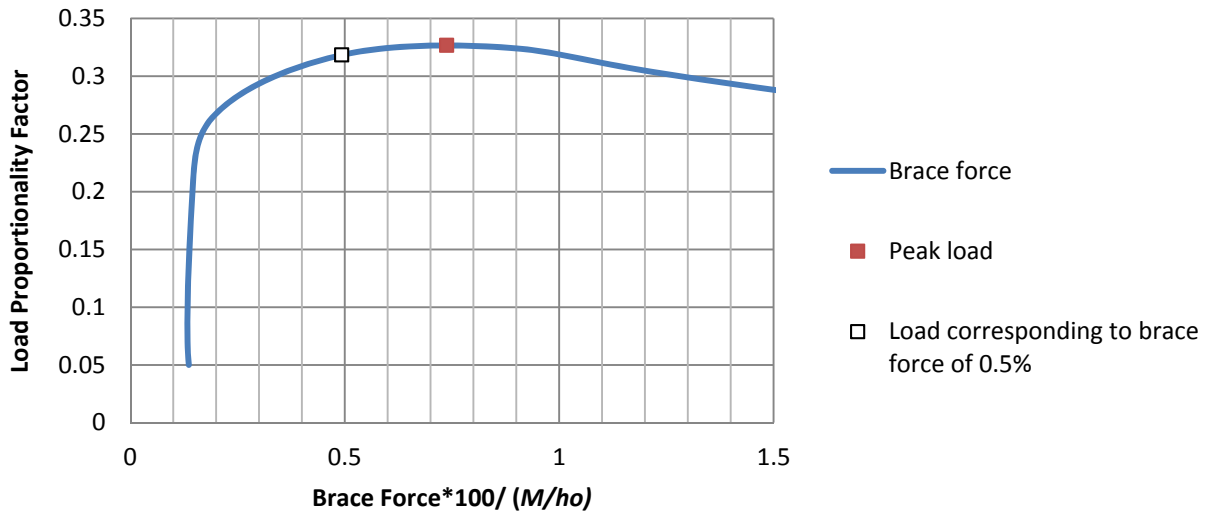


Figure 4.4. Brace force vs. the Load Proportionality Factor for B_MG1p_RB_n2_Lb5 with $\beta_L = \beta_{brL}$.

- The brace force versus brace stiffness curves in Fig. 4.3 show that the current AISC torsional bracing Eq. (4-6) substantially overestimates the strength requirements for the long unbraced length, where the response is more dominated by elastic stability effects. However, for the short unbraced length, where the beam experiences significant distributed yielding at its strength limit, AISC Eq. (4-6) significantly underestimates the strength requirements. This is consistent with the findings by Prado and White (2015). The brace strength requirement at the test limit load is consistently close to 1 % for the all beams considered in these Moment Gradient 1 tests. This is smaller than the requirements observed for the uniform bending cases studied by Prado and White, where a brace force $0.02M_r/h_o$ worked well as a base requirement.

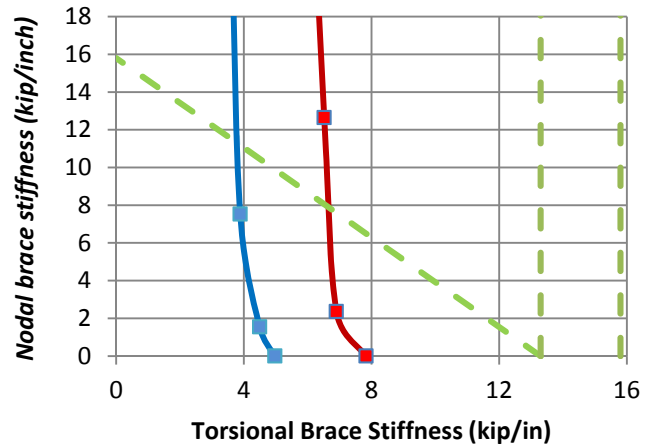
4.5.2 Beams with Moment Gradient 1 Loading, Combined Bracing Cases, Positive Bending

Figures 4.5 and 4.6 show the bracing stiffness interaction plots for combined bracing cases subjected to Moment Gradient 1 loading. The method of generating the interaction plots is discussed in Section 1.2. Knuckle curve and brace force versus brace stiffness plots for each of the combined bracing cases are provided in the Appendix of this report. The following observations can be gleaned from the positive bending results shown on the left-hand side of these figures (the negative bending results are addressed in the next section):

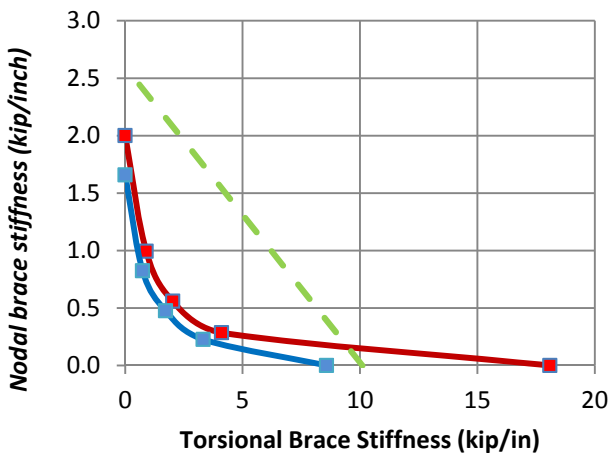
- For beams subjected to positive bending, the interaction between the combined lateral (nodal or shear panel) and torsional bracing stiffness requirements is represented accurately to conservatively by a simple linear interaction between the AISC lateral and torsional bracing stiffness requirements for all the cases studied.



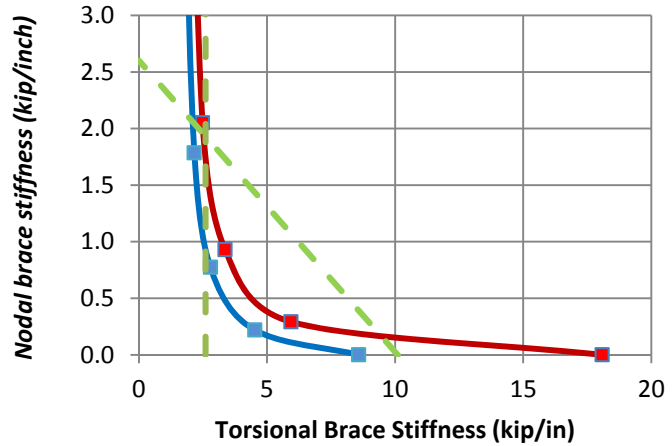
a) 5 ft unbraced length (Positive bending)



b) 5 ft unbraced length (Negative bending)



c) 15 ft unbraced length (Positive bending)



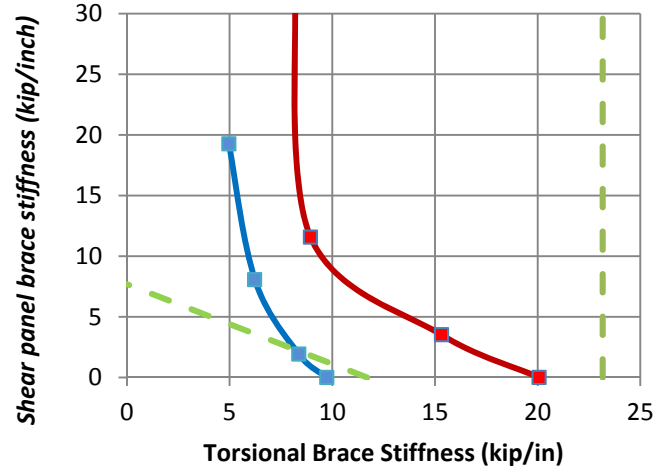
d) 15 ft unbraced length (Negative bending)

- Simulation-based stiffness interaction corresponding to 98 % of rigidly-braced strength
- Simulation-based stiffness interaction corresponding to 96 % of rigidly-braced strength
- - - Recommended design approximation

Figure 4.5. Point (nodal) lateral and point torsional bracing stiffness interactions for Moment Gradient 1 loading and $n = 1$ (B_MG1p_CNTB_n1* and B_MG1n_CNTB_n1*).



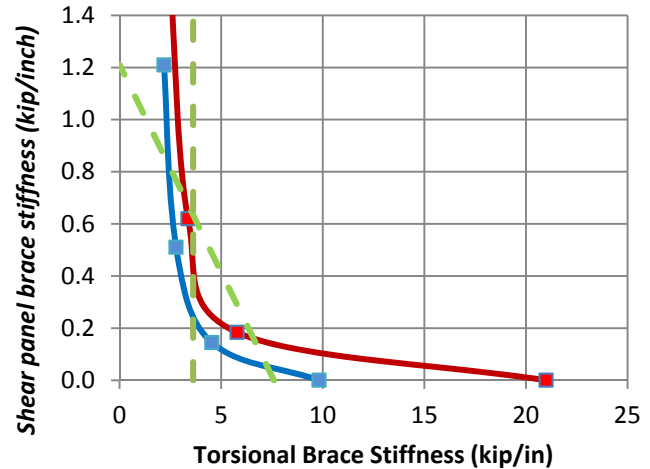
a) 5 ft unbraced length (Positive bending)



b) 5 ft unbraced length (Negative bending)



c) 15 ft unbraced length (Positive bending)



d) 15 ft unbraced length (Negative bending)

- Simulation-based stiffness interaction corresponding to 98 % of rigidly-braced strength
- Simulation-based stiffness interaction corresponding to 96 % of rigidly-braced strength
- - - Recommended design approximation

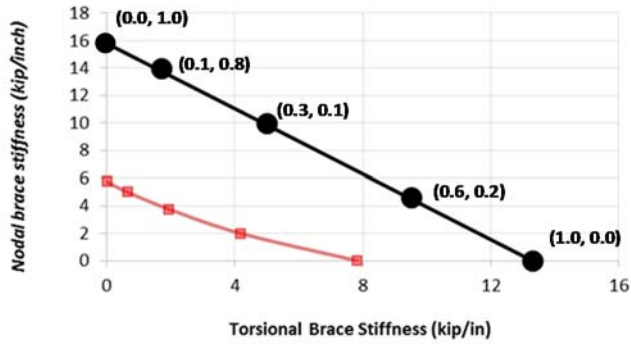
Figure 4.6. Shear panel (relative) lateral and point torsional bracing stiffness interactions for Moment Gradient 1 loading and $n = 2$ (B_MG1_CRTB_n2* and B_MG1n_CRTB_n2*).

- The AISC torsional bracing stiffness requirement for full bracing (i.e., the intercept of the suggested linear AISC stiffness interaction curve with the horizontal axis in the plots) is close to β_{F96} , the bracing stiffness corresponding to 96 % of the beam rigidly-braced strength, for all of the cases with the exception of B_MG1p_CNTB_n1_Lb5 in Fig. 4.5a. This is consistent with the findings by Prado and White (2015). The case shown in Fig. 4.5a appears to be a bit of an outlier. The AISC equation predictions are significantly conservative for this case. It should also be noted that B_MG1p_CNTB_n1_Lb5 exhibited substantial convergence difficulties in a number of the corresponding FEA test simulations (this is the reason why only a β_{F98} curve is shown in Fig. 4.5a. Also, it should be noted that the earlier base torsional bracing results in Fig. 4.3 are reported only for beams with $n = 1$. However, the interaction results in Fig. 4.6 are for $n = 2$, and include the results from torsional bracing tests not shown in the earlier figures.
- The AISC point lateral bracing requirement for full bracing (i.e., the intercept of the suggested linear AISC stiffness interaction curve with the vertical axis in the plots) is 2.77 times the β_{F98L} value in Fig. 4.5a (based on Table 4.6, β_{brL}/β_{F96L} is 4.16 for this case). The AISC required full bracing stiffness β_{br} for point lateral bracing is $1.30\beta_{F98L}$ and $1.62\beta_{F96L}$ in Fig. 4.5c. This is consistent with the results from Prado and White (2015) for uniform bending, which showed that brace stiffnesses only slightly larger than the ideal point lateral brace stiffness ($\beta_{iF.AISC}$) were sufficient to develop 98 % of the rigidly-braced beam strengths. However, stiffnesses close to $\beta_{brL} = 2\beta_{iF.AISC}$ were found to be necessary to avoid the onset of significant increases in the required brace forces at the beam limit loads. (The brace force - brace stiffness simulation results in Fig. 4.1 suggest that for Moment Gradient 1, there is no significant increase in the brace forces as β_L is reduced below $\beta_{brL} = 2\beta_{iF.AISC}$. However, this is only one of many sets of test results.)
- Comparable results to the above are obtained for the intercept of the recommended linear interaction curve with the vertical axis in the shear panel lateral torsional bracing

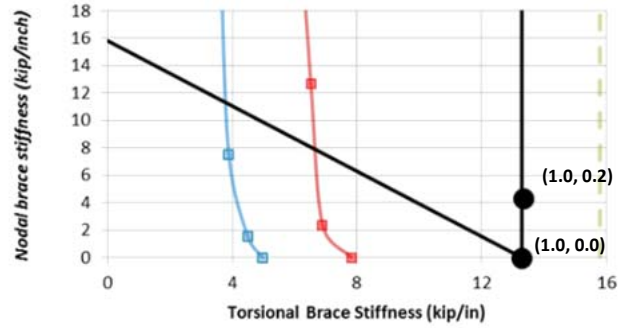
interaction plots of Fig. 4.5. That is $\beta_{brL} = 2.44\beta_{F96L}$ in Fig. 4.6a and $1.50\beta_{F96L}$ in Fig. 4.6c, as previously indicated in Table 4.6.

Ultimately, to fully validate the recommended linear stiffness interaction between the AISC torsional and lateral full bracing full bracing stiffness values, it is important to evaluate the component brace forces associated with the corresponding recommended combined bracing full bracing stiffness limits. These results are summarized on the plots shown in Figs. 4.7 and 4.8, in which the recommended interaction curves are shown by dark bold lines and data points corresponding to test simulations having the stiffness values associated with these curves are indicated by the circular markers on these curves. The corresponding required brace forces at the limit load of these tests are shown by the (M_{br}, P_{br}) or (M_{br}, V_{br}) tuples provided for each data point.

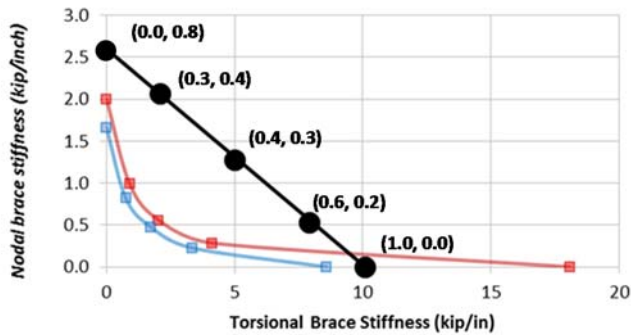
From the positive moment cases shown on the left-hand side of Figs. 4.7 and 4.8, one can observe that the separate torsional and lateral brace forces increase monotonically from zero, when the bracing component has zero stiffness, to values discussed previously for the basic torsional only or lateral only bracing cases when the bracing component has a stiffness corresponding to the AISC Appendix 6 requirements and the other brace stiffness is zero. The most critical case in Fig. 4.7 and 4.8 occurs in Fig. 4.8 in the limit that the torsional brace stiffness goes to zero. In this case, the maximum shear panel bracing force is $0.007M/h_o$. However, when the brace force - Load Proportionality Factor curve is considered for this problem (shown in Fig. 4.4 and discussed in Section 4.5.1), one can observe that greater than 96 % of the beam's rigidly-braced strength is developed when the recommended brace strength requirement of $0.005M/h_o$ is reached.



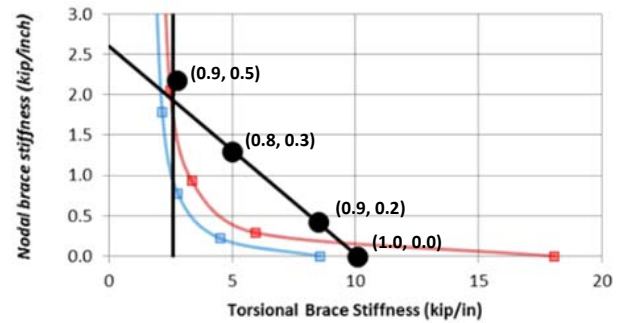
a) 5 ft unbraced length (Positive bending)



b) 5 ft unbraced length (Negative bending)



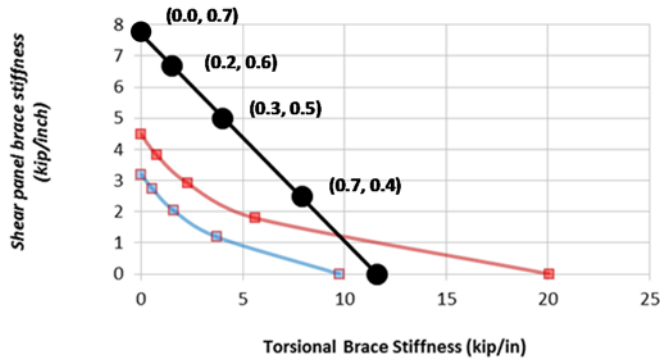
c) 15 ft unbraced length (Positive bending)



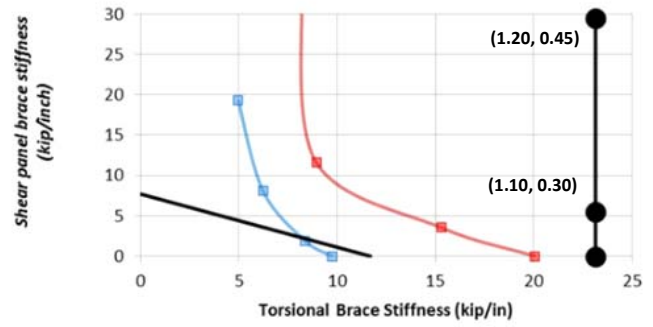
d) 15 ft unbraced length (Negative bending)

- Simulation-based stiffness interaction corresponding to 98 % of rigidly-braced strength
- Simulation-based stiffness interaction corresponding to 96 % of rigidly-braced strength
- Recommended design approximation

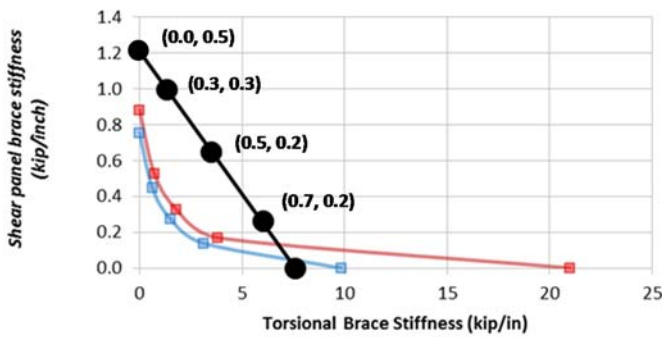
Figure 4.7. Point torsional and point lateral force tuples (M_{br} , P_{br}) corresponding to different combinations of recommended point (nodal) lateral and point torsional bracing stiffnesses from Fig. 4.5 for Moment Gradient 1 loading and $n = 1$ (B_MG1p_CNTB_n1* and B_MG1n_CNTB_n1*).



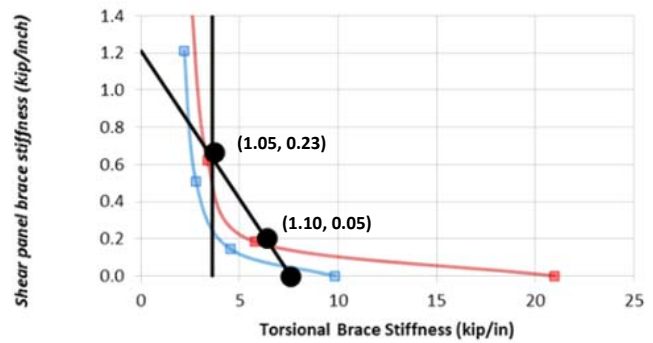
a) 5 ft unbraced length (Positive bending)



b) 5 ft unbraced length (Negative bending)



c) 15 ft unbraced length (Positive bending)



d) 15 ft unbraced length (Negative bending)

- Simulation-based stiffness interaction corresponding to 98 % of rigidly-braced strength
- Simulation-based stiffness interaction corresponding to 96 % of rigidly-braced strength
- Recommended design approximation

Figure 4.8. Point torsional and shear panel lateral force tuples (M_{br} , V_{br}) corresponding to different combinations of recommended shear panel lateral and point torsional bracing stiffnesses from Fig. 4.6 for Moment Gradient 1 loading and $n = 2$ (B_MG1p_CRTB_n2* and B_MG1n_CRTB_n2*).

4.5.3 Beams with Moment Gradient 1 Loading, Combined Bracing Cases, Negative Bending

When a member with combined lateral (nodal or shear panel) and torsional bracing is subjected to negative bending, where the laterally-braced top flange is in tension and the bottom flange is in compression, the interaction between the two bracing stiffness requirements is different. In this case, the lateral brace to the tension flange provides negligible benefit to the stability behavior of the beam in the limit that the torsional brace stiffness approaches zero. However, as explained by Prado and White (2015), in the limit that the lateral brace stiffness is rigid, the torsional brace (when modeled as a relative brace between the top and bottom flanges) effectively becomes a point (nodal) lateral brace to the bottom compression flange. This is because the idealization for a point (nodal) lateral brace is simply a grounded spring. In the limit that the lateral brace to the tension flange is rigid, the relative brace between the top and bottom flange is indeed such a grounded spring.

Upon establishing the above concept, then in the limit that the lateral bracing to the tension flange is rigid, one can surmise that the minimum torsional bracing stiffness requirement, expressed as an equivalent relative bracing (i.e., shear spring) stiffness between the top and bottom flange, can be specified simply as the point (nodal) lateral bracing stiffness requirement. However, the lateral bracing stiffness at the tension flange will need to be very large before the torsional brace actually works as a lateral brace. Therefore, a minimum torsional bracing stiffness equal to the nodal bracing value from Eq. (4-1) is recommended.

From Figs. 4.5 and 4.6, it is observed that the behavior for the Moment Gradient 1 cases considered here is similar to that observed by Prado and White (2015) for uniform bending tests. A vertical line at stiffness equal to that from Eq. (4-1) for a point (nodal) lateral brace, illustrated by the green dashed vertical line in the negative moment based plots on the right-hand side of the above figures, provides an accurate to somewhat conservative minimum limit for the torsional bracing stiffness as the lateral bracing stiffness becomes relatively large. With the exception of

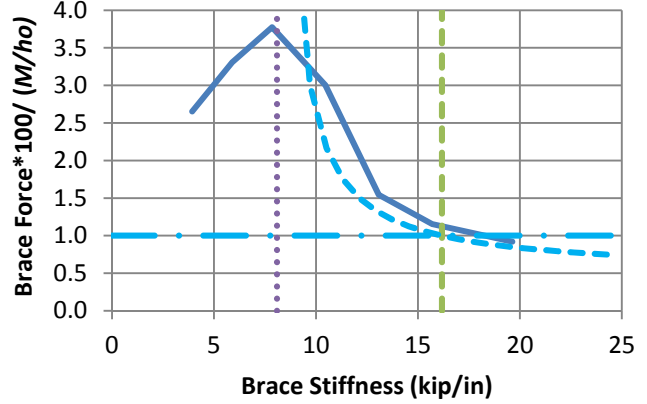
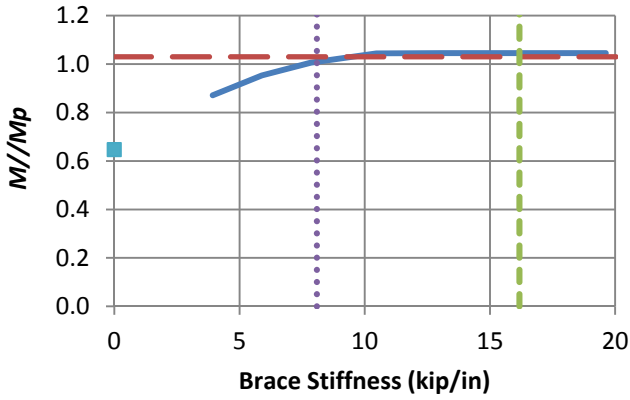
this minimum limit, the torsional bracing stiffness requirement can be reduced by providing a relatively small lateral bracing stiffness, by the same linear interpolation function as shown for the positive moment based plots. One can observe that for some cases, e.g. Fig. 4.5b, the stiffness from Eq. (4-1), is greater than the torsional bracing stiffness requirement. In such cases it is recommended that no reduction in the torsional bracing stiffness should be taken to account for benefits from lateral bracing at the tension flange. For ease of understanding, the interaction plots for such cases show two green dashed vertical lines. It is recommended to use the smaller of the corresponding two stiffnesses as the minimum limit i.e. for cases where the stiffness from Eq. (4-1), is greater than the torsional bracing stiffness requirement, one should simply require the full torsional bracing stiffness irrespective of the value of nodal bracing stiffness.

The plots on the right-hand side of Figs. 4.7 and 4.8 show the implications of the recommended design approximations for the bracing stiffness interaction for the negative moment cases. One can observe that the lateral brace forces generally become zero as the lateral brace stiffness goes to zero, as must be the case. However, the reduction in the required torsional brace forces (moments) is minimal at best, and the torsional brace forces can actually increase with increasing torsional brace stiffness in some situations. Nevertheless, both the lateral and torsional brace forces are maintained at values consistent with the predictions from the AISC full bracing force prediction Eqs. (4-2), (4-3) and (4-6).

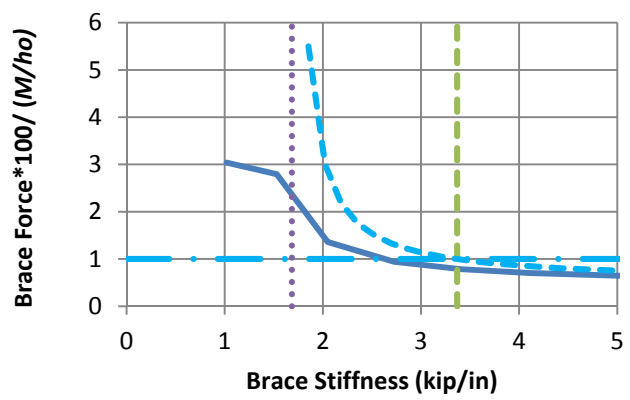
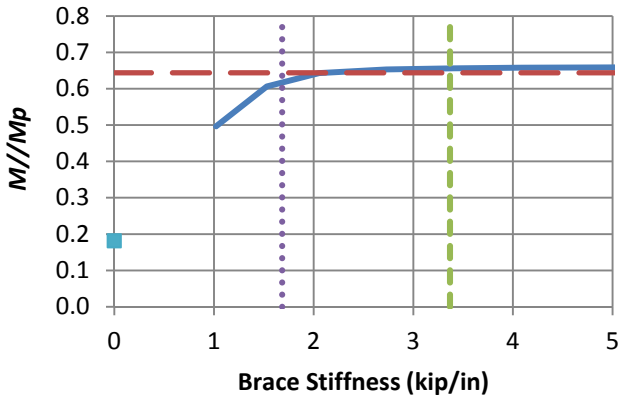
4.5.4 Beams with Moment Gradient 2 Loading, Basic Bracing Cases

The results for Moment Gradient 2 loading are shown for the basic point lateral and torsional bracing cases in Figs. 4.9 and 4.10. As noted in Section 2.2.3, the behavior of shear panel bracing with panels on one-half the point lateral bracing stiffness at the beam mid-span is identical to the corresponding behavior for point lateral bracing when n is equal to 1. Table 4.7 compares the bracing stiffness results from Figs. 4.9 and 4.10 to the corresponding estimates from the AISC bracing equations presented in Section 4.4 and reports the maximum brace forces as a percentage of M/h_o for the tests with $\beta_L = \beta_{brL}$ or $\beta_T = \beta_{brT}$. It can be observed that the AISC Appendix 6 Eq. (4-1) provides a conservative estimate of the stiffness required to reach 96 % of the rigidly-braced strength, β_{F96L} , for the beams with point (nodal) lateral bracing. However, β_{brT} from Eq. (4-5) is slightly smaller than β_{F96T} for the 15 ft torsionally braced case in Fig. 4.10b. Furthermore, for the short unbraced length torsional bracing case B_MG2pc_TB_n1_Lb5 presented in Fig. 4.10a, the knuckle curve approaches the rigidly-braced strength very gradually with increases in the brace stiffness. In this case, a torsional brace stiffness of 35.9 kip/in is required to develop 96 % of the rigidly-braced resistance, whereas β_{brT} is only 7.8 kip/in from Eq. (4-5). At $\beta_T = \beta_{brT}$, the beam strength is still slightly less than 90 % of the rigidly-braced strength for this test (approximately 88 %). This behavior is considered marginal. A substantial increase in the torsional bracing stiffness is necessary to achieve 96 % of the rigidly-braced beam strength in this problem.

It appears that the above behavior is related to the underlying assumption in the development of Eq. (4-5) that the elastic lateral stiffness of the beam is available to assist in resisting the brace point displacements. However, the beams corresponding to Fig. 4.10a are heavily plastified at their mid-span at the development of their limit loads. The above reduction in the beam strength relative to the rigidly-braced strength is more severe than the reductions encountered for the uniform bending cases studied by Prado and White (2015) as well as that shown in Fig. 4.3 for the Moment Gradient 1 loading in this research, where the strengths developed by the torsional bracing β_{brT} are close to or greater than 96 % of the rigidly-braced strengths.



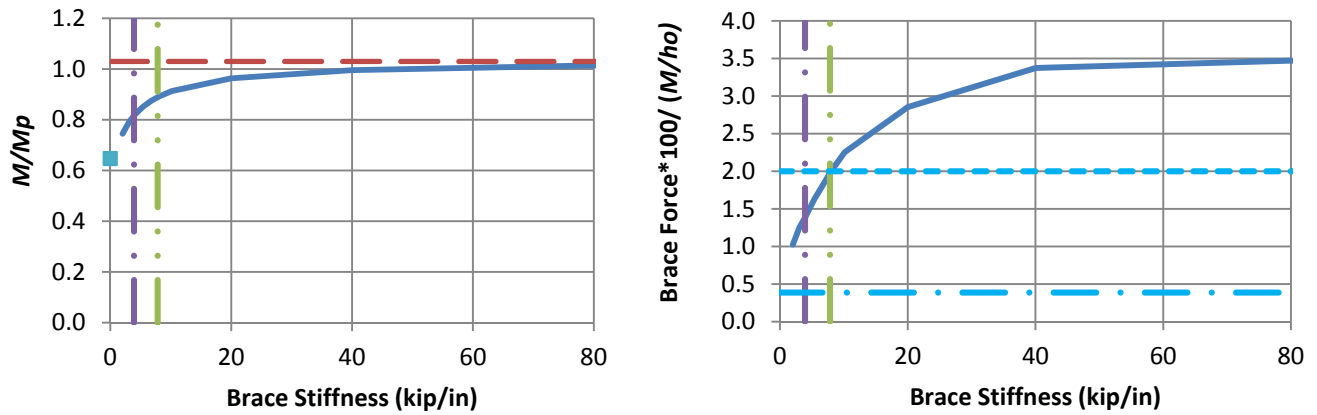
a) B_MG2pc_NB_n1_Lb5



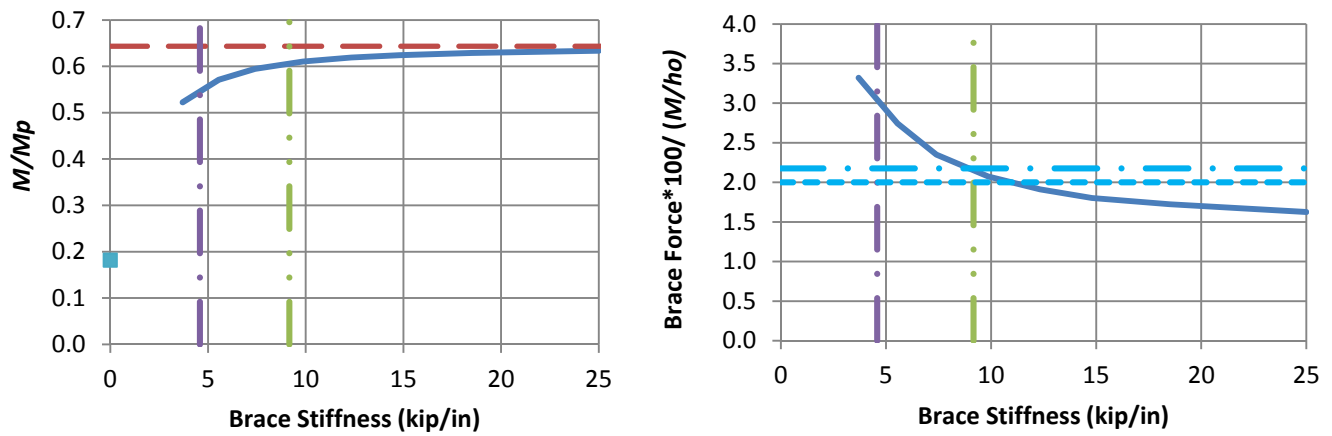
b) B_MG2pc_NB_n1_Lb15

- Test simulation results
- - Rigidly-braced strength
- ⋯ AISC ideal full bracing stiffness
- - $\beta_{brL} = 2x$ AISC ideal full bracing stiffness
- Test simulation strength at zero brace stiffness
- · Base AISC required strength corresponding to $\beta = \beta_{brL}$
- · - Refined estimate of required using Eqs. (4-1) and (4-4)

Figure 4.9. Beam knuckle curves and brace force vs. brace stiffness plots for point (nodal) lateral bracing cases with $n = 1$, Moment Gradient 2, and centroidal loading.



a) B_MG2pc_TB_n1_Lb5



b) B_MG2pc_TB_n1_Lb15

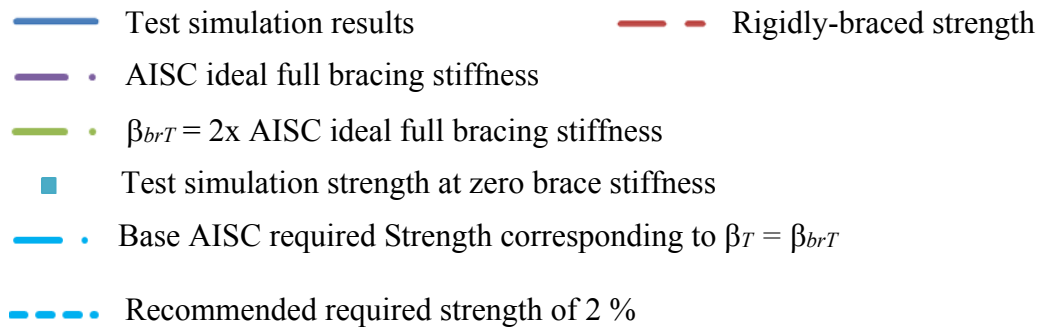


Figure 4.10. Beam knuckle curves and brace force vs. brace stiffness plots for torsional bracing cases with $n = 1$, Moment Gradient 2, and centroidal loading.

Table 4.7. Comparison of β_{br} to β_{F98} and β_{F96} and summary of braced forces at $\beta = \beta_{br}$ for Moment Gradient 2 basic bracing cases with transverse loading at the beam centroid.

Case	β_{F98} (kip/in)	β_{F96} (kip/in)	β_{br} (kip/in)	β_{br} / β_{F96}	Brace force as a percentage of M/h_o at $\beta = \beta_{br}$
B_MG2pc_NB_n1_Lb5	8.10	7.20	16.20	2.25	1.05
B_MG2pc_NB_n1_Lb15	1.90	1.70	3.40	2.00	0.90
B_MG2pc_TB_n1_Lb5	70.10	35.90	7.80	0.22	2.00
B_MG2pc_TB_n1_Lb15	21.20	12.00	9.20	0.77	2.10

The following observations can be gleaned from the brace force - brace stiffness plots in Figs. 4.9 and 4.10:

- The brace force versus brace stiffness curves in Fig. 4.9 show good correlation between the AISC required point lateral brace strength estimates and the test simulation results. As summarized in Table 4.7, the bracing forces are 1.05 and 0.90 % of M/h_o at the limit load of these tests when $\beta_L = \beta_{brL}$.
- Figure 4.10 shows that the torsional bracing strength requirements are estimated well by the base 2 % bracing requirement recommended by Prado and White (2015) for the 15 ft unbraced length case when $\beta_T \geq \beta_{brT}$. Also, the ANSI/AISC 360-10 Appendix 6 base requirement of 2.2 % is an accurate predictor of the brace force requirement at $\beta_T = \beta_{brT}$ for this case.
- For the short unbraced length case in Fig. 4.10, the base torsional bracing strength requirement of $0.02M_r$ recommended by Prado and White (2015) works well at $\beta_T = \beta_{brT}$. However, in this case, if the torsional brace stiffness is larger than β_{brT} , a torsional bracing strength of up to 3.5 % of the beam moment is required to develop the limit load in the test. Figure 4.11 shows the Load Proportionality Factor versus the brace force for the case from Fig. 4.10a where $\beta = 80$ kip/in, which maximizes the torsional brace force as shown in Fig. 4.10b. (The Load

Proportionality Factor is the fraction of a specified reference load that has been applied at a given stage of the structural analysis). One can observe that at a brace force of $0.02M_r$, a strength very close to that of the beam rigidly-braced strength is developed. This is considered to be acceptable behavior for stability bracing design for static loads. However, as noted above, the beam strength developed at $\beta_T = \beta_{brT}$ in this problem is approximately 88 % of the rigidly-braced strength.

- The AISC Commentary prediction based on Eq. (4-6) results in a substantially underestimated torsional brace strength requirement of less than 0.5 % for all values of the brace stiffness for the problem in Fig. 4.10. This is consistent with the findings by Prado and White (2015) and is due to the implicit assumption, in Eq. (4-5), that the elastic stiffness of the beam is available to assist the torsional bracing in resisting the brace point movements. For the short unbraced length case in Fig. 4.10b, the beam is heavily plastified at its strength limit and is not able to provide this elastic resistance to the brace point movement.

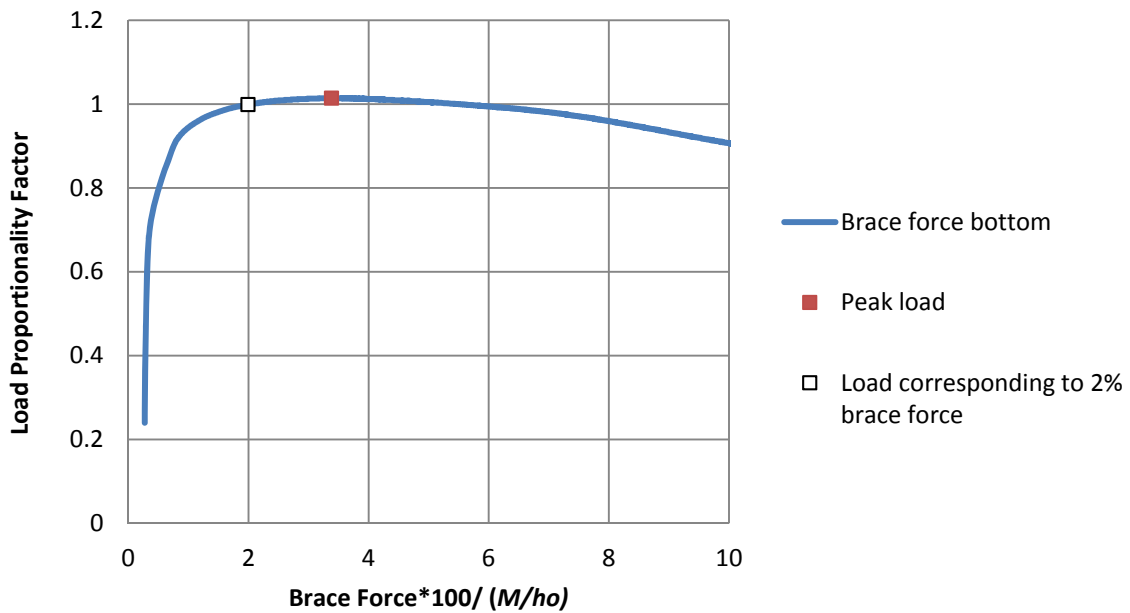


Figure 4.11. Brace force vs. the Load Proportionality Factor for B_MG2pc_TB_n1_Lb5 with $\beta = 80$ kip/in.

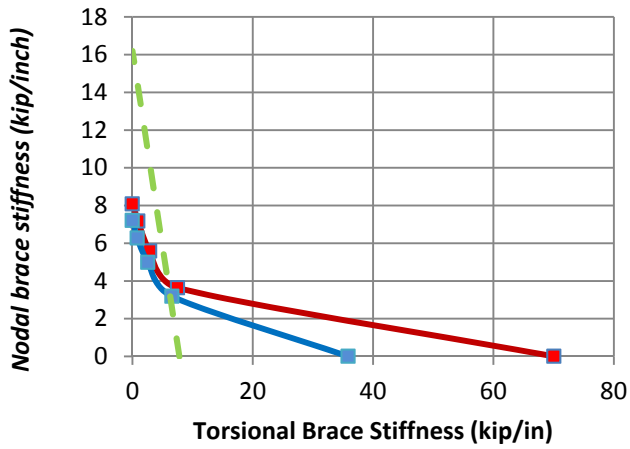
4.5.5 Beams with Moment Gradient 2 Loading, Combined Bracing Cases

Figure 4.12 shows the bracing stiffness interaction plot for combined point (nodal) lateral and torsional bracing cases subjected to Moment Gradient 2 loading. The knuckle curves and brace force versus brace stiffness plots corresponding to the combined bracing cases in this figure are provided in the Appendix of this report. Figure 4.13 shows the brace forces corresponding to different combinations of lateral and torsional bracing stiffnesses used in the interaction plot in Fig. 4.12. In Fig. 4.13 the first tuple value is the torsional brace force, and the second term is the lateral brace force.

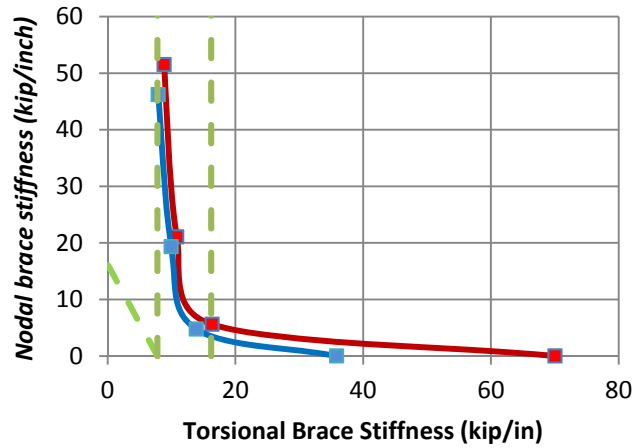
Based on the results in Figs. 4.9, 4.10 and 4.13 it can be concluded that with the exception of a few cases, the brace forces for the lateral and torsional bracing combinations are within the predicted brace strength limits. For the few cases where the brace forces are exceeding the predicted values, it can be shown that the brace strength requirements of 0.5 %, 1 % and 2 % for nodal lateral, shear panel lateral and torsional bracing respectively, are sufficient to develop member strengths very close to the test limit loads. Example cases are discussed below.

From Fig. 4.13a it can be observed that for one case, lateral brace force is 1.8 % and hence exceeds the predicted brace strength of 1 % of P . Figure 4.14 shows the lateral brace force versus the Load Proportionality Factor for this case. From Fig. 4.14 it can be observed that a lateral brace strength requirement of 1 % of P is sufficient to develop member strength very close to the test limit load.

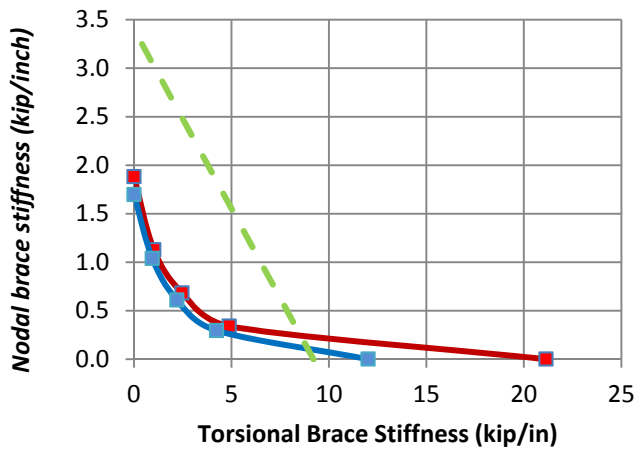
From Fig. 4.13b it can be observed that for one case ($\beta_T = 7.8$ kip/in, $\beta_L = 46$ kip/in), the lateral brace force is 3.0 % and torsional brace force is 3.8 %, exceeding both the predicted brace strengths of 1 % and 2 % respectively. Figure 4.15 shows the point lateral brace force versus the Load Proportionality Factor for this case. From Fig. 4.15 it can be observed that a lateral brace strength requirement of 1 % of P is sufficient to develop member strength very close to the test limit load.



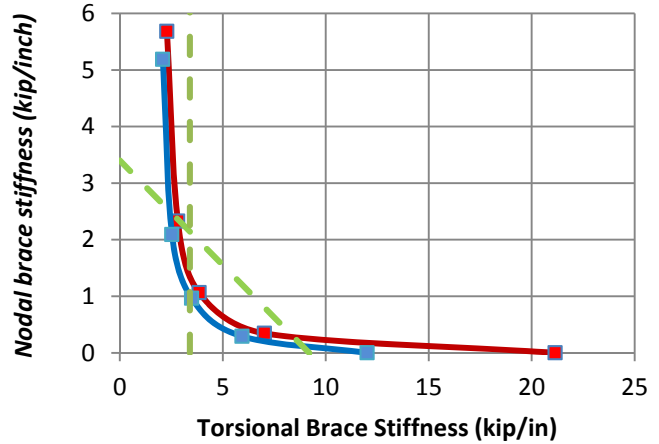
a) 5 ft unbraced length (Positive bending)



b) 5 ft unbraced length (Negative bending)



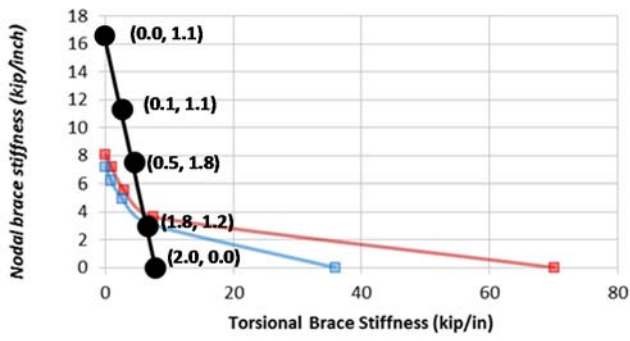
c) 15 ft unbraced length (Positive bending)



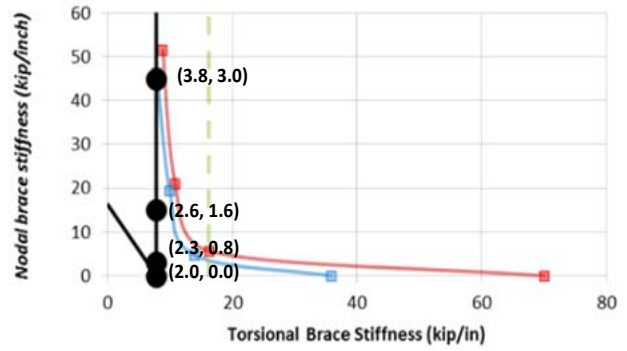
d) 15 ft unbraced length (Negative bending)

- Simulation-based stiffness interaction corresponding to 98 % of rigidly-braced strength
- Simulation-based stiffness interaction corresponding to 96 % of rigidly-braced strength
- - -■- - - Recommended design approximation

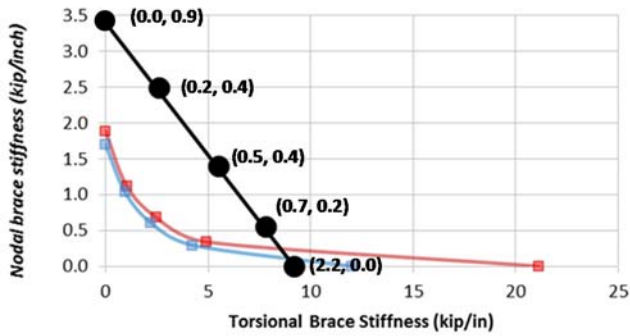
Figure 4.12. Point (nodal) lateral and point torsional bracing stiffness interactions for Moment Gradient 2, centroidal loading and $n = 1$ ($B_MG2*c_CNTB_n1^*$).



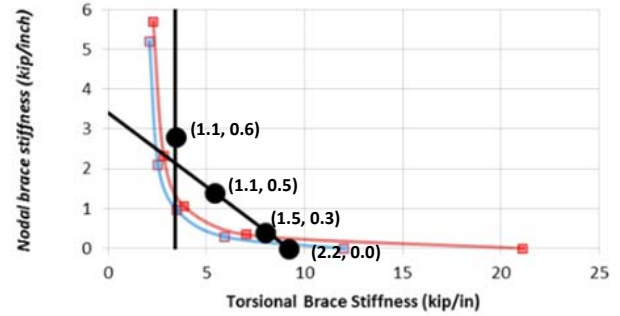
a) 5 ft unbraced length (Positive bending)



b) 5 ft unbraced length (Negative bending)



c) 15 ft unbraced length (Positive bending)



d) 15 ft unbraced length (Negative bending)

- Simulation-based stiffness interaction corresponding to 98 % of rigidly-braced strength
- Simulation-based stiffness interaction corresponding to 96 % of rigidly-braced strength
- Recommended design approximation

Figure 4.13. Brace forces corresponding to different combinations of point (nodal) lateral and point torsional bracing stiffnesses used in the interaction plots for Moment Gradient 2 loading and $n = 1$ ($B_MG2*c_CNTB_n1^*$) in Fig. 4.11.

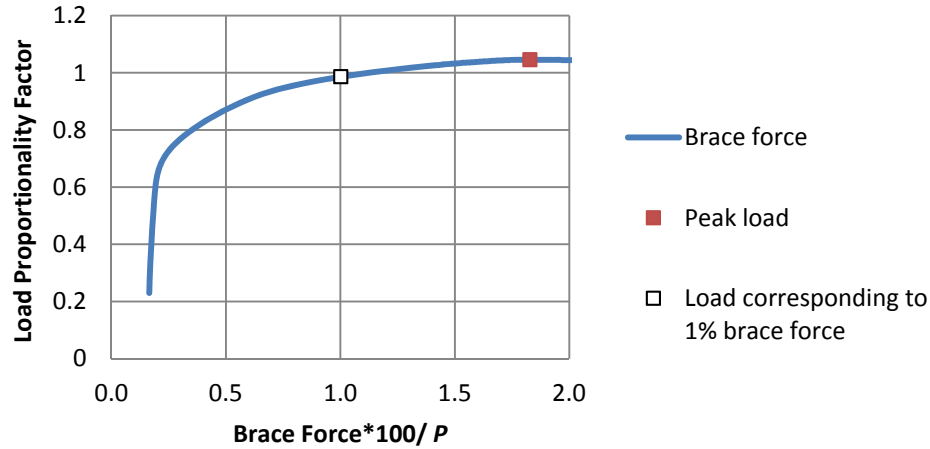


Figure 4.14. Point lateral brace force vs. the Load Proportionality Factor for the case in Fig. 4.13a (B_MG2pc_CNTB_n1_Lb5_TLBSR1) where the lateral brace force at peak load is 1.8 % of P .

Similarly, Fig. 4.16 shows the torsional brace force versus the Load Proportionality Factor for this case. From Fig. 4.16 it can be observed that a torsional brace strength requirement of 2 % is sufficient to develop member strength very close to the test limit load. Combining the more critical result in Fig. 4.15 with the knuckle curve for this critical case from Fig. 4.13b (see Fig. A.11c), it can be observed that 94 % of the beam’s rigidly-braced strength is developed when the point lateral brace force reaches $0.01M/h_o$ in this problem.

Based on the results from Figs. 4.5 through 4.8, Figs. 4.12 and 4.13, and the results for uniform bending from Prado and White (2015), the following recommendations can be made for the bracing stiffness requirements for beams with combined lateral and torsional bracing. When the lateral bracing is on the flange subjected to flexural compression (i.e., positive bending), the provided lateral and torsional bracing stiffnesses should satisfy the requirement

$$\frac{\beta_T}{\beta_{To}} + \frac{\beta_L}{\beta_{Lo}} \geq 1.0 \quad (4-8)$$

where:

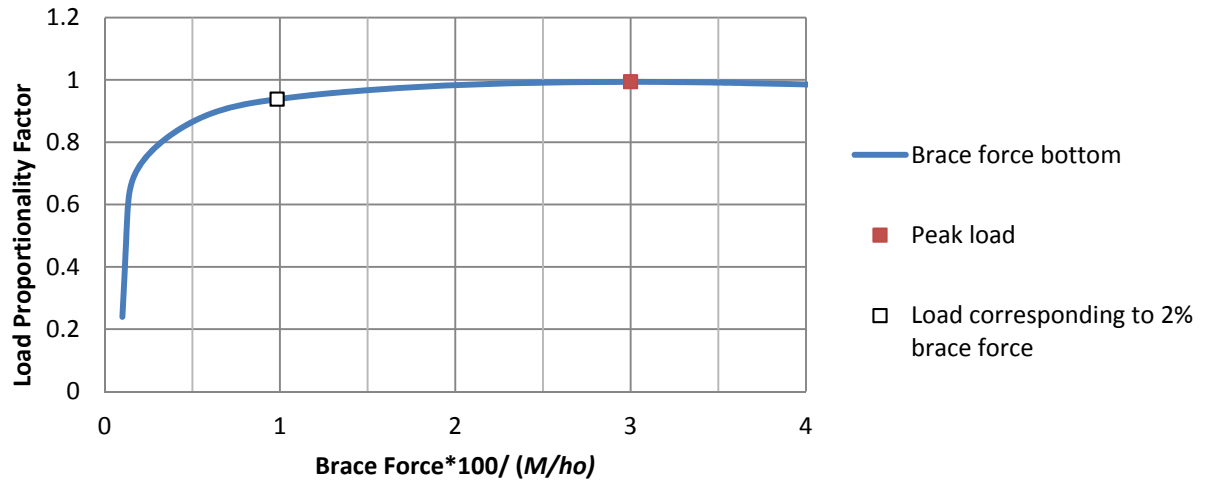


Figure 4.15. Point lateral brace force vs. the Load Proportionality Factor for the critical case in Fig. 4.13b (B_MG2nc_CNTB_n1_Lb5_TLBSR0.33) where the lateral brace force is 3.0 % of P and the torsional brace moment is 3.8 % of M at the peak load.

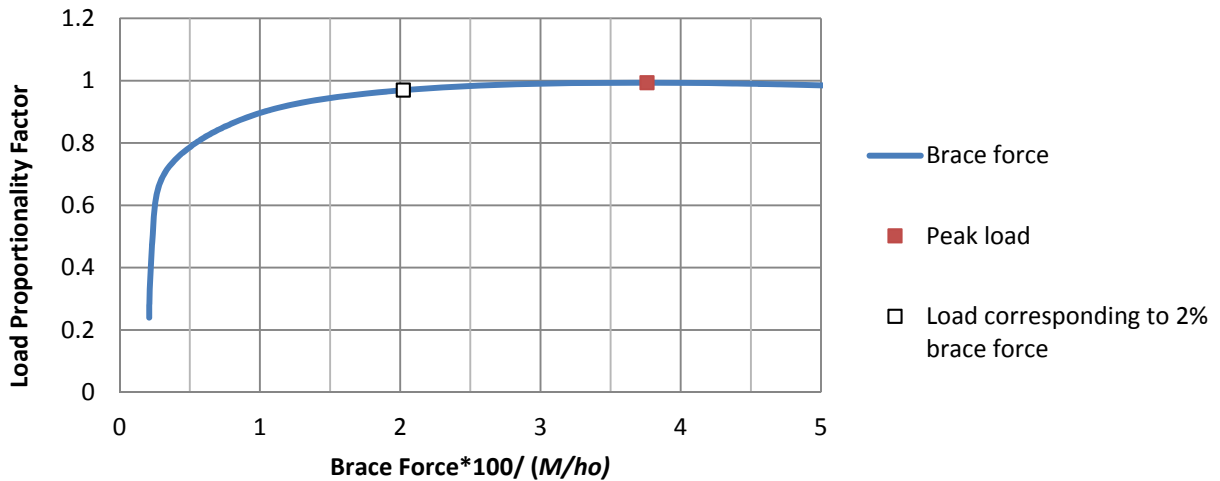


Figure 4.16. Point torsional brace force vs. the Load Proportionality Factor for the critical case in Fig. 4.13b (B_MG2nc_CNTB_n1_Lb5_TLBSR0.33) where the lateral brace force is 3.0 % of P and the torsional brace force is 3.8 % of M at the peak load.

β_L = Provided lateral bracing stiffness.

β_T = Provided torsional bracing stiffness.

β_{Lo} = Base required lateral bracing stiffness for full bracing per the AISC 360-10 Appendix 6 (AISC 2010a) rules, assuming the member is laterally braced only, including the refinements specified in the Appendix 6 Commentary, i.e., Eq. (4-1).

β_{To} = Base required torsional bracing stiffness for full bracing per the AISC 360-10 Appendix 6 (AISC 2010a) rules, assuming the member is torsionally braced only, including the refinements specified in the Appendix 6 Commentary. When expressed as a rotational stiffness, i.e., the torsional brace moment divided by the twist rotation at the torsional brace location, this stiffness is given by Eq. (4-5) times h_o^2 . When expressed as an equivalent shear panel or relative brace in the vertical direction between the two flanges, this stiffness is given directly by Eq. (4-5).

When the lateral bracing is on the flange subjected to flexural tension (i.e., negative bending), the provided lateral and torsional bracing stiffnesses should satisfy the above interaction Eq. (4-8). In addition, for cases with negative bending the following requirement should be satisfied,

- i) For cases where β_{To} , expressed as a rotational stiffness, is greater than h_o^2 times the point (nodal) lateral bracing stiffness requirement per AISC, the required torsional brace stiffness (β_T) should be greater than or equal to h_o^2 times the point (nodal) lateral bracing stiffness requirement per AISC, i.e., β_{brL} from Eq. (4-1).
- ii) For cases where β_{To} , expressed as a rotational stiffness, is smaller than h_o^2 times the point (nodal) lateral bracing stiffness requirement per AISC, the required torsional brace stiffness (β_T) should be greater than or equal to β_{To} .

AISC Appendix 6 Eqs. (4-2) and (4-3) should be employed to estimate the lateral brace strength requirements and the recommendation from Prado and White (2015) of $0.02M$ should be employed for the torsional brace strength requirement for combined lateral and torsional bracing. The

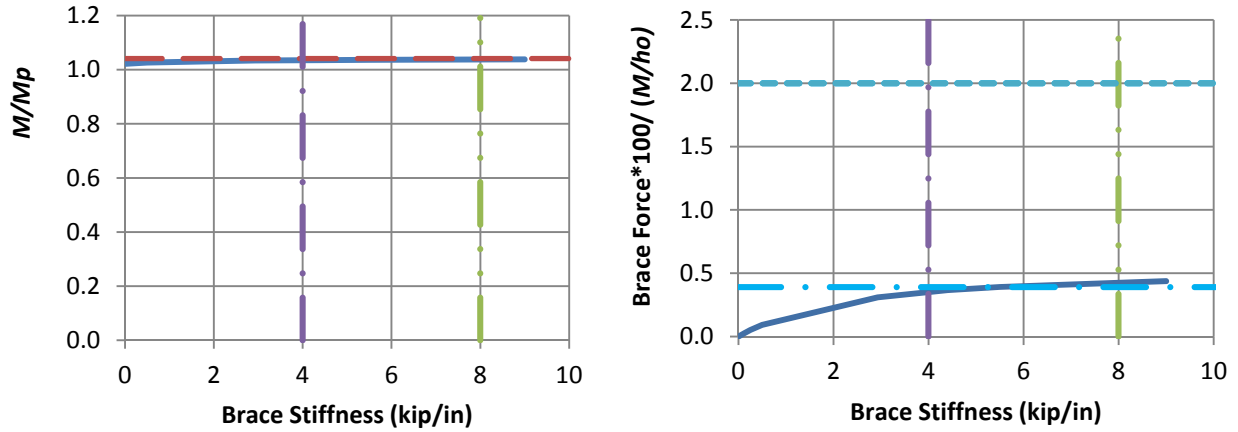
variation in the strength requirements with different combinations of bracing stiffness is nonlinear in general, with a large number of combined bracing cases showing strength requirements on the individual components comparable to the recommended values for torsional and lateral bracing alone. For this reason, as well as for the reason that the recommended individual component stability bracing force values are already relatively small, it is suggested that no interaction effects be considered in calculating the combined bracing strength requirements. The behavior of the combined bracing cases under the additional Moment Gradient 3 loading is discussed in the next section.

4.5.6 Beams with Moment Gradient 3 Loading

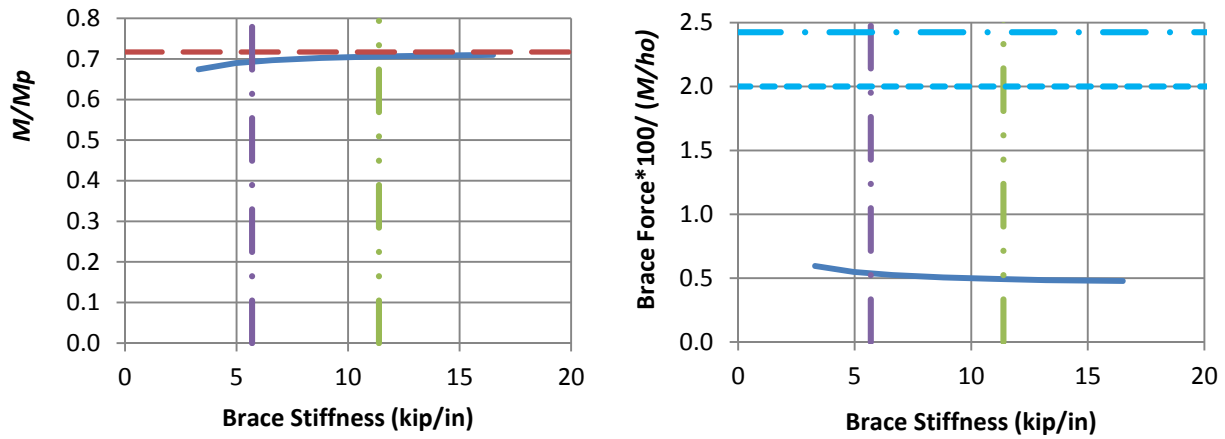
The results for beam Moment Gradient 3 loading are discussed in the following subsections.

a) Torsional bracing only

Figure 4.17 shows the knuckle curve and brace force versus brace stiffness plots for beams with torsional bracing and Moment Gradient 3 loading. From the knuckle curve in Fig 4.17a it can be observed that because of the moment gradient effect (large C_b factor), this member is able to reach the plateau strength even when the bracing stiffness is zero (i.e., unbraced length of 10 ft). From the knuckle curve in Fig. 4.17b, the β_{brT} value from AISC Appendix 6 Eq. (4-5) is 2.32 times the brace stiffness required to reach 96 % of the simulation rigidly-braced strength. Thus Eq. (4-5) gives a conservative estimate of the stiffness required to reach 96 % of the rigidly-braced strength for beams with Moment Gradient 3 loading and torsional bracing.



a) B_MG3_TB_n1_Lb5



b) B_MG3_TB_n1_Lb15

- Test simulation results
- AISC ideal full bracing stiffness
- $\beta_{brT} = 2x$ AISC ideal full bracing stiffness
- Base AISC Required Strength corresponding to $\beta = \beta_{brT}$
- - - Recommended required strength of 2 %
- - - Rigidly-braced strength

Figure 4.17. Beam knuckle curves and brace force vs. brace stiffness plots for point torsional bracing cases with $n = 1$ and Moment Gradient 3 loading.

The brace force versus brace stiffness curves in Fig. 4.17 show that the current AISC Eq. (4-6) substantially overestimates the strength requirements for the long unbraced length ($L_b = 15$ ft) case, where the response is more dominated by elastic stability effects. This is consistent with the findings by Prado and White (2015). However, Eq. (4-6) gives an accurate prediction of the required torsional bracing moment at $\beta_T = \beta_{brT}$ for the short unbraced length ($L_b = 5$ ft) case. The basic torsional bracing strength requirement of $0.02M$ recommended by Prado and White (2015) is substantially conservative relative to the test simulation results in both of the above problems.

b) Combined point (nodal) lateral and point torsional bracing

Figure 4.18 shows the bracing stiffness interaction plot for beams with combined point lateral and torsional bracing and Moment Gradient 3 loading. From this figure, it can be inferred that when bracing is located at an inflection point, providing a torsional brace at this location is sufficient and that no significant benefit is gained in terms of reducing the torsional bracing stiffness requirement by providing an additional nodal lateral brace at this position. In fact, it can be observed that as lateral bracing stiffness is increased to a large value, the torsional bracing stiffness requirement does not go to zero. This is related to the AISC Appendix 6 requirement that, if only lateral bracing is provided near an inflection point, both flanges must be laterally braced. It is also related to the behavior observed in the previous sections for negative bending moment. The unbraced length on one side of the brace point is subjected to negative bending for the case of the Moment Gradient 3 loading. Based on the plot in Fig. 4.18, it is recommended that for beams subjected to reverse curvature bending, the combined lateral and torsional bracing should be designed using the recommendations for negative bending, which are summarized at the end of Section 4.5.5.

Figure 4.19 shows the knuckle curves and brace force versus brace stiffness plots corresponding to the combined bracing cases in Fig. 4.18. No bracing stiffness interaction plot is provided corresponding to the knuckle curves for the 5 ft unbraced length because, similar to the behavior in Fig. 4.17a, the member is able to reach the plateau strength even when the bracing stiffness is zero (i.e., unbraced length of 10 ft) due to the moment gradient effect (large C_b factor).

Figure 4.20 shows the brace forces corresponding to different combinations of lateral and torsional bracing stiffnesses used in the interaction plot in Fig. 4.18. In Fig. 4.20 the first tuple value is the torsional brace force, and the second term is the lateral brace force. It can be observed from Fig. 4.20 that for all the combinations of lateral and torsional bracing considered, the brace forces are well within the brace strength requirements given by the AISC Appendix 6 equations. In fact, the lateral brace force is practically zero in all of these cases.

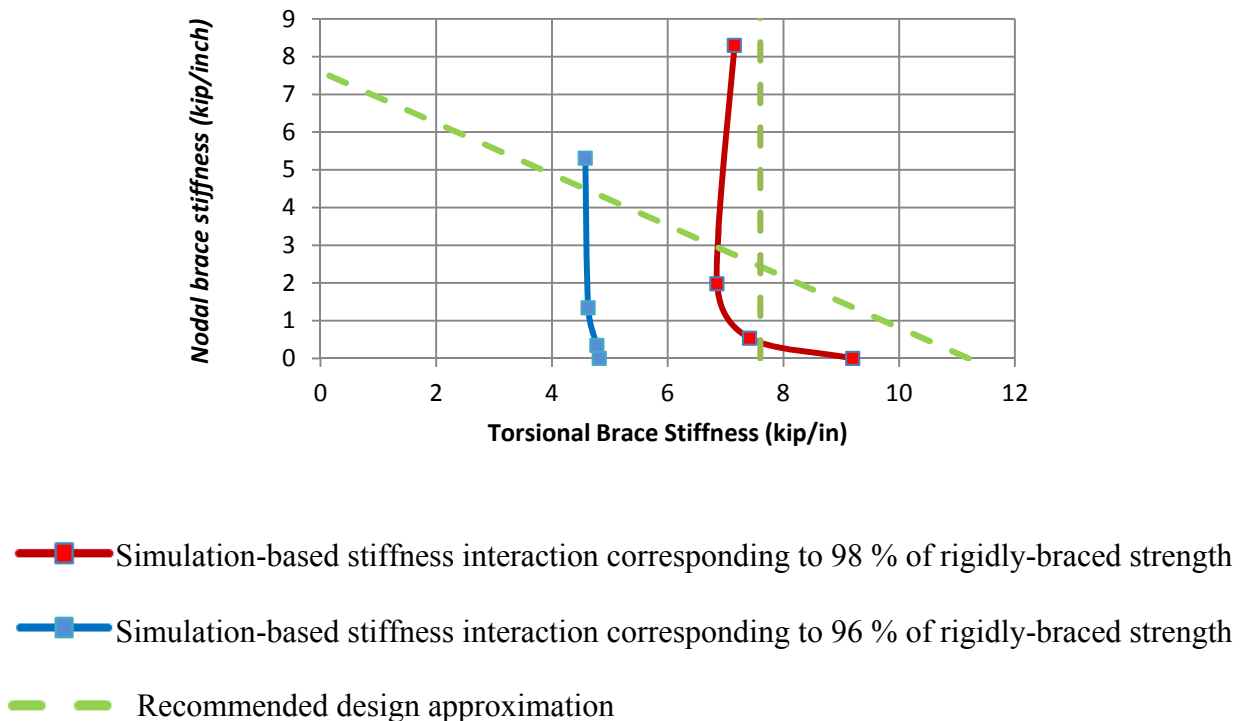
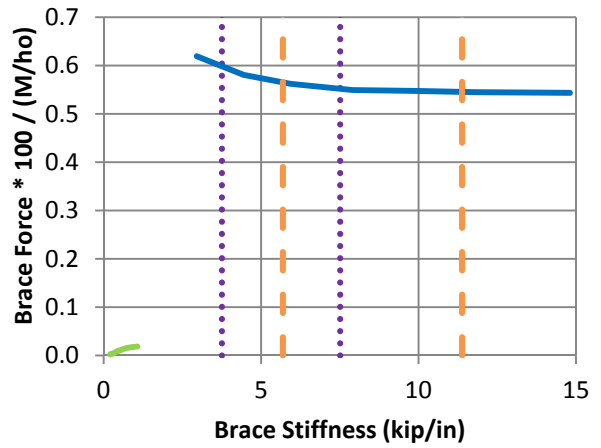
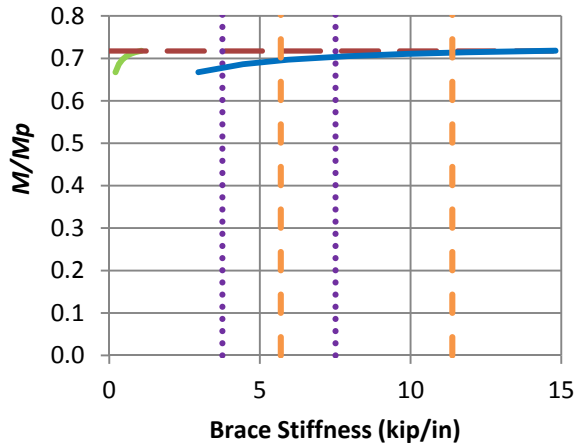
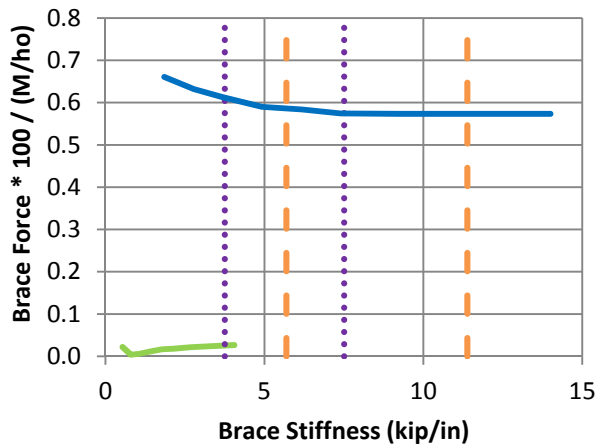
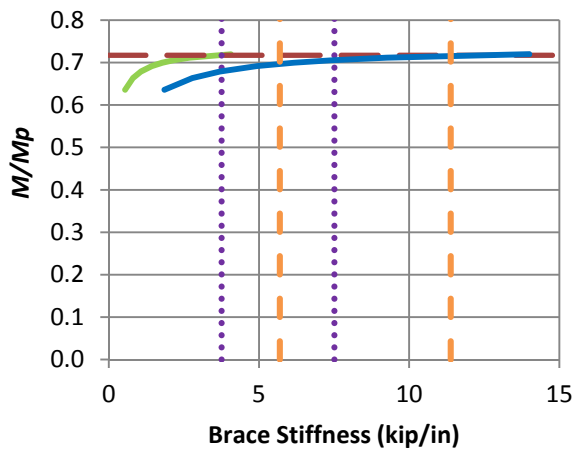


Figure 4.18. Point (nodal) lateral and point torsional bracing stiffness interaction for Moment Gradient 3 loading, $n = 1$ and $L_b = 15$ ft (B_MG3_CNTB_n1_Lb15*).



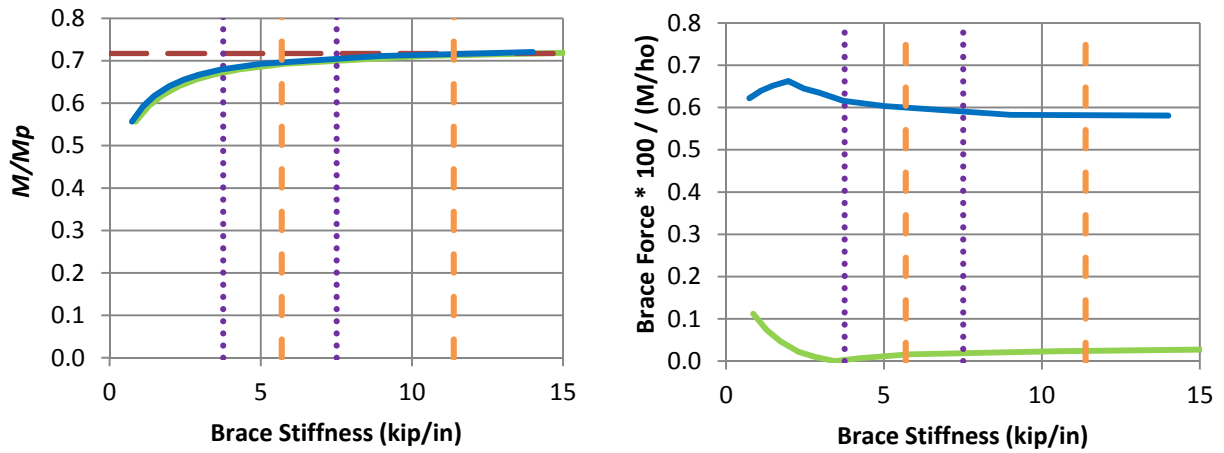
a) B_MG3_CNTB_n1_Lb15_TLBSR4



b) B_MG3_CNTB_n1_Lb15_TLBSR1

- Rigidly-braced strength
- Test simulation results corresponding to torsional brace
- Test simulation results corresponding to lateral brace
- β_{brL} and $0.5\beta_{brL}$ for point lateral bracing
- β_{brT} and $0.5\beta_{brT}$ for point torsional bracing

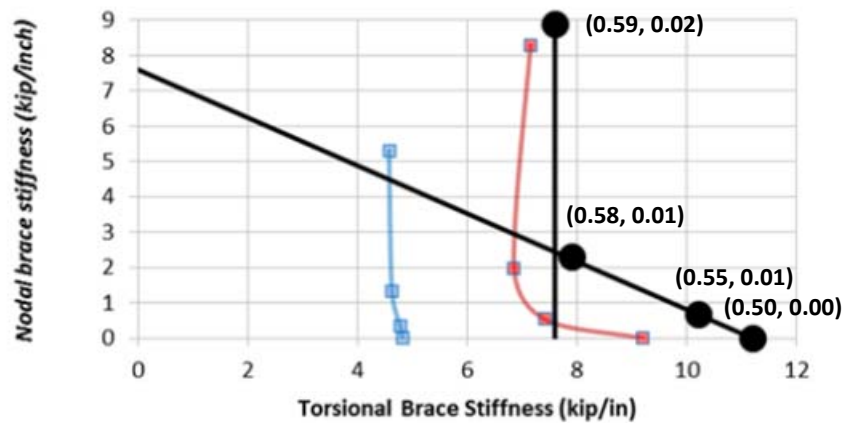
Figure 4.19. Beam knuckle curves and brace force vs. brace stiffness plots for combined point (nodal) lateral and point torsional bracing cases with $n = 1$, Moment Gradient 3 loading and $L_b = 15$ ft.



c) B_MG3_CNTB_n1_Lb15_TLBSR0.25

- Rigidly-braced strength
- Test simulation results corresponding to torsional brace
- Test simulation results corresponding to lateral brace
- β_{brL} and $0.5\beta_{brL}$ for point lateral bracing
- β_{brT} and $0.5\beta_{brT}$ for point torsional bracing

Fig. 4.19 (continued). Beam knuckle curves and brace force vs. brace stiffness plots for combined point (nodal) lateral and point torsional bracing cases with $n = 1$, Moment Gradient 3 loading and $L_b = 15$ ft.



- Simulation-based stiffness interaction corresponding to 98 % of rigidly-braced strength
- Simulation-based stiffness interaction corresponding to 96 % of rigidly-braced strength
- Recommended design approximation

Figure 4.20. Brace forces corresponding to different combinations of point (nodal) lateral and point torsional bracing stiffnesses used in the Fig. 4.18 interaction plots for Moment Gradient 3 loading and $n = 1$ (B_MG3_CNTB_n1_Lb15*).

c) Combined shear panel (relative) lateral and torsional bracing

Figure 4.21 shows the bracing stiffness interaction plot for beams with combined shear panel (relative) lateral and torsional bracing and Moment Gradient 3 loading. Figure 4.22 shows the knuckle curves and brace force versus brace stiffness plots corresponding to each of the combined bracing data points in Fig. 4.21.-Figure 4.23 shows the brace forces corresponding to different combinations of lateral and torsional bracing stiffnesses used in the interaction plot in Fig. 4.21. In Fig. 4.23 the first tuple value is the torsional brace force, and the second term is the lateral brace force.

It can be observed that the recommended design approximations provide a conservative estimate of the required torsional bracing stiffness as the lateral bracing stiffness is increased to a large value. As one might expect for some situations, depending on the nature of the problem, the lateral bracing on one of the flanges at the inflection point does provide some benefit, and there is a finite lateral bracing stiffness level that is sufficient to develop 96 % of the rigidly-braced strength without any torsional bracing. In this case, this shear panel stiffness value to satisfy this requirement is 4.1 kip/in. However, generally speaking, from the interaction plots in Figs. 4.18 and 4.20 it can be concluded that for beams subjected to reverse curvature bending, the combined lateral and torsional bracing should be designed using the recommendations for negative bending, which are summarized at the end of Section 4.5.5. It can be observed from Fig. 4.23 that for the combinations of lateral and torsional bracing, the brace forces are within the predicted brace strength limits. Very slightly less than 96 % of the beam’s rigidly-braced strength is developed in the limit that the shear panel brace stiffness approaches zero in Fig. 4.23.

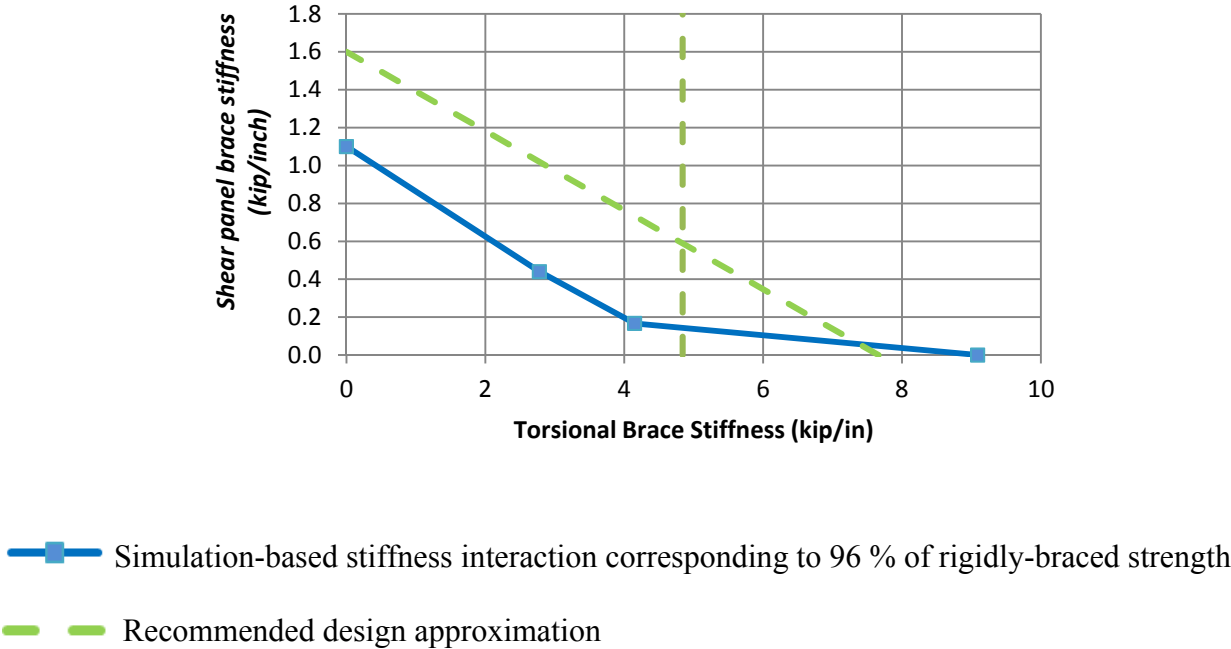
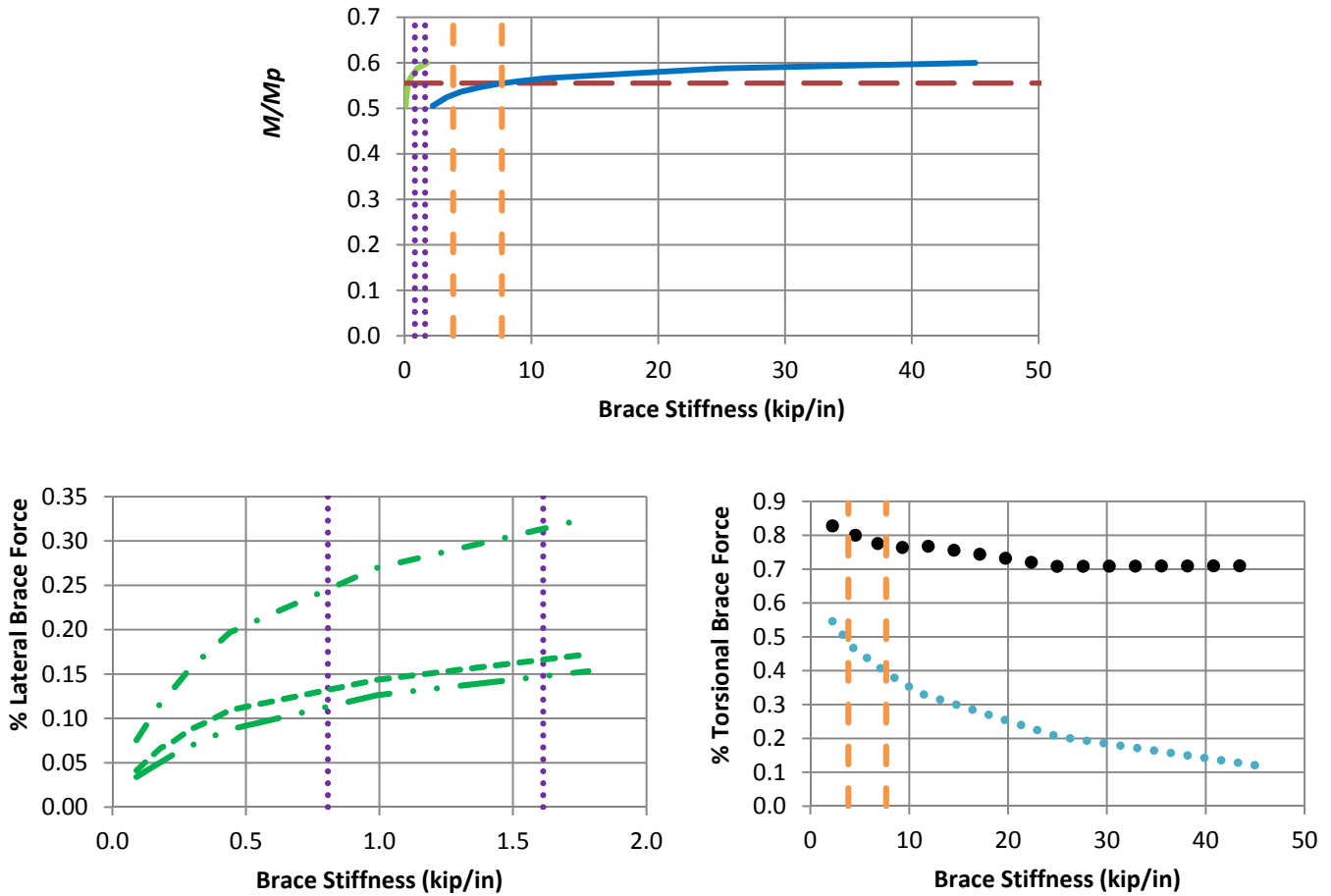


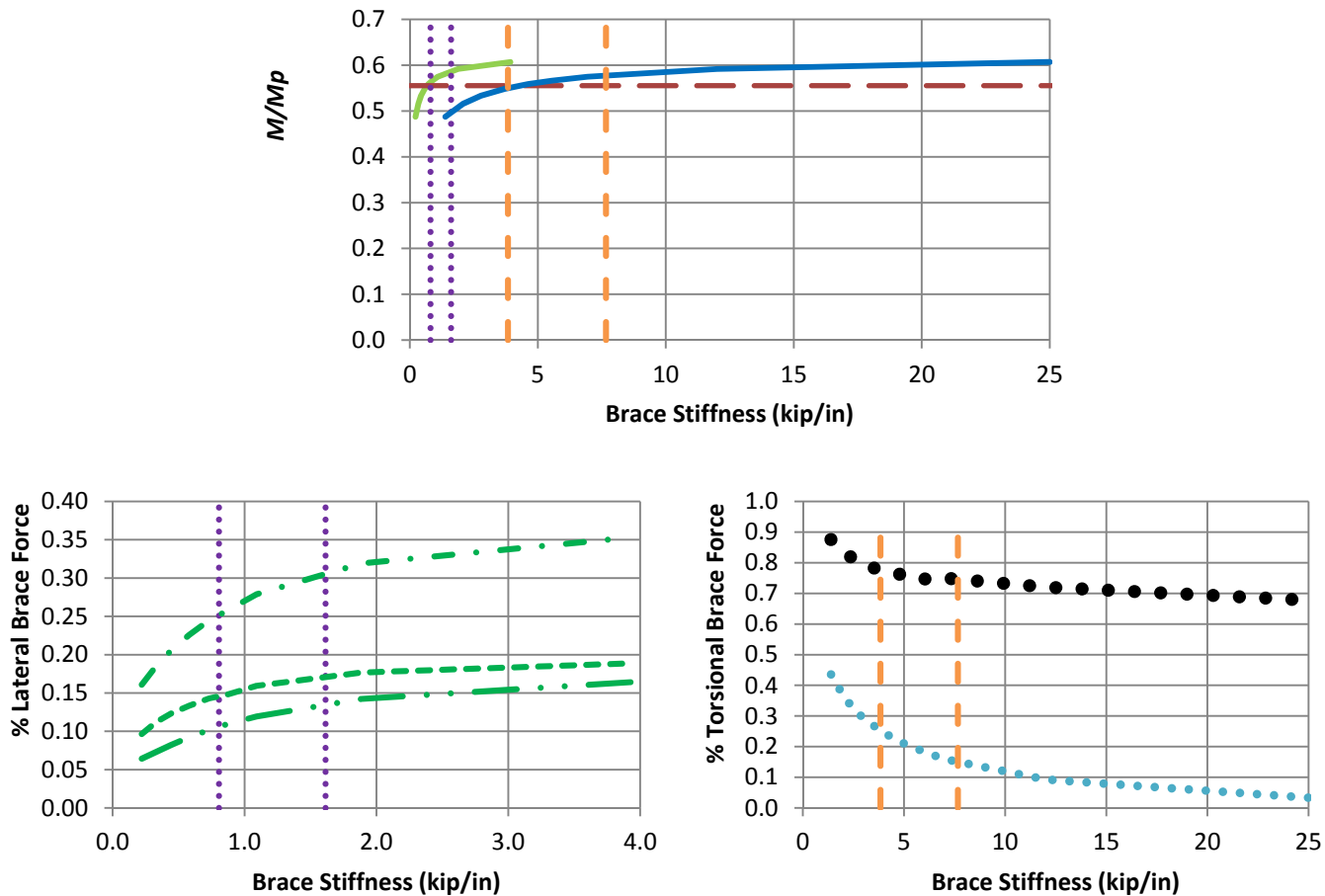
Figure 4.21. Shear panel (relative) lateral and point torsional bracing stiffness interaction for Moment Gradient 3 loading, $n = 2$ and $L_b = 15$ ft (B_MG3_CRTB_n2_Lb15*).



a) B_MG3_CRTB_n2_Lb15_TLBSR4

- Rigidly-braced strength
- Test simulation results corresponding to torsional brace
- Test simulation results corresponding to lateral brace
- β_{brL} and $0.5\beta_{brL}$ for point lateral bracing
- β_{brT} and $0.5\beta_{brT}$ for point torsional bracing
- Left end panel shear force
- Right end panel shear force
- Middle panel shear force
- Torsional brace force 1
- Torsional brace force 2

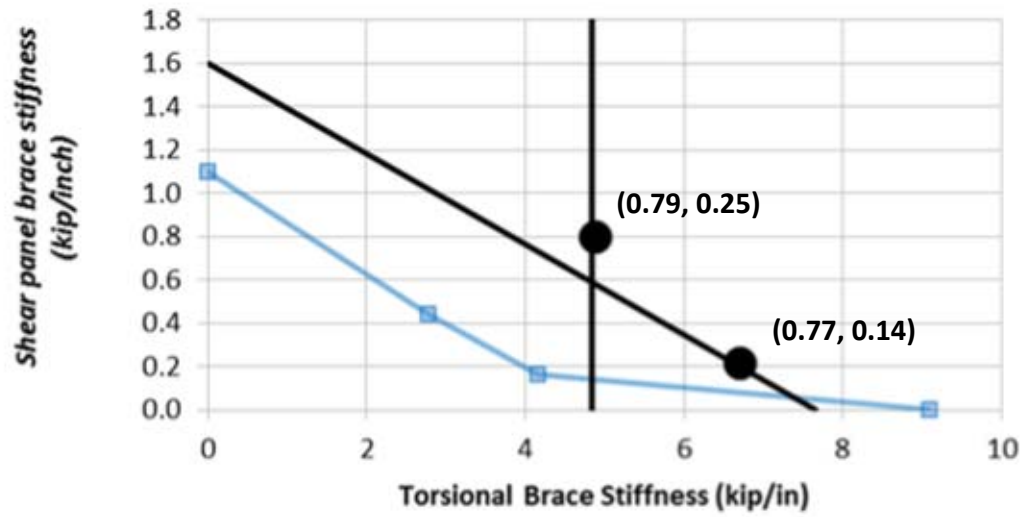
Figure 4.22. Beam knuckle curves and brace force vs. brace stiffness plots for combined shear panel (relative) lateral and point torsional bracing cases with $n = 2$, Moment Gradient 3 loading and $L_b = 15$ ft.



b) B_MG3_CRTB_n2_Lb15_TLBSR1

- Rigidly-braced strength
- Test simulation results corresponding to torsional brace
- Test simulation results corresponding to lateral brace
- β_{brL} and $0.5\beta_{brL}$ for point lateral bracing
- β_{brT} and $0.5\beta_{brT}$ for point torsional bracing
- Left end panel shear force
- Right end panel shear force
- Middle panel shear force
- Torsional brace force 1
- Torsional brace force 2

Fig. 4.22 (continued). Beam knuckle curves and brace force vs. brace stiffness plots for combined shear panel (relative) lateral and point torsional bracing cases with $n = 2$, Moment Gradient 3 loading and $L_b = 15$ ft.



- Simulation-based stiffness interaction corresponding to 96 % of rigidly-braced strength
- Recommended design approximation

Figure 4.23. Brace forces corresponding to different combinations of shear panel (relative) lateral and point torsional bracing stiffnesses used in the Fig. 4.21 interaction plots for Moment Gradient 3 loading and $n = 2$ (B_MG3_CRTB_n2_Lb15*).

CHAPTER 5 BEAMS WITH TOP FLANGE LOADING

5.1 Overview

This chapter addresses the second major objective of this research, evaluation of the bracing of beams subjected to an intermediate transverse load applied at the top flange, thus causing an additional destabilizing effect. Section 5.2 gives details of the cases considered. Section 5.3 presents the test simulation results.

5.2 Detailed Study Design

The cases considered in this research, to study the influence of the height of an intermediate transverse load, are listed below. The corresponding cases summarized in Section 4.2 for the Moment Gradient 2 loading involve transverse concentrated load applied at the centroidal axis of the members. The following cases involve a transverse concentrated load applied at the top flange level of the mid-span cross-section, Moment Gradient 2 loading.

- Positive moment loading, basic bracing types:

B_MG2pt_NB_n1_Lb5
B_MG2pt_NB_n1_Lb15
B_MG2pt_TB_n1_Lb5
B_MG2pt_TB_n1_Lb15

- Positive moment loading, combined point (nodal) lateral and point torsional bracing:

B_MG2pt_CNTB_n1_Lb5_TLBSR4
B_MG2pt_CNTB_n1_Lb5_TLBSR1
B_MG2pt_CNTB_n1_Lb5_TLBSR0.25
B_MG2pt_CNTB_n1_Lb15_TLBSR4
B_MG2pt_CNTB_n1_Lb15_TLBSR1
B_MG2pt_CNTB_n1_Lb15_TLBSR0.25

- Negative moment loading, combined point (nodal) lateral and point torsional bracing:

B_MG2nt_CNTB_n1_Lb5_TLBSR5.67
B_MG2nt_CNTB_n1_Lb5_TLBSR1
B_MG2nt_CNTB_n1_Lb5_TLBSR0.33
B_MG2nt_CNTB_n1_Lb5_TLBSR0.11
B_MG2nt_CNTB_n1_Lb15_TLBSR5.67
B_MGnt_CNTB_n1_Lb15_TLBSR1
B_MG2nt_CNTB_n1_Lb15_TLBSR0.33
B_MG2nt_CNTB_n1_Lb15_TLBSR0.11

5.3 Results

The results for beams with intermediate transverse load applied at centroid of the mid-span cross section are discussed in Section 4.5. The knuckle curves and brace force - brace stiffness curves for beams with intermediate transverse load applied at top flange level of the mid-span cross section are shown in Figs. 5.1 through 5.2.

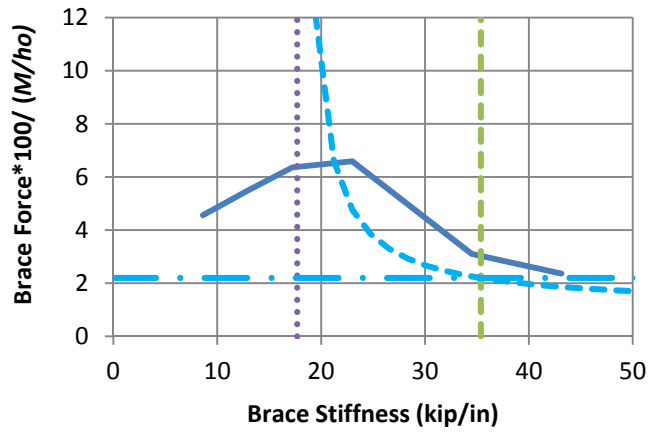
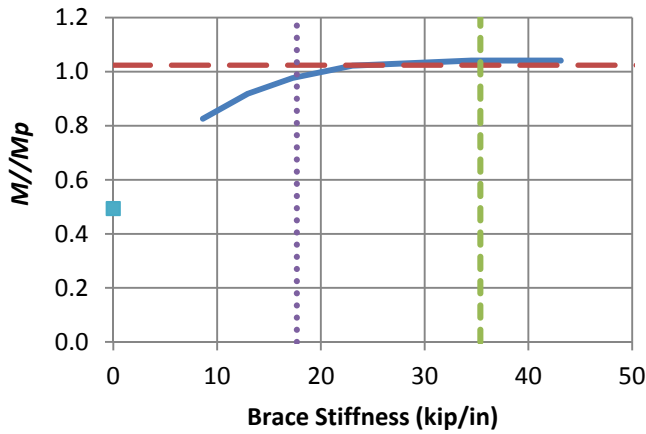
Equations (4-1) through (4-3) include a C_{tL} factor to account for the impact of transverse load height on the bracing stiffness and strength requirements. This factor is equal to 1.0 for centroidal loading is equal to 2.2 for top flange loading when $n = 1$, as explained in Section 4.4. Similarly, Eq. (4-5) has a C_{tT} factor that accounts for transverse load height effects on torsional bracing. This factor is equal to 1.2 for top flange loading, as explained in Section 4.4. The ANSI/AISC 360-10

torsional bracing strength requirement indicated by Eq. (4-6) is impacted by the C_{IT} via its inclusion of the torsional bracing β_{brT} . The AISC full bracing stiffness and strength requirements shown in Figs. 5.1 to 5.3 include the impact of the above C_{IL} and C_{IT} values.

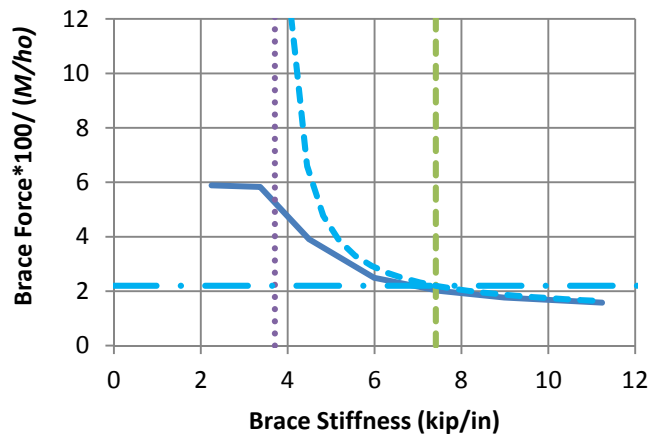
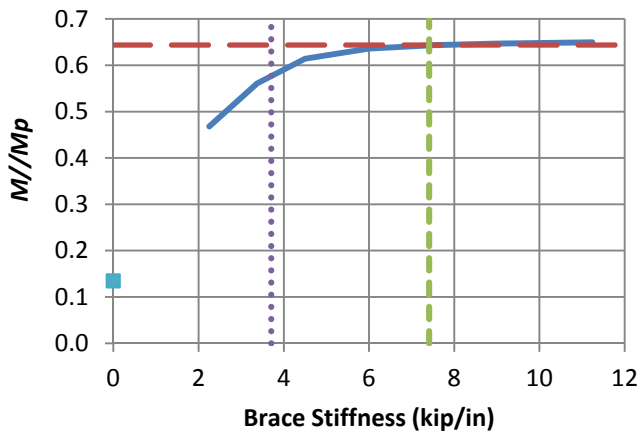
Table 5.1 compares the bracing stiffness values β_{F98} and β_{F96} from Figs. 5.1 and 5.2 to the corresponding estimates from the AISC bracing equations presented in Section 4.4 for the basic point lateral and point torsional bracing cases. It also summarizes the maximum brace forces at the beam limit load when $\beta_L = \beta_{brL}$ or $\beta_T = \beta_{brT}$. Since the β_{F96}/β_{br} values in Table 5.1 are approximately equal to the corresponding values in Table 4.6, it can be concluded that the C_{IL} and C_{IT} factors do a good job of estimating the impact of transverse load height on the bracing stiffness requirements.

From Figs. 4.9 and 5.1, one can observe that the C_{IL} factor does not fully account for the impact of the load height on the bracing strength requirements. The required brace strength corresponding to a brace stiffness of β_{br} in Fig. 5.1 versus the comparable value in Fig 4.9 is 2.73 (3.0/1.1) for the case with 5 ft unbraced length, and it is 2.5 (2.0/0.8) for the case with 15 ft unbraced length, instead of the C_{IL} value of 2.2. However, the AISC C_{IL} value may be accepted as a reasonable approximation of the test simulation values. Furthermore, it is important to note that both the AISC Specification (AISC 2010a) equations as well as the test simulation models do not account for the benefits of tipping restraint from the applied loading. In many physical situations, the load is applied through secondary members or a slab or deck. This loading condition commonly provides a beneficial tipping restraint effect. Additional discussion of tipping restraint effects is provided by Yura (2001).

It can be observed from Fig. 5.1a and Table 5.1 that the maximum brace force as a percentage of M/h_o is larger than the base requirement of $0.01C_{IL} = 0.022$ also for the point lateral bracing case with $L_b = 5$ ft. The same arguments posed above regarding the underestimate of the brace stiffness requirement for this case can also be applied to this overestimate of the point lateral brace strength requirement.



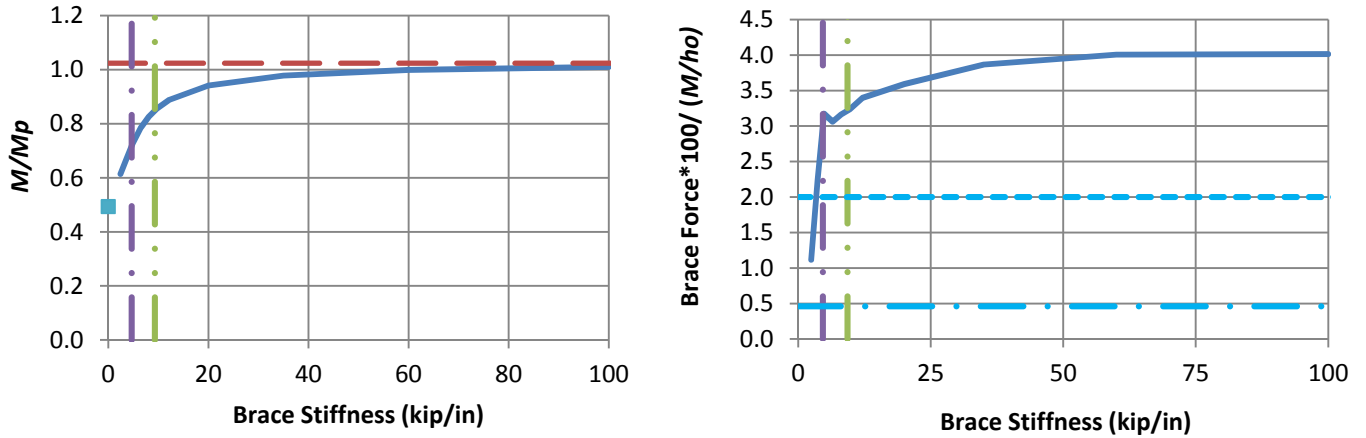
a) B_MG2pt_NB_n1_Lb5



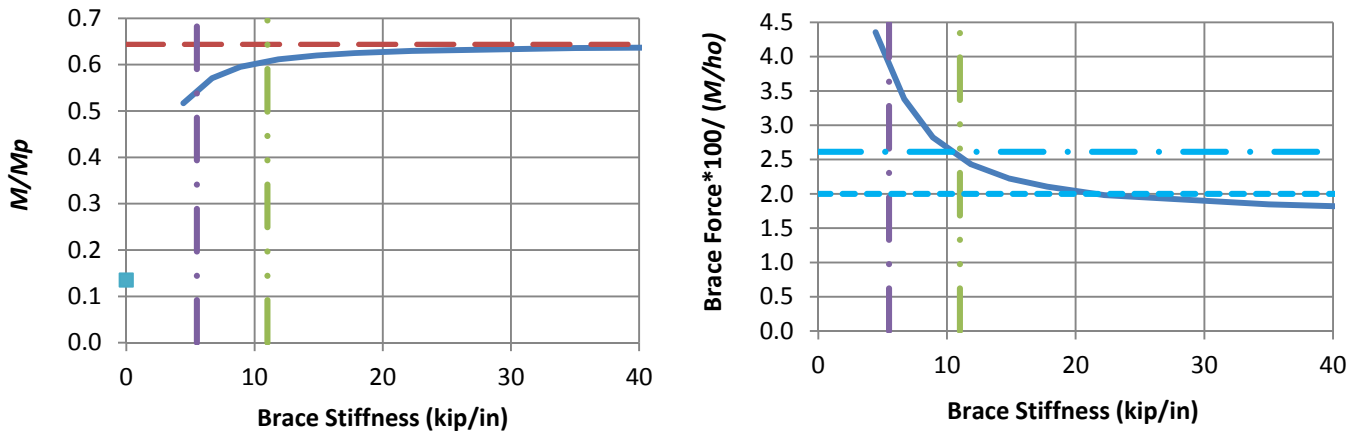
b) B_MG2pt_NB_n1_Lb15

- Test simulation results
- - Rigidly-braced strength
- ⋯ AISC ideal full bracing stiffness
- - $\beta_{brL} = 2x$ AISC ideal full bracing stiffness
- Test simulation strength at zero brace stiffness
- · Base AISC Required Strength Corresponding to $\beta_L = \beta_{brL}$
- - · Refined estimate of required strength using Eqs. (4-1) and (4-4)

Figure 5.1. Beam knuckle curves and brace force vs. brace stiffness plots for point (nodal) lateral bracing cases with $n = 1$, Moment Gradient 2, and top flange loading.



a) B_MG2pt_TB_n1_Lb5



b) B_MG2pt_TB_n1_Lb15

- Test simulation results
- • AISC ideal full bracing stiffness
- • $\beta_{brT} = 2x$ AISC ideal full bracing stiffness
- Test simulation strength at zero brace stiffness
- • Base AISC Required Strength corresponding to $\beta_T = \beta_{brT}$
- - - Recommended required strength of 2 %
- - - Rigidly-braced strength

Figure 5.2. Beam knuckle curves and brace force vs. brace stiffness plots for point torsional bracing cases with $n = 1$, Moment Gradient 2, and top flange loading.

Table 5.1. Comparison of β_{br} to β_{F98} and β_{F96} and summary of brace forces at $\beta = \beta_{br}$ for Moment Gradient 2 basic bracing cases involving top flange loading.

Case	β_{F98} (kip/in)	β_{F96} (kip/in)	β_{br} (kip/in)	β_{br}/β_{F96}	Brace force as a percentage of M/h_o for $\beta = \beta_{br}$
B_MG2pt_NB_n1_Lb5	20.70	18.10	35.40	1.96	3.00
B_MG2pt_NB_n1_Lb15	5.60	4.80	7.40	1.54	2.00
B_MG2pt_TB_n1_Lb5	76.40	41.20	9.20	0.22	3.20
B_MG2pt_TB_n1_Lb15	24.90	14.10	11.00	0.78	2.50

The most critical of the above cases corresponds to test B_MG2pt_TB_n1_Lb5. It can be observed from Fig. 5.2a and Table 5.1 that the torsional base strength requirement of $0.02M$ recommended by Prado and White (2015) is unconservative at $\beta_T = \beta_{brT}$ for the torsional bracing case with $L_b = 5$ ft. Furthermore, Fig. 5.3 shows the Load Proportionality Factor versus brace force plot for B_MG2pt_TB_n1_Lb5 with $\beta_T = \beta_{brT}$. (The Load Proportionality Factor is the fraction of a specified reference load that has been applied at a given stage of the structural analysis.) It can be observed that at a brace force of $0.02M$, the applied load level is very close to the limit load. Combining the results from Fig. 5.3 with the knuckle curve value at $\beta_T = \beta_{brT}$, it can be observed that only 82 % of the beam's rigidly-braced strength is developed at the brace strength limit of $0.02M$. This case is discussed further at the end of Chapter 8, Summary and Conclusions.

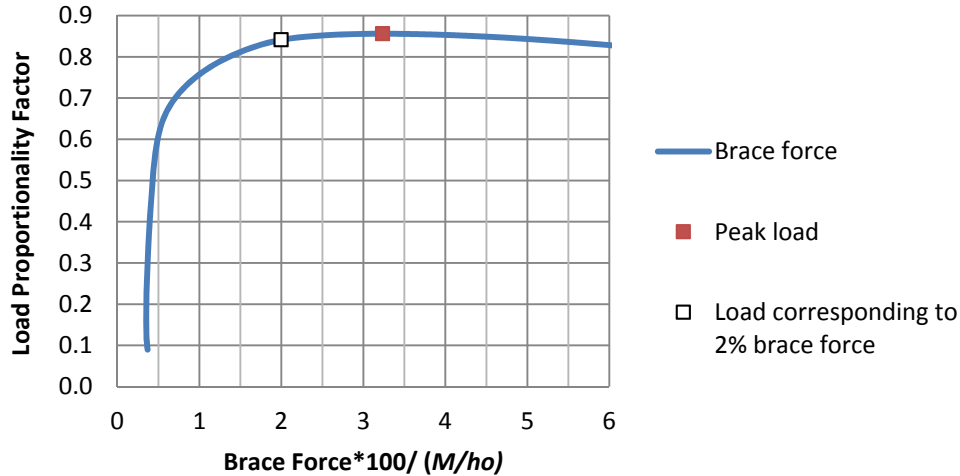
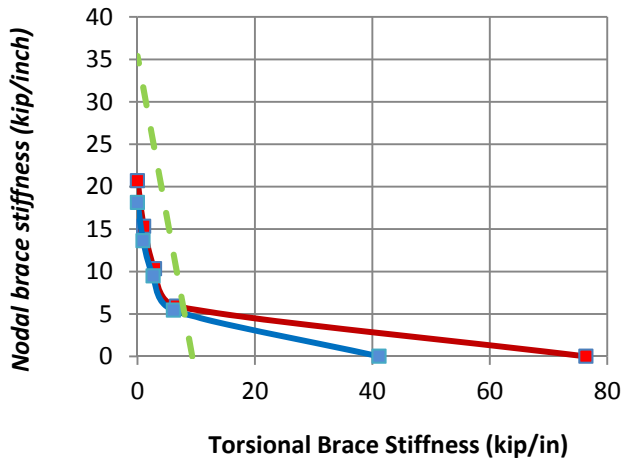


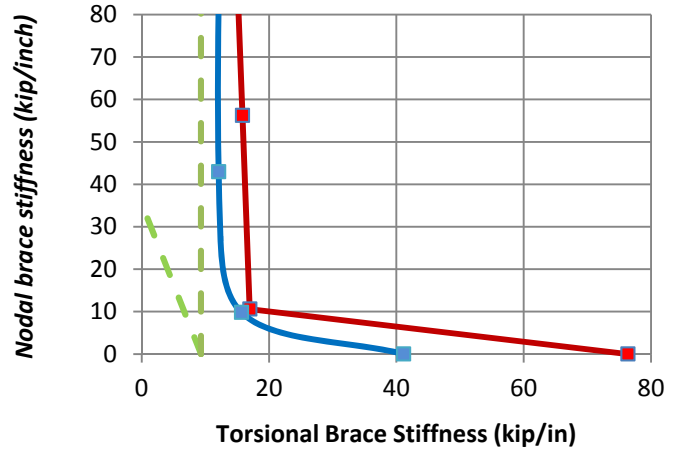
Figure 5.3. Brace force vs. the Load Proportionality Factor for B_MG2pt_TB_n1_Lb5 with $\beta_T = \beta_{brT}$.

Figures 4.11 and 5.4 show the bracing stiffness interaction plots for the combined bracing cases with centroidal transverse load and top flange transverse load respectively. The knuckle curves and brace force versus brace stiffness plots corresponding to the combined bracing data points in these interaction plots are shown in the Appendix of this report. Figure 5.5 shows the brace forces corresponding to different combinations of lateral and torsional bracing stiffnesses used in the interaction plot in Fig. 5.3. In Fig. 5.5 the first term of the tuples is the torsional brace force, and the second term is the lateral brace force.

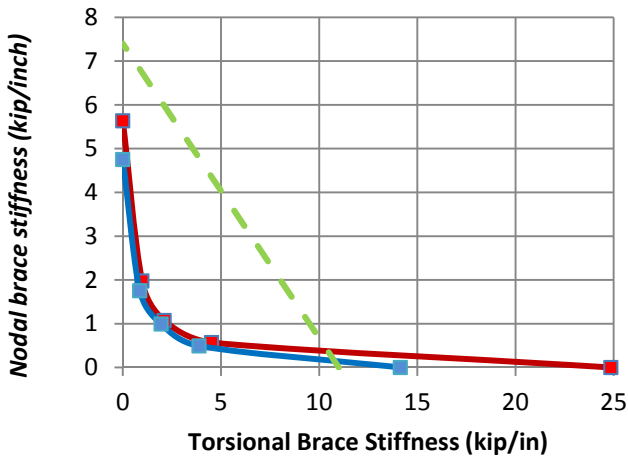
For top flange loading the required braced strengths are multiplied by factors $C_{IL} = 2.2$ and $C_{IT} = 1.2$ for lateral and torsional bracing respectively. Similar to the discussion at the end of Section 4.5.4, based on the results shown in Fig. 5.5, it can be concluded that with the exception of a few cases, the brace forces for the lateral and torsional bracing combinations are within the predicted brace strength limits. For the few cases where the brace forces exceed the predicted values, it can be shown that the brace strength requirements of 0.5 %, 1 % and 2 % for nodal lateral, shear panel lateral and torsional bracing respectively, are sufficient to develop member strength very close to the test limit load. An example case is discussed below.



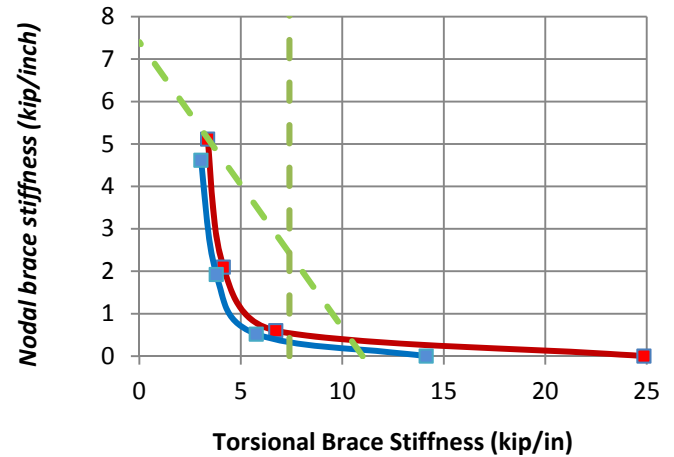
a) 5 ft unbraced length (Positive bending)



b) 5 ft unbraced length (Negative bending)



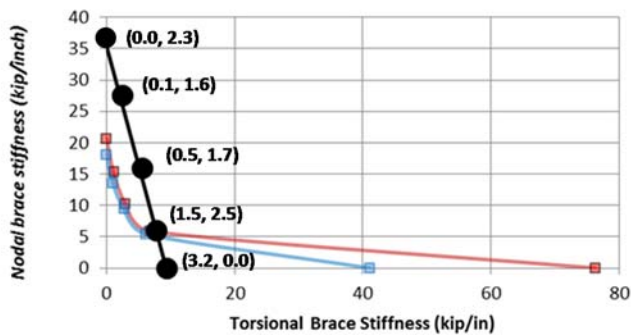
c) 15 ft unbraced length (Positive bending)



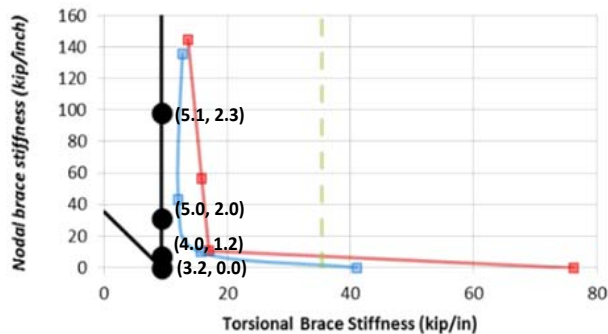
d) 15 ft unbraced length (Negative bending)

- Simulation-based stiffness interaction corresponding to 98 % of rigidly-braced strength
- Simulation-based stiffness interaction corresponding to 96 % of rigidly-braced strength
- - -■- - - Recommended design approximation

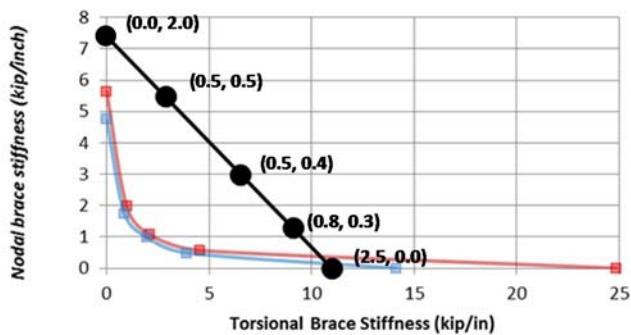
Figure 5.4. Point (nodal) lateral and point torsional bracing stiffness interactions for Moment Gradient 2, top flange loading and $n = 1$ (B_MG2pt_CNTB_n1*).



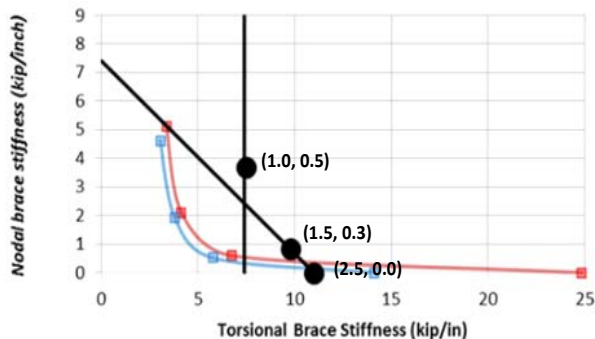
a) 5 ft unbraced length (Positive bending)



b) 5 ft unbraced length (Negative bending)



c) 15 ft unbraced length (Positive bending)



d) 15 ft unbraced length (Negative bending)

- Simulation-based stiffness interaction corresponding to 98 % of rigidly-braced strength
- Simulation-based stiffness interaction corresponding to 96 % of rigidly-braced strength
- Recommended design approximation

Figure 5.5. Brace forces corresponding to different combinations of point (nodal) lateral and point torsional bracing stiffnesses used in the interaction plots for Moment Gradient 2 loading and $n = 1$ ($B_{MG2} \cdot t_{CNTB_n1}$) in Fig. 5.3.

From Fig. 5.5b it can be observed that for one case ($\beta_T = 9.3$ kip/in and $\beta_L = 98$ kip/in) the torsional brace force is 5.1 %, which exceeds the predicted brace strength. Fig. 5.6 shows the torsional brace force versus the Load Proportionality Factor from the test simulation for this case. (As noted above, the Load Proportionality Factor is the fraction of a specified reference load that has been applied at a given stage of the structural analysis.) From Fig. 5.6 it can be observed that a torsional brace strength requirement of 2 % is sufficient to develop member strength very close to the test limit load. Combining these results with the knuckle curve provided in Fig. A.15b, it can be observed that approximately 91 % of the beam's rigidly-braced strength is developed when the brace moment reaches $0.02M$ for the case where the brace stiffnesses satisfy the rules summarized at the end of Section 4.5.5.

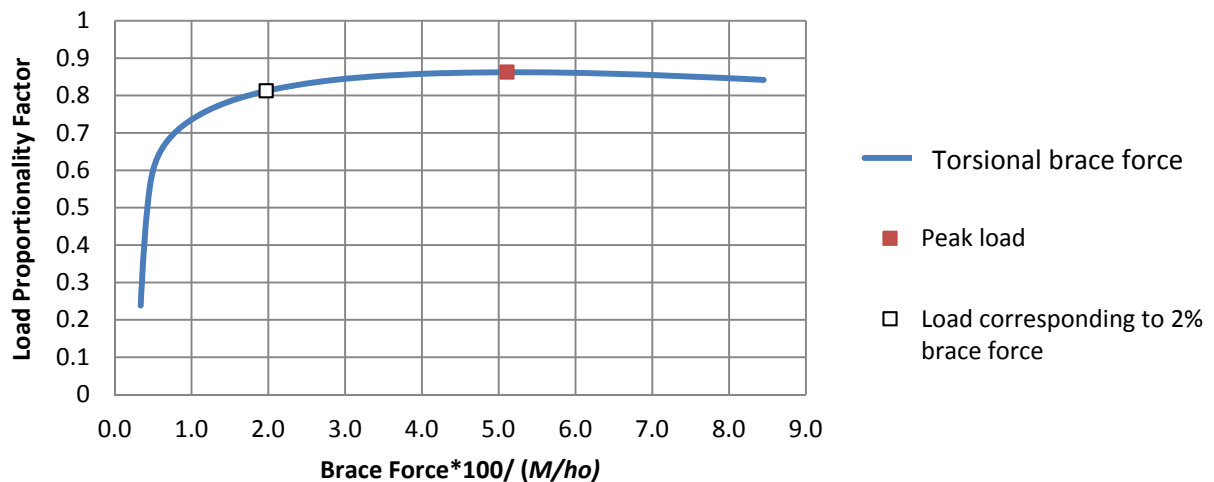


Figure 5.6. Point torsional brace force vs. the Load Proportionality Factor for the case B_MG2nt_CNTB_n1_TLBSR1 in Fig. 5.5b where torsional brace force at peak load is 5.1 %.

Based on the above results, it can be concluded that the recommendations for consideration of the interaction between the lateral and torsional brace stiffnesses explained at the end of Section 4.5.5 can also be applied to cases where the transverse loads are applied at the top flange, causing additional destabilizing effects.

CHAPTER 6 BEAM-COLUMNS SUBJECTED TO UNIFORM BENDING MOMENT

6.1 Overview

This chapter addresses the third major objective of this research, assessment of bracing requirements for beam-columns subjected to axial load and uniform bending moment. Section 6.2 gives details of the cases considered. Section 6.3 summarizes the recommended beam-column stiffness and strength calculations developed in this research. Section 6.4 presents the evaluation of these equations using a wide range of test simulation results.

6.2 Detailed Study Design

The cases considered in this research to study the bracing requirements for beam-columns subjected to axial load and uniform bending moment are listed below.

- Basic bracing types, with positive moment loading and only one flange in net compression:

BC_UMp_NB_n1_Lb5_FFR-0.67
BC_UMp_NB_n1_Lb5_FFR-0.33
BC_UMp_NB_n1_Lb5_FFR0
BC_UMp_NB_n1_Lb10_FFR-0.67
BC_UMp_NB_n1_Lb10_FFR-0.33
BC_UMp_NB_n1_Lb10_FFR0
BC_UMp_NB_n1_Lb15_FFR-0.67
BC_UMp_NB_n1_Lb15_FFR-0.33
BC_UMp_NB_n1_Lb15_FFR0
BC_UMp_RB_n2_Lb5_FFR-0.67
BC_UMp_RB_n2_Lb5_FFR-0.33

BC_UMp_RB_n2_Lb5_FFR0
BC_UMp_RB_n2_Lb10_FFR-0.67
BC_UMp_RB_n2_Lb10_FFR-0.33
BC_UMp_RB_n2_Lb10_FFR0
BC_UMp_RB_n2_Lb15_FFR-0.67
BC_UMp_RB_n2_Lb15_FFR-0.33
BC_UMp_RB_n2_Lb15_FFR0

- Basic bracing types, positive moment loading and both flanges in net compression:

BC_UMp_NB_n1_Lb5_FFR0.5
BC_UMp_NB_n1_Lb5_FFR1
BC_UMp_NB_n1_Lb10_FFR0.5
BC_UMp_NB_n1_Lb10_FFR1
BC_UMp_NB_n1_Lb15_FFR0.5
BC_UMp_NB_n1_Lb15_FFR1
BC_UMp_RB_n2_Lb5_FFR0.5
BC_UMp_RB_n2_Lb5_FFR1
BC_UMp_RB_n2_Lb10_FFR0.5
BC_UMp_RB_n2_Lb10_FFR1
BC_UMp_RB_n2_Lb15_FFR0.5
BC_UMp_RB_n2_Lb15_FFR1

- Combined lateral and torsional bracing, with positive moment loading and only one flange in net compression:

BC_UMp_CNTB_n1_Lb5_FFR-0.67
BC_UMp_CNTB_n1_Lb5_FFR-0.33
BC_UMp_CNTB_n1_Lb5_FFR0
BC_UMp_CNTB_n1_Lb15_FFR-0.67
BC_UMp_CNTB_n1_Lb15_FFR-0.33
BC_UMp_CNTB_n1_Lb15_FFR0
BC_UMp_CRTB_n2_Lb5_FFR-0.67
BC_UMp_CRTB_n2_Lb5_FFR-0.33
BC_UMp_CRTB_n2_Lb5_FFR0
BC_UMp_CRTB_n2_Lb15_FFR-0.67
BC_UMp_CRTB_n2_Lb15_FFR-0.33
BC_UMp_CRTB_n2_Lb15_FFR0

- Combined lateral and torsional bracing, with positive moment loading and both flanges in net compression:

BC_UMp_CNTB_n1_Lb5_FFR0.5
BC_UMp_CNTB_n1_Lb5_FFR1
BC_UMp_CNTB_n1_Lb15_FFR0.5
BC_UMp_CNTB_n1_Lb15_FFR1
BC_UMp_CRTB_n2_Lb5_FFR0.5
BC_UMp_CRTB_n2_Lb5_FFR1
BC_UMp_CRTB_n2_Lb15_FFR0.5
BC_UMp_CRTB_n2_Lb15_FFR1

- Combined lateral and torsional bracing, with negative moment loading and only one flange in net compression:

BC_UMn_CNTB_n1_Lb5_FFR-0.67
BC_UMn_CNTB_n1_Lb5_FFR-0.33
BC_UMn_CNTB_n1_Lb5_FFR0
BC_UMn_CNTB_n1_Lb15_FFR-0.67
BC_UMn_CNTB_n1_Lb15_FFR-0.33
BC_UMn_CNTB_n1_Lb15_FFR0
BC_UMn_CRTB_n2_Lb5_FFR-0.67
BC_UMn_CRTB_n2_Lb5_FFR-0.33
BC_UMn_CRTB_n2_Lb5_FFR0
BC_UMn_CRTB_n2_Lb15_FFR-0.67
BC_UMn_CRTB_n2_Lb15_FFR-0.33
BC_UMn_CRTB_n2_Lb15_FFR0

- Combined lateral and torsional bracing, with negative moment loading and both flanges in net compression:

BC_UMn_CNTB_n1_Lb5_FFR0.5
BC_UMn_CNTB_n1_Lb5_FFR1
BC_UMn_CNTB_n1_Lb15_FFR0.5
BC_UMn_CNTB_n1_Lb15_FFR1
BC_UMn_CRTB_n2_Lb5_FFR0.5
BC_UMn_CRTB_n2_Lb5_FFR1
BC_UMn_CRTB_n2_Lb15_FFR0.5
BC_UMn_CRTB_n2_Lb15_FFR1

6.3 Recommended Beam-Column Bracing Requirements

As noted in Section 1.1, the implications of simply summing the AISC column and beam bracing requirements to obtain the bracing requirements for beam-column members are not clear. This is due to the impact of the lateral bracing position and the transverse load position through the cross-section depth, as well as the fact that both torsional and lateral restraint are important attributes of the general beam-column bracing problem. The true physical interaction of these factors with the member stability behavior can be quite complex. This research seeks to propose a number of simple rules for combining and distributing the requirements to different beam-column bracing elements, and to evaluate the efficacy of these rules by comparison to FEA test simulations. The proposed rules are based on logical combinations of the column and beam load effects along with preliminary inspection and evaluation of FEA test simulation results. The finalized rules evaluated in this research are listed below. Section 6.4 then proceeds with the comparison of the results from these rules to the output from a wide range of FEA test simulations. The proposed rules are subdivided into three sets:

- 1) Beam-columns with lateral bracing only on the flange in flexural compression, and in which the opposite flange is subjected to a net flexural tension throughout the member's length. This case corresponds to an effective Flange Force Ratio $FFR = P_{ft} / P_{fc} \leq 0$, as discussed previously in Section 2.2.5.2.
- 2) Beam-columns with lateral bracing only on the flange in flexural compression, and in which the opposite flange is subjected to a net flexural compression anywhere along the member's length. This case corresponds to an effective Flange Force Ratio $FFR > 0$.
- 3) Beam-columns restrained by a combination of lateral and torsional bracing.

These rules are described in the following sub-sections.

6.3.1 Beam-Columns with Lateral Bracing Only on the Flange in Flexural Compression and with $P_{ft}/P_{fc} \leq 0$

For a beam-column with lateral bracing only on the flange in flexural compression, and where $P_{ft}/P_{fc} \leq 0$, the opposite flange is subjected to a net flexural tension. In this case, the “column bracing” demands are reduced due to the net tension on the unbraced flange. As such, it is proposed that the lateral braces be designed using the following full-bracing stiffness and strength requirements:

$$\beta_{brL} = \frac{2N_i}{L_b} \left[\frac{P}{2} + \left(\frac{M_{max}}{h_o} \right) C_{tL} C_d \right] \quad (6-1)$$

$$R_{brL} = 0.01 \left[\frac{P}{2} + \left(\frac{M_{max}}{h_o} \right) C_{tL} C_d \right] \text{ for point (nodal) lateral bracing} \quad (6-2a)$$

$$= 0.005 \left[\frac{P}{2} + \left(\frac{M_{max}}{h_o} \right) C_{tL} C_d \right] \text{ for shear panel (relative) lateral bracing} \quad (6-2b)$$

where all of the above variables are as previously defined in Section 4.4, with the exception of P , which is the constant beam-column axial compression considered in this research.

6.3.2 Beam-Columns with Lateral Bracing Only on the Flange in Flexural Compression and with $P_{ft}/P_{fc} > 0$

For a beam-column with lateral bracing only on the flange in flexural compression, and where $P_{ft}/P_{fc} > 0$, the opposite flange is subjected to a net flexural compression. In this case, the “column bracing” demands are increased. The following requirements for full lateral bracing are evaluated for this case:

$$\beta_{brL} = \frac{2N_i}{L_b} \left[2.5P + \left(\frac{M_{max}}{h_o} \right) C_{tL} C_d \right] \quad (6-3)$$

$$R_{brL} = 0.01 \left[2.5P + \left(\frac{M_{max}}{h_o} \right) C_{tL} C_d \right] \text{ for point (nodal) lateral bracing} \quad (6-4a)$$

$$= 0.005 \left[2.5P + \left(\frac{M}{h_o} \right) C_{tL} C_d \right] \text{ for shear panel (relative) lateral bracing} \quad (6-4b)$$

6.3.3 Beam-Columns Restrained by a Combination of Lateral and Torsional Bracing

For a beam-column braced by a combination of lateral and torsional bracing, the lateral bracing system can be designed conceptually for the axial load P and the torsional bracing can be designed for the moment M_{max} . The moment can be assumed to have a negligible effect on the lateral bracing, but the axial force creates some additional demands on the torsional bracing. Therefore, the requirements for full bracing by the different bracing components may be written as follows:

$$\beta_{brL} = \frac{2N_i P}{L_b} \quad (6-5)$$

$$R_{brL} = 0.01P \text{ for point (nodal) lateral bracing} \quad (6-6a)$$

$$= 0.005P \text{ for shear panel (relative) lateral bracing} \quad (6-6b)$$

$$\beta_{brT} = \pi^2 \left[\frac{\left(\frac{M_{max}}{C_b h_o} + \frac{P}{2} \right)}{P_{ef,eff}} \right] \left[\frac{\left(\frac{M_{max}}{C_b h_o} + \frac{P}{2} \right)}{L_b} \right] \left[\frac{n_T + 1}{n_T} \right] C_{tT} \quad (6-7)$$

$$M_{brT} = 0.02 \left(M_{max} + \frac{P}{2} h_o \right) \quad (6-8)$$

where all of the above variables are as previously defined in Section 4.4, with the exception of P , which is the constant beam-column axial compression considered in this research.

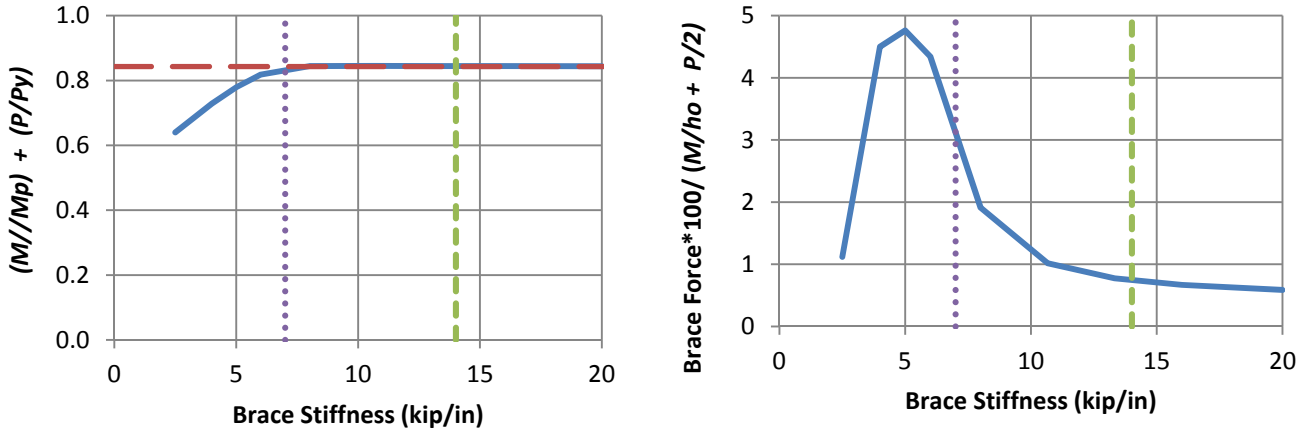
6.4 Results

6.4.1 Beam-Columns with Lateral Bracing Only on the Flange in Flexural Compression and with $P_{ft}/P_{fc} \leq 0$

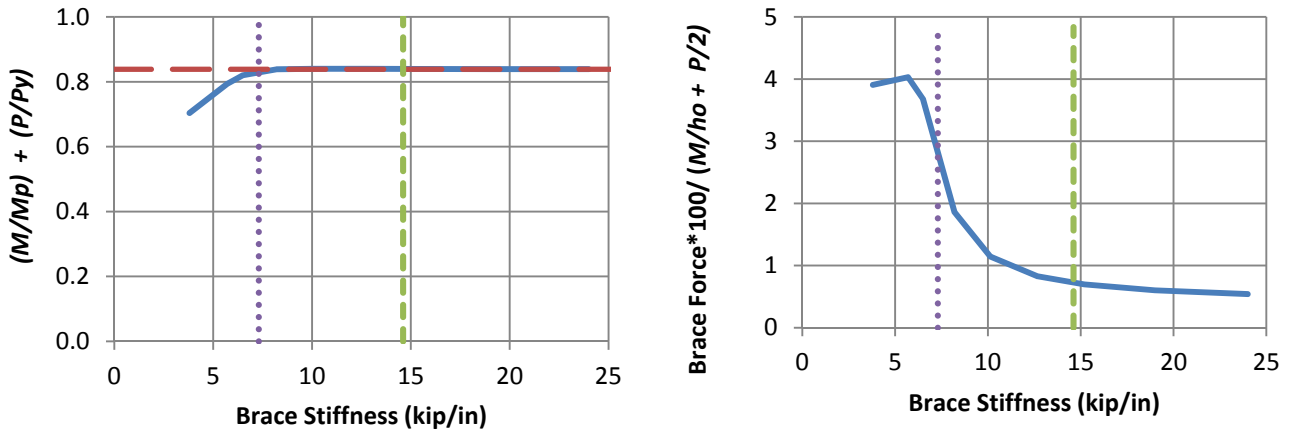
Figures 6.1 through 6.6 show the results from test simulation for the selected beam-column cases with lateral bracing only on the flange in flexural compression and with $P_{ft}/P_{fc} \leq 0$. The ordinate of the knuckle curve graphs is taken as $M/M_p + P/P_y$ in these figures. This is a reasonable normalized ordinate allowing the engineer to ascertain the effect of increasing the bracing stiffness values on the beam-column strength. The ordinate of the required brace force versus brace stiffness curves is normalized by $M/h_o + P/2$.

Table 6.1 compares the β_{brL} estimates from Eq. (6-1) to the stiffnesses corresponding to 96 % of the simulation rigidly-braced strengths, β_{F96L} , from Figs. 6.1 through 6.6. It also compares the estimated brace strength requirements at $\beta_L = \beta_{brL}$ from Eqs. (6-2) to the corresponding results from the test simulations.

Based on the results in Table 6.1, it can be observed that for all beam-column cases where the effective flange force ratio $P_{ft}/P_{fc} \leq 0$ (i.e., the unbraced flange is in net tension), the recommended bracing requirements are accurate to somewhat conservative. These results show that the use of an “effective member force” of $P/2 + M/h_o$ gives a bracing stiffness requirement that ranges from 1.14 to 2.42 for β_{brL}/β_{F96L} . For shear panel (relative) lateral bracing, it can be observed that a strength requirement of 0.5 % is more appropriate than the ANSI/AISC 360-10 value of 0.4 %, which is consistent with the findings from Prado and White (2015) and the recommendations in Section 4.5. The recommended rules for cases with $P_{ft}/P_{fc} \leq 0$ result in point bracing forces ranging from 0.70 to 0.83 % of $(P/2 + M/h_o)$ and maximum shear panel bracing forces ranging from 0.43 to 0.52 % of $(P/2 + M/h_o)$ at $\beta_L = \beta_{brL}$.



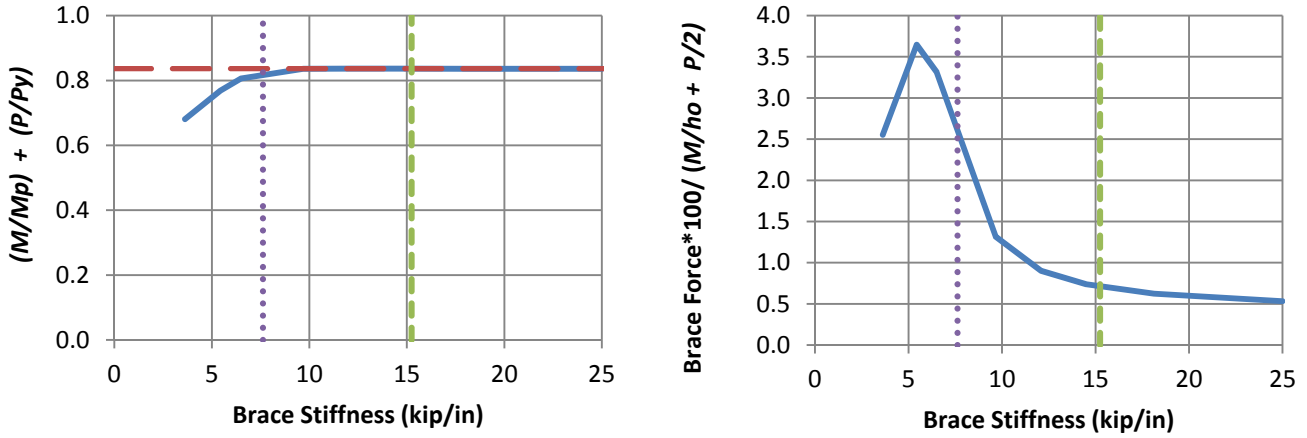
a) BC_UMp_NB_n1_Lb5_FFR-0.67



b) BC_UMp_NB_n1_Lb5_FFR-0.33

- Test simulation results
- - Rigidly-braced strength
- ⋯ $0.5\beta_{brL}$
- - β_{brL}

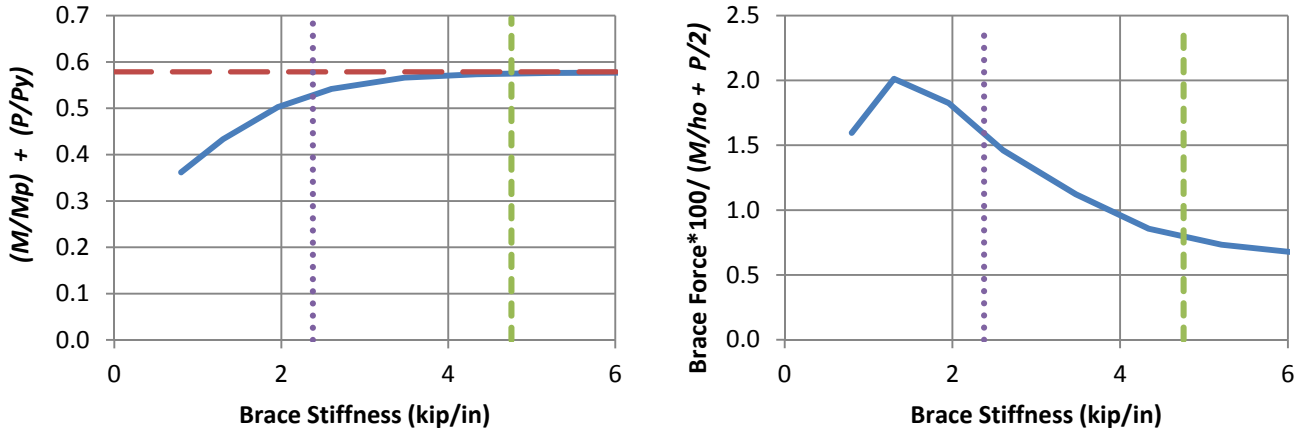
Figure 6.1. brace force vs. brace stiffness plots for point (nodal) lateral bracing cases with $n = 1$, uniform bending with an effective flange force ratio $P_{ft}/P_{fc} \leq 0$, and $L_b = 5$ ft.



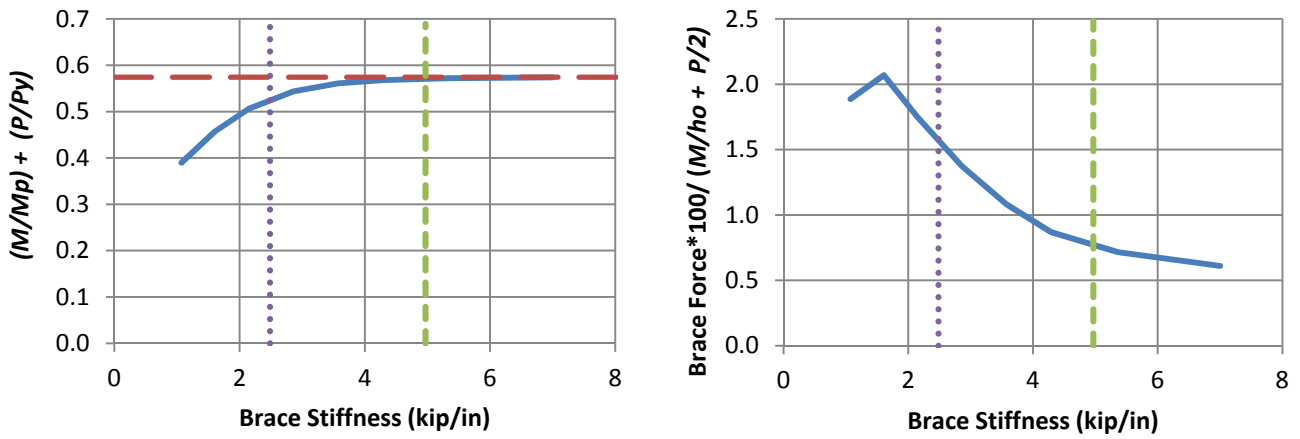
c) BC_UMp_NB_n1_Lb5_FFR0

- Test simulation results
- - Rigidly-braced strength
- ⋯ $0.5\beta_{brL}$
- - β_{brL}

Fig. 6.1 (continued). Beam-column knuckle curves and brace force vs. brace stiffness plots for point (nodal) lateral bracing cases with $n = 1$, uniform bending with an effective flange force ratio $P_{ft}/P_{fc} \leq 0$, and $L_b = 5$ ft.



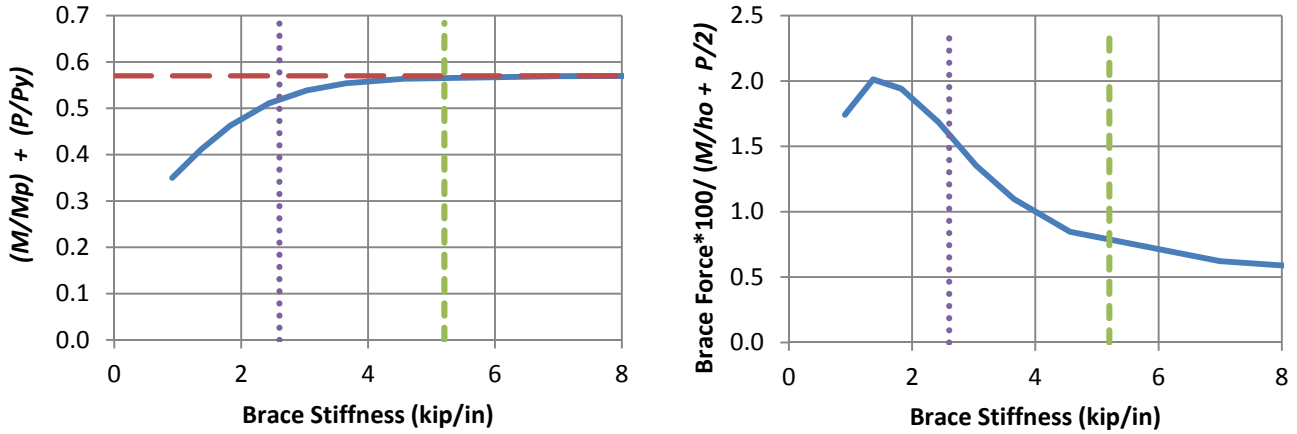
a) BC_UMp_NB_n1_Lb10_FFR-0.67



b) BC_UMp_NB_n1_Lb10_FFR-0.33

- Test simulation results
- - Rigidly-braced strength
- ⋯ $0.5\beta_{brL}$
- - β_{brL}

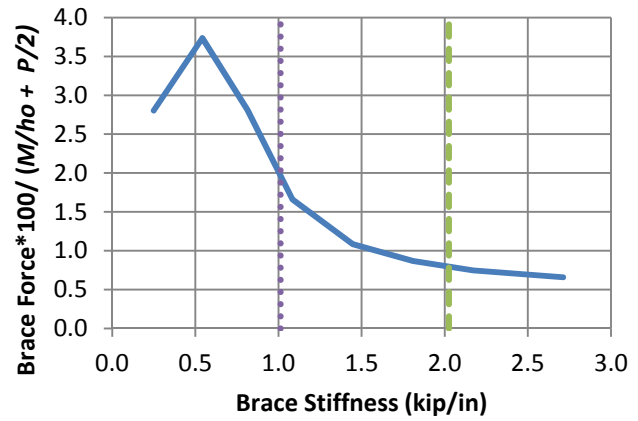
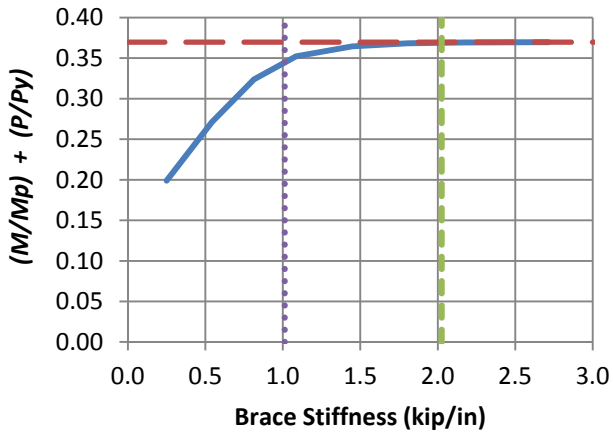
Figure 6.2. Beam-column knuckle curves and brace force vs. brace stiffness plots for point (nodal) lateral bracing cases with $n = 1$, uniform bending with an effective flange force ratio $P_{ft} / P_{fc} \leq 0$, and $L_b = 10$ ft.



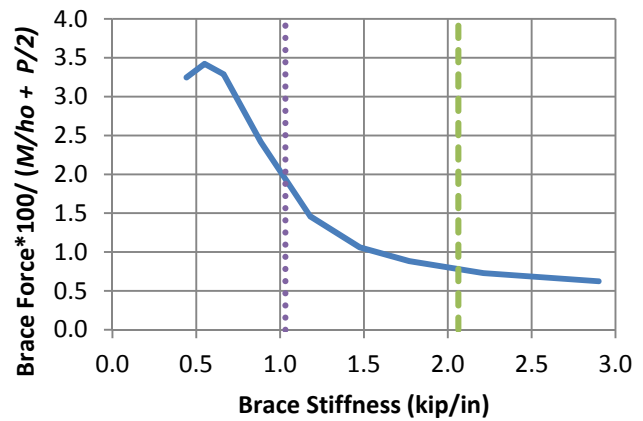
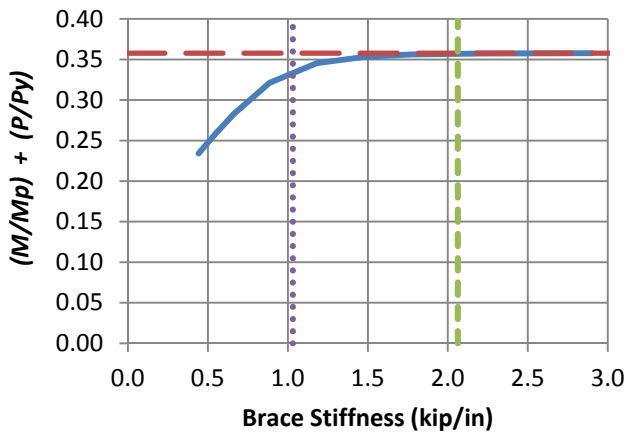
c) BC_UMp_NB_n1_Lb10_FFR0

- Test simulation results
- - Rigidly-braced strength
- ⋯ $0.5\beta_{brL}$
- - β_{brL}

Fig. 6.2 (continued). Beam-column knuckle curves and brace force vs. brace stiffness plots for point (nodal) lateral bracing cases with $n = 1$, uniform bending with an effective flange force ratio $P_{ft}/P_{fc} \leq 0$, and $L_b = 10$ ft.



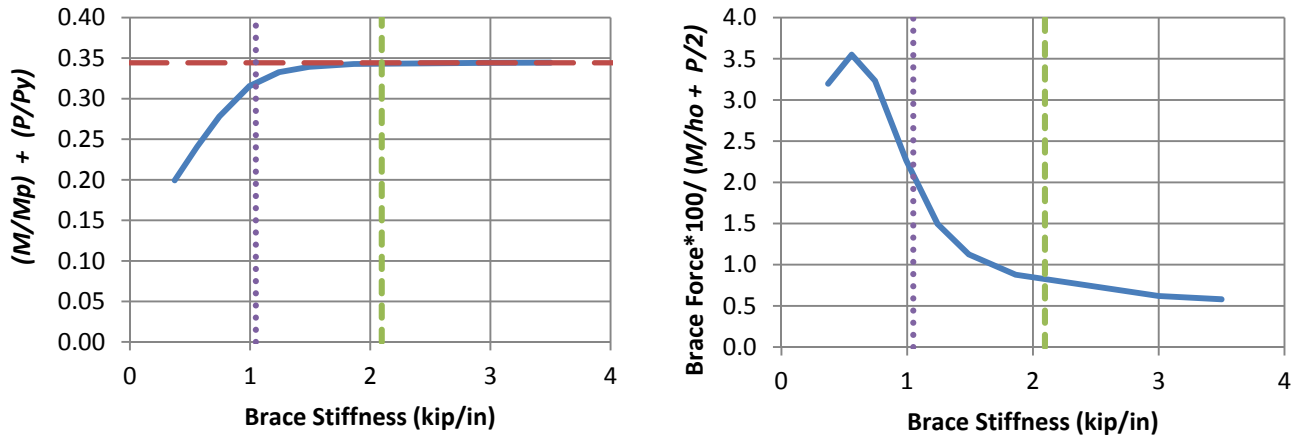
a) BC_UMp_NB_n1_Lb15_FFR-0.67



b) BC_UMp_NB_n1_Lb15_FFR-0.33

- Test simulation results
- - Rigidly-braced strength
- ⋯ $0.5\beta_{brL}$
- - β_{brL}

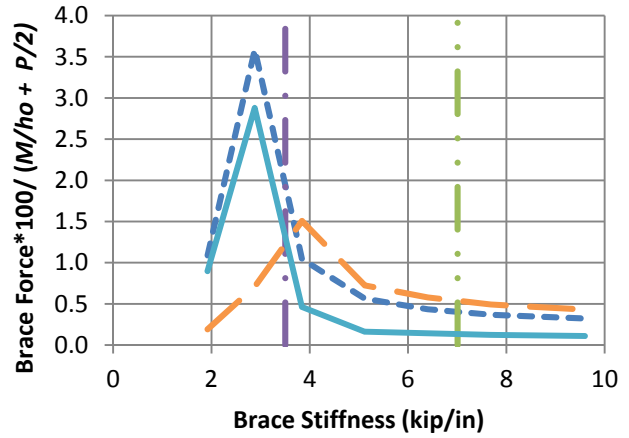
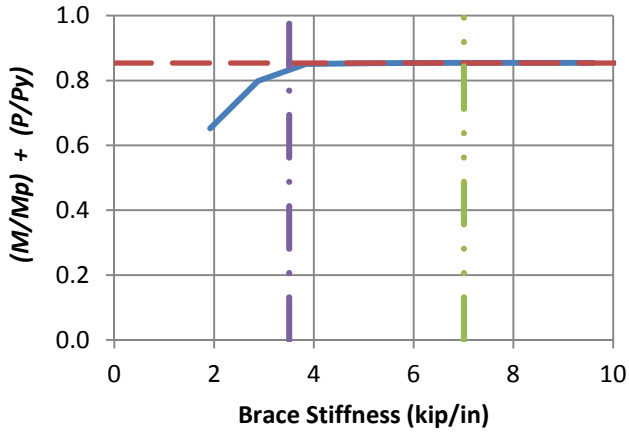
Figure 6.3. Beam-column knuckle curves and brace force vs. brace stiffness plots for point (nodal) lateral bracing cases with $n = 1$, uniform bending with an effective flange force ratio $P_{ft}/P_{fc} \leq 0$, and $L_b = 15$ ft.



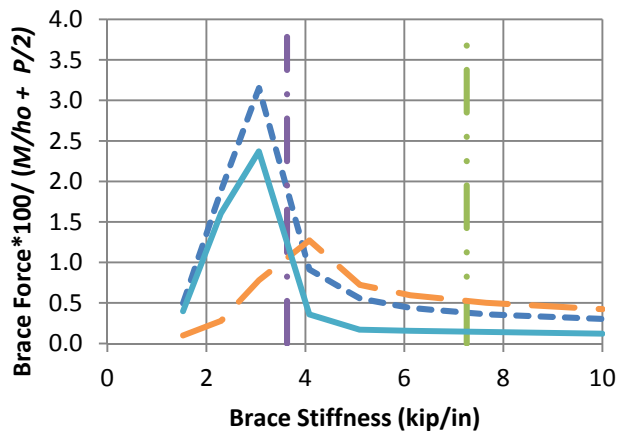
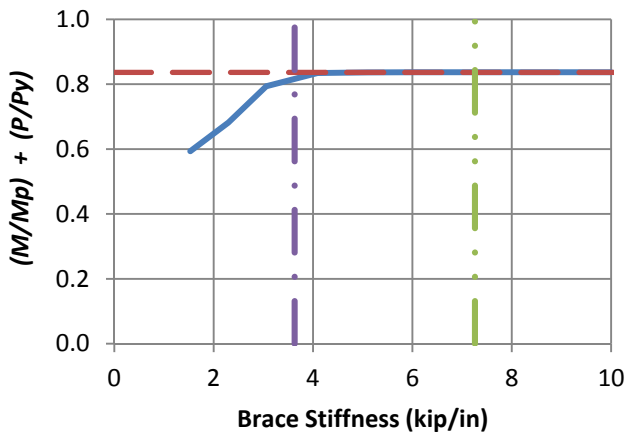
c) BC_UMp_NB_n1_Lb15_FFR0

- Test simulation results
- - Rigidly-braced strength
- ⋯ $0.5\beta_{brL}$
- - β_{brL}

Fig. 6.3 (continued). Beam-column knuckle curves and brace force vs. brace stiffness plots for point (nodal) lateral bracing cases with $n = 1$, uniform bending with effective flange force ratio $P_{ft}/P_{fc} \leq 0$, and $L_b = 15$ ft.



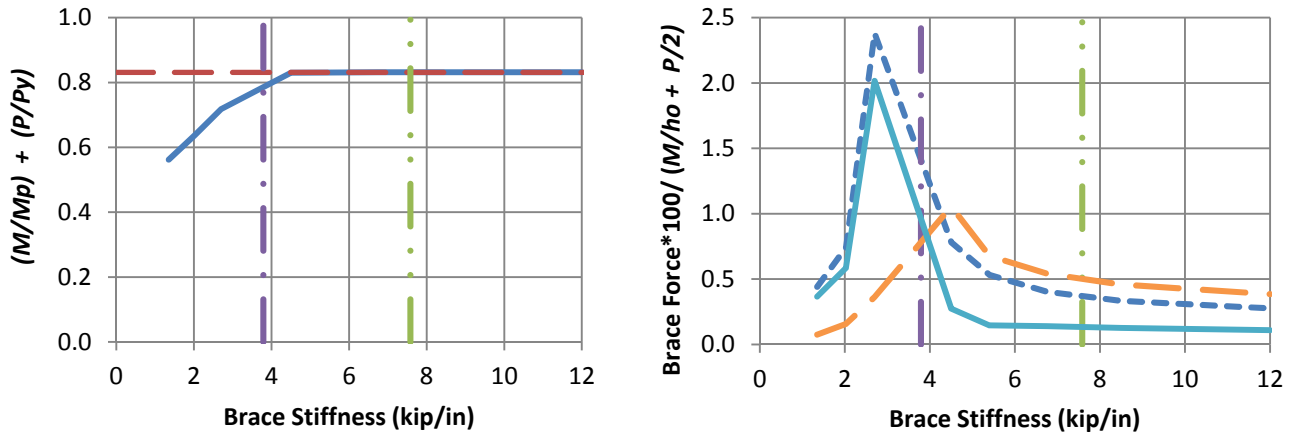
a) BC_UMp_RB_n2_Lb5_FFR-0.67



b) BC_UMp_RB_n2_Lb5_FFR-0.33



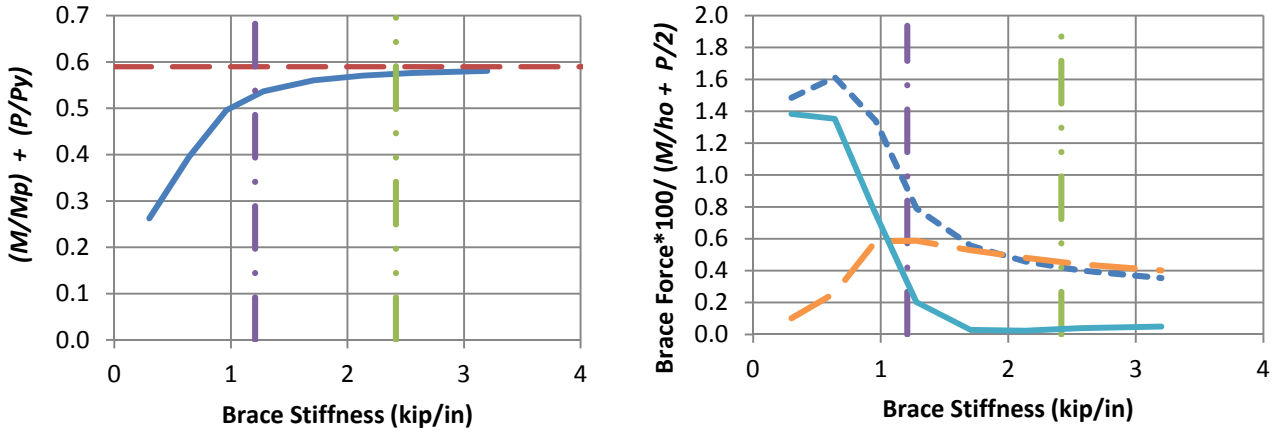
Figure 6.4. Beam-column knuckle curves and brace force vs. brace stiffness plots for shear panel (relative) lateral bracing cases with $n = 2$, uniform bending with an effective flange force ratio $P_{ft} / P_{fc} \leq 0$, and $L_b = 5$ ft.



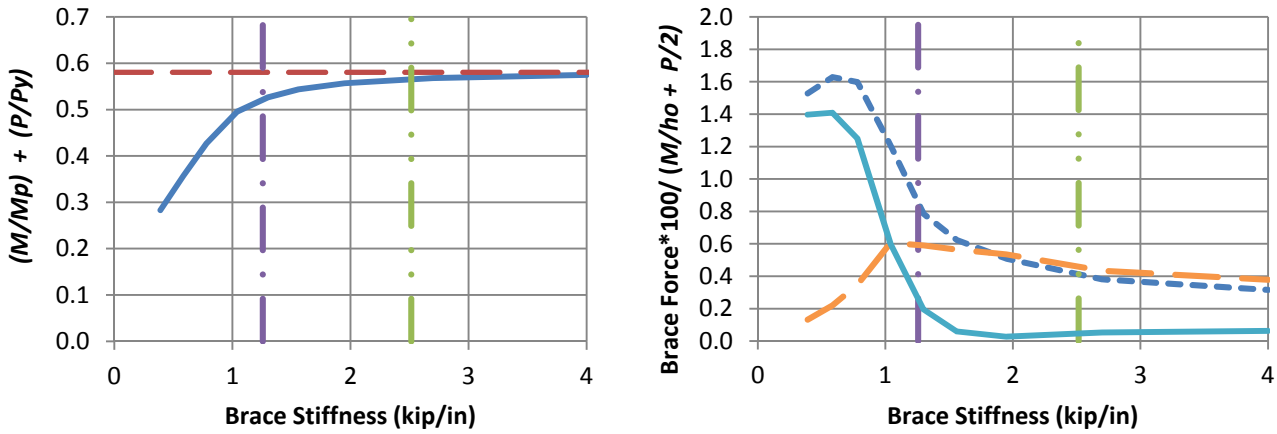
c) BC_UMp_RB_n2_Lb5_FFR0

- Test simulation results
- - Rigidly-braced strength
- $0.5\beta_{brL}$
- β_{brL}
- - - Left end panel shear force
- Right end panel shear force
- - Middle panel shear force

Fig. 6.4 (continued). Beam-column knuckle curves and brace force vs. brace stiffness plots for shear panel (relative) lateral bracing cases with $n = 2$, uniform bending with an effective flange force ratio $P_{ft}/P_{fc} \leq 0$, and $L_b = 5$ ft.



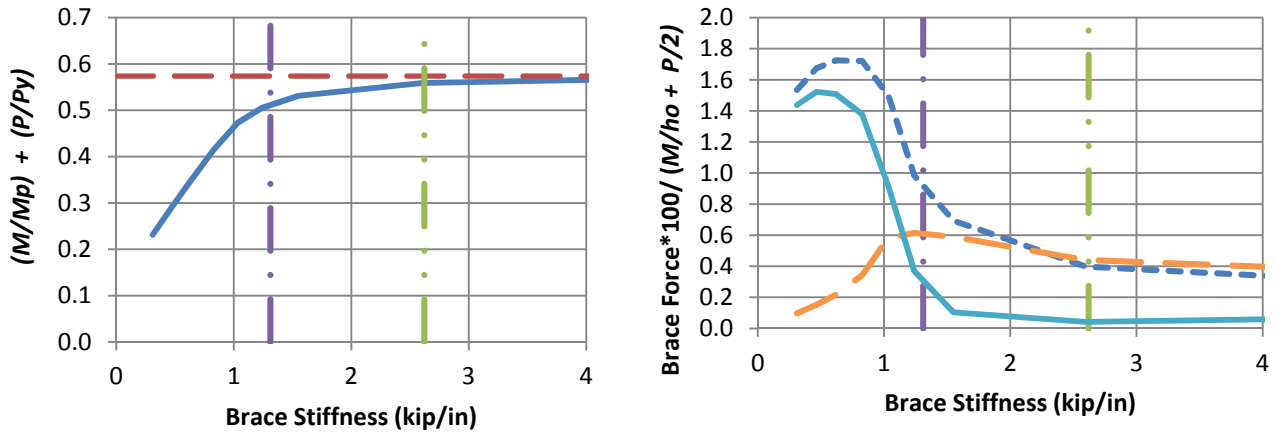
a) BC_UMp_RB_n2_Lb10_FFR-0.67



b) BC_UMp_RB_n2_Lb10_FFR-0.33



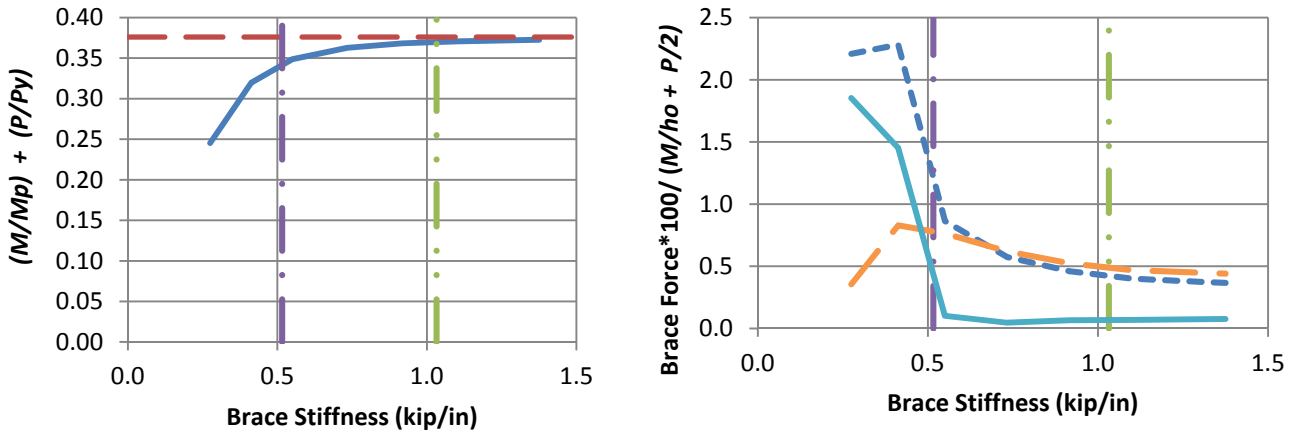
Figure 6.5. Beam-column knuckle curves and brace force vs. brace stiffness plots for shear panel (relative) lateral bracing cases with $n = 2$, uniform bending with an effective flange force ratio $P_{ft} / P_{fc} \leq 0$, and $L_b = 10$ ft.



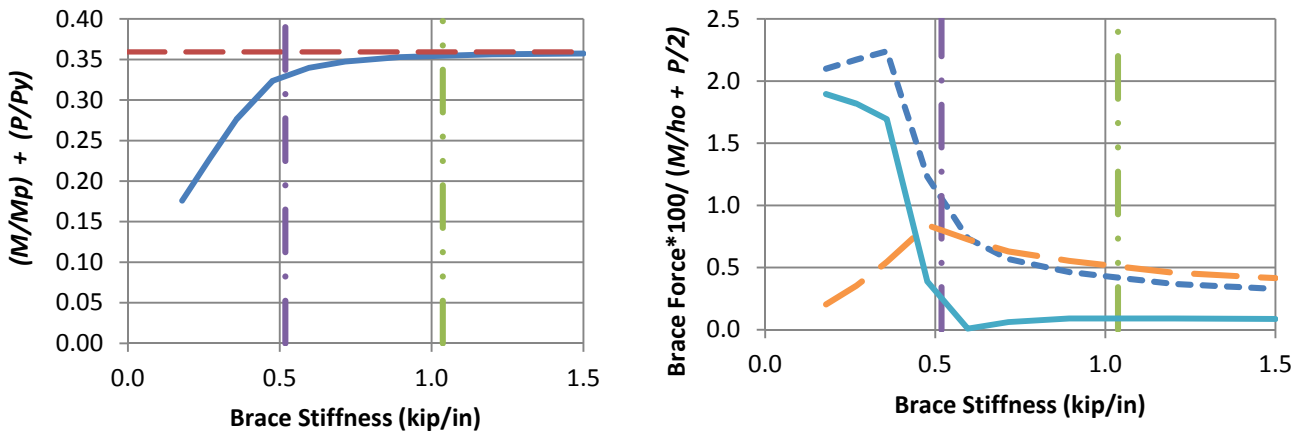
c) BC_UMp_RB_n2_Lb10_FFR0

- Test simulation results
- - Rigidly-braced strength
- $0.5\beta_{brL}$
- β_{brL}
- - - Left end panel shear force
- Right end panel shear force
- - Middle panel shear force

Fig. 6.5 (continued). Beam-column knuckle curves and brace force vs. brace stiffness plots for shear panel (relative) lateral bracing cases with $n = 2$, uniform bending with an effective flange force ratio $P_{ft} / P_{fc} \leq 0$, and $L_b = 10$ ft.



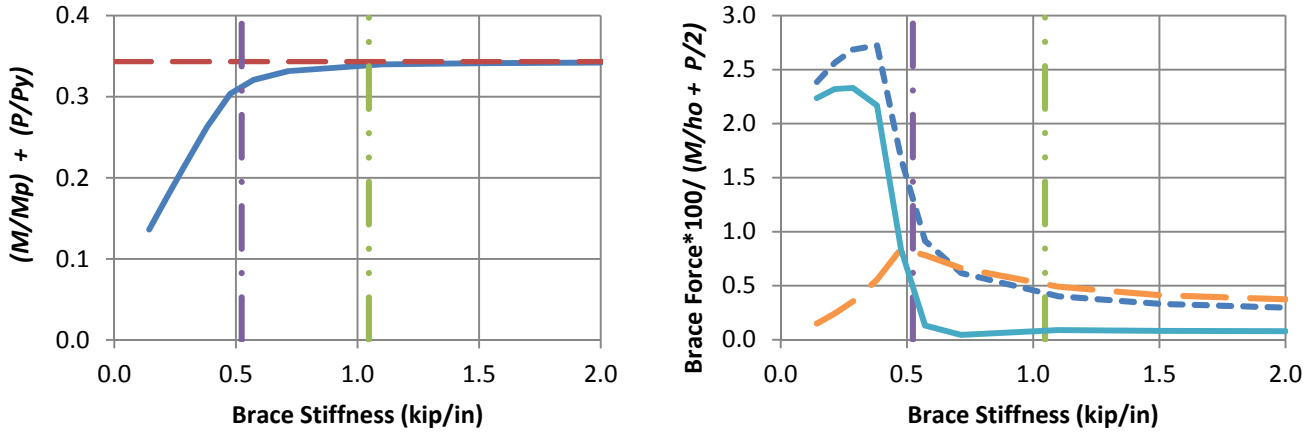
a) BC_UMp_RB_n2_Lb15_FFR-0.67



b) BC_UMp_RB_n2_Lb15_FFR-0.33



Figure 6.6. Beam-column knuckle curves and brace force vs. brace stiffness plots for shear panel (relative) lateral bracing cases with $n = 2$, uniform bending with an effective flange force ratio $P_{ft} / P_{fc} \leq 0$, and $L_b = 15$ ft.



c) BC_UMp_RB_n2_Lb15_FFR0

- Test simulation results
- - Rigidly-braced strength
- $0.5\beta_{brL}$
- β_{brL}
- - - Left end panel shear force
- Right end panel shear force
- - Middle panel shear force

Fig. 6.6 (continued). Beam-column knuckle curves and brace force vs. brace stiffness plots for shear panel (relative) lateral bracing cases with $n = 2$, uniform bending with an effective flange force ratio $P_{ft} / P_{fc} \leq 0$, and $L_b = 15$ ft.

Table 6.1. Brace stiffnesses β_{F96L} and β_{brL} and brace forces as a percentage of $(M/h_o + P/2)$ for beam-columns with lateral bracing only on the flange in flexural compression and with $P_{ft}/P_{fc} \leq 0$.

Case	β_{F96L} (kip/in)	β_{brL} (kip/in)	β_{brL}/β_{F96L}	% Brace Force at $\beta_L = \beta_{brL}$	Ratio of actual to estimated brace force at $\beta_L = \beta_{brL}$
BC_UMp_NB_n1_Lb5_FFR-0.67	5.78	14.00	2.42	0.76	0.76
BC_UMp_NB_n1_Lb5_FFR-0.33	6.05	14.60	2.41	0.70	0.70
BC_UMp_NB_n1_Lb5_FFR0	6.41	15.24	2.38	0.73	0.73
BC_UMp_NB_n1_Lb10_FFR-0.67	3.09	4.76	1.54	0.79	0.79
BC_UMp_NB_n1_Lb10_FFR-0.33	3.17	4.96	1.56	0.77	0.77
BC_UMp_NB_n1_Lb10_FFR0	3.38	5.20	1.54	0.79	0.79
BC_UMp_NB_n1_Lb15_FFR-0.67	1.17	2.02	1.73	0.81	0.81
BC_UMp_NB_n1_Lb15_FFR-0.33	1.16	2.06	1.78	0.77	0.77
BC_UMp_NB_n1_Lb15_FFR0	1.21	2.10	1.74	0.83	0.83
BC_UMp_RB_n2_Lb5_FFR-0.67	3.27	7.00	2.14	0.52	1.04
BC_UMp_RB_n2_Lb5_FFR-0.33	3.29	7.26	2.21	0.51	1.02
BC_UMp_RB_n2_Lb5_FFR0	3.99	7.58	1.90	0.50	1.00
BC_UMp_RB_n2_Lb10_FFR-0.67	1.94	2.42	1.25	0.45	0.90
BC_UMp_RB_n2_Lb10_FFR-0.33	1.98	2.52	1.27	0.46	0.92
BC_UMp_RB_n2_Lb10_FFR0	2.3	2.62	1.14	0.44	0.88
BC_UMp_RB_n2_Lb15_FFR-0.67	0.71	1.04	1.46	0.50	1.00
BC_UMp_RB_n2_Lb15_FFR-0.33	0.68	1.04	1.53	0.50	1.00
BC_UMp_RB_n2_Lb15_FFR0	0.69	1.04	1.51	0.50	1.00

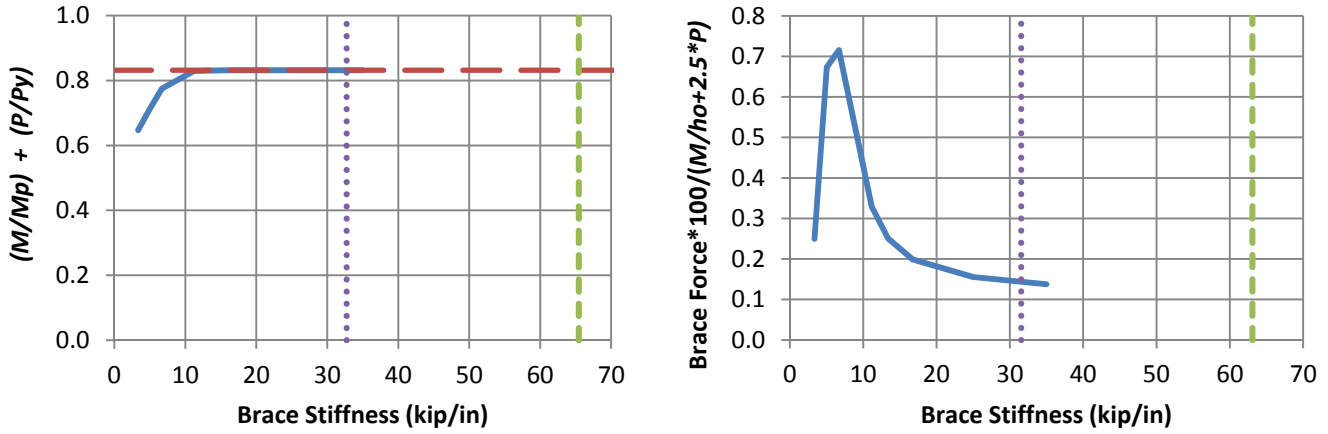
Based on Table 6.1, it can be observed that β_{brL} is sufficient to develop 96 % of the minimum rigidly-braced member strength for all of these bracing cases. In addition, the equations for R_{brL} do an accurate to slightly conservative job of estimating the brace strength requirements.

6.4.2 Beam-Columns with Lateral Bracing Only on the Flange in Flexural Compression and with $P_{ft}/P_{fc} > 0$

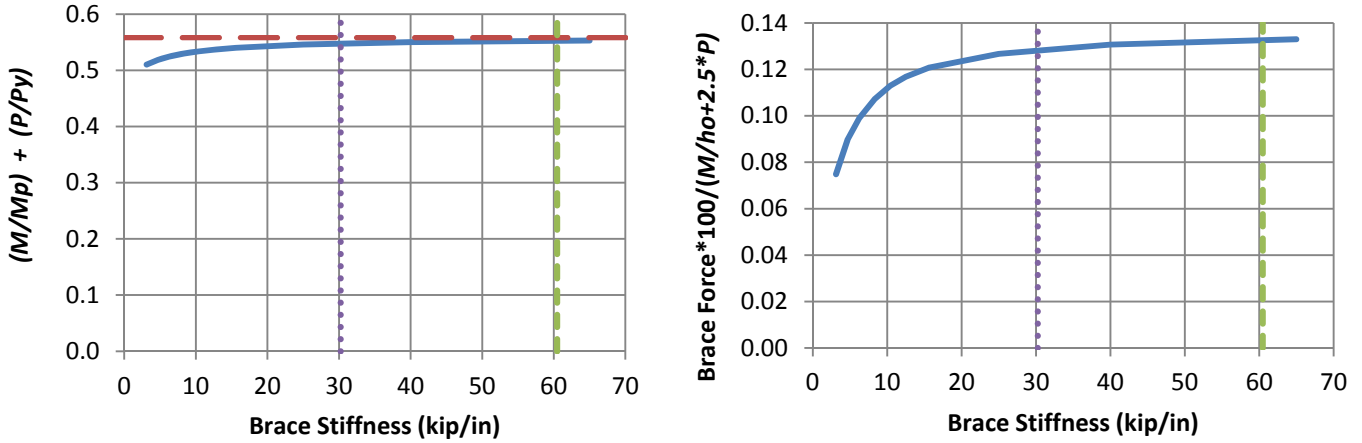
Figures 6.7 through 6.12 show the results from test simulation for the selected beam-column cases with lateral bracing only on the flange in flexural compression and with $P_{ft}/P_{fc} > 0$. The ordinate of the knuckle curve graphs is taken as $M/M_p + P/P_y$ in these figures. The ordinate of the required brace force versus brace stiffness curves is normalized by $M/h_o + 2.5P$.

Table 6.2 compares the β_{brL} estimates from Eq. (6-3) to the stiffnesses corresponding to 96 % of the simulation rigidly-braced strengths from Figs. 6.7 through 6.12. It also compares the estimated brace strength requirements at $\beta_L = \beta_{brL}$ from Eqs. (6-4) to the corresponding results from the test simulations.

Based on the results in Table 6.2, it can be observed that β_{brL} slightly underestimates β_{F96} for all the cases with $L_b = 15$ ft, and for two of the relative bracing cases with $L_b = 10$ ft. For the other cases (i.e., cases with one intermediate brace and unbraced lengths of 5 ft and 10 ft, and cases with two intermediate braces and an unbraced length of 5 ft) β_{brL} is a conservative estimate of β_{F96} . In addition, it can be observed that the recommended bracing strength calculation is conservative for all cases except for test BC_UMp_RB_n2_Lb15_FFR1, which involves zero bending, concentric axial compression, and $L_b = 15$ ft.



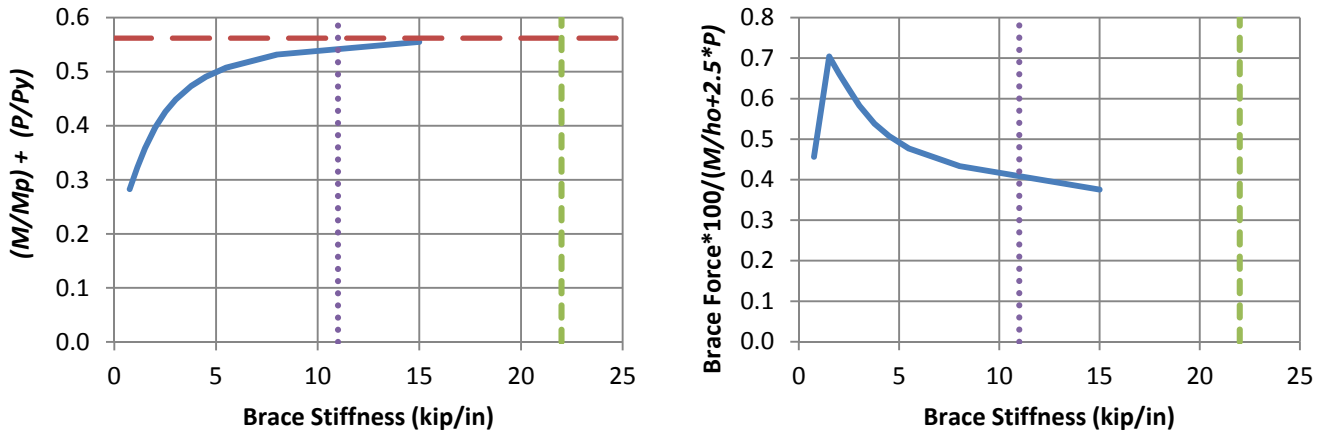
a) BC_UMp_NB_n1_Lb5_FFR0.5



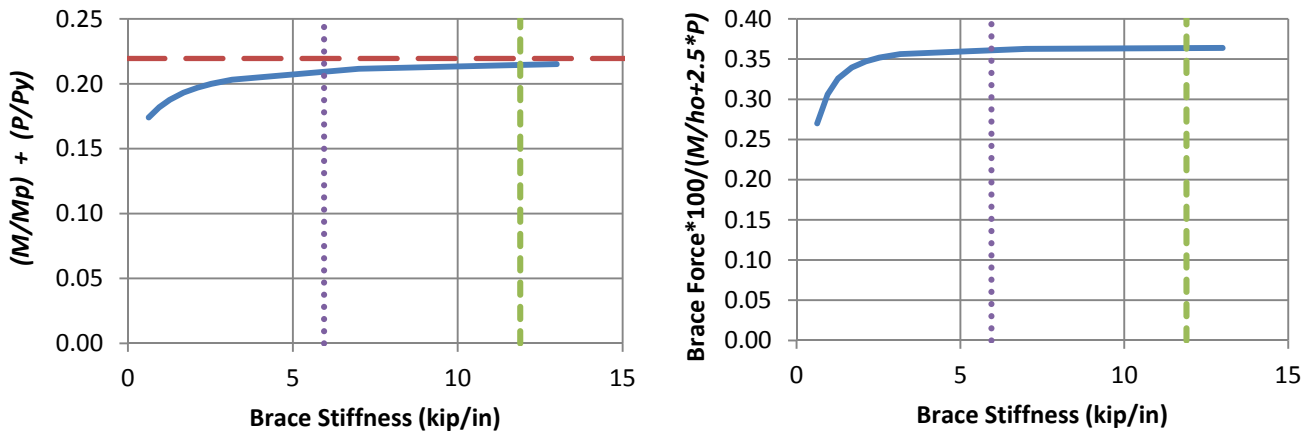
b) BC_UMp_NB_n1_Lb5_FFR1

- Test simulation results
- - Rigidly-braced strength
- ⋯ $0.5\beta_{brL}$
- - β_{brL}

Figure 6.7. Beam-column knuckle curves and brace force vs. brace stiffness plots for point (nodal) lateral bracing cases with $n = 1$, uniform bending with an effective flange force ratio $P_{ft}/P_{fc} > 0$, and $L_b = 5$ ft.



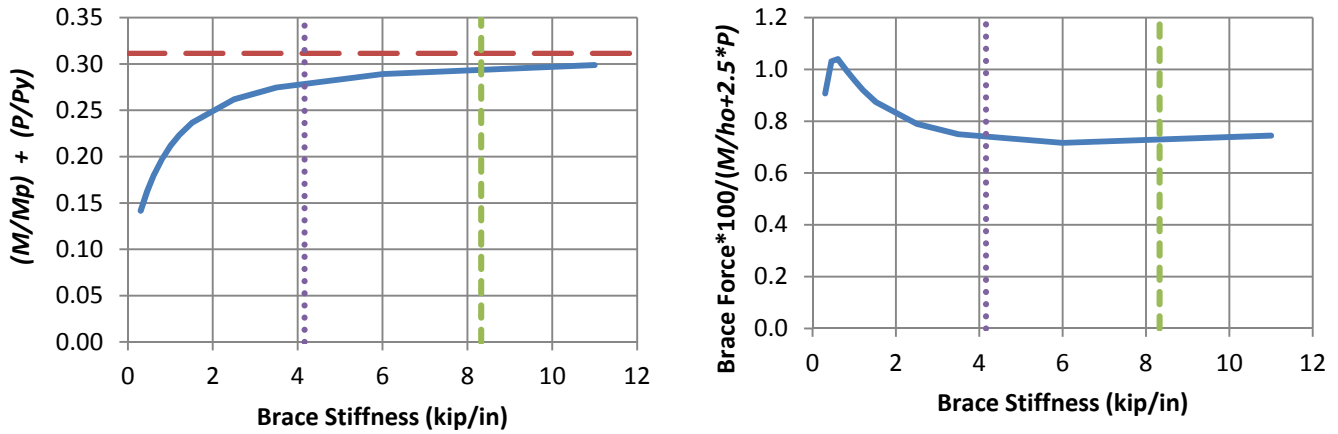
a) BC_UMp_NB_n1_Lb10_FFR0.5



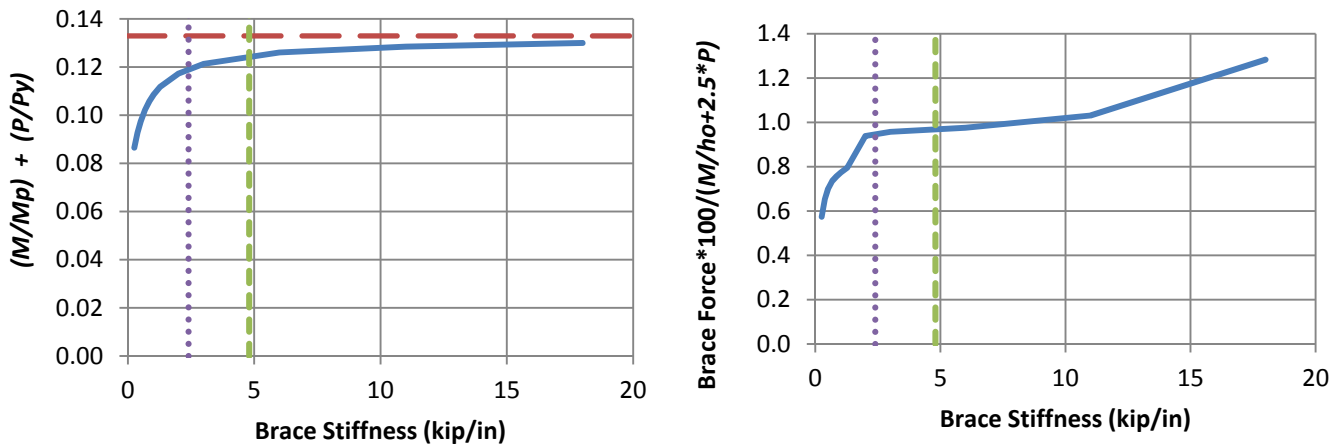
b) BC_UMp_NB_n1_Lb10_FFR1

- Test simulation results
- - Rigidly-braced strength
- ⋯ $0.5\beta_{brL}$
- - β_{brL}

Figure 6.8. Beam-column knuckle curves and brace force vs. brace stiffness plots for point (nodal) lateral bracing cases with $n = 1$, uniform bending with an effective flange force ratio $P_{ft} / P_{fc} > 0$, and $L_b = 10$ ft.



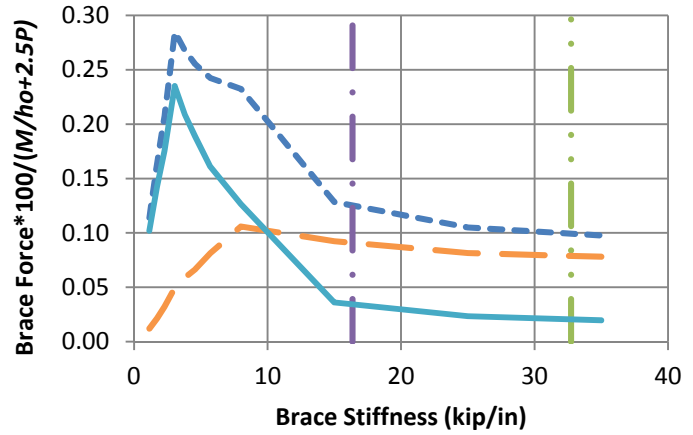
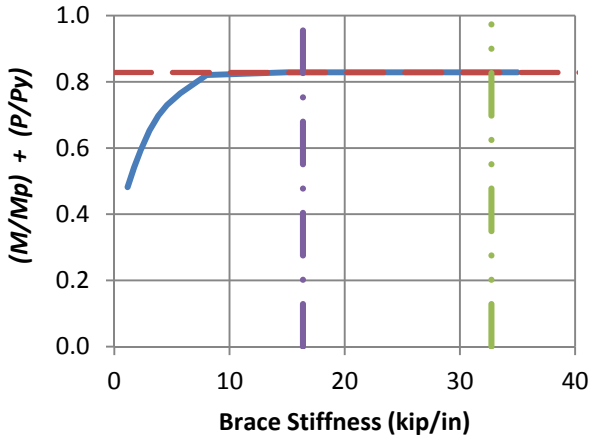
a) BC_UMp_NB_n1_Lb15_FFR0.5



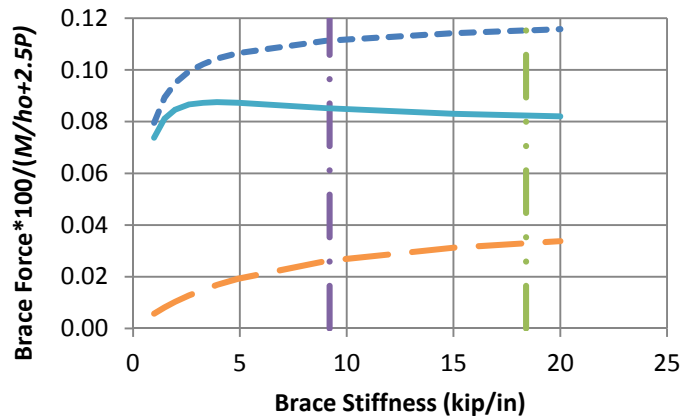
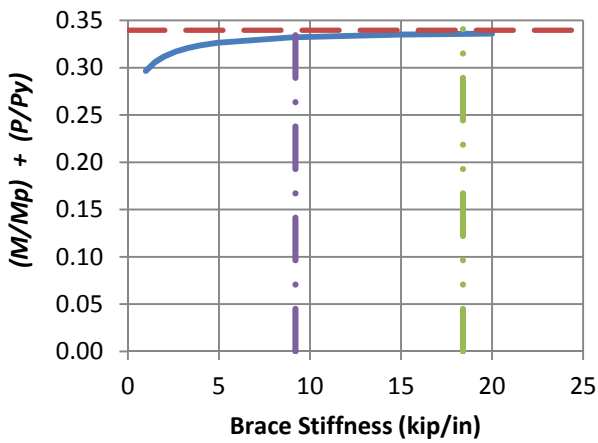
b) BC_UMp_NB_n1_Lb15_FFR1

- Test simulation results
- - Rigidly-braced strength
- ⋯ $0.5\beta_{brL}$
- - β_{brL}

Figure 6.9. Beam-column knuckle curves and brace force vs. brace stiffness plots for point (nodal) lateral bracing cases with $n = 1$, uniform bending with an effective flange force ratio $P_{ft} / P_{fc} > 0$, and $L_b = 15$ ft.



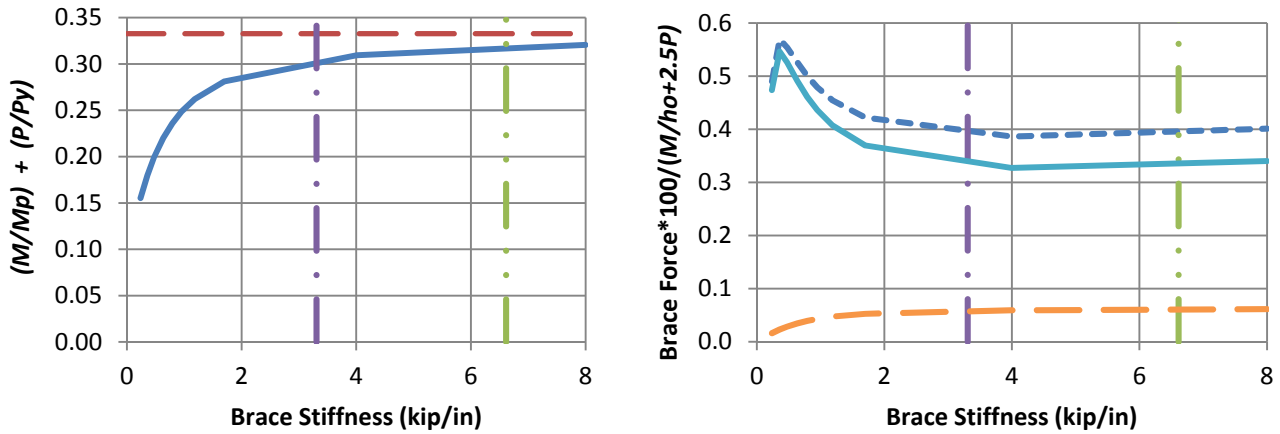
a) BC_UMp_RB_n2_Lb5_FFR0.5



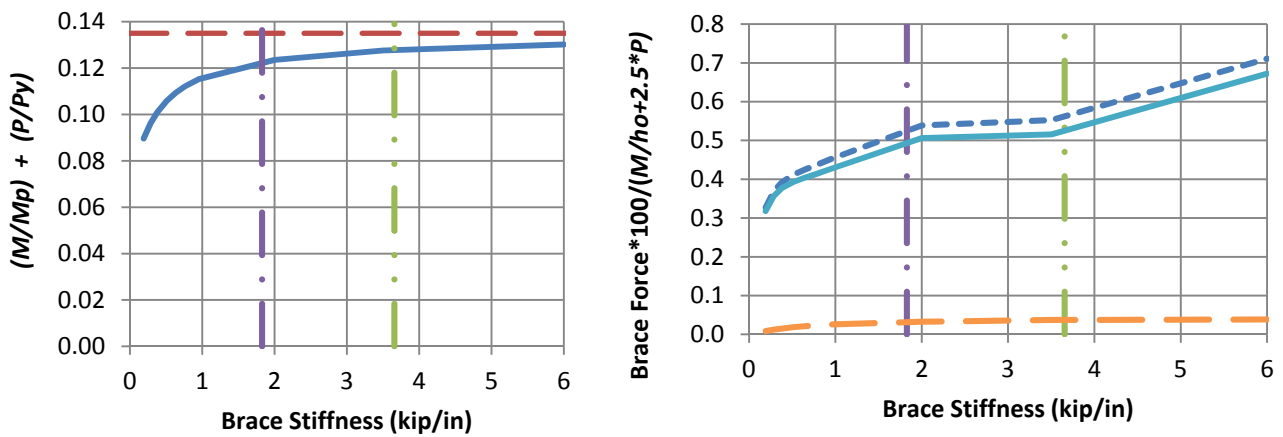
b) BC_UMp_RB_n2_Lb5_FFR1

- Test simulation results
- • $0.5\beta_{brL}$
- • β_{brL}
- - • Left end panel shear force
- - Middle panel shear force
- - Rigidly-braced strength
- Right end panel shear force

Figure 6.10. Beam-column knuckle curves and brace force vs. brace stiffness plots for shear panel (relative) lateral bracing cases with $n = 2$, uniform bending with an effective flange force ratio $P_{ft} / P_{fc} > 0$, and $L_b = 5$ ft.



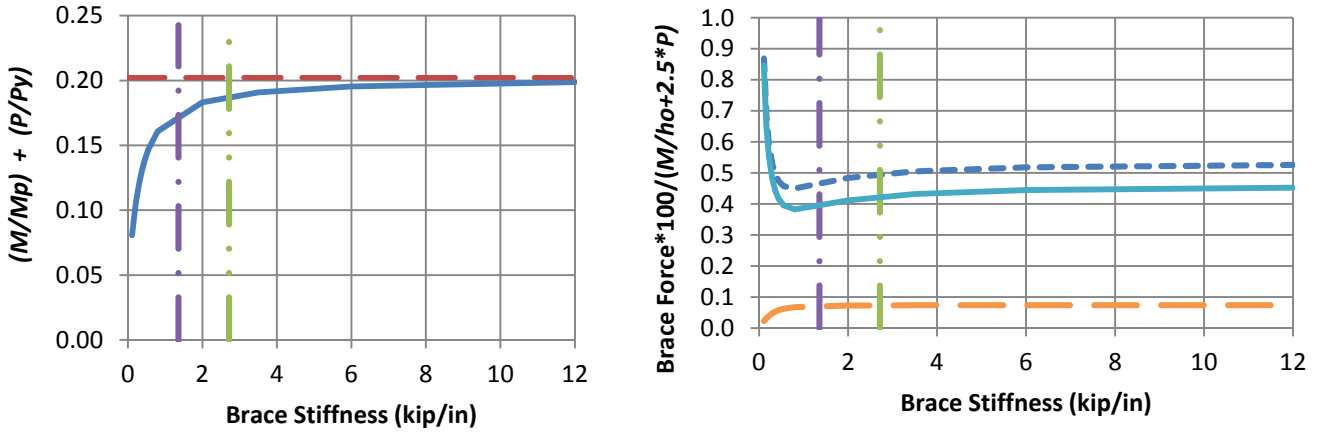
a) BC_UMp_RB_n2_Lb10_FFR0.5



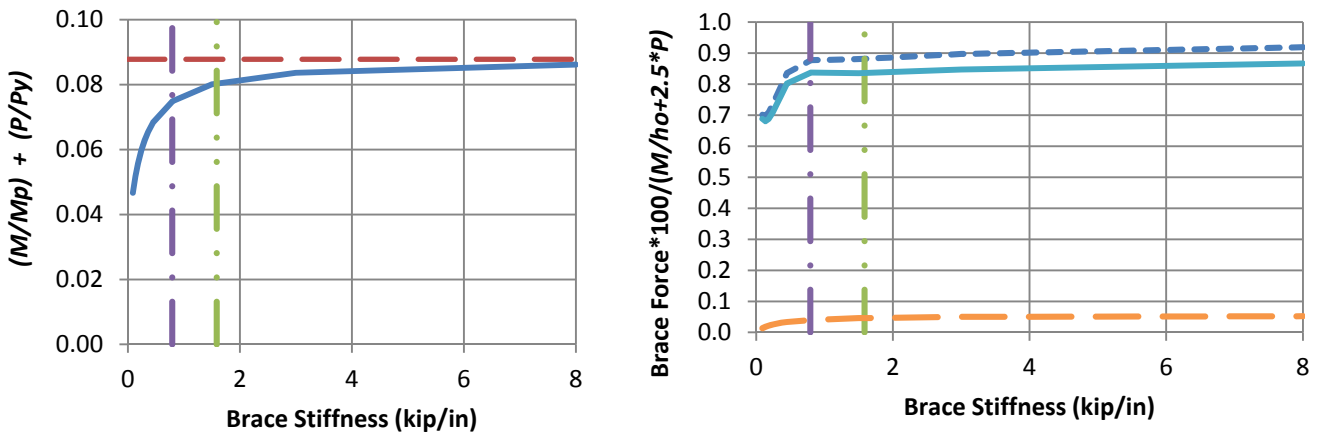
b) BC_UMp_RB_n2_Lb10_FFR1



Figure 6.11. Beam-column knuckle curves and brace force vs. brace stiffness plots for shear panel (relative) lateral bracing cases with $n = 2$, uniform bending with an effective flange force ratio $P_{ft} / P_{fc} > 0$, and $L_b = 10$ ft.



a) BC_UMp_RB_n2_Lb15_FFR0.5



b) BC_UMp_RB_n2_Lb15_FFR1



Figure 6.12. Beam-column knuckle curves and brace force vs. brace stiffness plots for shear panel (relative) lateral bracing cases with $n = 2$, uniform bending with an effective flange force ratio $P_{ft} / P_{fc} > 0$, and $L_b = 15$ ft.

Table 6.2. Brace stiffnesses β_{F96L} and β_{brL} and brace forces as a percentage of $(M/h_o + 2.5P)$ for beam-columns with lateral bracing only on the flange in flexural compression and with $P_{ft}/P_{fc} > 0$.

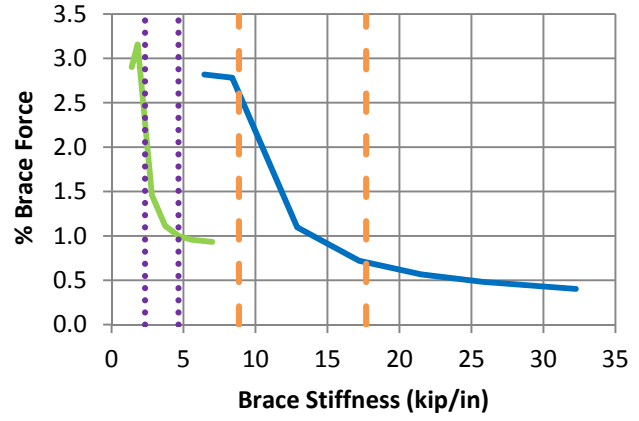
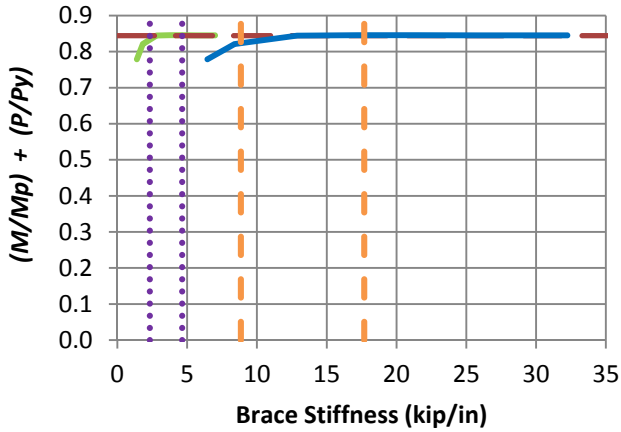
Case	β_{F96L} (kip/in)	β_{brL} (kip/in)	β_{brL}/β_{F96L}	% Brace Force at $\beta_L = \beta_{brL}$	Ratio of actual to estimated brace force at $\beta_L = \beta_{brL}$
BC_UMp_NB_n1_Lb5_FFR0.5	10.00	63.08	6.31	0.14	0.14
BC_UMp_NB_n1_Lb5_FFR1	11.89	60.48	5.09	0.13	0.13
BC_UMp_NB_n1_Lb10_FFR0.5	10.36	22.00	2.12	0.35	0.35
BC_UMp_NB_n1_Lb10_FFR1	6.67	11.90	1.78	0.36	0.36
BC_UMp_NB_n1_Lb15_FFR0.5	11.20	8.32	0.74	0.72	0.72
BC_UMp_NB_n1_Lb15_FFR1	9.16	4.80	0.52	0.97	0.97
BC_UMp_RB_n2_Lb5_FFR0.5	6.96	32.72	4.70	0.10	0.20
BC_UMp_RB_n2_Lb5_FFR1	4.80	18.40	3.83	0.12	0.24
BC_UMp_RB_n2_Lb10_FFR0.5	7.61	6.62	0.87	0.40	0.80
BC_UMp_RB_n2_Lb10_FFR1	5.43	3.66	0.67	0.55	1.10
BC_UMp_RB_n2_Lb15_FFR0.5	5.29	2.72	0.51	0.50	1.00
BC_UMp_RB_n2_Lb15_FFR1	4.31	1.58	0.37	0.84	1.68

It can be observed from Figs. 6.8 through 6.12 that in all cases where $\beta_{brL} / \beta_{F96L}$ is less than 1.0 (for which the cells are shaded grey in Table 6.2), the knuckle curve is relatively flat at $\beta_L = \beta_{brL}$. Therefore, the bracing stiffness requirement based on Eq. (6-3) is considered acceptable. BC_UMp_RB_n2_Lb15_FFR1 is the only test that causes significant concern, since the percent brace force of 0.84 at $\beta_L = \beta_{brL}$ is significantly larger than the recommended shear panel strength requirement of 0.5 %. It appears that the overall lateral buckling displacements of the long unbraced flange induces significant forces in the lateral braces on the opposite flange in this problem. However, it should be noted that the L/r_{yf} of the unbraced flange in this problem is equal to $(15 \text{ ft} \times 3 \times 12 \text{ in/ft}) / (1.88 \text{ in}) = 287$, where the radius of gyration of the flange $r_{yf} = 1.88 \text{ in}$. From tests BC_UMp_NB_n1_Lb15_FFR1 and BC_UMp_RB_n2_Lb10_FFR1, it can be inferred that when L/r_{yf} is less than 200, Eqs. (6-4a) and (6-4b) provide an accurate to conservative prediction of the bracing strength requirements from the test simulations. The most critical test with respect to the development of the beam strength is BC_UMp_NB_n1_Lb15_FFR1 where approximately 94 % of the beam's rigidly-braced strength is developed at the test limit load.

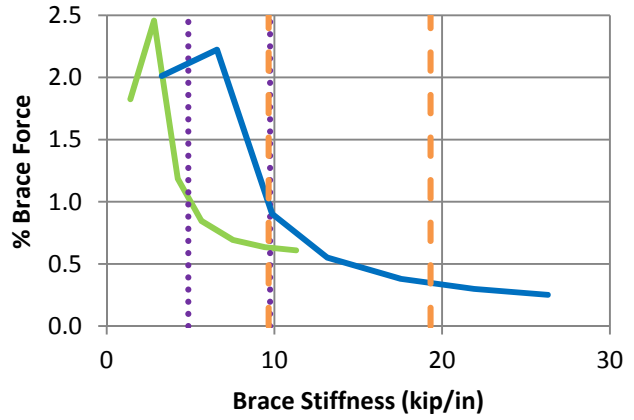
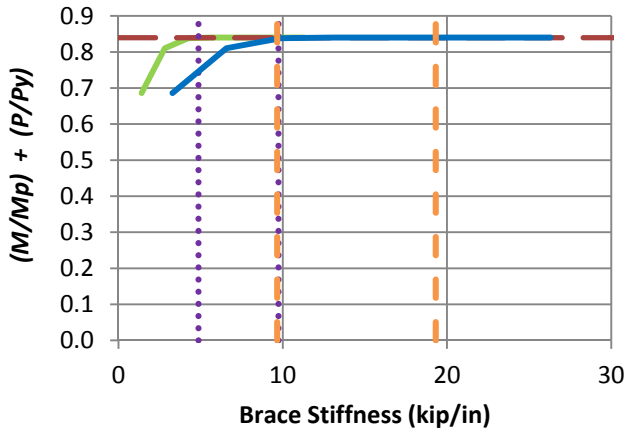
6.4.3 Beam-Columns Restrained by a Combination of Lateral and Torsional Bracing

Figures 6.13 through 6.20 show the results for beam-columns with combined lateral and torsional bracing. The lateral brace force in these figures is expressed as a percentage of P . The torsional brace force in these figures, considered as the corresponding shear force in the equivalent relative brace between the two member flanges, is expressed as percentage of $M/h_o + P/2$.

Tables 6.3 and 6.4 summarize the results for the bracing stiffness and strength requirements from Figs. 6.13 through 6.20. The lateral and torsional bracing stiffnesses corresponding to 96 % of the member rigidly braced strengths are denoted by the symbols β_{F96L} and β_{F96T} respectively.



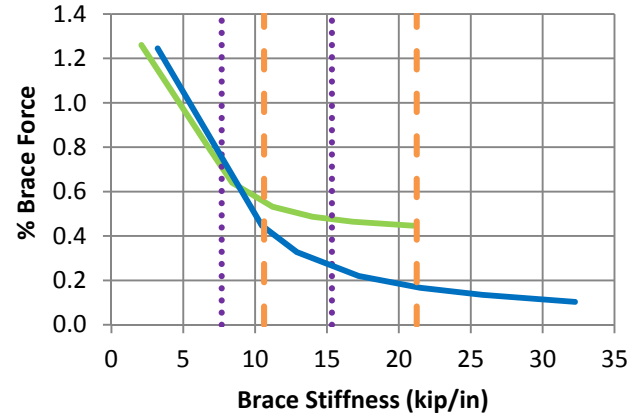
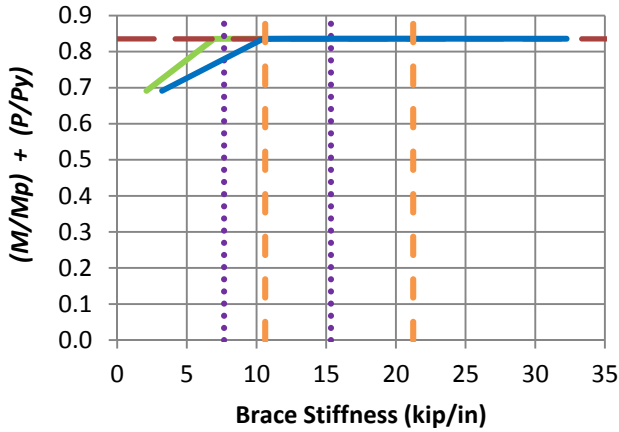
a) BC_UMp_CNTB_n1_Lb5_FFR-0.67



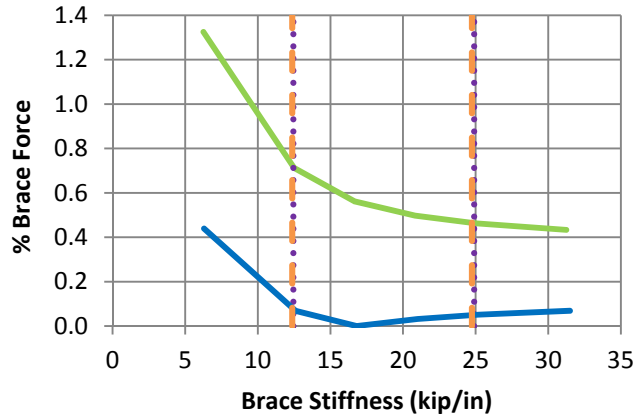
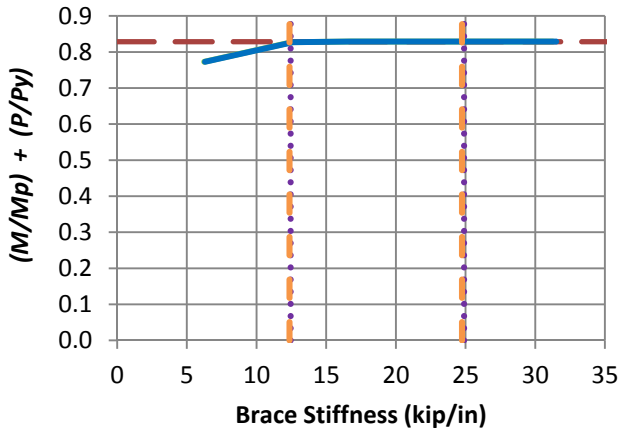
b) BC_UMp_CNTB_n1_Lb5_FFR-0.33

- - Rigidly-braced strength
- Test simulation results corresponding to torsional brace
- Test simulation results corresponding to lateral brace
- ⋯ β_{brL} and $0.5\beta_{brL}$
- - β_{brT} and $0.5\beta_{brT}$

Figure 6.13. Beam-column knuckle curves and brace force vs. brace stiffness plots for combined point (nodal) lateral and torsional bracing cases with $n = 1$, uniform bending with lateral bracing on the flange in flexural compression, and $L_b = 5$ ft.



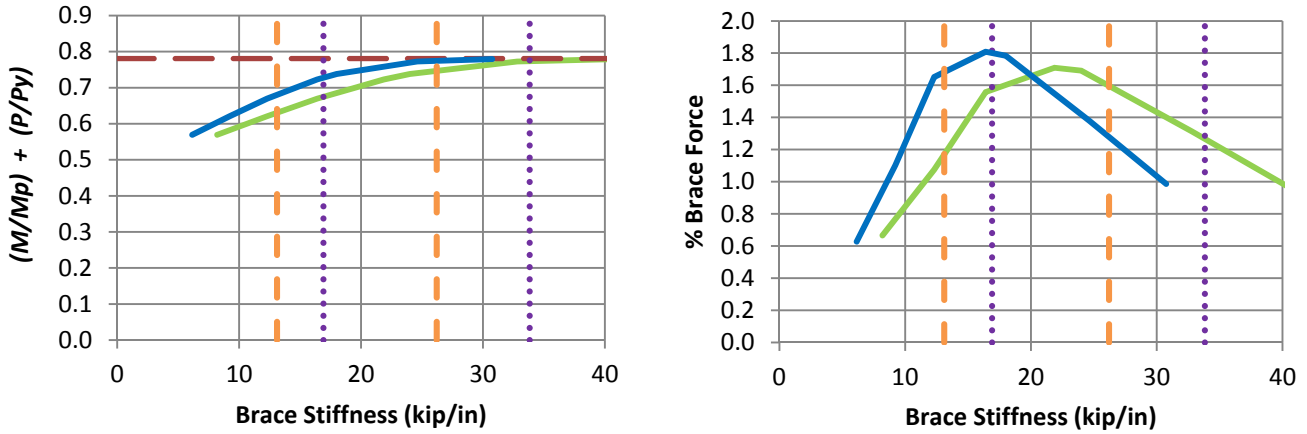
c) BC_UMp_CNTB_n1_Lb5_FFR0



d) BC_UMp_CNTB_n1_Lb5_FFR0.5

- — Rigidly-braced strength
- Test simulation results corresponding to torsional brace
- Test simulation results corresponding to lateral brace
- ⋯⋯⋯ β_{brL} and $0.5\beta_{brL}$
- - - β_{brT} and $0.5\beta_{brT}$

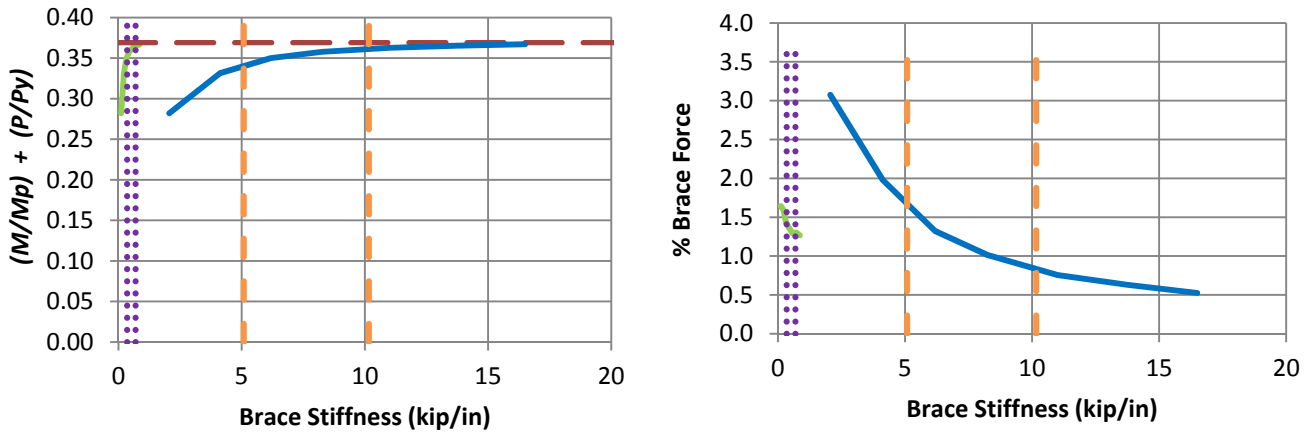
Fig. 6.13 (continued). Beam-column knuckle curves and brace force vs. brace stiffness plots for combined point (nodal) lateral and torsional bracing cases with $n = 1$, uniform bending with lateral bracing on the flange in flexural compression, and $L_b = 5$ ft.



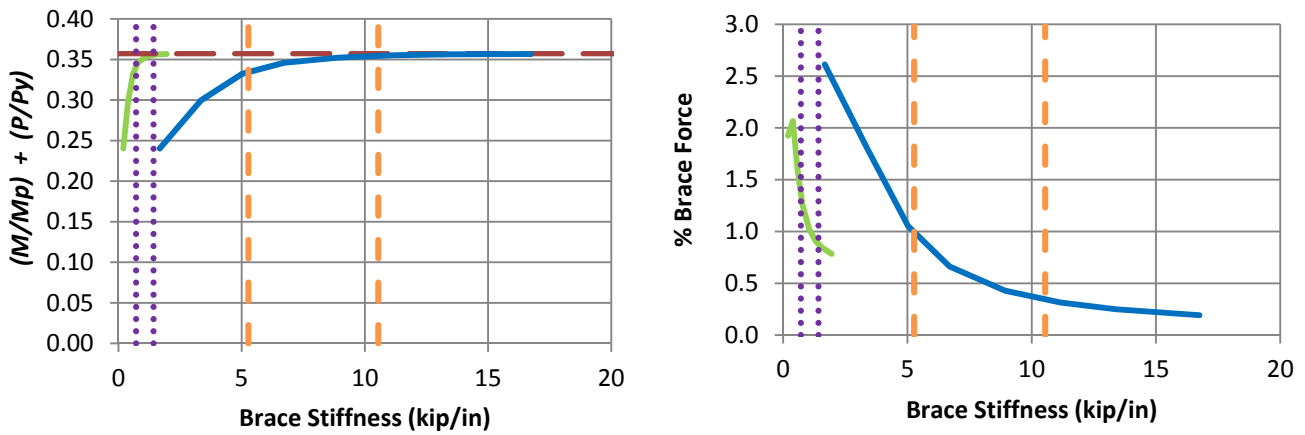
e) BC_UMp_CNTB_n1_Lb5_FFR1

- Rigidly-braced strength
- Test simulation results corresponding to torsional brace
- Test simulation results corresponding to lateral brace
- β_{brL} and $0.5\beta_{brL}$
- β_{brT} and $0.5\beta_{brT}$

Fig. 6.13 (continued). Beam-column knuckle curves and brace force vs. brace stiffness plots for combined point (nodal) lateral and torsional bracing cases with $n = 1$, uniform bending with lateral bracing on the flange in flexural compression, and $L_b = 5$ ft.



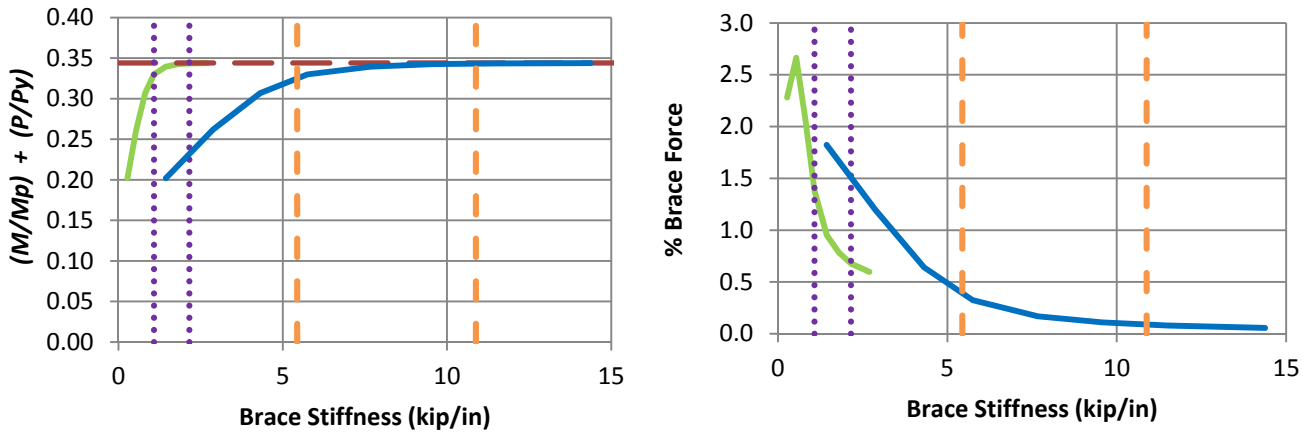
a) BC_UMp_CNTB_n1_Lb15_FFR-0.67



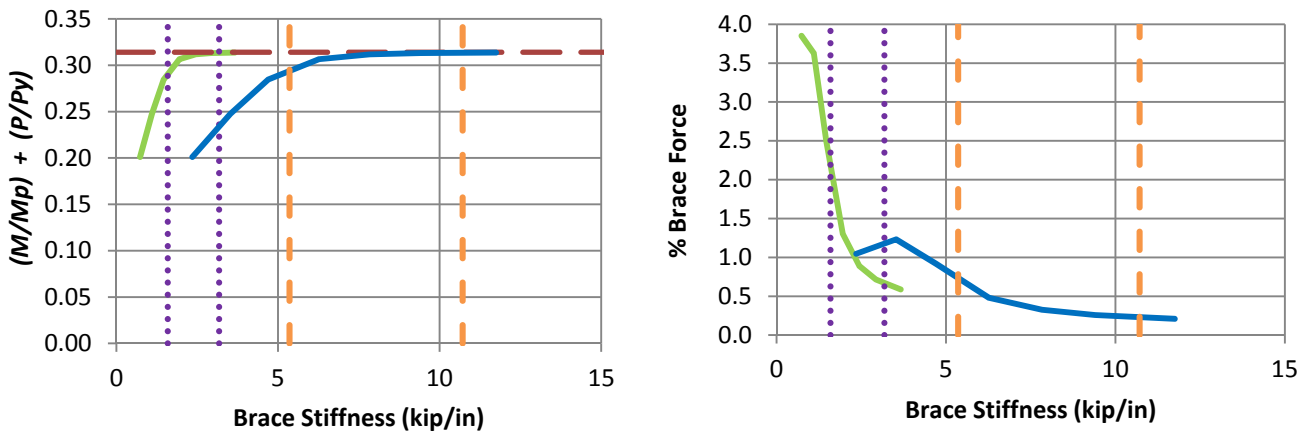
b) BC_UMp_CNTB_n1_Lb15_FFR-0.33

- Rigidly-braced strength
- Test simulation results corresponding to torsional brace
- Test simulation results corresponding to lateral brace
- β_{brL} and $0.5\beta_{brL}$
- β_{brT} and $0.5\beta_{brT}$

Figure 6.14. Beam-column knuckle curves and brace force vs. brace stiffness plots for combined point (nodal) lateral and torsional bracing cases with $n = 1$, uniform bending with lateral bracing on the flange in flexural compression, and $L_b = 15$ ft.



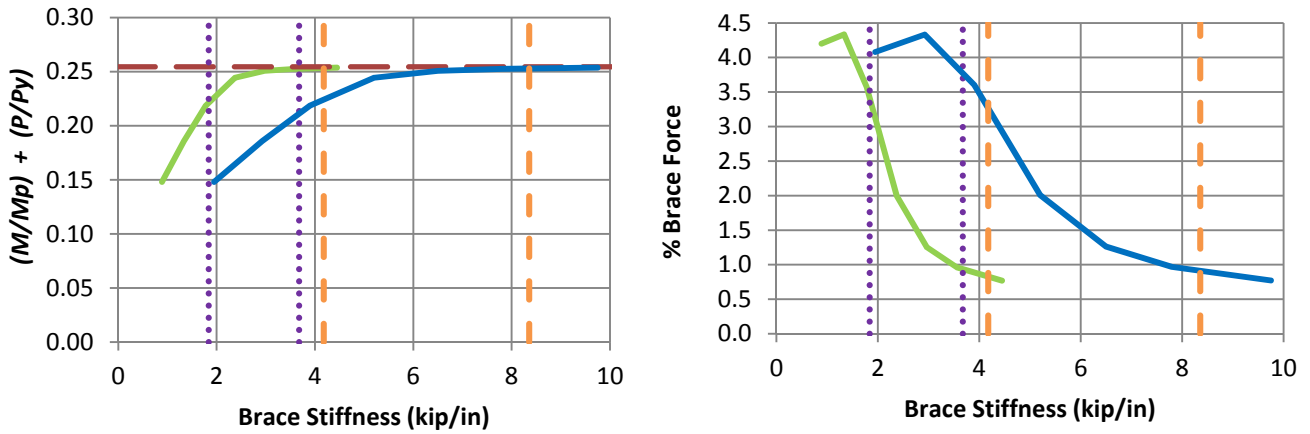
c) BC_UMp_CNTB_n1_Lb15_FFR0



d) BC_UMp_CNTB_n1_Lb15_FFR0.5

- Rigidly-braced strength
- Test simulation results corresponding to torsional brace
- Test simulation results corresponding to lateral brace
- β_{brL} and $0.5\beta_{brL}$
- - - β_{brT} and $0.5\beta_{brT}$

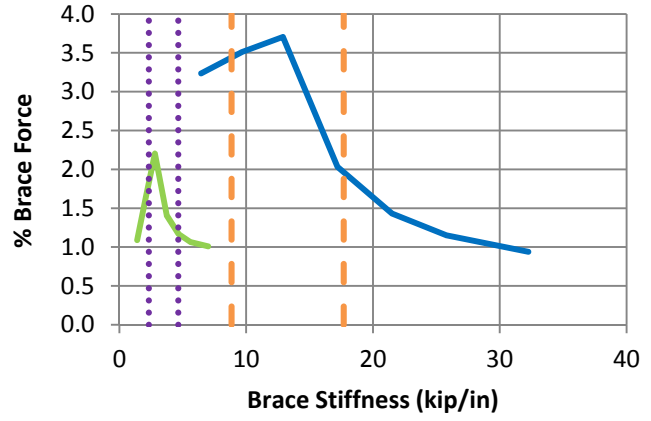
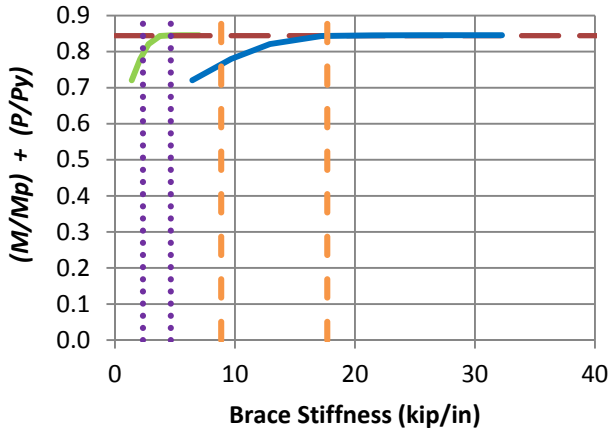
Fig. 6.14 (continued). Beam-column knuckle curves and brace force vs. brace stiffness plots for combined point (nodal) lateral and torsional bracing cases with $n = 1$, uniform bending with lateral bracing on the flange in flexural compression, and $L_b = 15$ ft.



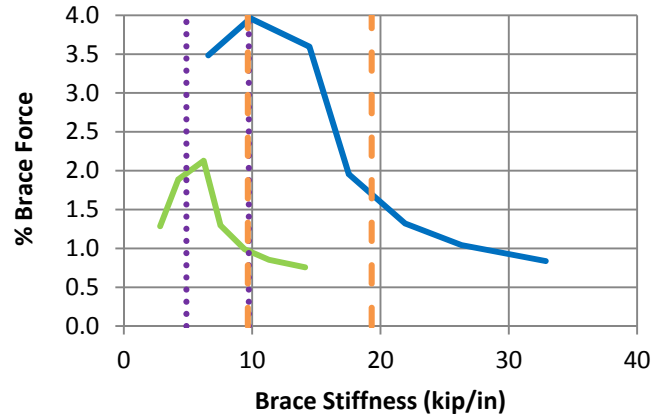
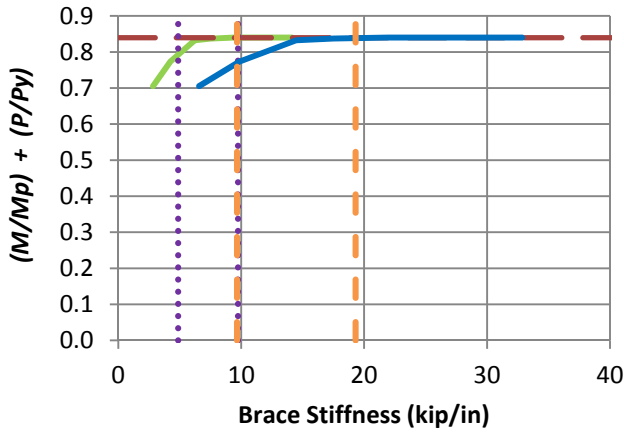
e) BC_UMp_CNTB_n1_Lb15_FFR1

- Rigidly-braced strength
- Test simulation results corresponding to torsional brace
- Test simulation results corresponding to lateral brace
- β_{brL} and $0.5\beta_{brL}$
- β_{brT} and $0.5\beta_{brT}$

Fig. 6.14 (continued). Beam-column knuckle curves and brace force vs. brace stiffness plots for combined point (nodal) lateral and torsional bracing cases with $n = 1$, uniform bending with lateral bracing on the flange in flexural compression, and $L_b = 15$ ft.



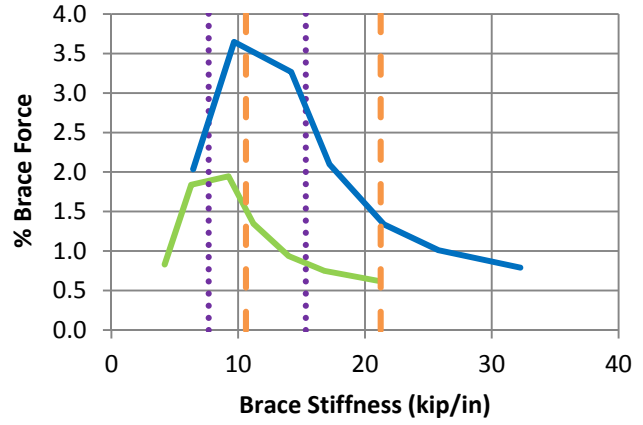
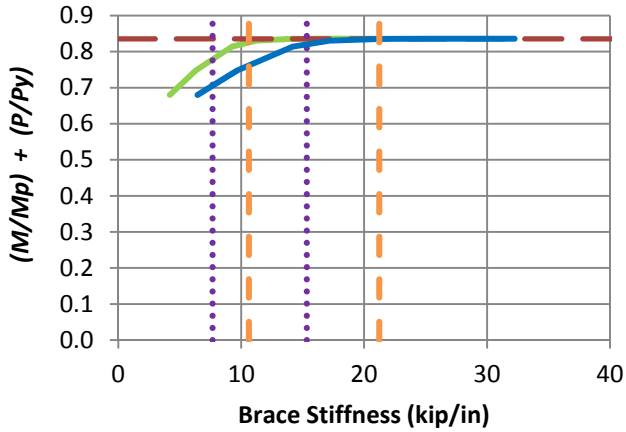
a) BC_UMn_CNTB_n1_Lb5_FFR-0.67



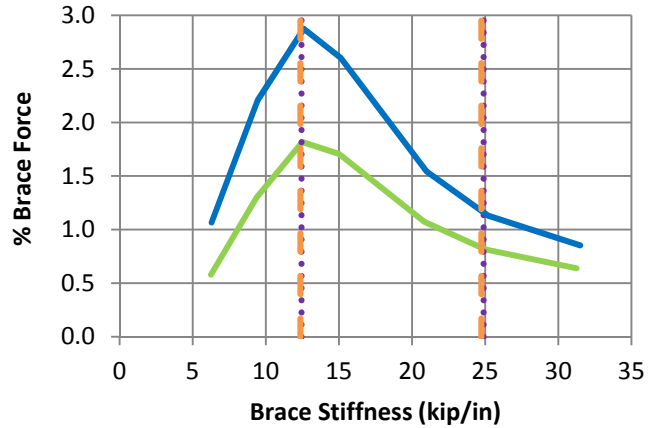
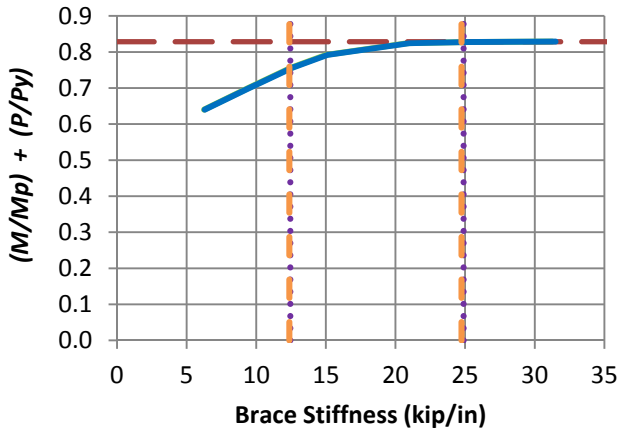
b) BC_UMn_CNTB_n1_Lb5_FFR-0.33

- — Rigidly-braced strength
- Test simulation results corresponding to torsional brace
- Test simulation results corresponding to lateral brace
- ⋯⋯⋯ β_{brL} and $0.5\beta_{brL}$
- - - β_{brT} and $0.5\beta_{brT}$

Figure 6.15. Beam-column knuckle curves and brace force vs. brace stiffness plots for combined point (nodal) lateral and torsional bracing cases with $n = 1$, uniform bending with lateral bracing on the flange in flexural tension, and $L_b = 5$ ft.



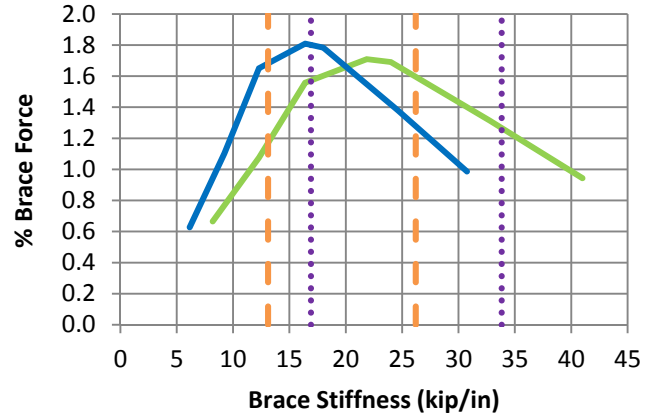
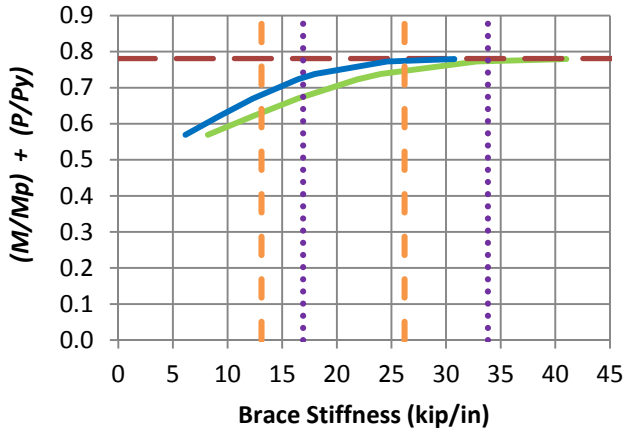
c) BC_UMn_CNTB_n1_Lb5_FFR0



d) BC_UMn_CNTB_n1_Lb5_FFR0.5

- Rigidly-braced strength
- Test simulation results corresponding to torsional brace
- Test simulation results corresponding to lateral brace
- β_{brL} and $0.5\beta_{brL}$
- β_{brT} and $0.5\beta_{brT}$

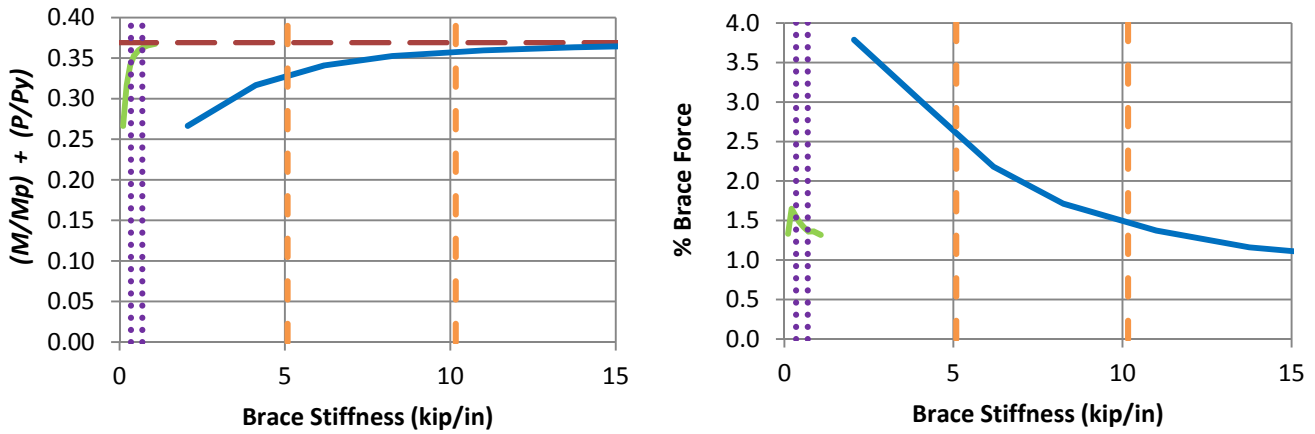
Fig. 6.15 (continued). Beam-column knuckle curves and brace force vs. brace stiffness plots for combined point (nodal) lateral and torsional bracing cases with $n = 1$, uniform bending with lateral bracing on the flange in flexural tension, and $L_b = 5$ ft.



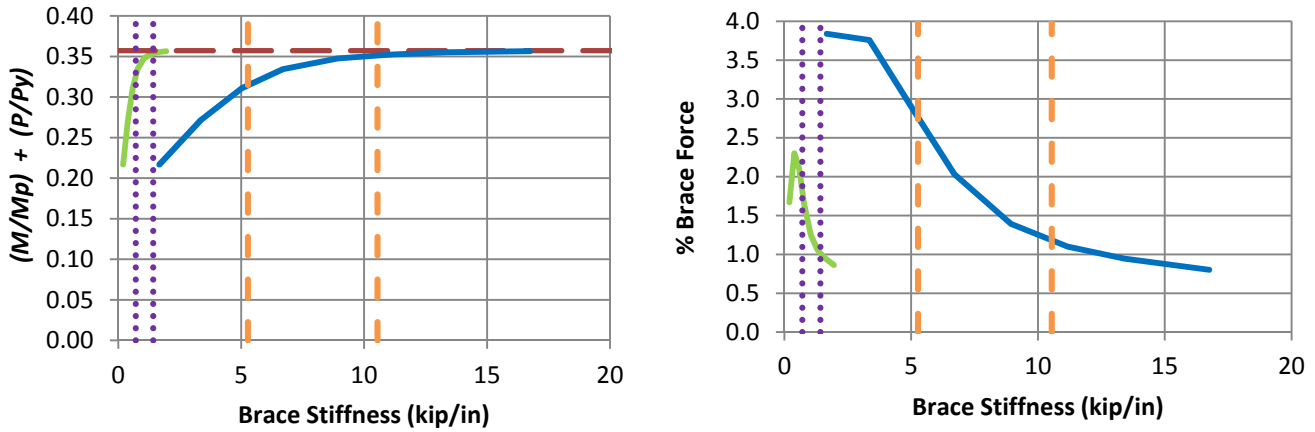
e) BC_UMn_CNTB_n1_Lb5_FFR1

- Rigidly-braced strength
- Test simulation results corresponding to torsional brace
- Test simulation results corresponding to lateral brace
- β_{brL} and $0.5\beta_{brL}$
- β_{brT} and $0.5\beta_{brT}$

Fig. 6.15 (continued). Beam-column knuckle curves and brace force vs. brace stiffness plots for combined point (nodal) lateral and torsional bracing cases with $n = 1$, uniform bending with lateral bracing on the flange in flexural tension, and $L_b = 5$ ft.



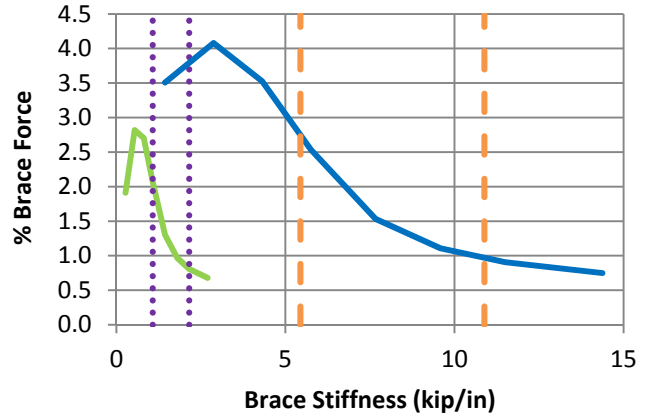
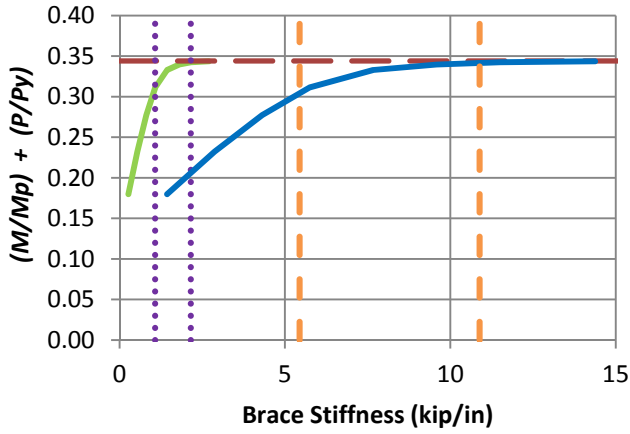
a) BC_UMn_CNTB_n1_Lb15_FFR-0.67



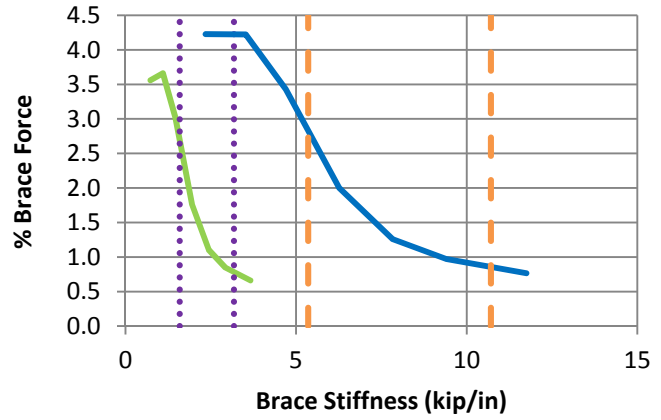
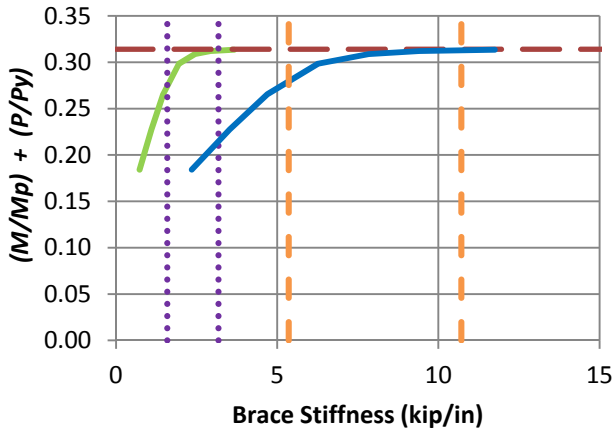
b) BC_UMn_CNTB_n1_Lb15_FFR-0.33

- Rigidly-braced strength
- Test simulation results corresponding to torsional brace
- Test simulation results corresponding to lateral brace
- β_{brL} and $0.5\beta_{brL}$
- β_{brT} and $0.5\beta_{brT}$

Figure 6.16. Beam-column knuckle curves and brace force vs. brace stiffness plots for combined point (nodal) lateral and torsional bracing cases with $n = 1$, uniform bending with lateral bracing on the flange in flexural tension, and $L_b = 15$ ft.



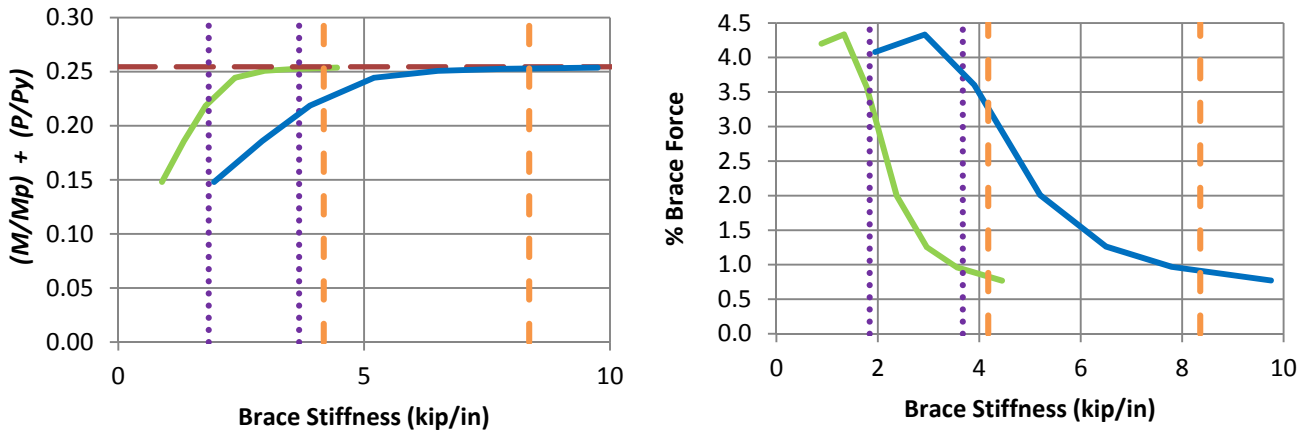
c) BC_UMn_CNTB_n1_Lb15_FFR0



d) BC_UMn_CNTB_n1_Lb15_FFR0.5

- Rigidly-braced strength
- Test simulation results corresponding to torsional brace
- Test simulation results corresponding to lateral brace
- β_{brL} and $0.5\beta_{brL}$
- — — β_{brT} and $0.5\beta_{brT}$

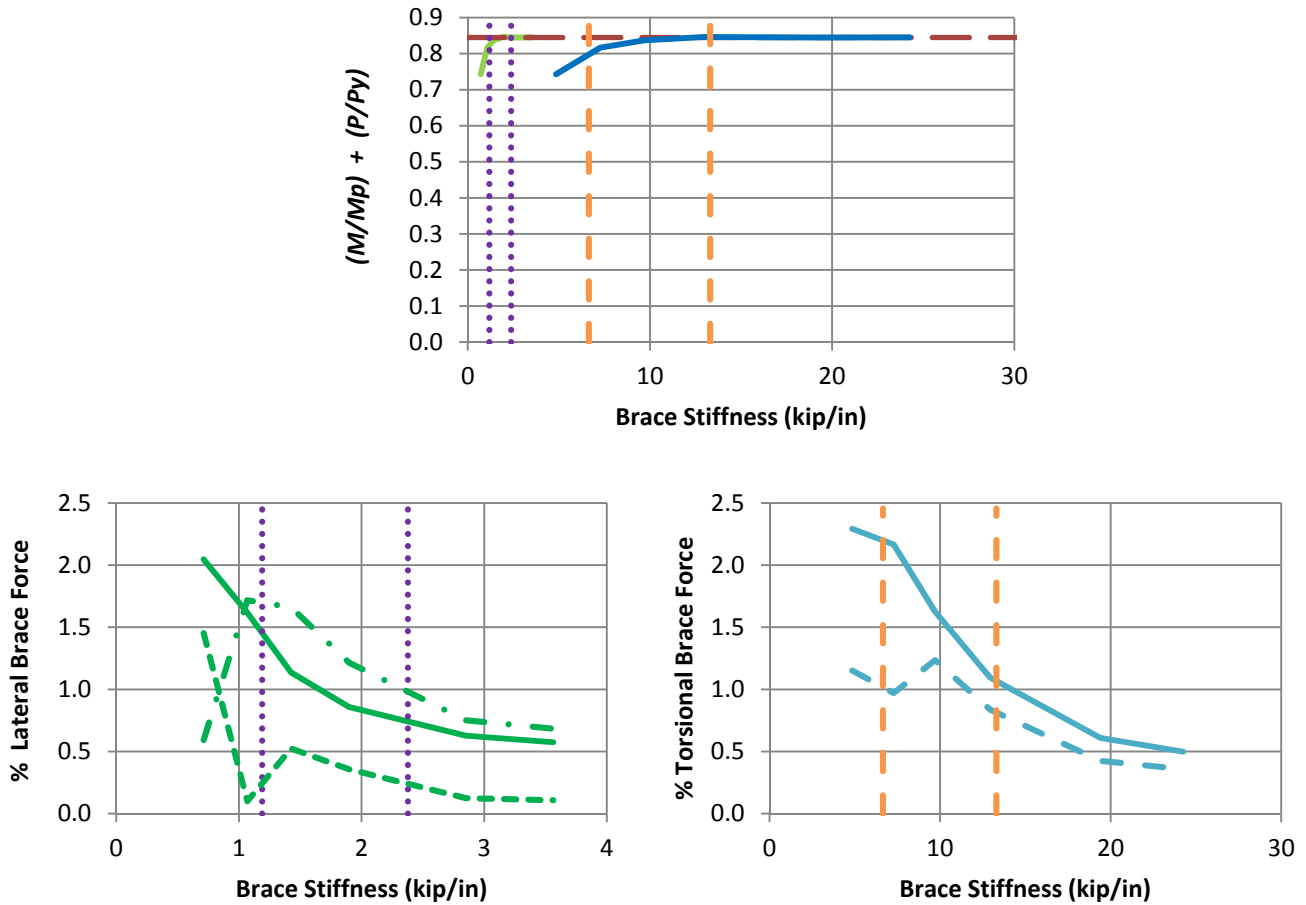
Fig. 6.16 (continued). Beam-column knuckle curves and brace force vs. brace stiffness plots for combined point (nodal) lateral and torsional bracing cases with $n = 1$, uniform bending with lateral bracing on the flange in flexural tension, and $L_b = 15$ ft.



e) BC_UMn_CNTB_n1_Lb15_FFR1

- Rigidly-braced strength
- Test simulation results corresponding to torsional brace
- Test simulation results corresponding to lateral brace
- β_{brL} and $0.5\beta_{brL}$
- β_{brT} and $0.5\beta_{brT}$

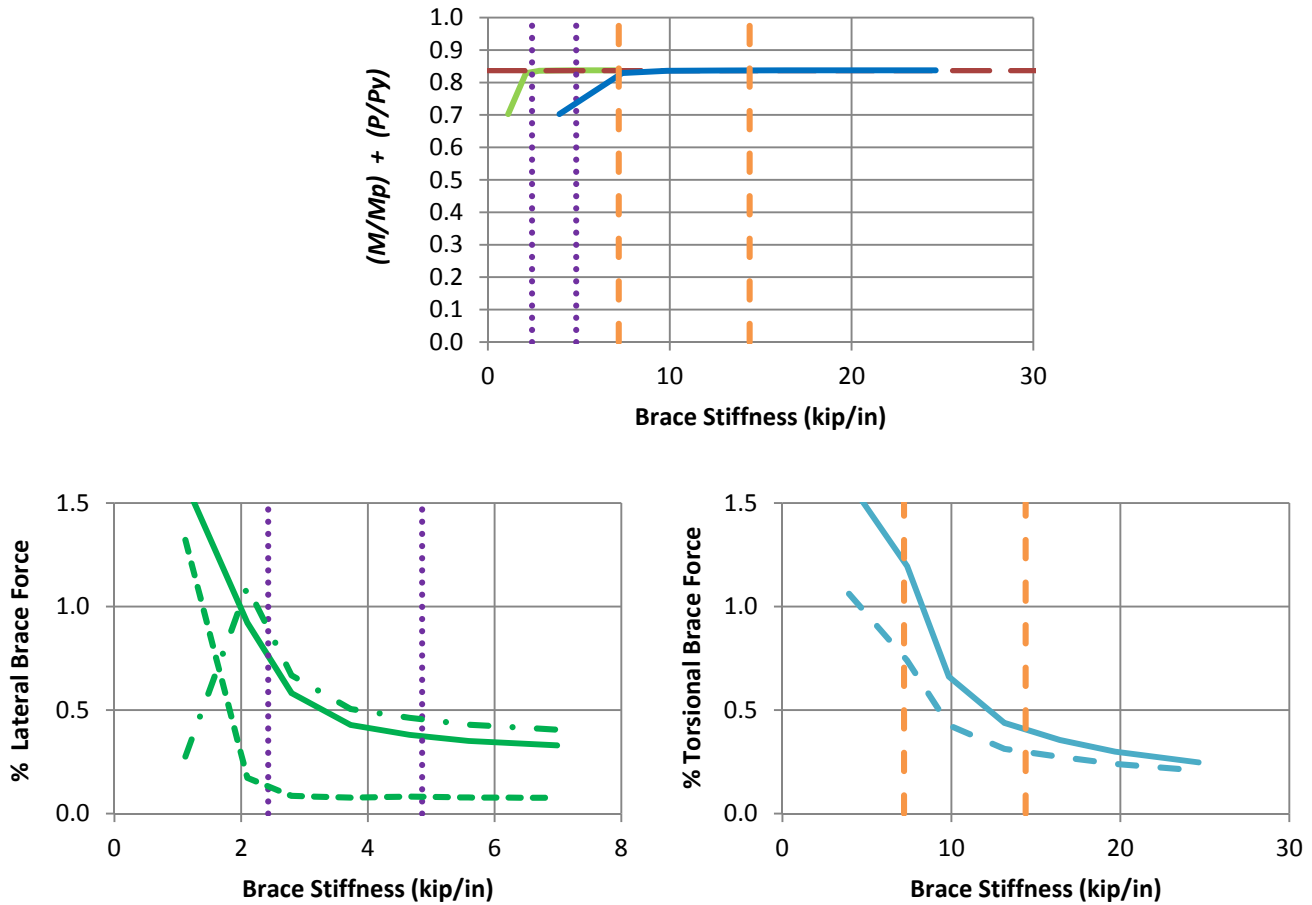
Fig. 6.16 (continued). Beam-column knuckle curves and brace force vs. brace stiffness plots for combined point (nodal) lateral and torsional bracing cases with $n = 1$, uniform bending with lateral bracing on the flange in flexural tension, and $L_b = 15$ ft.



a) BC_UMp_CRTB_n2_Lb5_FFR-0.67

- Rigidly-braced strength
- Test simulation results corresponding to torsional brace
- Test simulation results corresponding to lateral brace
- β_{brL} and $0.5\beta_{brL}$
- - - β_{brT} and $0.5\beta_{brT}$
- Left end panel shear force
- - - Right end panel shear force
- Torsional brace force 1
- - - Middle panel shear force
- - - Torsional brace force 2

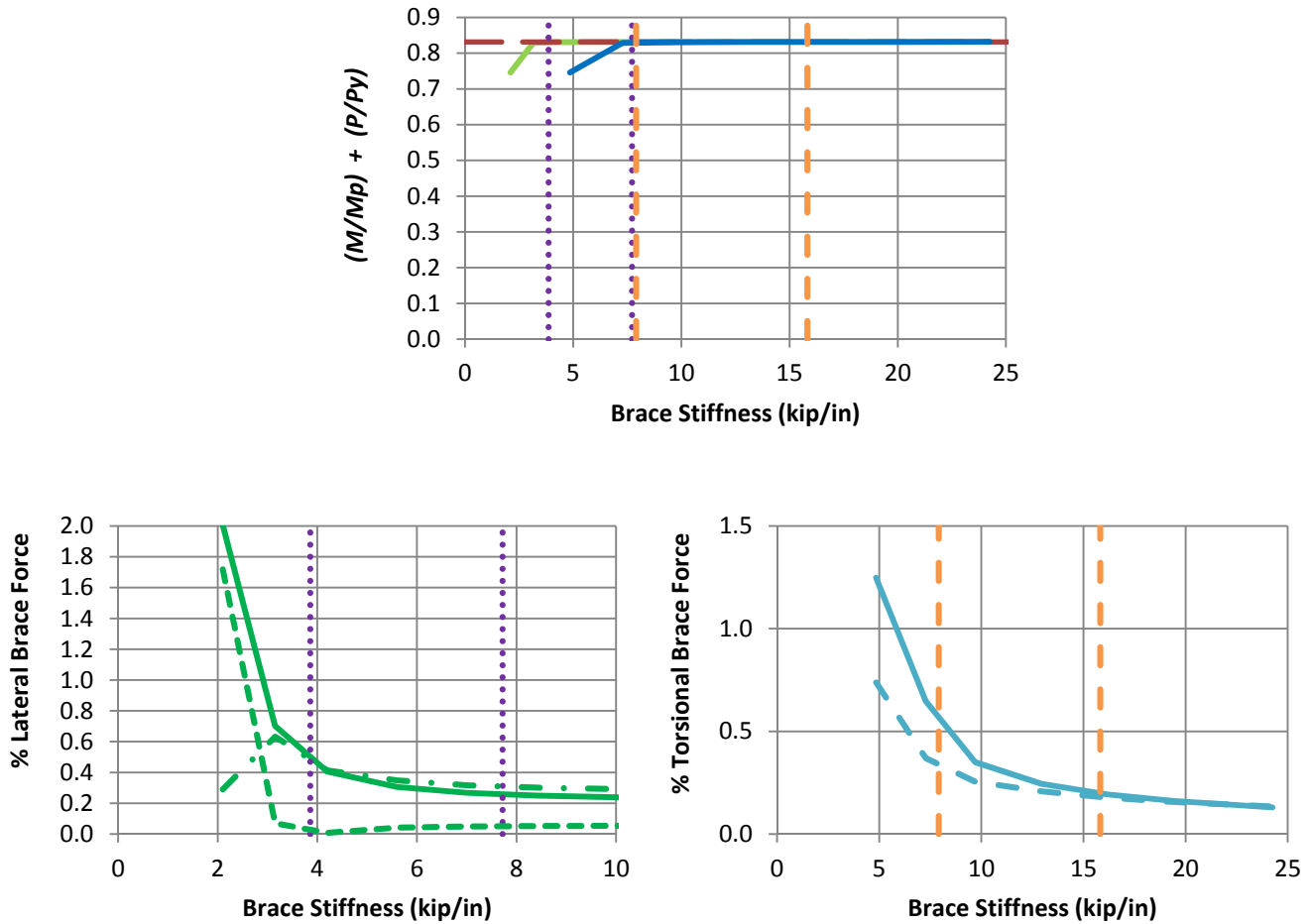
Figure 6.17. Beam-column knuckle curves and brace force vs. brace stiffness plots for combined shear panel (relative) lateral and torsional bracing cases with $n = 2$, uniform bending with lateral bracing on the flange in flexural compression, and $L_b = 5$ ft.



b) BC_UMp_CRTB_n2_Lb5_FFR-0.33

- Rigidly-braced strength
- Test simulation results corresponding to torsional brace
- Test simulation results corresponding to lateral brace
- ⋯ β_{brL} and $0.5\beta_{brL}$
- - β_{brT} and $0.5\beta_{brT}$
- Left end panel shear force
- - Right end panel shear force
- · - Middle panel shear force
- Torsional brace force 1
- - Torsional brace force 2

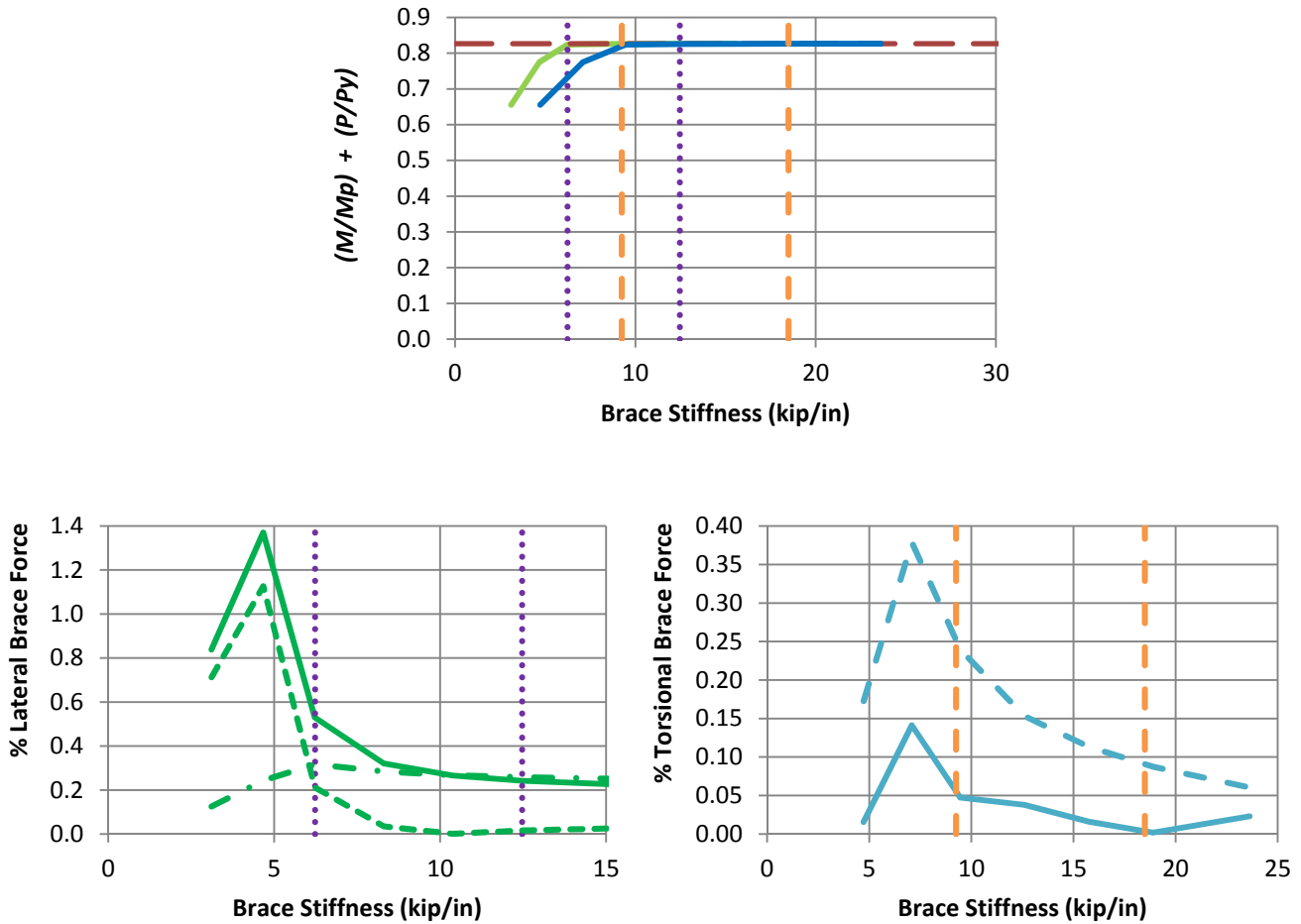
Fig. 6.17 (continued). Beam-column knuckle curves and brace force vs. brace stiffness plots for combined shear panel (relative) lateral and torsional bracing cases with $n = 2$, uniform bending with lateral bracing on the flange in flexural compression, and $L_b = 5$ ft.



c) BC_UMp_CRTB_n2_Lb5_FFR0

- Rigidly-braced strength
- Test simulation results corresponding to torsional brace
- Test simulation results corresponding to lateral brace
- β_{brL} and $0.5\beta_{brL}$
- β_{brT} and $0.5\beta_{brT}$
- Left end panel shear force
- Right end panel shear force
- Middle panel shear force
- Torsional brace force 1
- Torsional brace force 2

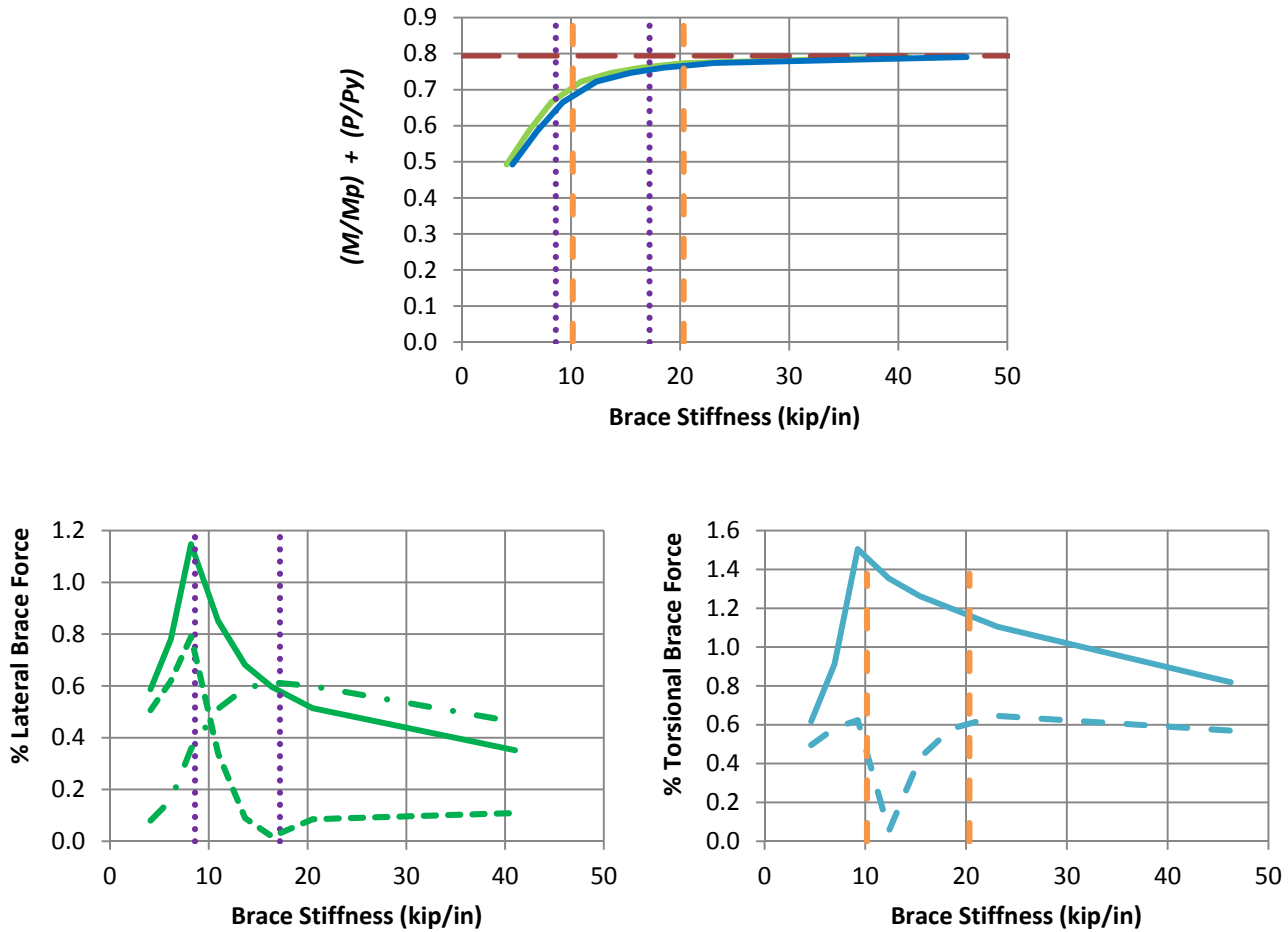
Fig. 6.17 (continued). Beam-column knuckle curves and brace force vs. brace stiffness plots for combined shear panel (relative) lateral and torsional bracing cases with $n = 2$, uniform bending with lateral bracing on the flange in flexural compression, and $L_b = 5$ ft.



d) BC_UMp_CRTB_n2_Lb5_FFR0.5

- Rigidly-braced strength
- Test simulation results corresponding to torsional brace
- Test simulation results corresponding to lateral brace
- β_{brL} and $0.5\beta_{brL}$
- - - β_{brT} and $0.5\beta_{brT}$
- Left end panel shear force
- - - Right end panel shear force
- . - Middle panel shear force
- Torsional brace force 1
- - - Torsional brace force 2

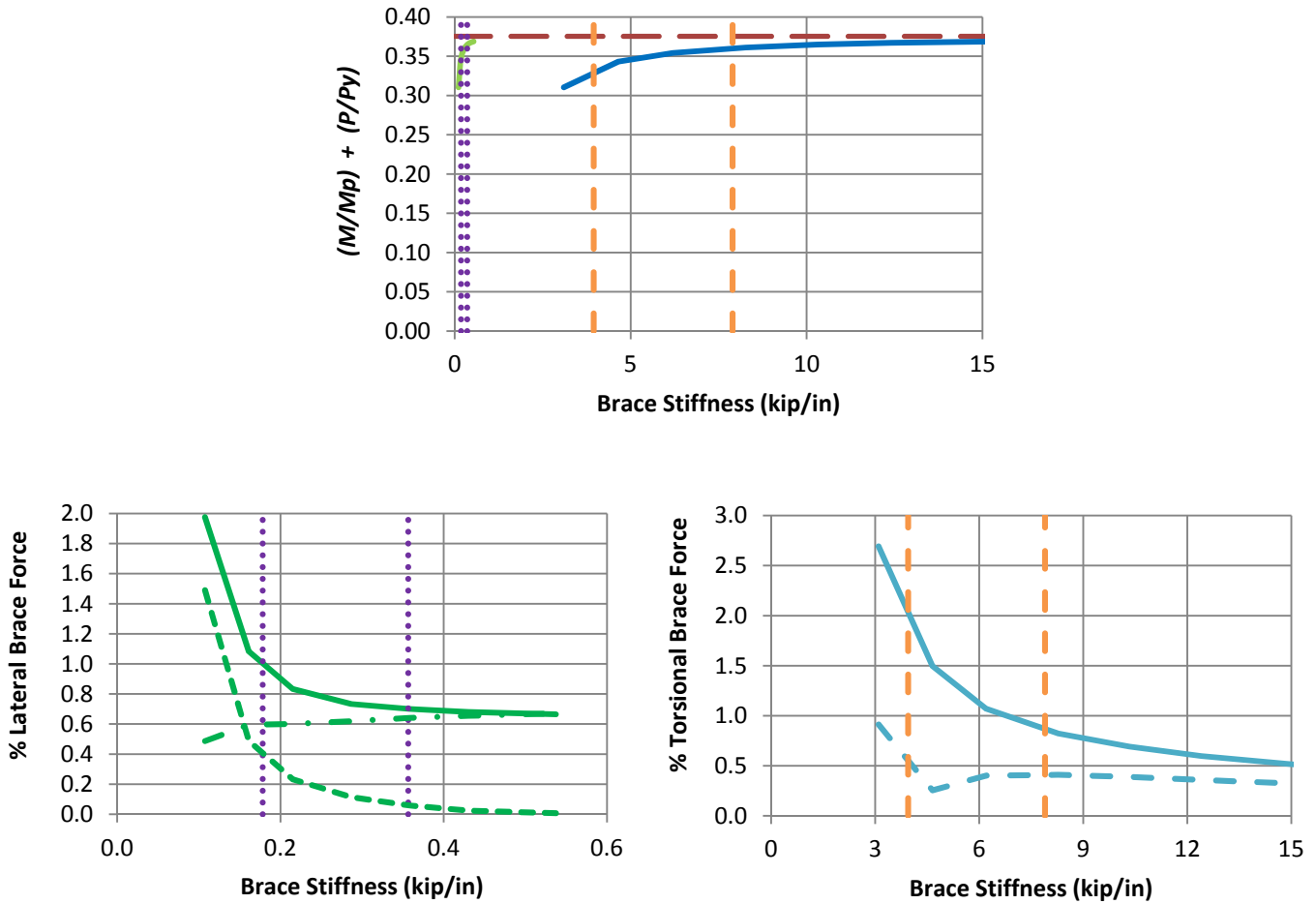
Fig. 6.17 (continued). Beam-column knuckle curves and brace force vs. brace stiffness plots for combined shear panel (relative) lateral and torsional bracing cases with $n = 2$, uniform bending with lateral bracing on the flange in flexural compression, and $L_b = 5$ ft.



e) BC_UMp_CRTB_n2_Lb5_FFR1

- Rigidly-braced strength
- Test simulation results corresponding to torsional brace
- Test simulation results corresponding to lateral brace
- β_{brL} and $0.5\beta_{brL}$
- - - β_{brT} and $0.5\beta_{brT}$
- Left end panel shear force
- - - Right end panel shear force
- . - Middle panel shear force
- Torsional brace force 1
- - - Torsional brace force 2

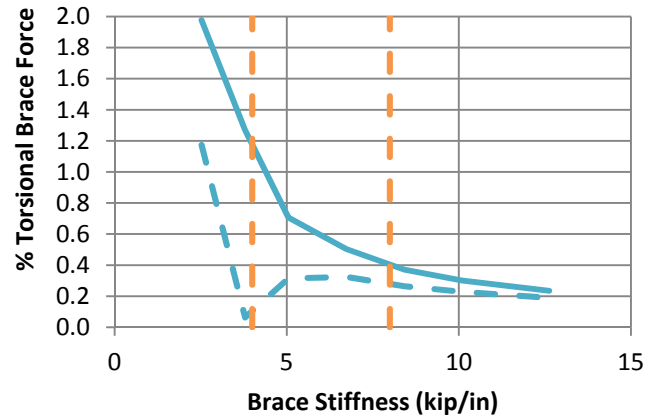
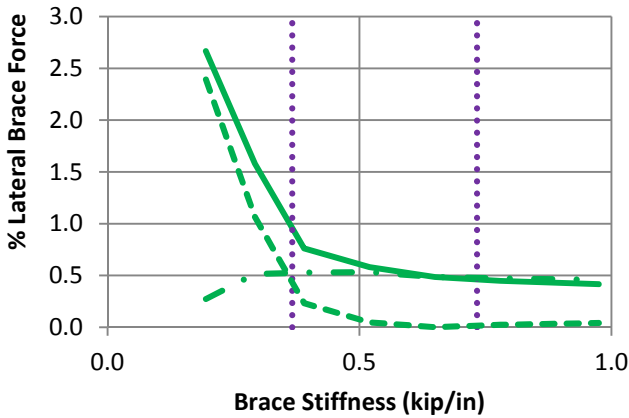
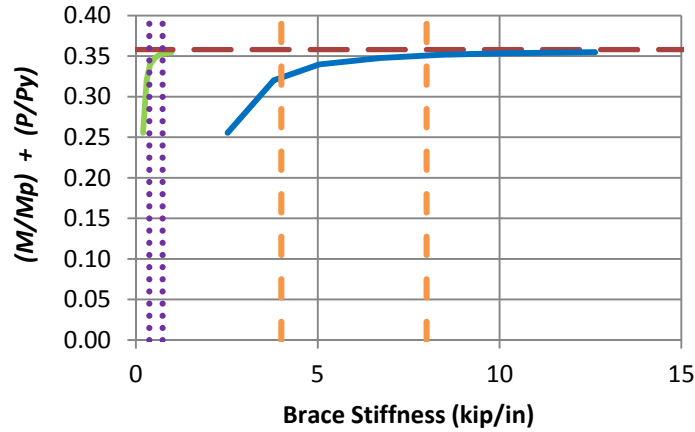
Fig. 6.17 (continued). Beam-column knuckle curves and brace force vs. brace stiffness plots for combined shear panel (relative) lateral and torsional bracing cases with $n = 2$, uniform bending with lateral bracing on the flange in flexural compression, and $L_b = 5$ ft.



a) BC_UMp_CRTB_n2_Lb15_FFR-0.67

- Rigidly-braced strength
- Test simulation results corresponding to torsional brace
- Test simulation results corresponding to lateral brace
- β_{brL} and $0.5\beta_{brL}$
- β_{brT} and $0.5\beta_{brT}$
- Left end panel shear force
- Right end panel shear force
- Middle panel shear force
- Torsional brace force 1
- Torsional brace force 2

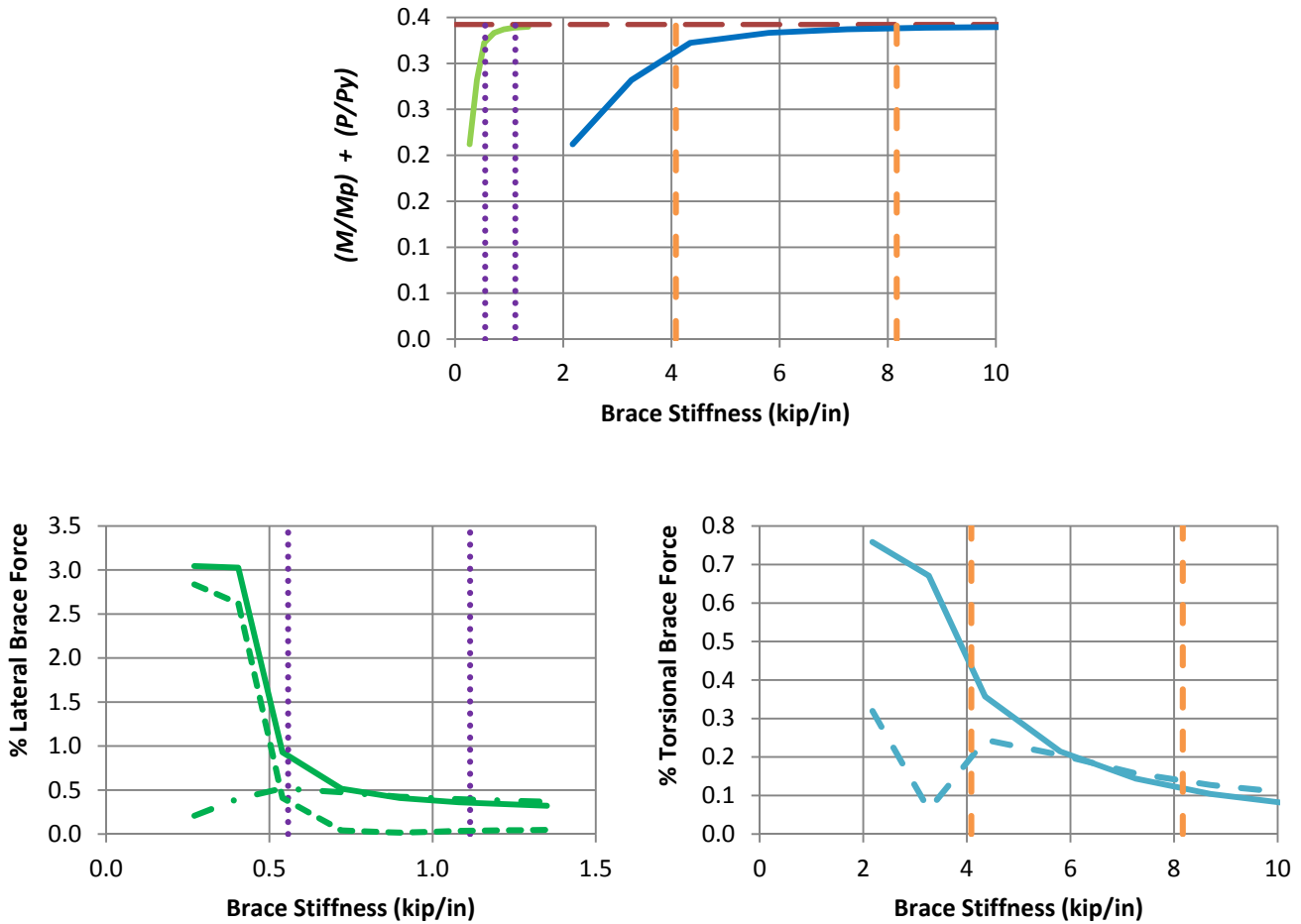
Figure 6.18. Beam-column knuckle curves and brace force vs. brace stiffness plots for combined shear panel (relative) lateral and torsional bracing cases with $n = 2$, uniform bending with lateral bracing on the flange in flexural compression, and $L_b = 15$ ft.



b) BC_UMp_CRTB_n2_Lb15_FFR-0.33

- — Rigidly-braced strength
- Test simulation results corresponding to torsional brace
- Test simulation results corresponding to lateral brace
- ⋯⋯⋯ β_{brL} and $0.5\beta_{brL}$
- - - β_{brT} and $0.5\beta_{brT}$
- Left end panel shear force
- - - Right end panel shear force
- · - Middle panel shear force
- Torsional brace force 1
- - - Torsional brace force 2

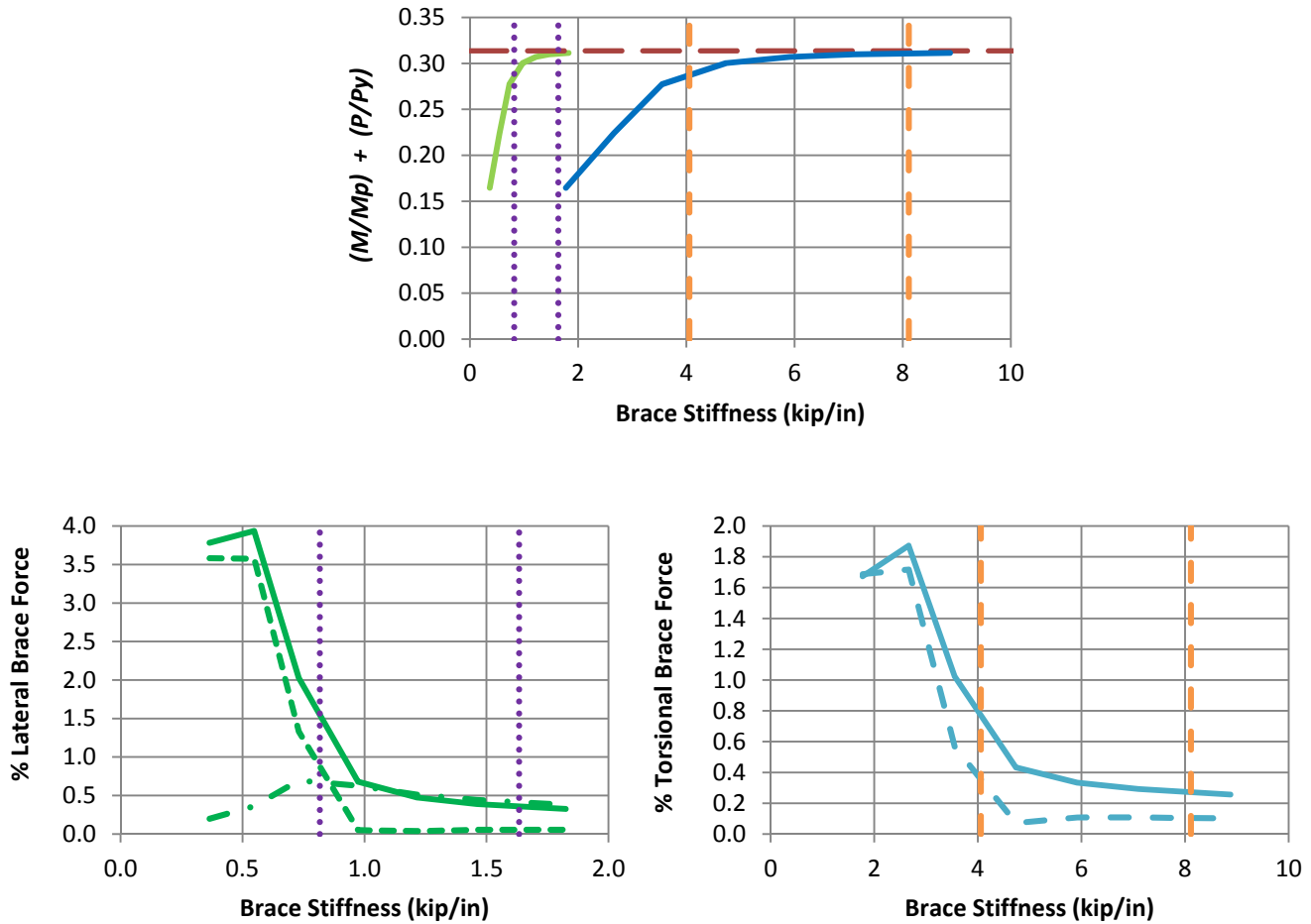
Fig. 6.18 (continued). Beam-column knuckle curves and brace force vs. brace stiffness plots for combined shear panel (relative) lateral and torsional bracing cases with $n = 2$, uniform bending with lateral bracing on the flange in flexural compression, and $L_b = 15$ ft.



c) BC_UMp_CRTB_n2_Lb15_FFR0

- Rigidly-braced strength
- Test simulation results corresponding to torsional brace
- Test simulation results corresponding to lateral brace
- β_{brL} and $0.5\beta_{brL}$
- β_{brT} and $0.5\beta_{brT}$
- Left end panel shear force
- Right end panel shear force
- Middle panel shear force
- Torsional brace force 1
- Torsional brace force 2

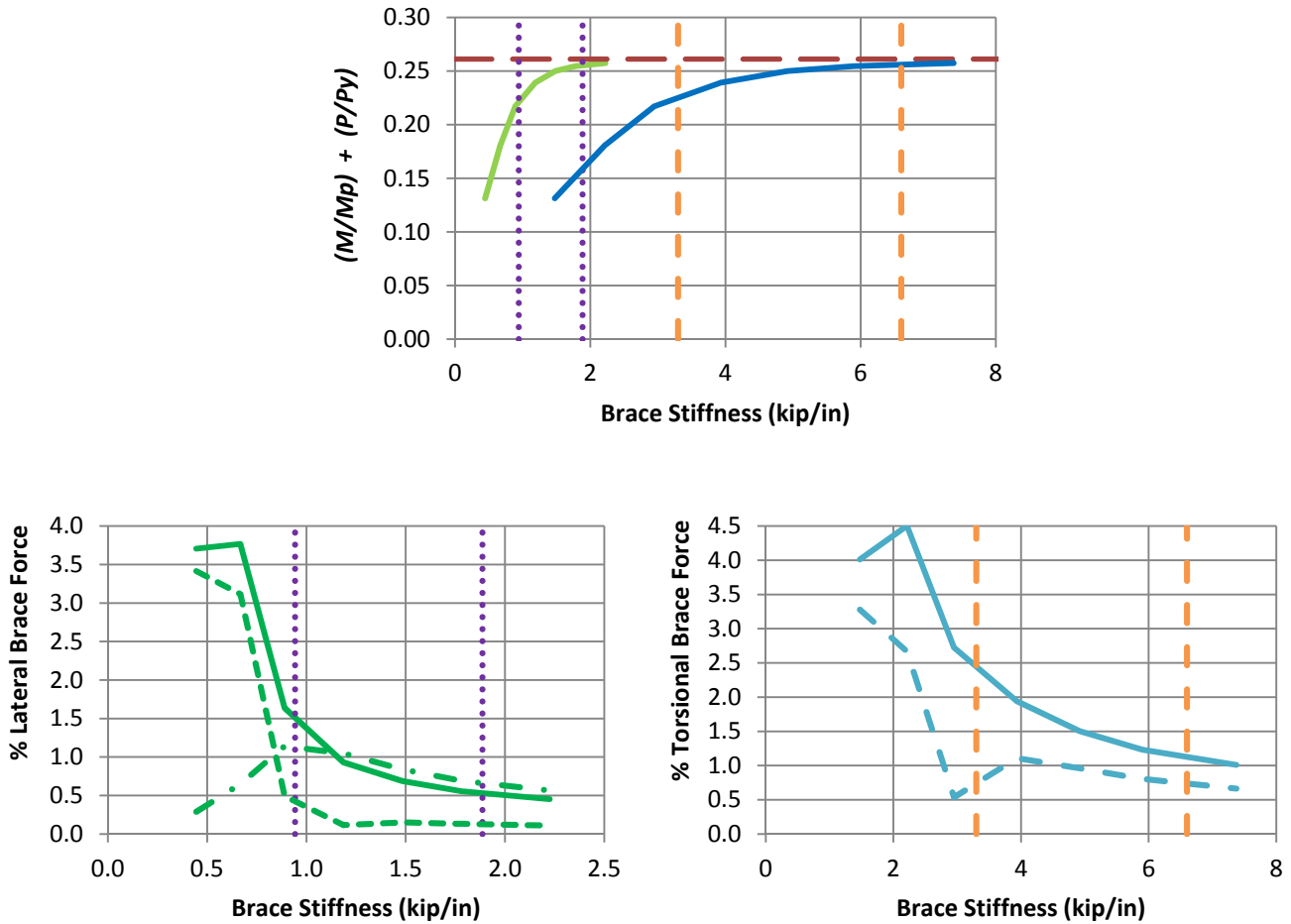
Fig. 6.18 (continued). Beam-column knuckle curves and brace force vs. brace stiffness plots for combined shear panel (relative) lateral and torsional bracing cases with $n = 2$, uniform bending with lateral bracing on the flange in flexural compression, and $L_b = 15$ ft.



d) BC_UMp_CRTB_n2_Lb15_FFR0.5

- Rigidly-braced strength
- Test simulation results corresponding to torsional brace
- Test simulation results corresponding to lateral brace
- β_{brL} and $0.5\beta_{brL}$
- — — β_{brT} and $0.5\beta_{brT}$
- Left end panel shear force
- — — Right end panel shear force
- • — Middle panel shear force
- Torsional brace force 1
- — — Torsional brace force 2

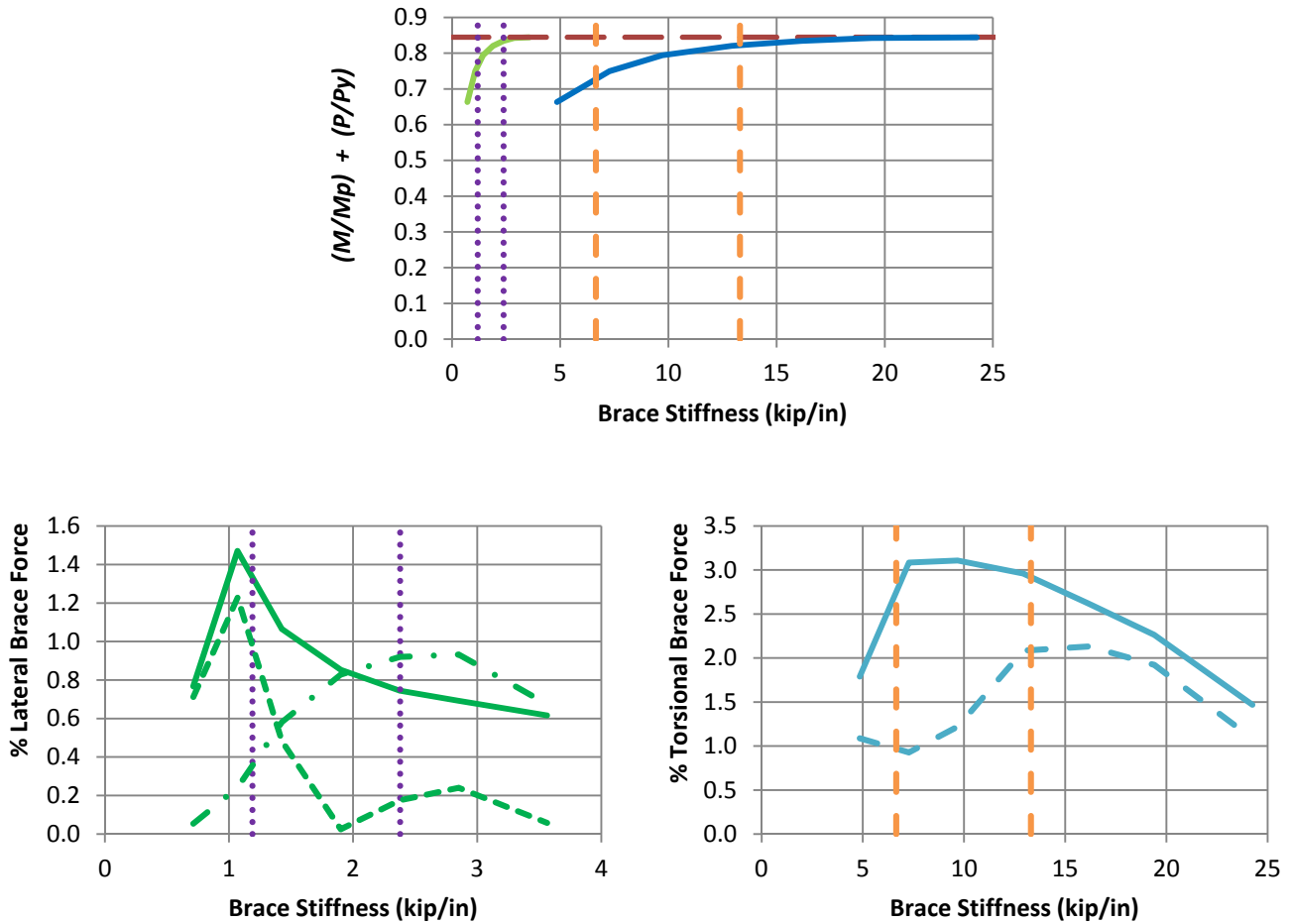
Fig. 6.18 (continued). Beam-column knuckle curves and brace force vs. brace stiffness plots for combined shear panel (relative) lateral and torsional bracing cases with $n = 2$, uniform bending with lateral bracing on the flange in flexural compression, and $L_b = 15$ ft.



e) BC_UMp_CRTB_n2_Lb15_FFR1

- Rigidly-braced strength
- Test simulation results corresponding to torsional brace
- Test simulation results corresponding to lateral brace
- β_{brL} and $0.5\beta_{brL}$
- β_{brT} and $0.5\beta_{brT}$
- Left end panel shear force
- Right end panel shear force
- Middle panel shear force
- Torsional brace force 1
- Torsional brace force 2

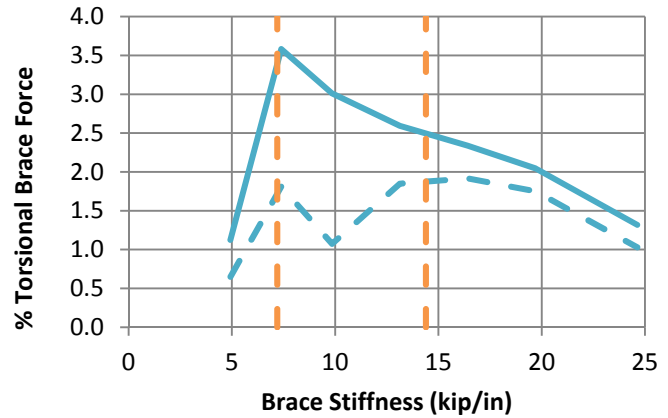
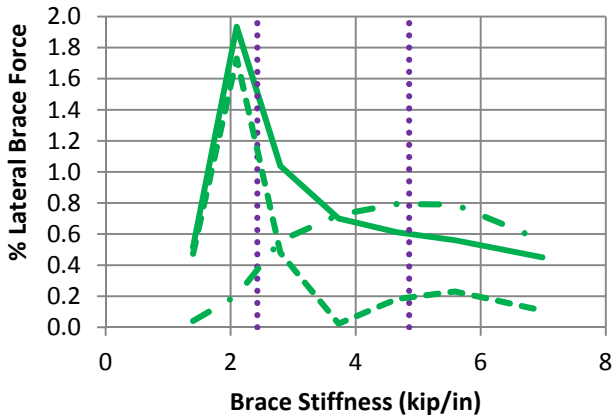
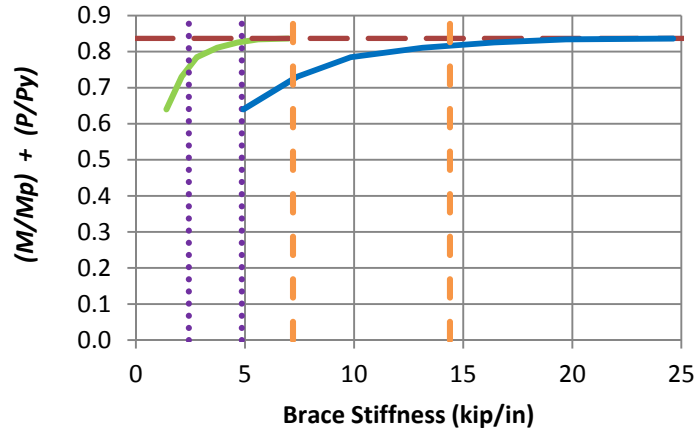
Fig. 6.18 (continued). Beam-column knuckle curves and brace force vs. brace stiffness plots for combined shear panel (relative) lateral and torsional bracing cases with $n = 2$, uniform bending with lateral bracing on the flange in flexural compression, and $L_b = 15$ ft.



a) BC_UMn_CRTB_n2_Lb5_FFR-0.67

- Rigidly-braced strength
- Test simulation results corresponding to torsional brace
- Test simulation results corresponding to lateral brace
- β_{brL} and $0.5\beta_{brL}$
- - - β_{brT} and $0.5\beta_{brT}$
- Left end panel shear force
- - - Right end panel shear force
- . - Middle panel shear force
- Torsional brace force 1
- - - Torsional brace force 2

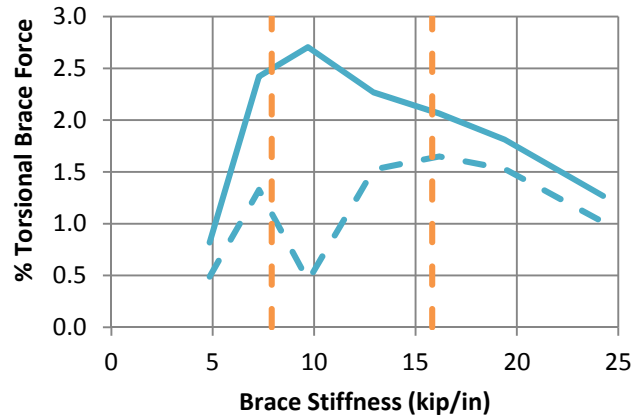
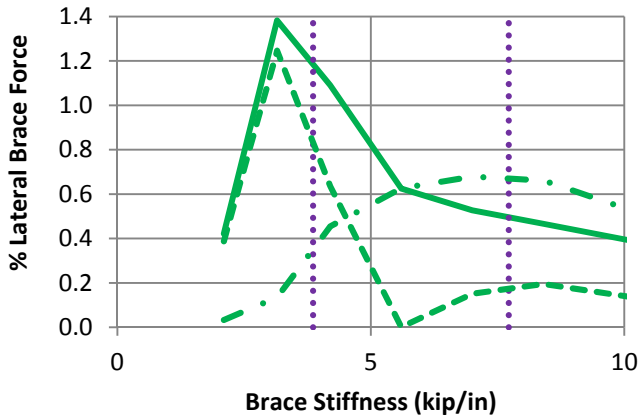
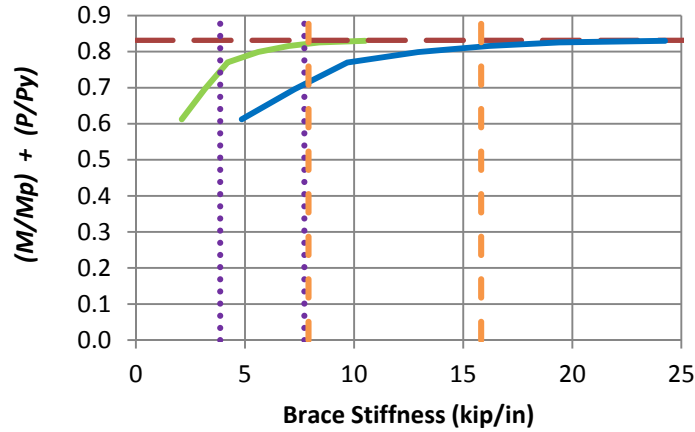
Figure 6.19. Beam-column knuckle curves and brace force vs. brace stiffness plots for combined shear panel (relative) lateral and torsional bracing cases with $n = 2$, uniform bending with lateral bracing on the flange in flexural tension, and $L_b = 5$ ft.



b) BC_UMn_CRTB_n2_Lb5_FFR-0.33

- - Rigidly-braced strength
- Test simulation results corresponding to torsional brace
- Test simulation results corresponding to lateral brace
- ⋯ β_{brL} and $0.5\beta_{brL}$
- - β_{brT} and $0.5\beta_{brT}$
- Left end panel shear force
- - Right end panel shear force
- · - Middle panel shear force
- Torsional brace force 1
- - Torsional brace force 2

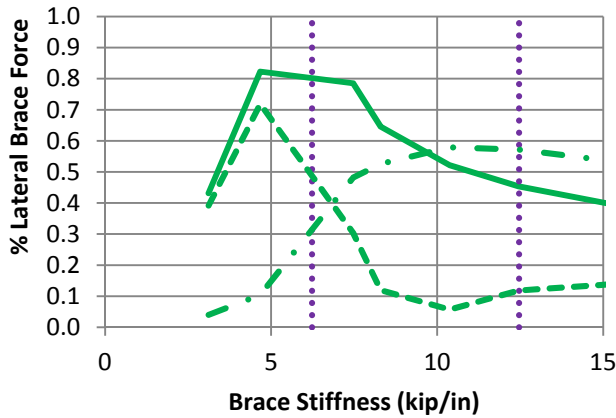
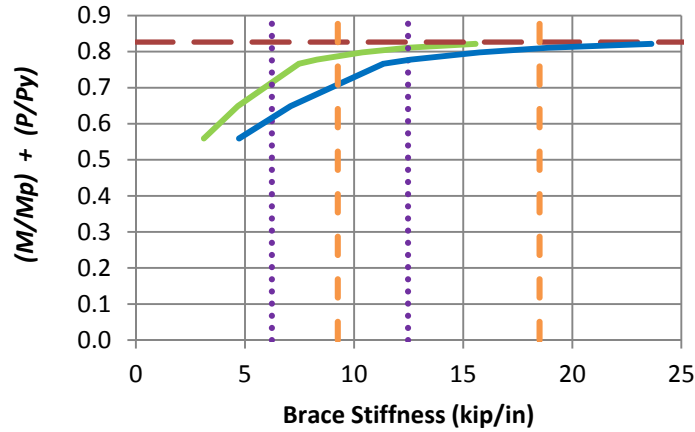
Fig. 6.19 (continued). Beam-column knuckle curves and brace force vs. brace stiffness plots for combined shear panel (relative) lateral and torsional bracing cases with $n = 2$, uniform bending with lateral bracing on the flange in flexural tension, and $L_b = 5$ ft.



c) BC_UMn_CRTB_n2_Lb5_FFR0

- - Rigidly-braced strength
- Test simulation results corresponding to torsional brace
- Test simulation results corresponding to lateral brace
- ⋯ β_{brL} and $0.5\beta_{brL}$
- - β_{brT} and $0.5\beta_{brT}$
- Left end panel shear force
- - Right end panel shear force
- · - Middle panel shear force
- Torsional brace force 1
- - Torsional brace force 2

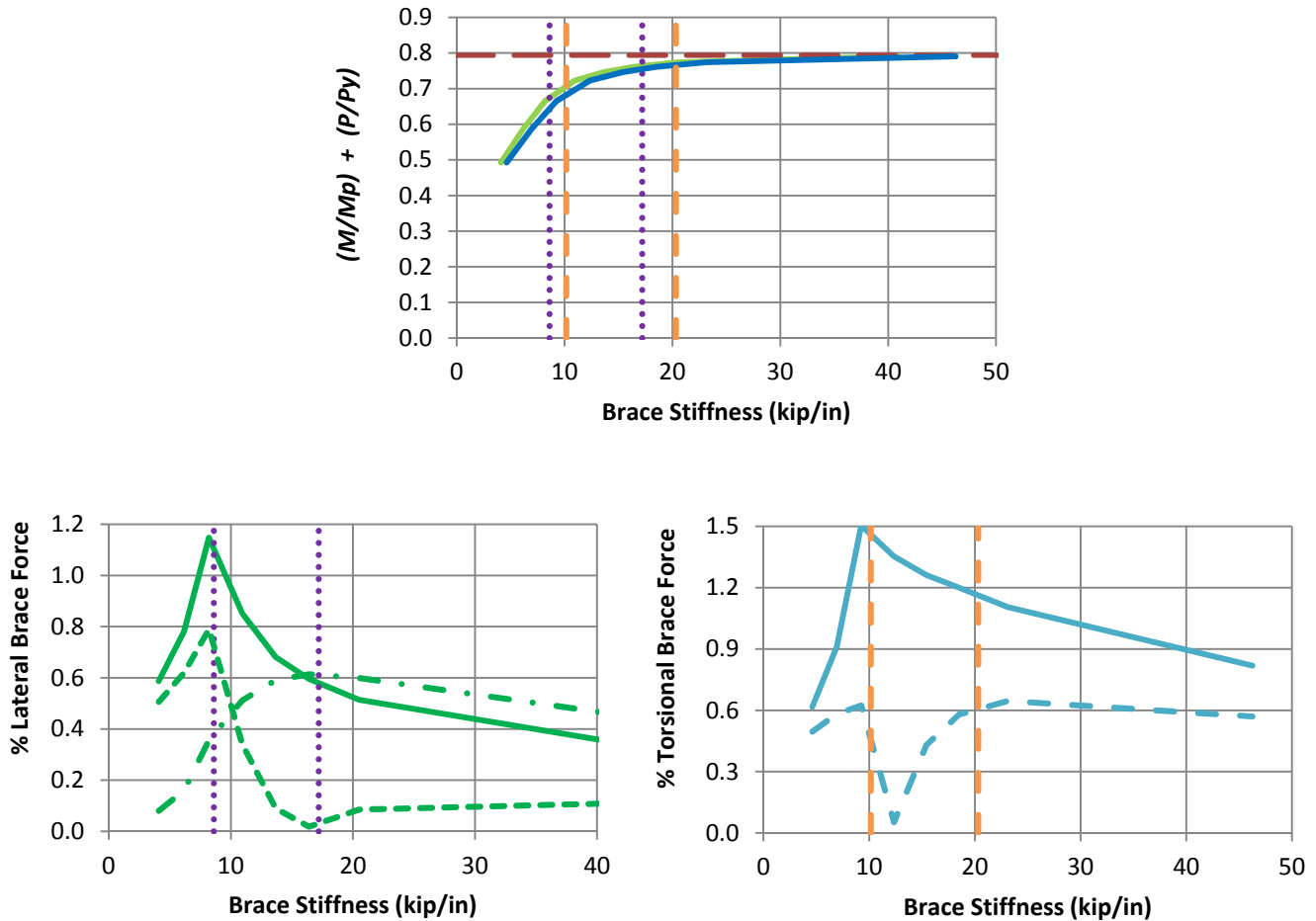
Fig. 6.19 (continued). Beam-column knuckle curves and brace force vs. brace stiffness plots for combined shear panel (relative) lateral and torsional bracing cases with $n = 2$, uniform bending with lateral bracing on the flange in flexural tension, and $L_b = 5$ ft.



d) BC_UMn_CRTB_n2_Lb5_FFR0.5

- Rigidly-braced strength
- Test simulation results corresponding to torsional brace
- Test simulation results corresponding to lateral brace
- β_{brL} and $0.5\beta_{brL}$
- — β_{brT} and $0.5\beta_{brT}$
- Left end panel shear force
- — Right end panel shear force
- • — Middle panel shear force
- Torsional brace force 1
- — Torsional brace force 2

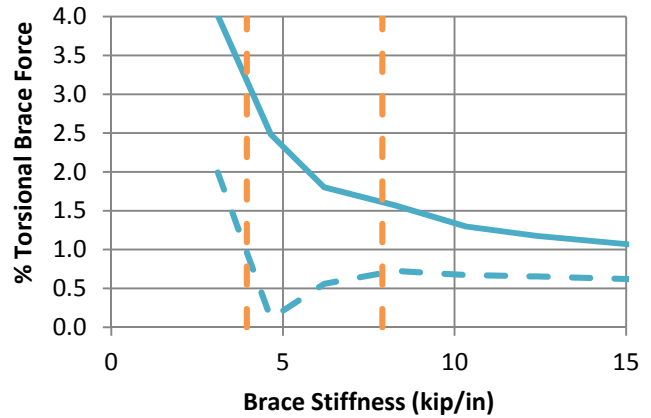
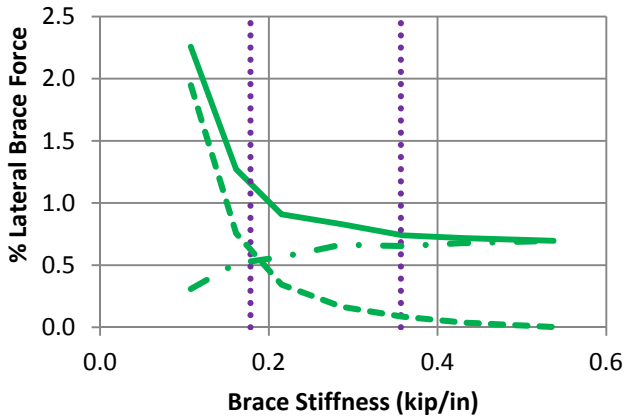
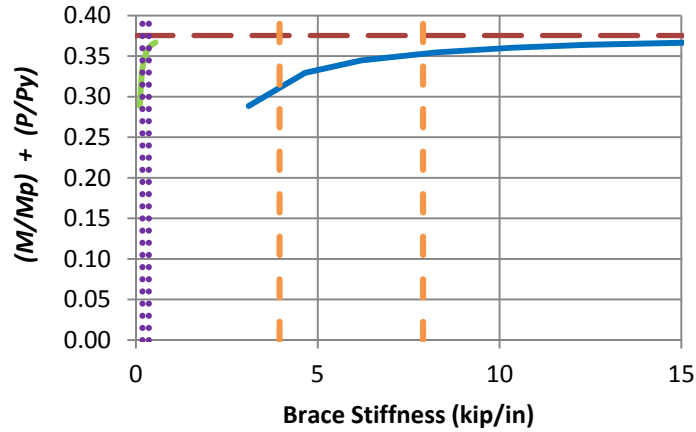
Fig. 6.19 (continued). Beam-column knuckle curves and brace force vs. brace stiffness plots for combined shear panel (relative) lateral and torsional bracing cases with $n = 2$, uniform bending with lateral bracing on the flange in flexural tension, and $L_b = 5$ ft.



e) BC_UMn_CRTB_n2_Lb5_FFR1

- Rigidly-braced strength
- Test simulation results corresponding to torsional brace
- Test simulation results corresponding to lateral brace
- β_{brL} and $0.5\beta_{brL}$
- - - β_{brT} and $0.5\beta_{brT}$
- Left end panel shear force
- - - Right end panel shear force
- . - Middle panel shear force
- Torsional brace force 1
- - - Torsional brace force 2

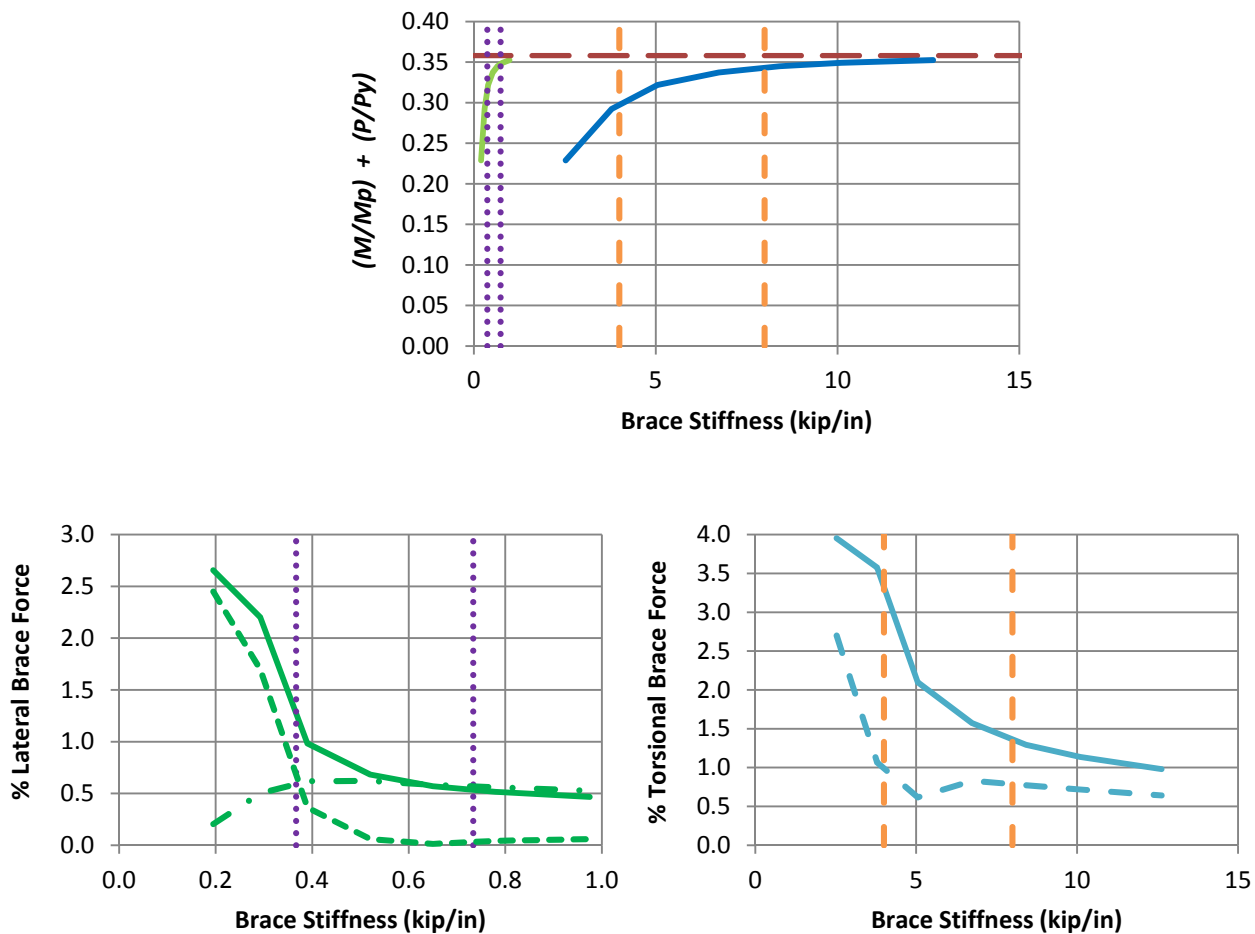
Fig. 6.19 (continued). Beam-column knuckle curves and brace force vs. brace stiffness plots for combined shear panel (relative) lateral and torsional bracing cases with $n = 2$, uniform bending with lateral bracing on the flange in flexural tension, and $L_b = 5$ ft.



a) BC_UMn_CRTB_n2_Lb15_FFR-0.67

- Rigidly-braced strength
- Test simulation results corresponding to torsional brace
- Test simulation results corresponding to lateral brace
- β_{brL} and $0.5\beta_{brL}$
- β_{brT} and $0.5\beta_{brT}$
- Left end panel shear force
- Right end panel shear force
- Middle panel shear force
- Torsional brace force 1
- Torsional brace force 2

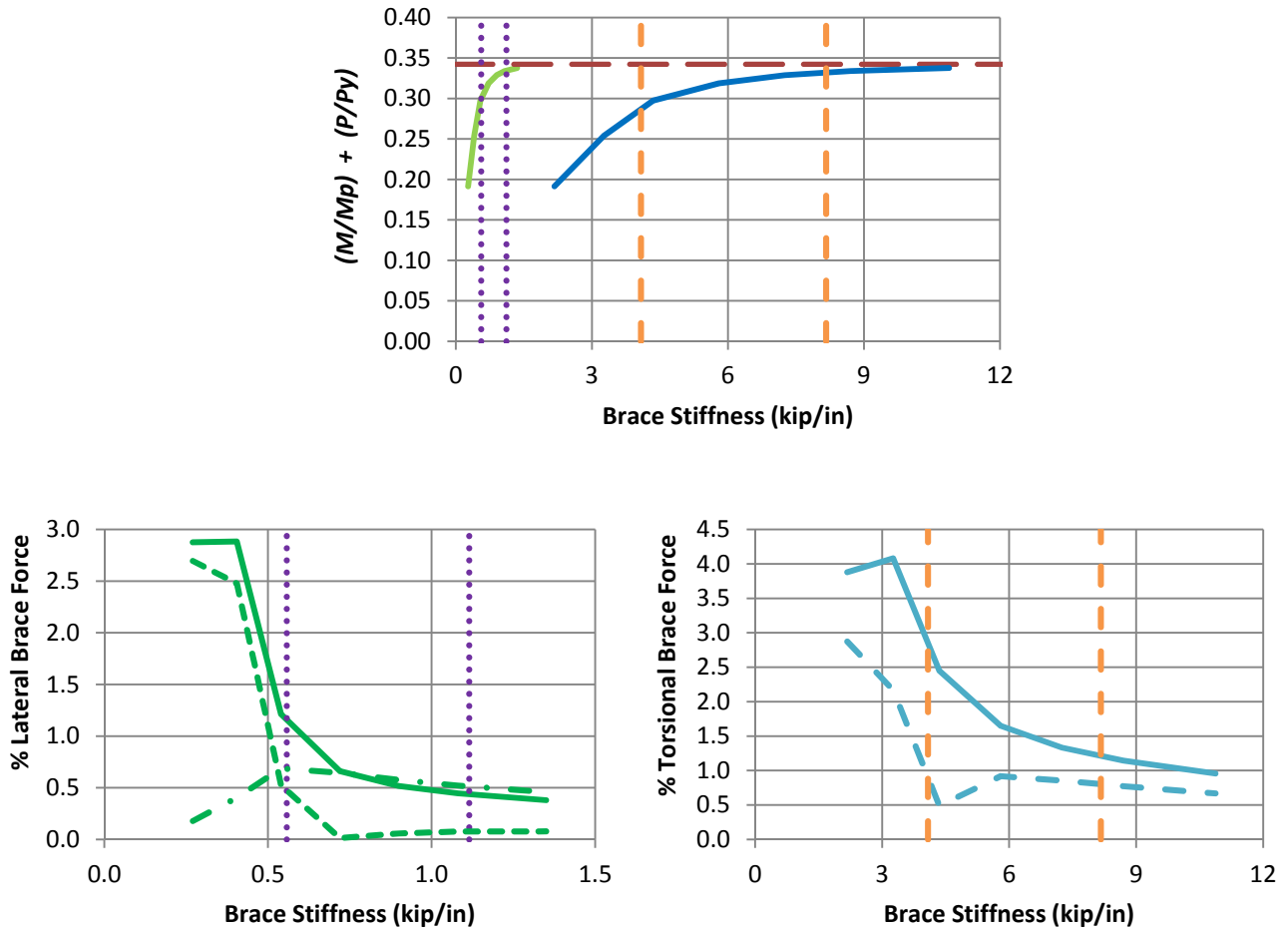
Figure 6.20. Beam-column knuckle curves and brace force vs. brace stiffness plots for combined shear panel (relative) lateral and torsional bracing cases with $n = 2$, uniform bending with lateral bracing on the flange in flexural tension, and $L_b = 15$ ft.



b) BC_UMn_CRTB_n2_Lb15_FFR-0.33

- Rigidly-braced strength
- Test simulation results corresponding to torsional brace
- Test simulation results corresponding to lateral brace
- β_{brL} and $0.5\beta_{brL}$
- - - β_{brT} and $0.5\beta_{brT}$
- Left end panel shear force
- - - Right end panel shear force
- . - Middle panel shear force
- Torsional brace force 1
- - - Torsional brace force 2

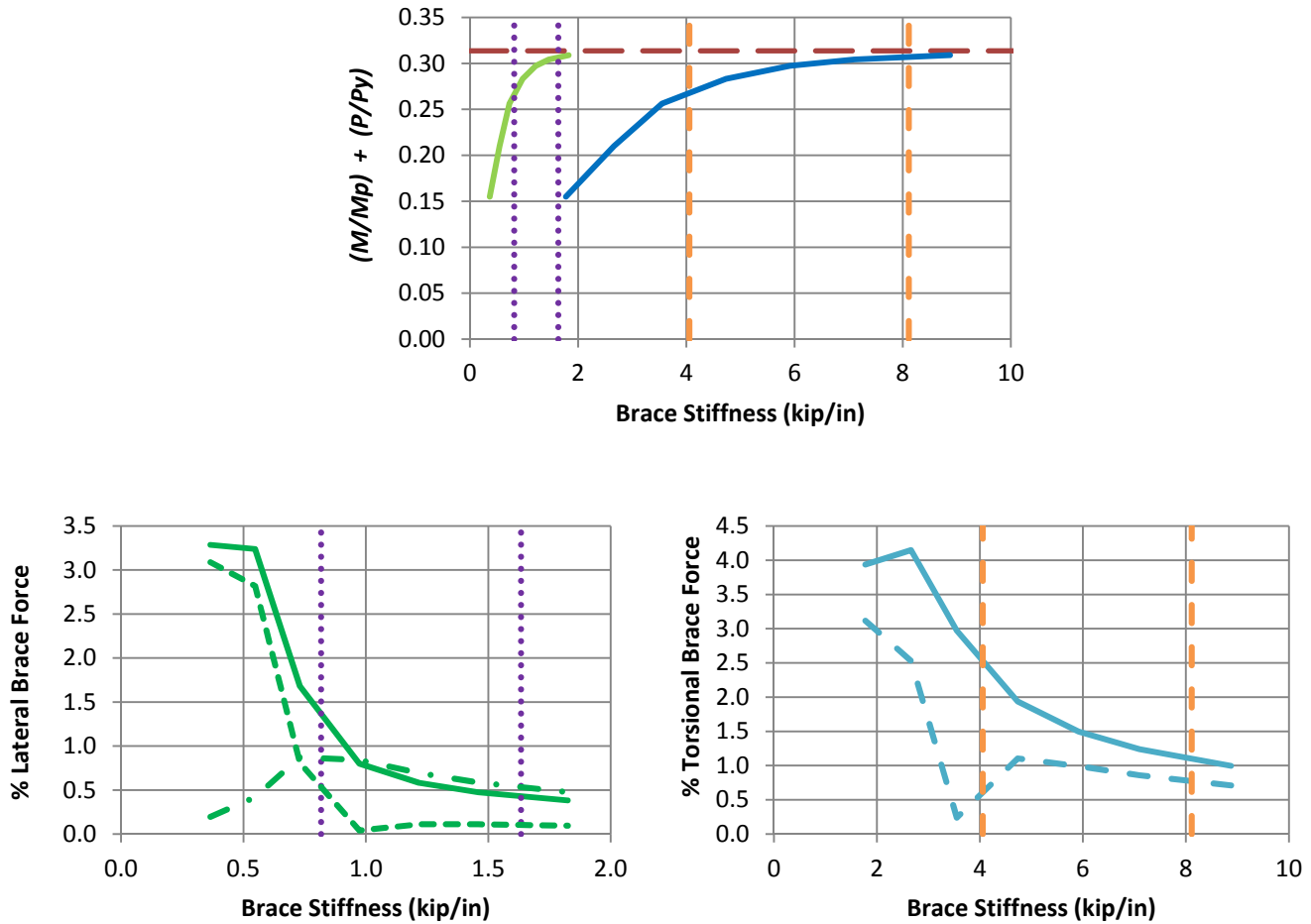
Fig. 6.20 (continued). Beam-column knuckle curves and brace force vs. brace stiffness plots for combined shear panel (relative) lateral and torsional bracing cases with $n = 2$, uniform bending with lateral bracing on the flange in flexural tension, $L_b = 15$ ft.



c) BC_UMn_CRTB_n2_Lb15_FFR0

- Rigidly-braced strength
- Test simulation results corresponding to torsional brace
- Test simulation results corresponding to lateral brace
- β_{brL} and $0.5\beta_{brL}$
- - - β_{brT} and $0.5\beta_{brT}$
- Left end panel shear force
- - - Right end panel shear force
- . - Middle panel shear force
- Torsional brace force 1
- - - Torsional brace force 2

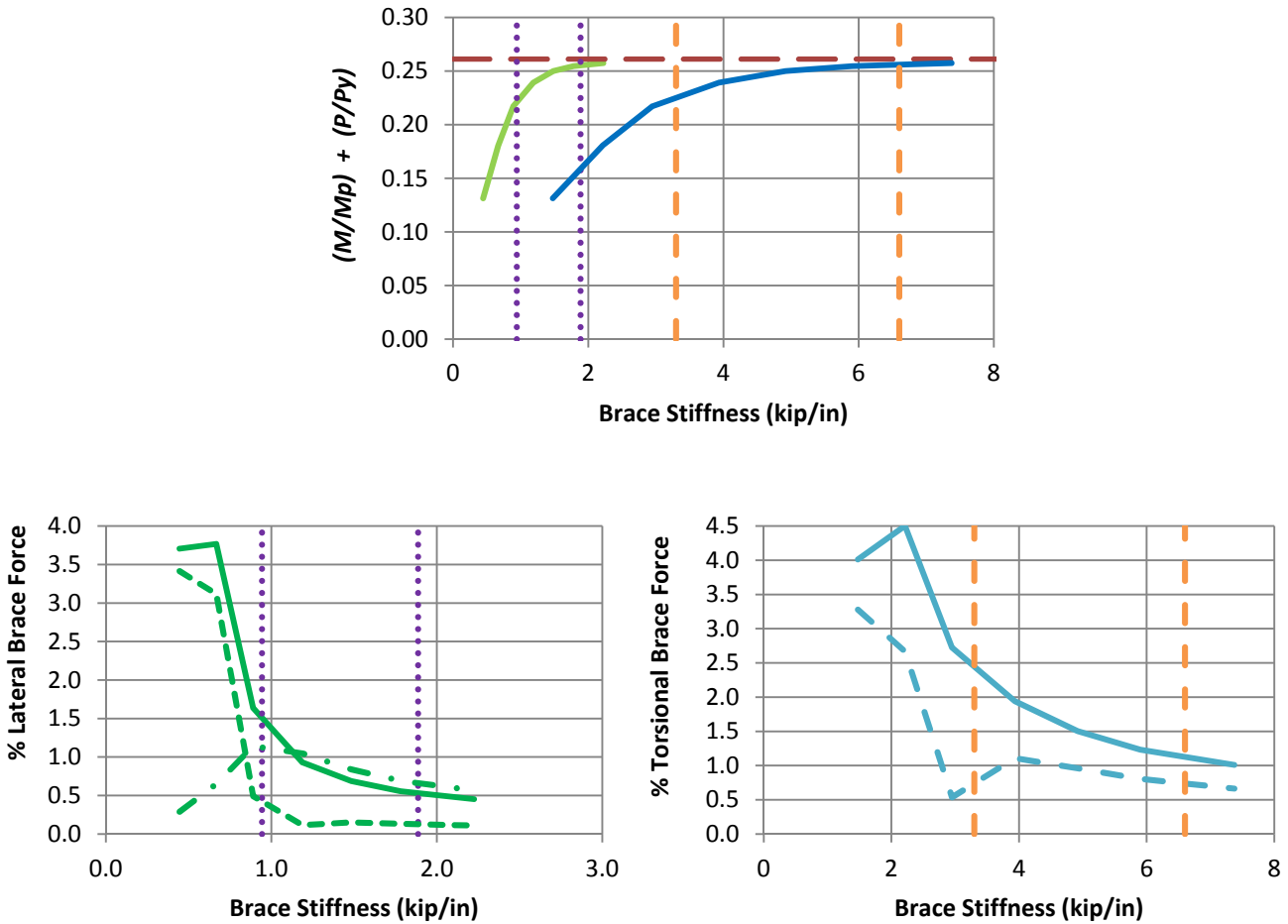
Fig. 6.20 (continued). Beam-column knuckle curves and brace force vs. brace stiffness plots for combined shear panel (relative) lateral and torsional bracing cases with $n = 2$, uniform bending with lateral bracing on the flange in flexural tension, and $L_b = 15$ ft.



d) BC_UMn_CRTB_n2_Lb15_FFR0.5

- Rigidly-braced strength
- Test simulation results corresponding to torsional brace
- Test simulation results corresponding to lateral brace
- β_{brL} and $0.5\beta_{brL}$
- - - β_{brT} and $0.5\beta_{brT}$
- Left end panel shear force
- - - Right end panel shear force
- . - Middle panel shear force
- Torsional brace force 1
- - - Torsional brace force 2

Fig. 6.20 (continued). Beam-column knuckle curves and brace force vs. brace stiffness plots for combined shear panel (relative) lateral and torsional bracing cases with $n = 2$, uniform bending with lateral bracing on the flange in flexural tension, and $L_b = 15$ ft.



e) BC_UMn_CRTB_n2_Lb15_FFR1

- Rigidly-braced strength
- Test simulation results corresponding to torsional brace
- Test simulation results corresponding to lateral brace
- β_{brL} and $0.5\beta_{brL}$
- — — β_{brT} and $0.5\beta_{brT}$
- Left end panel shear force
- Right end panel shear force
- Middle panel shear force
- Torsional brace force 1
- Torsional brace force 2

Fig. 6.20 (continued). Beam-column knuckle curves and brace force vs. brace stiffness plots for combined shear panel (relative) lateral and torsional bracing cases with $n = 2$, uniform bending with lateral bracing on the flange in flexural tension, and $L_b = 15$ ft.

Table 6.3. Brace stiffnesses β_{F96L} and β_{brL} and brace forces as a percentage of P for beam-columns with combined torsional and lateral bracing.

Case	β_{F96L} (kip/in)	β_{brL} (kip/in)	$\beta_{brL}/$ β_{F96L}	% Lateral Brace Force at $\beta_L = \beta_{brL}$ and $\beta_T = \beta_{brT}$	Ratio of Actual to Estimated Lateral Brace Force at $\beta_L = \beta_{brL}$ and $\beta_T = \beta_{brT}$
BC_UMp_CNTB_n1_Lb5_FFR-0.67	1.72	4.64	2.70	1.00	1.00
BC_UMp_CNTB_n1_Lb5_FFR-0.33	2.77	9.74	3.52	0.62	0.62
BC_UMp_CNTB_n1_Lb5_FFR0	5.81	15.34	2.64	0.47	0.47
BC_UMp_CNTB_n1_Lb5_FFR0.5	8.84	24.90	2.82	0.46	0.46
BC_UMp_CNTB_n1_Lb5_FFR1	26.91	33.82	1.26	1.29	1.29
BC_UMp_CNTB_n1_Lb15_FFR-0.67	0.38	0.68	1.79	1.30	1.30
BC_UMp_CNTB_n1_Lb15_FFR-0.33	0.74	1.42	1.92	0.88	0.88
BC_UMp_CNTB_n1_Lb15_FFR0	1.08	2.16	2.00	0.68	0.68
BC_UMp_CNTB_n1_Lb15_FFR0.5	1.84	3.18	1.73	0.68	0.68
BC_UMp_CNTB_n1_Lb15_FFR1	2.37	3.18	1.34	0.96	0.96
BC_UMp_CRTB_n2_Lb5_FFR-0.67	1.04	2.38	2.29	1.00	1.00
BC_UMp_CRTB_n2_Lb5_FFR-0.33	1.90	4.86	2.56	0.48	0.48
BC_UMp_CRTB_n2_Lb5_FFR0	2.76	7.72	2.80	0.38	0.38
BC_UMp_CRTB_n2_Lb5_FFR0.5	5.26	12.46	2.37	0.28	0.28
BC_UMp_CRTB_n2_Lb5_FFR1	16.75	17.20	1.03	0.60	0.60
BC_UMp_CRTB_n2_Lb15_FFR-0.67	0.28	0.36	1.29	0.70	0.70
BC_UMp_CRTB_n2_Lb15_FFR-0.33	0.45	0.74	1.64	0.50	0.50
BC_UMp_CRTB_n2_Lb15_FFR0	0.64	1.12	1.75	0.40	0.40

Table 6.3 (continued). Brace stiffnesses β_{F96L} and β_{brL} and brace forces as a percentage of P for beam-columns with combined torsional and lateral bracing.

Case	β_{F96L} (kip/in)	β_{brL} (kip/in)	β_{brL} / β_{F96}	% Lateral Brace Force at $\beta_L = \beta_{brL}$ and $\beta_T = \beta_{brT}$	Ratio of Actual to Estimated Lateral Brace Force at $\beta_L = \beta_{brL}$ and $\beta_T = \beta_{brT}$
BC_UMp_CRTB_n2_Lb15_FFR0.5	1.00	1.64	1.64	0.48	0.48
BC_UMp_CRTB_n2_Lb15_FFR1	1.53	1.88	1.23	0.65	0.65
BC_UMn_CNTB_n1_Lb5_FFR-0.67	2.62	4.64	1.77	1.10	1.10
BC_UMn_CNTB_n1_Lb5_FFR-0.33	5.33	9.74	1.83	1.00	1.00
BC_UMn_CNTB_n1_Lb5_FFR0	8.70	15.34	1.76	0.90	0.90
BC_UMn_CNTB_n1_Lb5_FFR0.5	15.63	24.90	1.59	0.80	0.80
BC_UMn_CNTB_n1_Lb5_FFR1	26.91	33.82	1.26	1.29	1.29
BC_UMn_CNTB_n1_Lb15_FFR-0.67	0.47	0.68	1.45	1.31	1.31
BC_UMn_CNTB_n1_Lb15_FFR-0.33	0.95	1.42	1.49	1.00	1.00
BC_UMn_CNTB_n1_Lb15_FFR0	1.40	2.16	1.54	0.90	0.90
BC_UMn_CNTB_n1_Lb15_FFR0.5	2.10	3.18	1.51	0.90	0.90
BC_UMn_CNTB_n1_Lb15_FFR1	2.37	3.18	1.34	1.00	1.00
BC_UMn_CRTB_n2_Lb5_FFR-0.67	1.73	2.38	1.38	0.90	0.90
BC_UMn_CRTB_n2_Lb5_FFR-0.33	3.46	4.86	1.40	0.80	0.80
BC_UMn_CRTB_n2_Lb5_FFR0	5.56	7.72	1.39	0.70	0.70
BC_UMn_CRTB_n2_Lb5_FFR0.5	9.91	12.46	1.26	0.60	0.60
BC_UMn_CRTB_n2_Lb5_FFR1	16.75	17.20	1.03	0.60	0.60
BC_UMn_CRTB_n2_Lb15_FFR-0.67	0.36	0.36	1.00	0.75	0.75
BC_UMn_CRTB_n2_Lb15_FFR-0.33	0.63	0.74	1.17	0.50	0.50
BC_UMn_CRTB_n2_Lb15_FFR0	0.89	1.12	1.26	0.50	0.50
BC_UMn_CRTB_n2_Lb15_FFR0.5	1.35	1.64	1.21	0.50	0.50
BC_UMn_CRTB_n2_Lb15_FFR1	1.53	1.88	1.23	0.70	0.70

Table 6.4. Brace stiffnesses β_{F96T} and β_{brT} and torsional brace force as a percentage of $(M/h_o + P/2)$ for beam-columns with combined torsional and lateral bracing.

Case	β_{F96T} (kip/in)	β_{brT} (kip/in)	$\beta_{brT}/$ β_{F96T}	% Torsional Brace Force at $\beta_L = \beta_{brL}$ and $\beta_T = \beta_{brT}$	Ratio of Actual to Estimated Torsional Brace Force at $\beta_L = \beta_{brL}$ and $\beta_T = \beta_{brT}$
BC_UMp_CNTB_n1_Lb5_FFR-0.67	7.91	17.70	2.24	0.70	0.35
BC_UMp_CNTB_n1_Lb5_FFR-0.33	6.45	19.32	3.00	0.38	0.19
BC_UMp_CNTB_n1_Lb5_FFR0	8.78	21.24	2.42	0.19	0.10
BC_UMp_CNTB_n1_Lb5_FFR0.5	8.91	24.74	2.78	0.05	0.03
BC_UMp_CNTB_n1_Lb5_FFR1	20.19	26.20	1.30	1.30	0.65
BC_UMp_CNTB_n1_Lb15_FFR-0.67	7.33	10.16	1.39	0.70	0.35
BC_UMp_CNTB_n1_Lb15_FFR-0.33	6.34	10.54	1.66	0.40	0.20
BC_UMp_CNTB_n1_Lb15_FFR0	5.78	10.88	1.88	0.10	0.05
BC_UMp_CNTB_n1_Lb15_FFR0.5	5.9	10.72	1.82	0.20	0.10
BC_UMp_CNTB_n1_Lb15_FFR1	5.2	10.72	2.06	0.95	0.48
BC_UMp_CRTB_n2_Lb5_FFR-0.67	7.09	13.30	1.88	1.00	0.50
BC_UMp_CRTB_n2_Lb5_FFR-0.33	6.69	14.40	2.15	0.45	0.23
BC_UMp_CRTB_n2_Lb5_FFR0	6.37	15.82	2.48	0.25	0.13
BC_UMp_CRTB_n2_Lb5_FFR0.5	7.99	18.50	2.32	0.09	0.05
BC_UMp_CRTB_n2_Lb5_FFR1	18.9	20.32	1.08	1.18	0.59
BC_UMp_CRTB_n2_Lb15_FFR-0.67	8.06	7.90	0.98	0.9	0.45
BC_UMp_CRTB_n2_Lb15_FFR-0.33	5.88	8.00	1.36	0.4	0.20
BC_UMp_CRTB_n2_Lb15_FFR0	5.17	8.16	1.58	0.15	0.08

Table 6.4 (continued). Brace stiffnesses β_{F96T} and β_{brT} and torsional brace force as a percentage of $(M/h_o + P/2)$ for beam-columns with combined torsional and lateral bracing.

Case	β_{F96T} (kip/in)	β_{brT} (kip/in)	$\beta_{F96T}/$ β_{brT}	% Torsional Brace Force at $\beta_L = \beta_{brL}$ and $\beta_T = \beta_{brT}$	Ratio of Actual to Estimated Torsional Brace Force at $\beta_L = \beta_{brL}$ and $\beta_T = \beta_{brT}$
BC_UMp_CRTB_n2_Lb15_FFR0.5	4.87	8.12	1.67	0.30	0.15
BC_UMp_CRTB_n2_Lb15_FFR1	5.08	6.60	1.30	1.20	0.60
BC_UMn_CNTB_n1_Lb5_FFR-0.67	12.09	17.70	1.46	2.00	1.00
BC_UMn_CNTB_n1_Lb5_FFR-0.33	12.41	19.32	1.56	1.60	0.80
BC_UMn_CNTB_n1_Lb5_FFR0	13.37	21.24	1.59	1.50	0.75
BC_UMn_CNTB_n1_Lb5_FFR0.5	15.75	24.74	1.57	1.10	0.55
BC_UMn_CNTB_n1_Lb5_FFR1	20.19	26.20	1.30	1.25	0.63
BC_UMn_CNTB_n1_Lb15_FFR-0.67	8.95	10.16	1.14	1.50	0.75
BC_UMn_CNTB_n1_Lb15_FFR-0.33	8.15	10.54	1.29	1.10	0.55
BC_UMn_CNTB_n1_Lb15_FFR0	7.44	10.88	1.46	1.00	0.50
BC_UMn_CNTB_n1_Lb15_FFR0.5	6.72	10.72	1.60	0.95	0.48
BC_UMn_CNTB_n1_Lb15_FFR1	5.20	10.72	2.06	0.95	0.48
BC_UMn_CRTB_n2_Lb5_FFR-0.67	11.78	13.30	1.13	2.90	1.45
BC_UMn_CRTB_n2_Lb5_FFR-0.33	12.18	14.40	1.18	2.50	1.25
BC_UMn_CRTB_n2_Lb5_FFR0	12.84	15.82	1.23	2.00	1.00
BC_UMn_CRTB_n2_Lb5_FFR0.5	15.05	18.50	1.23	1.60	0.80
BC_UMn_CRTB_n2_Lb5_FFR1	18.90	20.32	1.08	1.15	0.58
BC_UMn_CRTB_n2_Lb15_FFR-0.67	10.41	7.90	0.76	1.50	0.75
BC_UMn_CRTB_n2_Lb15_FFR-0.33	8.17	8.00	0.98	1.40	0.70
BC_UMn_CRTB_n2_Lb15_FFR0	7.21	8.16	1.13	1.25	0.63
BC_UMn_CRTB_n2_Lb15_FFR0.5	6.55	8.12	1.24	1.10	0.55
BC_UMn_CRTB_n2_Lb15_FFR1	5.08	6.60	1.30	1.10	0.15

The recommendations of Section 6.3.3 do an accurate to conservative job of predicting the bracing strength requirements for the combined bracing problem. They give slightly unconservative results in some cases. These cases are highlighted in grey in Tables 6.3 and 6.4. However, a close inspection of the brace force versus the Load Proportionality Factor for stiffnesses calculated from Eqs. (6-5) and (6-7) show that the corresponding bracing strength recommendations are sufficient to develop member strengths very close to the test limit loads. An example case is BC_UMp_CNTB_n1_Lb5_FFR1, the knuckle curve and brace force - brace stiffness curves for which are shown in Fig. 6.13e. The point lateral brace force versus the Load Proportionality Factor for this case with brace stiffnesses calculated from Eqs. (6-5) and (6-7) is shown in Fig. 6.21. It can be observed that a point lateral brace strength requirement of $0.01P$ is sufficient to develop member strength very close to the test limit load.

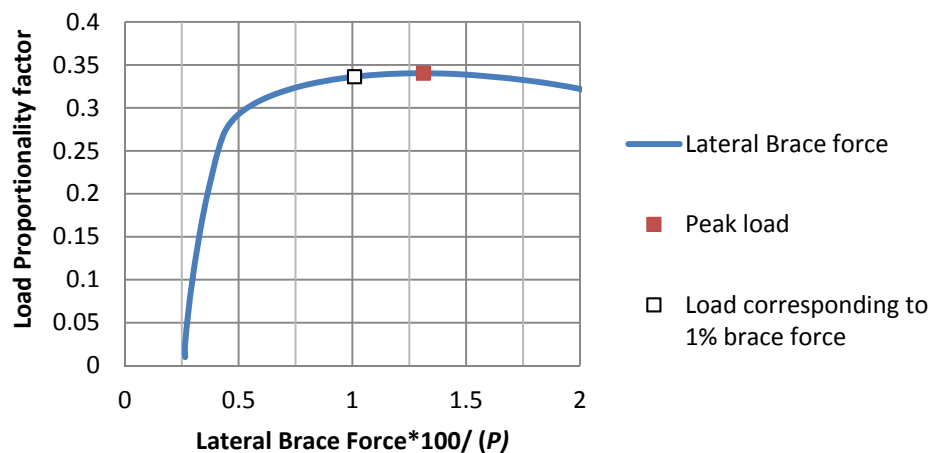


Figure 6.21. Point lateral brace force vs. the Load Proportionality Factor for BC_UMp_CNTB_n1_Lb5_FFR1 corresponding to a point lateral brace stiffness of $\beta_{brL} = 33.82$ kip/in from Eq. (6-5) and a point torsional brace stiffness of $\beta_{brT} = 26.20$ from Eq. (6-7).

Another example case is BC_UMn_CNTB_n1_Lb5_FFR-0.67, the knuckle curves and brace force - brace stiffness curves for which are shown in Fig. 6.15a. The point lateral brace force versus Load Proportionality Factor for this case with brace stiffnesses calculated from Eqs. (6-5) and (6-7) is shown in Fig. 6.22. Again, it can be observed that a lateral brace strength requirement of $0.01P$ is sufficient to develop member strength very close to the test limit load.

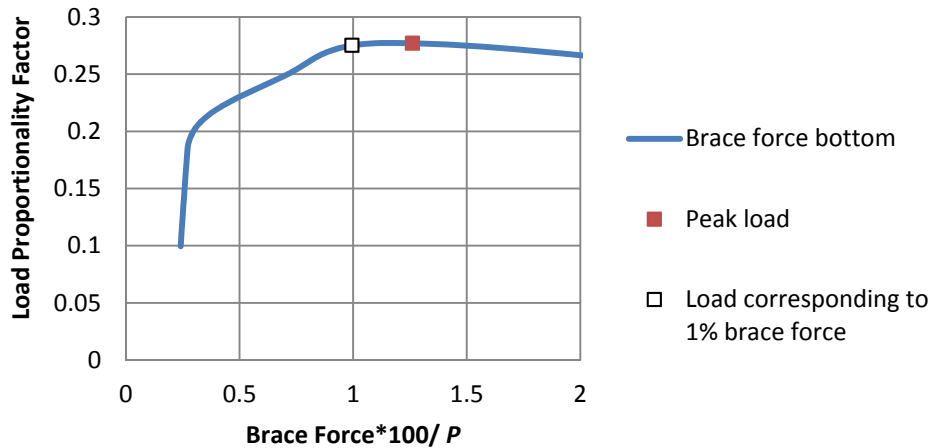


Figure 6.22. Point lateral brace force vs. the Load Proportionality Factor for BC_UMn_CNTB_n1_Lb5_FFR-0.67 corresponding to a point lateral brace stiffness of $\beta_{brL} = 4.64$ kip/in calculated from Eq. (6-5) and a point torsional brace stiffness of $\beta_{brT} = 12.09$ from Eq. (6-7).

A third example case is BC_UMp_CNTB_n1_Lb15_FFR-0.67, the knuckle and brace force - brace stiffness curves for which are shown in Fig. 6.14a. The point lateral brace force versus Load Proportionality Factor for this case with the brace stiffnesses calculated from Eq. (6-5) and (6-7) is shown in Fig. 6.23. It can be observed that a lateral brace strength requirement of $0.01P$ is sufficient to develop a member strength of only 81 % of the beam rigidly-braced strength in this problem (noting that the limit load in Fig. 6.23 corresponds essentially to the rigidly-braced in Fig. 6.14a). This is the most critical of the various study cases with respect to the lack of development of the limit load at the occurrence of the recommended design strength. When scrutinizing this problem, one might consider that the AISC required minimum brace stiffnesses for design by

LRFD are equal to the nominal β_{br} values divided by $\phi = 0.75$. As such, one might ask whether the beam strength corresponding to the point lateral brace reaching its required strength condition is larger if the brace stiffness is increased by $1/\phi$. Unfortunately, essentially the same brace force - Load Proportionality Factor curve as that shown in Fig. 6.23 is obtained when the lateral and torsional brace stiffnesses are increased by this amount. This result is consistent with the fact that the limit load in Fig. 6.23 corresponds essentially to the beam's rigidly-braced strength. It appears that the only way to avoid exceeding the recommended point lateral brace strength requirement in this problem is to increase the strength requirement of Eq. (6.6a) to $0.013P$. Correspondingly, the requirement from Eq. (6.6b) would need to be increased to $0.0065P$, since the single mid-span lateral brace is equivalent to two shear panel braces, one on each side of the mid-span. Test BC_UMp_CNTB_n1_Lb15_FFR-0.67 is discussed further at the end of Chapter 8, Summary and Conclusions.

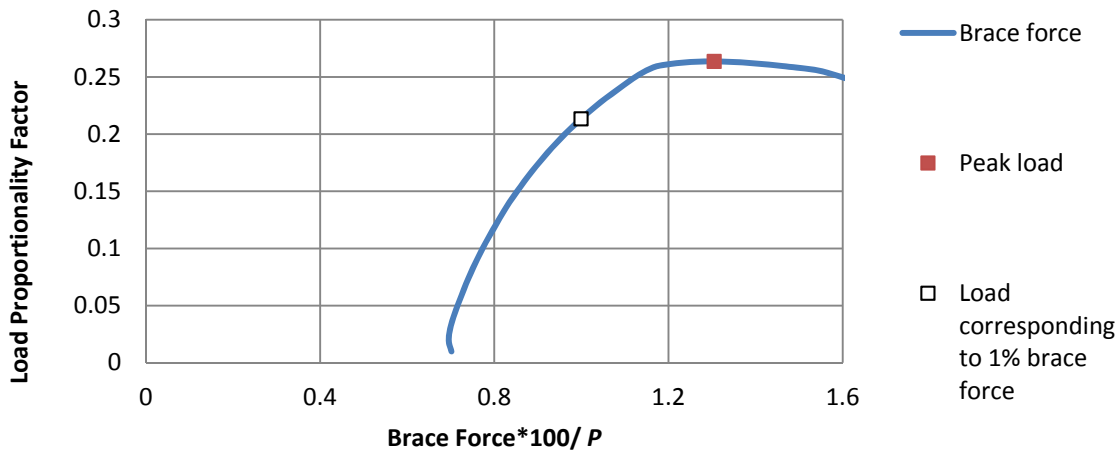


Figure 6.23. Point lateral brace force vs. the Load Proportionality Factor for BC_UMp_CNTB_n1_Lb15_FFR-0.67 corresponding to a point lateral brace stiffness $\beta_{brL} = 0.68$ kip/in from Eq. (6-5) and a point torsional brace stiffness $\beta_{brT} = 10.16$ kip/in.

Aside from the above problems where the brace force reaches the recommended required strength value prior to the beam reaching its limit load, the beams listed in Tables 6.3 and 6.4 perform well. It can be observed from Tables 6.3 and 6.4 that the stiffnesses recommended by Eqs. (6-5) and (6-7) are sufficient to reach 96 % of the rigidly-braced strength for all cases except BC_UMn_CRTB_n2_Lb15_FFR-0.67. However, when $\beta_L = \beta_{brL}$ and $\beta_T = \beta_{brT}$ in this problem, the member strength is at 93 % of the rigidly-braced strength. This is considered to be acceptable.

CHAPTER 7 BEAM-COLUMNS SUBJECTED TO MOMENT GRADIENT LOADING

7.1 Overview

This chapter addresses the fourth major part of this research, beam-columns subjected to axial load and moment gradient loading. Section 7.2 gives details of the cases considered. Section 7.3 presents the test simulation results.

7.2 Detailed Study Design

The cases considered in this research to study the bracing requirements for beam-columns subjected to axial load and moment gradient loading are listed below.

The cases considered for beam-columns with Moment Gradient 1 loading are as follows:

- Basic point and shear panel lateral bracing types, axial load and positive Moment Gradient 1 loading such that only one flange is in net compression:

BC_MG1p_NB_n1_Lb5_FFR-0.5
BC_MG1p_NB_n1_Lb5_FFR0
BC_MG1p_NB_n1_Lb15_FFR-0.5
BC_MG1p_NB_n1_Lb15_FFR0
BC_MG1p_RB_n2_Lb5_FFR-0.5
BC_MG1p_RB_n2_Lb5_FFR0
BC_MG1p_RB_n2_Lb15_FFR-0.5
BC_MG1p_RB_n2_Lb15_FFR0

- Combined lateral and torsional bracing, axial load and positive Moment Gradient 1 loading such that only one flange is in net compression:

BC_MG1p_CNTB_n1_Lb5_FFR-0.5
BC_MG1p_CNTB_n1_Lb5_FFR0
BC_MG1p_CNTB_n1_Lb15_FFR-0.5
BC_MG1p_CNTB_n1_Lb15_FFR0
BC_MG1p_CRTB_n2_Lb5_FFR-0.5
BC_MG1p_CRTB_n2_Lb5_FFR0
BC_MG1p_CRTB_n2_Lb15_FFR-0.5
BC_MG1p_CRTB_n2_Lb15_FFR0

- Combined lateral and torsional bracing, axial load and positive Moment Gradient 1 loading such that both flanges are in net compression:

BC_MG1p_CNTB_n1_Lb5_FFR0.5
BC_MG1p_CNTB_n1_Lb5_FFR1
BC_MG1p_CNTB_n1_Lb15_FFR0.5
BC_MG1p_CNTB_n1_Lb15_FFR1
BC_MG1p_CRTB_n2_Lb5_FFR0.5
BC_MG1p_CRTB_n2_Lb5_FFR1
BC_MG1p_CRTB_n2_Lb15_FFR0.5
BC_MG1p_CRTB_n2_Lb15_FFR1

- Combined lateral and torsional bracing, axial load and negative Moment Gradient 1 loading such that only one flange is in net compression:

BC_MG1n_CNTB_n1_Lb5_FFR-0.5
BC_MG1n_CNTB_n1_Lb5_FFR0
BC_MG1n_CNTB_n1_Lb15_FFR-0.5
BC_MG1n_CNTB_n1_Lb15_FFR0
BC_MG1n_CRTB_n2_Lb5_FFR-0.5
BC_MG1n_CRTB_n2_Lb5_FFR0
BC_MG1n_CRTB_n2_Lb15_FFR-0.5
BC_MG1n_CRTB_n2_Lb15_FFR0

- Combined lateral and torsional bracing, axial load and negative Moment Gradient 1 loading such that both flanges are in net compression:

BC_MG1n_CNTB_n1_Lb5_FFR0.5
BC_MG1n_CNTB_n1_Lb5_FFR1
BC_MG1n_CNTB_n1_Lb15_FFR0.5
BC_MG1n_CNTB_n1_Lb15_FFR1
BC_MG1n_CRTB_n2_Lb5_FFR0.5
BC_MG1n_CRTB_n2_Lb5_FFR1
BC_MG1n_CRTB_n2_Lb15_FFR0.5
BC_MG1n_CRTB_n2_Lb15_FFR1

Cases considered for beam-columns with Moment Gradient 2 loading are as follows:

- Basic point lateral bracing types, axial load and positive Moment Gradient 2 loading such that only one flange is in net compression:

BC_MG2p_NB_n1_Lb5_FFR-0.5
BC_MG2p_NB_n1_Lb5_FFR0
BC_MG2p_NB_n1_Lb15_FFR-0.5
BC_MG2p_NB_n1_Lb15_FFR0

- Combined lateral and torsional bracing, axial load and positive Moment Gradient 2 loading such that only one flange is in net compression:

BC_MG2p_CNTB_n1_Lb5_FFR-0.5
BC_MG2p_CNTB_n1_Lb5_FFR0
BC_MG2p_CNTB_n1_Lb15_FFR-0.5
BC_MG2p_CNTB_n1_Lb15_FFR0

- Combined lateral and torsional bracing, axial load and positive Moment Gradient 2 loading such that both flanges are in net compression:

BC_MG2p_CNTB_n1_Lb5_FFR0.5
BC_MG2p_CNTB_n1_Lb5_FFR1
BC_MG2p_CNTB_n1_Lb15_FFR0.5
BC_MG2p_CNTB_n1_Lb15_FFR1

- Combined lateral and torsional bracing, axial load and negative Moment Gradient 2 loading such that only one flange is in net compression:

BC_MG2n_CNTB_n1_Lb5_FFR-0.5
BC_MG2n_CNTB_n1_Lb5_FFR0
BC_MG2n_CNTB_n1_Lb15_FFR-0.5
BC_MG2n_CNTB_n1_Lb15_FFR0

- Combined lateral and torsional bracing, axial load and negative Moment Gradient 2 loading such that both flanges are in net compression:

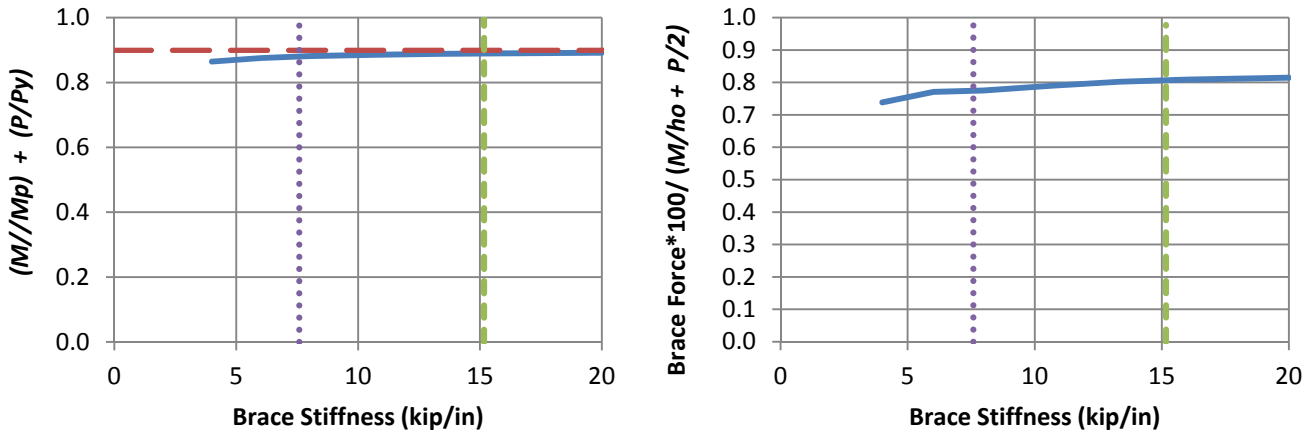
BC_MG2n_CNTB_n1_Lb5_FFR0.5
BC_MG2n_CNTB_n1_Lb5_FFR1
BC_MG2n_CNTB_n1_Lb15_FFR0.5
BC_MG2n_CNTB_n1_Lb15_FFR1

7.3 Results

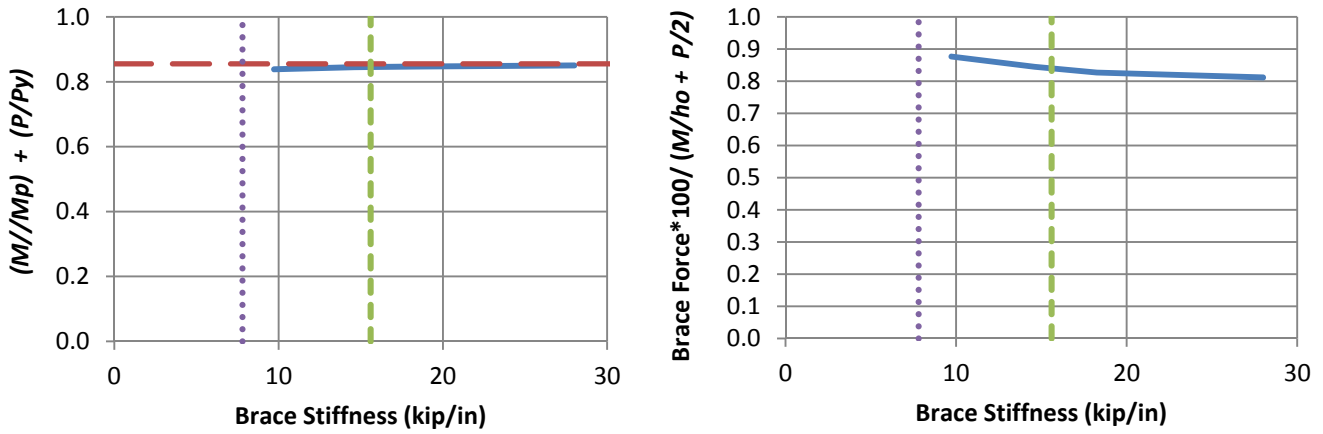
The results for the various beam-column moment gradient loading cases are presented in the following subsections.

7.3.1 Beam-Columns with Point Lateral Bracing Only on the Flange in Flexural Compression, Subjected to Moment Gradient 1 Loading

The knuckle curves and brace force - brace stiffness curves for beam-columns with Moment Gradient 1 loading and point lateral bracing only on one flange are shown in Figs. 7.1 through 7.4. Table 7.1 compares the brace stiffnesses β_{brL} calculated from Eq. (6-1) to the corresponding β_{F96} , and the recommended estimates of the brace force at $\beta_L = \beta_{brL}$ from Eq. (6-2a) to the simulation results from these figures.



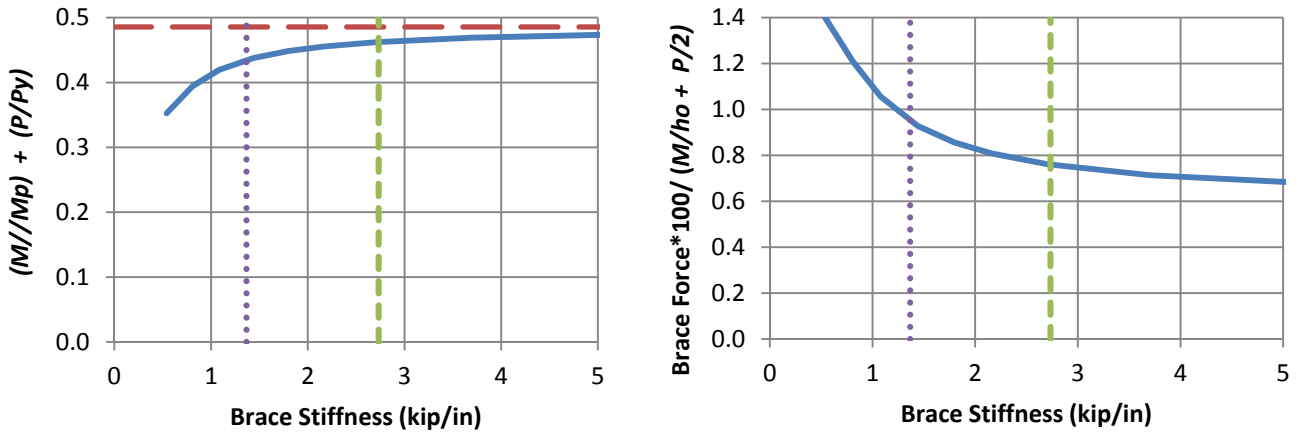
a) BC_MG1p_NB_n1_Lb5_FFR-0.5



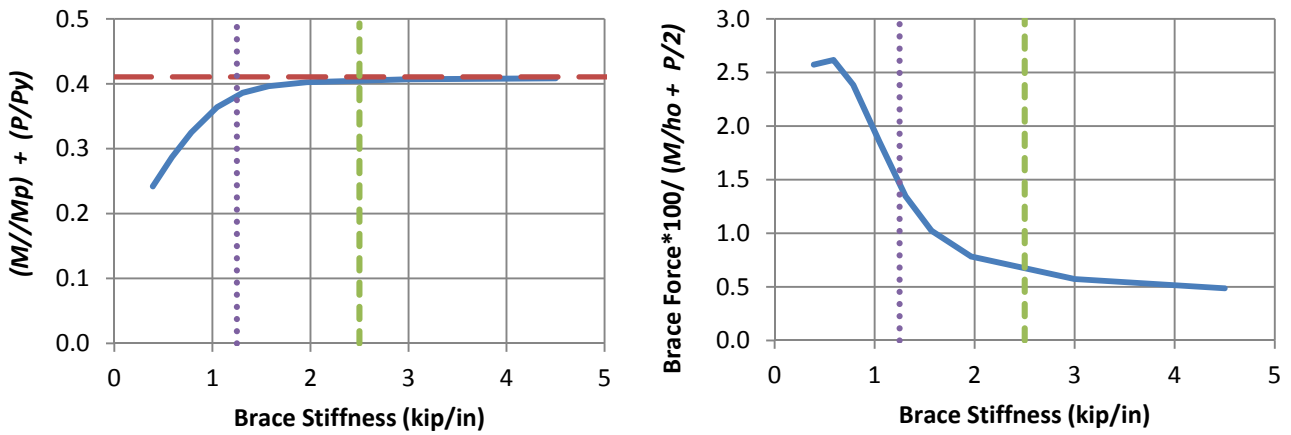
b) BC_MG1p_NB_n1_Lb5_FFR0

- Test simulation results
- - Rigidly-braced strength
- ⋯ 0.5 times bracing stiffness from Eq. (6-1)
- - Bracing stiffness from Eq. (6-1)

Figure 7.1. Beam-column knuckle curves and brace force vs. brace stiffness plots for point (nodal) lateral bracing cases with $n = 1$, Moment Gradient 1 loading, and $L_b = 5$ ft.



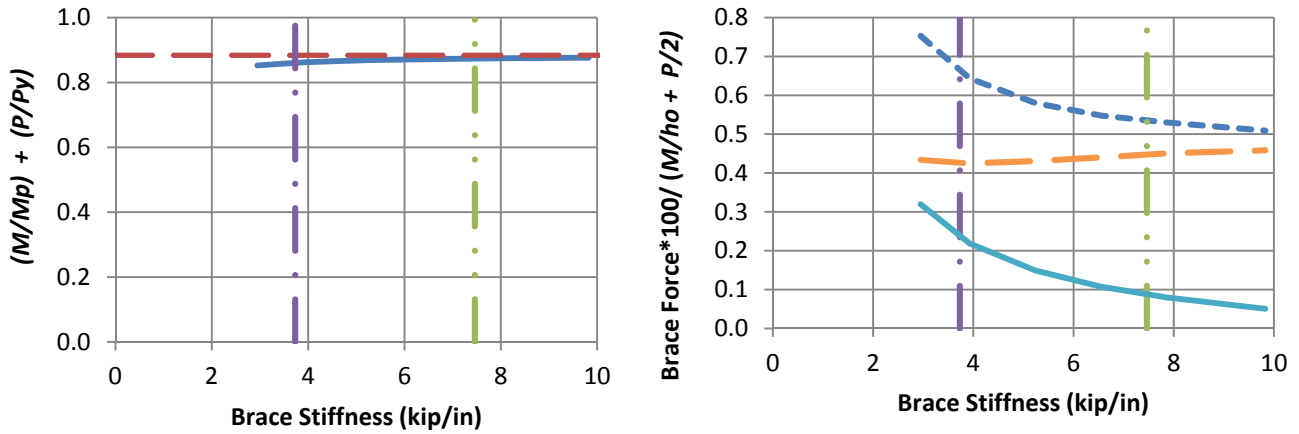
a) BC_MG1p_NB_n1_Lb15_FFR-0.5



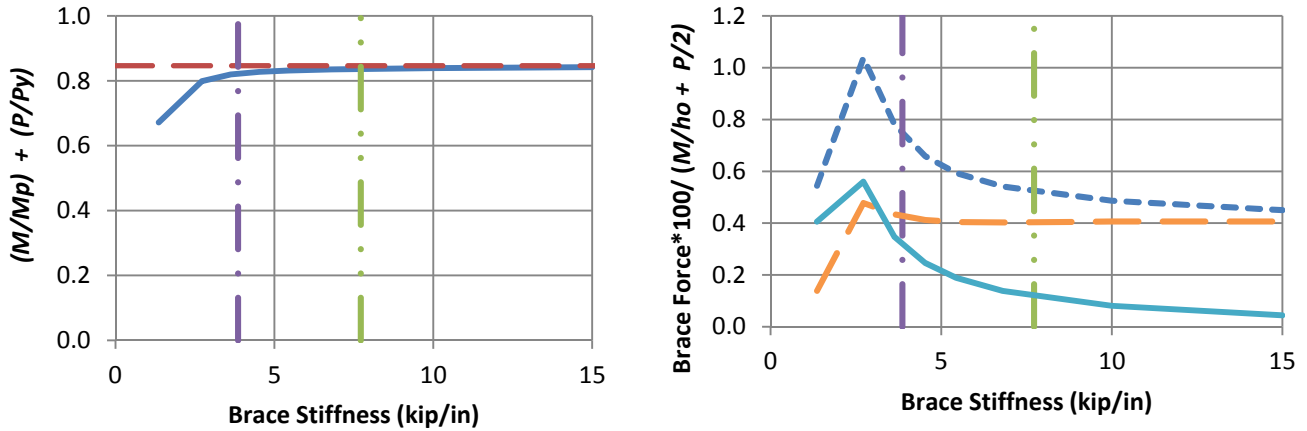
b) BC_MG1p_NB_n1_Lb15_FFR0

- Test simulation results
- - Rigidly-braced strength
- ⋯ 0.5 times bracing stiffness from Eq. (6-1)
- - Bracing stiffness from Eq. (6-1)

Figure 7.2. Beam-column knuckle curves and brace force vs. brace stiffness plots for point (nodal) lateral bracing cases with $n = 1$, Moment Gradient 1 loading, and $L_b = 15$ ft.



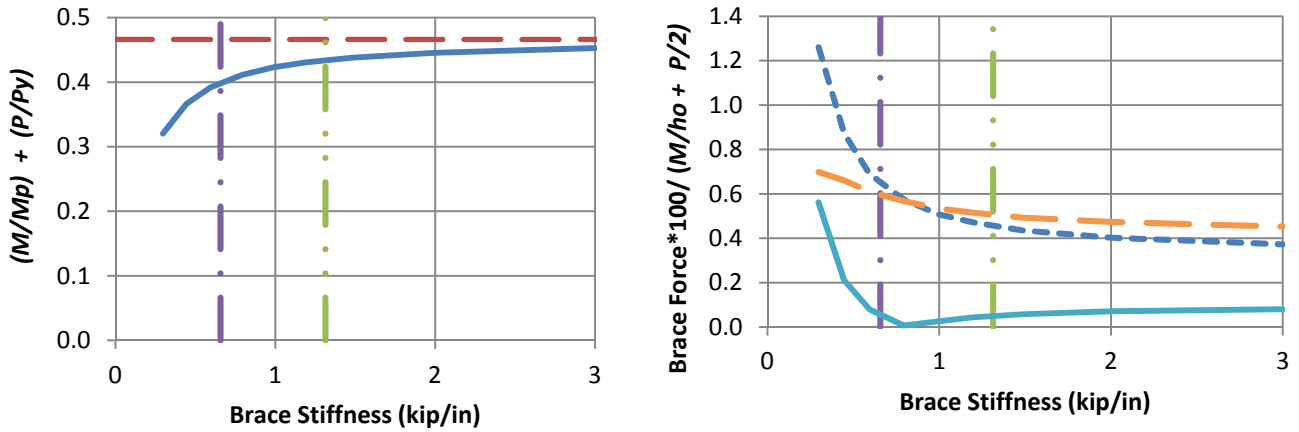
a) BC_MG1p_RB_n2_Lb5_FFR-0.5



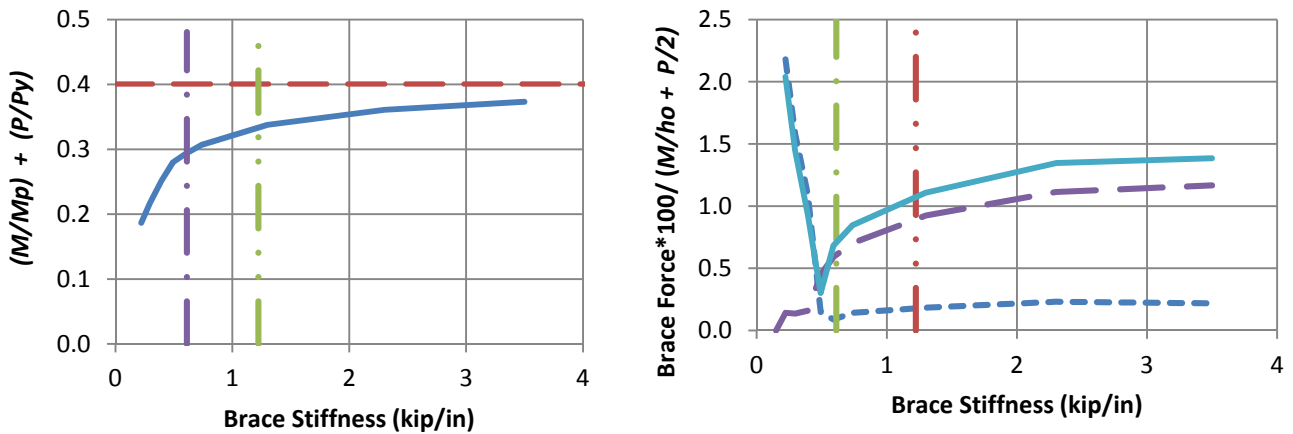
b) BC_MG1p_RB_n2_Lb5_FFR0

- Test simulation results
- - Rigidly-braced strength
- 0.5 times bracing stiffness from Eq. (6-1)
- Bracing stiffness from Eq. (6-1)
- - Left end panel shear force
- Right end panel shear force
- - Middle panel shear force

Figure 7.3. Beam-column knuckle curves and brace force vs. brace stiffness plots for shear panel (relative) lateral bracing cases with $n = 2$, Moment Gradient 1 loading, and $L_b = 5$ ft.



a) BC_MG1p_RB_n2_Lb15_FFR-0.5



b) BC_MG1p_RB_n2_Lb15_FFR0

- Test simulation results
- - Rigidly-braced strength
- 0.5 times bracing stiffness from Eq. (6-1)
- Bracing stiffness from Eq. (6-1)
- - Left end panel shear force
- Right end panel shear force
- - Middle panel shear force

Figure 7.4. Beam-column knuckle curves and brace force vs. brace stiffness plots for shear panel (relative) lateral bracing cases with $n = 2$, Moment Gradient 1 loading, and $L_b = 15$ ft.

Table 7.1. Brace stiffnesses β_{F96L} and β_{brL} , and brace forces as a percentage of $(M/h_o + P/2)$ for beam-columns with Moment Gradient 1 loading, lateral bracing only on the flange in flexural compression, and $P_{ft}/P_{fc} \leq 0$.

Case	β_{F96L} (kip/in)	β_{brL} (kip/in)	β_{brL} / β_{F96L}	% Brace Force at $\beta_L = \beta_{brL}$	Ratio of actual to estimated brace force at $\beta_L = \beta_{brL}$
BC_MG1p_NB_n1_Lb5_FFR-0.5	3.50	15.16	4.33	0.80	0.80
BC_MG1p_NB_n1_Lb5_FFR0	5.39	15.60	2.89	0.82	0.82
BC_MG1p_NB_n1_Lb15_FFR-0.5	3.29	2.74	0.83	0.76	0.76
BC_MG1p_NB_n1_Lb15_FFR0	1.52	2.50	1.64	0.70	0.70
BC_MG1p_RB_n2_Lb5_FFR-0.5	2.89	7.46	2.58	0.51	1.02
BC_MG1p_RB_n2_Lb5_FFR0	3.33	7.72	2.32	0.50	1.00
BC_MG1p_RB_n2_Lb15_FFR-0.5	2.29	1.32	0.58	0.50	1.00
BC_MG1p_RB_n2_Lb15_FFR0	1.74	1.22	0.70	1.05	2.10

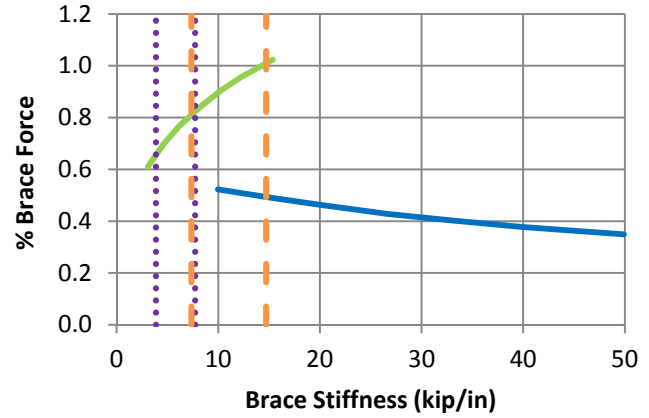
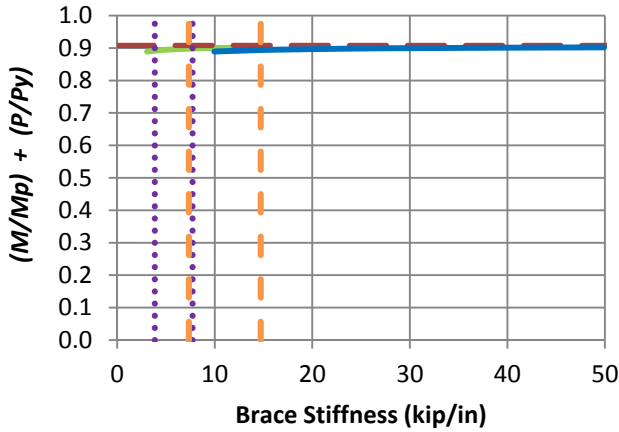
From Table 7.1, it can be observed that the bracing stiffness calculated by Eq. (6-1) is accurate to conservative for all cases except for those in which the L/r_{yf} of the unbraced flange (the flange loaded in flexural tension) is greater than 200 (i.e., the tests with $n = 2$ and $L_b = 15$ ft). This behavior is similar to that observed in Section 6.4.1 for beam-column members with lateral bracing only on one flange, subjected to uniform bending. BC_MG1p_NB_n1_Lb15_FFR-0.5 has a $\beta_{brL} / \beta_{F96L}$ slightly less than 1.0; however, one can observe from Fig. 7.2a that the knuckle curve is relatively flat at $\beta_L = \beta_{brL} = 2.74$ kip/in. Therefore, the bracing performance for this case is acceptable. Approximately 95 % of the beam rigidly-braced strength is developed at $\beta_L = \beta_{brL}$. Similarly from Figs. 7.1 through 7.4 and Table 7.1, it can be observed that the bracing strength calculated by Eq. (6-2) is accurate to slightly conservative for all cases except BC_MG1p_RB_n2_Lb15_FFR0, for which the L/r_{yf} of the unbraced flange greater than 200.

7.3.2 Beam-Columns with Combined Lateral and Torsional Bracing, Subjected to Moment Gradient 1 Loading

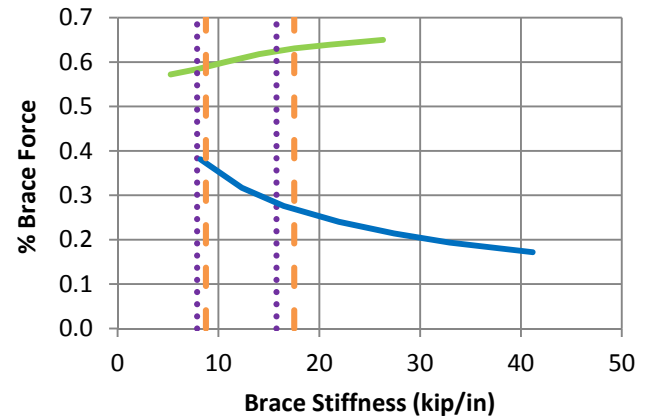
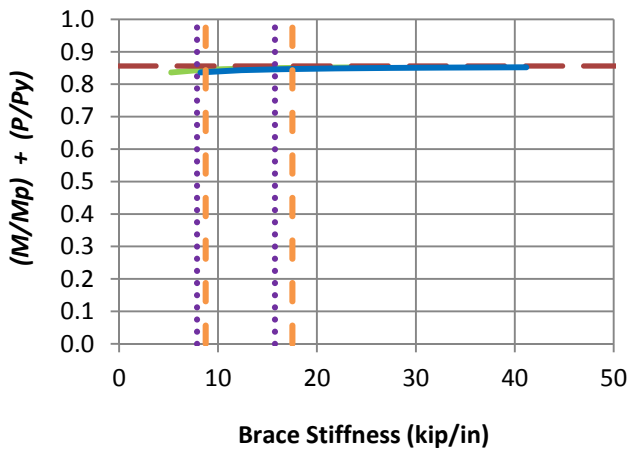
The knuckle curves and brace force - brace stiffness curves for beam-columns with Moment Gradient 1 loading and combined point lateral and torsional bracing are shown in Figs. 7.5 through 7.12. Tables 7.2 and 7.3 compare the estimated stiffness and strength requirements to the simulation results from these figures. The point lateral brace force in these figures and tables is expressed as percentage with respect to P . The point torsional brace force is expressed as percentage with respect to $M/h_o + P/2$.

From Tables 7.2 and 7.3, it can be observed that the bracing strength requirements predicted by Eqs. (6-6) and (6-8) are conservative for all cases except BC_MG1n_CNTB_n1_Lb15_FFR-0.5. The point lateral brace force versus the Load Proportionality Factor for this case, with the brace stiffnesses calculated from Eqs. (6-6) and (6-8) is shown in Fig. 7.13. It can be observed that a point lateral brace strength requirement of $0.01P$ is sufficient to develop member strength very close to the test limit load.

In addition, it can be observed from Tables 7.2 and 7.3 that the recommended lateral or torsional bracing stiffness is smaller than the stiffness required to reach 96 % of the rigidly-braced strength for a few cases. For these cases, Tables 7.4 and 7.5 show the peak load as a percentage of the rigidly-braced strength when $\beta_L = \beta_{brL}$ or $\beta_T = \beta_{brT}$, depending on which of these equalities corresponds to the smaller member strength in the test simulations. The cases shown in Table 7.4 are more critical with respect to the lateral bracing stiffness (i.e., the member strength is smaller when $\beta_L = \beta_{brL}$ than when $\beta_T = \beta_{brT}$), and the cases shown in Table 7.5 are more critical with respect to the torsional bracing stiffness (i.e., the member strength is smaller when $\beta_T = \beta_{brT}$ compared to when $\beta_L = \beta_{brL}$). (It should be noted that $\beta_L/\beta_T = \beta_{brL}/\beta_{brT}$ in these test simulations; however, the $\beta_{F96L}/\beta_{F96T}$ ratio depends on the physical characteristics of the problems as captured by the test simulations and generally is not the same as β_{brL}/β_{brT} .)



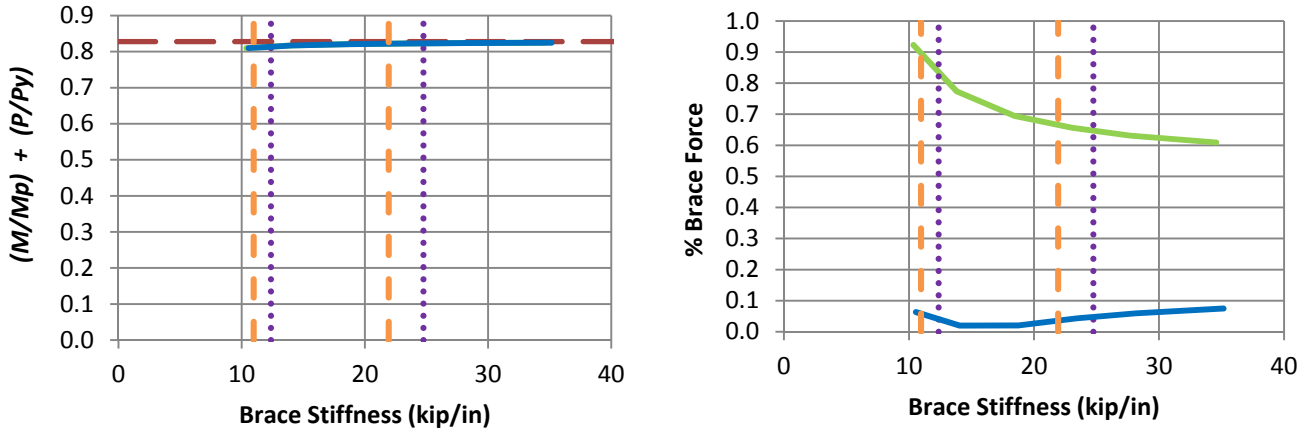
a) BC_MG1p_CNTB_n1_Lb5_FFR-0.5



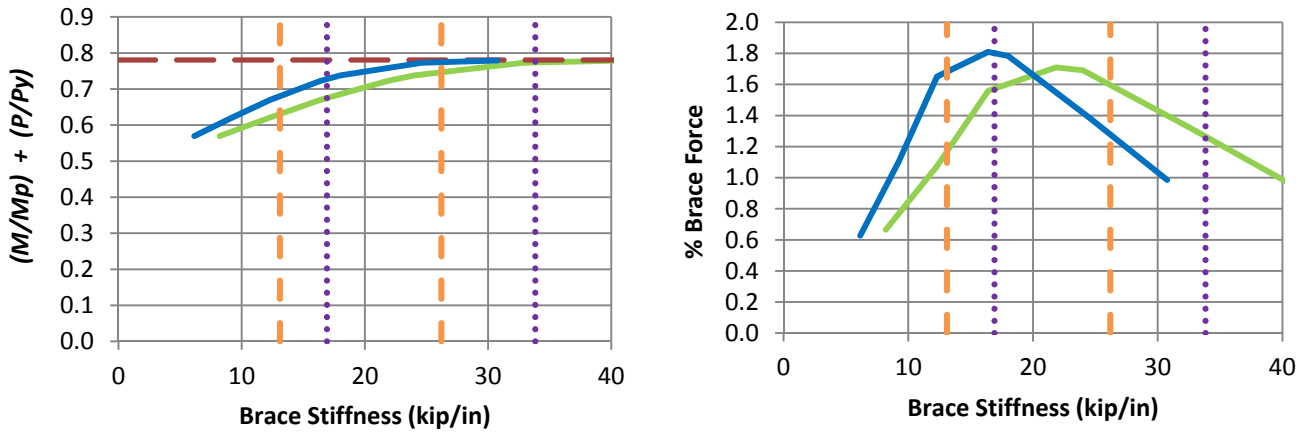
b) BC_MG1p_CNTB_n1_Lb5_FFR0

- Rigidly-braced strength
- Test simulation results corresponding to torsional brace
- Test simulation results corresponding to lateral brace
- 1x and 0.5x lateral bracing stiffness from Eq. (6-5)
- 1x and 0.5x torsional bracing stiffness from Eq. (6-7)

Figure 7.5. Beam-column knuckle curves and brace force vs. brace stiffness plots for combined point (nodal) lateral and torsional bracing cases with $n = 1$, Moment Gradient 1 loading with lateral bracing on the flange in flexural compression, and $L_b = 5$ ft.



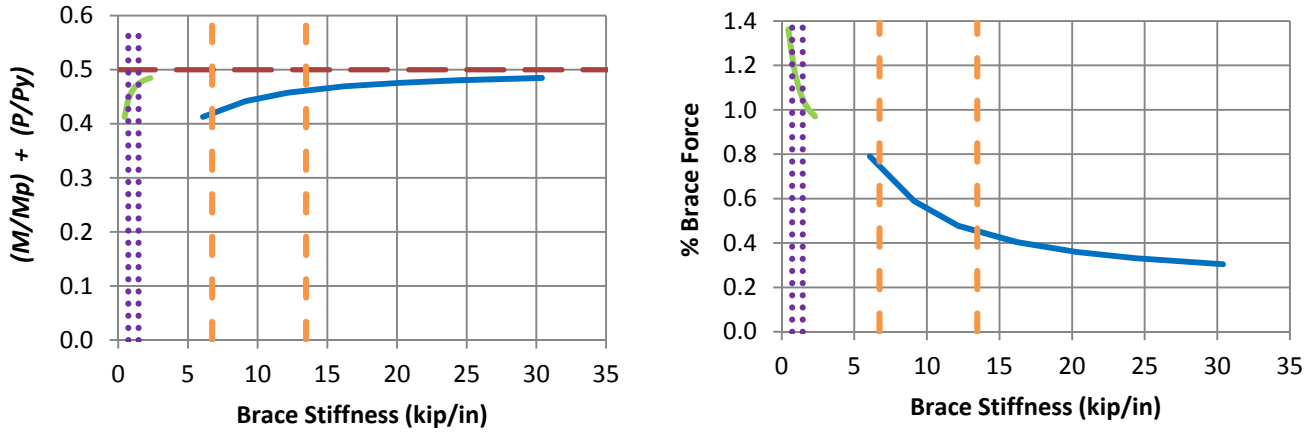
c) BC_MG1p_CNTB_n1_Lb5_FFR0.5



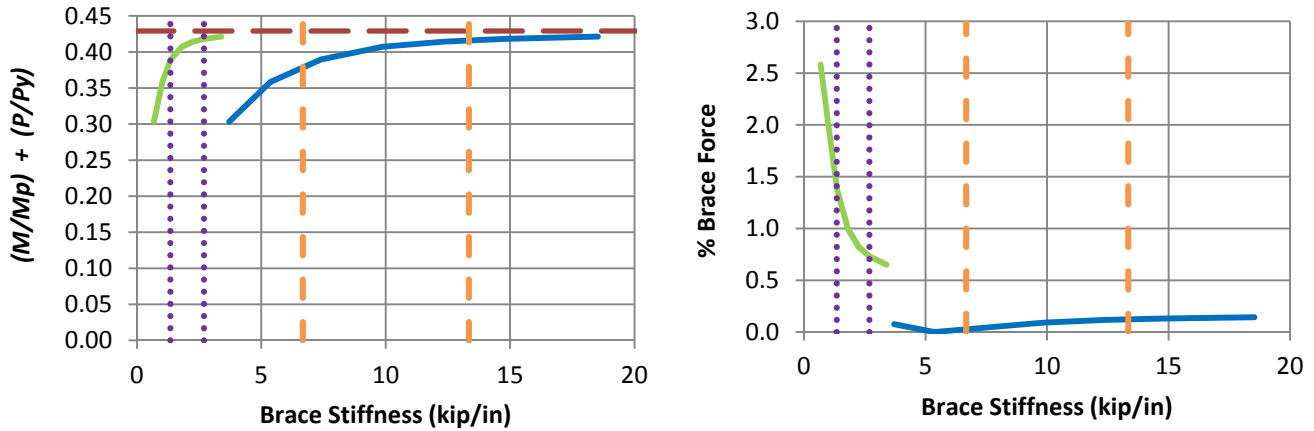
d) BC_MG1p_CNTB_n1_Lb5_FFR1

- Rigidly-braced strength
- Test simulation results corresponding to torsional brace
- Test simulation results corresponding to lateral brace
- 1x and 0.5x lateral bracing stiffness from Eq. (6-5)
- - - 1x and 0.5x torsional bracing stiffness from Eq. (6-7)

Fig. 7.5 (continued). Beam-column knuckle curves and brace force vs. brace stiffness plots for combined point (nodal) lateral and torsional bracing cases with $n = 1$, Moment Gradient 1 loading with lateral bracing on the flange in flexural compression, and $L_b = 5$ ft.



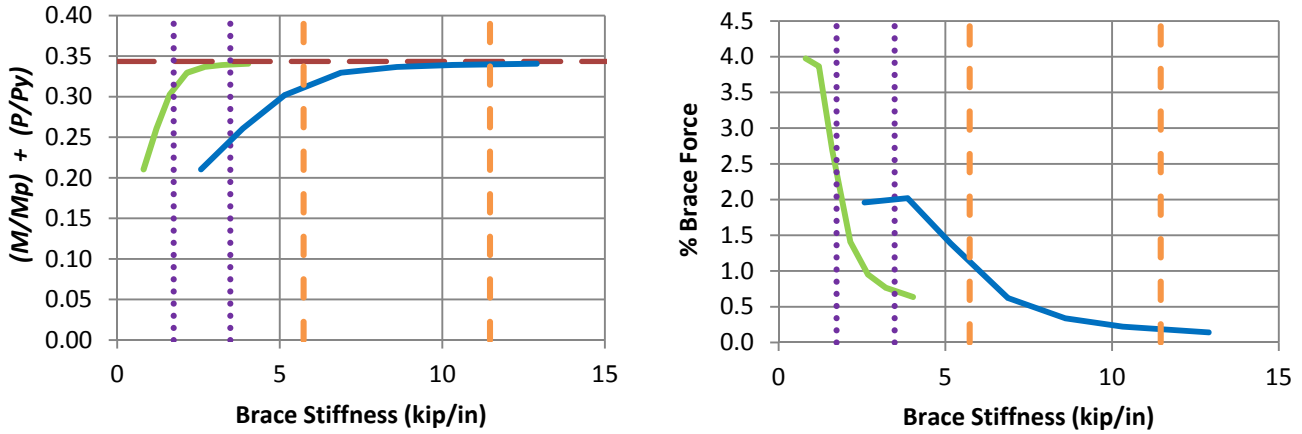
a) BC_MG1p_CNTB_n1_Lb15_FFR-0.5



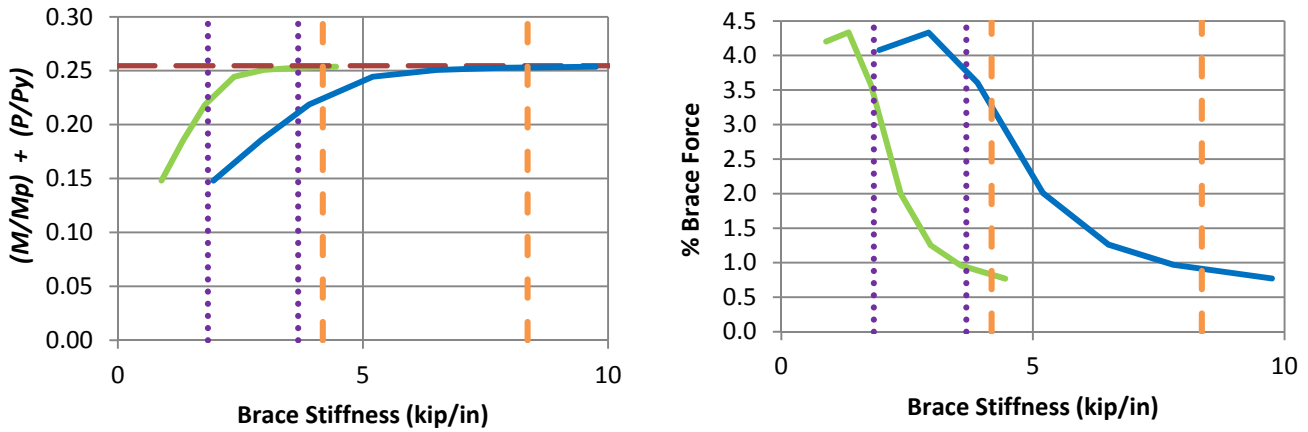
b) BC_MG1p_CNTB_n1_Lb15_FFR0

- Rigidly-braced strength — Test simulation results corresponding to torsional brace
- Test simulation results corresponding to lateral brace
- 1x and 0.5x lateral bracing stiffness from Eq. (6-5)
- - - 1x and 0.5x torsional bracing stiffness from Eq. (6-7)

Figure 7.6. Beam-column knuckle curves and brace force vs. brace stiffness plots for combined point (nodal) lateral and torsional bracing cases with $n = 1$, Moment Gradient 1 loading with lateral bracing on the flange in flexural compression, and $L_b = 15$ ft.



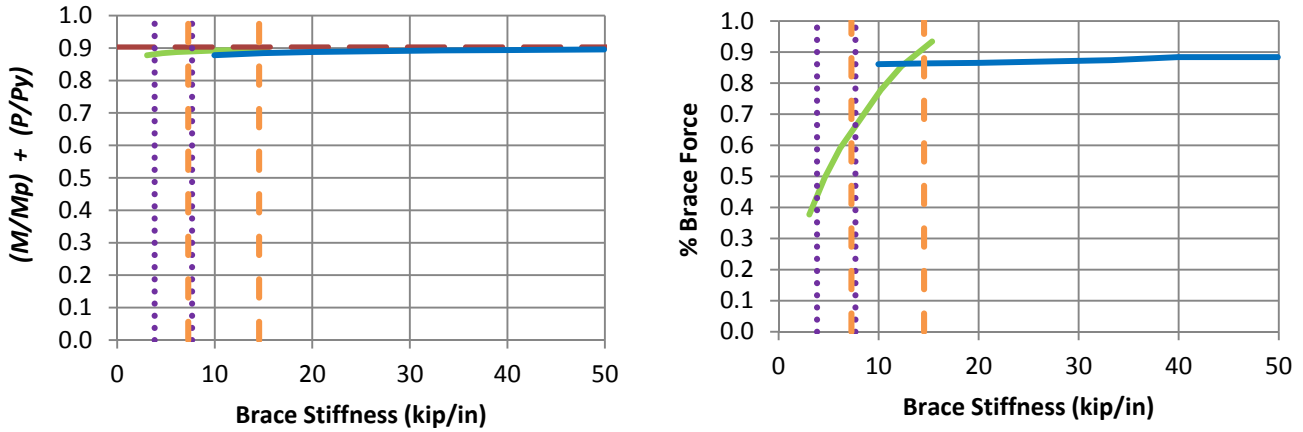
c) BC_MG1p_CNTB_n1_Lb15_FFR0.5



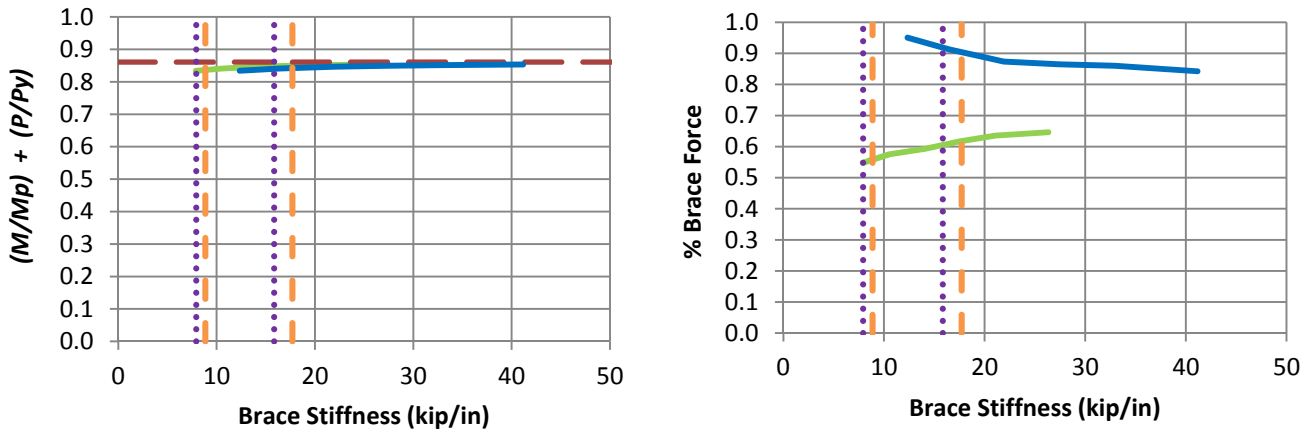
d) BC_MG1p_CNTB_n1_Lb15_FFR1

- Rigidly-braced strength
- Test simulation results corresponding to torsional brace
- Test simulation results corresponding to lateral brace
- ⋯ 1x and 0.5x lateral bracing stiffness from Eq. (6-5)
- 1x and 0.5x torsional bracing stiffness from Eq. (6-7)

Fig. 7.6 (continued). Beam-column knuckle curves and brace force vs. brace stiffness plots for combined point (nodal) lateral and torsional bracing cases with $n = 1$, Moment Gradient 1 loading with lateral bracing on the flange in flexural compression, and $L_b = 15$ ft.



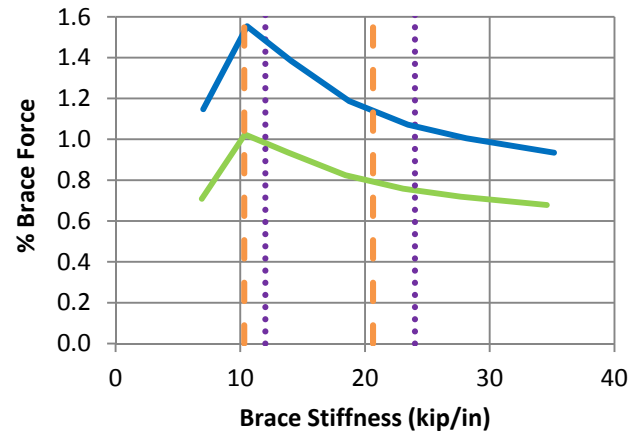
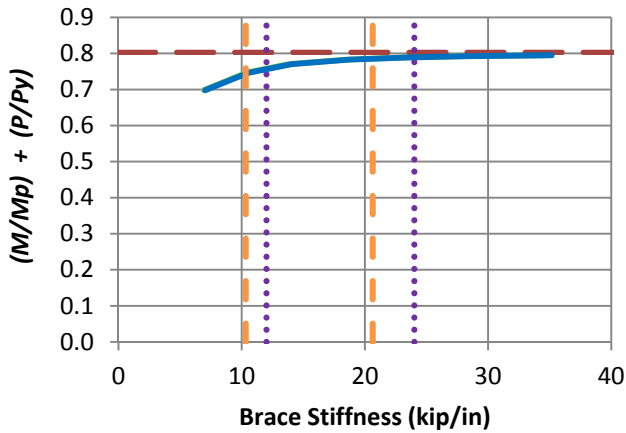
a) BC_MG1n_CNTB_n1_Lb5_FFR-0.5



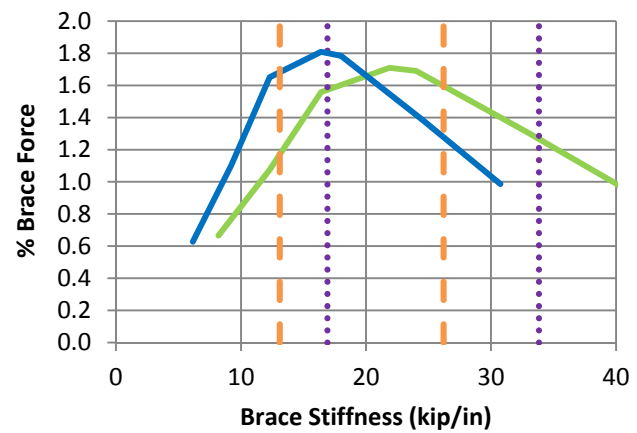
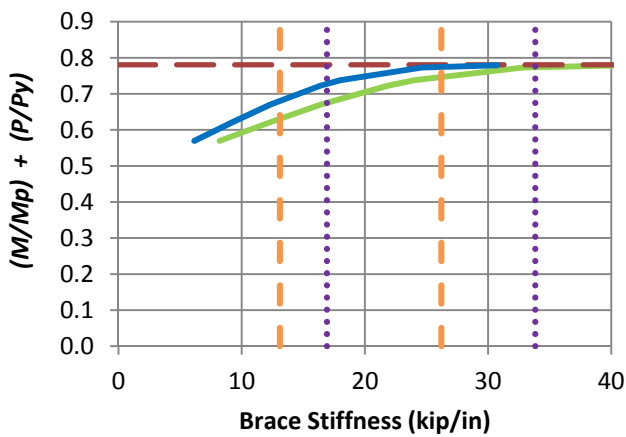
b) BC_MG1n_CNTB_n1_Lb5_FFR0

- Rigidly-braced strength
- Test simulation results corresponding to torsional brace
- Test simulation results corresponding to lateral brace
- 1x and 0.5x lateral bracing stiffness from Eq. (6-5)
- - - 1x and 0.5x torsional bracing stiffness from Eq. (6-7)

Figure 7.7. Beam-column knuckle curves and brace force vs. brace stiffness plots for combined point (nodal) lateral and torsional bracing cases with $n = 1$, Moment Gradient 1 loading with lateral bracing on the flange in flexural tension, and $L_b = 5$ ft.



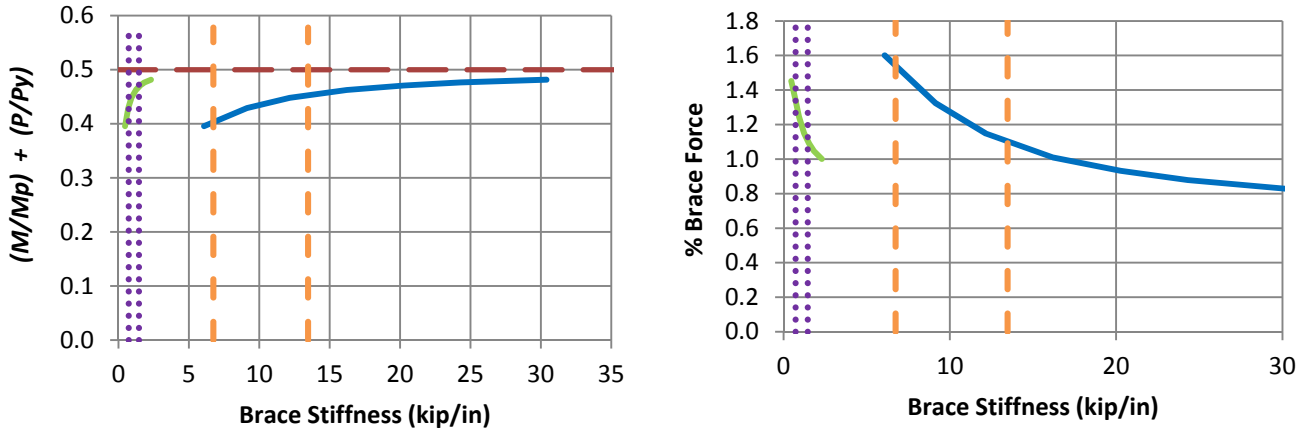
c) BC_MG1n_CNTB_n1_Lb5_FFR0.5



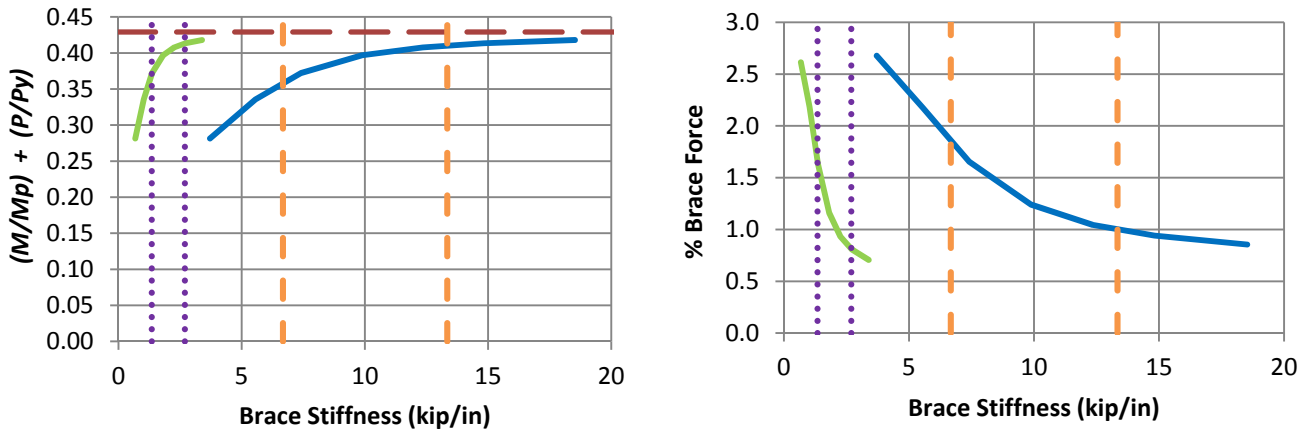
d) BC_MG1n_CNTB_n1_Lb5_FFR1

- Rigidly-braced strength
- Test simulation results corresponding to torsional brace
- Test simulation results corresponding to lateral brace
- 1x and 0.5x lateral bracing stiffness from Eq. (6-5)
- 1x and 0.5x torsional bracing stiffness from Eq. (6-7)

Fig. 7.7 (continued). Beam-column knuckle curves and brace force vs. brace stiffness plots for combined point (nodal) lateral and torsional bracing cases with $n = 1$, Moment Gradient 1 loading with lateral bracing on the flange in flexural tension, and $L_b = 5$ ft.



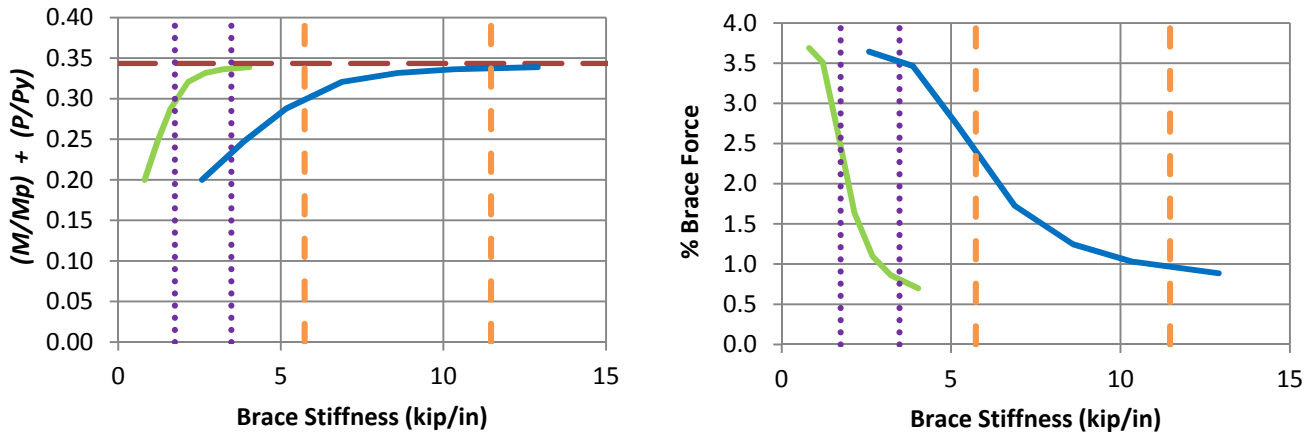
a) BC_MG1n_CNTB_n1_Lb15_FFR-0.5



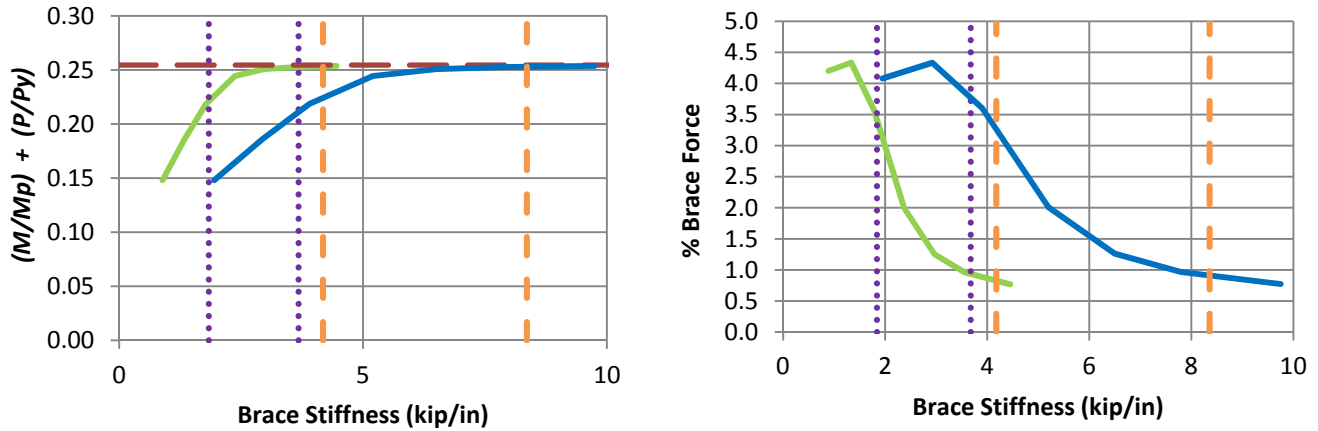
b) BC_MG1n_CNTB_n1_Lb15_FFR0

- Rigidly-braced strength
- Test simulation results corresponding to torsional brace
- Test simulation results corresponding to lateral brace
- 1x and 0.5x lateral bracing stiffness from Eq. (6-5)
- - - 1x and 0.5x torsional bracing stiffness from Eq. (6-7)

Figure 7.8. Beam-column knuckle curves and brace force vs. brace stiffness plots for combined point (nodal) lateral and torsional bracing cases with $n = 1$, Moment Gradient 1 loading with lateral bracing on the flange in flexural tension, and $L_b = 15$ ft.



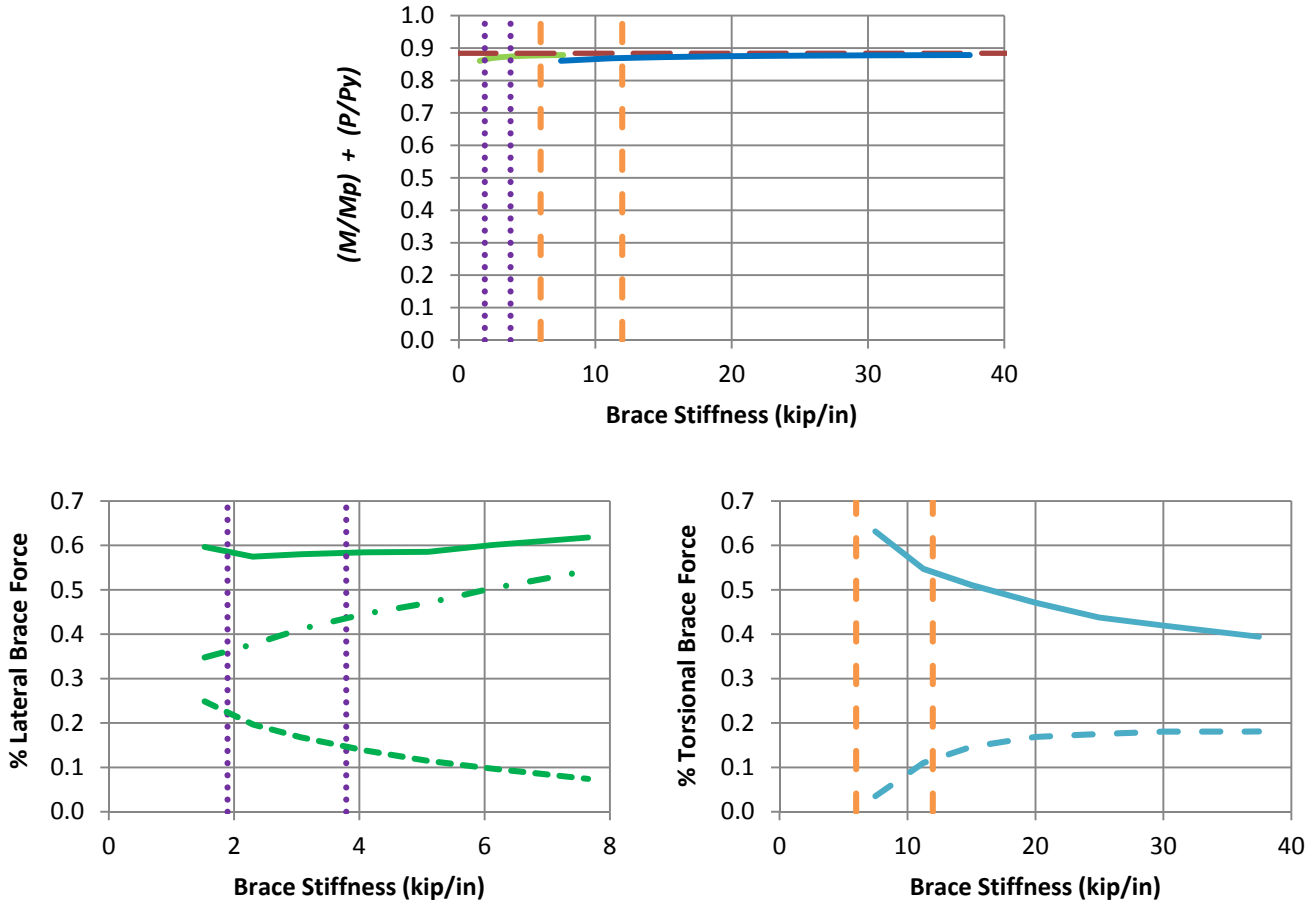
c) BC_MG1n_CNTB_n1_Lb15_FFR0.5



d) BC_MG1n_CNTB_n1_Lb15_FFR1

- Rigidly-braced strength
- Test simulation results corresponding to torsional brace
- Test simulation results corresponding to lateral brace
- 1x and 0.5x lateral bracing stiffness from Eq. (6-5)
- 1x and 0.5x torsional bracing stiffness from Eq. (6-7)

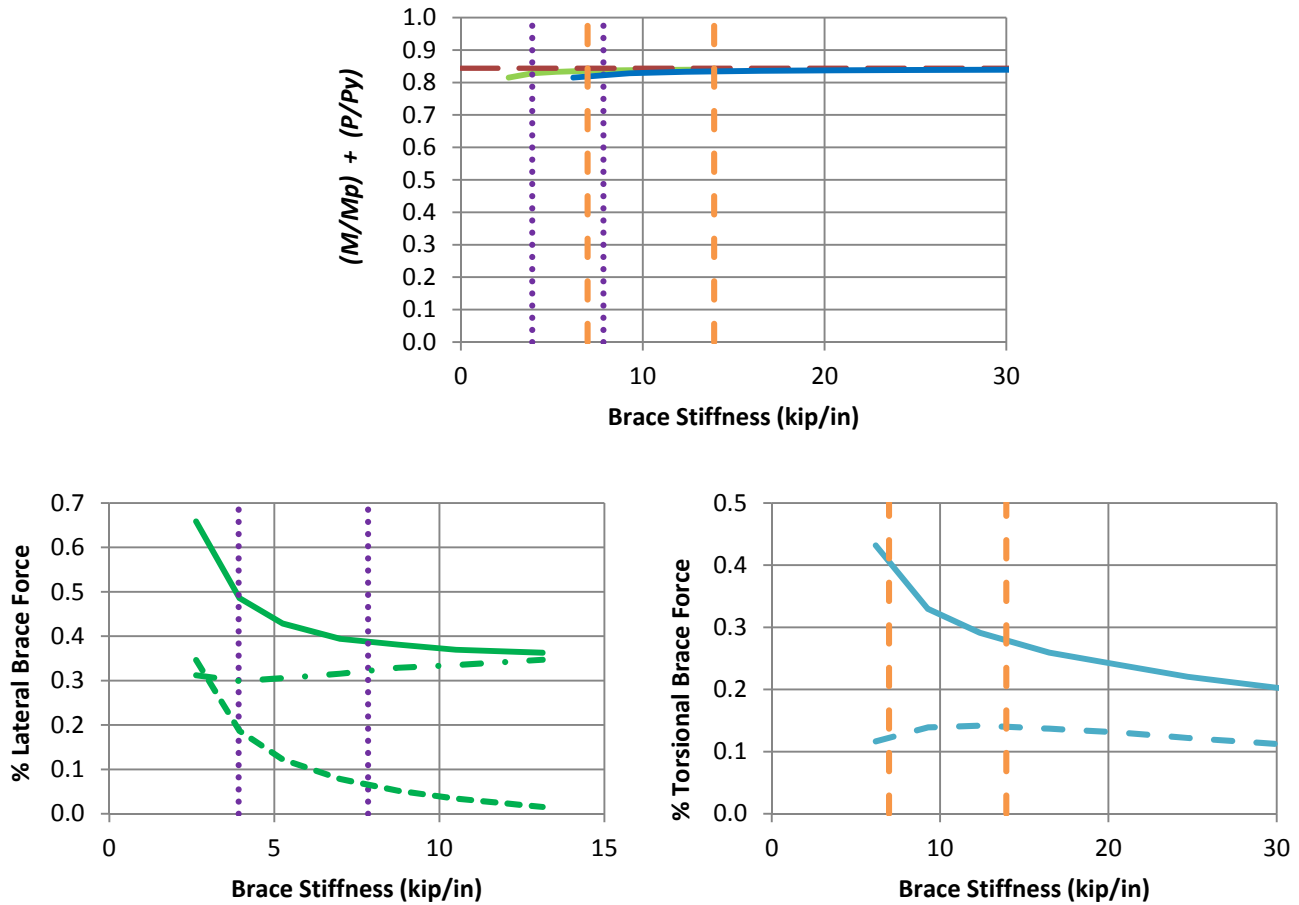
Fig. 7.8 (continued). Beam-column knuckle curves and brace force vs. brace stiffness plots for combined point (nodal) lateral and torsional bracing cases with $n = 1$, Moment Gradient 1 loading with lateral bracing on the flange in flexural tension, and $L_b = 15$ ft.



f) BC_MG1p_CRTB_n2_Lb5_FFR-0.5

- Rigidly-braced strength
- Test simulation results corresponding to torsional brace
- Test simulation results corresponding to lateral brace
- 1x and 0.5x lateral bracing stiffness from Eq. (6-5)
- 1x and 0.5x torsional bracing stiffness from Eq. (6-7)
- Left end panel shear force
- Right end panel shear force
- Middle panel shear force
- Torsional brace force 1
- Torsional brace force 2

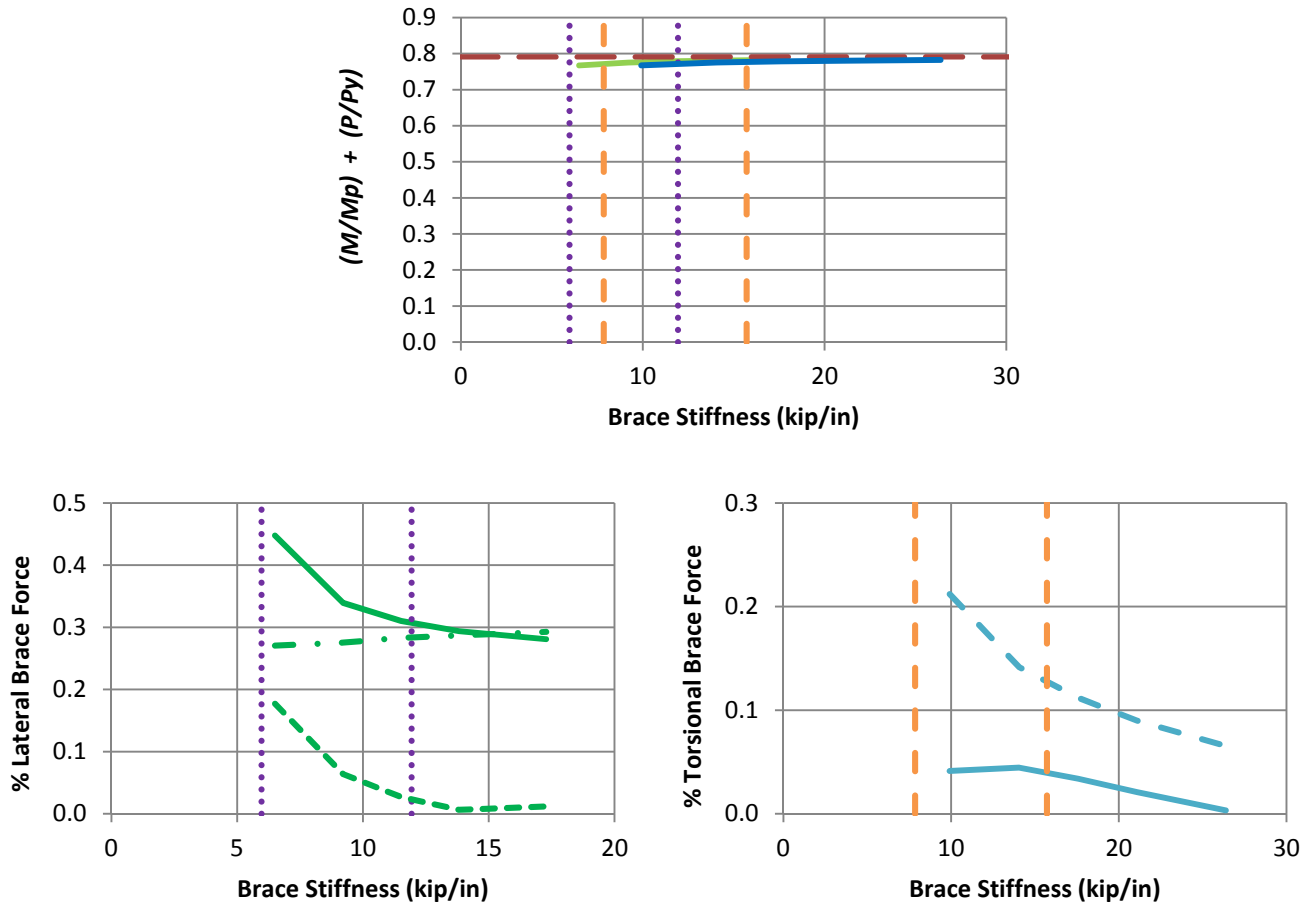
Figure 7.9. Beam-column knuckle curves and brace force vs. brace stiffness plots for combined shear panel (relative) lateral and torsional bracing cases with $n = 2$, Moment Gradient 1 loading with lateral bracing on the flange in flexural compression, and $L_b = 5$ ft.



g) BC_MG1p_CRTB_n2_Lb5_FFR0

- Rigidly-braced strength
- Test simulation results corresponding to torsional brace
- Test simulation results corresponding to lateral brace
- 1x and 0.5x lateral bracing stiffness from Eq. (6-5)
- - - 1x and 0.5x torsional bracing stiffness from Eq. (6-7)
- Left end panel shear force
- - - Right end panel shear force
- . - Middle panel shear force
- Torsional brace force 1
- - - Torsional brace force 2

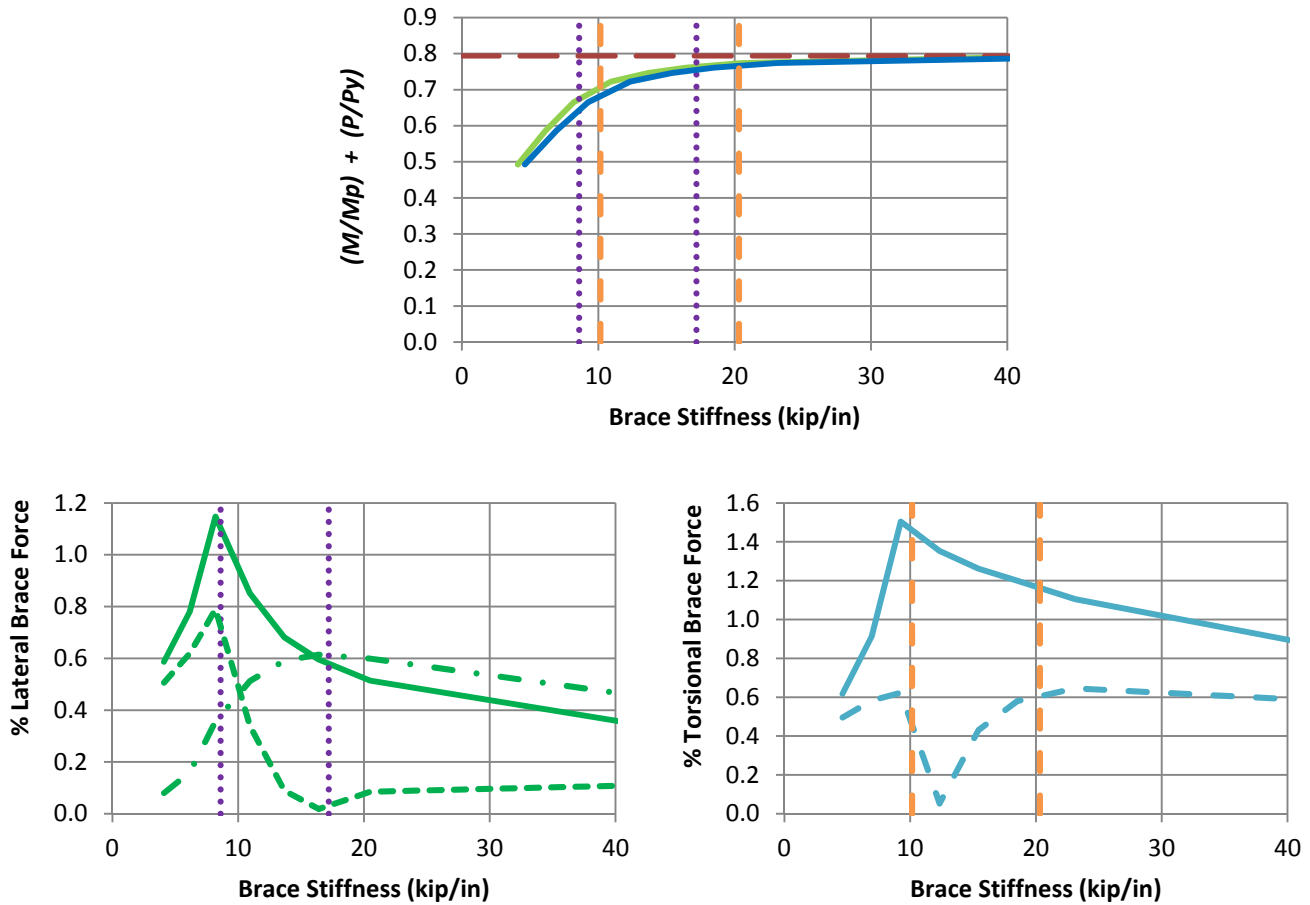
Fig. 7.9 (continued). Beam-column knuckle curves and brace force vs. brace stiffness plots for combined shear panel (relative) lateral and torsional bracing cases with $n = 2$, Moment Gradient 1 loading with lateral bracing on the flange in flexural compression, and $L_b = 5$ ft.



h) BC_MG1p_CRTB_n2_Lb5_FFR0.5

- Rigidly-braced strength
- Test simulation results corresponding to torsional brace
- Test simulation results corresponding to lateral brace
- 1x and 0.5x lateral bracing stiffness from Eq. (6-5)
- - - 1x and 0.5x torsional bracing stiffness from Eq. (6-7)
- Left end panel shear force
- - - Right end panel shear force
- . - Middle panel shear force
- Torsional brace force 1
- - - Torsional brace force 2

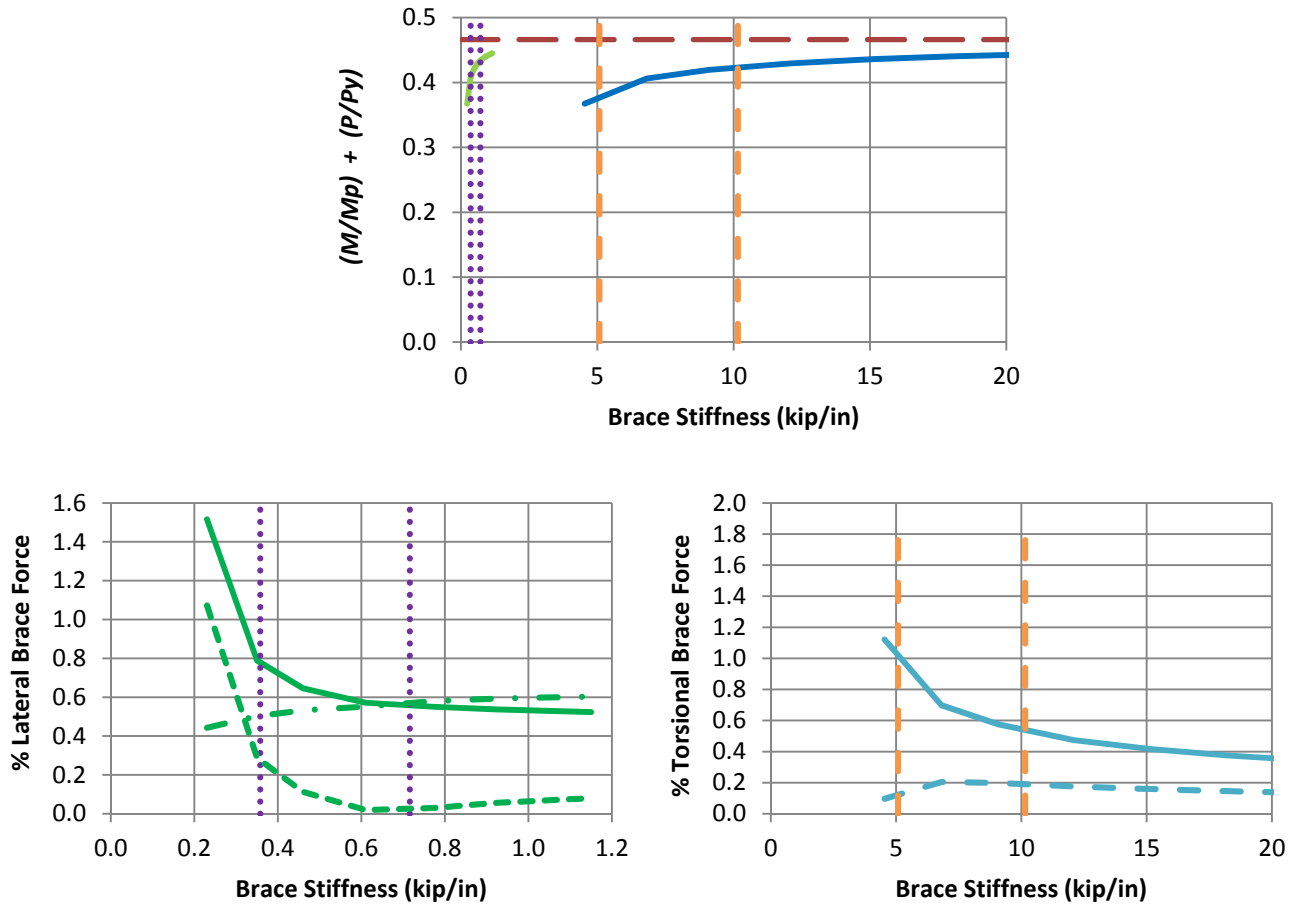
Fig. 7.9 (continued). Beam-column knuckle curves and brace force vs. brace stiffness plots for combined shear panel (relative) lateral and torsional bracing cases with $n = 2$, Moment Gradient 1 loading with lateral bracing on the flange in flexural compression, and $L_b = 5$ ft.



i) BC_MG1p_CRTB_n2_Lb5_FFR1

- Rigidly-braced strength
- Test simulation results corresponding to torsional brace
- Test simulation results corresponding to lateral brace
- 1x and 0.5x lateral bracing stiffness from Eq. (6-5)
- - - 1x and 0.5x torsional bracing stiffness from Eq. (6-7)
- Left end panel shear force
- - - Right end panel shear force
- . - Middle panel shear force
- Torsional brace force 1
- - - Torsional brace force 2

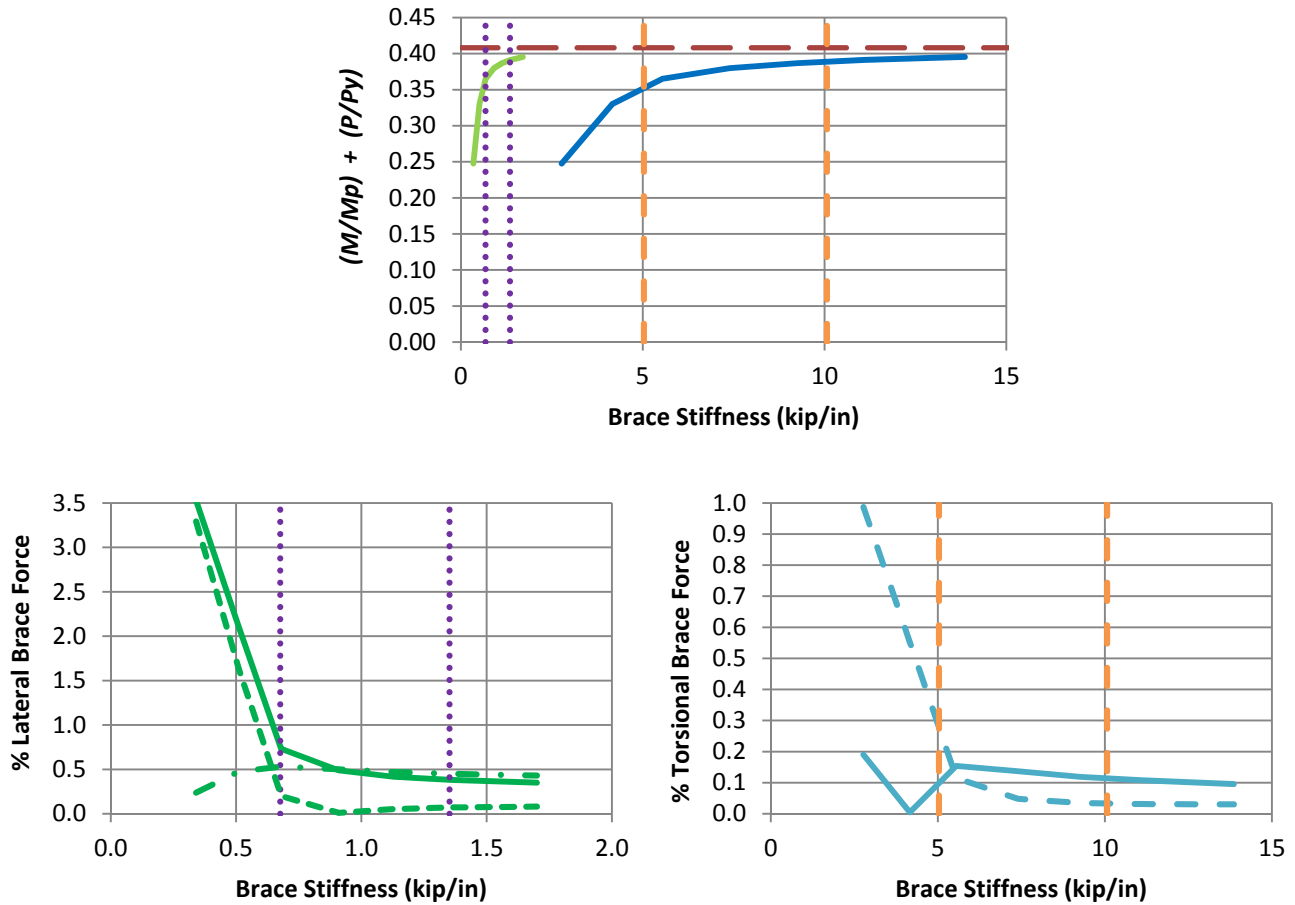
Fig. 7.9 (continued). Beam-column knuckle curves and brace force vs. brace stiffness plots for combined shear panel (relative) lateral and torsional bracing cases with $n = 2$, Moment Gradient 1 loading with lateral bracing on the flange in flexural compression, and $L_b = 5$ ft.



a) BC_MG1p_CRTB_n2_Lb15_FFR-0.5

- Rigidly-braced strength
- Test simulation results corresponding to torsional brace
- Test simulation results corresponding to lateral brace
- 1x and 0.5x lateral bracing stiffness from Eq. (6-5)
- - - 1x and 0.5x torsional bracing stiffness from Eq. (6-7)
- Left end panel shear force
- - - Right end panel shear force
- . - Middle panel shear force
- Torsional brace force 1
- Torsional brace force 2

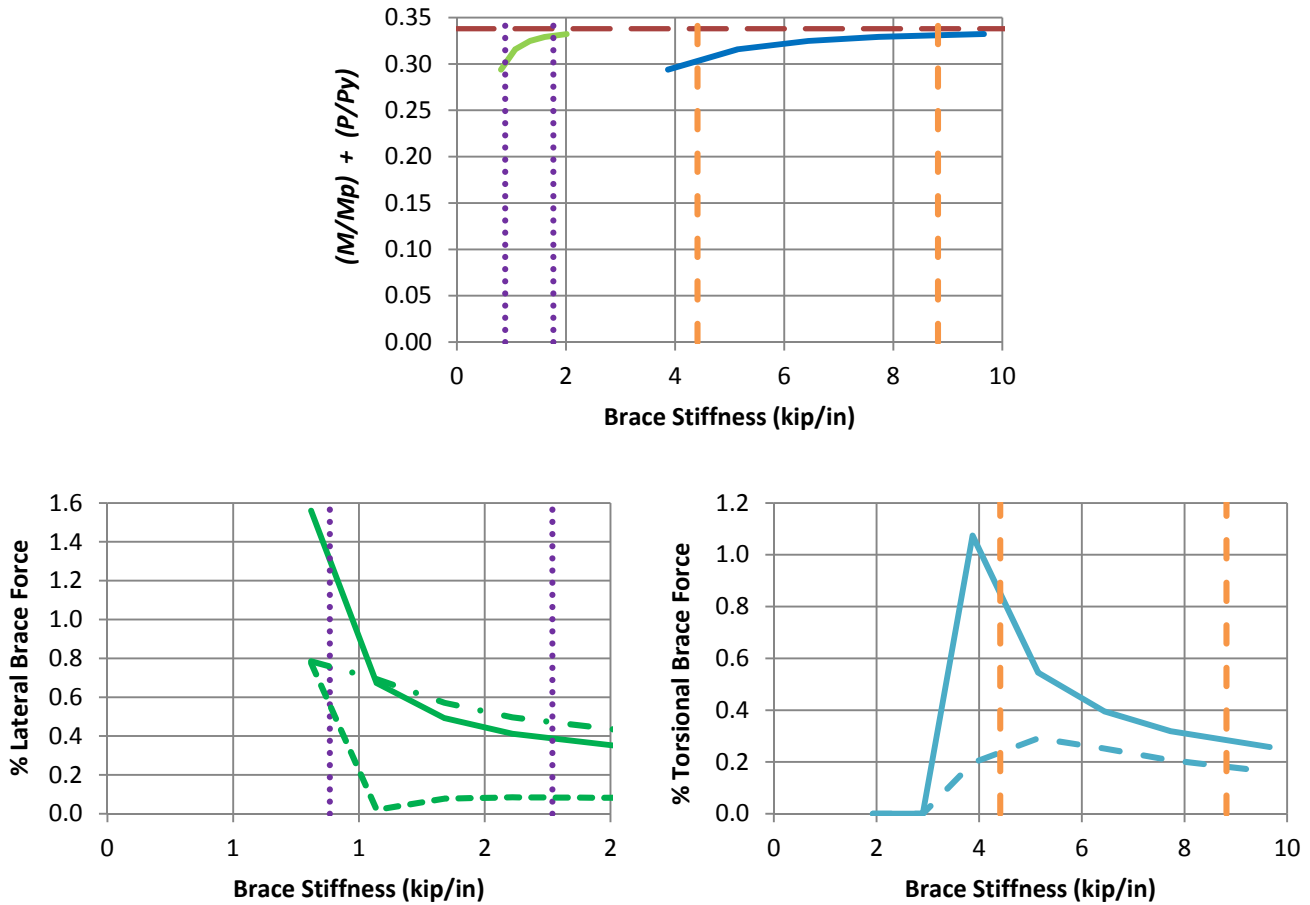
Figure 7.10. Beam-column knuckle curves and brace force vs. brace stiffness plots for combined shear panel (relative) lateral and torsional bracing cases with $n = 2$, Moment Gradient 1 loading with lateral bracing on the flange in flexural compression, and $L_b = 15$ ft.



b) BC_MG1p_CRTB_n2_Lb15_FFR0

- Rigidly-braced strength
- Test simulation results corresponding to torsional brace
- Test simulation results corresponding to lateral brace
- 1x and 0.5x lateral bracing stiffness from Eq. (6-5)
- - - 1x and 0.5x torsional bracing stiffness from Eq. (6-7)
- Left end panel shear force
- - - Right end panel shear force
- . - Middle panel shear force
- Torsional brace force 1
- - - Torsional brace force 2

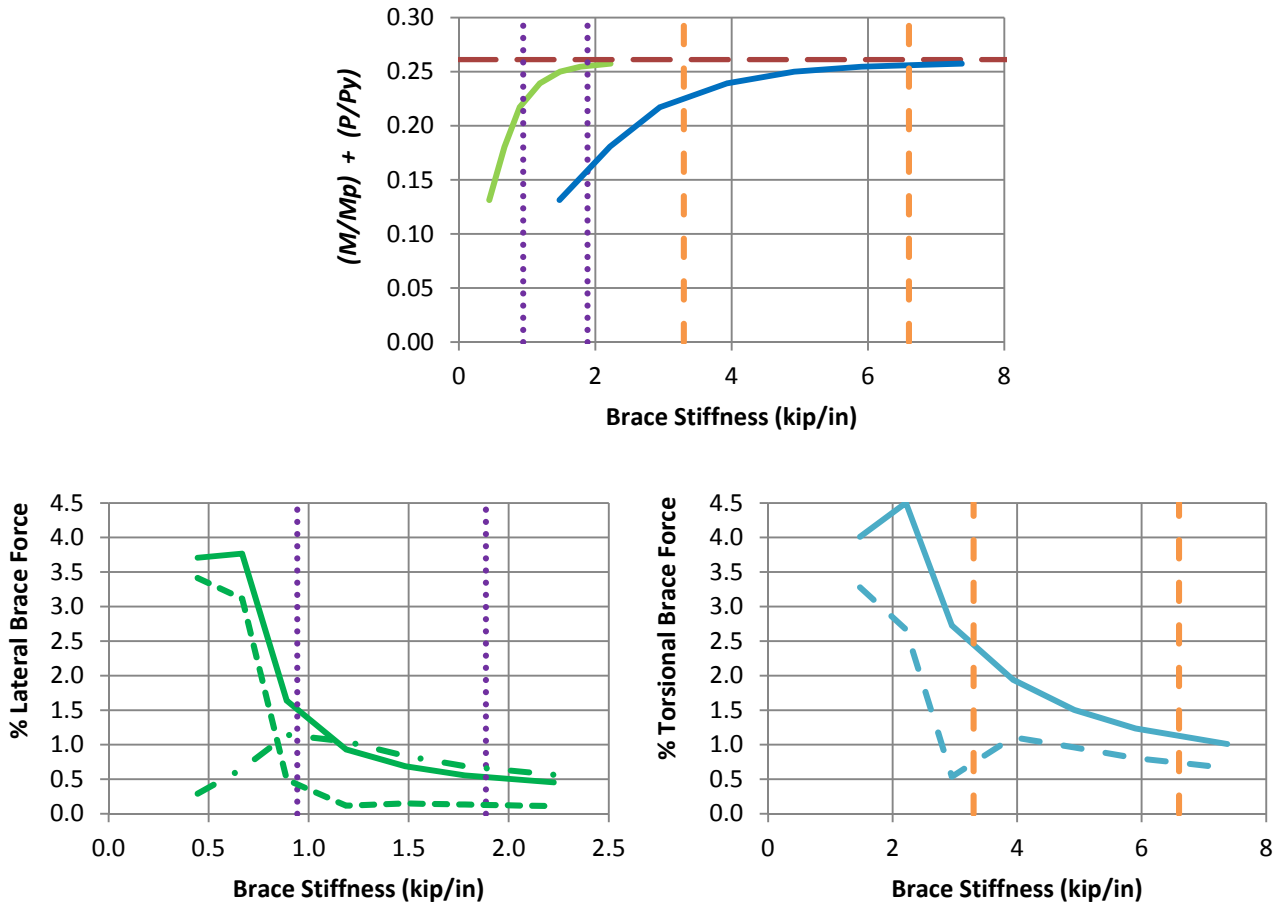
Fig. 7.10 (continued). Beam-column knuckle curves and brace force vs. brace stiffness plots for combined shear panel (relative) lateral and torsional bracing cases with $n = 2$, Moment Gradient 1 loading with lateral bracing on the flange in flexural compression, and $L_b = 15$ ft.



c) BC_MG1p_CRTB_n2_Lb15_FFR0.5

- Rigidly-braced strength
- Test simulation results corresponding to torsional brace
- Test simulation results corresponding to lateral brace
- 1x and 0.5x lateral bracing stiffness from Eq. (6-5)
- - - 1x and 0.5x torsional bracing stiffness from Eq. (6-7)
- Left end panel shear force
- - - Right end panel shear force
- . - Middle panel shear force
- Torsional brace force 1
- Torsional brace force 2

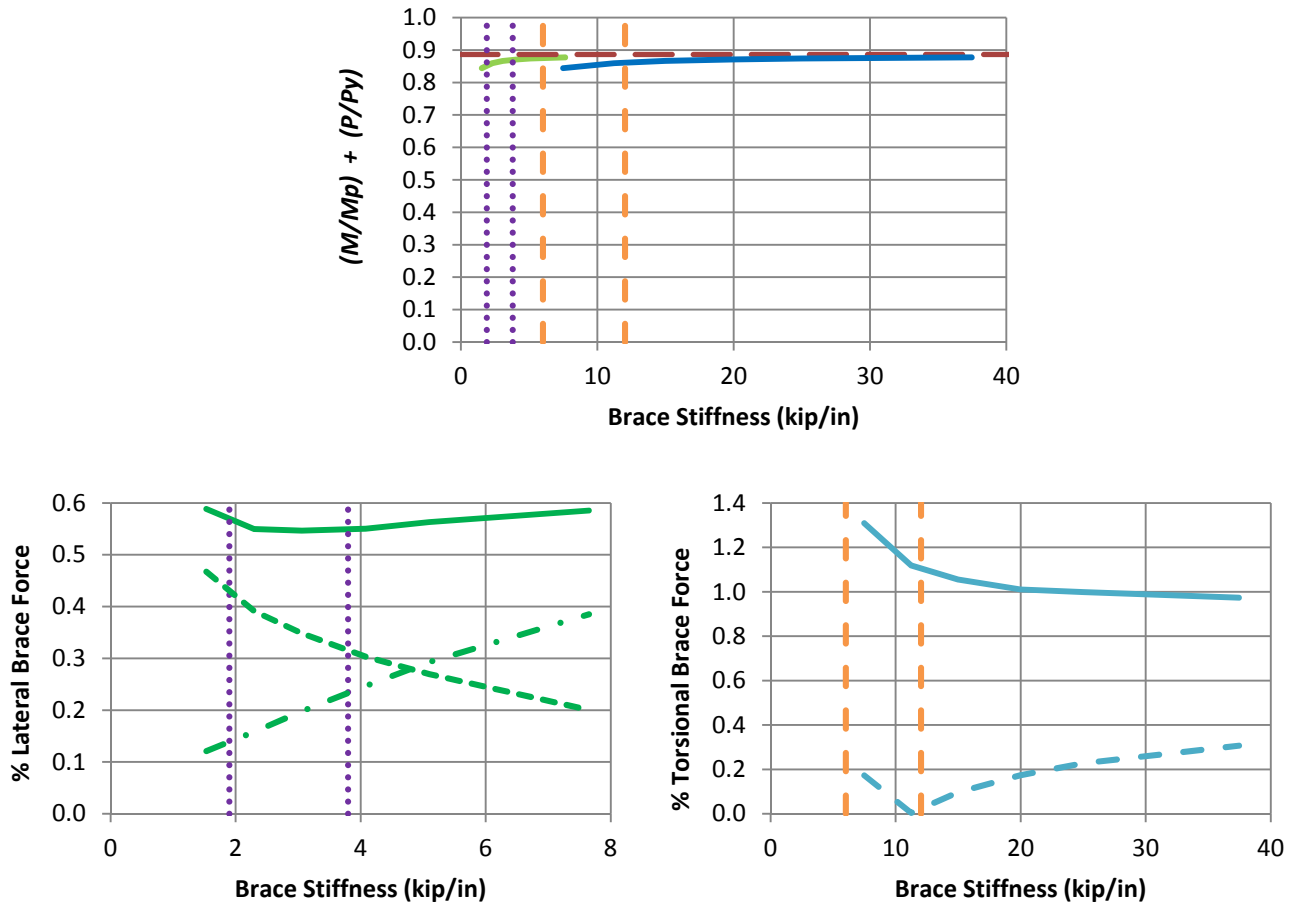
Fig. 7.10 (continued). Beam-column knuckle curves and brace force vs. brace stiffness plots for combined shear panel (relative) lateral and torsional bracing cases with $n = 2$, Moment Gradient 1 loading with lateral bracing on the flange in flexural compression, and $L_b = 15$ ft.



d) BC_MG1p_CRTB_n2_Lb15_FFR1

- Rigidly-braced strength
- Test simulation results corresponding to torsional brace
- Test simulation results corresponding to lateral brace
- 1x and 0.5x lateral bracing stiffness from Eq. (6-5)
- - - 1x and 0.5x torsional bracing stiffness from Eq. (6-7)
- Left end panel shear force
- - - Right end panel shear force
- . - Middle panel shear force
- Torsional brace force 1
- Torsional brace force 2

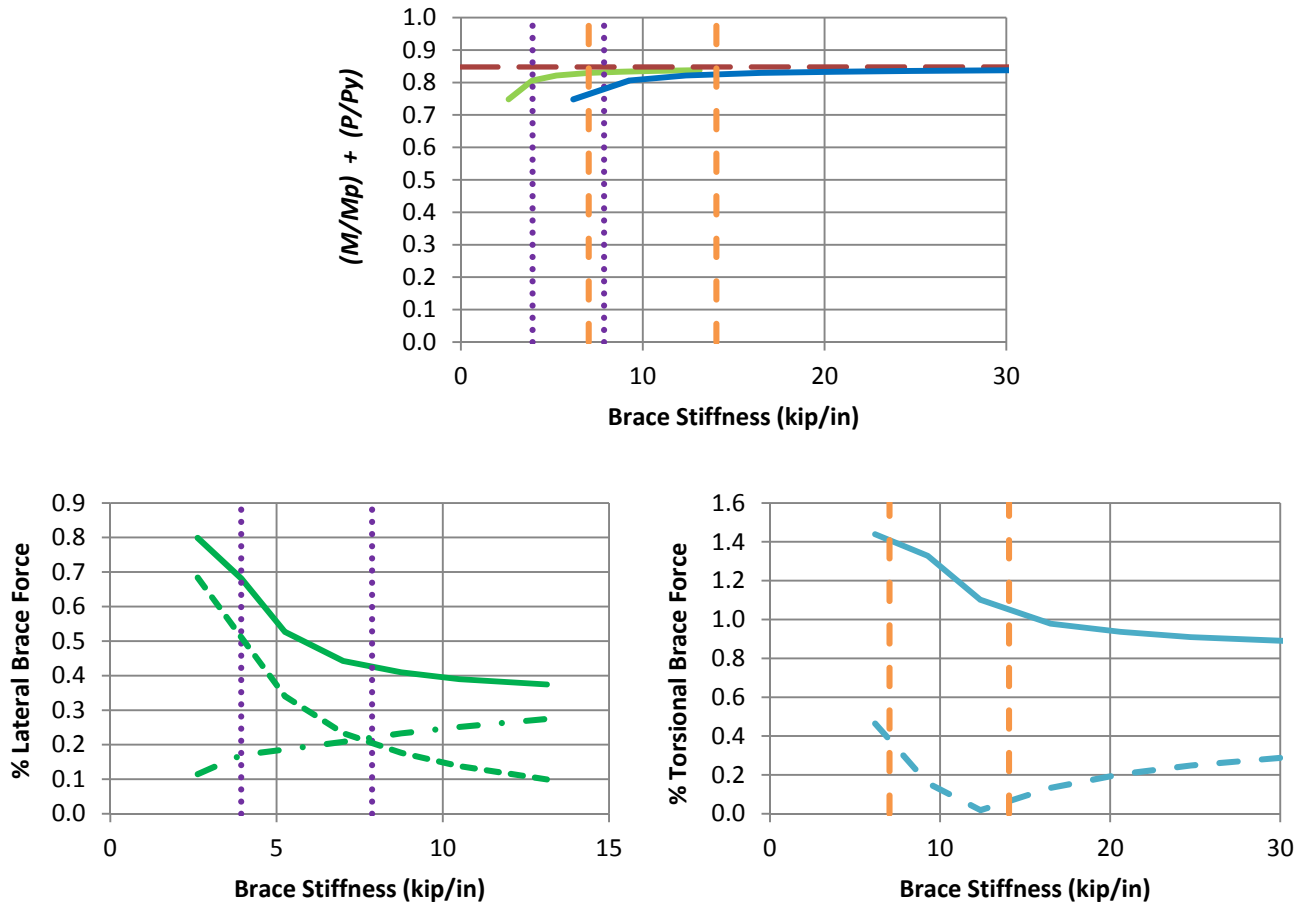
Fig. 7.10 (continued). Beam-column knuckle curves and brace force vs. brace stiffness plots for combined shear panel (relative) lateral and torsional bracing cases with $n = 2$, Moment Gradient 1 loading with lateral bracing on the flange in flexural compression, and $L_b = 15$ ft.



a) BC_MG1n_CRTB_n2_Lb5_FFR-0.5

- Rigidly-braced strength
- Test simulation results corresponding to torsional brace
- Test simulation results corresponding to lateral brace
- 1x and 0.5x lateral bracing stiffness from Eq. (6-5)
- 1x and 0.5x torsional bracing stiffness from Eq. (6-7)
- Left end panel shear force
- Right end panel shear force
- Middle panel shear force
- Torsional brace force 1
- Torsional brace force 2

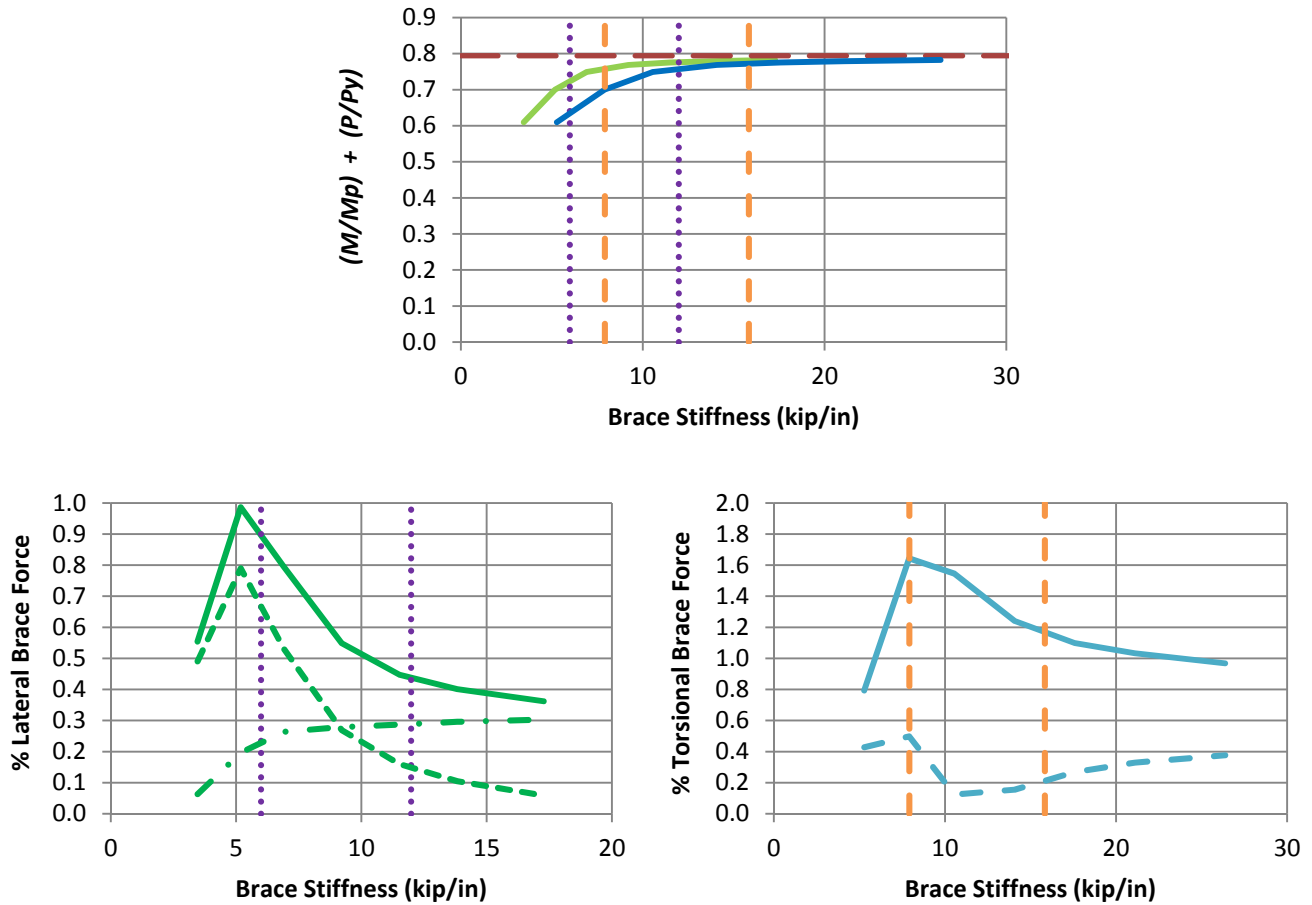
Figure 7.11. Beam-column knuckle curves and brace force vs. brace stiffness plots for combined shear panel (relative) lateral and torsional bracing cases with $n = 2$, Moment Gradient 1 loading with lateral bracing on the flange in flexural tension, and $L_b = 5$ ft.



b) BC_MG1n_CRTB_n2_Lb5_FFR0

- Rigidly-braced strength
- Test simulation results corresponding to torsional brace
- Test simulation results corresponding to lateral brace
- 1x and 0.5x lateral bracing stiffness from Eq. (6-5)
- - - 1x and 0.5x torsional bracing stiffness from Eq. (6-7)
- Left end panel shear force
- - - Right end panel shear force
- . - Middle panel shear force
- Torsional brace force 1
- - - Torsional brace force 2

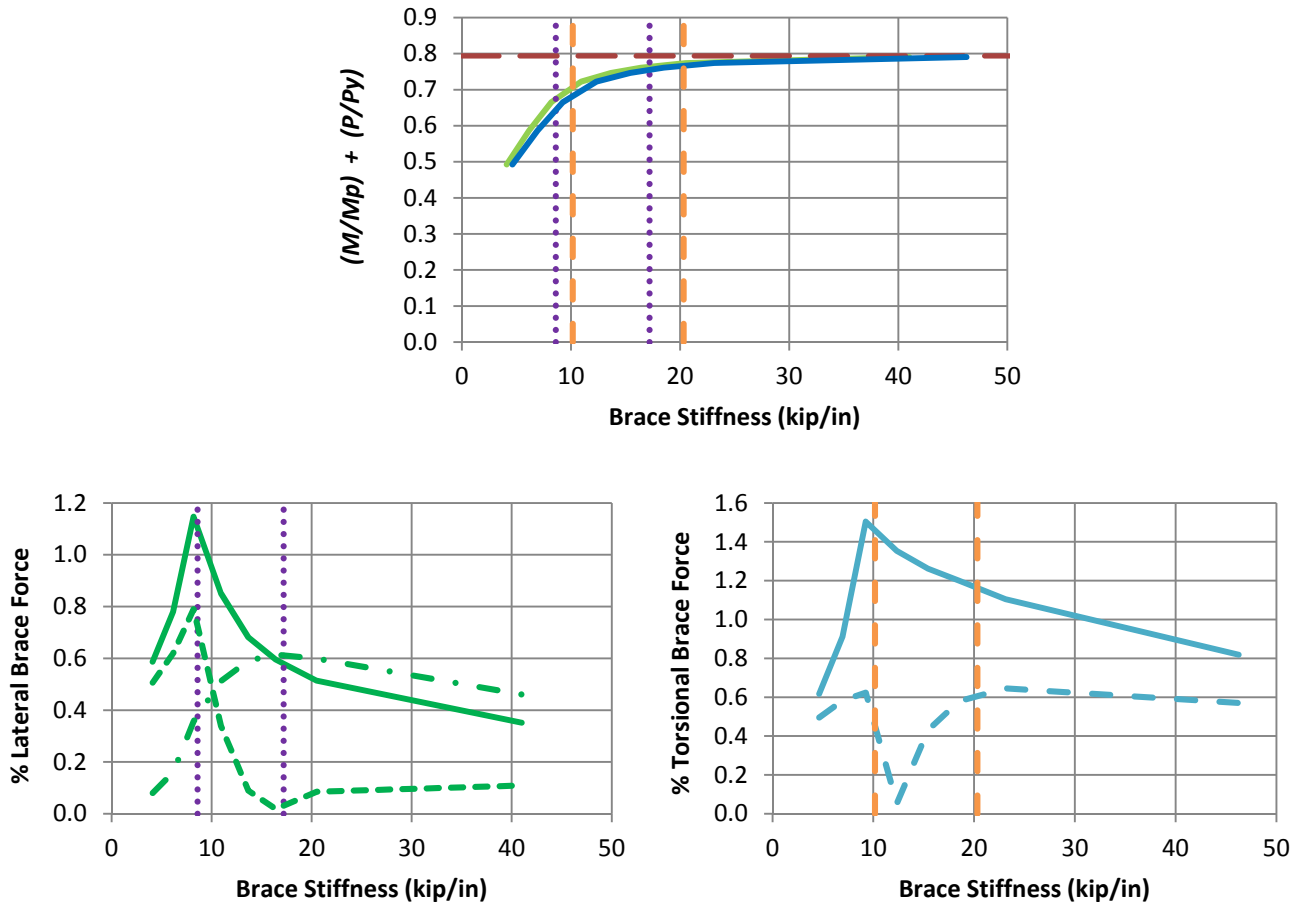
Fig. 7.11 (continued). Beam-column knuckle curves and brace force vs. brace stiffness plots for combined shear panel (relative) lateral and torsional bracing cases with $n = 2$, Moment Gradient 1 loading with lateral bracing on the flange in flexural tension, and $L_b = 5$ ft.



c) BC_MG1n_CRTB_n2_Lb5_FFR0.5

- Rigidly-braced strength
- Test simulation results corresponding to torsional brace
- Test simulation results corresponding to lateral brace
- 1x and 0.5x lateral bracing stiffness from Eq. (6-5)
- 1x and 0.5x torsional bracing stiffness from Eq. (6-7)
- Left end panel shear force
- Right end panel shear force
- Middle panel shear force
- Torsional brace force 1
- Torsional brace force 2

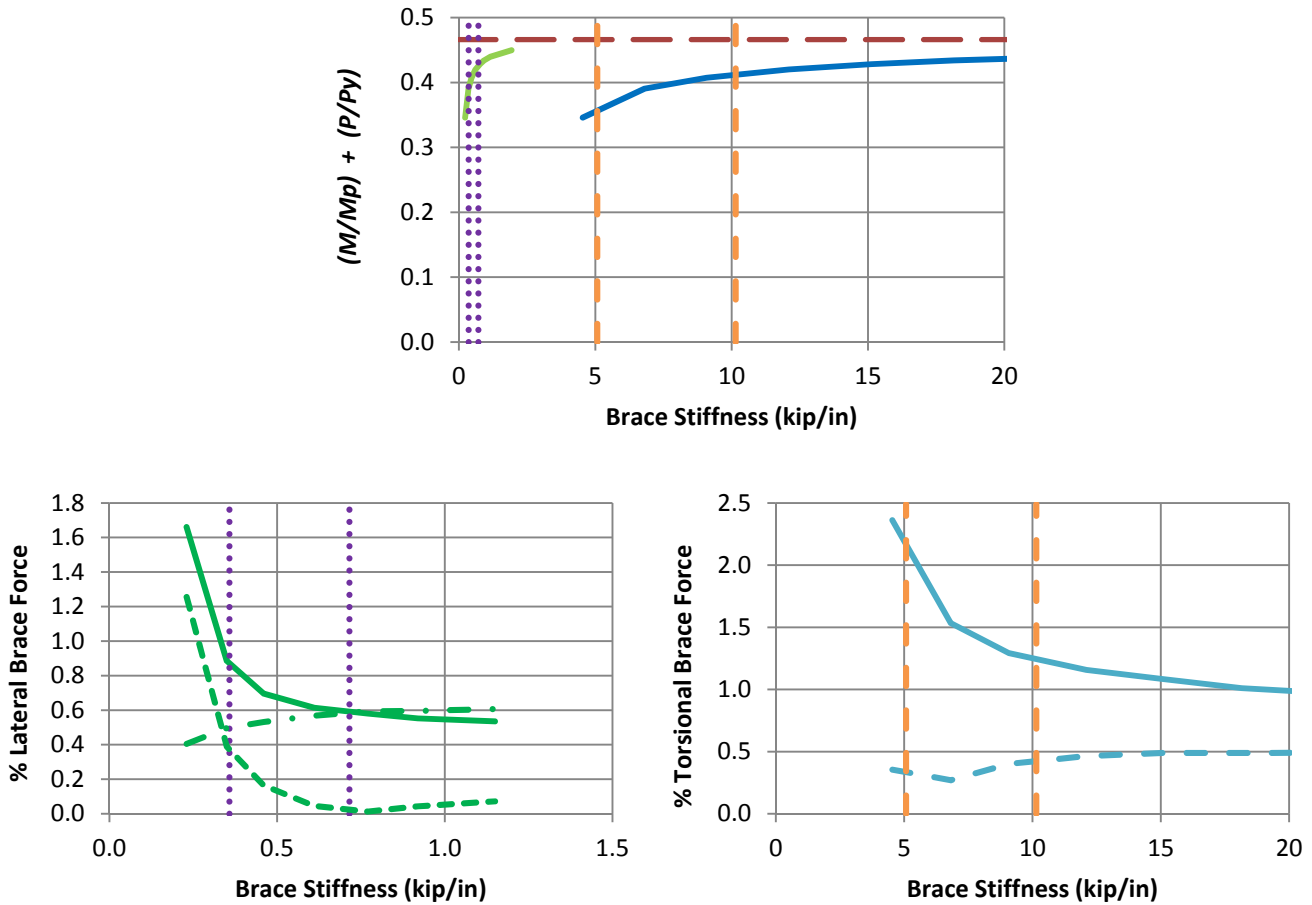
Fig. 7.11 (continued). Beam-column knuckle curves and brace force vs. brace stiffness plots for combined shear panel (relative) lateral and torsional bracing cases with $n = 2$, Moment Gradient 1 loading with lateral bracing on the flange in flexural tension, and $L_b = 5$ ft.



d) BC_MG1n_CRTB_n2_Lb5_FFR1

- Rigidly-braced strength
- Test simulation results corresponding to torsional brace
- Test simulation results corresponding to lateral brace
- 1x and 0.5x lateral bracing stiffness from Eq. (6-5)
- - - 1x and 0.5x torsional bracing stiffness from Eq. (6-7)
- Left end panel shear force
- - - Right end panel shear force
- . - Middle panel shear force
- Torsional brace force 1
- - - Torsional brace force 2

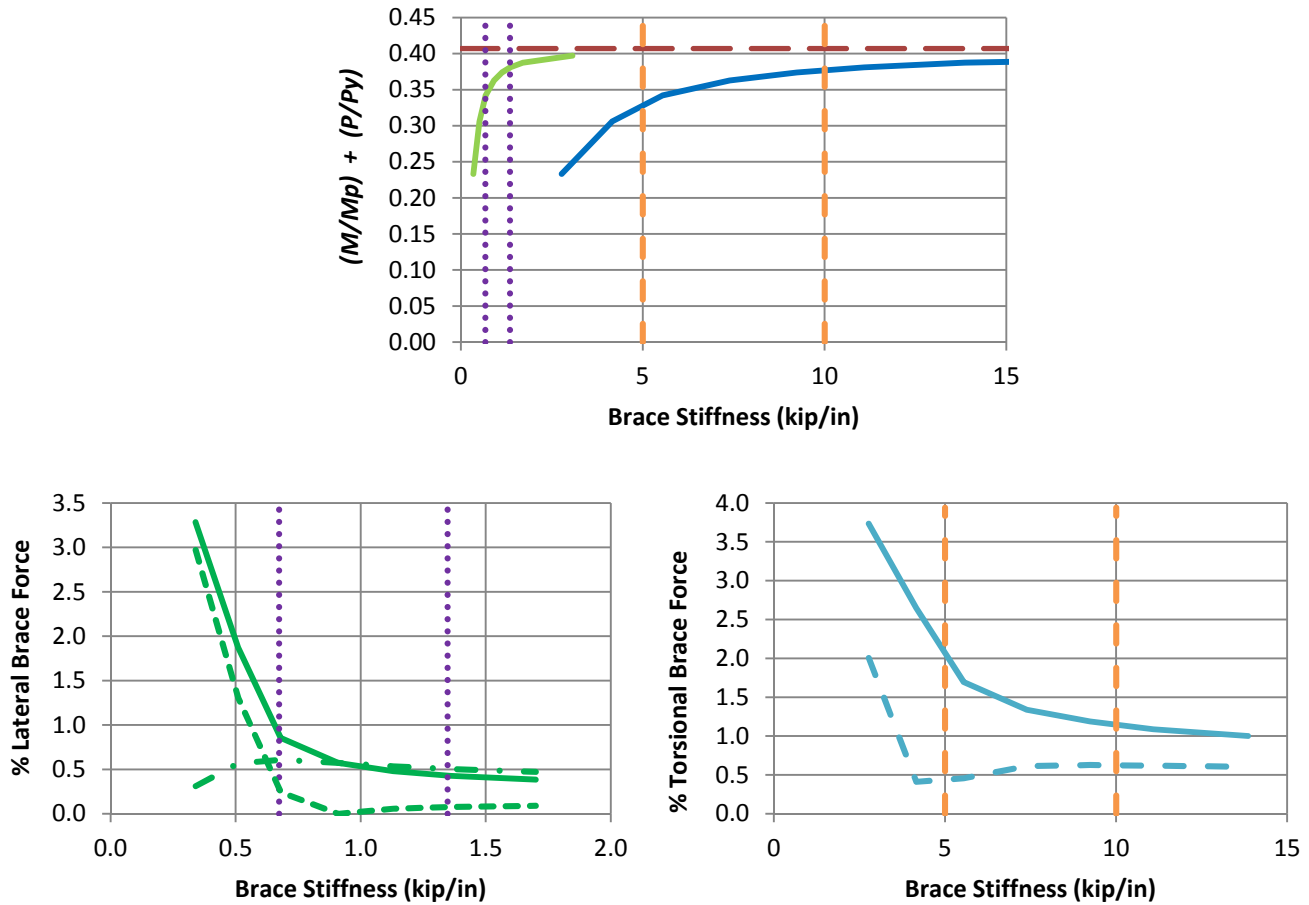
Fig. 7.11 (continued). Beam-column knuckle curves and brace force vs. brace stiffness plots for combined shear panel (relative) lateral and torsional bracing cases with $n = 2$, Moment Gradient 1 loading with lateral bracing on the flange in flexural tension, and $L_b = 5$ ft.



a) BC_MG1n_CRTB_n2_Lb15_FFR-0.5

- Rigidly-braced strength
- Test simulation results corresponding to torsional brace
- Test simulation results corresponding to lateral brace
- 1x and 0.5x lateral bracing stiffness from Eq. (6-5)
- 1x and 0.5x torsional bracing stiffness from Eq. (6-7)
- Left end panel shear force
- Right end panel shear force
- Middle panel shear force
- Torsional brace force 1
- Torsional brace force 2

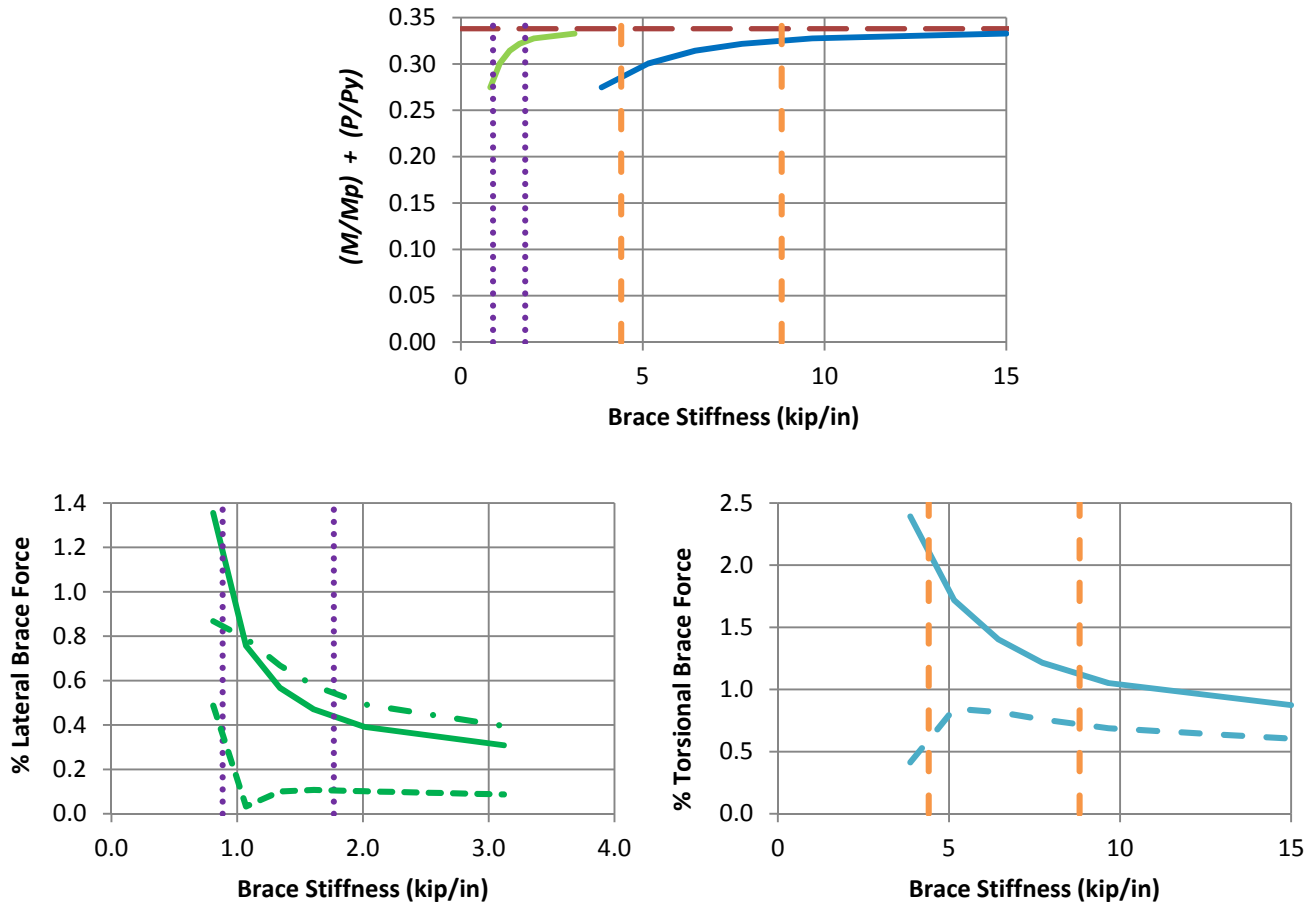
Figure 7.12. Beam-column knuckle curves and brace force vs. brace stiffness plots for combined shear panel (relative) lateral and torsional bracing cases with $n = 2$, Moment Gradient 1 loading with lateral bracing on the flange in flexural tension, and $L_b = 15$ ft.



b) BC_MG1n_CRTB_n2_Lb15_FFR0

- Rigidly-braced strength
- Test simulation results corresponding to torsional brace
- Test simulation results corresponding to lateral brace
- 1x and 0.5x lateral bracing stiffness from Eq. (6-5)
- - - 1x and 0.5x torsional bracing stiffness from Eq. (6-7)
- Left end panel shear force
- - - Right end panel shear force
- . - Middle panel shear force
- Torsional brace force 1
- - - Torsional brace force 2

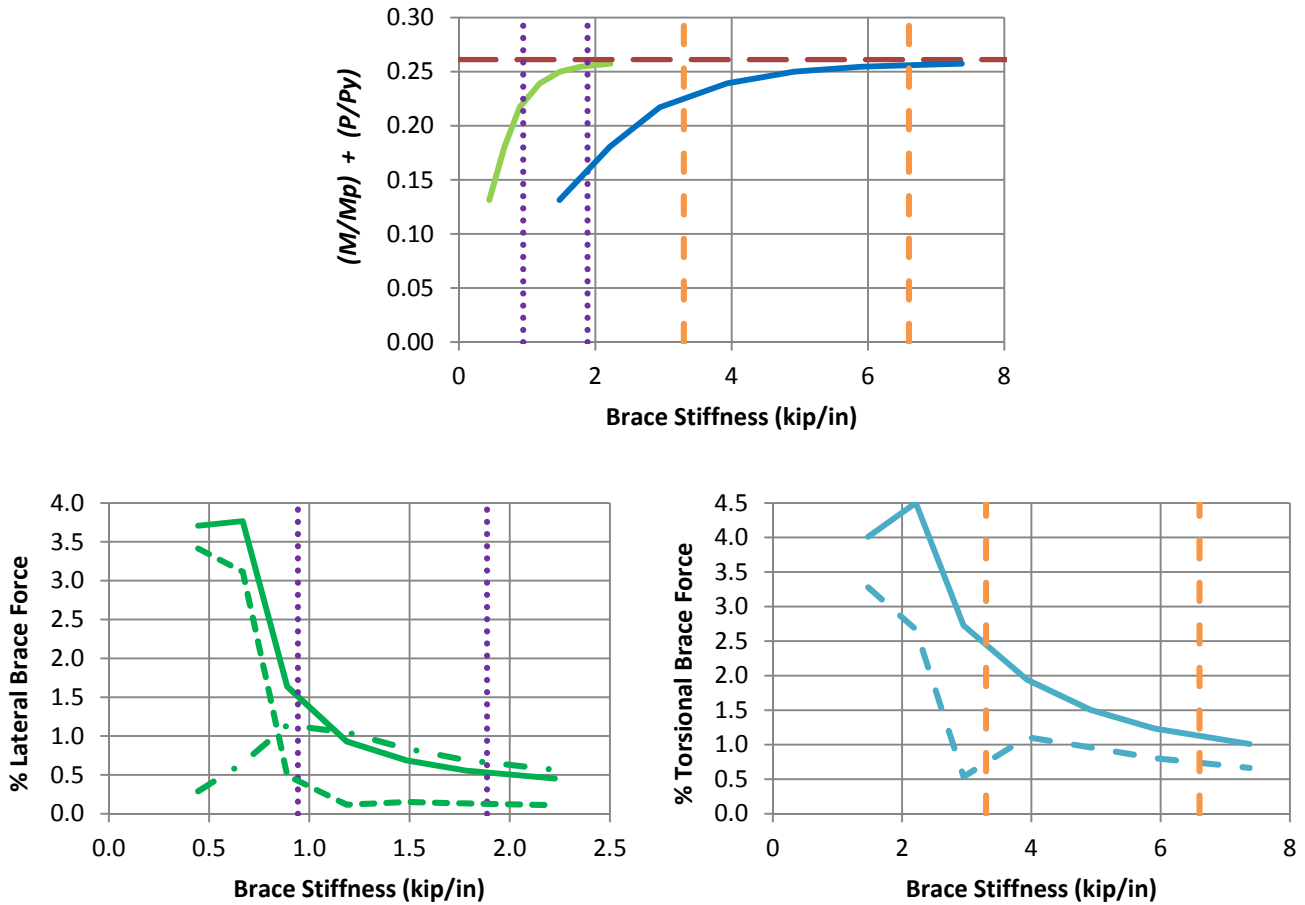
Fig. 7.12 (continued). Beam-column knuckle curves and brace force vs. brace stiffness plots for combined shear panel (relative) lateral and torsional bracing cases with $n = 2$, Moment Gradient 1 loading with lateral bracing on the flange in flexural tension, and $L_b = 15$ ft.



c) BC_MG1n_CRTB_n2_Lb15_FFR0.5

- Rigidly-braced strength
- Test simulation results corresponding to torsional brace
- Test simulation results corresponding to lateral brace
- ⋯ 1x and 0.5x lateral bracing stiffness from Eq. (6-5)
- 1x and 0.5x torsional bracing stiffness from Eq. (6-7)
- Left end panel shear force
- Right end panel shear force
- Middle panel shear force
- Torsional brace force 1
- Torsional brace force 2

Fig. 7.12 (continued). Beam-column knuckle curves and brace force vs. brace stiffness plots for combined shear panel (relative) lateral and torsional bracing cases with $n = 2$, Moment Gradient 1 loading with lateral bracing on the flange in flexural tension, and $L_b = 15$ ft.



d) BC_MG1n_CRTB_n2_Lb15_FFR1

- Rigidly-braced strength
- Test simulation results corresponding to torsional brace
- Test simulation results corresponding to lateral brace
- 1x and 0.5x lateral bracing stiffness from Eq. (6-5)
- 1x and 0.5x torsional bracing stiffness from Eq. (6-7)
- Left end panel shear force
- Right end panel shear force
- . - Middle panel shear force
- Torsional brace force 1
- Torsional brace force 2

Fig. 7.12 (continued). Beam-column knuckle curves and brace force vs. brace stiffness plots for combined shear panel (relative) lateral and torsional bracing cases with $n = 2$, Moment Gradient 1 loading with lateral bracing on the flange in flexural tension, and $L_b = 15$ ft.

Table 7.2. Brace stiffnesses β_{F96L} and β_{brL} and point lateral brace forces as a percentage of P for beam-columns with Moment Gradient 1 loading and combined lateral and torsional bracing.

Case	β_{F96L} (kip/in)	β_{brL} (kip/in)	β_{brL}/β_{F96L}	% Lateral Brace Force at $\beta_L = \beta_{brL}$ and $\beta_T = \beta_{brT}$	Ratio of Actual to Estimated Lateral Brace Force at $\beta_L = \beta_{brL}$ and $\beta_T = \beta_{brT}$
BC_MG1p_CNTB_n1_Lb5_FFR-0.5	1.40	7.70	5.50	0.80	0.80
BC_MG1p_CNTB_n1_Lb5_FFR0	3.21	15.76	4.91	0.62	0.62
BC_MG1p_CNTB_n1_Lb5_FFR0.5	7.09	24.76	3.49	0.65	0.65
BC_MG1p_CNTB_n1_Lb15_FFR-0.5	1.82	1.46	0.80	1.00	1.00
BC_MG1p_CNTB_n1_Lb15_FFR0	2.10	2.70	1.29	0.75	0.75
BC_MG1p_CNTB_n1_Lb15_FFR0.5	2.17	3.48	1.60	0.70	0.70
BC_MG1p_CNTB_n1_Lb15_FFR1	2.37	3.68	1.55	0.95	0.95
BC_MG1n_CNTB_n1_Lb5_FFR-0.5	2.10	7.66	3.65	0.68	0.68
BC_MG1n_CNTB_n1_Lb5_FFR0	6.50	15.86	2.44	0.60	0.60
BC_MG1n_CNTB_n1_Lb5_FFR0.5	14.00	24.00	1.71	0.76	0.76
BC_MG1n_CNTB_n1_Lb15_FFR-0.5	2.16	1.46	0.68	1.10	1.10
BC_MG1n_CNTB_n1_Lb15_FFR0	2.59	2.70	1.04	0.80	0.80
BC_MG1n_CNTB_n1_Lb15_FFR0.5	2.59	3.48	1.34	0.81	0.81
BC_MG1n_CNTB_n1_Lb15_FFR1	2.37	3.68	1.55	0.95	0.95
BC_MG1p_CRTB_n2_Lb5_FFR-0.5	1.11	3.78	3.41	0.58	0.58
BC_MG1p_CRTB_n2_Lb5_FFR0	2.57	7.84	3.05	0.40	0.40

Table 7.2 (continued). Brace stiffnesses β_{F96L} and β_{brL} and brace forces as a percentage of P for beam-columns with Moment Gradient 1 loading and combined lateral and torsional bracing.

Case	β_{F96L} (kip/in)	β_{brL} (kip/in)	β_{brL} / β_{F96L}	% Lateral Brace Force at $\beta_L = \beta_{brL}$ and $\beta_T = \beta_{brT}$	Ratio of Actual to Estimated Lateral Brace Force at $\beta_L = \beta_{brL}$ and $\beta_T = \beta_{brT}$
BC_MG1p_CRTB_n2_Lb5_FFR0.5	6.11	11.94	1.95	0.30	0.30
BC_MG1p_CRTB_n2_Lb5_FFR1	16.75	17.20	1.03	0.58	0.58
BC_MG1p_CRTB_n2_Lb15_FFR-0.5	1.40	0.72	0.51	0.48	0.48
BC_MG1p_CRTB_n2_Lb15_FFR0	1.41	1.36	0.96	0.48	0.48
BC_MG1p_CRTB_n2_Lb15_FFR0.5	1.33	1.76	1.32	0.44	0.44
BC_MG1p_CRTB_n2_Lb15_FFR1	1.53	1.88	1.23	0.57	0.57
BC_MG1n_CRTB_n2_Lb5_FFR-0.5	1.86	3.80	2.04	0.55	0.55
BC_MG1n_CRTB_n2_Lb5_FFR0	4.60	7.88	1.71	0.41	0.41
BC_MG1n_CRTB_n2_Lb5_FFR0.5	8.50	11.98	1.41	0.42	0.42
BC_MG1n_CRTB_n2_Lb5_FFR1	16.75	17.20	1.03	0.60	0.60
BC_MG1n_CRTB_n2_Lb15_FFR-0.5	1.74	0.72	0.41	0.60	0.60
BC_MG1n_CRTB_n2_Lb15_FFR0	2.16	1.34	0.62	0.50	0.50
BC_MG1n_CRTB_n2_Lb15_FFR0.5	1.80	1.76	0.98	0.50	0.50
BC_MG1n_CRTB_n2_Lb15_FFR1	1.53	1.88	1.23	0.57	0.57

Table 7.3. Brace stiffnesses β_{F96T} and β_{brT} and torsional brace forces as a percentage of $(M/h_o + P/2)$ for beam-columns with Moment Gradient 1 loading and combined lateral and torsional bracing.

Case	β_{F96T} (kip/in)	β_{brT} (kip/in)	β_{brT} $/\beta_{F96T}$	% Torsional Brace Force at $\beta_L = \beta_{brL}$ and $\beta_T = \beta_{brT}$	Ratio of Actual to Estimated Torsional Brace Force at $\beta_L = \beta_{brL}$ and $\beta_T = \beta_{brT}$
BC_MG1p_CNTB_n1_Lb5_FFR-0.5	4.23	14.70	3.48	0.50	0.25
BC_MG1p_CNTB_n1_Lb5_FFR0	5.02	17.52	3.49	0.27	0.14
BC_MG1p_CNTB_n1_Lb5_FFR0.5	7.21	21.94	3.04	0.05	0.03
BC_MG1p_CNTB_n1_Lb15_FFR-0.5	24.03	13.48	0.56	0.45	0.23
BC_MG1p_CNTB_n1_Lb15_FFR0	11.48	13.34	1.16	0.20	0.10
BC_MG1p_CNTB_n1_Lb15_FFR0.5	6.94	11.46	1.65	0.21	0.11
BC_MG1p_CNTB_n1_Lb15_FFR1	5.20	8.36	1.61	0.95	0.48
BC_MG1n_CNTB_n1_Lb5_FFR-0.5	6.83	14.56	2.13	0.86	0.43
BC_MG1n_CNTB_n1_Lb5_FFR0	10.16	17.72	1.74	0.90	0.45
BC_MG1n_CNTB_n1_Lb5_FFR0.5	14.24	20.64	1.45	1.15	0.58
BC_MG1n_CNTB_n1_Lb15_FFR-0.5	28.55	13.46	0.47	1.10	0.55
BC_MG1n_CNTB_n1_Lb15_FFR0	14.16	13.34	0.94	1.00	0.50
BC_MG1n_CNTB_n1_Lb15_FFR0.5	8.30	11.46	1.38	0.99	0.50
BC_MG1n_CNTB_n1_Lb15_FFR1	5.20	8.36	1.61	0.95	0.48
BC_MG1p_CRTB_n2_Lb5_FFR-0.5	5.42	11.98	2.21	0.52	0.26
BC_MG1p_CRTB_n2_Lb5_FFR0	6.05	13.94	2.30	0.27	0.14

Table 7.3 (continued). Brace stiffnesses β_{F96T} and β_{brT} and torsional brace forces as a percentage of $(M/h_o + P/2)$ for beam-columns with Moment Gradient 1 loading and combined lateral and torsional bracing.

Case	β_{F96T} (kip/in)	β_{brT} (kip/in)	β_{brT} / β_{F96T}	% Torsional Brace Forces at $\beta_L = \beta_{brL}$ and $\beta_T = \beta_{brT}$	Ratio of Actual to Estimated Torsional Brace Force at $\beta_L = \beta_{brL}$ and $\beta_T = \beta_{brT}$
BC_MG1p_CRTB_n2_Lb5_FFR0.5	9.33	15.72	1.68	0.12	0.06
BC_MG1p_CRTB_n2_Lb5_FFR1	18.90	20.32	1.08	1.18	0.59
BC_MG1p_CRTB_n2_Lb15_FFR-0.5	27.68	10.16	0.37	0.47	0.24
BC_MG1p_CRTB_n2_Lb15_FFR0	11.48	10.06	0.88	0.11	0.06
BC_MG1p_CRTB_n2_Lb15_FFR0.5	6.40	8.82	1.38	0.25	0.13
BC_MG1p_CRTB_n2_Lb15_FFR1	5.08	6.60	1.30	1.10	0.55
BC_MG1n_CRTB_n2_Lb5_FFR-0.5	9.11	12.04	1.32	1.10	0.55
BC_MG1n_CRTB_n2_Lb5_FFR0	10.84	14.06	1.30	1.05	0.53
BC_MG1n_CRTB_n2_Lb5_FFR0.5	12.99	15.84	1.22	1.20	0.60
BC_MG1n_CRTB_n2_Lb5_FFR1	18.90	20.32	1.08	1.15	0.58
BC_MG1n_CRTB_n2_Lb15_FFR-0.5	34.42	10.14	0.29	1.25	0.63
BC_MG1n_CRTB_n2_Lb15_FFR0	17.62	10.00	0.57	1.10	0.55
BC_MG1n_CRTB_n2_Lb15_FFR0.5	8.65	8.82	1.02	1.11	0.56
BC_MG1n_CRTB_n2_Lb15_FFR1	5.08	6.60	1.30	1.10	0.55

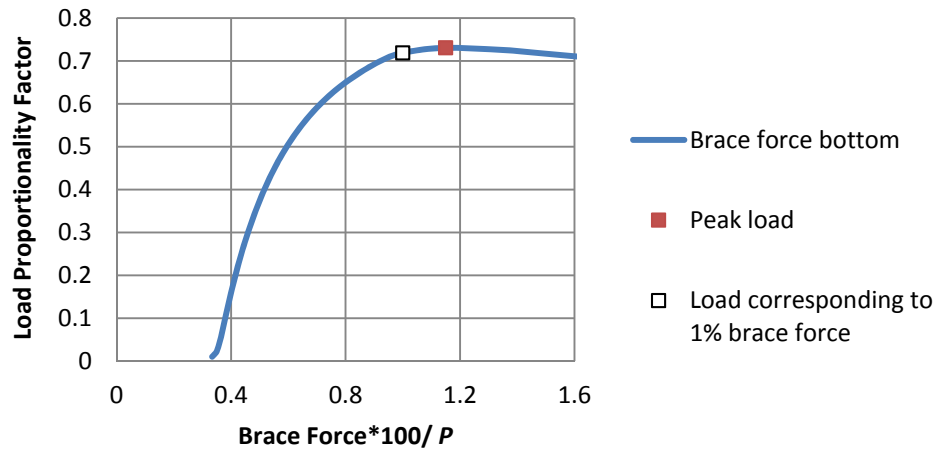


Figure 7.13. Point lateral brace force vs. the Load Proportionality Factor for BC_MG1n_CNTB_n1_Lb15_FFR-0.5 corresponding to a point lateral brace stiffness $\beta_{brL} = 1.46$ kip/in from Eq. (6-5) and a point torsional brace stiffness $\beta_{brT} = 13.46$ kip/in from Eq. (6-7).

Table 7.4. Peak load as a percentage of the rigidly-braced strength when $\beta_L = \beta_{brL}$.

Case	Peak load as a percentage of rigidly-braced strength when $\beta_L = \beta_{brL}$
BC_MG1p_CNTB_n1_Lb15_FFR-0.5	94.4
BC_MG1n_CNTB_n1_Lb15_FFR-0.5	93.6
BC_MG1p_CRTB_n2_Lb15_FFR-0.5	92.8
BC_MG1p_CRTB_n2_Lb15_FFR0	95.6
BC_MG1n_CRTB_n2_Lb15_FFR-0.5	91.4
BC_MG1n_CRTB_n2_Lb15_FFR0	93.4

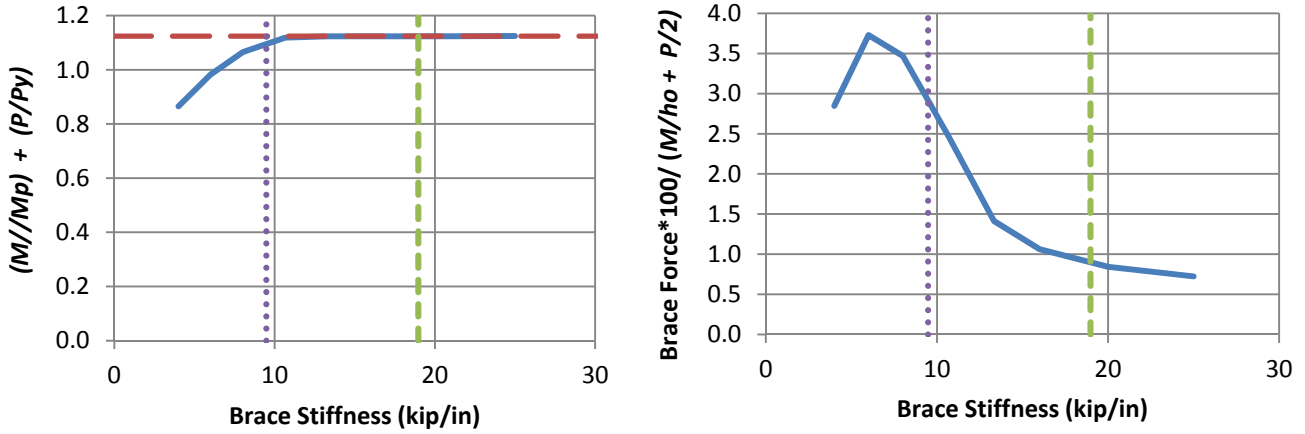
Table 7.5. Peak load as a percentage of the rigidly-braced strength when $\beta_T = \beta_{brT}$.

Case	Peak load as a percentage of rigidly-braced strength when $\beta_T = \beta_{brT}$
BC_MG1p_CNTB_n1_Lb15_FFR-0.5	92.2
BC_MG1n_CNTB_n1_Lb15_FFR-0.5	91.0
BC_MG1n_CNTB_n1_Lb15_FFR0	95.1
BC_MG1p_CRTB_n2_Lb15_FFR-0.5	91.2
BC_MG1p_CRTB_n2_Lb15_FFR0	94.4
BC_MG1n_CRTB_n2_Lb15_FFR-0.5	88.0
BC_MG1n_CRTB_n2_Lb15_FFR0	93.1

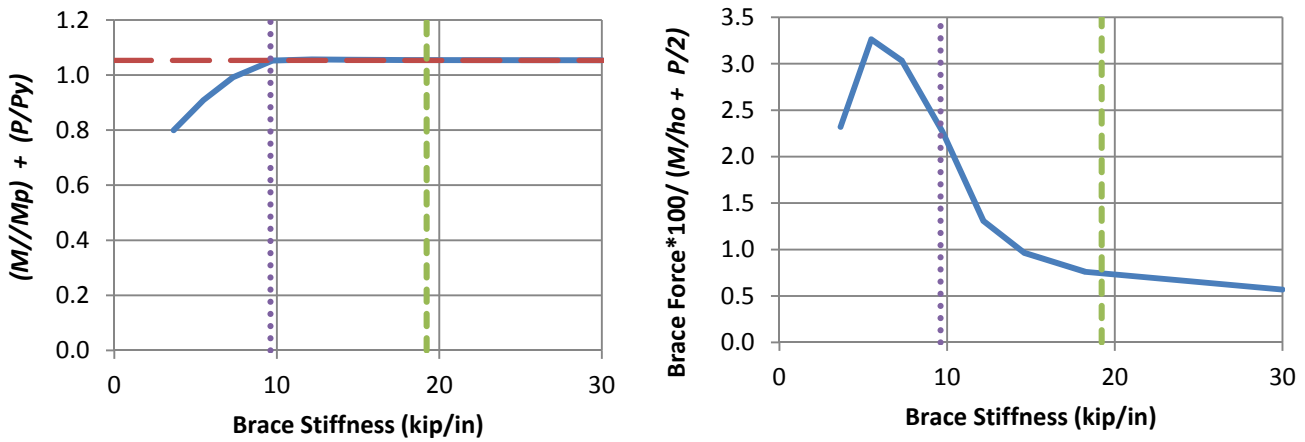
It can be observed that even for the critical cases summarized in Tables 7.4 and 7.5, strengths of 90.4 to 94.4 % of the rigidly-braced strengths are obtained with the exception of one case, and hence the results are considered to be acceptable. However, only 88.0 % of the rigidly-braced strength is obtained at $\beta_T = \beta_{brT}$ for BC_MG1n_CRTB_n2_Lb15_FFR-0.5. The knuckle curves and brace force - brace stiffness curves for this case are presented in Fig. 7.12a. It can be observed that the β_{brT} for this case is 10.14 kip/in and that the knuckle curve is reasonably flat within the vicinity of this stiffness. If one considers the increase in the required brace stiffness due to the division by $\phi = 0.75$ in LRFD, it can be observed that the beam develops 91.1 % of its rigidly-braced strength at the actual required design stiffness. These results are considered to be marginal, but acceptable.

7.3.3 Beam-Columns with Point Lateral Bracing Only on the Flange in Flexural Compression, Subjected to Moment Gradient 2 Loading

The knuckle and brace force - brace stiffness curves for beam-columns with Moment Gradient 2 loading and point lateral bracing only on one flange are shown in Figs. 7.14 and 7.15. Table 7.6 compares the β_{brL} calculated from Eq. (6-1) to β_{F96} , and the recommended estimates of the brace force at $\beta_L = \beta_{brL}$ from Eq. (6-2a) to the simulation results from these figures. From Table 7.6 it can be observed that the bracing stiffness calculated by Eq. (6-1) provides a conservative estimate of the targeted bracing stiffness. More than 96 % of the rigidly-braced strength is developed at $\beta_L = \beta_{brL}$ in all the cases shown in Table 7.6. From Figs. 7.14 and 7.15, it can be observed that the bracing strength calculated using Eq. (6-2a) is accurate to slightly conservative.



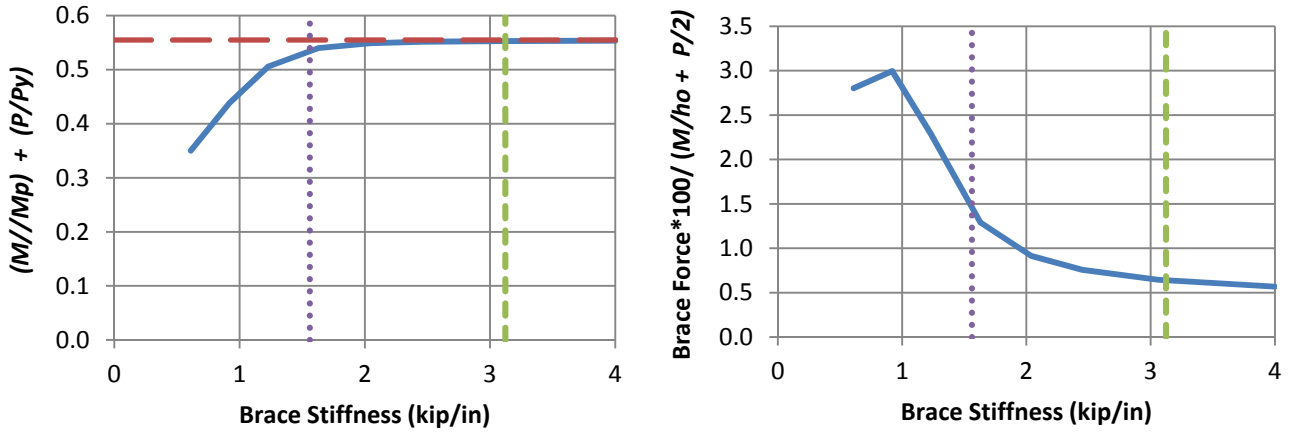
a) BC_MG2p_NB_n1_Lb5_FFR-0.5



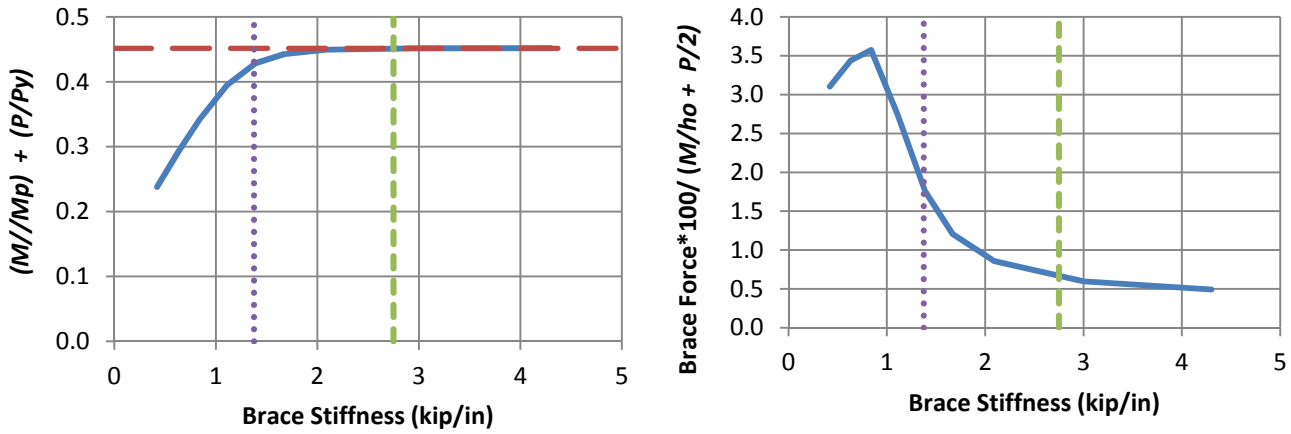
b) BC_MG2p_NB_n1_Lb5_FFR0

- Test simulation results
- - Rigidly-braced strength
- ⋯ 0.5 times bracing stiffness from Eq. (6-1)
- - Bracing stiffness from Eq. (6-1)

Figure 7.14. Beam-column knuckle curves and brace force vs. brace stiffness plots for point (nodal) lateral bracing cases with $n = 1$, Moment Gradient 2 loading, and $L_b = 5$ ft.



a) BC_MG2p_NB_n1_Lb15_FFR-0.5



b) BC_MG2p_NB_n1_Lb15_FFR0

- Test simulation results
- - Rigidly-braced strength
- ⋯ 0.5 times bracing stiffness from Eq. (6-1)
- - Bracing stiffness from Eq. (6-1)

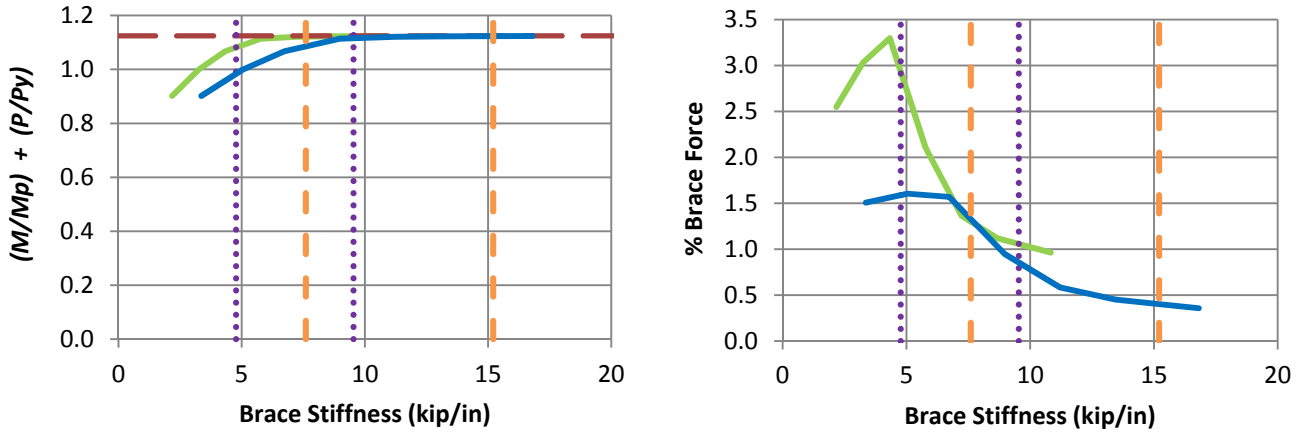
Figure 7.15. Beam-column knuckle curves and brace force vs. brace stiffness plots for point (nodal) lateral bracing cases with $n = 1$, Moment Gradient 2 loading, and $L_b = 15$ ft.

Table 7.6. Brace stiffnesses β_{F96L} and β_{brL} and brace forces as a percentage of $(M/h_o + P/2)$ for beam-columns with Moment Gradient 2 loading, lateral bracing only on the flange in flexural compression and $P_{ft}/P_{fc} \leq 0$.

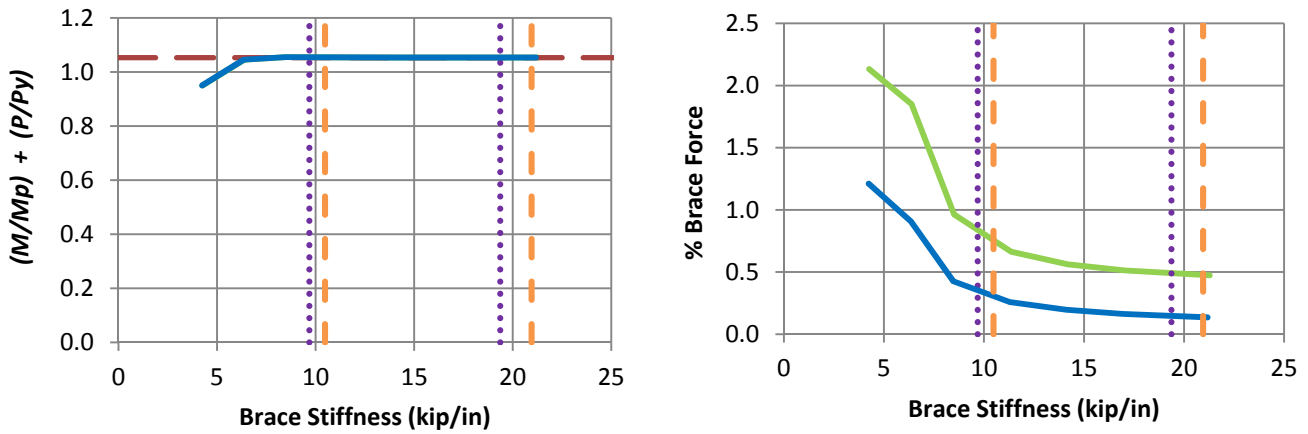
Case	β_{F96L} (kip/in)	β_{brL} (kip/in)	β_{brL}/β_{F96L}	% Brace Force at $\beta_L = \beta_{brL}$	Ratio of actual to estimated brace force at $\beta_L = \beta_{brL}$
BC_MG2p_NB_n1_Lb5_FFR-0.5	8.72	18.96	2.17	0.90	0.90
BC_MG2p_NB_n1_Lb5_FFR0	8.07	19.22	2.38	0.75	0.75
BC_MG2p_NB_n1_Lb15_FFR-0.5	1.54	3.12	2.03	0.60	0.60
BC_MG2p_NB_n1_Lb15_FFR0	1.49	2.74	1.84	0.65	0.65

7.3.4 Beam-Columns with Combined Lateral and Torsional Bracing, Subjected to Moment Gradient 2 Loading

The knuckle curves and brace-force - brace stiffness curves for beam-columns with combined lateral and torsional bracing, subjected to Moment Gradient 2 loading, are shown in Figs. 7.16 through 7.19. The lateral brace force in these figures is expressed as percentage of P . The torsional brace force in these figures is expressed as percentage of $M/h_o + P/2$. Tables 7.7 and 7.8 summarize the relationship the estimated stiffness and strength requirements and the simulation results from the above figures.



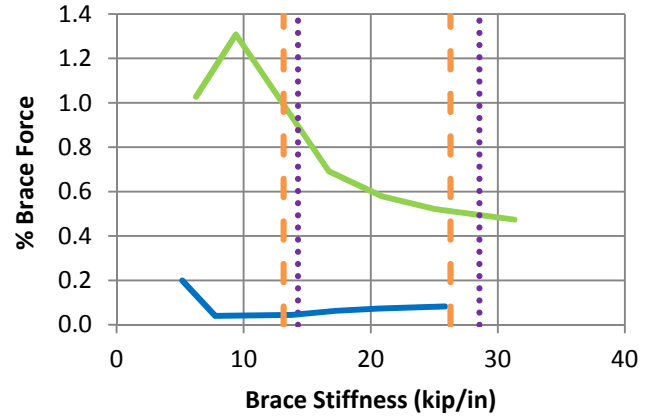
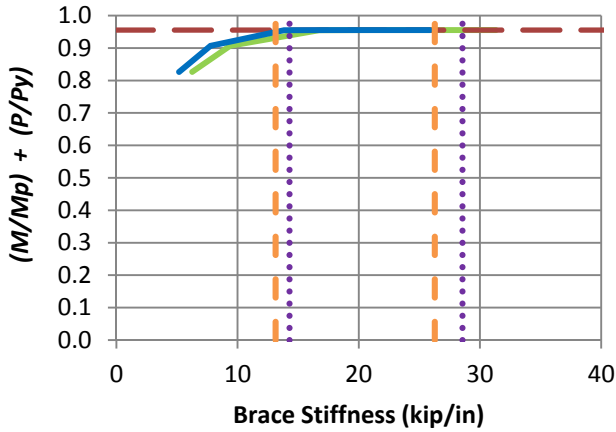
a) BC_MG2p_CNTB_n1_Lb5_FFR-0.5



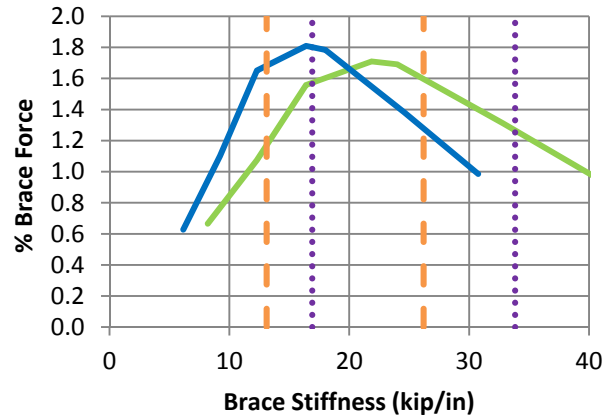
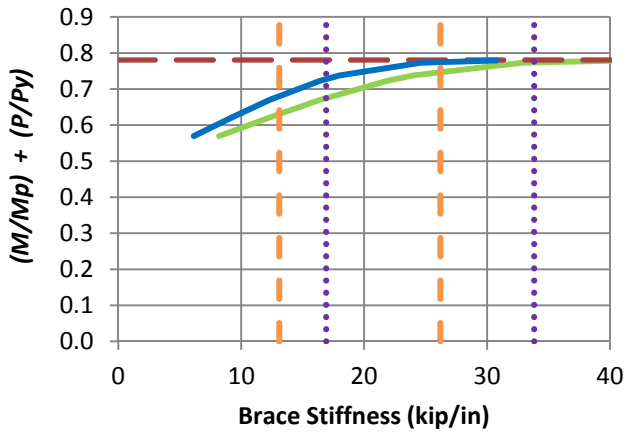
b) BC_MG2p_CNTB_n1_Lb5_FFR0

- Rigidly-braced strength
- Test simulation results corresponding to torsional brace
- Test simulation results corresponding to lateral brace
- 1x and 0.5x lateral bracing stiffness from Eq. (6-5)
- - - 1x and 0.5x torsional bracing stiffness from Eq. (6-7)

Figure 7.16. Beam-column knuckle curves and brace force vs. brace stiffness plots for combined point (nodal) lateral and torsional bracing cases with $n = 1$, Moment Gradient 2 loading with lateral bracing on the flange in flexural compression, and $L_b = 5$ ft.



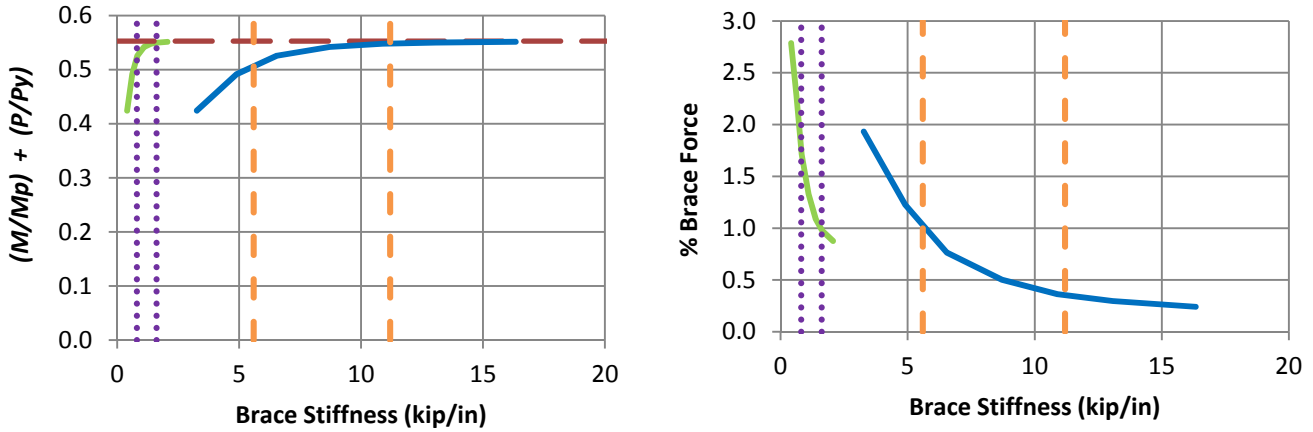
c) BC_MG2p_CNTB_n1_Lb5_FFR0.5



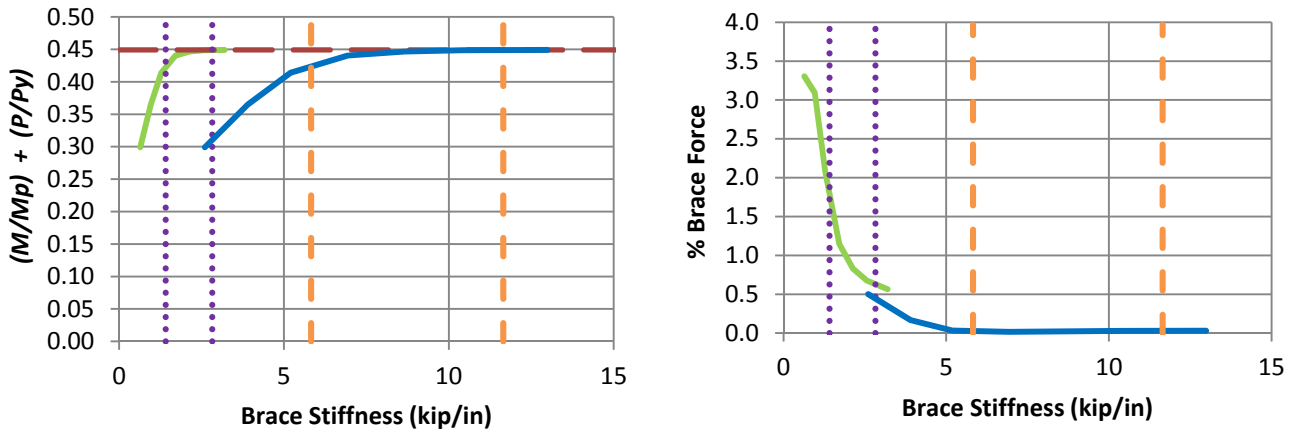
d) BC_MG2p_CNTB_n1_Lb5_FFR1

- Rigidly-braced strength
- Test simulation results corresponding to torsional brace
- Test simulation results corresponding to lateral brace
- 1x and 0.5x lateral bracing stiffness from Eq. (6-5)
- 1x and 0.5x torsional bracing stiffness from Eq. (6-7)

Fig. 7.16 (continued). Beam-column knuckle curves and brace force vs. brace stiffness plots for combined point (nodal) lateral and torsional bracing cases with $n = 1$, Moment Gradient 2 loading with lateral bracing on the flange in flexural compression, and $L_b = 5$ ft.



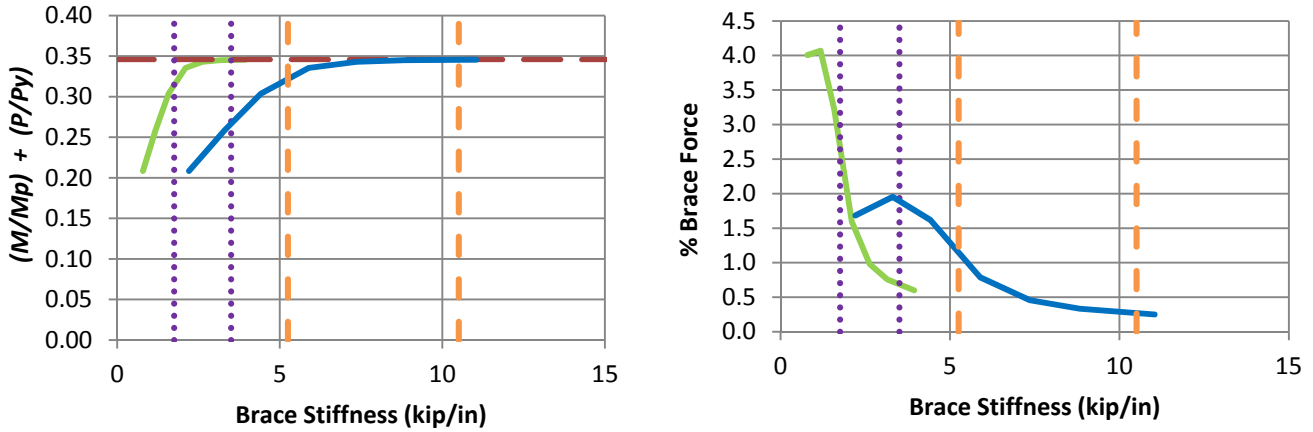
a) BC_MG2p_CNTB_n1_Lb15_FFR-0.5



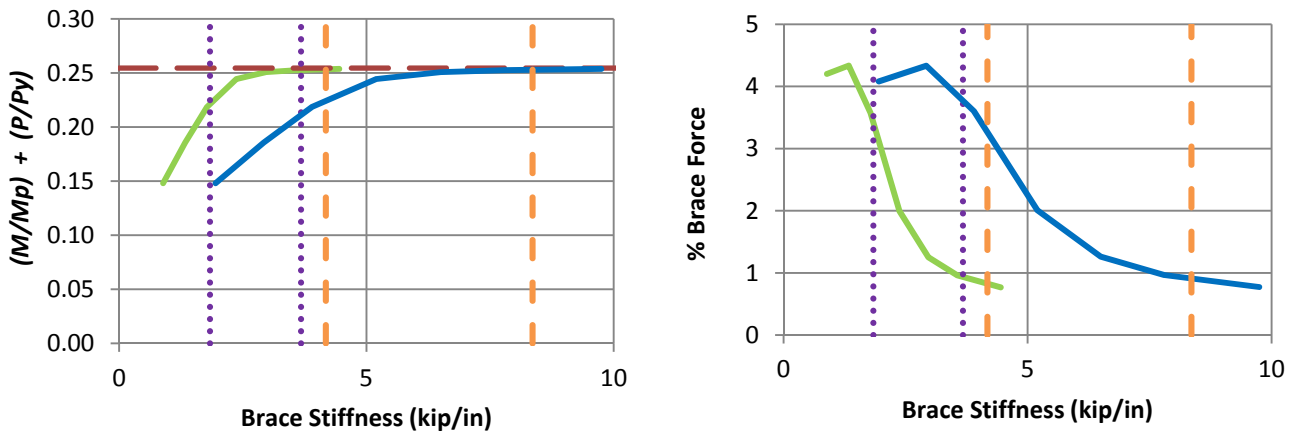
b) BC_MG2p_CNTB_n1_Lb15_FFR0

- Rigidly-braced strength
- Test simulation results corresponding to torsional brace
- Test simulation results corresponding to lateral brace
- ⋯ 1x and 0.5x lateral bracing stiffness from Eq. (6-5)
- 1x and 0.5x torsional bracing stiffness from Eq. (6-7)

Figure 7.17. Beam-column knuckle curves and brace force vs. brace stiffness plots for combined point (nodal) lateral and torsional bracing cases with $n = 1$, Moment Gradient 2 loading with lateral bracing on the flange in flexural compression, and $L_b = 15$ ft.



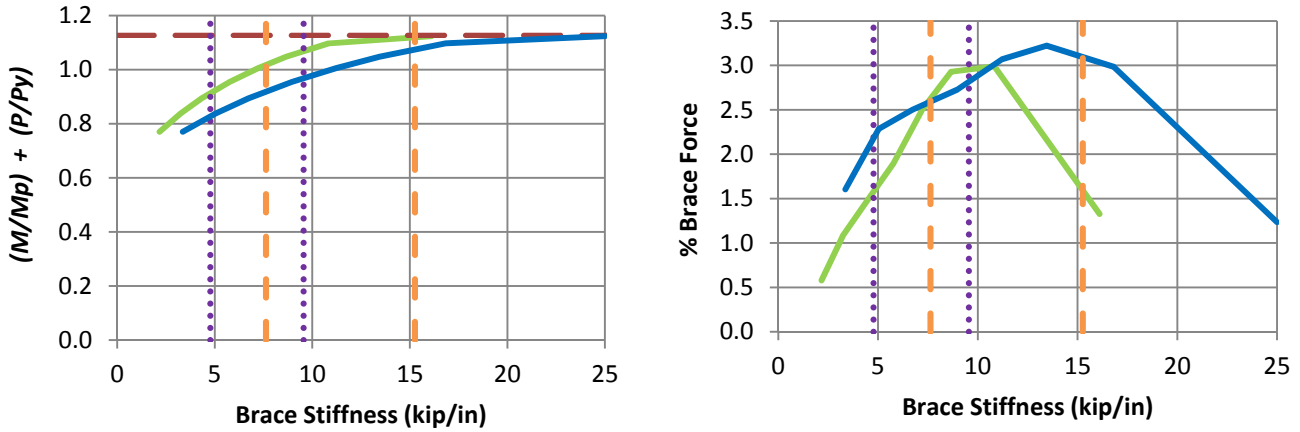
c) BC_MG2p_CNTB_n1_Lb15_FFR0.5



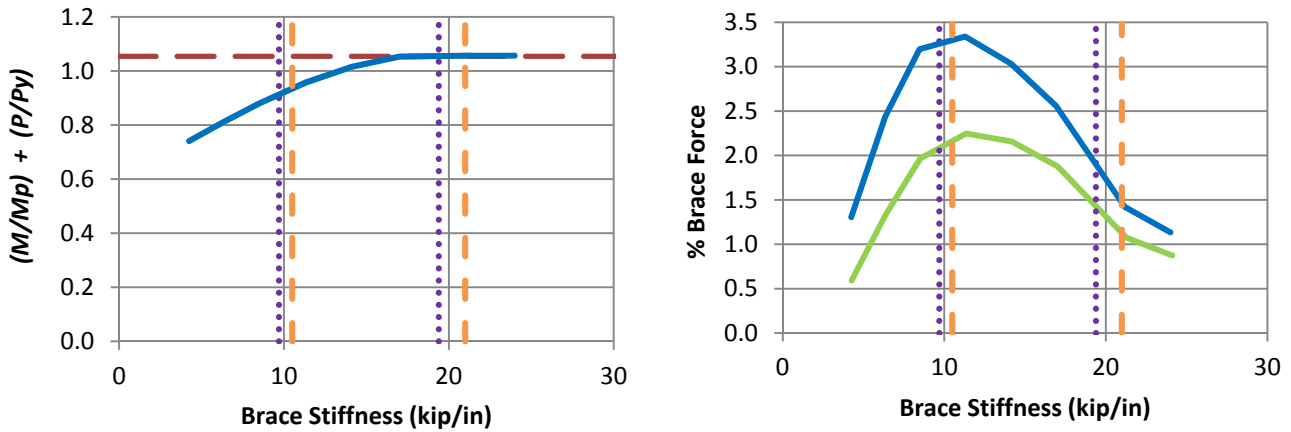
d) BC_MG2p_CNTB_n1_Lb15_FFR1

- Rigidly-braced strength
- Test simulation results corresponding to torsional brace
- Test simulation results corresponding to lateral brace
- 1x and 0.5x lateral bracing stiffness from Eq. (6-5)
- 1x and 0.5x torsional bracing stiffness from Eq. (6-7)

Fig. 7.17 (continued). Beam-column knuckle curves and brace force vs. brace stiffness plots for combined point (nodal) lateral and torsional bracing cases with $n = 1$, Moment Gradient 2 loading with lateral bracing on the flange in flexural compression, and $L_b = 15$ ft.



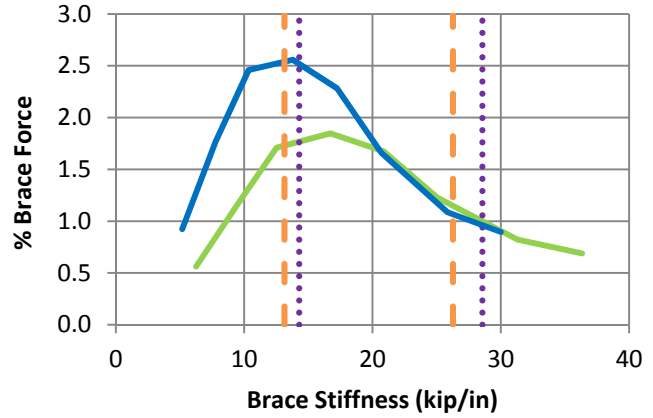
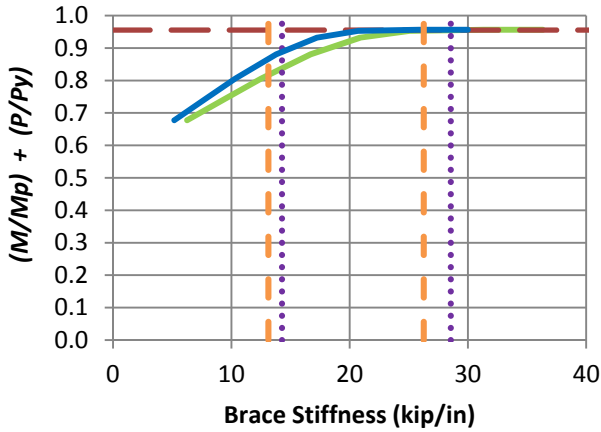
a) BC_MG2n_CNTB_n1_Lb5_FFR-0.5



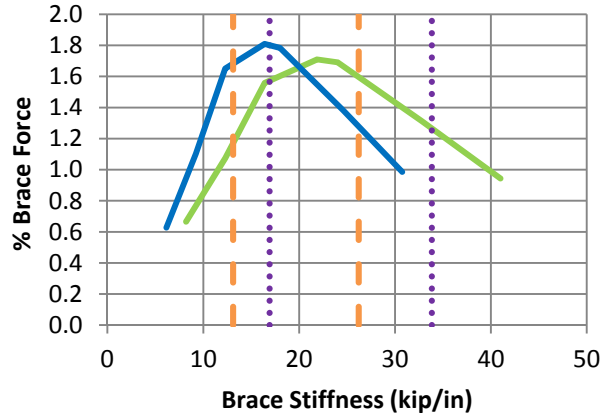
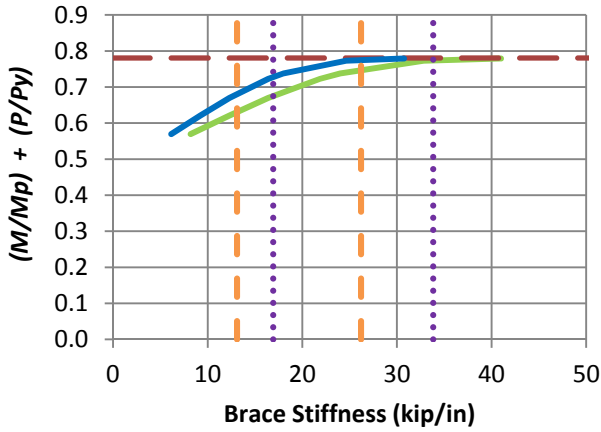
b) BC_MG2n_CNTB_n1_Lb5_FFR0

- Rigidly-braced strength
- Test simulation results corresponding to torsional brace
- Test simulation results corresponding to lateral brace
- 1x and 0.5x lateral bracing stiffness from Eq. (6-5)
- - - 1x and 0.5x torsional bracing stiffness from Eq. (6-7)

Figure 7.18. Beam-column knuckle curves and brace force vs. brace stiffness plots for combined point (nodal) lateral and torsional bracing cases with $n = 1$, Moment Gradient 2 loading with lateral bracing on the flange in flexural tension, and $L_b = 5$ ft.



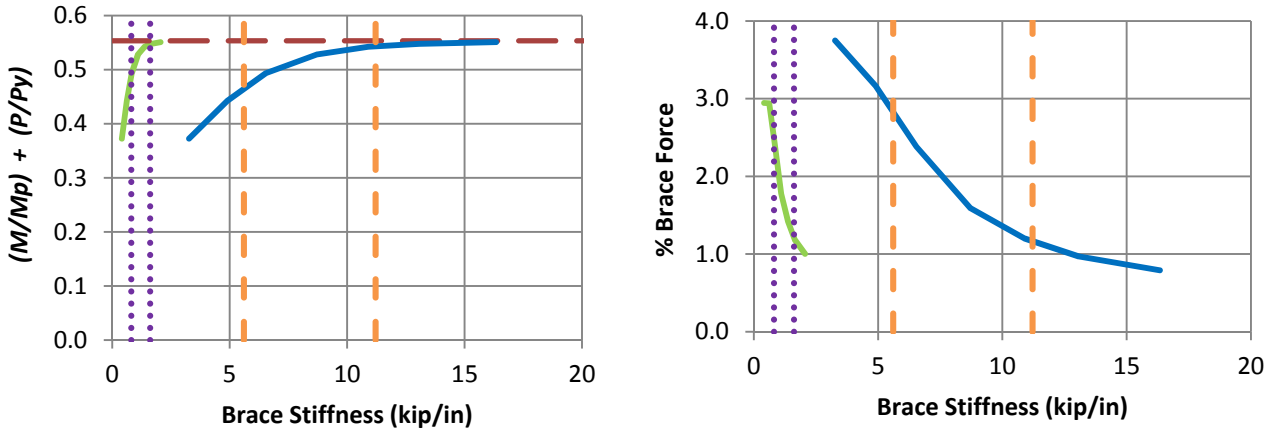
c) BC_MG2n_CNTB_n1_Lb5_FFR0.5



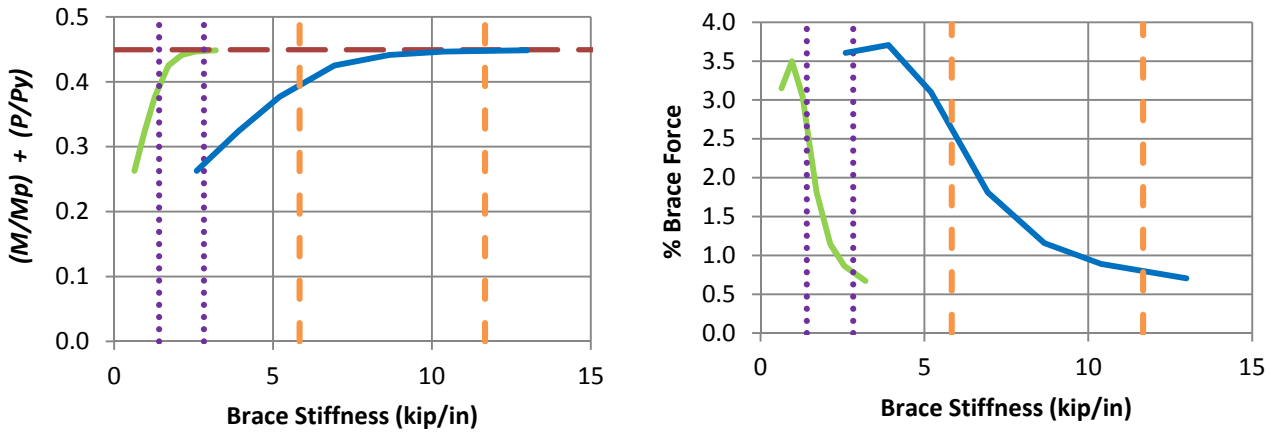
d) BC_MG2n_CNTB_n1_Lb5_FFR1

- Rigidly-braced strength
- Test simulation results corresponding to torsional brace
- Test simulation results corresponding to lateral brace
- 1x and 0.5x lateral bracing stiffness from Eq. (6-5)
- - - 1x and 0.5x torsional bracing stiffness from Eq. (6-7)

Fig. 7.18 (continued). Beam-column knuckle curves and brace force vs. brace stiffness plots for combined point (nodal) lateral and torsional bracing cases with $n = 1$, Moment Gradient 2 loading with lateral bracing on the flange in flexural tension, and $L_b = 5$ ft.



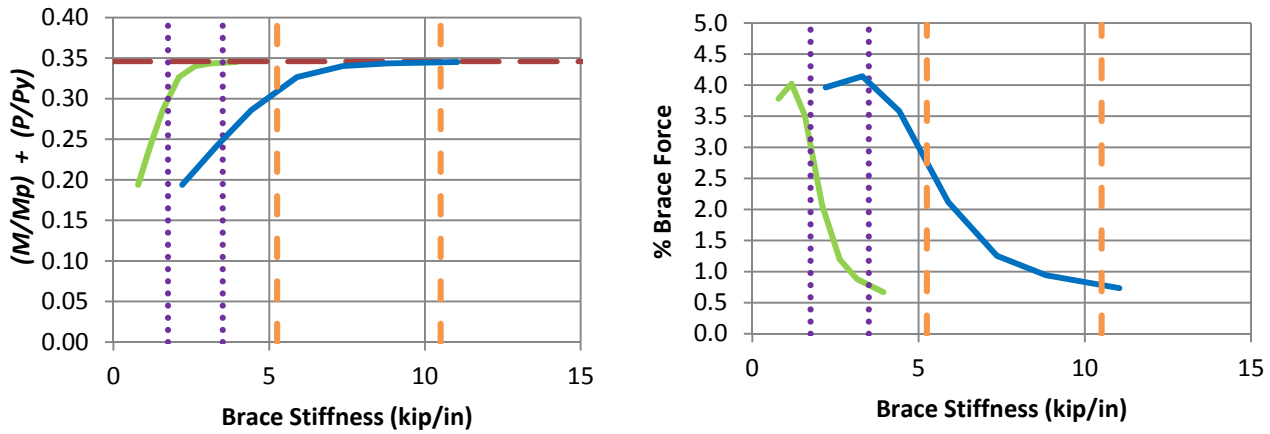
a) BC_MG2n_CNTB_n1_Lb15_FFR-0.5



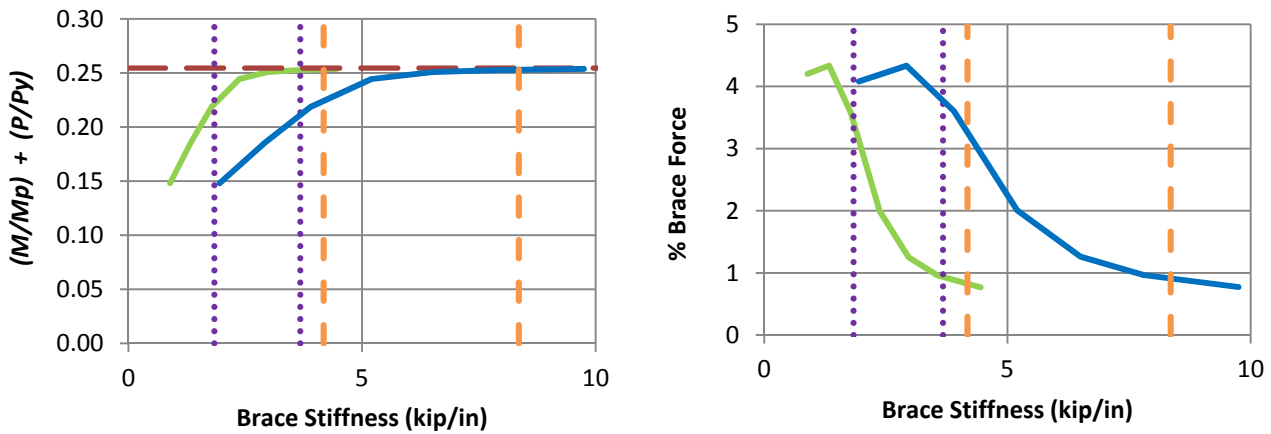
b) BC_MG2n_CNTB_n1_Lb15_FFR0

- Rigidly-braced strength
- Test simulation results corresponding to torsional brace
- Test simulation results corresponding to lateral brace
- ⋯ 1x and 0.5x lateral bracing stiffness from Eq. (6-5)
- 1x and 0.5x torsional bracing stiffness from Eq. (6-7)

Figure 7.19. Beam-column knuckle curves and brace force vs. brace stiffness plots for combined point (nodal) lateral and torsional bracing cases with $n = 1$, Moment Gradient 2 loading with lateral bracing on the flange in flexural tension, and $L_b = 15$ ft.



c) BC_MG2n_CNTB_n1_Lb15_FFR0.5



d) BC_MG2n_CNTB_n1_Lb15_FFR1

- Rigidly-braced strength
- Test simulation results corresponding to torsional brace
- Test simulation results corresponding to lateral brace
- 1x and 0.5x lateral bracing stiffness from Eq. (6-5)
- 1x and 0.5x torsional bracing stiffness from Eq. (6-7)

Fig. 7.19 (continued). Beam-column knuckle curves and brace force vs. brace stiffness plots for combined point (nodal) lateral and torsional bracing cases with $n = 1$, Moment Gradient 2 loading with lateral bracing on the flange in flexural tension, and $L_b = 15$ ft.

Table 7.7. Brace stiffnesses β_{F96L} and β_{brL} and brace forces as a percentage of P for beam-columns with Moment Gradient 2 loading and combined lateral and torsional bracing.

Case	β_{F96L} (kip/in)	β_{brL} (kip/in)	β_{brL} $/\beta_{F96L}$	% Lateral Brace Force at $\beta_L = \beta_{brL}$ and $\beta_T = \beta_{brT}$	Ratio of Actual to Estimated Lateral Brace Force at $\beta_L = \beta_{brL}$ and $\beta_T = \beta_{brT}$
BC_MG2p_CNTB_n1_Lb5_FFR-0.5	4.71	9.54	2.03	1.00	1.00
BC_MG2p_CNTB_n1_Lb5_FFR0	5.61	19.36	3.45	0.50	0.50
BC_MG2p_CNTB_n1_Lb5_FFR0.5	10.98	28.56	2.60	0.52	0.52
BC_MG2p_CNTB_n1_Lb5_FFR1	26.91	33.82	1.26	1.29	1.29
BC_MG2p_CNTB_n1_Lb15_FFR-0.5	0.92	1.62	1.76	1.00	1.00
BC_MG2p_CNTB_n1_Lb15_FFR0	1.56	2.82	1.81	0.60	0.60
BC_MG2p_CNTB_n1_Lb15_FFR0.5	2.04	3.50	1.72	0.58	0.58
BC_MG2p_CNTB_n1_Lb15_FFR1	2.37	3.68	1.55	0.98	0.98
BC_MG2n_CNTB_n1_Lb5_FFR-0.5	10.15	9.56	0.94	2.98	2.98
BC_MG2n_CNTB_n1_Lb5_FFR0	14.02	19.38	1.38	1.16	1.16
BC_MG2n_CNTB_n1_Lb5_FFR0.5	19.67	28.56	1.45	1.00	1.00
BC_MG2n_CNTB_n1_Lb5_FFR1	26.91	33.82	1.26	1.29	1.29
BC_MG2n_CNTB_n1_Lb15_FFR-0.5	1.16	1.62	1.40	1.06	1.06
BC_MG2n_CNTB_n1_Lb15_FFR0	1.88	2.82	1.50	0.75	0.75
BC_MG2n_CNTB_n1_Lb15_FFR0.5	2.31	3.50	1.52	0.80	0.80
BC_MG2n_CNTB_n1_Lb15_FFR1	2.37	3.68	1.55	0.98	0.98

Table 7.8. Brace stiffnesses β_{F96T} and β_{brT} and torsional brace forces as a percentage of $(M/h_o + P/2)$ for beam-columns with Moment Gradient 2 loading and combined lateral and torsional bracing.

Case	β_{F96T} (kip/in)	β_{brT} (kip/in)	β_{brL} / β_{F96T}	% Torsional Brace Force at $\beta_L = \beta_{brL}$ and $\beta_T = \beta_{brT}$	Ratio of Actual to Estimated Torsional Brace Force at $\beta_L = \beta_{brL}$ and $\beta_T = \beta_{brT}$
BC_MG2p_CNTB_n1_Lb5_FFR-0.5	7.33	15.20	2.07	0.48	0.24
BC_MG2p_CNTB_n1_Lb5_FFR0	5.58	20.96	3.76	0.10	0.05
BC_MG2p_CNTB_n1_Lb5_FFR0.5	9.07	26.28	2.90	0.08	0.04
BC_MG2p_CNTB_n1_Lb5_FFR1	20.19	26.20	1.30	1.22	0.61
BC_MG2p_CNTB_n1_Lb15_FFR-0.5	7.23	11.20	1.55	0.40	0.20
BC_MG2p_CNTB_n1_Lb15_FFR0	6.32	11.66	1.84	0.02	0.01
BC_MG2p_CNTB_n1_Lb15_FFR0.5	5.73	10.50	1.83	0.25	0.13
BC_MG2p_CNTB_n1_Lb15_FFR1	5.20	8.36	1.61	0.99	0.50
BC_MG2n_CNTB_n1_Lb5_FFR-0.5	15.75	15.26	0.97	3.10	1.55
BC_MG2n_CNTB_n1_Lb5_FFR0	13.96	21.00	1.50	1.50	0.75
BC_MG2n_CNTB_n1_Lb5_FFR0.5	16.24	26.28	1.62	1.05	0.53
BC_MG2n_CNTB_n1_Lb5_FFR1	20.19	26.20	1.30	1.23	0.62
BC_MG2n_CNTB_n1_Lb15_FFR-0.5	9.20	11.22	1.22	1.10	0.55
BC_MG2n_CNTB_n1_Lb15_FFR0	7.62	11.68	1.53	0.80	0.40
BC_MG2n_CNTB_n1_Lb15_FFR0.5	6.47	10.50	1.62	0.80	0.40
BC_MG2n_CNTB_n1_Lb15_FFR1	5.20	8.36	1.61	0.96	0.48

From Tables 7.7 and 7.8, it can be observed that the bracing stiffnesses predicted by Eqs. (6-5) and (6-7) are sufficient to develop 96 % of the minimum rigidly-braced member strength for all of the combined bracing cases. The brace demands calculated from the simulations are smaller than the predicted brace strengths for all cases except BC_MG2n_CNTB_n1_Lb5_FFR-0.5 and BC_MG2n_CNTB_n1_Lb5_FFR0. Figure 7.20 shows the lateral brace force versus the Load Proportionality Factor for BC_MG2n_CNTB_n1_Lb5_FFR-0.5 with brace stiffnesses calculated from Eq. (6-5) and (6-7). Figure 7.21 shows the corresponding plot for the torsional brace in this problem. It can be observed that a point lateral brace strength requirement of $0.01P$ is sufficient to develop member strength of 87.0 % of the test limit load in this case. Combining the results in Fig. 7.20 with the knuckle curve value corresponding to the recommended full bracing stiffnesses in Fig. 7.18a, it can be observed that the targeted bracing stiffnesses develop 83 % of the member rigidly-braced strength in this problem. This is the case that has the greatest lack of conservatism for the combined bracing problems studied with Moment Gradient 2 loading. Similar to other extreme cases discussed in the previous sections, if the increased stiffness associated with the multiplication by $1/\phi = 1/0.75$ is considered, the point lateral brace force at the test limit load is reduced to $0.022P$ and greater than 95 % of the member rigidly-braced strength is developed at the point lateral brace strength requirement of $0.01P$. In the corresponding Load Proportionality Factor vs torsional brace force plot (not shown), greater than 95 % of the member rigidly-braced strength is developed when the torsional brace reaches $0.02(P/2 + M/h_o)$.

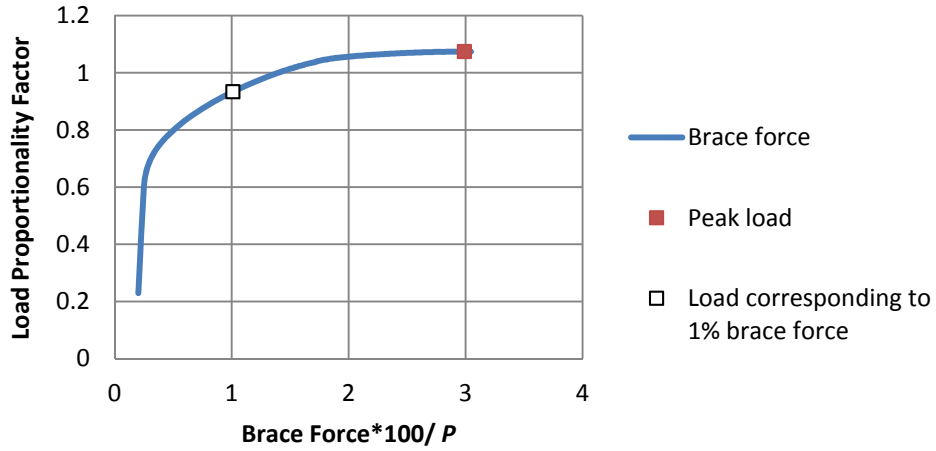


Figure 7.20. Point lateral brace force vs. the Load Proportionality Factor for BC_MG2n_CNTB_n1_Lb5_FFR-0.5 corresponding to a point lateral brace stiffness of $\beta_{brL} = 9.56$ kip/in from Eq. (6-5) and a point torsional brace stiffness of $\beta_{brT} = 15.26$ kip/in from Eq. (6-7).

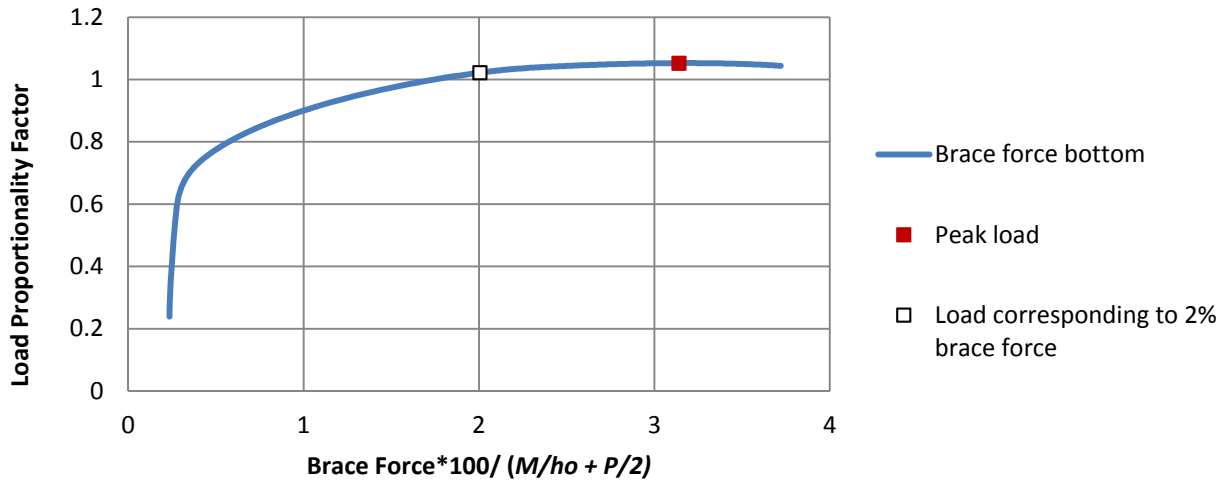


Figure 7.21. Point torsional brace force vs. the Load Proportionality Factor for BC_MG2n_CNTB_n1_Lb5_FFR-0.5 corresponding to a point lateral brace stiffness of $\beta_{brL} = 9.56$ kip/in from Eq. (6-5) and a point torsional brace stiffness of $\beta_{brT} = 15.26$ kip/in from Eq. (6-7).

CHAPTER 8 SUMMARY AND CONCLUSIONS

Based on the results from this research, the following recommendations are made for improving the AISC Appendix 6 (AISC 2010a) provisions:

- a) For combined lateral and torsional bracing systems of beams, the following bracing stiffness requirements are recommended:

When the lateral bracing is on the flange in subjected to flexural compression, the provided lateral and torsional bracing stiffnesses should satisfy the requirement

$$\frac{\beta_T}{\beta_{To}} + \frac{\beta_L}{\beta_{Lo}} \geq 1.0 \quad (4-8)$$

where:

β_L = Provided lateral bracing stiffness

β_T = Provided torsional bracing stiffness

β_{Lo} = Base required lateral bracing stiffness for full bracing per the AISC 360-10 Appendix 6 (AISC 2010a) rules, including the refinements specified in the Appendix 6 Commentary, i.e., Eq. (4-1), assuming the member is laterally braced only.

β_{To} = Base required torsional bracing stiffness for full bracing per the AISC 360-10 Appendix 6 (AISC 2010a) rules, assuming the member is torsionally braced only, including the refinements specified in the Appendix 6 Commentary. When expressed as a rotational stiffness, i.e., the torsional brace moment divided by the twist rotation at the torsional brace location, this stiffness is given by Eq. (4-5) times h_o^2 . When expressed as an equivalent

shear panel or relative brace in the vertical direction between the two flanges, this stiffness is given directly by Eq. (4-5).

When the lateral bracing is on the flange subjected to flexural tension, the provided lateral and torsional bracing stiffnesses should satisfy the above interaction Eq. (4-8) and, in addition, the required torsional brace stiffness, expressed as a rotational stiffness, shall be greater than or equal to the smaller of β_{T_0} or h_o^2 times the point (nodal) lateral bracing stiffness requirement as per AISC, obtained from Eq. (4-1) from the Appendix 6 (AISC 2010a) Commentary.

The base AISC Eqs. (4-2) and (4-3) should be employed to estimate the bracing lateral strength requirements. A base torsional bracing strength requirement of 2 % of the beam major-axis bending moment, or $0.02M/h_o$ of the couple force developed in the equivalent shear panel or relative bracing in the vertical direction between the I-section flanges. The variation in the strength requirements with different combinations of bracing stiffness is nonlinear in general, with a large number of combined bracing cases showing strength requirements on the individual components comparable to the recommended values for torsional and lateral bracing alone. For this reason, as well as for the reason that the recommended individual component stability bracing force values are already relatively small, it is suggested that no interaction effects be considered in calculating the combined bracing strength requirements.

b) For beam-column members, the following bracing requirements are recommended:

For beam-columns with lateral bracing only on the flange in flexural compression, the bracing requirements can be obtained from Eqs. (6-1) through (6-4):

- When the effective flange force ratio $P_{ft}/P_{fc} \leq 0$, such that the opposite flange is in net tension along its entire length,

$$\beta_{brL} = \frac{2N_i}{L_b} \left[\frac{P}{2} + \left(\frac{M_{max}}{h_o} \right) C_{tL} C_d \right] \quad (6-1)$$

$$R_{brL} = 0.01 \left[\frac{P}{2} + \left(\frac{M_{max}}{h_o} \right) C_{tL} C_d \right] \text{ for point (nodal) lateral bracing} \quad (6-2a)$$

$$= 0.005 \left[\frac{P}{2} + \left(\frac{M_{max}}{h_o} \right) C_{tL} C_d \right] \text{ for shear panel (relative) lateral bracing} \quad (6-2b)$$

where β_{brL} is the required lateral bracing stiffness, R_{brL} is the required lateral bracing strength, and all of the above variables are as defined in Section 4.4, with the exception of P , which is the constant beam-column axial compression considered in this research.

- When the effective flange force ratio $P_{fi} / P_{fc} > 0$, such that the opposite flange is subjected to a net compression force at any position along its length,

$$\beta_{brL} = \frac{2N_i}{L_b} \left[2.5P + \left(\frac{M_{max}}{h_o} \right) C_{tL} C_d \right] \quad (6-3)$$

$$R_{brL} = 0.01 \left[2.5P + \left(\frac{M_{max}}{h_o} \right) C_{tL} C_d \right] \text{ for point (nodal) lateral bracing} \quad (6-4a)$$

$$= 0.005 \left[2.5P + \left(\frac{M}{h_o} \right) C_{tL} C_d \right] \text{ for shear panel (relative) lateral bracing} \quad (6-4b)$$

For beam-columns restrained by combined lateral and torsional bracing the lateral bracing system can be designed conceptually for the axial load P and the torsional bracing can be designed for the moment M_{max} . The moment can be assumed to have a negligible effect on the lateral bracing, but the axial force creates some additional demands on the

torsional bracing. Therefore, the requirements for full bracing by the different bracing components may be written as follows:

$$\beta_{brL} = \frac{2N_i P}{L_b} \quad (6-5)$$

$$R_{brL} = 0.01P \text{ for point (nodal) lateral bracing} \quad (6-6a)$$

$$= 0.005P \text{ for shear panel (relative) lateral bracing} \quad (6-6b)$$

$$\beta_{brT} = \pi^2 \left[\frac{\left(\frac{M_{max}}{C_b h_o} + \frac{P}{2} \right)}{P_{ef,eff}} \right] \left[\frac{\left(\frac{M_{max}}{C_b h_o} + \frac{P}{2} \right)}{L_b} \right] \left[\frac{n_T + 1}{n_T} \right] C_{iT} \quad (6-7)$$

$$M_{brT} = 0.02 \left(M_{max} + \frac{P}{2} h_o \right) \quad (6-8)$$

where all of the above variables are as defined in Section 4.4, with the exception of P , which is the constant beam-column axial compression considered in this research.

Based on the test simulation studies conducted in this research, it can be stated that the above rules provide an accurate to conservative characterization of the stiffness and strength demands on the individual and/or combined bracing components. Syntheses of the test simulation studies have been presented that emphasize the percentage of the member rigidly-braced strengths developed either at the limit load of the tests where the recommended full bracing stiffness values are used, or in cases where the brace forces exceed the recommended brace strength requirements prior to the development of the member limit load with the brace stiffnesses set at the recommended full bracing values, the percentage of the member rigidly-braced strengths developed at the stage where the brace strength requirement is exceeded. The most critical cases identified in these syntheses are as follows:

- For beam members subjected to Moment Gradient 1 loading (see Fig. 2.1) and restrained by basic point lateral, shear panel lateral or point torsional bracing, approximately 97 % of the

beam rigidly-braced strength is developed in test B_MG1p_RB_n2_Lb5 when the maximum shear force in the bracing panels reaches $0.005M/h_o$ (see Figs. 4.4 and 4.2a).

- For beam members subjected to Moment Gradient 1 loading and restrained by combined lateral and torsional bracing, all of the study cases exceed 96 % of the rigidly-braced strengths when the recommended full bracing stiffness values are employed. In the combined bracing cases, the largest point lateral brace force is $0.008M/h_o$ (see Fig. 4.7a), the largest shear panel bracing force is $0.006M/h_o$ (see Fig. 4.8a) and the largest torsional bracing moment encountered is $0.012M$ (see Fig. 4.8b) at the test limit loads. Although the above shear panel bracing force exceeds the recommended required strength limit of $0.005M/h_o$, greater than 96 % of the member rigidly-braced strength is developed when this strength limit is reached.
- For beam members subjected to Moment Gradient 2 loading (see Fig. 2.2) and restrained by basic point lateral, shear panel lateral or point torsional bracing, with the transverse load applied at the mid-depth of the web, approximately 88 % of the beam rigidly-braced strength is developed in test B_MG2pc_TB_n1_Lb5 at the member limit load when the recommended torsional full bracing stiffness is used (see Figs. 4.11 and 4.10a). The torsional brace moment at the test limit load is predicted accurately by the recommended required strength of $0.02M$ in this problem when $\beta_T = \beta_{brT}$. Larger torsional brace moments are encountered at the test limit load for larger torsional brace stiffnesses in this problem; however, the brace force - Load Proportionality Factor curves are very flat at the limit load, such that the member develops very close to its limit load when the brace strength reaches $0.02M$.
- For beam members subjected to Moment Gradient 2 loading and restrained by combined lateral and torsional bracing, with the transverse load applied at the mid-depth of the web, approximately 94 % of the beam rigidly-braced strength is developed in test B_MG2pc_CNTB_n1_Lb5_TLBSR1 when the point lateral brace force reaches $0.01M/h_o$ (see Figs. 4.14 and 4.13a).
- For beam members subjected to Moment Gradient 2 loading and restrained by basic point lateral, shear panel lateral or point torsional bracing, with the transverse load applied at the top

flange, approximately 82 % of the beam rigidly-braced strength is developed in test B_MG2pt_TB_n1_Lb5 when the point torsional brace moment reaches $0.02M$ (see Figs. 5.3 and 5.2a). This case is considered further in the discussions below.

- For beam members subjected to Moment Gradient 2 loading and restrained by combined lateral and torsional bracing, with the transverse load applied at the top flange, approximately 91 % of the beam rigidly-braced strength is developed in test B_MG2nt_CNTB_n1_Lb5_TLBSR1 when the point torsional brace moment reaches $0.02M$ (see Figs. 5.6 and A.15b).
- For beam members subjected to Moment Gradient 3 loading and restrained by combined lateral and torsional bracing, more than 96 % of the beam rigidly-braced strength is developed in all cases, with the exception that as the shear panel brace stiffness approaches zero in B_MG3_CRTB_n2_Lb15, very slightly less than 96 % of the beam rigidly-braced strength is developed (see Fig. 4.23). In the combined bracing cases, the point lateral and the shear panel brace forces are very small (see Figs. 4.20 and 4.23) and the largest torsional bracing moment encountered is $0.0079M$ (see Fig. 4.23).
- For beam-columns with lateral bracing only on the flange in flexural compression and with $P_{ft}/P_{fc} \leq 0$, subjected to uniform primary moment such that the opposite flange is in net tension, the requirements given by Eqs. (6-1) and (6-2) develop more than 96 % of the member rigidly-braced strength in all cases, and the largest brace forces developed range from 0.70 to 1.04 of the estimated brace strength requirement (see Table 6.1).
- For beam-columns with lateral bracing only on the flange in flexural compression and with $P_{ft}/P_{fc} > 0$, subjected to uniform primary moment such that the opposite flange is in net compression, excluding cases with a slenderness of the opposite flange $L/r_{yf} > 200$, approximately 94 % of the member rigidly-braced strength is developed at the limit load of test BC_UMp_NB_n1_Lb15_FFR1 (see Table 6-2 and Fig. 6.9b). The point brace force from test simulation at this strength limit is essentially equal to the recommended design strength estimate, $0.01M/h_o$.

- For beam-columns restrained by combined lateral and torsional bracing, subjected to uniform primary moment, approximately 81 % of the beam rigidly-braced strength is developed in test BC_UMp_CNTB_n1_Lb15_FFR-0.67 when the point lateral brace force reaches $0.01P$ (see Figs. 6.23 and 6.14a). A brace force of $0.013P$ is required to develop the test limit load in this problem (see Fig. 6.23). In addition, the test limit load in this case is essentially equal to the beam-column rigidly-braced strength (see Fig. 6.14a). This case is considered further in the discussions below.
- For beam-columns with lateral bracing only on the flange in flexural compression, subjected to Moment Gradient 1 loading, excluding cases with a slenderness of the opposite flange $L/r_{yf} > 200$, approximately 95 % of the member rigidly-braced strength is developed at the limit load of test BC_MG1p_NB_n1_Lb15_FFR-0.5 (see Table 7-1 and Fig. 7-2a). The brace forces at the limit loads in the test simulation studies with $\beta_L = \beta_{brL}$ range from 0.70 to 1.02 of the recommended bracing strength requirement at in all of the tests of this type (see Table 7.1).
- For beam-columns with combined lateral and torsional bracing, subjected to Moment Gradient 1 loading, approximately 88 % of the member rigidly-braced strength is developed at the limit load of test BC_MB1n_CRTB_n2_Lb15_FFR-0.5 (see Table 7.5 and Fig. 7.12a). The lateral brace forces at the limit loads in the test simulation studies with $\beta_L = \beta_{brL}$ and $\beta_T = \beta_{brT}$ range from 0.30 to 1.10 of the recommended lateral brace strength requirements (see Table 7.2). The torsional brace moments at the limit loads in these test simulation studies range from 0.03 to 0.60 of the recommended torsional brace strength requirements (see Table 7.3).
- For beam-columns with lateral bracing only on the flange in flexural compression, subjected to Moment Gradient 2 loading, the requirements given by Eqs. (6-1) and (6-2) develop more than 96 % of the member rigidly-braced strength in all cases, and the largest brace forces developed range from 0.60 to 0.90 of the estimated brace strength requirements (see Table 7.6).

- For beam-columns with combined lateral and torsional bracing, subjected to Moment Gradient 2 loading, approximately 83 % of the member rigidly-braced strength is developed in test BC_MG2n_CNTB_n1_Lb5_FFR-0.5 when the point lateral brace reaches $0.01P$ (see Tables 7.7 and 7.8, and Figs. 7.2 and 7.18a).

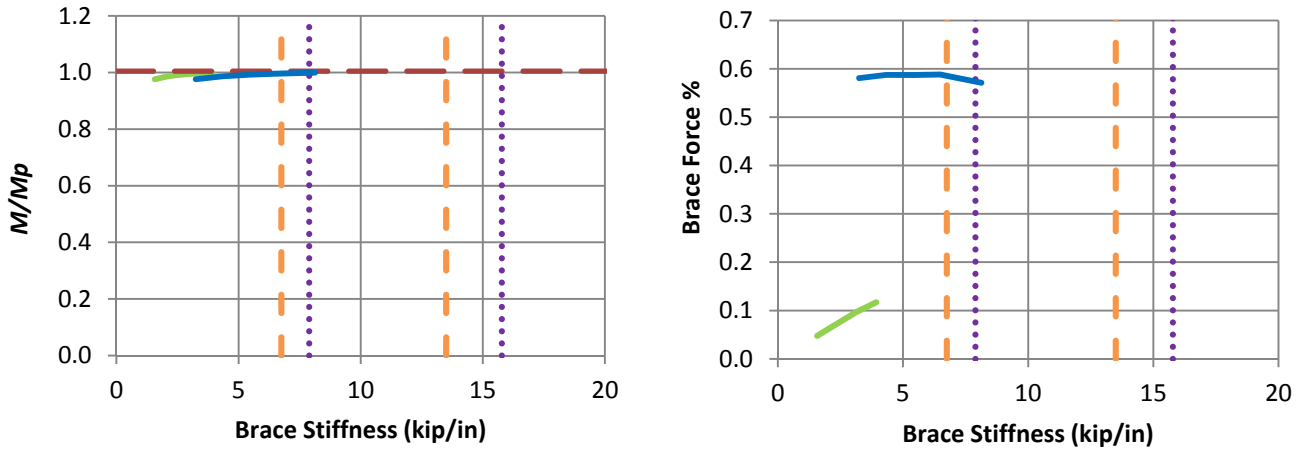
In the most demanding of the critical cases identified above, i.e., the cases exhibiting the greatest reduction from the member rigidly-braced strength at the limit load associated with the use of the recommended full bracing stiffness requirements, or the greatest reduction from the rigidly-braced strength when any of the brace forces exceed the recommended brace strength requirements for full bracing (using the recommended full bracing stiffness requirements), the fact that the design brace stiffness is increased by $1/\phi = 1/0.75 = 1.33$ in LRFD increases the member strength developed to greater than 90 % of the rigidly-braced strength in all cases with the exception of the following:

- 1) The torsionally braced beam test B_MG2pt_TB_n1_Lb5. The knuckle curve in this case exhibits the largest reduction in the beam strength from the rigidly-braced strength, plus this case exhibits relatively large torsional brace moments at the beam limit load (see Fig. 5.2a). However, as discussed in Section 5.3, other factors such as tipping restraint due to the manner in which the top flange load is typically applied can relieve the demands on the bracing in this problem. Alternatively, increasing the basic beam torsional bracing stiffness requirement by a factor of 1.5 in Eq. (4-5) increases the beam strength in this test to approximately 90 % of the rigidly-braced strength when the torsional bracing strength requirement of $0.02M$ is reached. Increasing the torsional bracing strength requirement has little effect in this problem since its brace force - Load Proportionality Factor curve is very flat in the vicinity of the limit load (see Fig. 4.11). This increase in the required torsional bracing stiffness would also increase the percentage of the rigidly-braced strength at which the torsional bracing strength of $0.02M$ is reached in test B_MG2nt_CNTB_n1_TLBSR1 to greater than 96 % of the rigidly-braced strength (see Figs. 5.6 and A.15b).

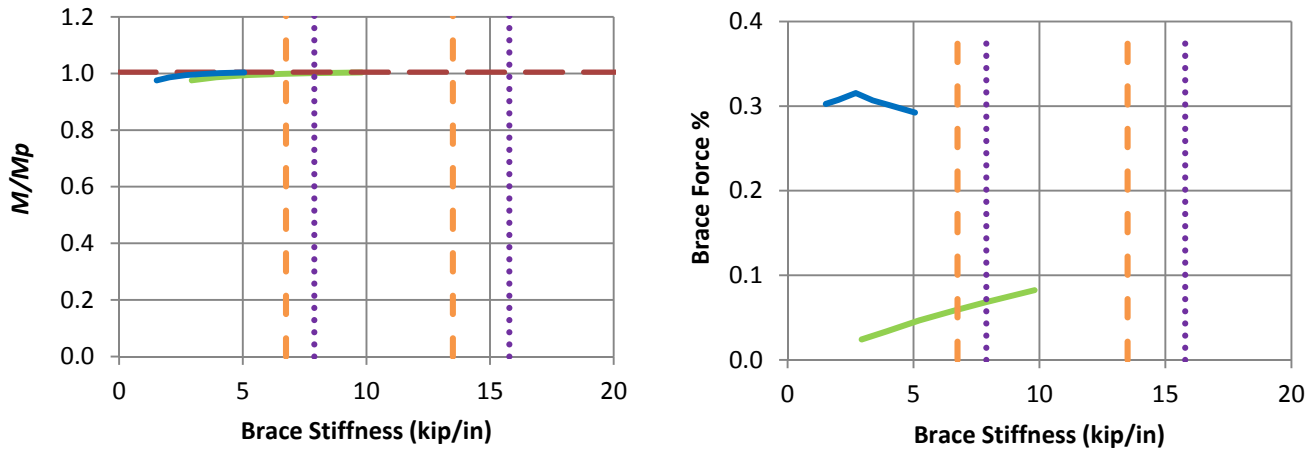
- 2) The combined lateral and torsional bracing beam-column test BC_UMp_CNTB_n1_Lb15_FFR-0.67. In this problem, essentially the same lateral brace force results shown in Fig. 6.23 are obtained when the stiffness of the lateral and torsional bracing is increased by $1/\phi = 1/0.75$. This result is consistent with the fact that the recommended bracing stiffness requirements develop this member's rigidly-braced strength for all practical purposes. To avoid exceeding the recommended lateral brace strength in this problem, the recommended point lateral brace strength requirement needs to be increased to $0.013P$. Correspondingly, the shear panel bracing strength requirement would need to be increased to $0.0065P$, since a single mid-span lateral brace is equivalent to two shear panel braces, one on each side of the mid-span.

CHAPTER 9 APPENDIX

The knuckle curves and brace force versus brace stiffness plots corresponding to the combined bracing data points on the interaction plots in Figs. 4.5, 4.6, 4.12 and 5.4 are shown below in Figs. A.1 through A.16.



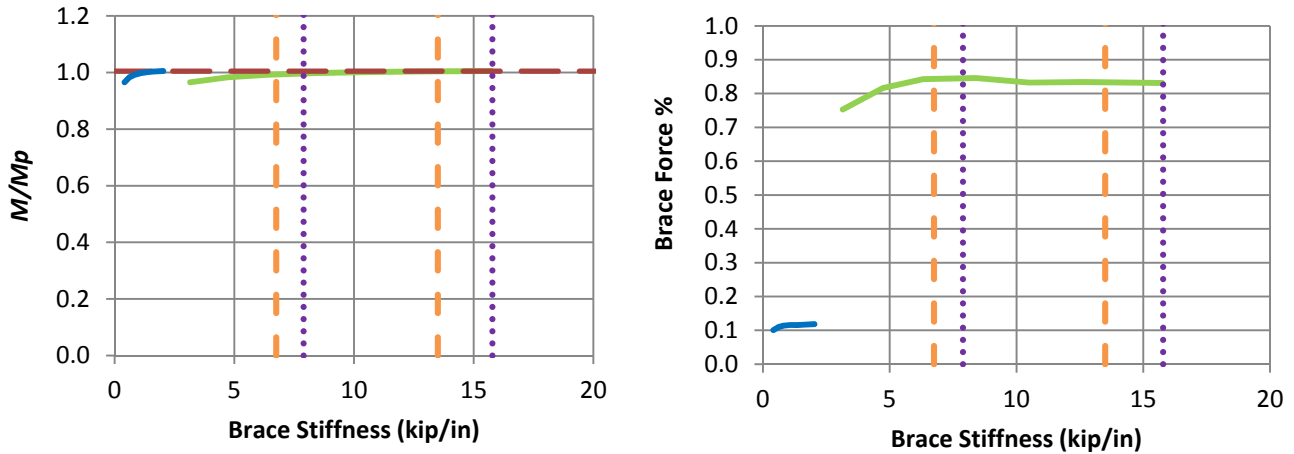
a) B_MG1p_CNTB_n1_Lb5_TLBSR4



b) B_MG1p_CNTB_n1_Lb5_TLBSR1

- Rigidly-braced strength
- Test simulation results corresponding to torsional brace
- Test simulation results corresponding to lateral brace
- 1x and 0.5x lateral bracing stiffness from Eq. (4-1)
- 1x and 0.5x torsional bracing stiffness from Eq. (4-5)

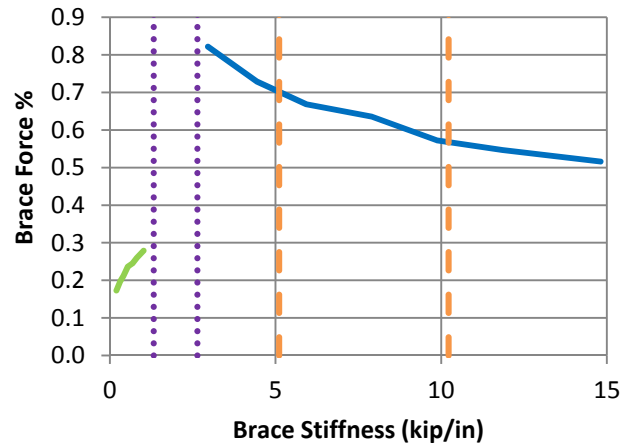
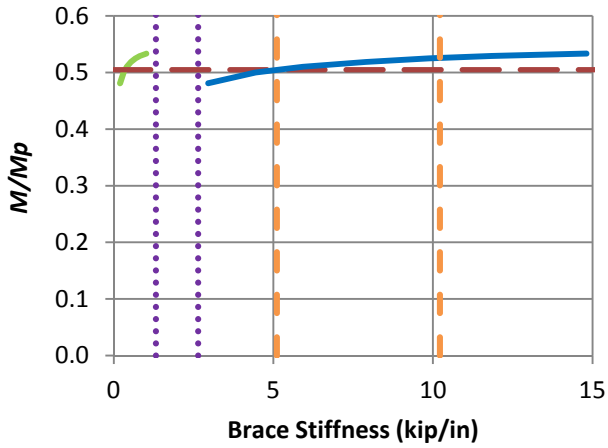
Figure A.1. Beam knuckle curves and brace force vs. brace stiffness plots for combined point (nodal) lateral and torsional bracing cases with $n = 1$, Moment Gradient 1 loading with lateral bracing on the flange in flexural compression, and $L_b = 5$ ft.



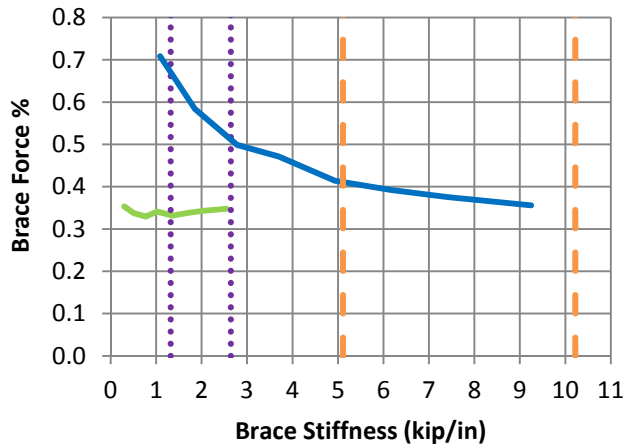
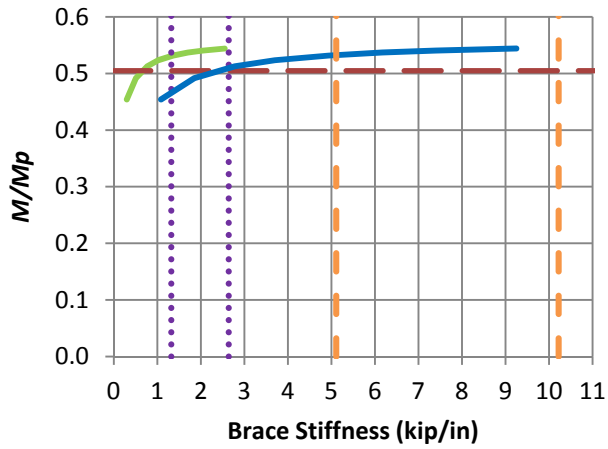
c) B_MG1p_CNTB_n1_Lb5_TLBSR0.25

- - Rigidly-braced strength
- Test simulation results corresponding to torsional brace
- Test simulation results corresponding to lateral brace
- ⋯ 1x and 0.5x lateral bracing stiffness from Eq. (4-1)
- - 1x and 0.5x torsional bracing stiffness from Eq. (4-5)

Fig. A.1 (continued). Beam knuckle curves and brace force vs. brace stiffness plots for combined point (nodal) lateral and torsional bracing cases with $n = 1$, Moment Gradient 1 loading with lateral bracing on the flange in flexural compression, and $L_b = 5$ ft.



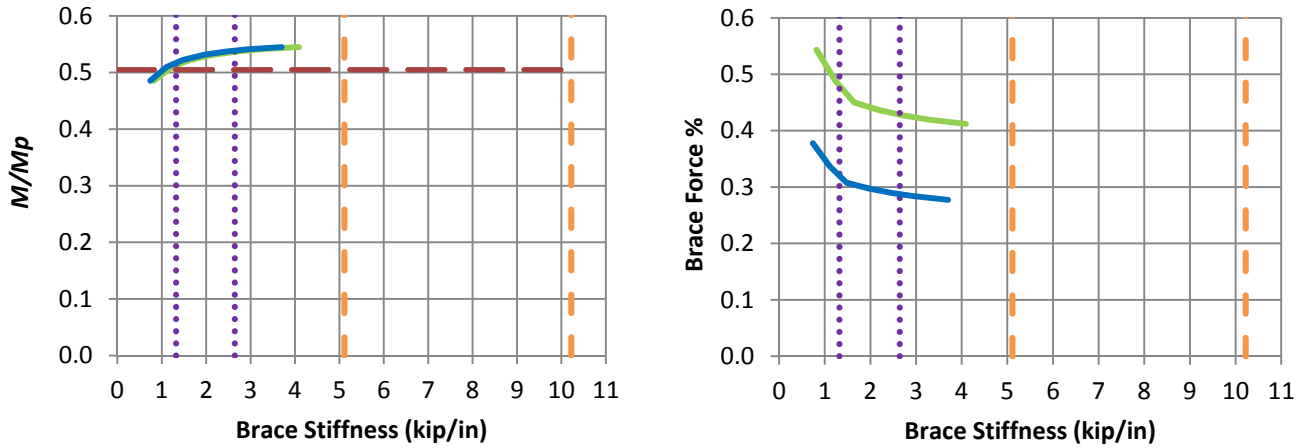
a) B_MG1p_CNTB_n1_Lb15_TLBSR4



b) B_MG1p_CNTB_n1_Lb15_TLBSR1

- Rigidly-braced strength
- Test simulation results corresponding to torsional brace
- Test simulation results corresponding to lateral brace
- 1x and 0.5x lateral bracing stiffness from Eq. (4-1)
- 1x and 0.5x torsional bracing stiffness from Eq. (4-5)

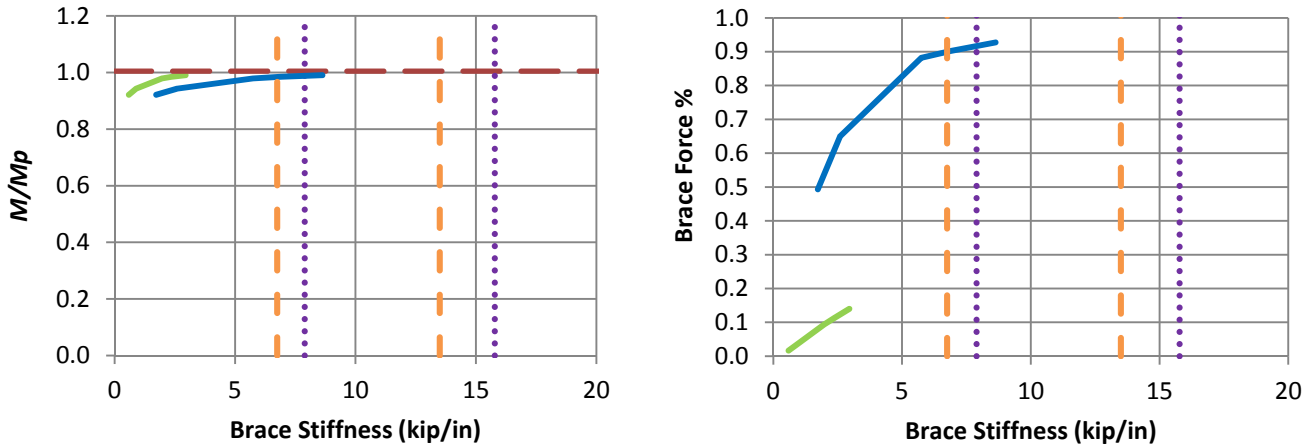
Figure A.2. Beam knuckle curves and brace force vs. brace stiffness plots for combined point (nodal) lateral and torsional bracing cases with $n = 1$, Moment Gradient 1 loading with lateral bracing on the flange in flexural compression, and $L_b = 15$ ft.



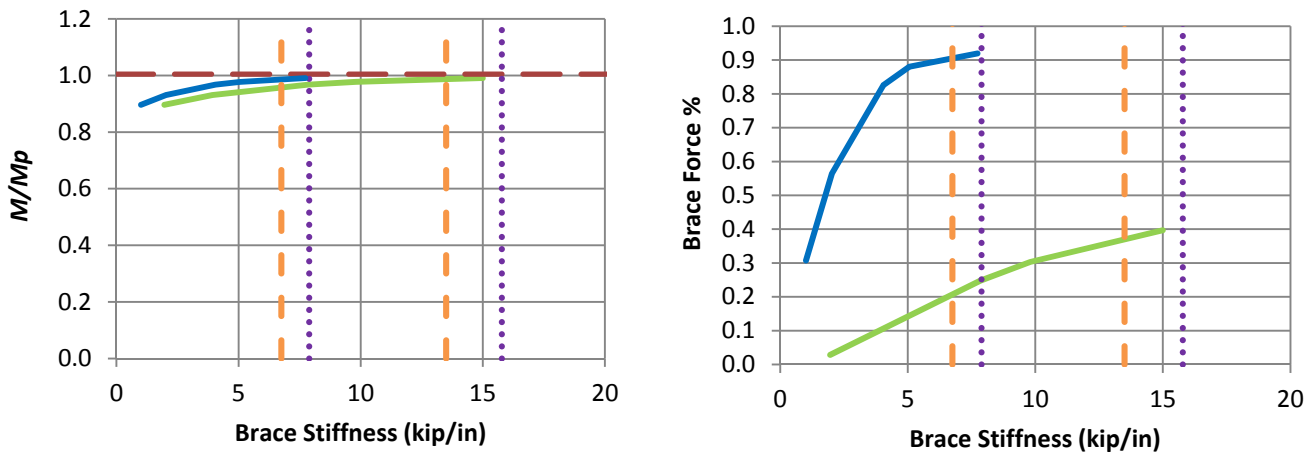
c) B_MG1p_CNTB_n1_Lb15_TLBSR0.25

- Rigidly-braced strength
- Test simulation results corresponding to torsional brace
- Test simulation results corresponding to lateral brace
- 1x and 0.5x lateral bracing stiffness from Eq. (4-1)
- 1x and 0.5x torsional bracing stiffness from Eq. (4-5)

Fig. A.2 (continued). Beam knuckle curves and brace force vs. brace stiffness plots for combined point (nodal) lateral and torsional bracing cases with $n = 1$, Moment Gradient 1 loading with lateral bracing on the flange in flexural compression, and $L_b = 15$ ft.



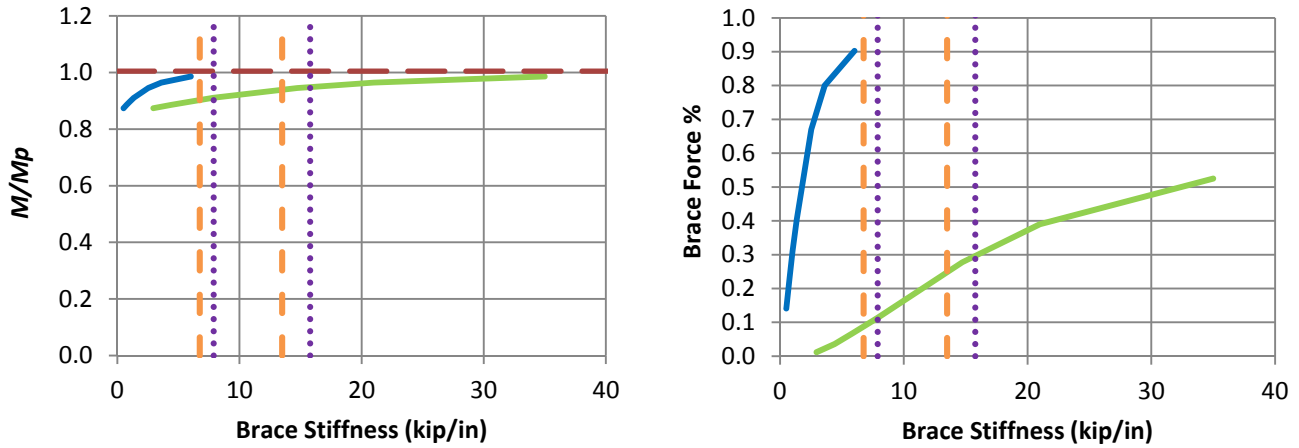
a) B_MG1n_CNTB_n1_Lb5_TLBSR5.67



b) B_MG1n_CNTB_n1_Lb5_TLBSR1

- Rigidly-braced strength
- Test simulation results corresponding to torsional brace
- Test simulation results corresponding to lateral brace
- 1x and 0.5x lateral bracing stiffness from Eq. (4-1)
- - - 1x and 0.5x torsional bracing stiffness from Eq. (4-5)

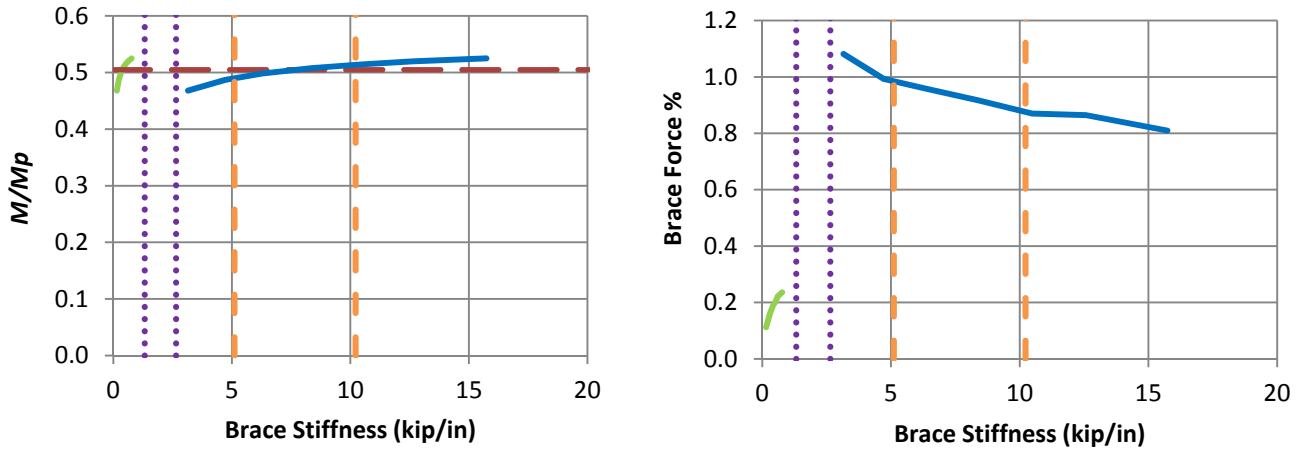
Figure A.3. Beam knuckle curves and brace force vs. brace stiffness plots for combined point (nodal) lateral and torsional bracing cases with $n = 1$, Moment Gradient 1 loading with lateral bracing on the flange in flexural tension, and $L_b = 5$ ft.



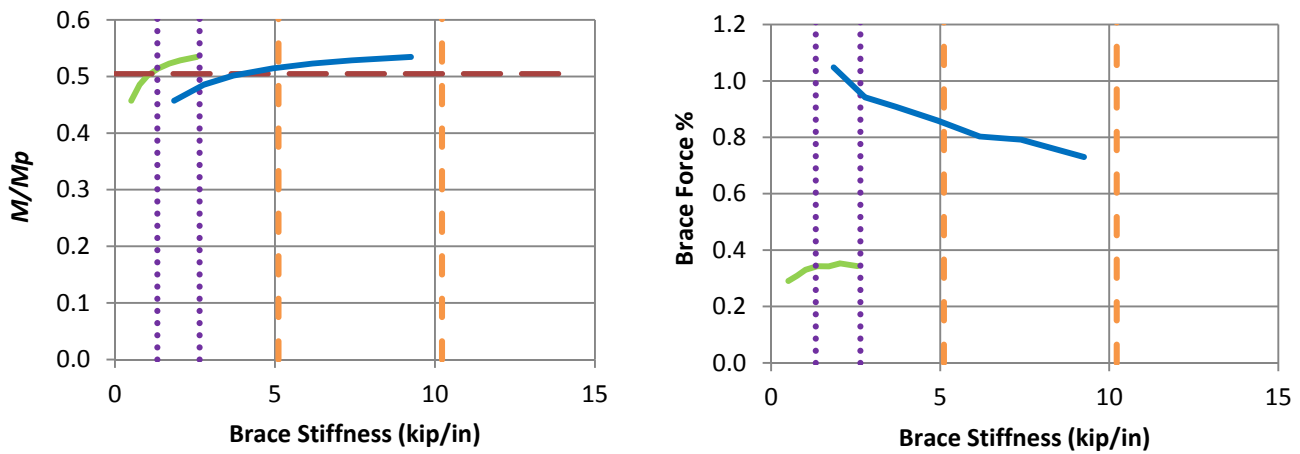
c) B_MG1n_CNTB_n1_Lb5_TLBSR0.33

- Rigidly-braced strength
- Test simulation results corresponding to torsional brace
- Test simulation results corresponding to lateral brace
- 1x and 0.5x lateral bracing stiffness from Eq. (4-1)
- 1x and 0.5x torsional bracing stiffness from Eq. (4-5)

Fig. A.3 (continued). Beam knuckle curves and brace force vs. brace stiffness plots for combined point (nodal) lateral and torsional bracing cases with $n = 1$, Moment Gradient 1 loading with lateral bracing on the flange in flexural tension, and $L_b = 5$ ft.



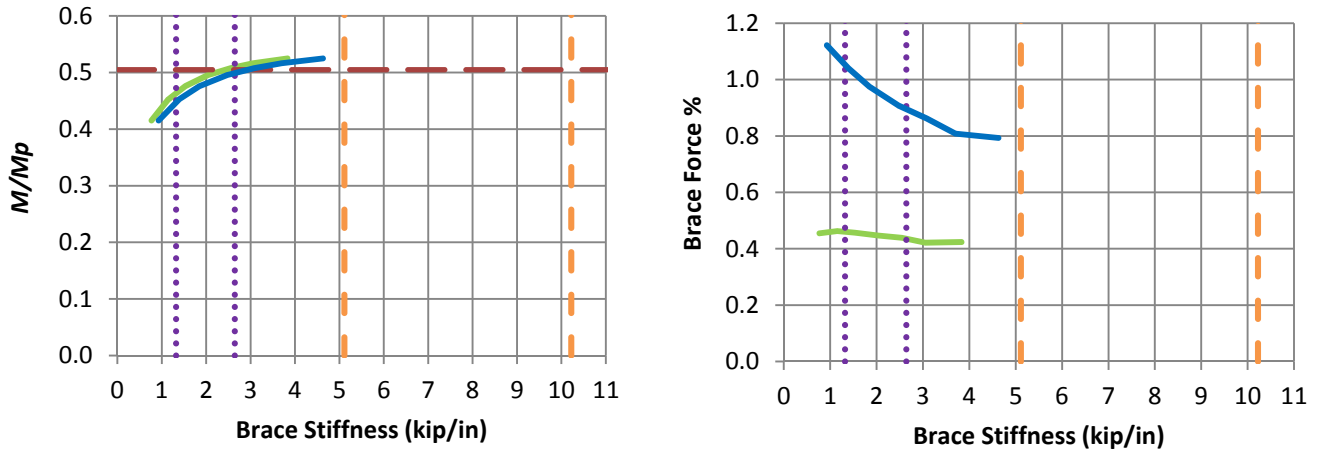
a) B_MG1n_CNTB_n1_Lb15_TLBSR5.67



b) B_MG1n_CNTB_n1_Lb15_TLBSR1

- Rigidly-braced strength
- Test simulation results corresponding to torsional brace
- Test simulation results corresponding to lateral brace
- 1x and 0.5x lateral bracing stiffness from Eq. (4-1)
- 1x and 0.5x torsional bracing stiffness from Eq. (4-5)

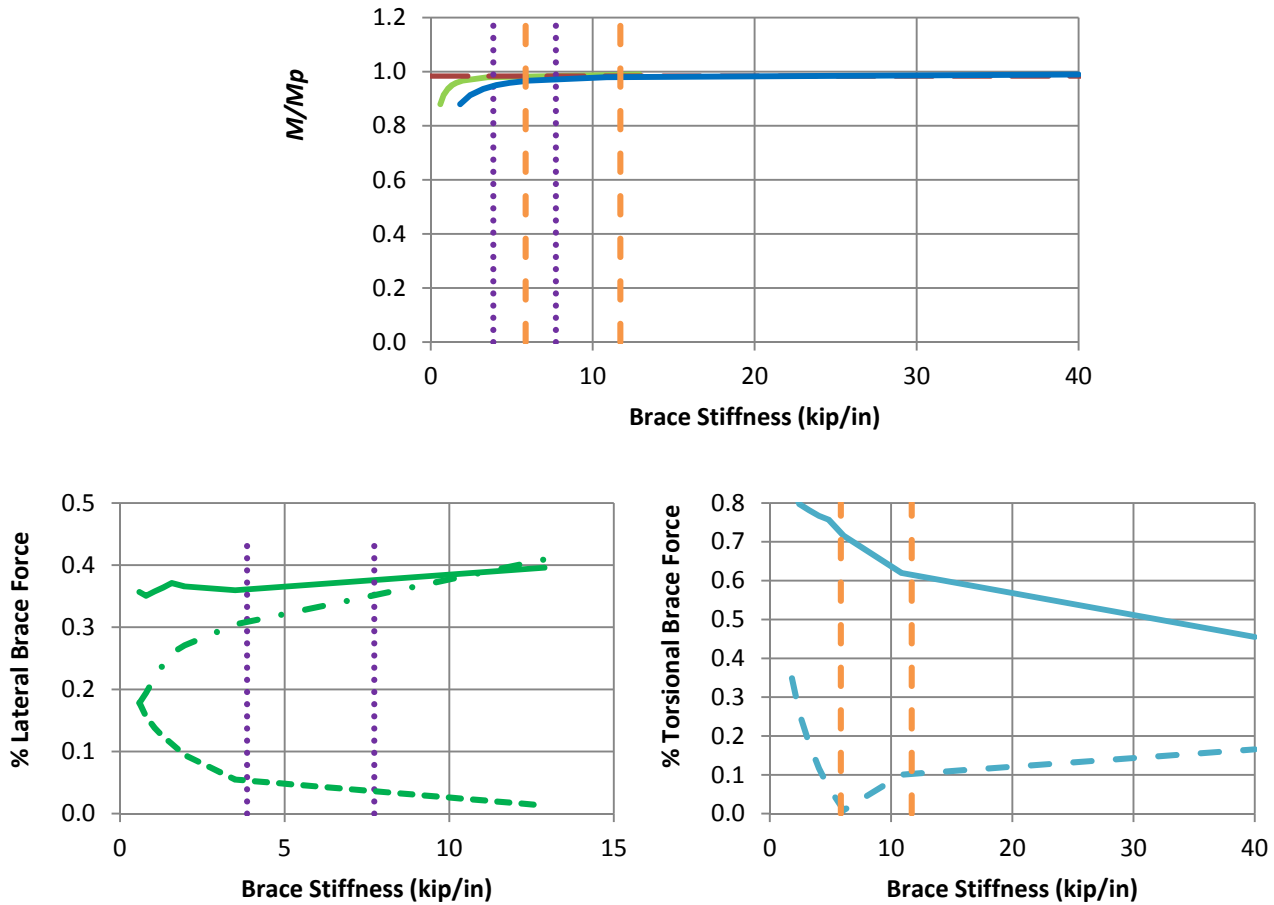
Figure A.4. Beam knuckle curves and brace force vs. brace stiffness plots for combined point (nodal) lateral and torsional bracing cases with $n = 1$, Moment Gradient 1 loading with lateral bracing on the flange in flexural tension, and $L_b = 15$ ft.



c) B_MG1n_CNTB_n1_Lb15_TLBSR0.33

- Rigidly-braced strength
- Test simulation results corresponding to torsional brace
- Test simulation results corresponding to lateral brace
- 1x and 0.5x lateral bracing stiffness from Eq. (4-1)
- 1x and 0.5x torsional bracing stiffness from Eq. (4-5)

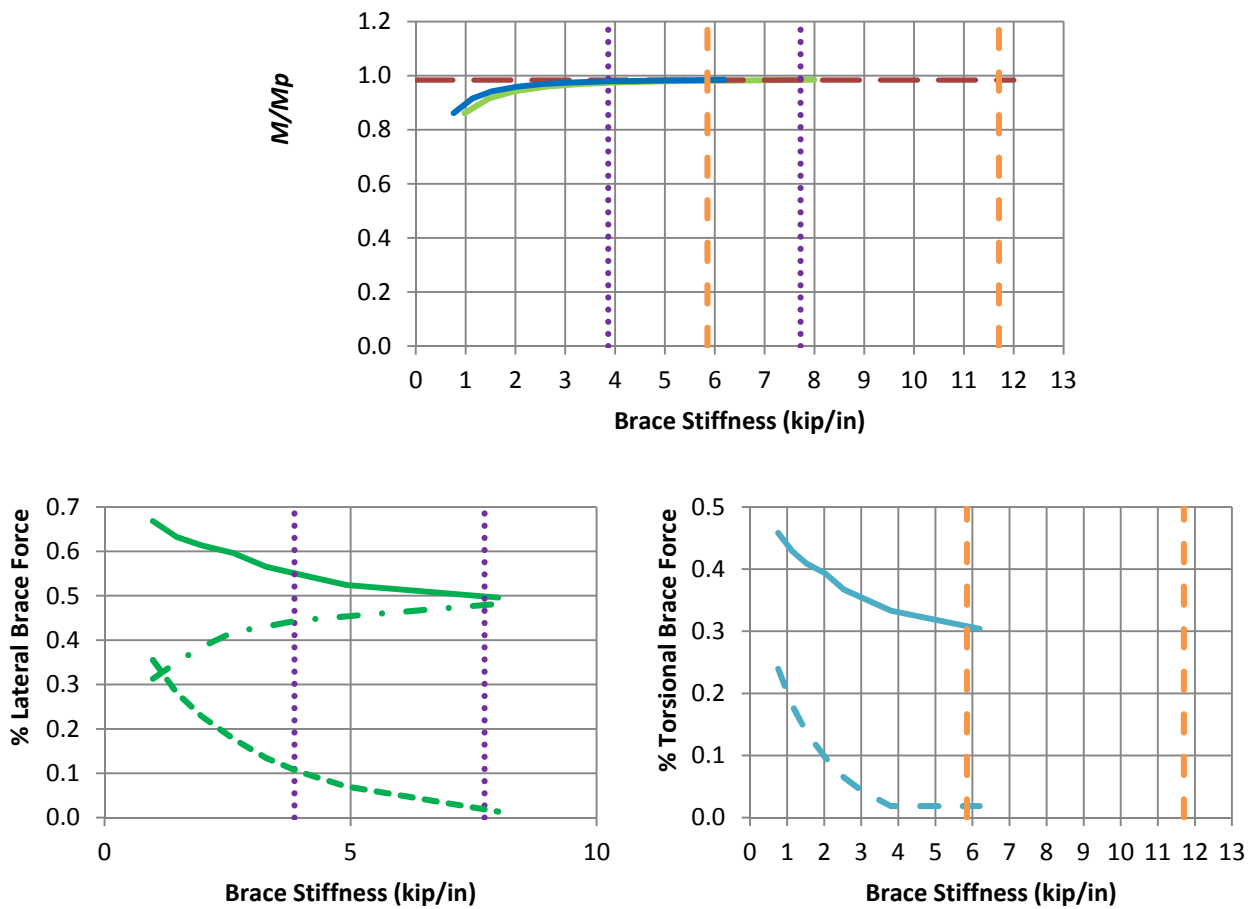
Fig. A.4 (continued). Beam knuckle curves and brace force vs. brace stiffness plots for combined point (nodal) lateral and torsional bracing cases with $n = 1$, Moment Gradient 1 loading with lateral bracing on the flange in flexural tension, and $L_b = 15$ ft.



a) B_MG1p_CRTB_n2_Lb5_TLBSR4

- Rigidly-braced strength
- Test simulation results corresponding to torsional brace
- Test simulation results corresponding to lateral brace
- 1x and 0.5x lateral bracing stiffness from Eq. (4-1)
- - - 1x and 0.5x torsional bracing stiffness from Eq. (4-5)
- Left end panel shear force
- - - Right end panel shear force
- . - Middle panel shear force
- Torsional brace force 1
- - - Torsional brace force 2

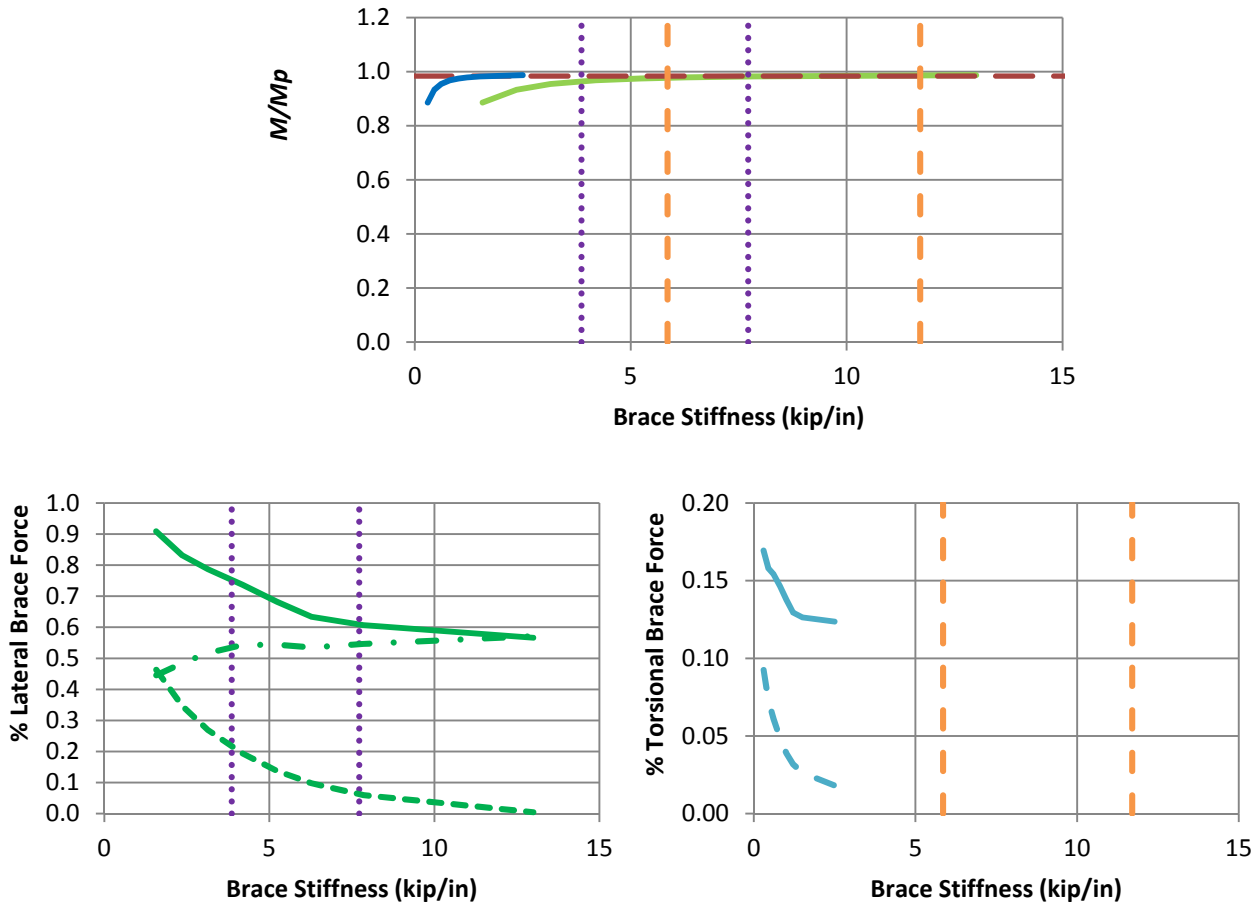
Figure A.5. Beam knuckle curves and brace force vs. brace stiffness plots for combined shear panel (relative) lateral and point torsional bracing cases with $n = 2$, Moment Gradient 1 loading with lateral bracing on the flange in flexural compression, and $L_b = 5$ ft.



b) B_MG1p_CRTB_n2_Lb5_TLBSR1

- Rigidly-braced strength
- Test simulation results corresponding to torsional brace
- Test simulation results corresponding to lateral brace
- ⋯ 1x and 0.5x lateral bracing stiffness from Eq. (4-1)
- 1x and 0.5x torsional bracing stiffness from Eq. (4-5)
- Left end panel shear force
- Right end panel shear force
- Middle panel shear force
- Torsional brace force 1
- Torsional brace force 2

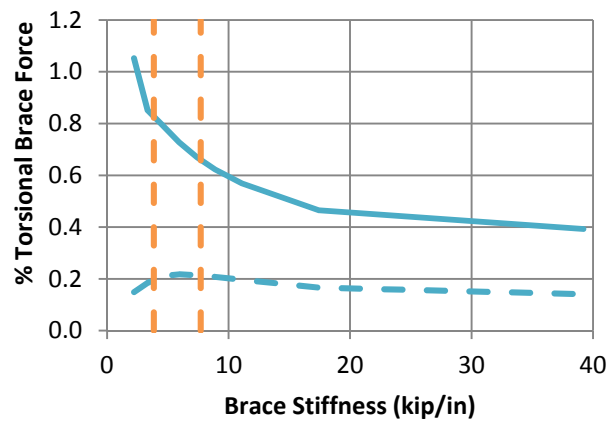
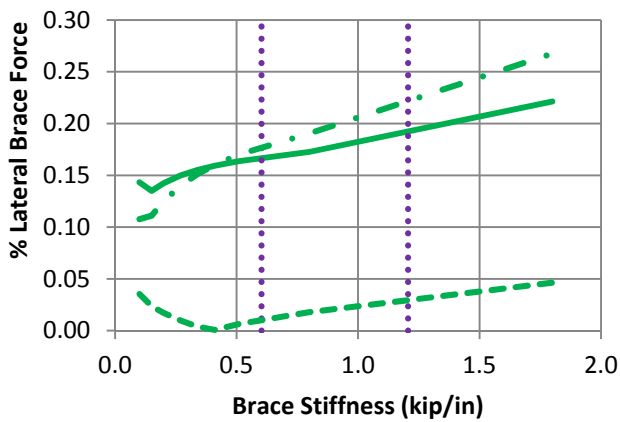
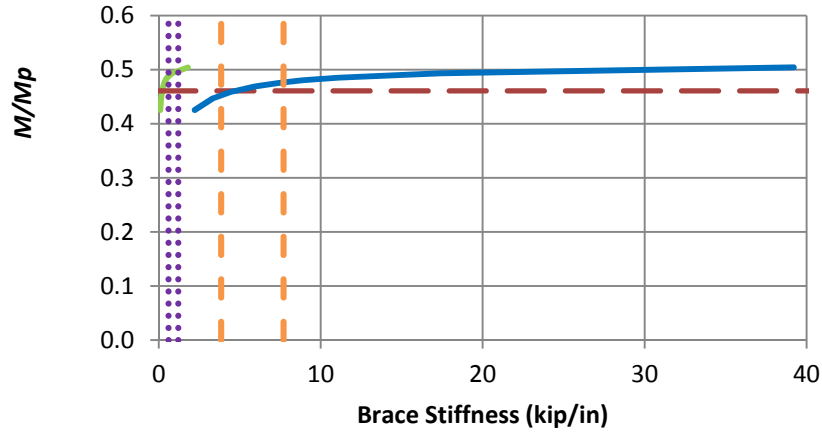
Fig. A.5 (continued). Beam knuckle curves and brace force vs. brace stiffness plots for combined shear panel (relative) lateral and point torsional bracing cases with $n = 2$, Moment Gradient 1 loading with lateral bracing on the flange in flexural compression, and $L_b = 5$ ft.



c) B_MG1p_CRTB_n2_Lb5_TLBSR0.25

- Rigidly-braced strength
- Test simulation results corresponding to torsional brace
- Test simulation results corresponding to lateral brace
- ⋯ 1x and 0.5x lateral bracing stiffness from Eq. (4-1)
- 1x and 0.5x torsional bracing stiffness from Eq. (4-5)
- Left end panel shear force
- Right end panel shear force
- Middle panel shear force
- Torsional brace force 1
- Torsional brace force 2

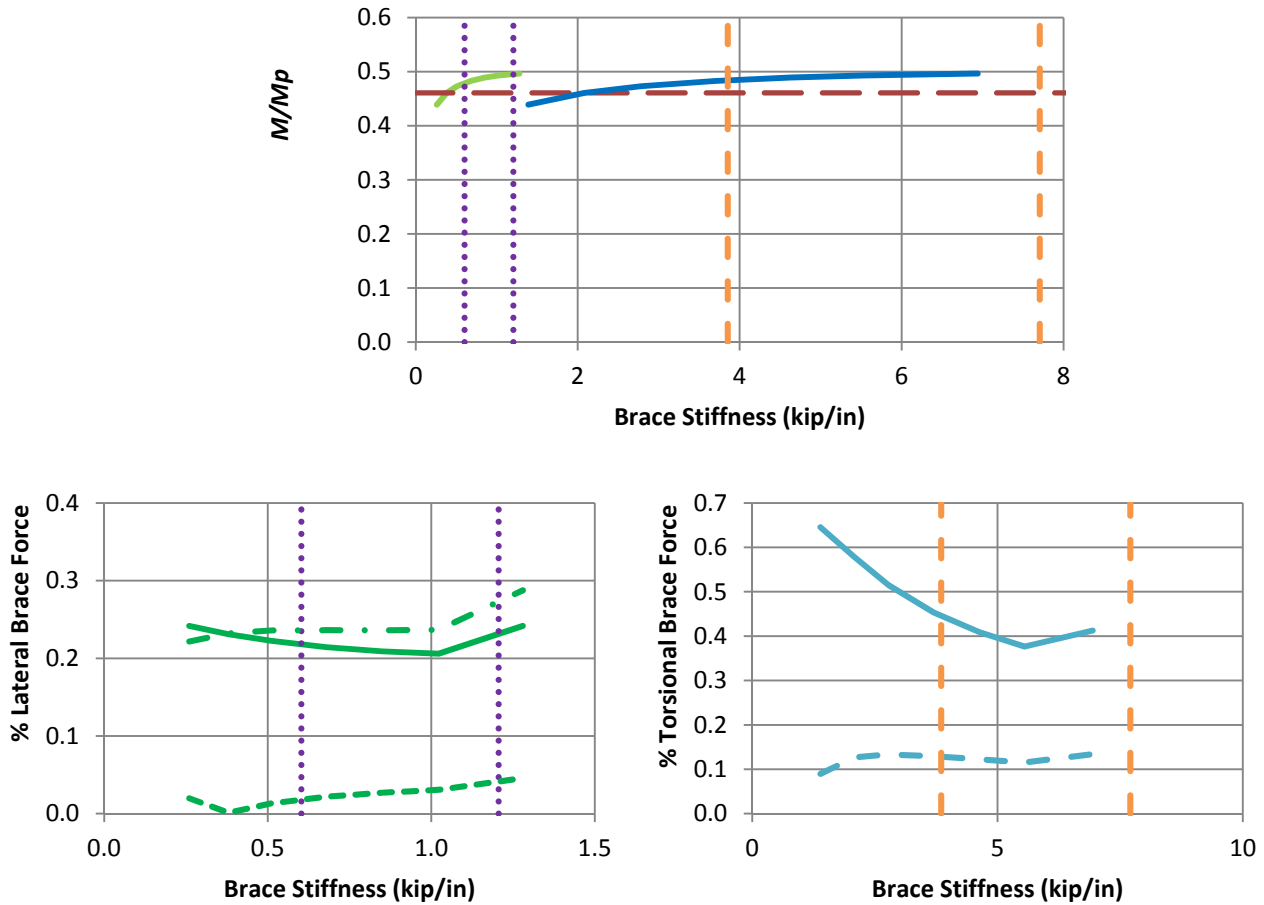
Fig. A.5 (continued). Beam knuckle curves and brace force vs. brace stiffness plots for combined shear panel (relative) lateral and point torsional bracing cases with $n = 2$, Moment Gradient 1 loading with lateral bracing on the flange in flexural compression, and $L_b = 5$ ft.



a) B_MG1p_CRTB_n2_Lb15_TLBSR4

- Rigidly-braced strength
- Test simulation results corresponding to torsional brace
- Test simulation results corresponding to lateral brace
- ⋯ 1x and 0.5x lateral bracing stiffness from Eq. (4-1)
- 1x and 0.5x torsional bracing stiffness from Eq. (4-5)
- Left end panel shear force
- Right end panel shear force
- . - Middle panel shear force
- Torsional brace force 1
- Torsional brace force 2

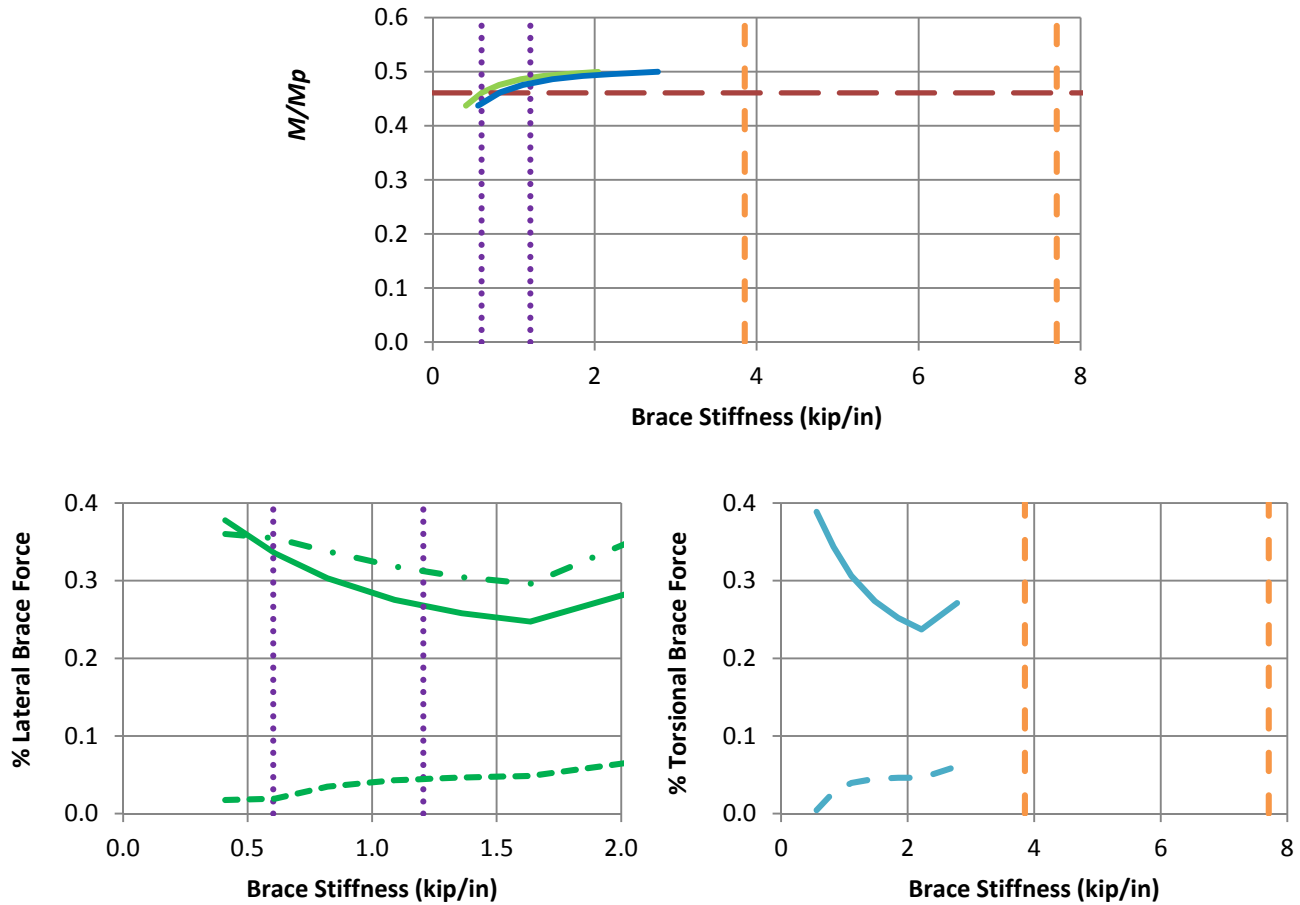
Figure A.6. Beam knuckle curves and brace force vs. brace stiffness plots for combined shear panel (relative) lateral and point torsional bracing cases with $n = 2$, Moment Gradient 1 loading with lateral bracing on the flange in flexural compression, and $L_b = 15$ ft.



b) B_MG1p_CRTB_n2_Lb15_TLBSR1

- Rigidly-braced strength
- Test simulation results corresponding to torsional brace
- Test simulation results corresponding to lateral brace
- ⋯ 1x and 0.5x lateral bracing stiffness from Eq. (4-1)
- 1x and 0.5x torsional bracing stiffness from Eq. (4-5)
- Left end panel shear force
- Right end panel shear force
- Middle panel shear force
- Torsional brace force 1
- Torsional brace force 2

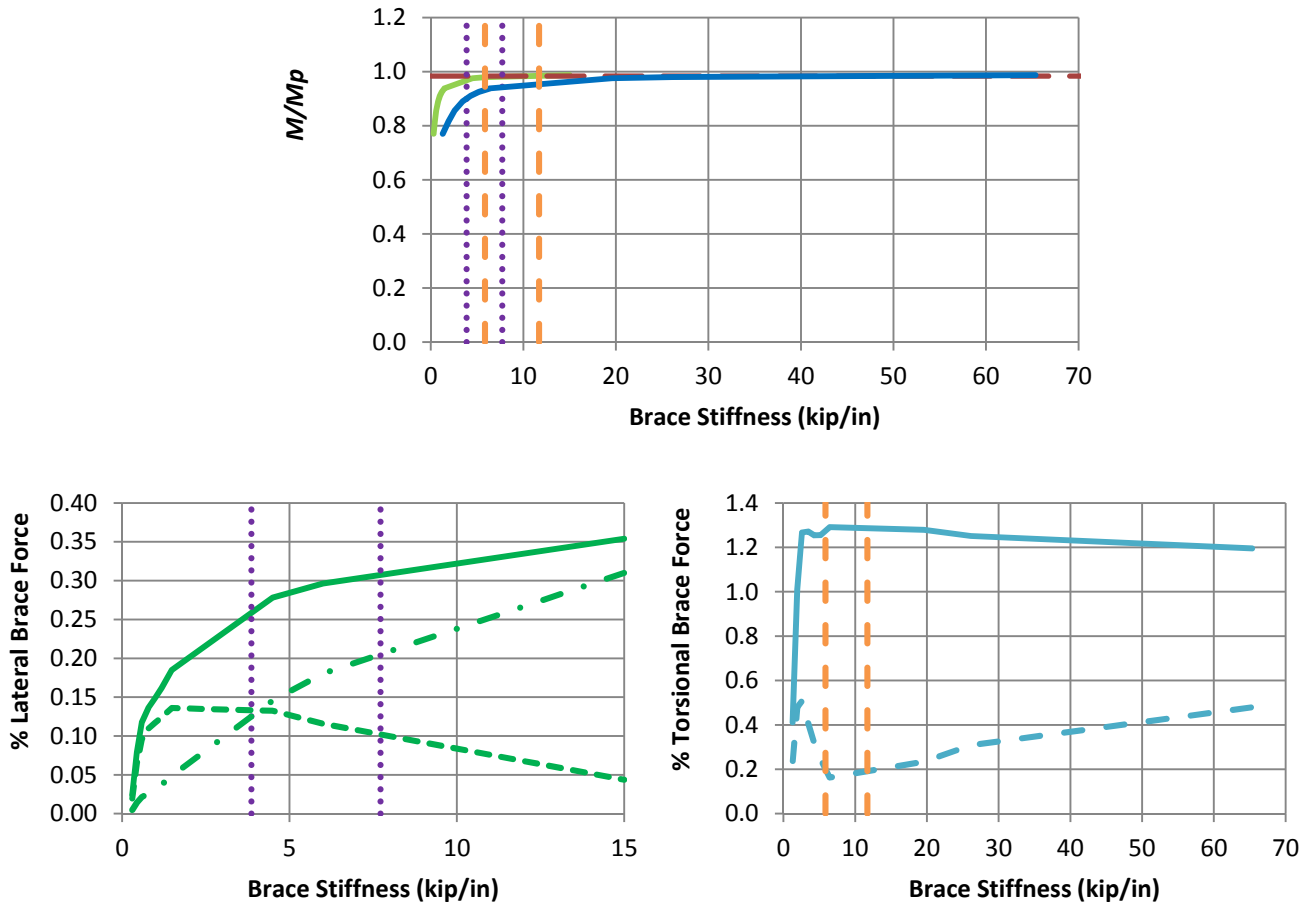
Fig. A.6 (continued). Beam knuckle curves and brace force vs. brace stiffness plots for combined shear panel (relative) lateral and point torsional bracing cases with $n = 2$, Moment Gradient 1 loading with lateral bracing on the flange in flexural compression, and $L_b = 15$ ft.



c) B_MG1p_CRTB_n2_Lb15_TLBSR0.25

- Rigidly-braced strength
- Test simulation results corresponding to torsional brace
- Test simulation results corresponding to lateral brace
- ⋯ 1x and 0.5x lateral bracing stiffness from Eq. (4-1)
- - - 1x and 0.5x torsional bracing stiffness from Eq. (4-5)
- Left end panel shear force
- - - Right end panel shear force
- . - Middle panel shear force
- Torsional brace force 1
- - - Torsional brace force 2

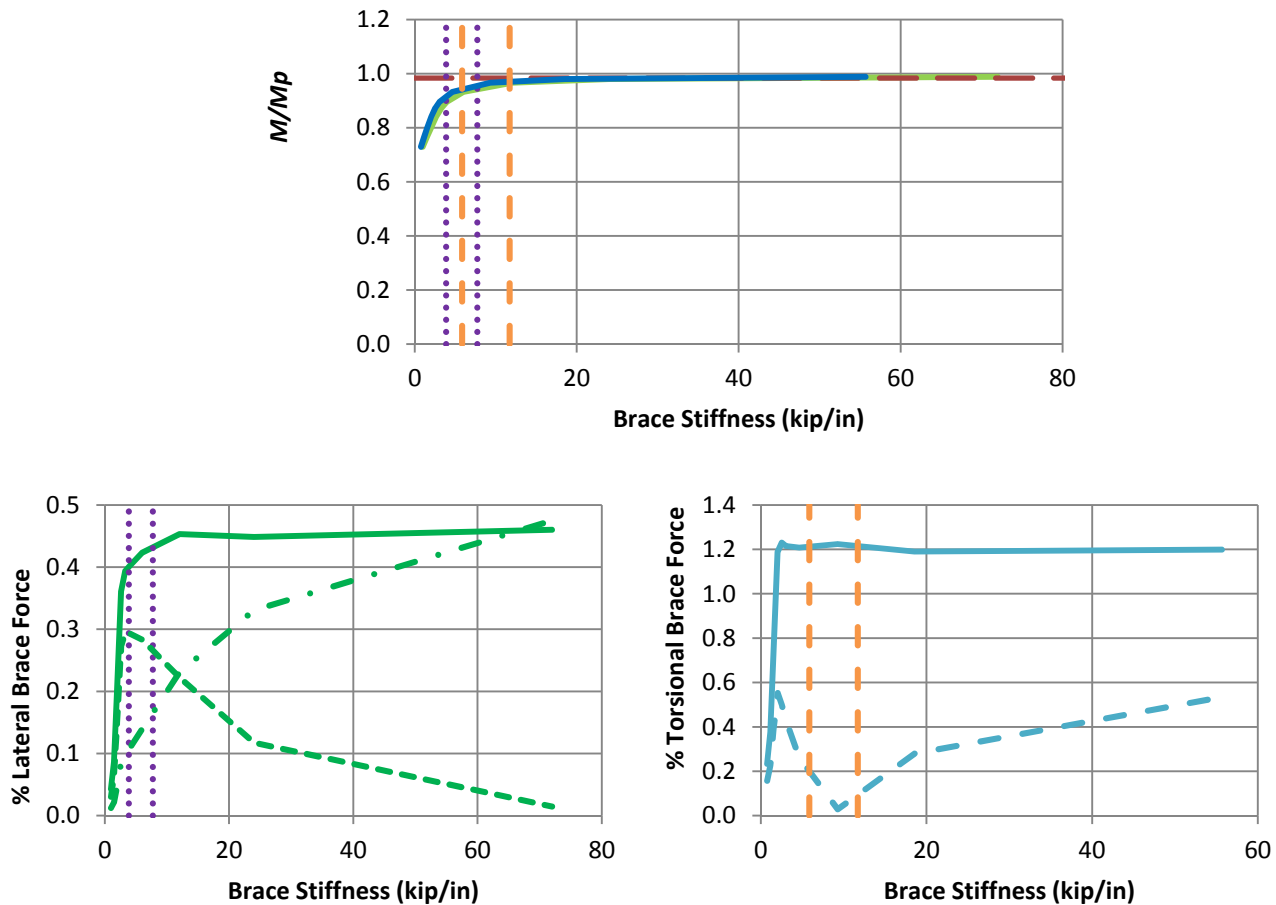
Fig. A.6 (continued). Beam knuckle curves and brace force vs. brace stiffness plots for combined shear panel (relative) lateral and point torsional bracing cases with $n = 2$, Moment Gradient 1 loading with lateral bracing on the flange in flexural compression, and $L_b = 15$ ft.



a) B_MG1n_CRTB_n2_Lb5_TLBSR5.67

- Rigidly-braced strength
- Test simulation results corresponding to torsional brace
- Test simulation results corresponding to lateral brace
- 1x and 0.5x lateral bracing stiffness from Eq. (4-1)
- - - 1x and 0.5x torsional bracing stiffness from Eq. (4-5)
- Left end panel shear force
- - - Right end panel shear force
- . - Middle panel shear force
- Torsional brace force 1
- Torsional brace force 2

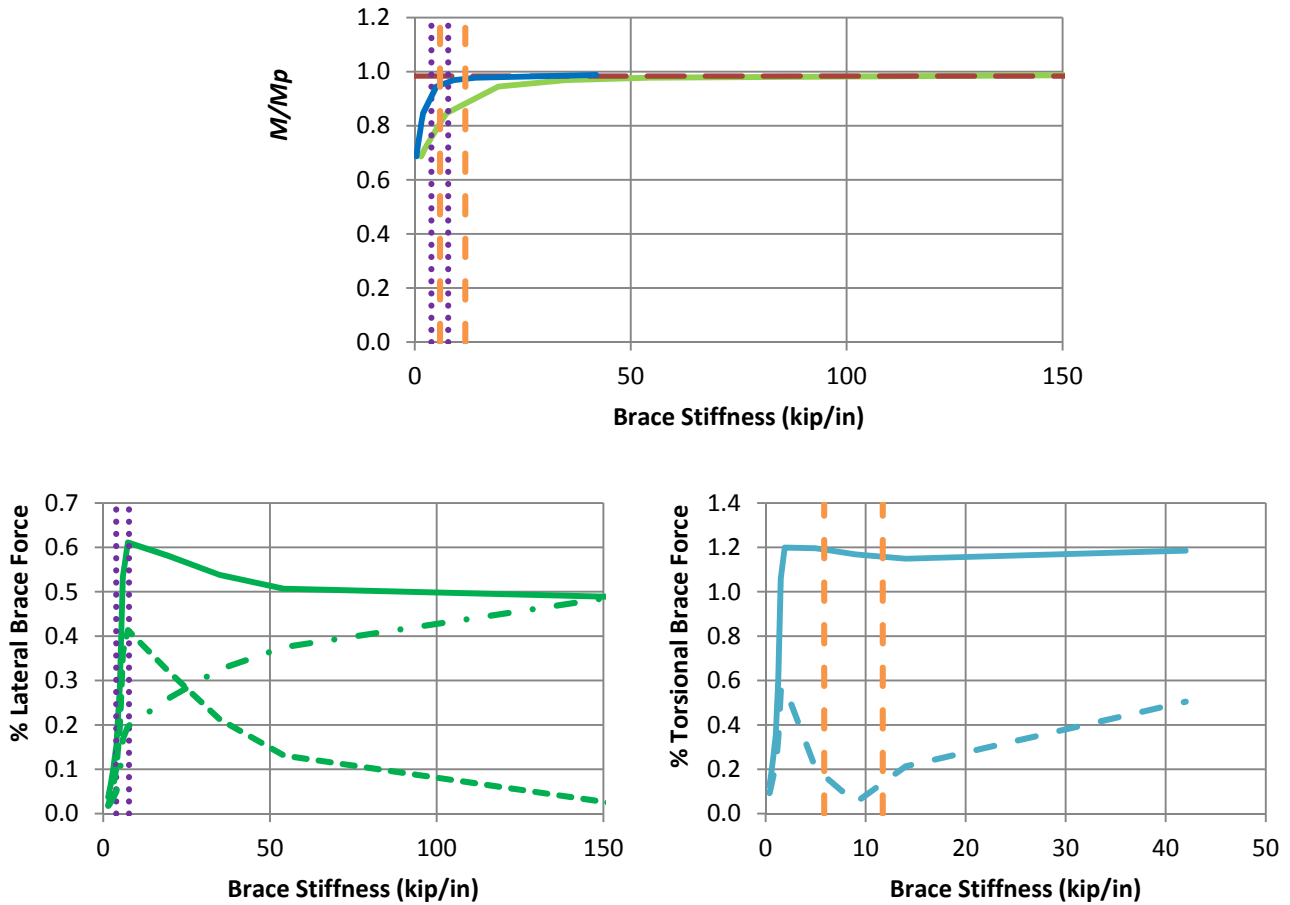
Figure A.7. Beam knuckle curves and brace force vs. brace stiffness plots for combined shear panel (relative) lateral and point torsional bracing cases with $n = 2$, Moment Gradient 1 loading with lateral bracing on the flange in flexural tension, and $L_b = 5$ ft.



b) B_MG1n_CRTB_n2_Lb5_TLBSR1

- Rigidly-braced strength
- Test simulation results corresponding to torsional brace
- Test simulation results corresponding to lateral brace
- 1x and 0.5x lateral bracing stiffness from Eq. (4-1)
- - - 1x and 0.5x torsional bracing stiffness from Eq. (4-5)
- Left end panel shear force
- - - Right end panel shear force
- . - Middle panel shear force
- Torsional brace force 1
- - - Torsional brace force 2

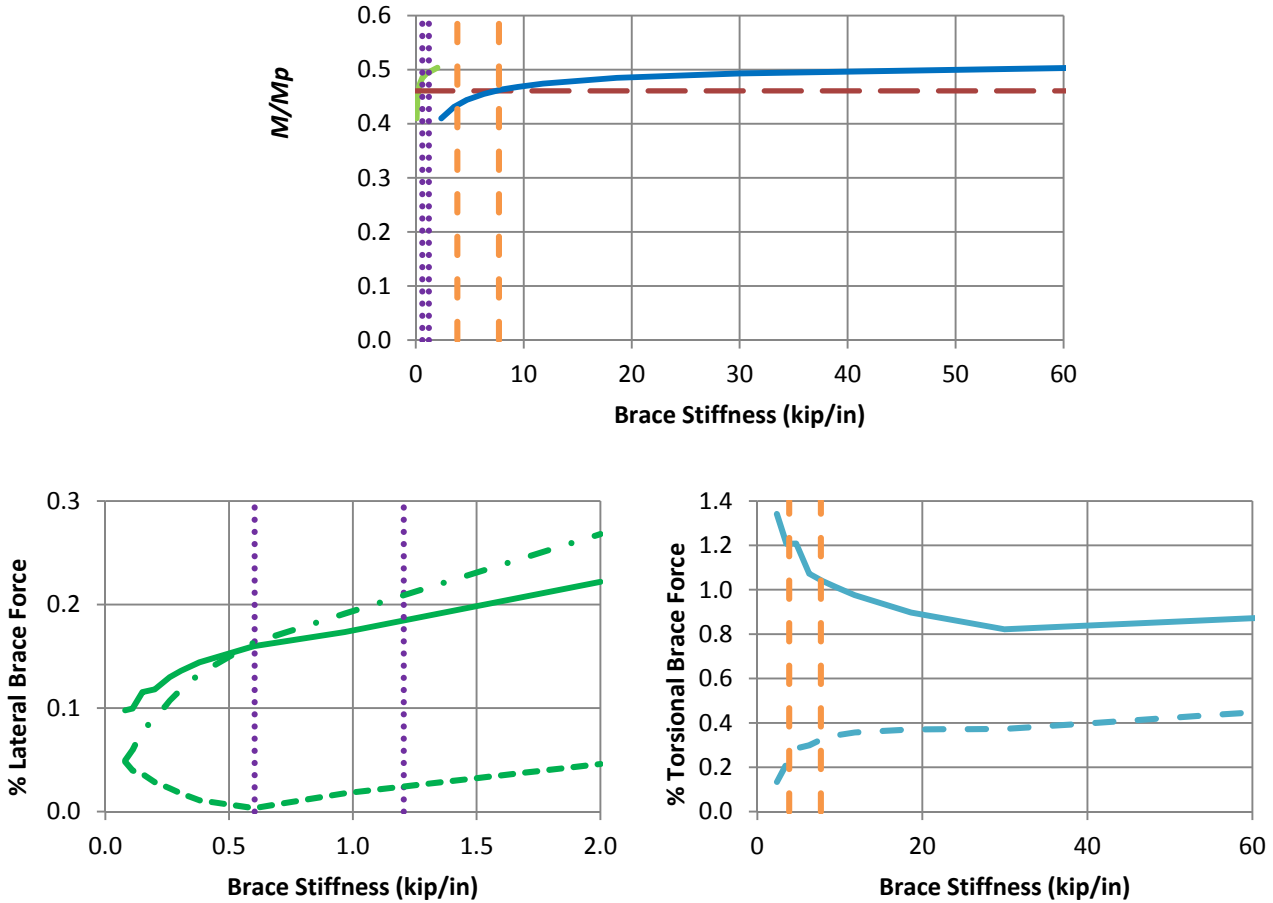
Fig. A.7 (continued). Beam knuckle curves and brace force vs. brace stiffness plots for combined shear panel (relative) lateral and point torsional bracing cases with $n = 2$, Moment Gradient 1 loading with lateral bracing on the flange in flexural tension, and $L_b = 5$ ft.



c) B_MG1n_CRTB_n2_Lb5_TLBSR0.33

- Rigidly-braced strength
- Test simulation results corresponding to torsional brace
- Test simulation results corresponding to lateral brace
- 1x and 0.5x lateral bracing stiffness from Eq. (4-1)
- - - 1x and 0.5x torsional bracing stiffness from Eq. (4-5)
- Left end panel shear force
- - - Right end panel shear force
- . - Middle panel shear force
- Torsional brace force 1
- - - Torsional brace force 2

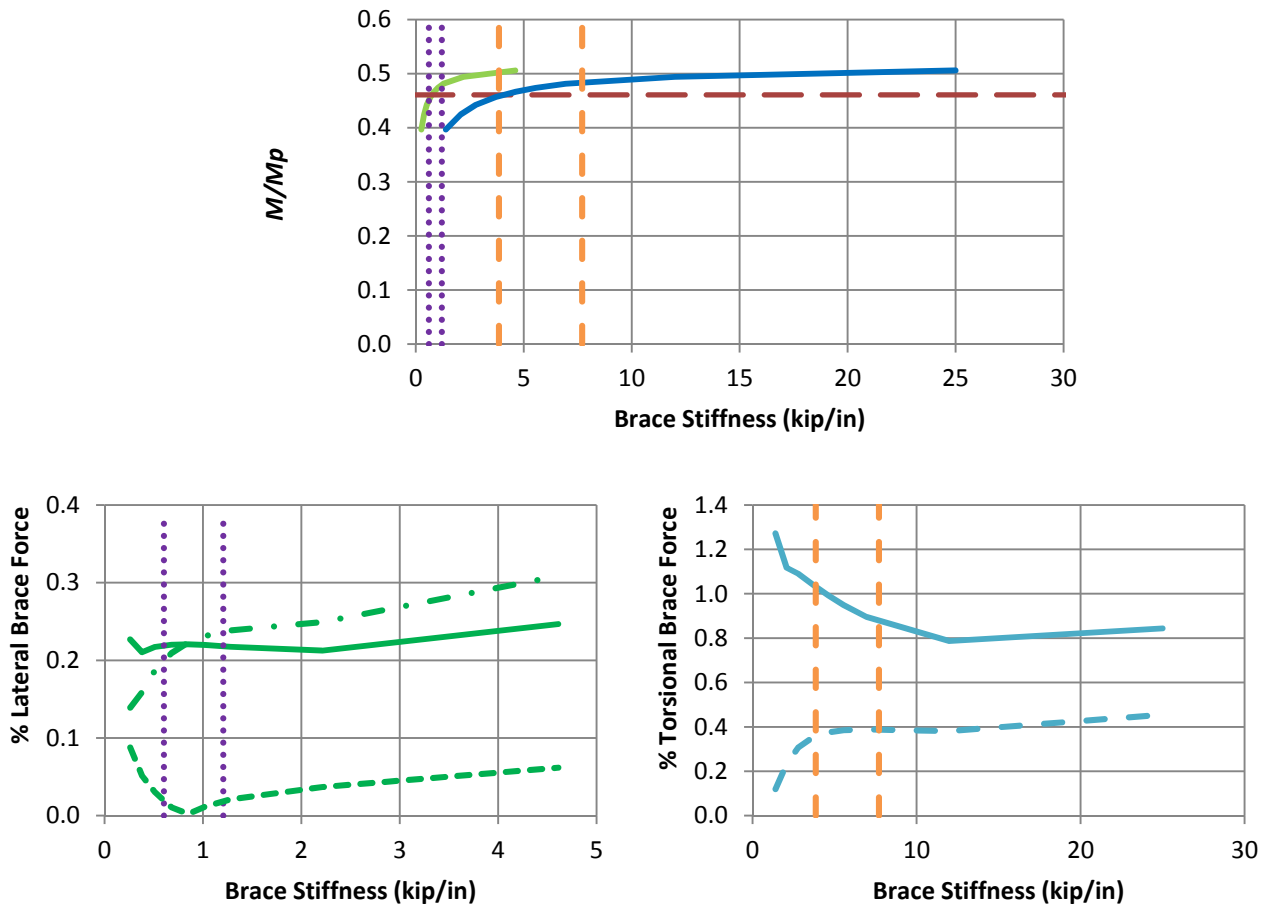
Fig. A.7 (continued). Beam knuckle curves and brace force vs. brace stiffness plots for combined shear panel (relative) lateral and point torsional bracing cases with $n = 2$, Moment Gradient 1 loading with lateral bracing on the flange in flexural tension, and $L_b = 5$ ft.



a) B_MG1n_CRTB_n2_Lb15_TLBSR5.67

- Rigidly-braced strength
- Test simulation results corresponding to torsional brace
- Test simulation results corresponding to lateral brace
- ⋯ 1x and 0.5x lateral bracing stiffness from Eq. (4-1)
- 1x and 0.5x torsional bracing stiffness from Eq. (4-5)
- Left end panel shear force
- Right end panel shear force
- · - Middle panel shear force
- Torsional brace force 1
- Torsional brace force 2

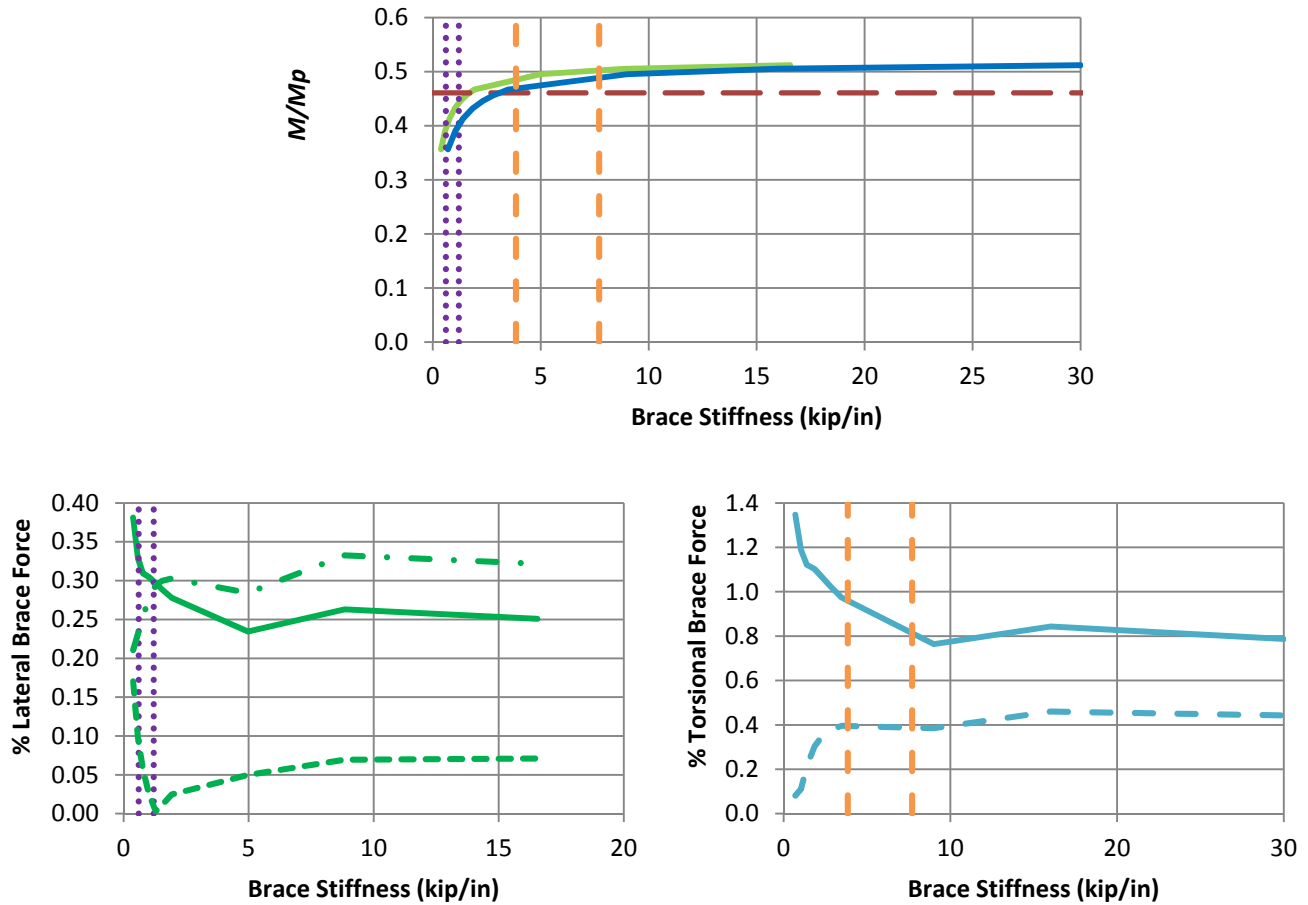
Figure A.8. Beam knuckle curves and brace force vs. brace stiffness plots for combined shear panel (relative) lateral and point torsional bracing cases with $n = 2$, Moment Gradient 1 loading with lateral bracing on the flange in flexural tension, and $L_b = 15$ ft.



b) B_MG1n_CRTB_n2_Lb15_TLBSR1

- Rigidly-braced strength
- Test simulation results corresponding to torsional brace
- Test simulation results corresponding to lateral brace
- 1x and 0.5x lateral bracing stiffness from Eq. (4-1)
- - - 1x and 0.5x torsional bracing stiffness from Eq. (4-5)
- Left end panel shear force
- - - Right end panel shear force
- . - Middle panel shear force
- Torsional brace force 1
- Torsional brace force 2

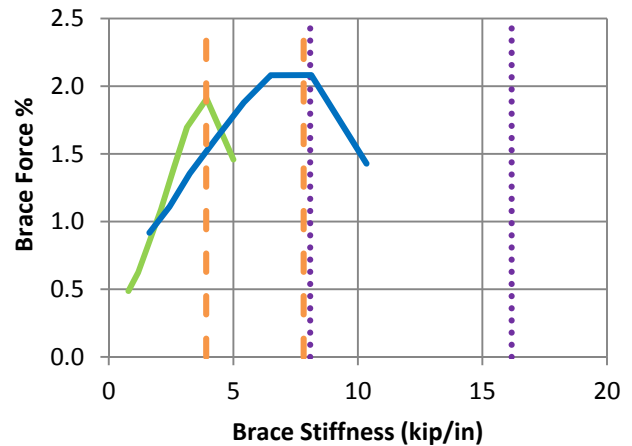
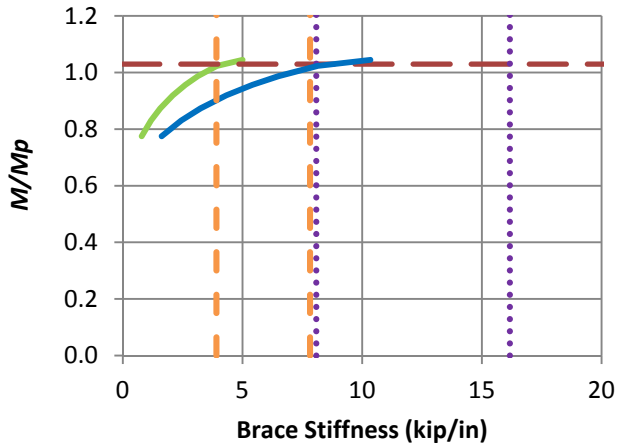
Fig. A.8 (continued). Beam knuckle curves and brace force vs. brace stiffness plots for combined shear panel (relative) lateral and point torsional bracing cases with $n = 2$, Moment Gradient 1 loading with lateral bracing on the flange in flexural tension, and $L_b = 15$ ft.



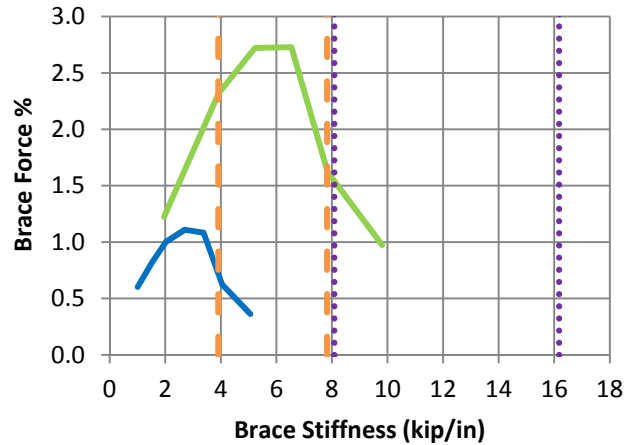
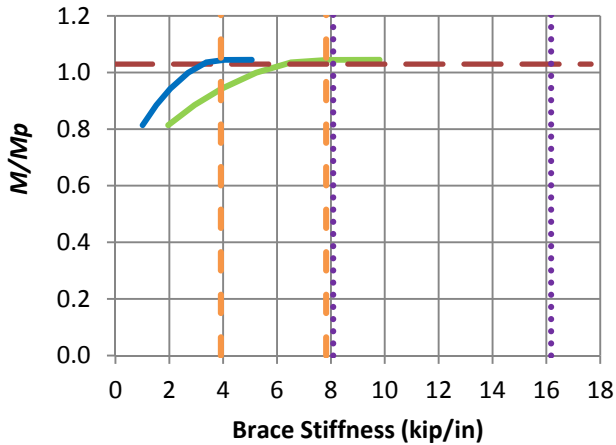
c) B_MG1n_CRTB_n2_Lb15_TLBSR0.33

- Rigidly-braced strength
- Test simulation results corresponding to torsional brace
- Test simulation results corresponding to lateral brace
- 1x and 0.5x lateral bracing stiffness from Eq. (4-1)
- 1x and 0.5x torsional bracing stiffness from Eq. (4-5)
- Left end panel shear force
- Right end panel shear force
- Middle panel shear force
- Torsional brace force 1
- Torsional brace force 2

Fig. A.8 (continued). Beam knuckle curves and brace force vs. brace stiffness plots for combined shear panel (relative) lateral and point torsional bracing cases with $n = 2$, Moment Gradient 1 loading with lateral bracing on the flange in flexural tension, and $L_b = 15$ ft.



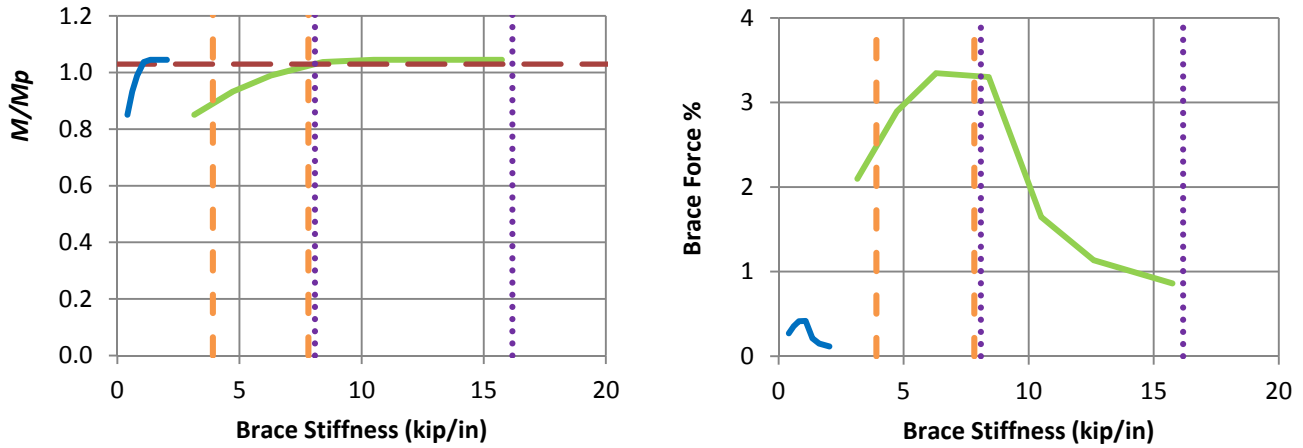
a) B_MG2pc_CNTB_n1_Lb5_TLBSR4



b) B_MG2pc_CNTB_n1_Lb5_TLBSR1

- Rigidly-braced strength
- Test simulation results corresponding to torsional brace
- Test simulation results corresponding to lateral brace
- 1x and 0.5x lateral bracing stiffness from Eq. C-A-6-5, AISC 360-10, with $C_b P_f$ taken equal to M_{max}/h_o
- 1x and 0.5x torsional bracing stiffness equal to (β_{Tbr} / h_o^2) , where β_{Tbr} is given in Eq. 4-1

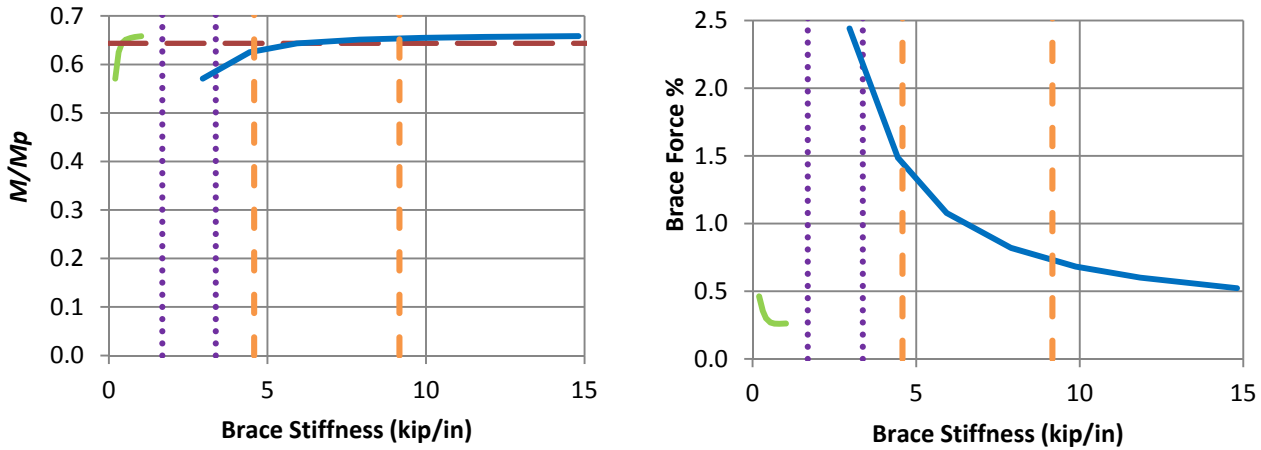
Figure A.9. Beam knuckle curves and brace force vs. brace stiffness plots for combined point (nodal) lateral and torsional bracing cases with $n = 1$, Moment Gradient 2 loading with lateral bracing on the flange in flexural compression, intermediate transverse load applied at centroid of the mid-span cross-section, and $L_b = 5$ ft.



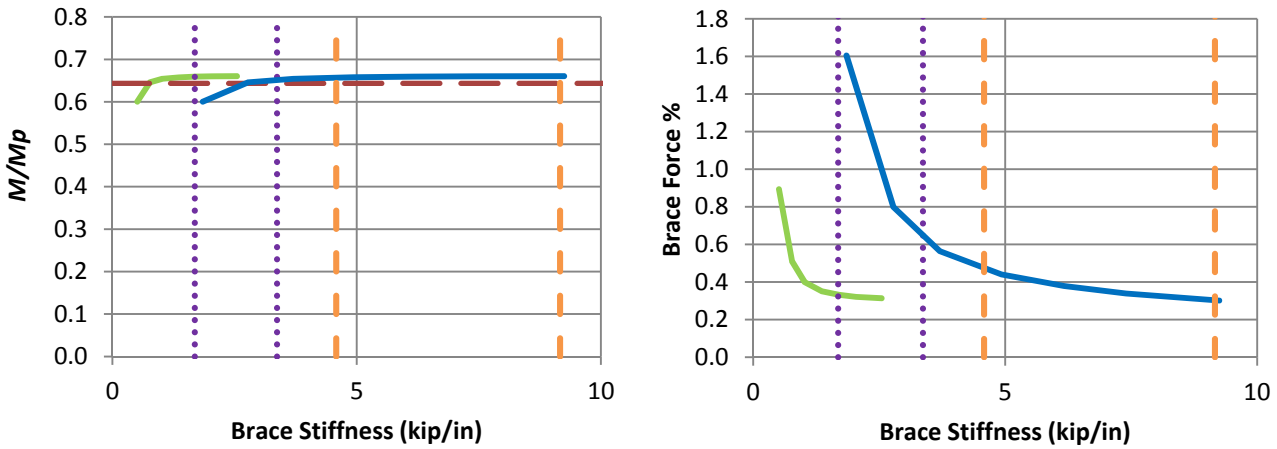
c) B_MG2pc_CNTB_n1_Lb5_TLBSR0.25

- Rigidly-braced strength
- Test simulation results corresponding to torsional brace
- Test simulation results corresponding to lateral brace
- 1x and 0.5x lateral bracing stiffness from Eq. (4-1)
- 1x and 0.5x torsional bracing stiffness from Eq. (4-5)

Fig. A.9 (continued). Beam knuckle curves and brace force vs. brace stiffness plots for combined point (nodal) lateral and torsional bracing cases with $n = 1$, Moment Gradient 2 loading with lateral bracing on the flange in flexural compression, intermediate transverse load applied at centroid of the mid-span cross-section, and $L_b = 5$ ft.



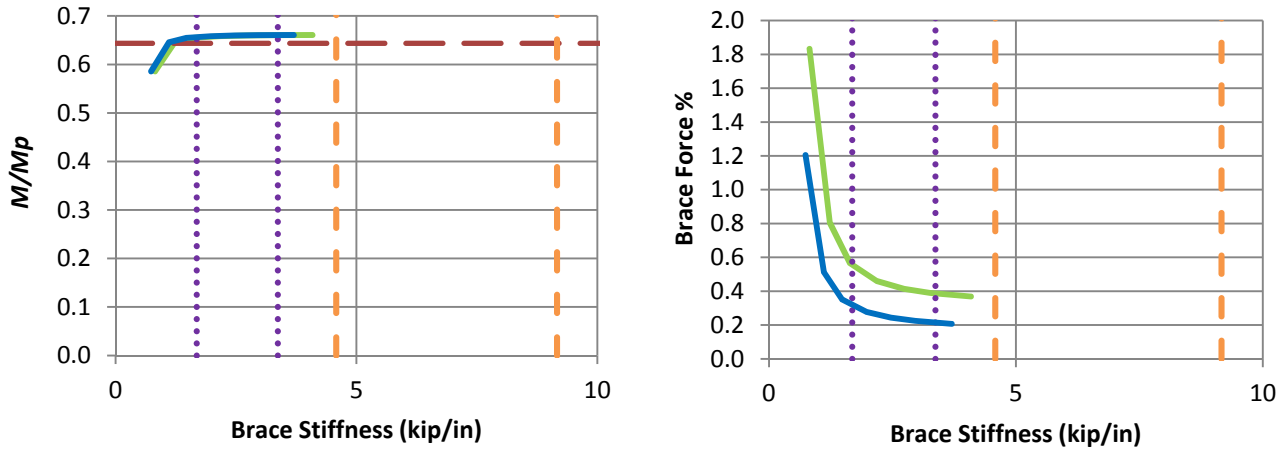
a) B_MG2pc_CNTB_n1_Lb15_TLBSR4



b) B_MG2pc_CNTB_n1_Lb15_TLBSR1

- Rigidly-braced strength
- Test simulation results corresponding to torsional brace
- Test simulation results corresponding to lateral brace
- 1x and 0.5x lateral bracing stiffness from Eq. (4-1)
- - - 1x and 0.5x torsional bracing stiffness from Eq. (4-5)

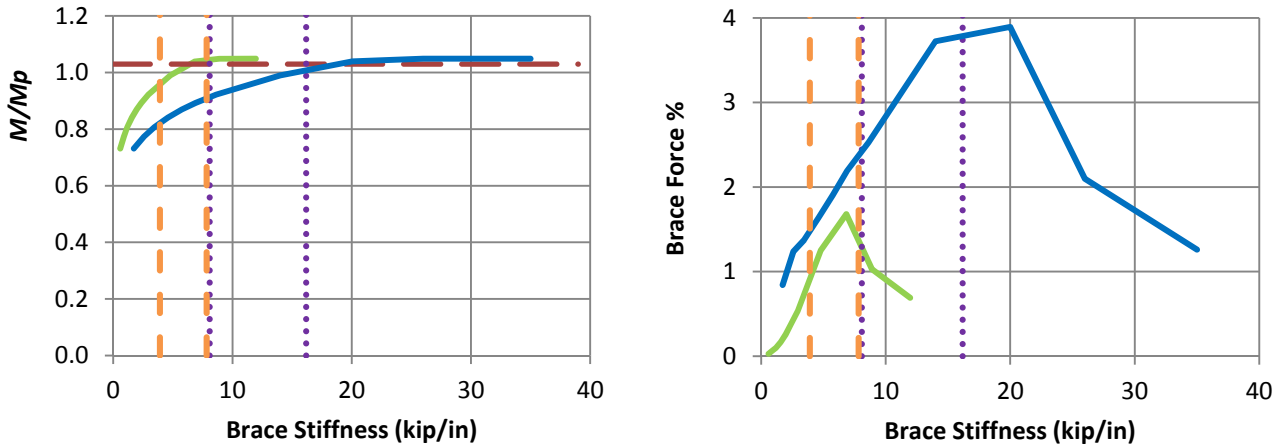
Figure A.10. Beam knuckle curves and brace force vs. brace stiffness plots for combined point (nodal) lateral and torsional bracing cases with $n = 1$, Moment Gradient 2 loading with lateral bracing on the flange in flexural compression, intermediate transverse load applied at centroid of the mid-span cross-section, and $L_b = 15$ ft.



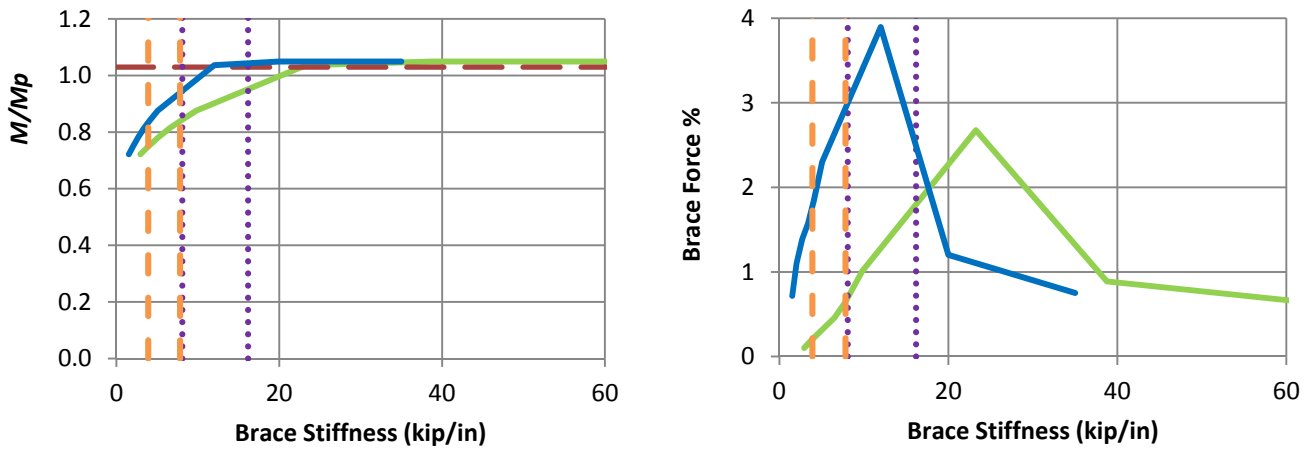
c) B_MG2pc_CNTB_n1_Lb15_TLBSR0.25

- Rigidly-braced strength
- Test simulation results corresponding to torsional brace
- Test simulation results corresponding to lateral brace
- 1x and 0.5x lateral bracing stiffness from Eq. (4-1)
- 1x and 0.5x torsional bracing stiffness from Eq. (4-5)

Fig. A.10 (continued). Beam knuckle curves and brace force vs. brace stiffness plots for combined point (nodal) lateral and torsional bracing cases with $n = 1$, Moment Gradient 2 loading with lateral bracing on the flange in flexural compression, intermediate transverse load applied at centroid of the mid-span cross-section, and $L_b = 15$ ft.



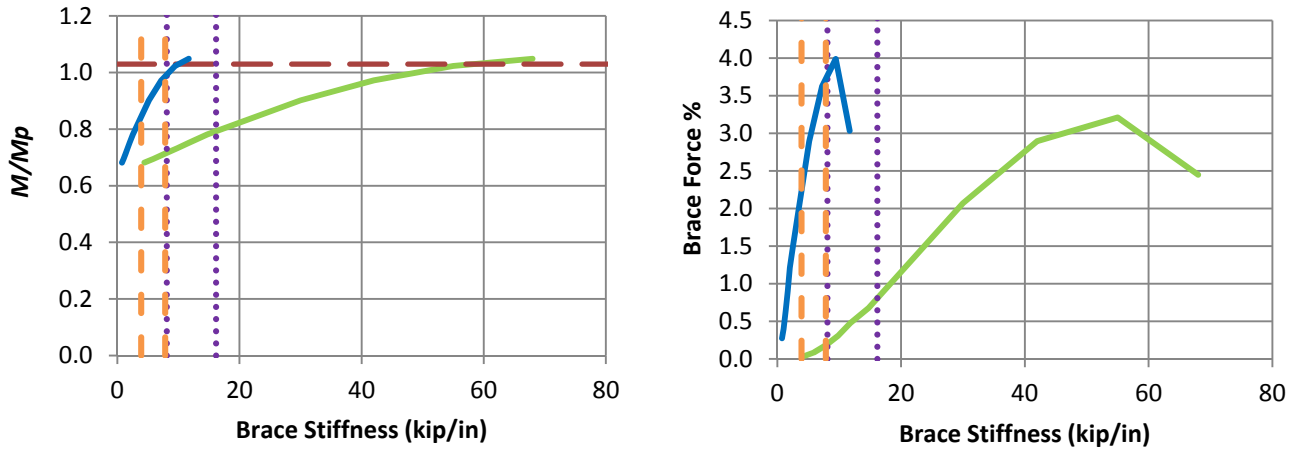
a) B_MG2nc_CNTB_n1_Lb5_TLBSR5.67



b) B_MG2nc_CNTB_n1_Lb5_TLBSR1

- Rigidly-braced strength
- Test simulation results corresponding to torsional brace
- Test simulation results corresponding to lateral brace
- 1x and 0.5x lateral bracing stiffness from Eq. (4-1)
- - - 1x and 0.5x torsional bracing stiffness from Eq. (4-5)

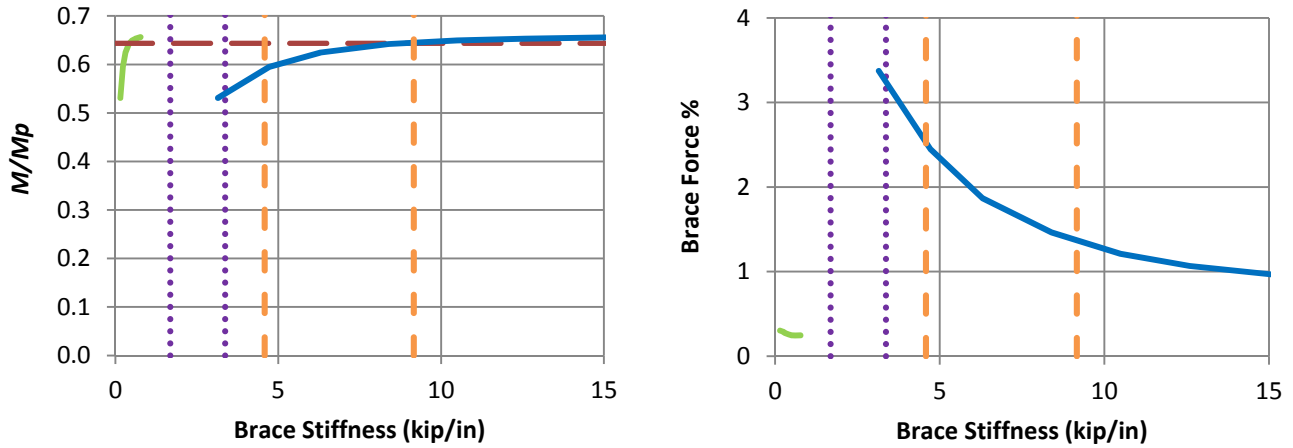
Figure A.11. Beam knuckle curves and brace force vs. brace stiffness plots for combined point (nodal) lateral and torsional bracing cases with $n = 1$, Moment Gradient 2 loading with lateral bracing on the flange in flexural tension, intermediate transverse load applied at centroid of the mid-span cross-section, and $L_b = 5$ ft.



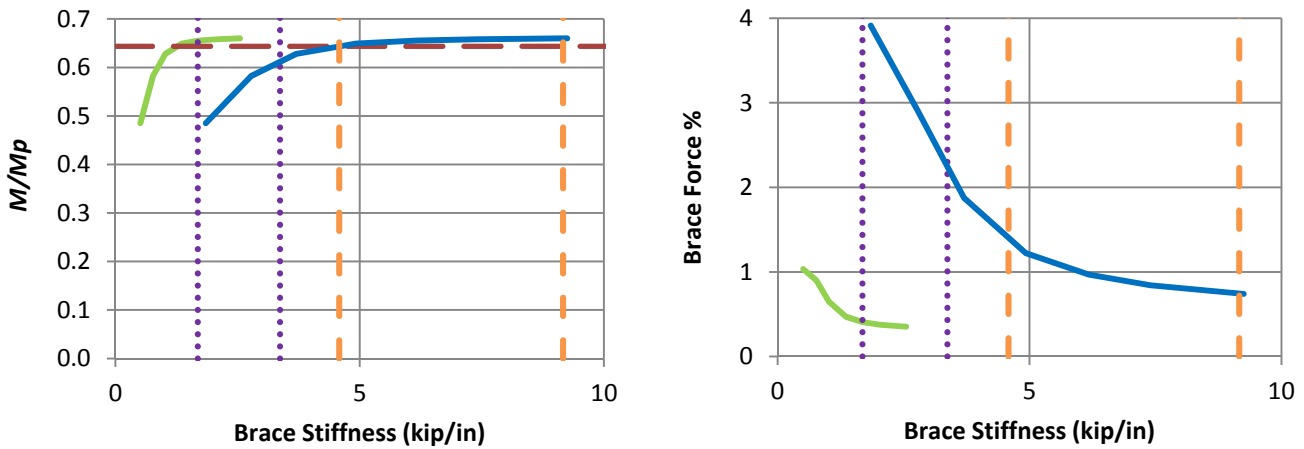
c) B_MG2nc_CNTB_n1_Lb5_TLBSR0.33

- — Rigidly-braced strength
- Test simulation results corresponding to torsional brace
- Test simulation results corresponding to lateral brace
- ⋯⋯⋯ 1x and 0.5x lateral bracing stiffness from Eq. (4-1)
- — 1x and 0.5x torsional bracing stiffness from Eq. (4-5)

Fig. A.11 (continued). Beam knuckle curves and brace force vs. brace stiffness plots for combined point (nodal) lateral and torsional bracing cases with $n = 1$, Moment Gradient 2 loading with lateral bracing on the flange in flexural tension, intermediate transverse load applied at centroid of the mid-span cross-section, and $L_b = 5$ ft.



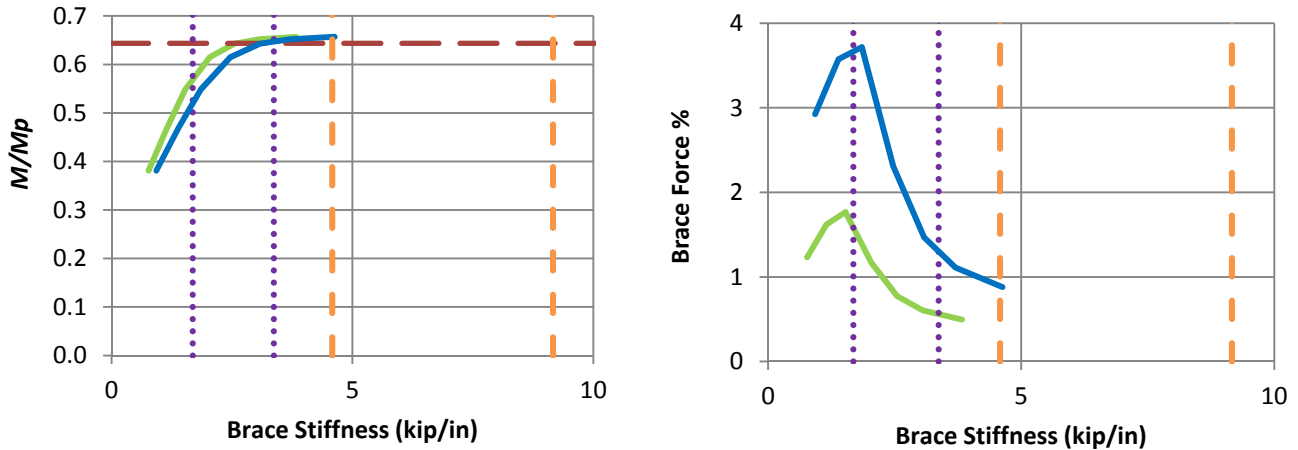
a) B_MG2nc_CNTB_n1_Lb15_TLBSR5.67



b) B_MG2nc_CNTB_n1_Lb15_TLBSR1

- Rigidly-braced strength
- Test simulation results corresponding to torsional brace
- Test simulation results corresponding to lateral brace
- 1x and 0.5x lateral bracing stiffness from Eq. (4-1)
- - - 1x and 0.5x torsional bracing stiffness from Eq. (4-5)

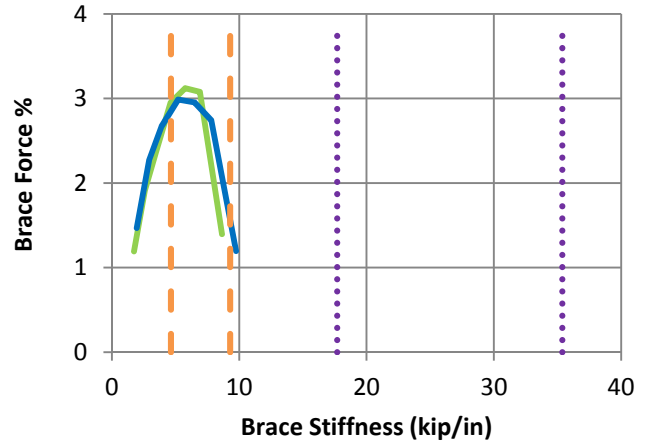
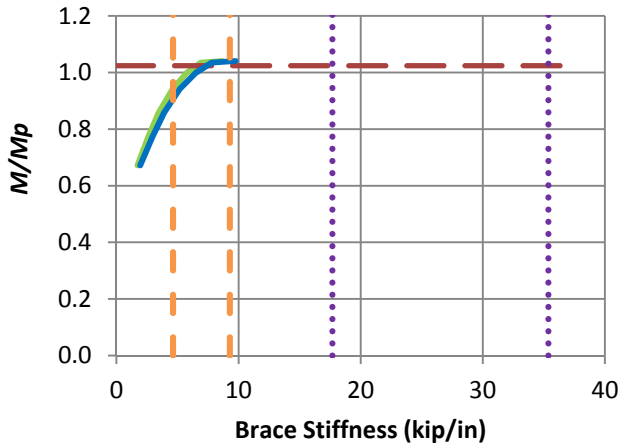
Figure A.12. Beam knuckle curves and brace force vs. brace stiffness plots for combined point (nodal) lateral and torsional bracing cases with $n = 1$, Moment Gradient 2 loading with lateral bracing on the flange in flexural tension, intermediate transverse load applied at centroid of the mid-span cross-section, and $L_b = 15$ ft.



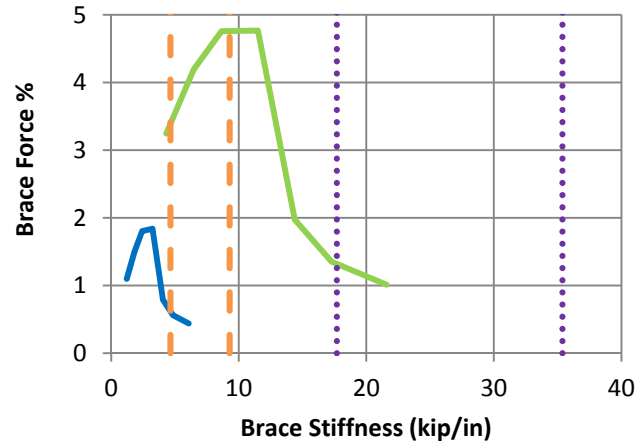
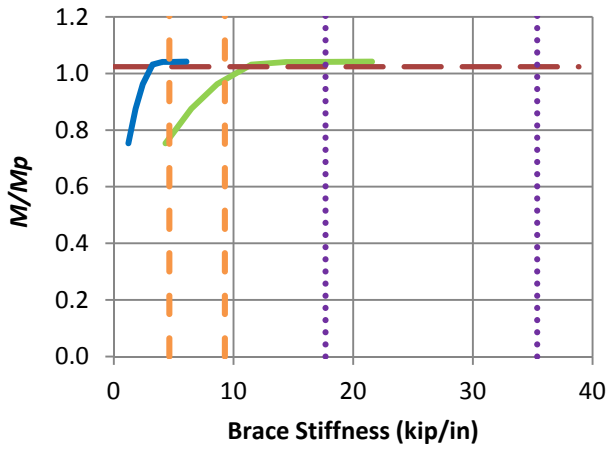
c) B_MG2nc_CNTB_n1_Lb15_TLBSR0.33

- Rigidly-braced strength
- Test simulation results corresponding to torsional brace
- Test simulation results corresponding to lateral brace
- 1x and 0.5x lateral bracing stiffness from Eq. (4-1)
- 1x and 0.5x torsional bracing stiffness from Eq. (4-5)

Fig. A.12 (continued). Beam knuckle curves and brace force vs. brace stiffness plots for combined point (nodal) lateral and torsional bracing cases with $n = 1$, Moment Gradient 2 loading with lateral bracing on the flange in flexural tension, intermediate transverse load applied at centroid of the mid-span cross-section, and $L_b = 15$ ft.



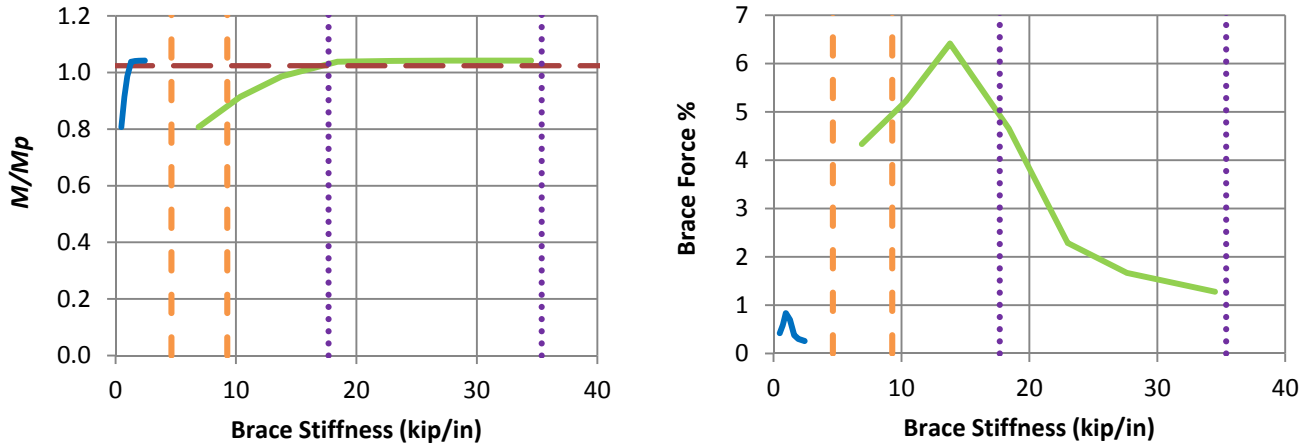
a) B_MG2pt_CNTB_n1_Lb5_TLBSR4



b) B_MG2pt_CNTB_n1_Lb5_TLBSR1

- Rigidly-braced strength
- Test simulation results corresponding to torsional brace
- Test simulation results corresponding to lateral brace
- 1x and 0.5x lateral bracing stiffness from Eq. (4-1)
- 1x and 0.5x torsional bracing stiffness from Eq. (4-5)

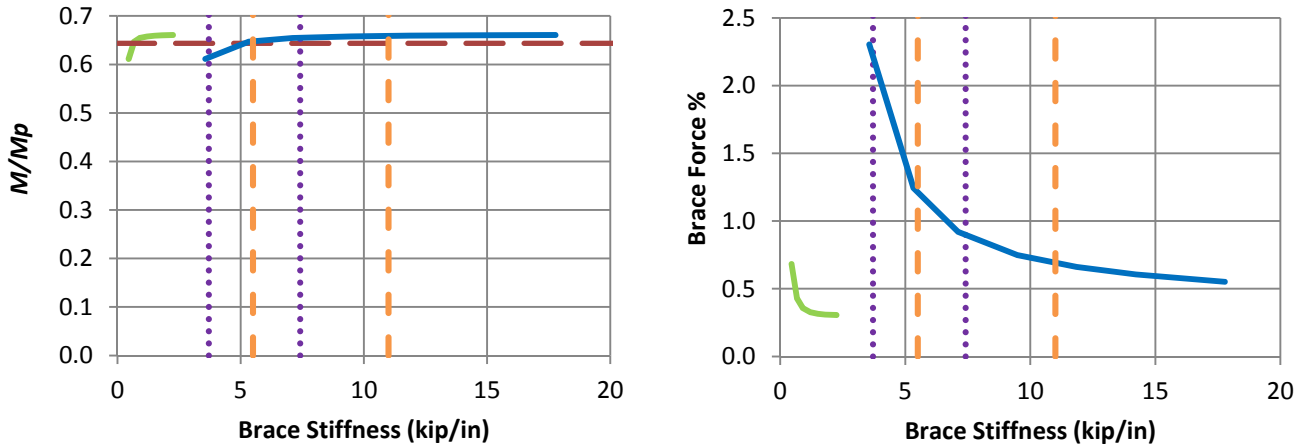
Figure A.13. Beam knuckle curves and brace force vs. brace stiffness plots for combined point (nodal) lateral and torsional bracing cases with $n = 1$, Moment Gradient 2 loading with lateral bracing on the flange in flexural compression, intermediate transverse load applied at top flange of the mid-span cross-section, and $L_b = 5$ ft.



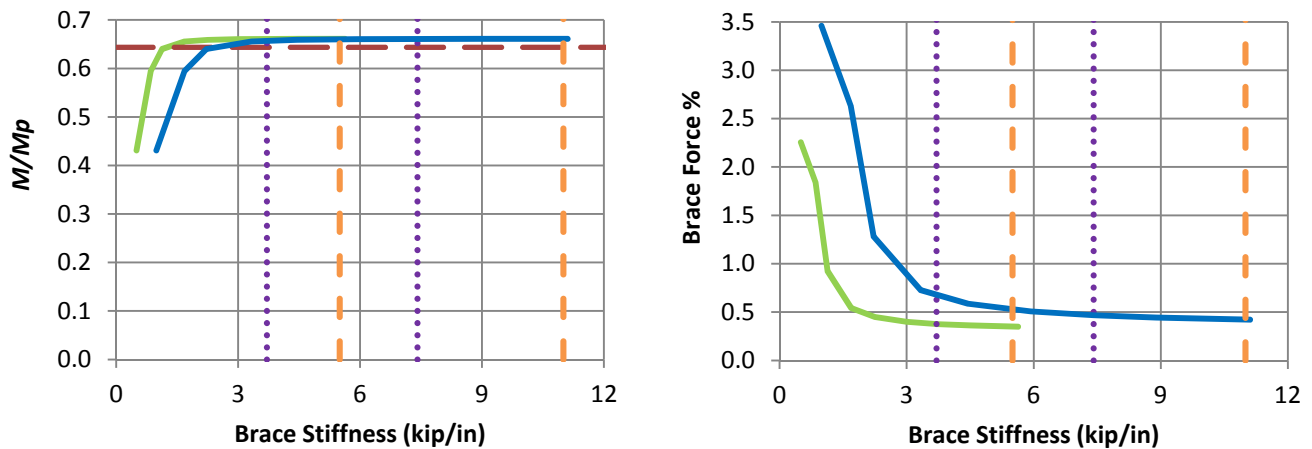
c) B_MG2pt_CNTB_n1_Lb5_TLBSR0.25

- Rigidly-braced strength
- Test simulation results corresponding to torsional brace
- Test simulation results corresponding to lateral brace
- 1x and 0.5x lateral bracing stiffness from Eq. (4-1)
- 1x and 0.5x torsional bracing stiffness from Eq. (4-5)

Fig. A.13 (continued). Beam knuckle curves and brace force vs. brace stiffness plots for combined point (nodal) lateral and torsional bracing cases with $n = 1$, Moment Gradient 2 loading with lateral bracing on the flange in flexural compression, intermediate transverse load applied at top flange of the mid-span cross-section, and $L_b = 5$ ft.



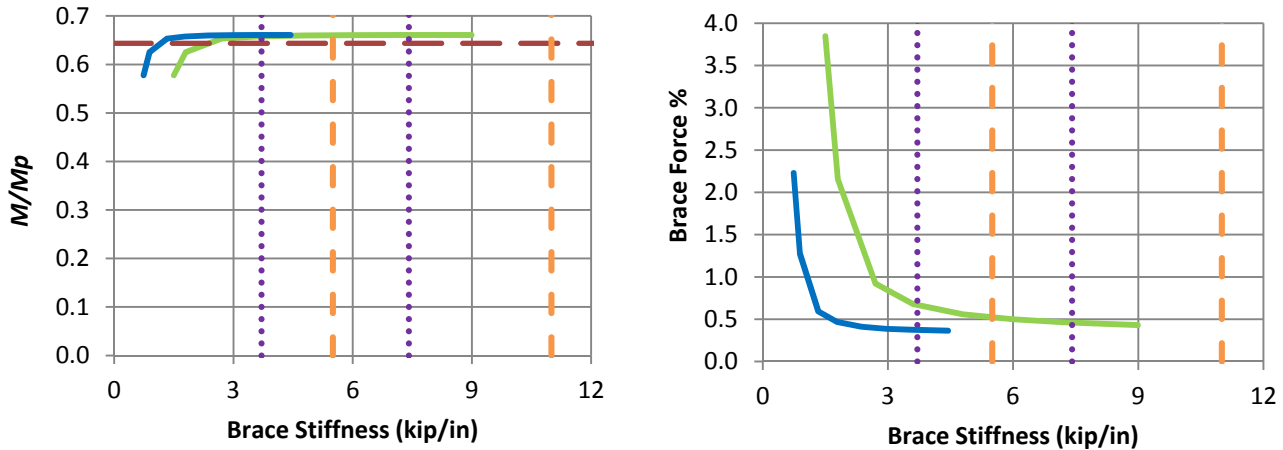
a) B_MG2pt_CNTB_n1_Lb15_TLBSR4



b) B_MG2pt_CNTB_n1_Lb15_TLBSR1

- Rigidly-braced strength
- Test simulation results corresponding to torsional brace
- Test simulation results corresponding to lateral brace
- 1x and 0.5x lateral bracing stiffness from Eq. (4-1)
- - - 1x and 0.5x torsional bracing stiffness from Eq. (4-5)

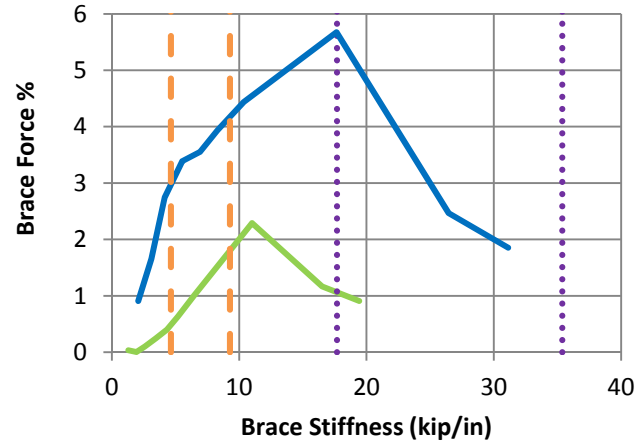
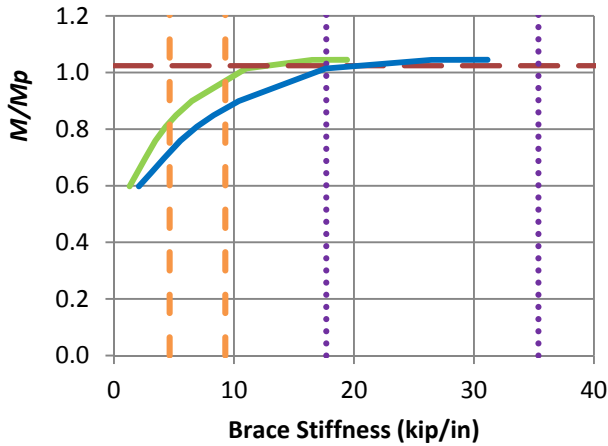
Figure A.14. Beam knuckle curves and brace force vs. brace stiffness plots for combined point (nodal) lateral and torsional bracing cases with $n = 1$, Moment Gradient 2 loading with lateral bracing on the flange in flexural compression, intermediate transverse load applied at top flange of the mid-span cross-section, and $L_b = 15$ ft.



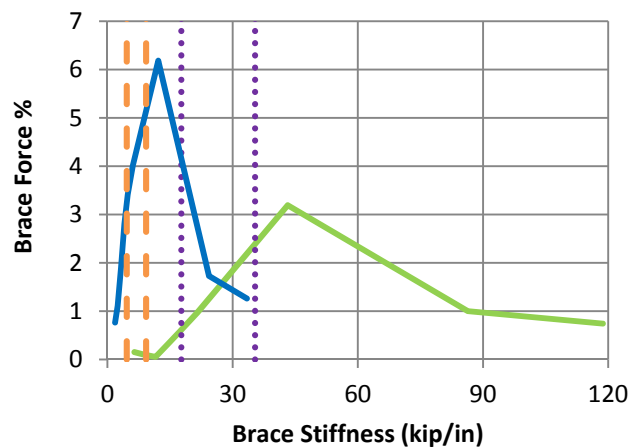
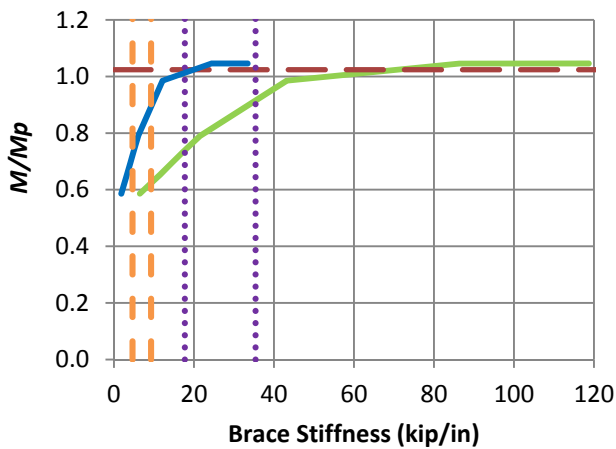
c) B_MG2pt_CNTB_n1_Lb15_TLBSR0.25

- Rigidly-braced strength
- Test simulation results corresponding to torsional brace
- Test simulation results corresponding to lateral brace
- 1x and 0.5x lateral bracing stiffness from Eq. (4-1)
- - - 1x and 0.5x torsional bracing stiffness from Eq. (4-5)

Fig. A.14 (continued). Beam knuckle curves and brace force vs. brace stiffness plots for combined point (nodal) lateral and torsional bracing cases with $n = 1$, Moment Gradient 2 loading with lateral bracing on the flange in flexural compression, intermediate transverse load applied at top flange of the mid-span cross-section, and $L_b = 15$ ft.



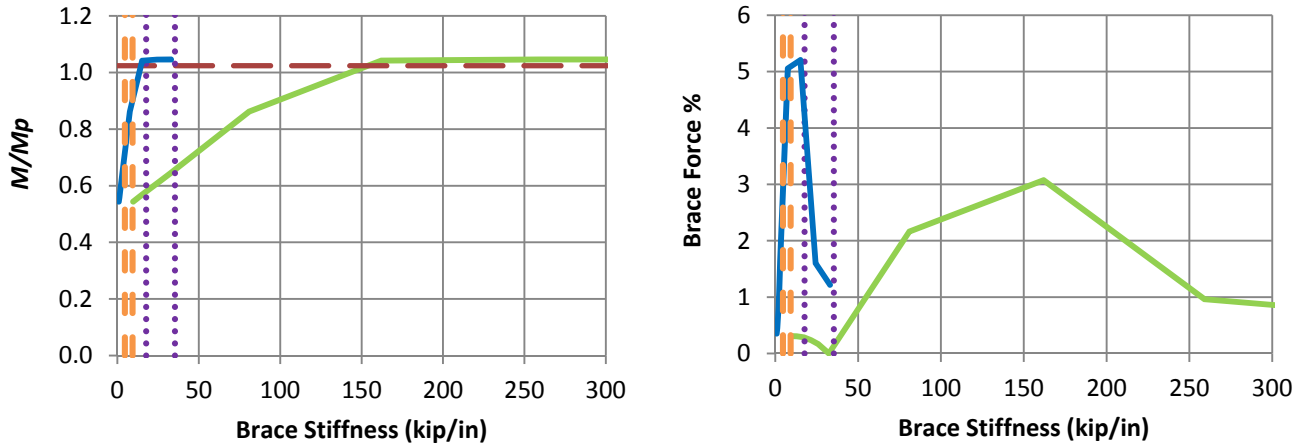
a) B_MG2nt_CNTB_n1_Lb5_TLBSR5.67



b) B_MG2nt_CNTB_n1_Lb5_TLBSR1

- Rigidly-braced strength
- Test simulation results corresponding to torsional brace
- Test simulation results corresponding to lateral brace
- 1x and 0.5x lateral bracing stiffness from Eq. (4-1)
- 1x and 0.5x torsional bracing stiffness from Eq. (4-5)

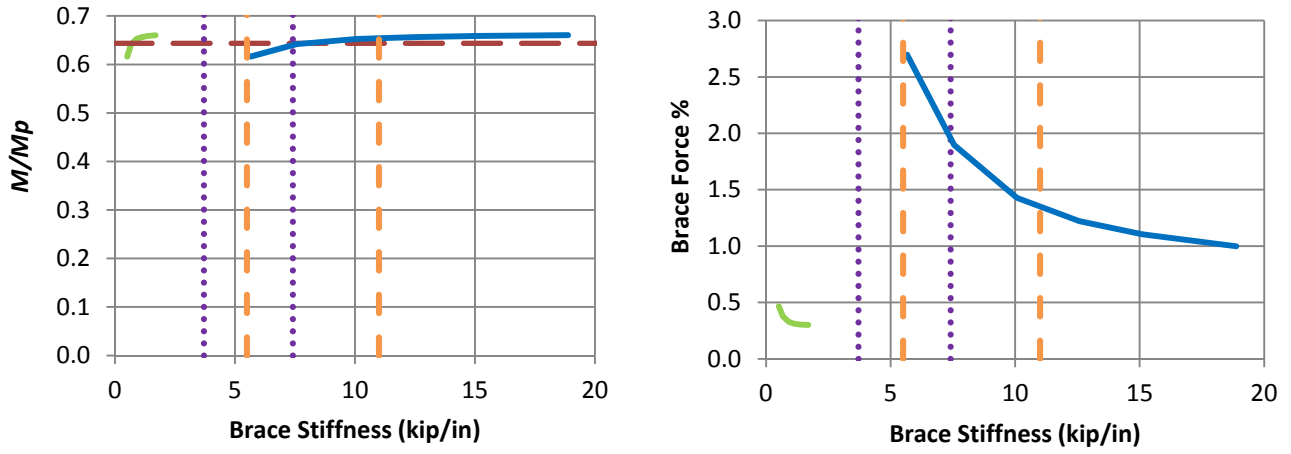
Figure A.15. Beam knuckle curves and brace force vs. brace stiffness plots for combined point (nodal) lateral and torsional bracing cases with $n = 1$, Moment Gradient 2 loading with lateral bracing on the flange in flexural tension, intermediate transverse load applied at top flange of the mid-span cross-section, and $L_b = 5$ ft.



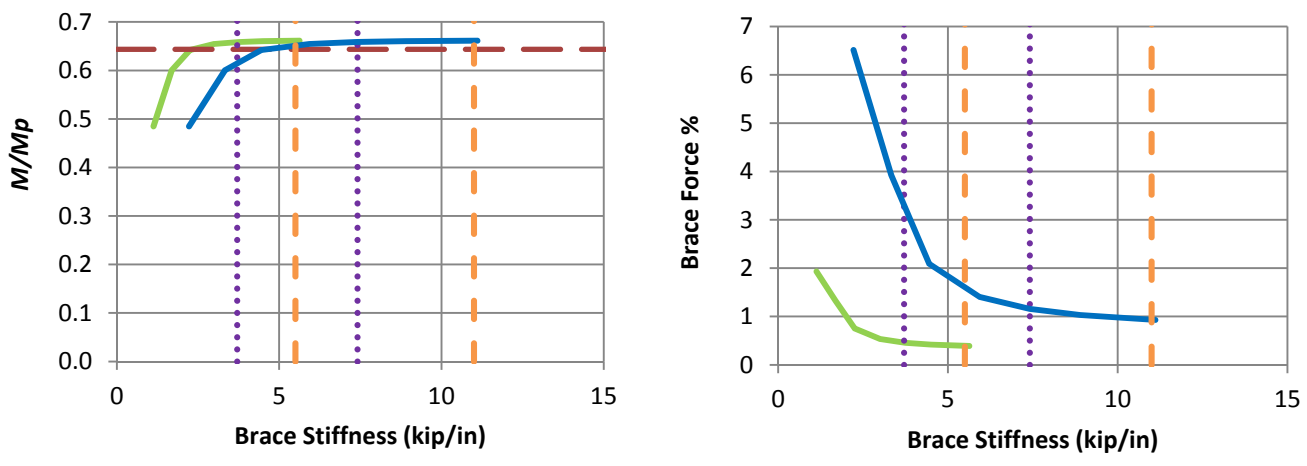
c) B_MG2nt_CNTB_n1_Lb5_TLBSR0.33

- Rigidly-braced strength
- Test simulation results corresponding to torsional brace
- Test simulation results corresponding to lateral brace
- 1x and 0.5x lateral bracing stiffness from Eq. (4-1)
- 1x and 0.5x torsional bracing stiffness from Eq. (4-5)

Fig. A.15 (continued). Beam knuckle curves and brace force vs. brace stiffness plots for combined point (nodal) lateral and torsional bracing cases with $n = 1$, Moment Gradient 2 loading with lateral bracing on the flange in flexural tension, intermediate transverse load applied at top flange of the mid-span cross-section, and $L_b = 5$ ft.



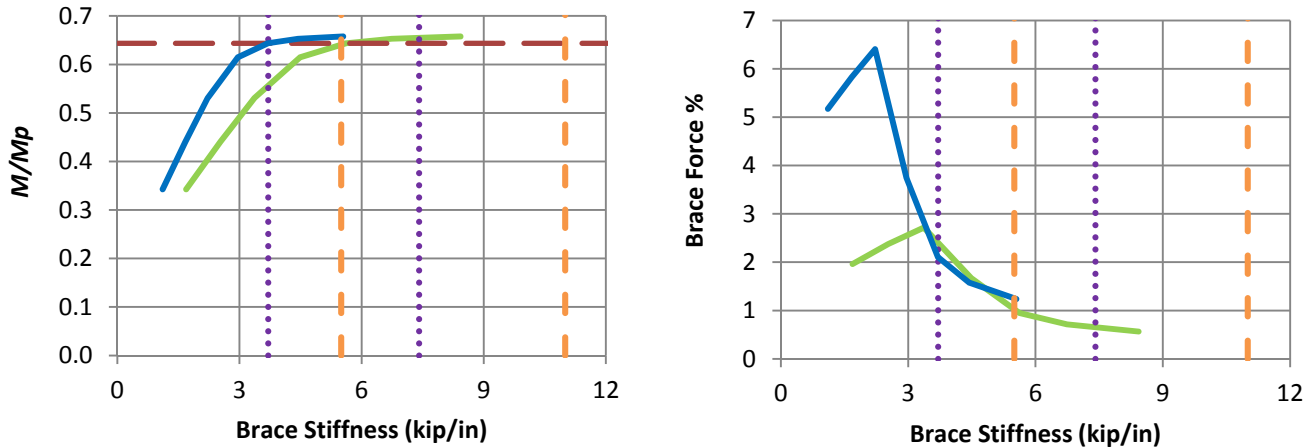
a) B_MG2nt_CNTB_n1_Lb15_TLBSR5.67



b) B_MG2nt_CNTB_n1_Lb15_TLBSR1

- Rigidly-braced strength
- Test simulation results corresponding to torsional brace
- Test simulation results corresponding to lateral brace
- 1x and 0.5x lateral bracing stiffness from Eq. (4-1)
- - - 1x and 0.5x torsional bracing stiffness from Eq. (4-5)

Figure A.16. Beam knuckle curves and brace force vs. brace stiffness plots for combined point (nodal) lateral and torsional bracing cases with $n = 1$, Moment Gradient 2 loading with lateral bracing on the flange in tension, intermediate transverse load applied at top flange of the mid-span cross-section, and $L_b = 15$ ft.



c) B_MG2nt_CNTB_n1_Lb15_TLBSR0.33

- Rigidly-braced strength
- Test simulation results corresponding to torsional brace
- Test simulation results corresponding to lateral brace
- 1x and 0.5x lateral bracing stiffness from Eq. (4-1)
- - - 1x and 0.5x torsional bracing stiffness from Eq. (4-5)

Fig. A.16 (continued). Beam knuckle curves and brace force vs. brace stiffness plots for combined point (nodal) lateral bracing cases with $n = 1$, Moment Gradient 2 loading with lateral bracing on the flange in flexural tension, intermediate transverse load applied at top flange of the mid-span cross-section, and $L_b = 15$ ft.

CHAPTER 10 REFERENCES

- AISC (2016). "Specification for Structural Steel Buildings", Ballot 3 Draft, American Institute of Steel Construction, Chicago, IL.
- AISC (2010a). "Specification for Structural Steel Buildings", ANSI/AISC 360-10, American Institute of Steel Construction, Chicago, IL.
- AISC (2010b). "Code of Standard Practice for Steel Buildings and Bridges", AISC 303-05 American Institute of Steel Construction, Chicago, IL.
- Bishop C.D. (2013). "Flange Bracing Requirements for Metal Building Systems" Doctoral Dissertation, Georgia Institute of Technology, Atlanta, GA.
- CEN (2005). Eurocode 3: Design of Steel Structures, Part 1-1: General Rules and rules for buildings, EN 1993-1-1:2005: E, Incorporating Corrigendum February 2006, European Committee for Standardization, Brussels, Belgium, 91 pp.
- Galambos, T.V. and Ketter, R. (1959). "Columns under Combined Bending and Thrust," *Journal of the Engineering Mechanics Division*, ASCE, 85(EM2), 135-152.
- Helwig, T.A. and Yura, J.A. (1999). "Torsional Bracing of Columns," *Journal of the Structural Engineering*, American Society of Civil Engineers, 125(5), 547-555.
- Nethercot, D.A and Trahair, N.S. (1976). "Lateral Buckling Approximations for Elastic Beams," *The Structural Engineer*, 54(6), 197-204.
- Prado E.P. and White, D.W. (2015). "Assessment of Basic Steel I-Section Beam Bracing Requirements by Test Simulation," Research Report, Georgia Institute of Technology, Atlanta, GA.
- Simulia (2013). ABAQUS, *Software and Analysis User's Manual*, Version 6.13.
- Stanway, G.S., Chapman, J.C., and Dowling, P.J. (1992a). "A simply supported imperfect column with a transverse elastic restraint at any position. Part 1: design models." *Proc. Instn. Civ. Engrs., Strucs. and Bldgs.*, 94(2), 217-218.
- Stanway, G.S., Chapman, J.C., and Dowling, P.J. (1992b). "A simply supported imperfect column with a transverse elastic restraint at any position. Part 1: behavior." *Proc. Instn. Civ. Engrs., Strucs. and Bldgs.*, 94(2), 205-216.
- Tran, D.Q. (2009). "Towards Improved Flange Bracing Requirements for Metal Building Frame Systems," MS Thesis, Georgia Institute of Technology, Atlanta, GA.
- Wang,L., and Helwig, T.A. (2005). "Critical Imperfections for Beam Bracing Systems," *ASCE Journal of Structural Division*, 131(6), 993-940.
- White, D.W., Sharma, A., Kim, Y.D. and Bishop, C.D. (2011). "Flange Stability Bracing Behavior in Metal Building Frame Systems," Final Research Report to Metal Building

Manufacturers Association, Structural Engineering, Mechanics and Materials Report No. 11-74, *School of Civil and Environmental Engineering*, Georgia Institute of Technology, Atlanta, GA, 361 PP.

Yura, J.A. (2001). "Fundamentals of Beam Bracing," *Engineering Journal*, AISC, 38(1), 11-26.

Yura, J.A., (1995), "Bracing for Stability – State-of-the-Art," Is Your Structure Suitably Braced? 1995 Conference, Structural Stability Research Council.

Yura, J. A. and Phillips, B. (1992). "Bracing Requirements for Elastic Steel Beams," *Report No. 1239-1*, Center for Transportation Research, University of Texas at Austin, May, 73 pp.

Yura, J.A., Philips, B., Raju, S., and Webb, S., (1992), "Bracing of Steel Beams in Bridges," Research Report 1239-4F, Center for Transportation Research, Univ. of Texas, October, 80 pp.